Gauge Theories and Geometry in Non-Perturbative String Theory

Wong, Jin-Mann

Awarding institution:
King's College London

KING'S COLLEGE LONDON

Gauge Theories and Geometry in Non-Perturbative String Theory

by

Jin-Mann Wong

A thesis submitted for the
degree of Doctor of Philosophy

in the
Department of Mathematics
School of Natural and Mathematical Sciences

July 2017

Abstract

The central theme in this thesis is compactifications: reductions of higher dimensional theories to lower dimensions and how the geometry of the compactification manifold determines features of the low energy physics. This is studied in the context of non-perturbative string theory in the framework of M-theory and F-theory.

Supersymmetry requires the compactification manifold in F-theory to be an elliptically fibered Calabi–Yau, where the complex structure of the elliptic fibration is identified with the complexified coupling constant in type IIB string theory. The non-perturbative nature of the theory originates from the strong-weak duality of type IIB, which manifests itself as the $SL(2,\mathbb{Z})$ modular transformation of the complex structure. Non-abelian gauge symmetries arise naturally in this framework and engineering Grand Unified Theories within F-theory has been an active area of research. Compactifications on Calabi–Yau four-folds give rise to gauge theories with $\mathcal{N} = 1$ supersymmetry in four dimensions coupled to gravity.

In the first part of this thesis we focus on abelian gauge symmetries in F-theory, which are essential in $SU(5)$ GUTs for forbidding couplings which result in fast proton decay. These arise from rational sections in the elliptic fibration and from the geometric constraints on these sections one can determine the set of possible $U(1)$ charges of GUT matter representations. Armed with this constrained set of charges we then proceed to study the phenomenology of these abelian gauge symmetries in the context of $SU(5)$ GUT models. We analyse their effectiveness at suppressing proton decay operators and explore the types of realistic flavour textures that can be generated using the Froggatt–Nielsen mechanism.

In the latter part of this thesis the focal point changes to M5-branes, one of the two fundamental objects of M-theory. The theory of multiple M5-branes is known to be a 6d $\mathcal{N} = (2,0)$ superconformal field theory, of which only the space-time symmetries and abelian equations of motion have been determined. In spite of this, fascinating correspondences have been shown to arise from the reduction of the M5-brane theory to lower dimensions. In particular, supersymmetric observables in the reduced theories capture non-trivial aspects of the geometry of the compactification manifold. The final chapter of this thesis studies the compactification of the 6d $\mathcal{N} = (2,0)$ theory on the two-sphere as a step towards deriving a correspondence related to four-manifolds.

Acknowledgements

I would like to express my immense gratitude to my supervisor Sakura Schäfer-Nameki for always driving me to learn and improve both academically and as a person. I could not have asked for a better supervisor.

My thanks also go to my fellow PhD students Christopher Couzens, Julius Eckhard, Moritz Küntzler, Craig Lawrie and Damiano Sacco for many enjoyable discussions and as sources for sharing misery and confusion when, as often happened, nothing seemed to be working.

Finally, I thank my family, in particular my brother and sisters, and Nicholas Fox for being my constant companions.

Contents

List of Tables

List of Figures

Chapter 1

Introduction

In 1921 Kaluza considered General Relativity extended to five space-time dimensions and showed that the dimensional reduction of the equations of motion to four dimensions yields both Einstein and Maxwell's equations, unifying gravity and electromagnetism into one theory [1]. In obtaining the four-dimensional equations of motion Kaluza made the crucial assumption,"the cylinder condition", that the five-dimensional metric is independent of the fifth dimension. This was later justified physically by Klein in 1926 using the recent developments in quantum mechanics at the time. By considering the fifth dimension to be compact and microscopic the momentum of components of the five-dimensional metric become quantised and the lowest lying states are exactly those satisfying the cylinder condition [2].

Since the introduction of Kaluza–Klein theory the number of compact dimensions has become greater, and therefore also the has complexity and richness. This is never more true than in the context of string theory. Born from models [3] constructed to explain hadrons and mesons, which we now know to be the theory of Quantum Chromodynamics, string theory has become the leading candidate for unifying the fundamental forces and has led to remarkable developments in mathematics. In its most elemental form it is a theory whose fundamental objects are one-dimensional strings instead of point particles. This however has remarkable consequences, one of which is the natural appearance of a massless spin-2 particle identified as the graviton.

The five string theories, which can all be unified under the umbrella of M-theory, are ten-dimensional. The existence of compact dimensions is then a requisite if the interactions we observe in nature, which are confined to four dimensions, are to have a UV completion in string theory. However, this is not the only basis to study compactifications in string theory and from a purely field theoretic perspective dimensions both larger and smaller than four are also of interest.

	Types of strings	No. of supercharges	Chiral/Non-chiral
Type I	Open+closed	16	Chiral
Type IIA	Open+closed	32	Non-chiral
Type IIB	Open+closed	32	Chiral
Heterotic $SO(32)$	Oriented closed	16	Chiral
Heterotic $E_8 \times E_8$	Oriented closed	16	Chiral

Table 1.1: The five supersymmetric string theories.

1.1 Theories of Superstrings

In the perturbative expansion of gravity as a quantum field theory one encounters an infinite number of divergences and the theory can not be regularised with a finite number of counter-terms i.e. it is non-renormalisable. This should be contrasted with Yang-Mills theories in dimensions $d \leq 4$, where the number of counter-terms required is finite. These divergences can be cured by the introduction of new physics appearing at high energies. In string theory this is the scale at which one can resolve the string and is related to the string tension. Below this scale the different modes of the string manifest themselves as point particles with different properties, such as spin. Of great consequence is of course the existence of a spin two particle among the massless states of the theory, which can play the role of the graviton.

String theory originated from models for the strong interactions and it was not until the work of Green and Schwarz [4] on anomaly cancellation in string theory that it gained stature as a possible candidate for being the fundamental description of nature. At the time only three of the five supersymmetric string theories had been discovered: type I, type IIA and type IIB [5]. The heterotic string was later derived by Gross, Harvey, Martinec and Rohm in [6], uncovering the two remaining supersymmetric string theories. The distinguishing features of the five supersymmetric string theories are summarised in table 1.1. They are determined by two conditions: consistency of the conformal field theory (CFT) on the worldsheet of the string and the absence of tachyons, which lead to an unstable vacuum[1]. String theories contain two parameters in which one can perform a perturbative expansion, the string tension and the string coupling, where the latter is associated to the quantum loop expansion. The low energy description is obtained by keeping only the massless modes in the full theory, and the presence of a graviton in the massless spectrum implies the effective action to the lowest order in the string tension and coupling is ten-dimensional supergravity.

[1] For the derivations we refer to the original papers [5, 6] and [7].

In 1995 Polchinksi realised that Dp-branes, $(p+1)$-dimensional hypersurfaces in space-time on which open strings can end, are in fact dynamical objects [8]. They arise as non-perturbative BPS solitons carrying Ramond-Ramond (RR) charge and couple electrically to the RR $(p+1)$-form in the string theory. The Dp-branes in each string theory are

String Theory	Dp-branes
Type I	$p = 1, 5, 9$
Type IIA	p even
Type IIB	$p = -1,$ odd

(1.1)

The two heterotic string theories have no RR potentials and therefore no Dp-branes. The presence of open strings in type II string theory is in fact a consequence of D-branes. In the type II string theories there only closed string fluctuations around the vacuum and the open strings arise as excitations around the non-perturbative D-branes. This should be contrasted with type I string theory which has both open and closed strings perturbations around the vacuum.

The five supersymmetric string theories are related by various dualities [9]. S-duality, which is a strong-weak duality between two theories, is a self-duality symmetry of type IIB string theory which relates the weak coupling and strong coupling regimes. S-duality forms part of the $SL(2,\mathbb{Z})$ symmetry of type IIB string theory, and is fundamental in the construction of F-theory, which is reviewed in section 2. In essence F-theory makes the action of $SL(2,\mathbb{Z})$ on the string coupling manifest in the compactification geometry, and is thereby able to capture non-perturbative aspects of type IIB string theory. Type IIA and type IIB are mapped into each other under the action of T-duality. A T-duality transformation of type IIA on a circle of radius R gives type IIB on a circle of radius proportional to $1/R$. Analogously, the two heterotic string theories are also exchanged under T-duality. For more details on the network of dualities see, for example, [10].

Analogous to the unification of gravity and electromagnetism in Kaluza–Klein theory, the five supersymmetric string theories can be unified in one dimension higher and obtained as perturbative limits of M-theory. M-theory, which first arose with the supermembrane [11], was discovered to be the non-perturbative limit of type IIA string theory in [12, 13] with the surprising feature that its low energy description is eleven-dimensional supergravity. The appearance of the additional dimension at the strong coupling limit of type IIA is very natural in the context of Kaluza–Klein reductions where the size of the compact dimensions often descends as the coupling constant in the lower dimensional theory. In this context the compact direction is a circle and the exact relation is given by

$$R_{10} = g_{IIA} l_s \,, \tag{1.2}$$

where R_{10} is the radius of the M-theory circle, g_{IIA} is the type IIA string coupling and l_s is the string length. From this we observe that the radius of the circle decompactifies in the limit $g_{\text{IIA}} \to \infty$.

Through the various dualities between the ten-dimensional string theories Witten was able show that type IIB, type I and Heterotic $SO(32)$ string theory also arise as different compactification limits of M-theory. The connection to Heterotic $E_8 \times E_8$ was later made in [14] completing the evidence for M-theory being the overarching non-perturbative theory from which the known string theories can be derived. However, due to the lack of a dimensionless coupling constant the theory does not admit a perturbative expansion and as a result not a great deal is known about M-theory itself. In chatper 5 we shall discuss its low energy description and the two fundamental objects in M-theory; M2-branes and M5-branes.

1.2 Supersymmetry and the MSSM

If string theory is to be a UV complete description of nature then it must incorporate the Standard Model which has been, both theoretically and experimentally, very successful [15]. Despite this great achievement the Standard Model is not an entirely satisfactory description and supersymmetry, which is naturally integrated into string theory, is a highly favoured extension of the Standard Model. One of the most prominent reasons for its popularity is that it provides a natural solution to the hierarchy problem, or the fine-tuning problem of the mass of the Higgs boson [16–19].

The observed mass of the Higgs boson, approximately 125GeV [20, 21], is a combination of the tree level mass and quantum loop corrections. It can be shown that the latter is proportional to the cut-off scale, the energy scale up to which the Standard Model remains an accurate description of fundamental interactions. In order to achieve the observed value of the Higgs mass one needs to cancel the quantum corrections with the tree level mass, which requires extreme fine-tuning. This problem can be resolved by the introduction of scalar superpartners for the fermions participating in the loop interactions. The loop contributions from the fermions and their superpartners cancel and the Higgs mass is protected from quantum corrections.

Despite all its theoretical favour there has been no evidence for supersymmetry at the first run of the Large Hadron Collider (LHC), which probed energies up to 8TeV. These searches have resulted in tighter constraints on the supersymmetry parameter space [22], which will be probed in the second run of the LHC with center of mass energies 13TeV.

Under the constraints of the current results the minimal supersymmetric extension of the Standard Model (MSSM) is not under pressure but other more constrained supersymmetric extensions have become highly disfavoured [23]. Irrespective of the final verdict on the phenomenological advantages of supersymmetry, supersymmetric gauge theories are irrefutably an interesting class of gauge theories in their own right, and we will only consider compactifications preserving supersymmetry in this thesis.

In order for a compactification to preserve supersymmetry the compactification manifold, X, must admit covariantly constant spinors, which satisfy (in the absence of flux)

$$\nabla_X \epsilon = 0\,, \tag{1.3}$$

where ϵ is a spinor. The existence of solutions to (1.3) means the manifold admits spinors which transform as scalars under the holonomy group of X. This is not possible for a manifold with general holonomy $SO(d)$, where $d = \dim X$, and therefore X must be a special holonomy manifold i.e. $\mathrm{Hol}(X) \subset SO(d)$. One class of such manifolds with holonomy contained in $SU(n)$ are the Calabi–Yau n-manifolds, Y_n, which can be specified by the topological condition of having trivial canonical bundle [24,25]. It was shown in [26] that compactifications of type I and heterotic string theories to four dimensions preserving at least $\mathcal{N} = 1$ supersymmetry required X to have holonomy $SU(3)$, i.e. a Calabi–Yau three-fold. Since the type II string theories have twice the number of supercharges in ten dimensions, they preserve 4d $\mathcal{N} = 2$ supersymmetry on Calabi–Yau three-folds. Reductions preserving $\mathcal{N} = 1$ in 4d can be obtained by taking orientifold quotients of Calabi–Yau three-fold compactifications.

The MSSM introduces, in addition to a superpartner for every particle in the Standard Model, two Higgs fields. These are referred to has the Higgs up, H_u, and Higgs down, H_d, and transform in the representations

Field	$G_{SM} = SU(3) \times SU(2) \times U(1)_Y$
H_u	$(\mathbf{1}, \mathbf{2})_{+\frac{1}{2}}$
H_d	$(\mathbf{1}, \mathbf{2})_{-\frac{1}{2}}$

(1.4)

The introduction of a second Higgs field is required for the masses of the up-type and down-type quarks to be supersymmetric [27, 28]. The allowed couplings in the superpotential consist of the Yukawa couplings, the μ-term

$$\mathcal{W}_{\mathrm{MSSM}} \supset \mu H_u H_d\,, \tag{1.5}$$

and also dangerous proton decay couplings. These undesirable couplings are forbidden by assigning the R-symmetry charges of the fields such that these couplings are not consistent

with the $U(1)$ R-symmetry transformation of the superpotential. These assignments also forbid the μ-term and only the Yukawa couplings remain.

One theoretical motivation for considering the MSSM is that it exhibits precision unification of gauge coupling constants around 10^{16}GeV [29] hinting at the presence of some higher rank unification group. The lowest rank Lie groups in which one can embed the MSSM are $SU(5), SO(10)$ and E_6, which all which have a simple realisation in F-theory [30, 31]. In this thesis we focus on $SU(5)$ GUT models in which one generation of quark and lepton representations in the MSSM fit exactly into one $\overline{\mathbf{5}}$ and $\mathbf{10}$ representation of $SU(5)$. The gauge bosons are obtained from the decomposition of the adjoint of $SU(5)$

$$\begin{aligned} SU(5) &\to G_{SM} = SU(3) \times SU(2) \times U(1)_Y \\ \mathbf{24} &\to (\mathbf{8},\mathbf{1})_0 \oplus (\mathbf{1},\mathbf{3})_0 \oplus (\mathbf{1},\mathbf{1})_0 \oplus (\mathbf{3},\overline{\mathbf{2}})_{-5} \oplus (\overline{\mathbf{3}},\mathbf{2})_{+5}\,. \end{aligned} \tag{1.6}$$

The first three representations correspond to the gauge bosons for the strong and electroweak interactions whereas the latter two representations are known as the XY bosons. These bosons are referred to as exotics as they do not appear in the matter spectrum of the MSSM.

The spectrum of quarks and leptons is obtained from the decompositions

$$\begin{aligned} \mathbf{10} &\to (\mathbf{3},\mathbf{2})_{1/6} \oplus (\overline{\mathbf{3}},\mathbf{1})_{-2/3} \oplus (\mathbf{1},\mathbf{1})_1 \\ \overline{\mathbf{5}} &\to (\overline{\mathbf{3}},\mathbf{1})_{1/3} \oplus (\mathbf{1},\mathbf{2})_{-1/2}\,. \end{aligned} \tag{1.7}$$

The Higgs sector in the MSSM also arises from decompositions of the (anti-)fundamental representation, however we also obtain exotic representations in the form of Higgs triplets. These representations can be seen in (1.7) and the issue of how the Higgs triplets become massive such that they do not appear in the spectrum after GUT breaking is the doublet-triplet splitting problem. In fact, as will be discussed in section 2.4, the resolution to this problem and the removal of the XY bosons can be built into the GUT breaking mechanism itself.

A pure $SU(5)$ GUT model is however not feasible as it predicts a proton lifetime much shorter than the lower bound of 10^{34} years [15]. Additional abelian symmetries which commute with the GUT group can be used to forbid dangerous proton decay operators, for example the dimension four coupling

$$\lambda^{(4)}\overline{\mathbf{5}}\overline{\mathbf{5}}\mathbf{10}\,, \tag{1.8}$$

if the $\mathbf{10}$ and $\overline{\mathbf{5}}$ representations are charged appropriately under the additional $U(1)$ symmetries. In the chapters 3 and 4 we shall determine the types of $U(1)$ symmetries which are realisable in the framework of F-theory and study the phenomenology of these additional symmetries with respect to constraints of proton decay in $SU(5)$ GUT models.

1.3 Outline of the Thesis

Following this short introduction to string theory the remainder of this thesis is structured as follows.

The first part of this thesis is centred on the study of abelian gauge symmetries in the context of GUT model building in F-theory. In chapter 2 we introduce F-theory as a framework for studying non-perturbative type IIB string theory in the presence of 7-branes. Of utmost importance will be the geometry of the compactification manifold, which is taken to be elliptically fibered Calabi–Yau three-folds and four-folds in this thesis. The mathematical implements required to extract the low energy physics from the geometry of the elliptic Calabi–Yau will be presented in this chapter with a focus on $SU(5)$ GUT models.

Using the dictionary between aspects of the elliptic Calabi–Yau and the lower dimensional theory discussed in chapter 2 we explore in chapter 3 how the $U(1)$ charges of GUT matter representations are constrained by the geometry. Additional $U(1)$ symmetries are engineered by additional rational sections in the elliptic fibration. By understanding the behaviour of the sections over loci where matter is localised we determine the possible charges of GUT matter under these additional abelian symmetries.

In chapter 4 the results from chapter 3 are used to study phenomenological aspects of $SU(5)$ GUT models with one and two additional $U(1)$ symmetries. The primary motivation for incorporating abelian symmetries into the low energy theory is for the prevention of proton decay couplings which plague $SU(5)$ GUT models. In this chapter we survey the effectiveness of the $U(1)$ charges determined in chapter 3 in suppressing proton decay and the feasibility of also generating favourable Yukawa textures via the Froggatt–Nielsen mechanism.

The final two chapters of this thesis change gear to the study of M5-branes in M-theory. The six-dimensional theory which describes the dynamics of multiple M5-branes has remained largely elusive. Chapter 5 begins with a review of what is currently known about these objects and then proceeds to describe their compactification to lower dimensions and the related correspondences which arise. It ends with a brief section on the subsequent derivation of these correspondences.

Chapter 6 discusses the compactification of a stack of k M5-branes on a two-sphere. The reduction is carried out by coupling the free theory to off-shell conformal supergravity in order to preserve supersymmetry. We proceed by first compactifying on a circle to five dimensions where a non-abelian action is obtained. The final result is a four-dimensional

topological sigma-model into the moduli space of Nahm's equations, or equivalently the moduli space of k $SU(2)$ monopoles, and the action for cases of one and two monopoles is obtained.

The material in chapters 3,4 and 6 are based on the papers [32–34]. The work [35] is not featured in this thesis but was also conducted during the course of the author's PhD.

Chapter 2

F-theory and Elliptic Fibrations

The twelve-dimensional theory describing non-perturbative type IIB string theory known as F-theory was constructed by Vafa in [36]. While dualities with heterotic string theory and related phenomenological aspects were explored in the early days of its discovery [36–44] , it was not until the three seminal papers [30,31,45] that F-theory started gathering attention as a powerful framework for constructing supersymmetric GUTs within type IIB string theory.

More recently, compactifications to six-dimensions have seen revived interest since the classification of 6d superconformal field theories (SCFTs) using F-theory [46,47]. Genuine 4d $\mathcal{N} = 3$ SCFTs were also obtained in [48] by considering D3-branes probing F-theory singularities. The general framework of F-theory has therefore been shown to have far reaching applications not solely limited to string phenomenology, however in this thesis we will only discuss the latter.

In this chapter F-theory is motivated by considering type IIB string theory in the presence of 7-branes. The mathematical framework of F-theory, centred around the geometry of elliptic fibrations, is introduced and a connection is made between various aspects of the geometry of the compactification manifold and features of the low energy physics. By employing the duality between M-theory and F-theory, non-abelian gauge symmetries can be seen to arise from singularities in the elliptic fibration. In addition matter multiplets and Yukawa couplings appear naturally from enhancements in the singularity.

In relation to F-theory, the primary focus of this thesis is the phenomenology of $SU(5)$ GUT models in the presence of additional $U(1)$ symmetries. Geometrically additional $U(1)$ symmetries are realised differently to the aspects of the low energy theory described above, and it is exactly the interaction between these different aspects of the geometry that is studied in chapter 3. The final ingredient we will be considering is fluxes, which

are essential for obtaining a chiral matter spectrum and for breaking the GUT group to the MSSM.

2.1 Type IIB String Theory and 7-branes

To motivate the F-theory construction we start in ten-dimensional type IIB string theory. The field content of type IIB contains the Neveu–Schwartz-Neveu–Schwartz (NSNS) and Ramond-Ramond fields (RR) [5]

NSNS	RR
Metric, g	Axion, C_0
Dilaton, ϕ	Two-form potential, C_2
Kalb–Ramond two-form, B_2	Four-form potential, C_4

(2.1)

where the dilaton is related to the string coupling by $g_s = e^{\phi}$. The ten-dimensional action has classical $SL(2,\mathbb{R})$ invariance, which is broken to $SL(2,\mathbb{Z})$ at the quantum level. The action of this duality symmetry on the fields takes a more compact form when the axion is combined with the string coupling into the axio-dilaton

$$\tau = C_0 + \frac{i}{g_s}\,. \tag{2.2}$$

The action of $SL(2,\mathbb{Z})$ then takes the form

$$\tau \to \frac{a\tau + b}{c\tau + d}\,, \quad \begin{pmatrix} C_2 \\ B_2 \end{pmatrix} \to \begin{pmatrix} aC_2 + bB_2 \\ cC_2 + dB_2 \end{pmatrix}\,, \quad C_4 \to C_4\,, \tag{2.3}$$

where $ad - bc = 1$. From the action of this symmetry we observe it contains the strong-weak duality, S-duality, which maps $\tau \to -1/\tau$ as mentioned in the introduction.

In [36] the transformation of the axio-dilaton under the duality symmetry of type IIB string theory was identified with the $SL(2,\mathbb{Z})$ modular transformations on the complex structure of a two-torus. This presented a natural way to encode the variation of the string coupling into the geometry of the compactification manifold. By considering a fibration of a two-torus over the compactification manifold the variation of the coupling is tracked by the complex structure of the T^2 [1]. In this way one is able to capture the non-perturbative regime of type IIB and the perturbative physics is recovered by taking the fibration to be trivial, so that the string coupling is constant, and taking g_s to be small. In generic fibrations the fiber can become singular and over these loci the complex structure can

[1] We will in fact be interested in fibrations where the fiber is an elliptic curve, which is a T^2 with a marked point. The resulting fibrations are known as elliptic fibrations and will be discussed in more detail in section 2.2.

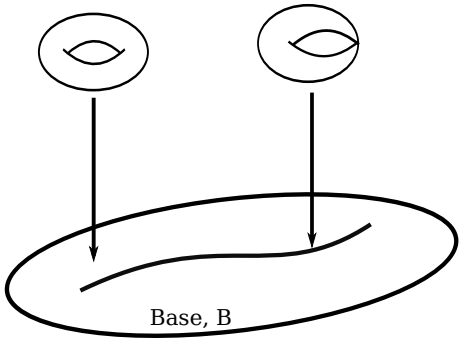

Figure 2.1: Over generic points on the base, B, the fiber is a smooth T^2. However the fiber can also become singular over special loci on the base where one of the 1-cycles on the T^2 shrinks to a point.

diverge. These singularities occur when one of the 1-cycles in the torus shrinks to a point as shown in figure 2.1. The physics of theses divergences can be understood by considering the coupling of the axio-dilaton to D7-branes.

The field strengths in the theory are given by

$$H_3 = dB_2\,, \quad F_{n+1} = dC_n\,, \text{ where } n = 0, 2, 4\,. \tag{2.4}$$

In additional one has the hodge dual of each field strength,

$$*\,F_{n+1} = F_{9-n} = dC_{8-n}\,. \tag{2.5}$$

The potentials C_{p+1} and C_{7-p} couple electrically and magnetically, respectively, to Dp-branes, for p odd[2]. In this way we see that the axio-dilaton couples magnetically to D7-branes. In the presence of a D7-brane the equation of motion for the field strength F_9 takes the form

$$d * F_9 = \delta^{(2)}(z - z_0)\,, \tag{2.6}$$

where z is a complex coordinate parametrising the plane transverse to the world-volume of the brane and z_0 is the location of the D7-brane.

The profile of the axio-dilaton which solves this equation of motion takes the form

$$\tau = \tau_0 + \frac{1}{2\pi i}\ln(z - z_0)\,, \tag{2.7}$$

where τ_0 is a constant and holomorphicity is imposed by its equation of motion. From this we observe that the axio-dilaton diverges logarithmically at the location of D7-branes, this is the physical interpretation of singularities in the fiber. Note that this solution for τ also means that the potential does not fall off to zero asymptotically far away from the

[2]This does not hold for the D9-brane in type IIB string theory, which couples to a ten-form potential. This ten-form does not appear in (2.1) as it is non-dynamical.

brane, as is the case for the other branes with $p < 7$. This means that the backreaction of the brane on the geometry is not negligible and in fact results in a deficit angle at infinity.

This framework allows for more general types of 7-branes known as (p, q)-7-branes on which (p, q)-strings end. In type IIB there are F1-strings and D1-strings which are charged under B_2 and C_2, respectively. As B_2 and C_2 are mixed by $SL(2, \mathbb{Z})$ transformations there exists (p, q)-strings which are charged under both two-form potentials where the fundamental string has charges $(1, 0)$ and the D1-string has charges $(0, 1)$. The existence of these strings means there is a corresponding generalisation of the objects on which the strings can end resulting in (p, q)-7-branes. The standard D7-brane on which fundamental strings end corresponds to a (1,0)-7-brane. The (p, q)-type of the brane changes under the action of $SL(2, \mathbb{Z})$, however it is not always possible in the presence of multiple (p, q)-7-branes to perform a transformation such that they are all of D7-type.

In this section we have motivated the study of elliptic fibrations in type IIB string theory. They provide a framework in which the variation of the axio-dilaton in the presence of 7-branes can be encoded into the compactification manifold and allow for the study of non-perturbative physics in type IIB. In the following sections we shall look at the geometry of these fibrations in more detail and how the low energy physics is dictated by various aspects of the geometry.

2.2 The F-theory Framework

As mentioned in the introduction, supersymmetry is preserved in compactifications of perturbative type IIB string theory on some manifold, B, when B admits covariantly constant spinors. Compactifying on a Calabi–Yau three-fold preserves $\mathcal{N} = 2$ in four dimensions. However, we now allow the axio-dilaton to vary over B as the complex structure of an elliptic curve, $\mathbb{E}_\tau$, fibered over B

$$\begin{array}{ccc} \mathbb{E}_\tau & \hookrightarrow & Y_n \\ & & \downarrow \pi \\ & & B_{n-1} \end{array} \tag{2.8}$$

In this framework one extends the ten dimensions of type IIB by two additional directions coming from the elliptic curve and F-theory is defined in twelve dimensions. The requirement for preserving supersymmetry in an F-theory compactification is that Y_n is a Calabi–Yau n-fold of real dimension $2n$. In particular this means that the base of the fibration B_{n-1} must be Kähler but not in general Ricci-flat. In fact only when the fibration is trivial is B_{n-1} a Calabi–Yau manifold.

In this thesis we shall only discuss elliptically fibered Calabi–Yau three-folds and four-folds relevant for constructing supersymmetric 6d and 4d vacua, respectively, of F-theory[3]

An elliptic curve is a non-singular genus one projective curve with a rational point. It can be written in Weierstrass form [52, 53]

$$P_W = wy^2 - x^3 - fxw^2 - gw^3 = 0\,, \tag{2.9}$$

where $[w : x : y]$ are projective coordinates in $\mathbb{P}^2$ and f, g are constants. The Weiestrass equation (2.9) has a rational point given by $[w : x : y] = [0 : 0 : 1]$.

To obtain an elliptic fibration in Weierstrass form we promote the constants f and g to sections of line bundles $\mathcal{O}(-4K_B)$ and $\mathcal{O}(-6K_B)$, respectively, where K_B is the canonical class of the the base. The constants f, g are chosen to be sections of these particular line bundles so that the resulting fibration is Calabi–Yau. In this way, f, g become functions of coordinates on the base. The projective coordinates also become sections of line bundles with classes

Section	Class
w	H
x	$H - 2K_B$
y	$H - 3K_B$

, (2.10)

where H is the hyperplane class of $\mathbb{P}^2$. The marked point of the elliptic curve defines a holomorphic section, σ_0, of the fibration, which is a map from the base to the fiber satisfying $\pi \circ \sigma_0 = id$. The Weierstrass equation (2.9) now cuts out a hypersurface in the ambient space

$$X = \mathbb{P}(\mathcal{O} \oplus K_B^{-2} \oplus K_B^{-3})\,, \tag{2.11}$$

where $\mathcal{O}$ is structure sheaf of B, which contains the data of all regular functions on open sets of B.

The fiber becomes singular when the discriminant, Δ, is zero,

$$\Delta = 4f^3 + 27g^2 = 0\,. \tag{2.12}$$

As the discriminant is also a section of some line bundle it generically vanishes over codimension one loci in the base. There can be many divisors[4] in the base, Σ_x, over which the discriminant vanishes. We shall denote the order to which the discriminant vanishes over Σ_x by δ_x. Recall from section 2.1 the complex structure diverges when the fiber is singular and this is associated with the presence of 7-branes. The 7-branes are

[3] Compactifications on Calabi–Yau five-folds, which gives rise to 2d $\mathcal{N} = (0, 2)$ gauge theories, were recently studied in [49–51].

[4] A (Weil) divisor on a normal variety X is a finite formal linear combination of integral hypersurfaces of X with integral coefficients [54].

wrapped on the codimension one loci Σ_x over which the discriminant vanishes with their remaining directions lying transverse to the elliptic Calabi–Yau. The number of 7-branes in the compactification and the types of singularities which can appear are constrained by requiring the elliptic fibration to be Calabi–Yau. The first chern class of Y can be expressed as [37]

$$c_1(Y) \simeq \pi^* \left(c_1(B) - \frac{1}{12} \sum_x \delta_x \omega_x \right) , \tag{2.13}$$

where $c_1(B)$ is the first chern class of the base and ω_x is the two-form Poincaré dual to Σ_x in the base. Vanishing of the first chern class requires

$$12 c_1(B) = \sum_x \delta_x \omega_x \, , \tag{2.14}$$

which constrains, for a particular choice of base, the types and number of singularities that can arise.

2.2.1 Singularities and Resolutions

From the discussion in the previous section singularities in the fiber indicate the presence of 7-branes. We are therefore interested in the types of singular fibers which can arise in elliptic fibrations. In all cases, with the exception of two, singularities in the fiber result in the total space of the fibration Y to also be singular. Recall that our Calabi–Yau is described by the hypersurface equation (2.9). The conditions for the Calabi–Yau to be singular are the vanishing of the first derivatives of (2.9) as this corresponds to a degeneration in the tangent space of Y. In this section we shall introduce the concept of a resolution or blow-up of singularities which will feature prominently in the upcoming sections.

Given an algebraic variety X, a resolution of singularities is a variety $\tilde{X}$ together with a projective morphism $f : \tilde{X} \to X$ such that

(1) $\tilde{X}$ is smooth and f is birational

(2) $f : f^{-1}(X_{ns}) \to X_{ns}$ is an isomorphism, and

(3) $f^{-1}(\text{Sing } X)$ is a divisor with simple normal crossings[5],

where Sing X is the set of singular points on X and $X_{ns} := X \setminus \text{Sing } X$ is the set of smooth points [55]. As we are concerned with Calabi–Yau manifolds we require the resolution to be crepant. Crepant resolutions preserve the canonical class of the manifold such that

[5]Let X be a smooth variety. A divisor $D \subset X$ is a simple normal crossings divisor if each irreducible component of D is smooth and all intersections are transverse.

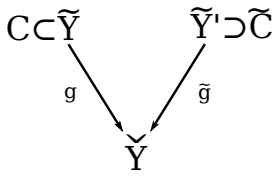

Figure 2.2: Two minimal resolution of singularities $\tilde{Y}$ and $\tilde{Y}'$ blow-down under g and $\tilde{g}$, respectively, to the singular space $\check{Y}$. Each blow-down contracts the contractible curve C and $\tilde{C}$ to a point in $\check{Y}$.

$K_X = K_{\tilde{X}}$. We can expand the divisor $f^{-1}(\text{Sing } X)$ into its irreducible components D_α as

$$f^{-1}(\text{Sing } X) = \sum_\alpha D_\alpha \,. \tag{2.15}$$

Often the divisors D_α are referred to as the exceptional divisors. An explicit example of a resolution of a singular elliptic fibration will be discussed in section 2.2.3.

A resolution of singularities can be obtained by a sequence of blow-ups, which is defined as follows: the blow-up of a variety X along some subvariety Z is a regular birational map $g : X' \to X$ associated to a subvariety $Z \subset X$ that is an isomorphism away from Z but may contain non-trivial fibers over Z. The exceptional divisor E is defined as

$$E = g^{-1}(Z) \subset X' \,. \tag{2.16}$$

Given a resolution of singularities $\tilde{X}$, one can obtain another resolution of singularities by blowing up a point of the exceptional divisor of $\tilde{X}$ [56]. One important class of such resolutions are the minimal ones, through which all other resolution of singularities factor. For singular varieties with complex dimension $d > 2$ there does not exist a unique minimal resolution as is true for the case of singular surfaces. The different minimal resolutions are connected by birational transformations called flips and flops [57, 58].

For Calabi–Yau varieties the relevant birational transformations are flops. Consider two minimal resolutions $\tilde{Y}$ and $\tilde{Y}'$ where each contains a contractible curve $C \subset \tilde{Y}$ and $\tilde{C} \subset \tilde{Y}'$, respectively, such that the blow-down of the contractible curve gives the singular space $\check{Y}$. This set-up is depicted in figure 2.2. The flop transition from $\tilde{Y}$ to $\tilde{Y}'$ is given by the composition $g \circ \tilde{g}^{-1}$, which has the effect of blowing down the curve C and performing a different blow-up of $\check{Y}$, which introduces the curve $\tilde{C}$.

2.2.2 Classification of Singular Fibers and Tate's Algorithm

Kodaira and Néron classified the singular fibers for elliptic surfaces [59–61]. In their classification each singularity is specified by the vanishing orders of (f, g, Δ). Their results

showed that the intersection matrix of the exceptional curves, obtained from the resolution, can only take the form of the zero matrix or one of the Cartan matrices of the simply laced affine Lie algebras. This classification can be generalised to codimension one singularities over higher dimensional bases [62].

Below are the fiber types and groups that will appear in this thesis, in particular I_5 singularities will feature prominently, where the exceptional curves in this case intersect in the affine Dynkin diagram of $\mathfrak{su}(5)$.

Fiber Type	Algebra	Vanishing Order of (f, g, Δ)
I_1	–	$(0, 0, 1)$
$I_{n>2}$	$\mathfrak{su}(n)$	$(0, 0, n)$
I_1^*	$\mathfrak{so}(10)$	$(2, 3, 7)$

(2.17)

The classification by Kodaira and Néron [59–61] was however not constructive and did not give the forms of f, g required to realise a singularity of a particular type. This was done for elliptic surfaces by Tate [62] who constructed an algorithm for determining the hypersurface equation required for a specific singularity. The work of [63, 64] then generalised this to higher dimensional bases. The algorithm, for an elliptic fibration with a section, is carried out by writing the hypersurface equation in Tate form

$$wy^2 + a_1wxy + a_3w^2y - x^3 - a_2wx^2 - a_4w^2x - a_6w^3 = 0\,, \tag{2.18}$$

where $[w : x : y]$ are coordinates in $\mathbb{P}^2$. The coefficients a_i are appropriate sections of line bundles over B. One then expands each of the coefficients as

$$a_i = \sum_{j=1}^{\infty} a_{i,j} z^j\,, \tag{2.19}$$

where z is a coordinate on the base and the $a_{i,j}$ are arbitrary coefficients independent of z. The discriminant then takes the form

$$\Delta = p_0 + p_1 z + p_1 z^2 + O(z^3)\,, \tag{2.20}$$

where p_0, p_1, p_2 are some polynomials in the coefficients $a_{i,j}$. Solving these to vanish order by order increases the vanishing order of the discriminant over $z = 0$. In the simplest cases this can be achieved by specifying a set of vanishing orders, n_{a_i}, for the coefficients a_i such that (2.19) becomes

$$a_i = \sum_{j=n_{a_i}}^{\infty} a_{i,j} z^j\,. \tag{2.21}$$

2.2.3 $SU(5)$ Example

In this section we shall give an example resolution of an I_5 singularity in a Calabi–Yau four-fold and discuss how intersections between divisors in the Calabi–Yau are computed. These intersections are relevant for determining key features of the low energy effective theory, as shall be made apparent in sections 2.2.4 and 2.2.5.

The hypersurface equation for the I_5 singularity is specified by the vanishing orders $(0, 1, 2, 3, 5)$ [63, 64] such that the Tate form is given by

$$wy^2 + a_1wxy + a_3z^2w^2y - x^3 - a_2zwx^2 - a_4z^3w^2x - a_6z^5w^3 = 0\,, \tag{2.22}$$

where the class of z is denoted SG. The discriminant vanishes as

$$\Delta = O(z^5)\,, \tag{2.23}$$

over the divisor $z = 0$ in the base. From the projective relation between the coordinates (w, x, y), the associated divisors can not intersect in the ambient five-fold. This implies an intersection relation on the homology classes of the divisors

$$H \cdot (H - 2K_B) \cdot (H - 3K_B) = 0\,. \tag{2.24}$$

Keeping track of these intersection relations is important for computing intersections between curves and divisors in the Calabi–Yau.

To see that this is an I_5 singularity we need to resolve the singularity and determine how the exceptional divisors from the resolution intersect. We will work in the patch $w = 1$. The hypersurface (2.22) is singular over $x = y = z = 0$, and we can perform a resolution where the coordinates x, y, z are replaced by,

$$x = \hat{x}\zeta_1,\ y = \hat{y}\zeta_1,\ z = \hat{z}\zeta_1\,, \tag{2.25}$$

where the new coordinates $[\hat{x} : \hat{y} : \hat{z}]$ can not vanish simultaneously. The singular locus $x = y = z = 0$ has been replaced with an exceptional divisor whose polynomial equation is $\zeta_1 = 0$. Denoting the class of the exception divisor as by $[\zeta_1] = E_1$, the classes of the new coordinates are given by

$$[\hat{x}] = H - 2K_B - E_1\,, \quad [\hat{y}] = H - 3K_B - E_1\,, \quad [\hat{z}] = SG - E_1\,. \tag{2.26}$$

The intersection relation between the new projective coordinates is given by

$$(H - 2K_B - E_1) \cdot (H - 3K_B - E_1) \cdot (SG - E_1) = 0\,. \tag{2.27}$$

The hypersurface equation after the blow-up takes the form

$$\zeta_1^2(\hat{y}^2 + a_1\hat{x}\hat{y} + a_3\hat{y}\hat{z}^2\zeta_1 - \hat{x}^3\zeta_1 - a_2\hat{x}^2\hat{z}\zeta_1 - a_4\hat{x}\hat{z}^3\zeta_1^2 - a_6\hat{z}^5\zeta_1^3) = 0\,. \tag{2.28}$$

However, this equation does not define a Calabi–Yau anymore as the resolution was not crepant. In order for this to be a crepant resolution we need to take the proper transform, which requires dividing by ζ_1^2 leaving us with only the irreducible component. The space is still singular after this resolution and in order to reach a fully resolved space we must perform three further blow-ups. The final two blow-ups are small resolutions, which resolve codimension two, and are not unique. The distinct smooth Calabi–Yau varieties which arise from each choice of small resolutions are related by the flop transitions [65] discussed in section 2.2.1.

One choice of resolutions is given by,

$$\begin{aligned} \text{Res}_2\text{:}\quad & x = x\zeta_2, \quad y = y\zeta_2, \quad z = z\zeta_2 \\ \text{Res}_3\text{:}\quad & y = y\zeta_3, \quad \zeta_1 = \zeta_1\zeta_3 \\ \text{Res}_4\text{:}\quad & y = y\zeta_4, \quad \zeta_2 = \zeta_2\zeta_4\,, \end{aligned} \tag{2.29}$$

where we have dropped the hat notation on the coordinates and instead keep track of the intersection relations. Introducing the classes E_m for the exceptional divisors D_{F_m}, defined by $\zeta_m = 0$, the additional relations are

$$\begin{aligned} (H - 2K_B - E_1 - E_2)\cdot(H - 3K_B - E_1 - E_2)\cdot(SG - E_1 - E_2) &= 0 \\ (H - 3K_B - E_1 - E_2 - E_3)\cdot(E_1 - E_3) &= 0 \\ (H - 3K_B - E_1 - E_2 - E_3 - E_4)\cdot(E_2 - E_4) &= 0\,. \end{aligned} \tag{2.30}$$

Each of the four resolutions required to resolve the singularity introduces a new exceptional divisor D_{F_m} in Y. These divisors are of the form,

$$\begin{array}{c} \mathbb{P}_1 \\ \downarrow \\ S_{GUT} \end{array} \tag{2.31}$$

where S_{GUT} is the divisor in the base defined by $z = 0$. We denote the rational curves (the $\mathbb{P}_1$s) by F_m, where $m = 1, \cdots, 4$. These are sometimes referred to as the exceptional curves. The associated exceptional divisors D_{F_m} are obtained by fibering F_m over the singularity locus, S_{GUT}. The fiber is there a collection of curves consisting of the exceptional curves and the curve, F_0, distinguished by its non-trivial intersection with the section of the fibration. Together these are referred to as fibral curves, denoted by F_i where $i = (0, m)$, and the associated divisors are fibral divisors.

We would now like to compute the intersection of the fibral divisors to confirm that they intersect in the affine Dynkin diagram of $\mathfrak{su}(5)$. In order to do so we note that the intersection relations (2.24), (2.27) and (2.30) allow us to replace triple intersections of H, E_1 and E_2 with lower powers of each. A similar statement is true for the double intersections of E_3 and E_4. The only non-trivial intersections in the ambient five-fold are then of the form

$$H^2 \cdot D_1 \cdot D_2 \cdot D_3 \,, \tag{2.32}$$

where $D_{1,2,3}$ are pullbacks of divisors in the base. The intersections computed in chapters 3 and 4 were carried out using the Mathematica package `Smooth` [66]. One can check explicitly that the fibral curves intersect to give the affine Dynkin diagram of $\mathfrak{su}(5)$, where the curve F_0 corresponds to the affine node.

The Kodaira-Nerón classification allows us to determine the singularity type by resolving the singularity and computing the intersection matrix of the exceptional divisors. However we note that the resolved space is not the relevant one for F-theory compactifications. The relevant space is obtained by taking the F-theory singular limit [37] of the smooth elliptic Calabi–Yau, which contracts all curves in the fiber which do not intersect the section σ_0 i.e. the F_m's. The remaining singular fibration has only a single Kähler parameter associated with the volume of the component which remains large in the singular limit F_0.

2.2.4 M/F-duality and Non-abelian Gauge Symmetries

There is a correspondence between the Lie algebra of ADE type associated with the singularities in the fiber and the gauge group living on the stack of 7-branes wrapping the discriminant locus. To see how these are related we will need to make use of the duality between M-theory and F-theory [67].

The duality proceeds as follows. We begin in M-theory, which is eleven-dimensional, compactified on a $T^2 = S^1_A \times S^1_B$. Taking S^1_A to be the M-theory circle we obtain perturbative type IIA on S^1_B by shrinking the radius $r_A \to 0$. T-dualising type IIA on S^1_B gives type IIB on $\tilde{S}^1_B$ where the radii of the two S^1_B and $\tilde{S}^1_B$ are inversely proportional. The decompactification limit is given by $\tilde{r}_B \to \infty$ which corresponds to shrinking the remaining cycle in the M-theory T^2 to zero size. As the volume of the T^2 is now zero there are no Kähler moduli, however there is still the complex structure $\tau = iR_A/R_B$ which is related to the string coupling g_s in type IIB. This is extended to a duality between M-theory and F-theory by taking the T^2 in M-theory to be fibered over some base B and then performing the above steps fiberwise.

Armed with the understanding of the relation between M-theory and F-theory we return to the question of how gauge degrees of freedom arise from the singularities in the fiber. Let us consider M-theory compactified on an elliptic four-fold, Y_4. This preserves $\mathcal{N} = 2$ supersymmetry in three dimensions. If the fibration is singular one needs to resolve the Calabi–Yau as described in section 2.2.1. The divisors D_{F_m} obtained from the resolutions are Poincaré dual in Y_4 to $(1,1)$-forms, w_m, and the reduction of the M-theory C_3 potential gives one-forms A^m,

$$C_3 = A^m \wedge w_m \,. \tag{2.33}$$

These one-forms are associated with the degrees of freedom from the Cartan subalgebra of the gauge group. The remaining generators come from M2-branes wrapping chains of $\mathbb{P}_1$s in the fiber, which become massless when the volume of the fiber is taken to zero. Using M/F-duality, the singular limit decompactifies the circle in type IIB and the low energy theory is four-dimensional. The number of supercharges remains the same so we obtain $\mathcal{N} = 1$ supersymmetry.

We should note that $U(1)$ symmetries in the low energy effective theory are not engineered from singularities in the fiber. Although single 7-branes correspond to I_1 singularities in the fiber the total space of the fibration is not singular. One can see this explicitly by looking at the Tate form for an I_1 singularity [64]

$$T_{I_1} = y^2 + a_1 xy + a_3 yz - x^3 - a_2 x^2 - a_4 xz - a_6 z = 0 \,. \tag{2.34}$$

In order for the total space to be singular the Tate form and its first derivatives need to vanish. The obstruction to the space being singular is the derivative with respect to z

$$\partial_z T_{I_1} = a_3 y - a_4 x - a_6 \,, \tag{2.35}$$

which is non-vanishing for $a_6 \neq 0$. Forcing a_6 to vanish to a higher order in z increases the vanishing order of the discriminant and one obtains an I_2 singularity. Since the Calabi–Yau is smooth there is no need to resolve and one obtains no new divisors in the geometry. In fact abelian gauge symmetries arise geometrically in a different way, which is the topic of section 2.3.

2.2.5 Appearance of Matter and Yukawa Couplings

We have just seen how codimension one singularities in the fiber determine the non-abelian gauge symmetries on the stack of 7-branes wrapping the discriminant locus. As the bases we consider are either complex two- or three-dimensional one can consider what happens over higher codimension. Over codimension two loci in the base the vanishing order of the

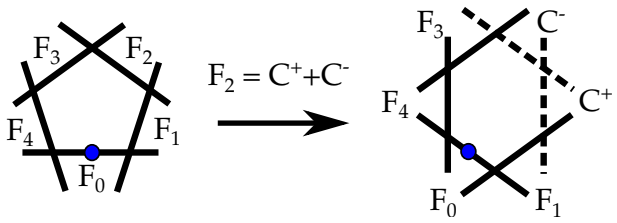

Figure 2.3: One possible splitting of the curves in the I_5 fiber over a codimension two enhancement to I_6 [69, 65].

discriminant can increase which corresponds to an enhancement in the singularity. These loci are associated with matter [68] transforming in some representation, $\mathbf{R}$, of the gauge group.

To illustrate this let us consider an I_5 singularity. Over codimension two the singularity can enhance generically in one of two ways, evident from the discriminant

$$\Delta = P_5 P_{10} z^5 + P_{10} z^6 + z^7 + \cdots . \tag{2.36}$$

The singularity enhances to I_6 and I_1^* over $P_5 = 0$ and $P_{10} = 0$, respectively. Over these loci it was observed in [69] that the curves in the I_5 fiber become reducible. Let us consider the enhancement over $P_5 = 0$. In this case one of the fibral curves splits into two irreducible curves

$$F_i \to C^+ + C^- . \tag{2.37}$$

We shall consider the splitting depicted in figure 2.3. One can compute the intersection of $C^\pm$ with the exceptional divisors

	D_{F_1}	D_{F_2}	D_{F_3}	D_{F_4}
C^+	0	-1	1	0
C^-	1	-1	0	0

(2.38)

and we obtain weights of the $\mathbf{5}$ and $\overline{\mathbf{5}}$ representation of $\mathfrak{su}(5)$. The new set of irreducible curves $(F_0, F_1, C^+, C^-, F_3, F_4)$ intersect in the affine Dynkin diagram of $\mathfrak{su}(6)$, the Lie algebra associated to an I_6 singularity.

The matter representations can be determined from the group theoretic decomposition of the adjoint representation of $\mathfrak{su}(6)$ into $\mathfrak{su}(5)$

$$\mathbf{35} \to \mathbf{24}_0 + \overline{\mathbf{5}}_{-6} + \mathbf{5}_6 + \mathbf{1}_0 , \tag{2.39}$$

which gives the adjoint of $\mathfrak{su}(5)$ as well as the fundamental and anti-fundamental representations. Analogously, the enhancement over $P_{10} = 0$ gives rise to the antisymmetric representation from the decomposition of adjoint of the associated Lie algebra $\mathfrak{so}(10)$

$$\mathbf{45} \to \mathbf{24}_0 + \overline{\mathbf{10}}_{-4} + \mathbf{10}_4 + \mathbf{1}_0 . \tag{2.40}$$

In order to understand how these additional curves arising from the splitting of codimension one fiber components correspond to massless matter we employ M/F-Theory duality. Consider M-theory compactified on the same elliptic Calabi–Yau. The massless modes transforming in some representation $\mathbf{R}$ under $\mathfrak{g}$ arise from M2-branes wrapping these additional curves in the fiber over codimension two. Matter is therefore localised to the codimension two loci over which the discriminant enhances. The additional curves in the fiber arising from the splitting of the fibral curves will be referred to as matter curves.

The possible splittings of the fibral curves over codimension two were studied in [70]. These splittings were determined by analysing the phases of the classical Coulomb branch of the $3d$ $\mathcal{N}=2$ gauge theory arising from the compactification of M-theory on a Calabi–Yau four-fold. The presence of matter charged under the gauge group subdivides the Coulomb branch giving rise to the different phases which correspond to different resolutions of the singular Calabi–Yau three-fold. The different phases/resolutions were encoded in the so-called decorated box graphs associated to each codimension two fiber. The splitting for a codimension one singularity, with associated Lie algebra $\mathfrak{g}$, follows the rules for the decomposition of the simple roots of $\mathfrak{g}$ into the weights of the representation $\mathbf{R}$ of $\mathfrak{g}$ [71].

In elliptic four-folds the discriminant can enhance further over codimension three loci, which are points in the base. These special points are the intersections of curves in the base over which matter is localised and correspond to Yukawa couplings between the matter representations. For an I_5 singularity these enhancements produce couplings between $\mathbf{5}$, $\overline{\mathbf{5}}$ and $\mathbf{10}$ representations producing the usual top and bottom Yukawa couplings

$$\begin{aligned} &\lambda^{t}_{iab}\mathbf{5}_i\mathbf{10}_a\mathbf{10}_b \\ &\lambda^{b}_{ija}\overline{\mathbf{5}}_i\overline{\mathbf{5}}_j\mathbf{10}_a\,. \end{aligned} \tag{2.41}$$

2.3 The Mordell–Weil Group and $U(1)$ Symmetries

Abelian gauge symmetries arise from the presence of additional rational sections in the elliptic fibration [37,38]. A rational point on an elliptic curve, a solution to the Weierstrass equation where the coordinates take rational values, lifts to a rational section for an elliptic fibration. This a map from the base to the fiber, which defines a $\mathbb{Q}$-divisor in the Calabi–Yau. The explicit fibrations we have considered so far have only a single holomorphic section called the zero-section, σ_0. One can also consider fibrations with rational sections, in addition to the zero-section, and these give rise to abelian gauge symmetries.

The rational sections of an elliptic fibration form a group, the Mordell–Weil group which is a finitely generated abelian group [72, 73]. The group law is given by the group law

of rational points on elliptic curves, where the zero-section plays the role of the identity. In order to generate a rank 1 Mordell–Weil group one must have in addition to the zero-section an additional rational section. For each rational section, σ_α, one can define the Shioda map,

$$S(\sigma_\alpha) = \sigma_0 - \sigma_\alpha + S_f \tag{2.42}$$

where S_f is a linear combination of the exceptional divisors D_{F_m} and pullbacks of divisors in the base. It is determined by the condition

$$S(\sigma_\alpha) \cdot_Y F_i = 0\,, \quad \text{where } i = 0, \cdots, 4\,, \tag{2.43}$$

where $\cdot_Y$ denotes an intersection in the Calabi–Yau. The Shioda map defines an additional divisor in Y with dual $(1,1)$-form, w_α. Using M/F-theory duality the dimensional reduction of the C_3-form along this $(1,1)$-form by (2.33) gives an additional gauge field A^α associated to an abelian gauge factor [38]. The condition (2.43) ensures that the non-abelian gauge bosons are uncharged under these additional $U(1)$ symmetries.

In codimension one both holomorphic and rational sections intersect the fiber transversely in a point. They are distinguished over codimension two matter loci where rational sections exhibit two types of behaviours

(1) Intersects the fiber transversely in a point.

(2) Contains curves in the fiber.

In comparison a holomorphic section can only continue to intersect the fiber in a point. It is exactly this feature of rational sections that will be exploited in the analysis in chapter 3 to obtain the possible $U(1)$ charges for **5** and **10** matter. The $U(1)$ charges of the matter representations are computed by intersecting the Shioda map with the matter curves which arise from the splitting of codimension one fiber components. For the example considered in section 2.2.5, where the splitting was given by $F_2 \to C^+ + C^-$, the $U(1)$ charges of the corresponding $\overline{\mathbf{5}}$ and **5** matter are determined by

$$q_\alpha(C^\pm) = S(\sigma_\alpha) \cdot_Y C^\pm\,. \tag{2.44}$$

We note that discrete gauge symmetries also play an important role in GUT model building and can be used to prevent fast proton decay in $SU(5)$ GUT models. Examples of such discrete symmetries include R-parity and baryon triality [74]. In this thesis we will not consider abelian or non-abelian discrete symmetries beyond commenting on how they can be obtained by Higgsing additional $U(1)$ symmetries. Discrete symmetries arise from genus one fibrations, elliptic fibrations without a section, which are beyond the scope of this thesis. These have been studied in [75–82].

2.4 GUT Breaking and Fluxes

We have now seen how GUT groups and matter representations arise from singularities in the elliptic fibration. However, in order arrive at the MSSM a mechanism for breaking the GUT group needs to be employed. In addition the matter representations arising from codimension two enhancements come in pairs $\mathbf{R} \oplus \overline{\mathbf{R}}$ for some representation $\mathbf{R}$, which means that the spectrum has no chirality. An additional ingredient is required for obtaining a chiral spectrum, which is G_4-flux [30, 31, 83]. In this section we shall review how fluxes can be employed to break the GUT group as well as generate chirality in the matter spectrum.

There are three main mechanisms for breaking the GUT group in string theory, summarised in [30]. We will briefly review them here focussing on $SU(5)$ GUT models in Calabi–Yau four-fold compactifications breaking to the MSSM.

- Higgs Field
  In this scenario the GUT group is broken by giving a vacuum expectation value to a Higgs field transforming in the adjoint representation of the GUT group. Engineering this is possible in F-theory, however this mechanism suffers from the doublet-triplet splitting problem. Recall the decomposition of the fundamental of $SU(5)$ into the representations of the MSSM is

$$\begin{aligned} SU(5) &\to G_{SM} = SU(3) \times SU(2) \times U(1)_Y \\ \mathbf{5} &\to (\mathbf{3}, \mathbf{1})_{-\frac{1}{3}} \oplus (\mathbf{1}, \mathbf{2})_{\frac{1}{2}} \,, \end{aligned} \tag{2.45}$$

  with a similar decomposition for the anti-fundamental representation. The doublet we obtain has the correct transformation for the Higgs up, H_u, however the triplet is an exotic. The existence of the triplet is problematic as it participates in proton decay couplings and in order for these to be sufficiently suppressed the mass of the triplet has to be large. The double-triplet problem is therefore a question of how to make the triplet representations sufficiently massive while keeping the masses of the doublets of the order of the electroweak scale.

- Wilson Line Breaking
  This mechanism has been used heavily in Heterotic GUT model building as it has the virtue of splitting the Higgs doublet and triplets providing a natural solution to the doublet-triplet splitting problem. GUT breaking in F-theory using Wilson lines (flat line bundles) was first proposed in [30, 45] while a more detailed study was carried out in [84, 85]. These models require the surface S_{GUT} wrapped by the 7-branes in the Calabi–Yau four-fold to have non-trivial fundamental group. Models obtained

from Wilson line breaking in the hypercharge direction $U(1)_Y$, the commutant of G_{SM} inside $SU(5)$, are however also not phenomenologically ideal as they contain light exotic matter in the form of the XY bosons [30]. These are states arising from the decomposition of the adjoint of $SU(5)$

$$\begin{aligned} SU(5) &\to G_{SM} = SU(3) \times SU(2) \times U(1)_Y \\ \mathbf{24} &\to (\mathbf{8},\mathbf{1})_0 \oplus (\mathbf{1},\mathbf{3})_0 \oplus (\mathbf{1},\mathbf{1})_0 \oplus (\mathbf{3},\overline{\mathbf{2}})_{-5} \oplus (\overline{\mathbf{3}},\mathbf{2})_{+5}\,, \end{aligned} \tag{2.46}$$

where the latter two representations are the exotic XY bosons. When the line bundle is not flat the reasoning in [30] is no longer valid, however in these scenarios there is a tension between engineering a massless photon and gauge coupling unification, which was studied in [86].

- $U(1)$ Fluxes
  Lastly, one can consider turning on fluxes for a $U(1)$ factor inside the GUT group which commutes with the standard model gauge group. In the case of $SU(5)$ GUT models the commutant is $U(1)_Y$, which breaks $SU(5)$ to G_{SM}. This line of study was initiated in [87, 84, 45]. In order for the hypercharge gauge field to be massless there is a topological constraint on the associated line bundle $\mathcal{L}_Y$: the 2-cycle, Ξ, Poinaré dual to $c_1(\mathcal{L}_Y)$ inside S_{GUT} must be a non-trivial two-cycle in the GUT surface but trivial in the base. Formally this means that there is a 3-chain in the base with boundary Ξ. The advantage of this method is that it does not lead to a double-triplet splitting problem and can avoid massless XY bosons.

In chapter 4, hypercharge flux will be used for decomposing $SU(5)$ GUT models with additional $U(1)$ symmetries to the MSSM. In order to obtain a chiral spectrum we also need non-trivial G_4-flux. The flux quantisation condition for the four-form flux G_4 was determined by Witten in [88] and reads

$$G_4 + \frac{1}{2}c_2(Y) \in H^4(Y,\mathbb{Z})\,, \tag{2.47}$$

where $c_2(Y)$ is the second Chern class of the smooth Calabi–Yau. For Calabi–Yau three-folds the second Chern class is always divisible by two [89, 90] and the flux quantisation condition reduces to a constraint on G_4 only. In the Calabi–Yau four-fold case the implication of (2.47) is that depending on the topology of the Calabi–Yau the G_4-flux may necessarily be non-vanishing.

The chirality of a representation $\mathbf{R}$ of the MSSM, denoted $\chi(\mathbf{R})$, induced from the presence of non-trivial G_4-flux and hypercharge flux is given by [45, 84]

$$\chi(\mathbf{R}) = \int_\Sigma c_1(V_\Sigma \otimes \mathcal{L}_Y^{q_\mathbf{R}^Y})\,, \tag{2.48}$$

where Σ is the codimension two curve in the base over which matter is localised, V_Σ is the vector bundle associated with the G_4-flux, $\mathcal{L}_Y$ is the line bundle for the $U(1)$ hypercharge flux and $q^Y_{\mathbf{R}}$ is the $U(1)_Y$ charge of the representation $\mathbf{R}$. The chirality can be expressed in terms of two parameters

$$\chi(\mathbf{R}) = \mathcal{M}_\Sigma + q^Y_{\mathbf{R}}\mathcal{N}_\Sigma\,, \tag{2.49}$$

where $\mathcal{M}_\Sigma$ and $\mathcal{N}_\Sigma$ are the contributions to the chirality from the G_4-flux and hypercharge flux, respectively. They are the same for all MSSM representations which originate from the same GUT matter representation and from these we can define the chirality of the MSSM spectrum to be

$SU(5)$ representation	MSSM representation	Particle	Chirality
$\mathbf{10}_a$	$(\mathbf{3},\mathbf{2})_{1/6}$	Q	M_a
	$(\bar{\mathbf{3}},\mathbf{1})_{-2/3}$	$\bar{u}$	$M_a - N_a$
	$(\mathbf{1},\mathbf{1})_{1}$	$\bar{e}$	$M_a + N_a$
$\overline{\mathbf{5}}_i$	$(\bar{\mathbf{3}},\mathbf{1})_{1/3}$	$\bar{d}$	M_i
	$(\bar{\mathbf{1}},\mathbf{2})_{-1/2}$	L	$M_i + N_i$

(2.50)

where M_a, M_i, N_a, N_i can be expressed in terms of $\mathcal{M}_\Sigma, \mathcal{N}_\Sigma$.

Various constraints on the parameters determining the chirality of each MSSM representation arise from the cancellation of anomalies and the absence of exotics. From the absence of MSSM anomalies the the chiralities are required to satisfy

$$\sum_a M_a = \sum_i M_i\,, \qquad \sum_a N_a = \sum_i N_i = 0\,. \tag{2.51}$$

In pure $SU(5)$ GUT models, i.e. no additional $U(1)$ symmetries, there only exists a single curve in the base over which $\mathbf{10}$ and $\overline{\mathbf{5}}$ representations are localised i.e. $a = i = 1$ and the absence of exotics requires $M_{10} = M_5 = 3$ and $N_{10} = N_5 = 0$. However, in the presence of additional $U(1)$ symmetries there can be multiple codimension two loci with matter in the $\mathbf{10}$ and $\overline{\mathbf{5}}$ representations with different $U(1)$ charges. Mixed anomalies between the additional abelian symmetries and the MSSM gauge groups must now be cancelled which leads to constraints on the chirality parameters and the $U(1)$ charges of GUT matter. These will be discussed in detail in chapter 4.

Chapter 3

F-theory and All Things Rational: Surveying $U(1)$ Symmetries with Rational Sections

3.1 Introduction

Recent years have seen much progress towards refining F-theory compactifications, including the realisation of symmetries of the low energy effective theory that allow more realistic model building. These developments have been fuelled by increasingly sophisticated mathematical techniques that are required to construct the geometries underlying such F-theory compactifications. In lockstep with this, there has been a definite trend towards characterizing universal aspects of string compactifications, with a view to going beyond an example-driven approach. One of the areas where a universal characterisation would be particularly bountiful is that of additional symmetries, such as abelian and discrete gauge symmetries, due to the direct phenomenological impact.

The main result of this chapter is to provide such a universal characterisation of possible $U(1)$ symmetries and associated matter charges in F-theory. Furthermore, we obtain a characterisation of $U(1)$-charged singlets, which in turn can be used to Higgs abelian gauge groups to discrete symmetries.

The framework we are working within is F-theory compactifications on elliptically fibered Calabi–Yau three- and four-folds, where non-abelian gauge groups are modelled in terms of singularities above codimension one loci in the base of the fibration [36]. Applications include the modelling of six-dimensional $\mathcal{N} = (1, 0)$ or four-dimensional $\mathcal{N} = 1$ supersymmetric gauge theories, whose gauge group is determined by the Kodaira type of the singularity [60, 59, 61]. Matter is engineered from codimension two singularities, whose

fibers are characterised in terms of representation theoretic data, associated to the representation graph of the matter multiplet [70]. Abelian symmetries, which for instance are important model building tools for four-dimensional GUT models in F-theory [30, 31, 45], are realised mathematically in terms of rational sections of the elliptic fibrations, i.e. maps from the base to the fiber [38]. The rational sections, under the elliptic curve group law, form an abelian group, the Mordell–Weil group, $\mathbb{Z}^r \oplus \Gamma$, where Γ is a discrete group, the origin of which is the zero-section σ_0. Such a rank r Mordell–Weil group gives rise to r abelian gauge factors in the low energy effective theory, by reducing the M-theory C_3-form upon the $(1,1)$-cycles that are dual to the rational sections.

Numerous examples of F-theory compactifications with $U(1)$ symmetries are by now well-studied starting with the general theory of realising the elliptic fiber with one [91], two [92–95] and three [96] rational sections, toric constructions of various kinds [97–100], models based on refined Weierstrass fibrations [101–103, 76], as well as a survey of all local spectral cover constructions [104] or from Higgsing of E_8 [105]. Unfortunately, none of these approaches are both comprehensive, i.e. explore the complete set of possible $U(1)$ symmetries, and at the same time global (in the case of the spectral cover survey and E_8 embedding, which are general but only in terms of local models).

Clearly it is highly desirable to determine the possible $U(1)$ symmetries in general, as these impose vital phenomenological input, and can lead to potentially non-standard physics beyond the Standard Model (see e.g. [106]). Furthermore, from a conceptual point of view, it is very appealing to be able to constrain these symmetries from the analysis of the fiber alone. One avenue that would lead in principle to such a general result is to determine the possible realisations of non-abelian gauge groups via Tate's algorithm [63, 64] applied to the elliptic fibrations with extra sections in [91, 93, 94]. This program was pursued in [107, 108], resulting in a large class of new Tate-like models, however, in order to be able to carry out the algorithm, some technical simplifications had to be made, thus potentially jeopardizing the universality of the result.

In this thesis, we propose and provide a systematic analysis and universal characterisation of such $U(1)$ symmetries in F-theory. Recall, that matter in a representation $\mathbf{R}$ of the gauge group, arises from wrapping M2-branes on irreducible components of the fiber in codimension two. The $U(1)$ charges of such matter multiplets are computed by intersecting the $U(1)$ generator, which is constructed from the rational sections, with these fiber components. To classify the possible charges, one requires the following input: firstly, a complete understanding of the types of codimension two fibers that realise matter, which is now available in [70], and secondly, the possible configurations that the rational sec-

tions can take within these fibers. As we will demonstrate, the latter can be constrained in terms of general consistency requirements on $\mathbb{P}^1$s, i.e. rational curves, in Calabi–Yau varieties.

The possible codimension two fibers in an elliptic fibration with a holomorphic zero-section can be characterised in terms of classical Coulomb phases of $d = 5$ or $d = 3$ $\mathcal{N} = 2$ supersymmetic gauge theories [109–113,65], in terms of so-called box graphs [70]. In particular, the box graphs characterise all possible splittings of the codimension one Kodaira fibers into codimension two fibers, which realise matter. In terms of the singular Weierstrass model, these characterise distinct small resolutions, which are connected by flop transitions.

A rational section is characterised by the property that its intersection with the fiber is one. In codimension one, this implies that the section intersects a single rational curve in the Kodaira fiber transversally in a point[1]. In codimension two, the section can again transversally intersect a single rational curve in the fiber, however, in addition, it can also contain components of the fiber. This effect has been referred to in the existing literature as the section *wrapping* the fiber component. This phenomenon was first observed in [91], where these fibers were shown to produce $U(1)$ charges distinct from fibers where both the zero-section and the additional section intersect transversally.

For each section σ there are two configurations that can occur in codimension two. Either the section intersects a single component transversally, or it contains (i.e. wraps) fiber components. The wrapping is highly constrained by the requirement that the intersection of σ with the fiber remains one, which we shall see translates into conditions on the normal bundle degrees of the wrapped curves. Concretely, we consider smooth elliptic Calabi–Yau varieties Y of dimension three and four and, subject to the following constraint, we determine the possible section configurations: intersections of σ with fiber components in codimension one are preserved in codimension two, in particular, they are consistent with the splitting as dictated by the box graphs.

For purposes of F-theory model building our main focus will be on $SU(n)$ gauge theories with fundamental and anti-symmetric matter, and in fact large parts of this chapter will focus on $n = 5$ with the view to realise $SU(5)$ GUT models in F-theory with additional $U(1)$ symmetries. We determine all possible section configurations in codimension two fibers for these matter representations, and thereby the $U(1)$ charges. For $SU(5)$ with one $U(1)$ there are three distinct codimension one configurations of the zero-section σ_0,

[1] In principle, the section could contain codimension one fiber components, however, it would then not be irreducible.

relative to the additional rational section σ_1, where they intersect transversally the same $\mathbb{P}^1$ $I_5^{(01)}$, nearest $I_5^{(0|1)}$ and next to nearest $I_5^{(0||1)}$ neighbor $\mathbb{P}^1$s of the I_5 Kodaira fiber (see figure 3.3).

We determine all section configurations for $\bar{\mathbf{5}}$ and $\mathbf{10}$ matter, under the assumption that the sections remain smooth divisors in the Calabi–Yau geometry – the precise setup that enters this discussion is summarised in section 3.4.1. The resulting charges are as follows:

$$\begin{aligned} U(1) \text{ charges of } \bar{\mathbf{5}} \text{ matter for } & \begin{cases} I_5^{(01)} \in \{-3,-2,-1,0,+1,+2,+3\} \\ I_5^{(0|1)} \in \{-14,-9,-4,+1,+6,+11\} \\ I_5^{(0||1)} \in \{-13,-8,-3,+2,+7,+12\} \end{cases} \\ U(1) \text{ charges of } \mathbf{10} \text{ matter for } & \begin{cases} I_5^{(01)} \in \{-3,-2,-1,0,+1,+2,+3\} \\ I_5^{(0|1)} \in \{-12,-7,-2,+3,+8,+13\} \\ I_5^{(0||1)} \in \{-9,-4,+1,+6,+11\} \ . \end{cases} \end{aligned} \tag{3.1}$$

This result holds for both three- and four-folds alike, which we will carefully derive using the constraints on the normal bundles of rational curves in Calabi–Yau varieties. For four-folds we also discuss some extension to Yukawa couplings, which arise in codimension three, and show how the box graph analysis generalises as well as how the $U(1)$ charges of the interacting matter representations are consistent with the section configuration in codimension three fibers.

At this juncture we should clarify an important point regarding the normalisation of the charges. The rational section, σ_1, gives rise to a $\mathbb{Q}$-divisor that is suitably orthogonal to the divisors associated to the $SU(5)$ singular fibers, using the homomorphism between the Mordell–Weil group and the $\mathbb{Q}$-divisors written in [114], $\phi(\sigma_1)$. The generator of a $U(1)$ symmetry is an integral divisor and must be a multiple of the above $\mathbb{Q}$-divisor to be orthogonal to the gauge group, that is, it must have the form $m\phi(\sigma_1)$ where m is such that the divisor is integral. Normalisation of the $U(1)$ charges fixes the multiplier: there must not exist another integral divisor $D \in H^2(Y,\mathbb{Z})$ such that $m\phi(\sigma_1) = m'D$ for any non-unit $m' \in \mathbb{Z}$. With a $U(1)$ generator so defined and normalised the $U(1)$ charges will be in the possibilities listed in (3.1).

One key realisation here is that the analysis of the section configuration holds true for any rational section, and thereby models with multiple sections and thus $U(1)^n$ additional gauge symmetry, can be obtained by combining the configurations in our classification. We discuss several examples with multiple $U(1)$s in section 3.9. All matter charges and fiber types in codimension two known from explicit models in the literature with one or more $U(1)$ symmetries appear in our classification, however these form a strict subset of

possible charges, and it would indeed be very interesting to construct explicit realisations for the new fiber types. We also compare our charges to the ones obtained from Higgsing E_8 in [105], and find that our class of models is strictly larger than the ones arising from E_8. Regarding the singlets in [105], we provide realisations for all charges of singlets in terms of I_2 fibers with rational sections. A detailed discussion of the comparison to E_8 can be found in appendix A.2.

Furthermore, we are able to determine the fiber configurations for singlets, i.e. enhancements from I_1 fibers in codimension one to I_2 fibers in codimension two. Contrary to the remaining part of the chapter, this analysis is general only for three-folds. One important criterion for determining the singlets is the contractibility of curves, which is known for three-folds, but not to our knowledge, in the case of four-folds. However, we determine all possible codimension two I_2 fibers with rational sections, without imposing any constraints on the normal bundle degree. This result can be seen as a general study of singlets, and imposing further constraints on the normal bundle to impose contractibility should then reduce these to the set of singlets in four-folds. Finally, we discuss flops of fibers with rational sections. It appears that flops can map out of the class of fibers where the section remains a smooth divisor in the Calabi–Yau, and it would be particularly interesting to study such singular flops in the future.

Finally, we discuss the possibility, based on the singlet curve classification, to study more general Higgsings of the $U(1)$ symmetry to discrete symmetries, by giving $U(1)$-charged singlets a vacuum expectation value (vev). The case of charge $q = 2, 3$ singlets and the Higgsing to $\mathbb{Z}_q$ has recently appeared in [79–81]. We provide both singlet fibers for higher charges, as well as determine the realisation of the various KK-charges, i.e. intersections with the zero-section.

The plan of this chapter is as follows. In section 3.2 we summarise all the necessary information about codimension two fibers from [70]. Furthermore, we extend that analysis, and determine the Coulomb phases for $SU(n)$ gauge theories with a general (not necessarily the one arising from $U(n)$) additional $U(1)$ symmetry. In section 3.3, we discuss rational curves in Calabi–Yau three- and four-folds, and determine constraints on their normal bundles. These results will be an important input and constraining factor in our analysis. We then argue at the beginning of section 3.4 that the constraints on the rational curves contained in a rational section, turn out to be identical in elliptic three- and four-folds[2], thus allowing us in the remainder of this section to perform full classification of the codimension two fibers for both dimensions simultaneously. The case of fundamental matter

[2]This is true only in this specific context of elliptically fibered Calabi–Yau geometries and we make the complete setup clear in section 3.3. It is by far not true, for rational curves in general Calabi–Yau varieties.

for $SU(n)$ is discussed in the second half of section 3.4 and the anti-symmetric matter for $n = 5$ is discussed in section 3.5 and appendix A.1. The latter can of course also be generalised to $n > 5$, however we leave this for the enterprising reader. Flops among these fibers are discussed in section 3.6. Singlets are discussed in section 3.7 and multiple $U(1)$s, as well as Higgsing to discrete subgroups are the subject of section 3.9. For four-folds we generalise our results to codimension three, and describe some of the Yukawa couplings and section compatibility conditions in section 3.8. We close with discussions and future directions in section 3.10.

To summarise the applicability of our results to three- and four-folds: sections 3.4 and 3.5 on charges of fundamental and anti-symmetric matter apply to both three- and four-folds. The section on flops is applicable to three-folds, the section on singlets 3.7.2 to three-folds and section 3.7.3 to four-folds. Finally, the section on codimension three to four-folds, only.

3.2 Coulomb Phases and Fibers

Before discussing rational sections we will review the results in [70], which give a comprehensive characterisation of the singular fibers in codimension two of an elliptic fibration. The main idea is that the classical Coulomb phases of a 5d $\mathcal{N} = 1$ or 3d $\mathcal{N} = 2$ supersymmetric gauge theory with matter obtained by compactifying M-theory on an elliptically fibered Calabi–Yau three- or four-fold, encode the information about the structure of singular fibers in codimensions one, two, and three. Distinct Coulomb phases, which are separated by walls characterised by additional light matter, correspond to distinct smooth Calabi–Yau varieties, which are related by flop transitions.

For this chapter, the main case of interest is $\mathfrak{su}(5)$[3] and we shall restrict our attention in section 3.2.1 to explaining the correspondence between singular fibers, gauge theory phases, and box graphs to the case of $\mathfrak{su}(5)$ with matter in the $\overline{\mathbf{5}}$ and $\mathbf{10}$ representations, respectively. For more general results see [70]. In addition, in section 3.2.3 we will also extend the analysis of Coulomb phases to $\mathfrak{su}(5) \oplus \mathfrak{u}(1)$.

3.2.1 Box Graphs and Coulomb Phases

Our main interest regarding the results in [70] is the characterisation of the fibers in codimension two in an elliptically fibered Calabi–Yau variety of dimension three or four.

[3] From the point of view of the box graphs, and also the elliptic fibration, it is more natural to consider the Lie algebra, rather than group.

We will assume that any such fibration has at least one section. The generic codimension one fibers in such a variety are either smooth elliptic curves, or singular fibers, which are collections of rational curves, i.e. smooth $\mathbb{P}^1$s, intersecting in an affine Dynkin diagram of an ADE Lie algebra $\mathfrak{g}$. This classification, due to Kodaira and Néron [59–61], holds true in codimension one, however fibers in higher codimension can deviate from this. The main result in [70], is to map the problem of determining the codimension two fibers to the problem of characterizing the Coulomb branch phases of a 3d $\mathcal{N} = 2$ or 5d $\mathcal{N} = 1$ supersymmetric gauge theory with matter in a representation $\mathbf{R}$ of the gauge algebra $\mathfrak{g}$ [109–113].

Let us first discuss briefly the connection between Coulomb phases and resolutions of singular elliptic Calabi–Yau varieties. The topologically distinct crepant resolutions, i.e. resolutions preserve keep the Calabi–Yau condition, of a singular Calabi–Yau variety are parameterised by the phases of the classical Coulomb branch of the 3d $\mathcal{N} = 2$ gauge theory[4] obtained from the compactification of M-theory on the four-fold [113, 65, 70].

The 3d $\mathcal{N} = 2$ vector multiplet V in the adjoint of the gauge algebra $\mathfrak{g}$ has bosonic components given by the vector potential A and a real scalar ϕ. We are interested in the theory with additional chirals Q, transforming in a representation $\mathbf{R}$ of $\mathfrak{g}$. The classical Coulomb branch is characterised by giving the scalars ϕ a vacuum expectation value, which breaks the gauge algebra $\mathfrak{g}$ to the Cartan subalgebra, where ϕ is such that

$$\langle \phi, \alpha_k \rangle \geq 0 \,, \tag{3.2}$$

and α_k are the simple roots of $\mathfrak{g}$. The Coulomb branch is therefore characterised by the Weyl chamber of the gauge algebra $\mathfrak{g}$.

The presence of the chiral multiplets Q in a representation $\mathbf{R}$ of $\mathfrak{g}$ adds a substructure to the Coulomb branch. The vevs of ϕ give rise to a real mass term for the chiral multiplets,

$$L \supset |\langle \phi, \lambda \rangle|^2 |Q|^2 \,, \tag{3.3}$$

where λ is a weight of the representation $\mathbf{R}$. The mass term vanishes along walls

$$\langle \phi, \lambda \rangle = 0 \,. \tag{3.4}$$

A classical Coulomb phase of the 3d gauge theory is then one of the subwedges of the Weyl chamber delineated by the walls where chiral multiplets become massless. A phase associated to the representation $\mathbf{R}$ is then specified by a map

$$\begin{aligned} \varepsilon : \quad \mathbf{R} &\to \{\pm 1\} \\ \lambda &\mapsto \varepsilon(\lambda) \,, \end{aligned} \tag{3.5}$$

[4] A similar statement is true for Calabi–Yau three-folds in terms of the phases of the associated 5d gauge theory.

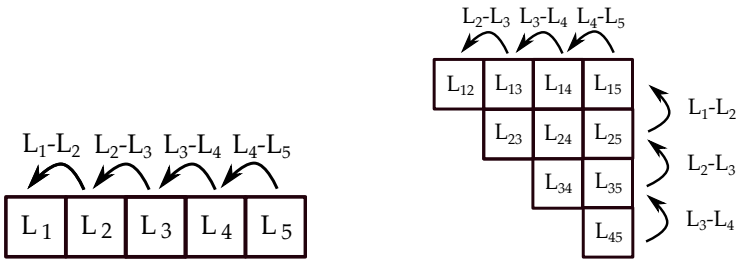

Figure 3.1: The **5** and **10** representation of $SU(5)$. Each box represents a weight L_i ($L_i + L_j$) of the fundamental (anti-symmetric) representation and the walls inbetween each box correspond to the action of the simple roots $\alpha_k = L_k - L_{k+1}$ on the weights as indicated by the arrows. The direction of the arrow indicates the addition of the corresponding simple root.

such that $\langle \phi, \lambda \rangle$ has a definite sign $\varepsilon(\lambda)$, i.e.

$$\varepsilon(\lambda)\langle \phi, \lambda \rangle > 0\,. \tag{3.6}$$

Solutions for ϕ will not exist for every possible sign assignment ε, i.e. the phases are the non-empty subwedges of the Weyl chamber satisfying (3.6). In particular the condition (3.6) means that the weight $\varepsilon(\lambda)\lambda$ is in this subwedge that characterises the corresponding phase. In [70] the phases for $\mathfrak{g}$ of ADE type were determined with various representations $\mathbf{R}$, and shown to be characterised in terms of sign-decorated representation graphs, so-called box graphs, of $\mathbf{R}$, which are essentially a graphical depiction of the maps ε. It was shown that there are simple, combinatorial rules for determining the box graphs corresponding to non-empty subwedges, and that furthermore these encode vital information about the elliptic Calabi–Yau geometry (the intersection ring and relative cone of effective curves in the elliptic fiber).

For our purposes $\mathfrak{g} = \mathfrak{su}(5)$ and $\mathbf{R} = \mathbf{5}$ or $\mathbf{10}$. We denote the weights of these representations in terms of the fundamental weights L_i

$$\mathbf{5}: \quad \lambda \in \{L_1, L_2, L_3, L_4, L_5\}\,, \qquad \mathbf{10}: \quad \lambda \in \{L_i + L_j |\ i < j;\ i, j = 1, \cdots, 5\}\,, \tag{3.7}$$

where $\sum_i L_i = 0$. The simple roots of $\mathfrak{su}(5)$ in this basis are

$$\alpha_k = L_k - L_{k+1}\,. \tag{3.8}$$

The result of [70] applied to $\mathfrak{g} = \mathfrak{su}(5)$ with $\mathbf{R} = \mathbf{5}$ can be summarised as follows: each consistent phase Φ_ε is characterised by a map ε as in (3.5), subject to the constraint that it satisfies

$$\mathbf{5} \text{ flow rules}: \quad \begin{cases} \varepsilon(L_i) = + & \Rightarrow \quad \varepsilon(L_j) = + \quad \text{for all } j < i \\ \varepsilon(L_i) = - & \Rightarrow \quad \varepsilon(L_j) = - \quad \text{for all } j > i \end{cases} \tag{3.9}$$

This results in phases that also include all $+$ or all $-$ sign assignments to the weights. These are in fact phases of the $\mathfrak{su}(5) \oplus \mathfrak{u}(1)$ theory. The phases for the $\mathfrak{su}(5)$ theory need to satisfy an additional constraint, which ensures that the sum of all the L_i vanishes (trace condition) [70]. In this chapter we are interested in the phases for the theory with additional abelian factors. It is a priori not clear that all phases of any $\mathfrak{su}(5) \oplus \mathfrak{u}(1)$ theory can be characterised in terms of the phases above, and we will prove this fact in section 3.2.3.

Likewise, for $\mathbf{R} = \mathbf{10}$ a sign assignment ε gives rise to a phase, if and only if

$$\mathbf{10} \text{ flow rules}: \quad \begin{cases} \varepsilon(L_i + L_j) = + & \Rightarrow \quad \varepsilon(L_k + L_l) = + \quad \text{for all } (k,l), \quad k \leq i\,,\ l \leq j \\ \varepsilon(L_i + L_j) = - & \Rightarrow \quad \varepsilon(L_k + L_l) = - \quad \text{for all } (k,l), \quad k \geq i\,,\ l \geq j \end{cases} \tag{3.10}$$

Again for $\mathfrak{su}(5)$ there is an additional trace condition, which however we do not impose as we are interested in theories with $\mathfrak{u}(1)$ factors. The connection between Coulomb phases and box graphs is then formulated as follows (see [70] and section 3.2.3):

Fact 3.2.1 *The classical Coulomb phases for 3d $\mathcal{N} = 2$ supersymmetric $\mathfrak{su}(5) \oplus \mathfrak{u}(1)$ gauge theories with matter in the $\mathbf{R} = \mathbf{5}$ or $\mathbf{10}$ representation are in one-to-one correspondence with maps ε as in (3.5), satisfying the flow rules (3.9) or (3.10), respectively. We will denote these by $\Phi_\varepsilon^{\mathbf{R}}$.*

Each phase $\Phi_\varepsilon^{\mathbf{R}}$ associated to such a map ε can be represented graphically in terms of a box graph $\mathcal{B}_\varepsilon^{\mathbf{R}}$.

Definition 3.2.1 *A box graph $\mathcal{B}_\varepsilon^{\mathbf{R}}$ for a Coulomb phase $\Phi_\varepsilon^{\mathbf{R}}$ is given in terms of the representation graph of $\mathbf{R}$, i.e. a graph where each weight λ of $\mathbf{R}$ is represented by a box, and two weights are adjacent if they are mapped into each other by the action of a simple root, together with a sign assignment/coloring, given by $\varepsilon(\lambda)$.*

Generically we will draw these by coloring $+$ as blue and $-$ as yellow. The representation graphs for $\mathbf{5}$ and $\mathbf{10}$ of $\mathfrak{su}(5)$ are shown in figure 3.1. The phases/box graphs for $\mathbf{5}$ are shown in figure 3.2, for $\mathbf{10}$ in appendix A.1.

3.2.2 Box Graphs and Singular Fibers

The Coulomb phases encode information about the effective curves of the elliptic fibration in codimension two. Let us begin with a few useful definitions. In the following Y is a smooth elliptic Calabi–Yau variety of dimension at least three with a section, which guarantees the existence of a Weierstrass model for this fibration. The information about the Coulomb phases can be reformulated in terms of the geometric data of a certain

relative subcone inside the cone of effective curves. A curve is defined to be *effective* if it can be written in terms of a positive integral linear combination of integral curves (i.e. actual complex one-dimensional subspaces) of Y. The cone of effective curves in Y is denoted by $NE(Y)$.[5] For an elliptic fibration, the notion of relative cone of curves is of particular importance. Let W be the singular Weierstrass model, associated to Y. In fact, for a given singular Weierstrass model there are generically several, topologically distinct smooth models, Y_i. The singular limit corresponds, in codimension one, to the maps

$$\pi_i : \quad Y_i \quad \to \quad W\,, \tag{3.11}$$

such that all rational curves in the singular Kodaira fibers, which do not meet the section, are contracted [115]. Associated to this, there is the notion of a relative cone of effective curves (see e.g. [54]):

Definition 3.2.2 *The relative cone of curves $NE(\pi_i)$ of the morphism π_i in (3.11) is the convex subcone of the cone of effective curves $NE(Y_i)$ generated by the curves that are contracted by π_i.*

The phases/box graphs are in one-to-one correspondence with pairs (Y_i, π_i), specified in the following way: Each fiber in codimension one is characterised by rational curves F_k associated to the simple roots of the gauge group G. In codimension two some of the F_k become reducible and split into a collection of rational curves

$$F_k \quad \to \quad C_1 + \cdots + C_\ell\,, \tag{3.12}$$

where each C_j is associated to $\varepsilon(\lambda)\lambda$ for λ a weight of the representation $\mathbf{R}$, or to a simple root. The main result in [70] can then be stated as follows:

Fact 3.2.2 *There is a one-to-one correspondence between consistent phases or box graphs $\mathcal{B}^{\mathbf{R}}_{\varepsilon_i}$ characterised by the sign assignments ε_i satisfying the conditions in Fact 3.2.1 and crepant resolution of W, (Y_i, π_i). In particular, the box graphs determine the relative cone of effective curves for the maps π_i as*

$$NE(\pi_i) = \left\langle \; \{F_k \mid k = 0, \cdots, \mathit{rank}(\mathfrak{g})\} \; \cup \; \{C_{\varepsilon_i(\lambda)\lambda} \mid \lambda \text{ weight of } \mathbf{R}\} \; \right\rangle_{\mathbb{Z}^+}. \tag{3.13}$$

The extremal generators of this cone are

1. *The rational curves F_k, that remain irreducible in codimension two.*
2. *$C_{\varepsilon_i(\lambda)\lambda}$ is extremal if there exists a j such that $\mathcal{B}^{\mathbf{R}}_{\varepsilon_j} = \mathcal{B}^{\mathbf{R}}_{\varepsilon_i}|_{\varepsilon_j(\lambda)=-\varepsilon_i(\lambda)}$, i.e. there is another consistent box graph or phase, such that the only sign change occurs in the weight λ.*

[5] These are numerically effective curves, where we mod out by the equivalence that two curves are identified if they have the same intersections with all Cartier divisors.

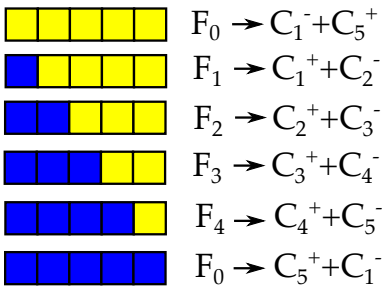

Figure 3.2: Box graphs for $\mathfrak{u}(5)$ phases with **5** matter. On the left are the splittings that occur over matter loci for the corresponding phase.

From the box graphs we can determine which F_k remain irreducible: F_k, associated to the simple roote α_k, remains irreducible, if any weight λ, for which $\lambda + \alpha_k$ is another weight in the representation $\mathbf{R}$, the weight $\lambda + \alpha_k$ has the same sign assignment, i.e.[6]

$$\varepsilon(\lambda) = \varepsilon(\lambda + \alpha_k)\,. \tag{3.14}$$

Fact 3.2.3 *Two crepant resolutions (Y_i, π_i) and (Y_j, π_j) of the singular Weierstrass model W are related by a simple flop, if the corresponding box graphs are related by a single sign change*

$$\mathcal{B}^{\mathbf{R}}_{\varepsilon_j} = \mathcal{B}^{\mathbf{R}}_{\varepsilon_i}|_{\varepsilon_j(\lambda)=-\varepsilon_i(\lambda)} \tag{3.15}$$

for some weight λ. I.e. they correspond to single box changes of signs, which map one extremal generator to minus itself.

In the remainder of this chapter, it will be very important to understand the degrees of normal bundles of curves in the fibers of elliptic Calabi–Yau varieties. The description of the codimension two fibers in terms of box graphs allows us to determine the intersections of the extremal generators with the so-called Cartan divisors, D_{F_k}, which are F_k fibered over the codimension one discriminant locus. They are dual to the rational curves F_k, with which they intersect in the Calabi–Yau Y in the negative Cartan matrix $-C_{kl}$ of the gauge algebra

$$D_{F_k} \cdot_Y F_l = -C_{kl}\,. \tag{3.16}$$

Consider now a codimension two fiber where F_k splits as in (3.12). Then

$$D_{F_m} \cdot_Y C_a = \varepsilon\left(\lambda^{(a)}\right)\lambda^{(a)}_m\,, \qquad m = 1, \cdots, \mathrm{rank}(\mathfrak{g})\,, \tag{3.17}$$

i.e. it intersects with the rational curves C_a in a weight $\lambda^{(a)}$ of the representation $\mathbf{R}$. Which weight this is, i.e. the intersections of the fiber components with the Cartan divisors, and with which sign assignment it occurs can be determined from the box graphs.

[6] This condition is formulated in [70] as adding the simple root does not cross the anti-Dyck path that separates the + and - sign assigned weights in the box graph.

Fact 3.2.4 *Let C be an extremal generator of the cone $NE(\pi_i)$ for a pair (Y_i, π_i), associated to the box graph $\mathcal{B}^{\mathbf{R}}_{\varepsilon_i}$ as in Fact 3.2.2, associated to a weight λ of the representation $\mathbf{R}$. The Dynkin labels $\varepsilon_i(\lambda)\lambda_m = D_{F_m} \cdot_Y C$ can be computed from the box graph $\mathcal{B}^{\mathbf{R}}_{\varepsilon_i}$ as follows: If $\lambda \pm \alpha_m$ is not a weight in the representation then $D_{F_m} \cdot_Y C = 0$. Else:*

1. *If $\varepsilon_i(\lambda) = \varepsilon_i(\lambda \pm \alpha_m)$ then $D_{F_m} \cdot_Y C = +1$.*
2. *If $\varepsilon_i(\lambda) = -\varepsilon_i(\lambda \pm \alpha_m)$ then $D_{F_m} \cdot_Y C = -1$.*

This fact together with $D_{F_m} \cdot_Y F_m = -2$, will be used quite regularly in the analysis of the normal bundles in sections 3.4 and 3.5.

Finally, let us note that the number $N^{\mathbf{R}_q}$ of phases, i.e. pairs (Y_i, π_i), with matter in the representation $\mathbf{R}$ and $\mathfrak{u}(1)$ charge q under the gauge algebra $\mathfrak{g} \oplus \mathfrak{u}(1)$ is given in terms of the quotiented Weyl group:

Fact 3.2.5 *The number $N^{\mathbf{R}}_q$ of classical Coulomb phases for gauge algebras $\mathfrak{g} \oplus \mathfrak{u}(1)$ and representation $\mathbf{R}$ with $\mathfrak{u}(1)$ charge q is*

$$N^{\mathbf{R}_q} = \left| \frac{W_{\widetilde{\mathfrak{g}}}}{W_{\mathfrak{g}}} \right| , \tag{3.18}$$

where $\widetilde{\mathfrak{g}}$ is the Lie algebra characterizing the local enhancement in codimension two, i.e. decomposing its adjoint into representations of the gauge algebra contains the representation $\mathbf{R}_q$ and its conjugate as follows

$$\begin{aligned} \widetilde{\mathfrak{g}} &\rightarrow \mathfrak{g} \oplus \mathfrak{u}(1) \\ Adj(\widetilde{\mathfrak{g}}) &\rightarrow Adj(\mathfrak{g}) \oplus Adj(\mathfrak{u}(1)) \oplus \mathbf{R}_q \oplus \overline{\mathbf{R}}_{-q} . \end{aligned} \tag{3.19}$$

For $\mathfrak{g} = \mathfrak{su}(5)$ and $\mathbf{R} = \mathbf{5}$ or $\mathbf{10}$, $\widetilde{\mathfrak{g}} = \mathfrak{su}(6)$ or $\mathfrak{so}(10)$ and $N^{\mathbf{5}} = 6$ and $N^{\mathbf{10}} = 16$. For $\mathfrak{su}(5)$ with $\mathbf{5}$ we summarised the phases in figure 3.2, including which of the F_k split. The components into which they split are precisely those adjacent to the sign change, which is clear from the statements in Fact 3.2.2. The curves $C_i^{\pm}$ correspond to the weights $\pm L_i$, which are generators of the cone defined by $\Phi^{\mathbf{R}}_{\varepsilon}$. Note that the $\mathbf{5}$ representation can also arise from a higher rank enhancement e.g. to $\mathfrak{su}(n)$, $n > 6$. Such enhancements when realised in the geometry would require very special tuning of the complex structure, with the fibers corresponding to monodromy-reduced I_n fibers. These will not be considered here, but the reader is referred to [116]. The structure of splittings in codimension two for $\mathbf{10}$ matter are listed in appendix A.1, tables A.1 and A.2, which include all the information about the splitting in codimension two, the extremal generators of the relative cone of effective curves, and the associated box graphs.

3.2.3 $U(1)$-Extended Coulomb Phases

In [70] the phases for the $\mathfrak{su}(5) \oplus \mathfrak{u}(1)$ theory were determined in the case where the $\mathfrak{u}(1)$ corresponds to $\sum_{i=1}^{5} L_i$, where the L_i are the fundamental weights introduced in the previous section, i.e. this $\mathfrak{u}(1)$ corresponds to the trace of the $\mathfrak{u}(5)$. In this section we show that the analysis there holds more generally for the classical Coulomb phases of $\mathfrak{su}(5) \oplus \mathfrak{u}(1)$, where the $U(1)$ does not necessarily have this origin[7]. Note that the phases for the $\mathfrak{su}(5) \oplus \mathfrak{u}(1)$ theory are one-to-one with the elements of the quotiented Weyl group $W_{\tilde{\mathfrak{g}}}/W_{\mathfrak{su}(5)}$, as summarised in Fact 3.2.5, which is strictly larger than the number of phases for the theory without an abelian factor.

Let $\mathbf{R}_q$ be a representation $\mathbf{R}$ of $\mathfrak{su}(5)$ with charge q under the $\mathfrak{u}(1)$. Let us consider the maps $\varepsilon : \mathbf{R}_q \to \{\pm 1\}$ corresponding to a consistent, non-empty, subwedge of the fundamental Weyl chamber. The walls of these subwedges are characterised by

$$\langle \phi, (\lambda_i; q) \rangle \equiv \langle \phi, \lambda_i \rangle + q\phi_u = 0\,, \tag{3.20}$$

where ϕ_u is the additional component of ϕ along the $\mathfrak{u}(1)$ generator. Consider the $\mathbf{5}_q$ representation of $\mathfrak{su}(5) \oplus \mathfrak{u}(1)$. The fundamental weights of $\mathfrak{su}(5)$, the L_i, in the Cartan-Weyl basis take the form

$$\begin{aligned} \lambda_1 &: \quad (1,0,0,0) \\ \lambda_2 &: \quad (-1,1,0,0) \\ \lambda_3 &: \quad (0,-1,1,0) \\ \lambda_4 &: \quad (0,0,-1,1) \\ \lambda_5 &: \quad (0,0,0,-1)\,. \end{aligned} \tag{3.21}$$

In the same basis the simple roots of the $\mathfrak{su}(5)$ are

$$\alpha_1 : (2,-1,0,0)\,, \quad \alpha_2 : (-1,2,-1,0)\,, \quad \alpha_3 : (0,-1,2,-1)\,, \quad \alpha_4 : (0,0,-1,2)\,. \tag{3.22}$$

To reiterate, to determine the maps ε which correspond to non-empty phases it is needed to find the maps $\varepsilon : \mathbf{5}_q \to \{\pm 1\}$ such that the inequalities

$$\begin{aligned} \langle \phi, \alpha_i \rangle &> 0 \\ \varepsilon((\lambda_i; q))\langle \phi, (\lambda_i; q) \rangle &> 0 \end{aligned} \tag{3.23}$$

have integral solutions for ϕ.

Similarly to the derivation of the flow rules alluded to in the earlier parts of this section one can show that if $\varepsilon((\lambda_i; q)) = -1$ and $\varepsilon((\lambda_{i+1}; q)) = +1$ then there would be no such

[7] There can corrections to the classical Coulomb phase analysis with additional abelian factors, as discussed in $6d$ in [117, 118], which will not play a role here.

solutions: for such an ε it would be the case that

$$\langle \phi, \lambda_{i+1} \rangle + q\phi_u - (\langle \phi, \lambda_i \rangle + q\phi_u) > 0 \quad \Leftrightarrow \quad \langle \phi, \lambda_{i+1} - \lambda_i \rangle > 0 \,. \tag{3.24}$$

However, the simple roots are $\alpha_i = \lambda_i - \lambda_{i+1}$ and the first of the inequalities in (3.23) implies

$$\langle \phi, \lambda_i - \lambda_{i+1} \rangle > 0 \,. \tag{3.25}$$

Obviously there is no such ϕ which solves these inequalities: all subwedges of the fundamental Weyl chamber defined by this map ε are empty. This leads to the same flow rules as listed in (3.9).

Again there are six phases, of which two have all positive or all negative signs, and are only non-empty in the theory with a $\mathfrak{u}(1)$ symmetry in addition to the $\mathfrak{su}(5)$, indeed these extra phases occur precisely for matter charged under the additional $\mathfrak{u}(1)$. Consider now the phase associated to the map $\varepsilon((\lambda_i; q)) = +1$ for all i. Then, using that $\sum \lambda_i = 0$, as can be seen explicitly above from the presentation in the Cartan-Weyl basis,

$$\sum_{i=1}^{5} (\langle \phi, \lambda_i \rangle + q\phi_u) > 0 \quad \Leftrightarrow \quad q\phi_u > 0 \,. \tag{3.26}$$

Such inequalities can only be solved if $q \neq 0$, and similiarly for the all negative phase. These are the two additional phases for charged matter.

One can also consider the $\mathbf{10}_q$ representation of $\mathfrak{su}(5) \oplus \mathfrak{u}(1)$ in the same way. Similarly to the case when of the $\mathbf{5}_q$ representation one finds an augmented set of maps ε when q is non-zero. There are sixteen phases when $q \neq 0$ and eight when $q = 0$. These sets of phases correspond to the different sets of phases in [70], except here there is no assumption that the generator of the $\mathfrak{u}(1)$ symmetry is necessarily that in the $\mathfrak{u}(5)$.

To summarise if the matter is charged under the $\mathfrak{u}(1)$ symmetry then there are additional phases of the classical Coulomb branch for the $\mathfrak{su}(5) \oplus \mathfrak{u}(1)$ theory with fundamental or anti-symmetric matter. The additional phases imply that there are additional distinct resolved geometries associated to the singular Calabi–Yau four-fold, induced by the specialisation of complex structure necessary to produce matter charged under the additional $\mathfrak{u}(1)$, i.e. geometrically, the existence of additional rational sections.

3.3 Rational Curves in Calabi–Yau Varieties

The goal of this chapter is to constrain the possible $U(1)$ charges of matter in 4d and 6d F-theory compactifications, by determining the possible codimension two fibers with

rational sections. The relevant characteristic of the codimension two fibers that determine the $U(1)$ charge are the intersection numbers between the rational curves in the fiber and the section. We constrain these by combining the input from the box graphs on the codimension two fibers with general constraints on the normal bundles of rational curves in projective varieties. From section 3.2 we obtain the information about the relative cone of effective curves $NE(\pi_i)$, for each resolution (Y_i, π_i) of a singular Weierstrass model W. All curves in $NE(\pi_i)$ are rational, i.e. they are smooth $\mathbb{P}^1$s in Y_i. In the following we will summarise several Theorems that we use in the later sections to constrain the fibers with rational sections for Calabi–Yau three- and four-folds. The protagonist in this discussion is the normal bundle of rational curves in Calabi–Yau varieties.

3.3.1 Rational Curves and Normal Bundles

In this section we collect useful results about rational curves in Calabi–Yau varieties, in particular related to the normal bundle, which will allow us to constrain the fibers with rational sections. Unless otherwise stated Y is a smooth Calabi–Yau variety.

The first theorem constrains the degree of the normal bundle of a rational curve in a Calabi–Yau variety.

Theorem 3.3.1 *Let Y be a smooth Calabi–Yau variety of dimension n and C a smooth rational curve in Y. Then the normal bundle of C in Y, $N_{C/Y}$, is*

$$N_{C/Y} = \bigoplus_{i=1}^{n-1} \mathcal{O}(a_i)\,, \quad \textit{with} \quad \sum_{i=1}^{n-1} a_i = -2\,.$$

Proof: E.g. for $n = 3$ see [119]. Let Y be of dimension n, then $N_{C/Y}$ is defined by the short exact sequence

$$0 \to T_C \to T_Y|_C \to N_{C/Y} \to 0\,, \tag{3.27}$$

where T denotes the respective tangent bundles. This implies that $N_{C/Y}$ is a rank $n-1$ vector bundle on C which, by the Birkhoff-Grothendieck Theorem [120], can be written uniquely up to permutations, as a direct sum of line bundles on C,

$$N_{C/Y} = \bigoplus_{i=1}^{n-1} \mathcal{O}(a_i)\,.$$

By the Calabi–Yau condition on Y, the canonical bundle is trivial and thus, $c_1(T_Y|_C) = 0$. Combining this with $c_1(T_C) = 2$ the exact sequence gives that $c_1(N_{C/Y}) = -2$. Thus $\sum a_i = -2$. □

In the following we will encounter rational curves which are contained within divisors, for instance, Cartan divisors associated to the elliptic fibration, which we introduced in (3.16). They are ruled by the rational curves F_k associated to simple roots of the gauge algebra, above the codimension one discriminant locus. Likewise we will see that the section, which we will assume to be a smooth divisor in the Calabi–Yau, can contain rational curves in the fiber that occur above codimension two. In all such instances it will be crucial to relate the normal bundle of the curve in the Calabi–Yau to the normal bundle in the divisor. This is achieved using the following exact sequence of normal bundles:

Theorem 3.3.2 *Let Y be a smooth projective variety, D a non-singular divisor in Y, and C a smooth rational curve contained in D. Then there is a short exact sequence of normal bundles*

$$0 \to \; N_{C/D} \to N_{C/Y} \to N_{D/Y}\big|_C \to 0\,. \tag{3.28}$$

Proof: [121], 19.1.5. □

One of the goals in later sections will be to determine the intersection of the rational section with various curves in the fiber. In particular, when these rational curves are contained in the section, this intersection is determined by the degree of the normal bundle of the divisor as follows – here C does not necessarily have to be a rational curve:

Theorem 3.3.3 *Let Y be a smooth projective variety, D a divisor in Y and C a curve $C \subset D \subset Y$. Then*

$$D \cdot_Y C = deg\left(N_{D/Y}\big|_C\right) \tag{3.29}$$

Proof: [122], Theorem 15.1. □

Combining these properties, we can in fact relate the intersection of any non-singular divisor and a smooth rational curve contained inside it in terms of the degree of the normal bundle of the curve inside the divisor.

Corollary 3.3.4 *Let Y be a smooth Calabi–Yau n-fold and C a rational curve contained inside a smooth divisor D in Y. Then*

$$D \cdot_Y C = -2 - deg\left(N_{C/D}\right)\,. \tag{3.30}$$

Proof: By Theorem 3.3.1 the degree of $N_{C/Y}$ is -2, which by Theorem 3.3.2 has to be the sum of the degrees $-2 = \deg(N_{C/D}) + \deg(N_{D/Y}|_C) = \deg(N_{C/D}) + D \cdot_Y C$ by Theorem

3.3.3. □

With these general results we now turn to determining the possible degrees of normal bundles of rational curves in Calabi–Yau three-folds and four-folds in the next two sections, respectively. In particular we will constrain the normal bundles of rational curves in divisors, for instance rational sections, which by the above corollary will imply constraints on the intersections and thereby $U(1)$ charges.

3.3.2 Calabi–Yau Three-folds

In this section, let Y be a smooth Calabi–Yau three-fold. Some results in rational curves in elliptically fibered three-folds (not necessarily Calabi–Yau varieties) can be found in Miranda [123], which however does not discuss rational sections, or the generalisation to higher dimensional varieties, which we will be important for us. Let D be a smooth divisor in Y, and C a smooth rational curve contained in D. Then it follows directly from Corollary 3.3.4 that[8]

$$D \cdot_Y C = -2 - C \cdot_D C \,. \tag{3.31}$$

We will often encounter the following situation: consider a rational curve C in a smooth elliptic Calabi–Yau variety Y. From the box graph analysis, we know its normal bundle in Y. We can then ask what normal bundles the curve can have in a divisor D – for instance the section. By the Corollary 3.3.4, the degree of the normal bundle $N_{C/D}$ is linked directly to the intersection in Y of the divisor with the curve, which in the case when D is a section determine the $U(1)$ charge. Thus, constraining the normal bundles of C in the rational section results in constraints on the possible charges. The following theorem determines what the possible normal bundles of rational curves in divisors can be, given the normal bundle of the curve in Y. We furthermore summarise the bounds that are then implied upon the intersection of the divisor with the curve.

Theorem 3.3.5 *Let Y be a smooth Calabi–Yau three-fold, D a non-singular divisor in Y, and C a rational curve contained in D.*

(i) Let $(C)^2_D = deg(N_{C/D}) = k$. If $k \geq -1$ the short exact sequence of normal bundles in Theorem 3.3.2 splits and

$$N_{C/Y} = \mathcal{O}(k) \oplus \mathcal{O}(-2-k) \,. \tag{3.32}$$

[8] We will most of the time refrain from using $(C)^2_D = C \cdot_D C$ as this does not generalise to higher dimensional varieties.

(ii) Let $N_{C/Y} = \mathcal{O}(-1) \oplus \mathcal{O}(-1)$. *If* D *is a smooth divisor containing* C, *then*

$$N_{C/D} = \mathcal{O}(k)\,, \qquad k \leq -1\,, \tag{3.33}$$

and there exists a non-trivial embedding

$$\mathcal{O}(k) \;\hookrightarrow\; N_{C/Y} = \mathcal{O}(-1) \oplus \mathcal{O}(-1)\,, \tag{3.34}$$

and

$$D \cdot_Y C = -2 - k \geq -1\,. \tag{3.35}$$

(iii) Let $N_{C/Y} = \mathcal{O} \oplus \mathcal{O}(-2)$. *If* D *is a smooth divisor containing* C, *then*

$$N_{C/D} = \mathcal{O}(k)\,, \qquad k = 0 \quad \textit{or} \quad k \leq -2\,, \tag{3.36}$$

and there exists a non-trivial embedding

$$\mathcal{O}(k) \;\hookrightarrow\; N_{C/Y} = \mathcal{O} \oplus \mathcal{O}(-2)\,, \tag{3.37}$$

and

$$D \cdot_Y C = -2 - k = \begin{cases} -2 & k = 0 \\ \geq 0 & k \leq -2 \end{cases}\,. \tag{3.38}$$

(iv) More generally, there is an embedding (without loss of generality $m \geq -1$*)*

$$\mathcal{O}(k) \;\hookrightarrow\; \mathcal{O}(m) \oplus \mathcal{O}(-2-m) \qquad \textit{for } k = m \quad \textit{or} \quad k \leq -2 - m\,. \tag{3.39}$$

Proof: To show (i) note that by Theorem 3.3.1 the degrees of the normal bundle have to sum to -2, so $N_{C/Y} = \mathcal{O}(a) \oplus \mathcal{O}(-2-a)$, where without loss of generality $a \leq -1$. By assumption $N_{C/D} = \mathcal{O}(k)$. The map $\mathcal{O}(k) \to \mathcal{O}(a)$ with $k \geq -1 \geq a$ is trivial map, unless $a = k$, in which case the Theorem follows. Else, if $a \neq k$ then $\mathcal{O}(k)$ needs to embed into $\mathcal{O}(-2-a)$ and therefore $k = -2 - a$. Part (ii) follows by applying (i) which implies that if $k > -1$ then the normal bundle $N_{C/Y}$ cannot be $\mathcal{O}(-1) \oplus \mathcal{O}(-1)$. Thus $k \leq -1$, and there is an embedding of $\mathcal{O}(k)$ into $\mathcal{O}(-1) \oplus \mathcal{O}(-1)$. Similar arguments show parts (iii) and (iv). □

Finally, the following theorem, which we will only make use of in our analysis of singlets, determines the normal bundles of contractible curves in three-folds:

Theorem 3.3.6 *Let* C *be a smooth, rational curve that can be contracted in a smooth three-fold* Y. *Then the normal bundle is*

$$N_{C/Y} = \mathcal{O}(a) \oplus \mathcal{O}(b)\,, \qquad (a,b) = (-1,-1),\ (-2,0),\ \textit{or}\ \ (-3,1)\,. \tag{3.40}$$

Such a curve is referred to as a $(-2)-$*curve.*

Proof: [124, 125].

3.3.3 Calabi–Yau Four-folds

For applications to 4d F-theory compactifications, including GUT model building, it is crucial to determine constraints for Calabi–Yau four-folds. In the following section, let Y be a smooth Calabi–Yau four-fold, and C a rational curve, contained in a smooth divisor D. For elliptic fibrations, we will in fact be interested in a slightly more specialised situation, where inside the divisor D there is a surface S which is ruled by C. Specifically, we have in mind what is usually referred to as matter surface, which is a $\mathbb{P}^1$-fibration, i.e. a ruled surface, over the matter curve (the codimension two locus in the base). These matter surfaces are contained within the Cartan divisors, which are dual to the rational curves F_i in the notation of section 3.2. In this setup, we will now show that the classification for three-folds will in fact carry over directly to four-folds in codimension two. [9]

Again, the goal is to connect the intersection of divisors (in particular the section) with a rational curve C in Y to the degrees of the normal bundle of C in Y. Recall the short exact sequence of normal bundles from Theorem 3.3.2 [121]

$$0 \;\to\; N_{C/D} \;\to\; N_{C/Y} \;\to\; N_{D/Y}|_C \;\to\; 0\,. \tag{3.41}$$

By Theorem 3.3.1, the normal bundle is a direct sum of line bundles, where the sum of degrees needs to add up to -2

$$N_{C/Y} = \mathcal{O}(a) \oplus \mathcal{O}(b) \oplus \mathcal{O}(-2-a-b)\,. \tag{3.42}$$

To determine the degrees a and b, there are two cases of interest when C is a rational curve in a codimension two fiber in an elliptic Calabi–Yau four-fold: either the rational curve C corresponds to one of the curves that split in codimension two, or it remains irreducible. From the box graphs, we can determine the intersection of the Cartan divisors with the curves, $D \cdot_Y C$, which in turn by Theorem 3.3.3, constrain $N_{D/Y}|_C$. The following theorem determines the normal bundle $N_{C/Y}$ given the information about $N_{D/Y}|_C$:

Theorem 3.3.7 *Let C be a smooth rational curve, contained in a smooth divisor D in a smooth Calabi–Yau four-fold Y.*

(i) If $N_{D/Y}|_C = \mathcal{O}(-1)$ and D contains a surface S, which is ruled by C, then

$$N_{C/D} = \mathcal{O} \oplus \mathcal{O}(-1)\,, \tag{3.43}$$

and the short exact sequence (3.41) splits

$$N_{C/Y} = \mathcal{O} \oplus \mathcal{O}(-1) \oplus \mathcal{O}(-1)\,. \tag{3.44}$$

[9] It would appear that in fact it holds in codimension two for any elliptic Calabi–Yau n-fold.

(ii) Likewise for $N_{D/Y}|_C = \mathcal{O}(-2)$ *and* D *is ruled by* C *then*

$$N_{C/D} = \mathcal{O} \oplus \mathcal{O}\,, \tag{3.45}$$

and

$$N_{C/Y} = \mathcal{O} \oplus \mathcal{O} \oplus \mathcal{O}(-2)\,. \tag{3.46}$$

Proof: (i) If there is a surface in D which is ruled by C then there is an embedding

$$\mathcal{O} \;\hookrightarrow\; N_{C/D}\,. \tag{3.47}$$

If $N_{D/Y}|_C = \mathcal{O}(-1)$ and given that the degrees in $N_{C/Y}$ sum to -2, it follows that

$$N_{C/D} = \mathcal{O}(m) \oplus \mathcal{O}(-1-m)\,. \tag{3.48}$$

As $\mathcal{O} = N_{C/S}$ needs to embed into $N_{C/D}$, it follows that $m = 0$. The extension group of $\mathcal{O} \oplus \mathcal{O}(-1)$ and $\mathcal{O}(-1)$ is trivial, and thereby the exact sequence splits. (ii) By similar arguments as in (i) $N_{C/D} = \mathcal{O}(m) \oplus \mathcal{O}(-m)$, and for $\mathcal{O}$ to embed into this $m = 0$. Again the extension group is trivial and the normal bundle sequence splits. □

For σ a rational section, which contains curves in the fiber, we can now constrain the possible normal bundle degrees of C in σ. The last theorem provides us with the information about the normal bundles $N_{C/Y}$. As in Theorem 3.3.5, we now determine the constraints on the intersection numbers $\sigma \cdot_Y C$ (where σ will be now be a rational section) by constraining the degrees of the normal bundle of C in σ, which are related by Corollary 3.3.4.

Theorem 3.3.8 *Let* σ *be a smooth divisor in* Y*, a smooth Calabi–Yau four-fold, and* $C \subset \sigma$ *a rational curve.*

(i) If $N_{C/Y} = \mathcal{O} \oplus \mathcal{O}(-1) \oplus \mathcal{O}(-1)$*, then there is an embedding*

$$N_{C/\sigma} = \mathcal{O}(a) \oplus \mathcal{O}(b) \;\hookrightarrow\; N_{C/Y} = \mathcal{O} \oplus \mathcal{O}(-1) \oplus \mathcal{O}(-1) \tag{3.49}$$

and

$$\sigma \cdot_Y C = -2 - a - b\,. \tag{3.50}$$

The values for a *and* b *are constrained to be (wlog* $a \geq b$*)*

$$a \leq 0\,, \quad b \leq -1\,, \quad a + b \leq -1\,, \tag{3.51}$$

which implies that

$$\sigma \cdot_Y C \geq -1\,. \tag{3.52}$$

(ii) If $N_{C/Y} = \mathcal{O} \oplus \mathcal{O} \oplus \mathcal{O}(-2)$*, then there is an injection*

$$N_{C/\sigma} = \mathcal{O}(a) \oplus \mathcal{O}(b) \;\hookrightarrow\; N_{C/Y} = \mathcal{O} \oplus \mathcal{O} \oplus \mathcal{O}(-2) \tag{3.53}$$

and

$$\sigma \cdot_Y C = -2 - a - b\,. \tag{3.54}$$

The values for a *and* b *are constrained to be*

$$a = b = 0 \qquad or \qquad a \leq 0\,,\; b \leq 0\,,\; a + b \leq -2\,, \tag{3.55}$$

which implies that

$$\sigma \cdot_Y C = \begin{cases} -2 & a = b = 0 \\ \geq 0 & a + b \leq -2 \end{cases}\,. \tag{3.56}$$

Proof: This follows directly from the short exact sequence (3.41) and Corollary 3.3.4. □

This concludes our summary of properties of rational curves. We now turn to combining these constraints on the intersection numbers and normal bundles, with the constraints from the box graphs that specify how codimension one fibers split in codimension two. The next two sections will discuss this in the case of $SU(n)$ with various matter representations.

3.4 $SU(5) \times U(1)$ with $\overline{\mathbf{5}}$ Matter

The ultimate physics application of our analysis of codimension two fibers is the case of $SU(5)$ GUTs with additional $U(1)$ symmetries. The constraints on the section and codimension two fiber structure provide a systematic way to obtain a comprehensive list of all possible $U(1)$ charges for matter in the $\overline{\mathbf{5}}$ and $\mathbf{10}$ representation of the GUT group $SU(5)$. In this section we will first focus on fundamental matter.

Throughout this section let Y be an elliptically fibered Calabi–Yau variety. The zero-section of the fibration will be denoted by σ_0, and the additional rational section needed for there to be a $U(1)$ symmetry as σ_1.

3.4.1 Setup and Scope

There are a few assumptions that go into this analysis, and to make it clear what the scope of the results in this chapter are, we will now list them.

(1.) We assume that each section in codimension one intersects exactly one fiber component transversally once, i.e. the sections do not contain components of codimension one fibers[10].

(2.) The rational sections, as divisors in Y, will always be assumed to be smooth.

(3.) The codimension one locus in the base of the fibration, above which there are singular fibers I_5, is smooth.

(4.) The $U(1)$ generator is an integral divisor normalised as described after (3.62).

Within the setup outlined above, the following can be regarded as complete classification of codimension two fibers for both Calabi–Yau three- and four-folds with one extra rational section, and thereby the possible matter charges.

3.4.2 Codimension one Fibers with Rational Sections

The codimension one fibers for $SU(5)$ GUTs realised in F-theory are fibers of Kodaira type I_5. These fibers consist of a ring of five smooth rational curves, F_i for $i = 0, \cdots, 4$.

Further, as these curves are the components of the fiber over generic points above a codimension one locus in the base, S_{GUT}, one can define divisors in Y, which are ruled by the curves F_i over S_{GUT}. These divisors, D_{F_i}, are called the Cartan divisors, and satisfy

$$D_{F_i} \cdot_Y F_j = -C_{ij}\,, \tag{3.57}$$

where C_{ij} is the Cartan matrix of affine $SU(5)$.

Let σ be a rational section of the elliptic fibration, i.e. it has to satisfy

$$\sigma \cdot_Y \text{Fiber} = 1\,. \tag{3.58}$$

Throughout this chapter it shall be assumed, see section 3.4.1, that this condition is satisfied by σ having exactly one transversal intersection with one of the components of the generic codimension one fiber and having no intersection with the other components. The section thus intersects, say, the mth component of the fiber

$$\sigma \cdot_Y F_i = \begin{cases} 1 & i = m \\ 0 & i \neq m\,. \end{cases} \tag{3.59}$$

It shall always be supposed, without loss of generality, that one section, the zero-section, shall intersect the component F_0. Up to inverting the order of the simple roots there

[10] This in fact seems to not be a real constraint, as wrapping in codimension one would imply that the section is either ruled by rational curves in the fiber (and thereby would contract to a curve in the singular limit) or not be irreducible.

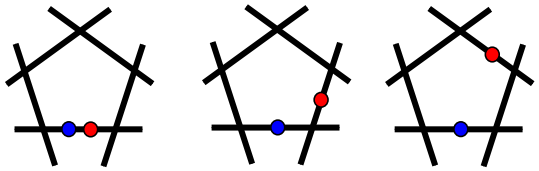

Figure 3.3: Three types of codimension one I_5 fibers with sections σ_0 (blue) and σ_1 (red) distributed as $I_5^{(01)}$, $I_5^{(0|1)}$ and $I_5^{(0||1)}$, respectively.

are three distinct codimension one fiber types once this information about the additional rational section is included. These are, using the notation introduced in [107],

$$\begin{aligned} I_5^{(01)}: &\qquad \sigma_0 \cdot_Y F_0 = \sigma_1 \cdot_Y F_0 = 1 \\ I_5^{(0|1)}: &\qquad \sigma_0 \cdot_Y F_0 = \sigma_1 \cdot_Y F_1 = 1 \\ I_5^{(0||1)}: &\qquad \sigma_0 \cdot_Y F_0 = \sigma_1 \cdot_Y F_2 = 1\,, \end{aligned} \tag{3.60}$$

corresponding to the three configurations shown in figure 3.3.

The $U(1)$ generator comes from the Shioda map as applied to the extra rational section, σ_1. The Shioda map associates to a rational section σ_1 an element $\mathcal{S}(\sigma_1)$ in $H_{2d-2}(Y,\mathbb{Z})$, where d is the complex dimension of Y, which is perpendicular to all horizontal divisors (i.e. divisors pulled back from the base), the zero-section as well as the Cartan divisors, associated to the F_i, which ensures that the non-abelian $SU(5)$ gauge bosons are uncharged under the $U(1)$ [91]. In order to compute $U(1)$ charges of matter, we are interested in the intersection of the Shioda map with curves in the fiber, for which the subtractions from contributions of horizontal divisors are not relevant, and we therefore define $S(\sigma_1)$ to be such that

$$S(\sigma_1) \cdot_Y C = q(C)\,, \tag{3.61}$$

the charge under the $U(1)$. In this way the Shioda map is specified by the codimension one data of the fibration. For $SU(5)$ with Mordell–Weil group rank one the Shioda divisors are

$$\begin{aligned} I_5^{(01)}: &\qquad S(\sigma_1) = \sigma_1 - \sigma_0 \\ I_5^{(0|1)}: &\qquad S(\sigma_1) = 5\sigma_1 - 5\sigma_0 + 4D_{F_1} + 3D_{F_2} + 2D_{F_3} + D_{F_4} \\ I_5^{(0||1)}: &\qquad S(\sigma_1) = 5\sigma_1 - 5\sigma_0 + 3D_{F_1} + 6D_{F_2} + 4D_{F_3} + 2D_{F_4}\,. \end{aligned} \tag{3.62}$$

To arrive at the specific forms above some further assumptions need to be made for the divisor $S(\sigma_1)$ that generates the $U(1)$ symmetry from the Shioda map. Imposing orthogonality to the $SU(5)$ Cartan divisors specifies the above up to a multiplicative constant. This constant is fixed by the requirement that $S(\sigma_1)$ should be integral, and that there should be no other integral divisor D such that $S(\sigma_1) = m'D$ for some $|m'| > 1$. The last condition is required for the $U(1)$ symmetry to be normalised appropriately.

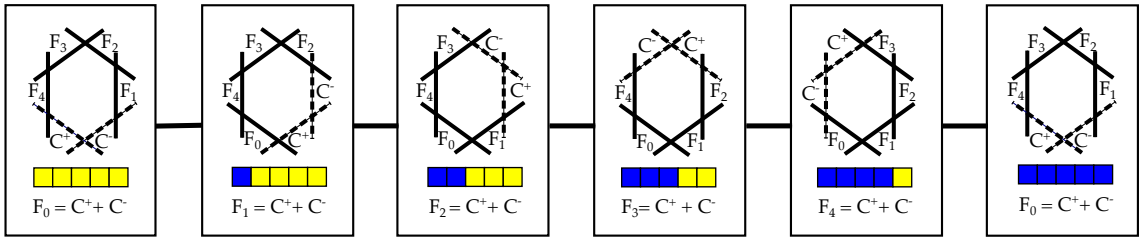

Figure 3.4: Box graphs and codimension two fibers where the F_j that split into $C^{\pm}$ in codimension two are shown with dashed lines, for the $\mathfrak{su}(5) \oplus \mathfrak{u}(1)$ theory with matter in the fundamental representation.

Assumption (4.) in section 3.4.1 is precisely that there does not exist such an integral divisor D.

3.4.3 Normal Bundles in Elliptic Calabi–Yau Varieties

We start with an I_5 fiber, with components F_i, intersecting in the affine Dynkin diagram of $SU(5)$. Along codimension two enhancement loci, some fiber components become reducible. The resulting codimension two fibers, which give rise to matter in the fundamental representation, were determined in section 3.2, from the Coulomb phases/box graphs, where one of the F_j curves splits as follows

$$F_j \to C^+ + C^- \,. \tag{3.63}$$

In the case of $SU(5)$ with $\overline{\mathbf{5}}$ these are shown in figure 3.4, including the fibers that split, shown as dashed lines.

In this analysis we allow for a non-holomorphic zero-section [93,97] which means that over codimension two σ_0 can also contain curves in the fiber. Let σ denote either σ_0 or σ_1. We will now determine the fibers including the rational sections in codimension two. In addition to intersecting the components of the codimension two fiber transversally, the section can contain entire fiber components $C \subset \sigma$, which in the existing literature is refered to as *wrapping*. In addition to consistency of the embedding of the rational curves into the divisors σ, we will use two constraints to determine all possible fibers:

1. If $\sigma \cdot_Y F_i = 0$ or 1, then this holds also in codimension two, in particular when the curve F_i splits it is necessary that the sum of the two curves, C^+ and C^-, intersects with the section as F_i did.

2. $\sigma \cdot_Y \text{Fiber} = 1$.

Denote by F_p the codimension one fiber component that splits

$$F_p \;\to\; C^+ + C^- \,. \tag{3.64}$$

From the box graph analysis it is known that the intersection with D_{F_p} of these curves is

$$D_{F_p} \cdot_Y C^{\pm} = -1\,. \tag{3.65}$$

For the case where a curve F_i in the fiber remains irreducible, again from the box graph analysis, we have that

$$D_{F_i} \cdot_Y F_i = -2\,. \tag{3.66}$$

We will now determine, using (3.65) and (3.66), the normal bundles of the curves $C^{\pm}$ and F_i in Y, which will in turn fix the possible intersection of these curves with the section.

Three-folds

First consider the case where Y is a Calabi–Yau three-fold. Then by Theorem 3.3.5 (i), (3.65) fixes the normal bundles to be

$$N_{C^{\pm}/Y} = \mathcal{O}(-1) \oplus \mathcal{O}(-1)\,. \tag{3.67}$$

If a curve $C = C^{\pm}$ is contained in the divisor σ, $C \subset \sigma$, then from Theorem 3.3.5 (ii) it follows that

$$N_{C/\sigma} = \mathcal{O}(k)\,, \quad k \leq -1\,, \tag{3.68}$$

and this in turn bounds the intesection of the curve with the section

$$\sigma \cdot_Y C = -2 - k \geq -1\,. \tag{3.69}$$

On the other hand, if σ does not contain one of the curves $C = C^{\pm}$, then $\sigma \cdot_Y C \geq 0$. In summary we can conclude that the intersection number of σ with the two curves $C^{\pm}$ is always bounded below as follows

$$\sigma \cdot_Y C^{\pm} \geq -1\,. \tag{3.70}$$

If F_i is irreducible and $F_i \subset \sigma$ then its normal bundle in Y is given by

$$N_{F_i/Y} = \mathcal{O} \oplus \mathcal{O}(-2)\,, \tag{3.71}$$

and by (3.66) and Theorem 3.3.5 (iii)

$$N_{F_i/\sigma} = \mathcal{O}(k), \qquad k = 0 \quad \text{or} \quad k \leq -2\,, \tag{3.72}$$

and

$$\sigma \cdot_Y F_i = \begin{cases} -2 & k = 0 \\ \geq 0 & k \leq -2 \end{cases}\,. \tag{3.73}$$

Four-folds

Likewise we can consider the case when Y is a smooth Calabi–Yau four-fold. We will now show that the constraints on the intersections of the section with the fiber components in this case are the same as the ones we derived for three-folds. In section 3.4.3 we started by considering a rational F_p in the fiber, which in codimension two splits and

$$D_{F_p} \cdot_Y C^{\pm} = -1\,. \tag{3.74}$$

Let $S^{\pm}$ be the surfaces ruled by $C^{\pm}$ over the codimension two locus in the base. Then $S^{\pm} \subset D_{F_p}$ which implies by Theorem 3.3.7 (i), that

$$N_{C^{\pm}/D_{F_p}} = \mathcal{O} \oplus \mathcal{O}(-1)\,. \tag{3.75}$$

and that the normal bundle to these curves in the four-fold is

$$N_{C^{\pm}/Y} = \mathcal{O} \oplus \mathcal{O}(-1) \oplus \mathcal{O}(-1)\,. \tag{3.76}$$

Consider now the situation that $S = S^{\pm}$ is contained in σ, and thereby $C = C^{\pm} \subset \sigma$. There is a normal bundle exact sequence

$$0 \to N_{C/S} \to N_{C/\sigma} \to N_{S/\sigma}|_C \to 0\,. \tag{3.77}$$

As S is ruled by C we know that $N_{C/S} = \mathcal{O}$. On the other hand, we know that by the normal bundle exact sequence for $C \subset \sigma \subset Y$

$$0 \to N_{C/\sigma} \to \; N_{C/Y} = \mathcal{O} \oplus \mathcal{O}(-1) \oplus \mathcal{O}(-1) \; \to N_{\sigma/Y}|_C \to 0\,, \tag{3.78}$$

thus writing $N_{C/\sigma} = \mathcal{O}(a) \oplus \mathcal{O}(b)$ Theorem 3.3.8 (i) states that $a \leq 0$, $b \leq -1$ and $a + b \leq -1$. However, from (3.77), we know that $\mathcal{O} \hookrightarrow \mathcal{O}(a) \oplus \mathcal{O}(b)$, therefore we must have $a = 0$ and $b \leq -1$, i.e.

$$N_{C^{\pm}/\sigma} = \mathcal{O} \oplus \mathcal{O}(k)\,, \qquad k \leq -1\,. \tag{3.79}$$

This proves that the conditions on the normal bundle degrees of $N_{C/\sigma}$ for four-folds are exactly the same as the ones we derived in the case of three-folds (3.69) resulting in the same bounds on $\sigma \cdot_Y C^{\pm}$ as in (3.70).

Likewise, when $F_i \subset S_i$ is contained in the section, where S_i is the surface ruled by F_i over the codimension two locus in the base, then $D_{F_i} \cdot_Y F_i = -2$ and by Theorem 3.3.7 (ii)

$$N_{F_i/Y} = \mathcal{O} \oplus \mathcal{O} \oplus \mathcal{O}(-2)\,. \tag{3.80}$$

Again applying the normal bundle exact sequences to $F_i \subset S_i \subset \sigma$ as well as $F_i \subset \sigma \subset Y$ we infer from 3.3.8 (ii) that

$$N_{F_i/\sigma} = \mathcal{O} \oplus \mathcal{O}(k)\,, \qquad k = 0 \quad \text{or} \quad k \leq -2\,, \tag{3.81}$$

which again is identical to the constraints that we had on the normal bundle degree for $F_i \subset \sigma$ in the three-fold case in (3.72) and thus the bound on $\sigma \cdot_Y F_i$ is also identical to that case and depends only on k.

It seems that similar arguments will hold for elliptic Calabi–Yau n-folds in codimension two, quite generally for $n \geq 3$, where instead of a ruled surface $S^{\pm}$, there is a ruled $n-2$ dimensional sub-variety, which is ruled by the rational curves in the fiber. This seems to only add additional $\mathcal{O}$ summands to the normal bundle, and the constraints on the intersections would appear to be the same as the ones we derived for $n = 3$ and $n = 4$.

3.4.4 Codimension two Fibers with Rational Sections

In the last section we have shown that the conditions on the normal bundle degrees for rational curves in the elliptic fibration which are contained in the section, are characterised, for both three- and four-folds by one integer, namely, the degree of the normal bundle $N_{C/\sigma} = \mathcal{O}(k)$ for three-folds, and $N_{C/\sigma} = \mathcal{O} \oplus \mathcal{O}(k)$, for four-folds, respectively, where k is bounded as described in the previous section. The happy fact, that the degrees in three-and four-folds (in this specifc context), are constrained in the same way, allows us to carry out a full classification simultaneously for both cases. The only important input is the degree of the normal bundles $\deg(N_{C/\sigma}) = k$, upon which the charges will depend. One last word of caution before we start our analysis: in the case of four-folds, whenever a rational curve C in the fiber is contained in σ, we mean this to imply always, that there is a surface S, which is ruled by C over the codimension two locus, which is also contained in σ (i.e. in compliance with the general discussion in section 3.4.3).

The two cases to consider now separately are

$$\sigma \cdot_Y F_p = \sigma \cdot_Y (C^+ + C^-) = \begin{cases} 0 & \text{Case (a)} \\ 1 & \text{Case (b)} \end{cases}\,. \tag{3.82}$$

(a) $\sigma \cdot_Y F_p = 0$:

From (3.69) it follows that $\sigma \cdot_Y C^{\pm} \geq -1$. There are three solutions to $\sigma \cdot_Y F_p = 0$:

$$(\sigma \cdot_Y C^+, \sigma \cdot_Y C^-) = (-1,1)\,,\ (0,0) \ \text{ and } \ (1,-1)\,. \tag{3.83}$$

There are several ways that each of these intersections can be realised: $\sigma \cdot_Y C^+ = -1$ implies $C^+ \subset \sigma$ and the degree of the normal bundle of C^+ in σ is $\deg(N_{C^+/\sigma}) = -1$.

Likewise, $\sigma \cdot_Y C^+ = 0$ implies $C^+ \subset \sigma$ and $\deg(N_{C^+/\sigma}) = -2$ or $C^+ \not\subset \sigma$ with no transverse intersection. On the other hand the intersections for C^- can be realised as follows: $\sigma \cdot_Y C^- = 1$ implies either, that $C^- \not\subset \sigma$, and intersects σ transversally once, or $C^- \subset \sigma$ and $\deg(N_{C^-/\sigma}) = -3$. The case for $\sigma \cdot_Y C^+ = 1$ proceeds in the same fashion, by swapping C^+ and C^-. The intersection $\sigma \cdot_Y C^- = 0$ implies either, that $C^- \not\subset \sigma$, and does not intersects σ, or $C^- \subset \sigma$ and $\deg(N_{C^-/\sigma}) = -2$.

In the last case, it is important to note that by the structure of the codimension two fiber the two curves $C^\pm$, which are both contained in the divisor D_{F_p}, intersect

$$C^+ \cdot_{D_{F_p}} S^- = 1\,, \tag{3.84}$$

where S^- is the matter surface, which is ruled by C^- in the case of four-folds, and is equal to C^- for three-folds. I.e. if one of the curves is contained in the section, then the other curve will automatically acquire an intersection with the section. Thus the combinations $C^+ \subset \sigma$, $\deg(N_{C^+/\sigma}) = -2$ and $C^- \not\subset \sigma$, $\sigma \cdot_Y C^- = 0$ do not have any solution in an I_6 fiber.

In summary we obtain the following configurations:

$\sigma \cdot_Y C^+$	$\sigma \cdot_Y C^-$	C^+ configuration	C^- configuration
-1	1	$C^+ \subset \sigma\,,\ \deg(N_{C^+/\sigma}) = -1$	$C^- \not\subset \sigma\,,\ \sigma \cdot_Y C^- = 1$
		$C^+ \subset \sigma\,,\ \deg(N_{C^+/\sigma}) = -1$	$C^- \subset \sigma\,,\ \deg(N_{C^-/\sigma}) = -3$
0	0	$C^+ \subset \sigma\,,\ \deg(N_{C^+/\sigma}) = -2$	$C^- \subset \sigma\,,\ \deg(N_{C^-/\sigma}) = -2$
		$C^+ \not\subset \sigma\,,\ \sigma \cdot_Y C^+ = 0$	$C^- \not\subset \sigma\,,\ \sigma \cdot_Y C^- = 0$
1	-1	$C^+ \not\subset \sigma\,,\ \sigma \cdot_Y C^+ = 1$	$C^- \subset \sigma\,,\ \deg(N_{C^-/\sigma}) = -1$
		$C^+ \subset \sigma\,,\ \deg(N_{C^+/\sigma}) = -3$	$C^- \subset \sigma\,,\ \deg(N_{C^-/\sigma}) = -1$

(3.85)

(b) $\sigma \cdot_Y F_p = 1$:
Making use again of the bound (3.69), the solutions to $\sigma \cdot_Y (C^+ + C^-) = 1$ are

$$(\sigma \cdot_Y C^+, \sigma \cdot_Y C^-) = (-1, 2)\,,\ (0, 1)\,,\ (1, 0) \ \text{ and } \ (2, -1)\,. \tag{3.86}$$

The only new configuration that has not already appeared in case (a) is $\sigma \cdot_Y C^- = 2$. One configuration that realises this is $C^- \not\subset \sigma$, but C^- has two transverse intersection points with σ. Note that in this case C^+ is contained in σ, and thus contributes an intersection by (3.84). If $C^- \subset \sigma$ then $\deg(N_{C^-/\sigma}) = -4$. The complete set of

section configurations in this case are summarised in the following table[11]:

$\sigma \cdot_Y C^+$	$\sigma \cdot_Y C^-$	C^+ configuration	C^- configuration
-1	2	$C^+ \subset \sigma\,,\ \deg(N_{C^+/\sigma}) = -1$	$C^- \not\subset \sigma\,,\ \sigma \cdot_Y C^- = 2$
		$C^+ \subset \sigma\,,\ \deg(N_{C^+/\sigma}) = -1$	$C^- \subset \sigma\,,\ \deg(N_{C^-/\sigma}) = -4$
0	1	$C^+ \subset \sigma\,,\ \deg(N_{C^+/\sigma}) = -2$	$C^- \not\subset \sigma\,,\ \sigma \cdot_Y C^- = 1$ $(*)$
		$C^+ \subset \sigma\,,\ \deg(N_{C^+/\sigma}) = -2$	$C^- \subset \sigma\,,\ \deg(N_{C^-/\sigma}) = -3$
		$C^+ \not\subset \sigma\,,\ \sigma \cdot_Y C^+ = 0$	$C^- \not\subset \sigma\,,\ \sigma \cdot_Y C^- = 1$
1	0	$C^+ \not\subset \sigma\,,\ \sigma \cdot_Y C^+ = 1$	$C^- \subset \sigma\,,\ \deg(N_{C^-/\sigma}) = -2$ $(*)$
		$C^+ \subset \sigma\,,\ \deg(N_{C^+/\sigma}) = -3$	$C^- \subset \sigma\,,\ \deg(N_{C^-/\sigma}) = -2$
		$C^+ \not\subset \sigma\,,\ \sigma \cdot_Y C^+ = 1$	$C^- \not\subset \sigma\,,\ \sigma \cdot_Y C^- = 0$
2	-1	$C^+ \not\subset \sigma\,,\ \sigma \cdot_Y C^+ = 2$	$C^- \subset \sigma\,,\ \deg(N_{C^-/\sigma}) = -1$
		$C^+ \subset \sigma\,,\ \deg(N_{C^+/\sigma}) = -4$	$C^- \subset \sigma\,,\ \deg(N_{C^-/\sigma}) = -1$

(3.87)

Note that for each value of $\sigma \cdot_Y C^\pm$ there are two realisations in terms of different configurations, and in the following we will only consider one of these.

Furthermore, we need to discuss the remaining fiber components. From the box graphs, we know that the intersection of rational curves in the fiber in codimension two is that of an I_6 Kodaira fiber. Thus, if a component $C^\pm$ is contained in σ it induces intersections of the section with the adjacent fiber components. Depending on the position of the section in codimension one, there are two cases again to consider: let F_q be such that it remains an irreducible fiber component in codimension two. Then

(a) $\sigma \cdot_Y F_q = 0$:
Either $F_q \not\subset \sigma$ and has no transverse intersections, or $F_q \subset \sigma$ then $\deg(N_{F_q/\sigma}) = -2$.

(b) $\sigma \cdot_Y F_q = 1$:
Either $F_q \not\subset \sigma$ and has one transverse intersection, or $F_q \subset \sigma$ then $\deg(N_{F_q/\sigma}) = -3$.

We can now determine the complete set of fibers in codimension two with a rational section σ. Again, $F_p \to C^+ + C^-$ is the rational curve that becomes reducible in codimension two:

(i) $C^+, C^- \not\subset \sigma$:

(a) $\sigma \cdot_Y F_p = 0$ and $\sigma \cdot_Y F_m = 1$, $p \neq m$:
It follows from table 3.85 that the only configuration is

$$C^+, C^- \not\subset \sigma\,, \quad \sigma \cdot_Y C^\pm = 0\,. \tag{3.88}$$

[11] We will see that the intersection configurations with $(*)$ in fact do not have a realisation in an I_6 fiber.

The section does not intersect either of the split components, indeed it must merely remain on the component that it originally intersected in codimension one, F_m. Figures 3.5 and 3.10 (i) represent this configuration.

(b) $\sigma \cdot_Y F_p = 1$:
From table 3.87 the only two solutions are

$$C^+, C^- \not\subset \sigma\,, \quad \sigma \cdot_Y C^{\pm} = 1\,, \quad \sigma \cdot_Y C^{\mp} = 0\,. \tag{3.89}$$

In this case the section intersects one of the split components transversally, and does not contain any curves in the fiber. This is shown in figure 3.5, and more generally, in figures 3.11, (i) and (ii), respectively.

(ii) $C^+ \subset \sigma$, $C^- \not\subset \sigma$:

(a) $\sigma \cdot_Y F_p = 0$ and $\sigma \cdot_Y F_m = 1$, $p \neq m$:
The configuration from table 3.85 is

$$\begin{aligned} &C^+ \subset \sigma\,,\ \deg(N_{C^+/\sigma}) = -1 \\ &C^- \not\subset \sigma\,,\ \sigma \cdot_Y C^- = 1\,. \end{aligned} \tag{3.90}$$

The positive intersection of σ with C^- arises from the single point of intersection between the curves C^+ and C^-. Any fiber components, F_i, which are positioned in the ring between C^+ and F_m must also be contained in σ, so that $\sigma \cdot_Y F_i = 0$. This can be seen by considering first the intersection point of C^+ with the curve F_i, which is adjacent to it in the ring. Clearly this would have $\sigma \cdot_Y F_i = 1$, which would be inconsistent with codimension one unless $i = m$. Therefore F_i must be contained in σ, with $F_i \cdot_\sigma D_{F_i} = -2$, so that it has zero intersection number in Y. This is consistent with Theorems 3.3.5 and 3.3.8. Identically, such wrapping must continue until the section meets the fiber component that it intersects in codimension one. This configuration is depicted in figure 3.5 and, more generally, for I_n, in figure 3.10 (ii).

(b) $\sigma \cdot_Y F_p = 1$:
There are two solutions in this case from table 3.87, however we will see only the following gives rise to a consistent fiber:

$$\begin{aligned} &C^+ \subset \sigma\,,\ \deg(N_{C^+/\sigma}) = -1 \\ &C^- \not\subset \sigma\,,\ \sigma \cdot_Y C^- = 2\,. \end{aligned} \tag{3.91}$$

The second solution characterised by $C^+ \subset \sigma\,,\ \deg(N_{C^+/\sigma}) = -2$ and $C^- \not\subset \sigma\,,\ \sigma \cdot_Y C^- = 1$ would imply that the section wraps C^+, and thus by the argument in the last paragraph, would gain a non-trivial intersection with all

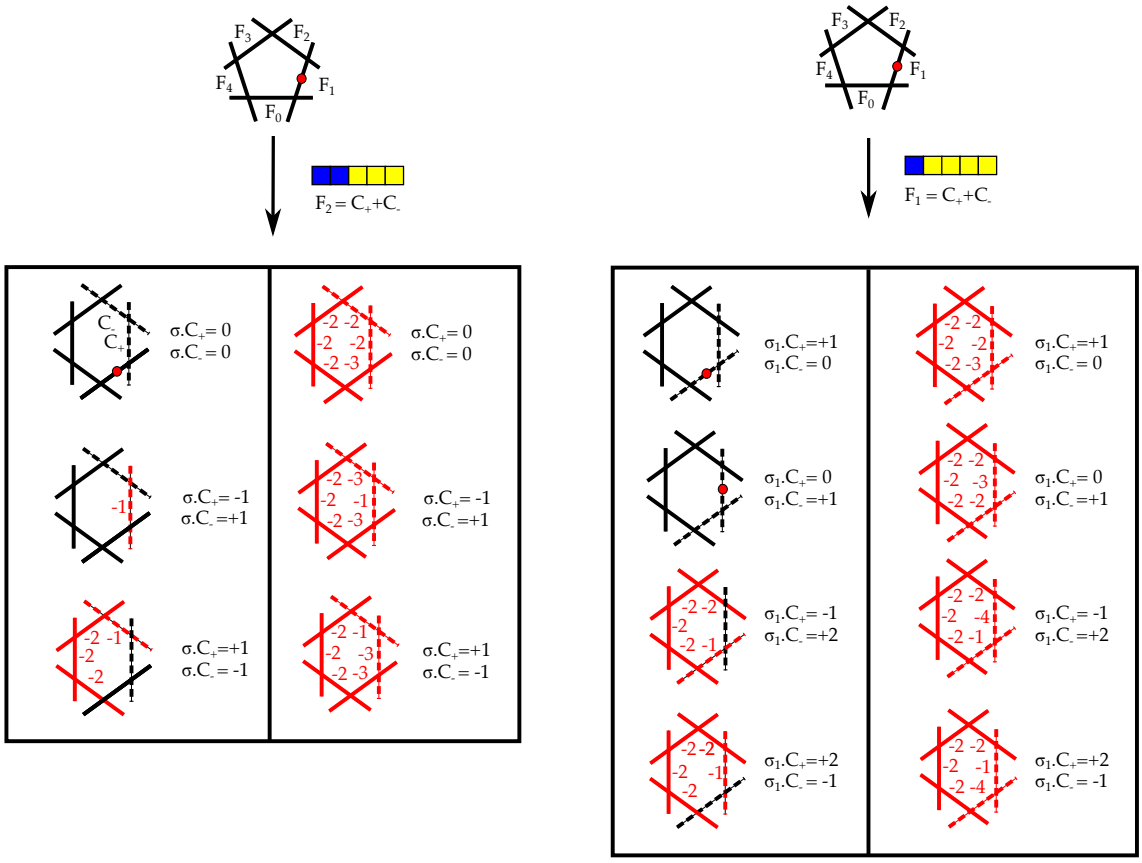

Figure 3.5: I_5 fiber with rational section σ, shown intersecting F_1 in codimension one. The left hand side shows the case $F_2 \to C^+ + C^-$ in codimension two and all the the section configurations that are consistent, which correspond to all case (a) in the main text. The fiber components that are contained in σ are colored red, and the numbers next to it refer to the degree of the normal bundle of the curves inside σ. Furthermore, in each row the two configurations give rise to the same intersection of $\sigma \cdot_Y C^{\pm}$, and are thus, from the point of view of $U(1)$ charges, identical. Note that for one of these configurations the entire fiber is contained in the section. The right hand side shows the case when the fiber component F_1, which intersects the section in codimension one, becomes reducible in codimension two. Again, for each pair $(\sigma \cdot_Y C^+, \sigma \cdot_Y C^-)$ there are two configurations realising those intersection numbers.

F_i between C^+ and C^- unless, all of these curves are contained in σ with normal bundle degree -2, so that $\sigma \cdot_Y F_i = 0$. However, then C^- would be the only not contained fiber component, and would have intersection 2 with the section, which would be in contradiction. Thus we are left with the only configuration (3.91). Again, by the same arguments as given in the previous paragraph the section must contain all the F_i between C^+ and C^-. If there were to be some F_i which was not contained in σ then it would have a strictly positive intersection number with σ from its neighbour in the ring, contradicting codimension one. C^- then has one intersection point with σ from the intersection with C^+ and one from the intersection with the F_i on its other side, giving the required intersection number of $+2$. The fiber is represented in figure 3.5 and for I_n in figure 3.11 (iv).

(iii) $C^- \subset \sigma$, $C^+ \not\subset \sigma$:

The analysis in the case is essentially identical to the analysis in case (ii), by exchanging the roles of C^+ and C^-, and we do not repeat it here.

(a) $\sigma \cdot_Y F_p = 0$:

See figure 3.5 and figure 3.10 (iii).

(b) $\sigma \cdot_Y F_p = 1$:

See figure 3.5 and figure 3.11 (iii).

(iv) $C^+, C^- \subset \sigma$:

(a) $\sigma \cdot_Y F_p = 0$ and $\sigma \cdot_Y F_m = 1$, $p \neq m$:

From table 3.85 there are three configurations, corresponding to degree of the normal bundle of the curves in σ

$$\big(\deg(N_{C^+/\sigma}),\ \deg(N_{C^-/\sigma})\big) = (-1,-3)\,,\ (-2,-2)\,,\ (-3,-1)\,. \tag{3.92}$$

In all of these cases, all F_i need to be contained in σ, which again follows by noting that if only $C^\pm$ were contained in σ, then both F_{p-1} and F_{p+1} gain an intersection from the wrapping of $C^\pm$. Thus in order for all but F_m to have zero intersection with σ, the entire fiber needs to be contained in σ with

$$\deg(N_{F_m/\sigma}) = -3\,, \qquad \deg(N_{F_i/\sigma}) = -2\,, \quad i \neq m, p\,. \tag{3.93}$$

The degree of $\deg(N_{F_m/\sigma})$ ensures that this component has, consistently with codimension one, intersection $+1$ with σ. See figure 3.5 and figure 3.10 parts (iv)-(vi).

(b) $\sigma \cdot_Y F_p = 1$:

Table 3.87 implies there are four configurations of this type:

$$\big(\deg(N_{C^+/\sigma}),\ \deg(N_{C^-/\sigma})\big) = (-1,-4)\,,\ (-2,-3)\,,\ (-3,-2)\,,\ (-4,-1)\,. \tag{3.94}$$

Again, just as in the last paragraph, the entire fiber needs to be contained in σ with

$$\deg(N_{F_i/\sigma}) = -2\,, \qquad i \neq p\,. \tag{3.95}$$

See figure 3.5 and figure 3.11 parts (v)-(viii).

This completes the analysis of what fiber configurations in codimension two are possible with one rational section.

3.4.5 Compilation of Fibers

The analysis in the last section allows us now to characterise all possible fibers in codimension two for an $SU(5)$ model with one rational section. There are in total three distinct codimension one configurations for the section, up to inverting the order of the curves F_i in codimension one. For each of these, we now determine the fibers with rational section in codimension two. As shown in tables 3.85 and 3.87, for each value of $(\sigma \cdot_Y C^+, \sigma \cdot_Y C^-)$ there are two realisations in terms of fibers, see e.g. figure 3.5. As these are indistinguishable from the point of view of $U(1)$ charges, in the following, we will only consider the fibers with minimal wrapping. The different configurations are drawn for each phase of each codimension one fiber type in figure 3.6. These tables contain information about

- Phase: given in terms of the box graph as well as the splitting $F_i = C^+ + C^-$ for each phase.
- Codimension two fiber: in the present case for fundamental matter, the enhancement is to an I_6 fiber, i.e. $SU(6)$. The intersection of the exceptional $\mathbb{P}^1$s is shown, including the curves $C^\pm$ that arise from the splitting are marked by dashed lines.
- All possible codimension two fibers with section: a dot on one of the $\mathbb{P}^1$s corresponds to a section intersecting the fiber component transversally in $+1$. If a fiber component is contained in the section σ, then it is colored (blue or red). The "wrapped" components carry a numerical label, which indicates the normal bundle degree of the curve inside the section σ.
- Matter intersections: finally, the table contains the information about the intersection of the section σ with the curves $C^\pm$, which will then be used to compute the

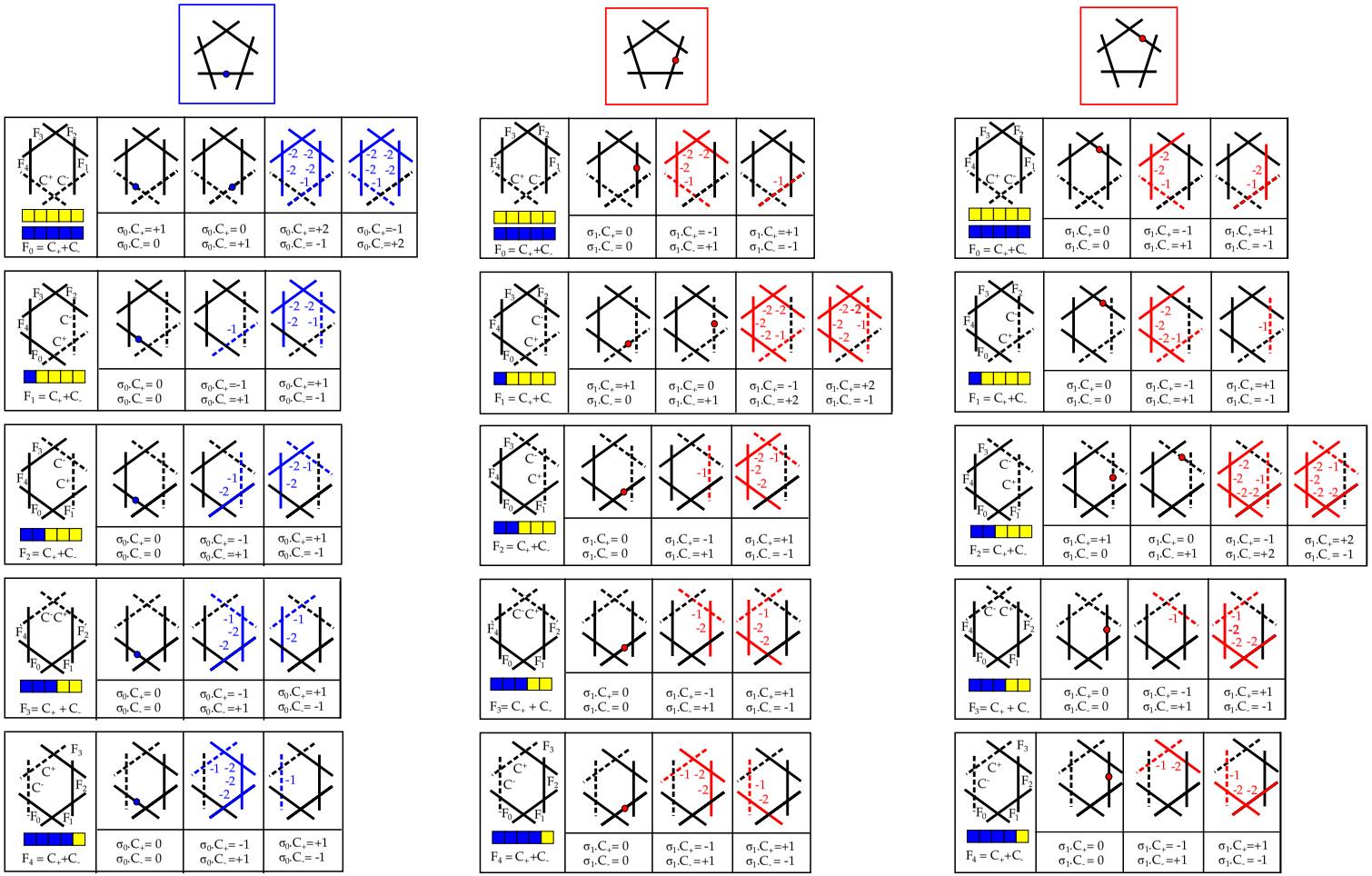

Figure 3.6: For each phase/box graph we show the full set of codimension two I_6 fibers with rational sections, for the codimension one fiber where the section intersects F_0, F_1 and F_2, respectively, shown at the top. The components that split are shown by dashed lines, and colored (either blue or red) components correspond to rational curves that are contained in the section, with the numbers indicating the degrees of the normal bundle in the section. Dots indicate transverse intersections of the section with the fiber components. We list the intersection numbers $\sigma \cdot_Y C^{\pm}$. More details can be found in the main text.

$U(1)$ charges.

Knowing the various configurations one can read off the values of $\sigma \cdot_Y C^{\pm}$ in each case. It is these values which determine the $U(1)$ charges, after the application of the Shioda map, as shall be seen in the subsequent section. In the phase where the codimension one component F_p splits the possible values of $\sigma \cdot_Y C^{\pm}$ are

(a) $\sigma \cdot_Y F_p = 0$

$$\sigma \cdot_Y C^{\pm} \in \{-1, 0, 1\}\,. \tag{3.96}$$

(b) $\sigma \cdot_Y F_p = 1$

$$\sigma \cdot_Y C^{\pm} \in \{-1, 0, 1, 2\}\,. \tag{3.97}$$

These values are the contributions to the $U(1)$ charges from the rational sections. One sees that there is an additional value for $\sigma \cdot_Y C$ when the codimension one curve that splits, F_p, had the rational section intersecting it in codimension one. We should then anticipate seeing additional $U(1)$ charges in those phases where such a component of the I_5 fiber splits. Indeed we will see this in the next section.

3.4.6 $U(1)$ Charges

The $U(1)$ charges of the curves $C^{\pm}$, which are labelled by the weights of the fundamental representation, are obtained by intersecting them with the Shioda map of the section σ_1

$$S(\sigma_1) = 5(\sigma_1 - \sigma_0) + S_f\,, \tag{3.98}$$

where σ_0 is the zero-section. Here, S_f depends on the codimension one fibers and is determined by requiring that for all i

$$S(\sigma_1) \cdot_Y F_i = 0\,. \tag{3.99}$$

In particular, if $F_i \to C^+ + C^-$ splits then $(C^+ + C^-) \cdot_Y S(\sigma_1) = 0$ is required. The $U(1)$ charges of C^+ and C^- is given by $S(\sigma_1) \cdot_Y C^+$ and $S(\sigma_1) \cdot_Y C^-$ respectively, and are always conjugate. For $I_5^{(01)}$, S_f is trivial, and for the remaining codimension one fiber types they are listed in tables 3.1 and 3.2.

In the section 3.4.4 we determined a comprehensive list of possible fibers in codimension two, given that a rational section σ intersects either F_0, F_1, or F_2 in codimension one, respectively. In a model with one $U(1)$, we apply this analysis to the zero-section σ_0 and additional section σ_1. Without loss of generality, $\sigma_0 \cdot_Y F_0 = 1$, and thus the possible codimension two fibers are listed in figure 3.6. Depending on which codimension one fiber

Phase	S_f	$S_f \cdot_Y C^+$	$S_f \cdot_Y C^-$
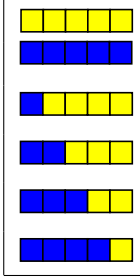	$4D_{F_1} + 3D_{F_2} + 2D_{F_3} + D_{F_4}$	$+1$	$+4$
		-4	-1
		$+1$	-1
		$+1$	-1
		$+1$	-1

Table 3.1: Values for $S_f \cdot_Y C^{\pm}$ for $I_5^{(0|1)}$ local enhancement to I_6.

Phase	S_f	$S_f \cdot_Y C^+$	$S_f \cdot_Y C^-$
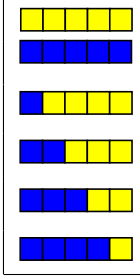	$3D_{F_1} + 6D_{F_2} + 4D_{F_3} + 2D_{F_4}$	$+2$	$+3$
		-3	$+3$
		-3	-2
		$+2$	-2
		$+2$	-2

Table 3.2: Values for $S_f \cdot_Y C^{\pm}$ for $I_5^{(0||1)}$ local enhancement to I_6.

type (3.60) we start with, in addition the section σ_1 can be in one of the configurations in figures 3.6. Obviously, only fiber types in the same phase can be combined.

The charge is computed by intersecting the Shioda map $S(\sigma_1)$ (3.98) with the split curves C^+ and C^-. The result is shown for all codimension one fiber types in figures 3.7, 3.8, and 3.9. Each of the figures contains the information

Caption for Figures 3.7, 3.8, and 3.9: (3.100)

- The phase, specified by the box graph, and the fiber in codimension two that results, without the section information.
- The horizontal (vertical) axis shows the different configurations for curves of the fiber in the section σ_1 (σ_0).
- The entries of the tables contain the $U(1)$ charges $(a, -a)$ determined by $S(\sigma_1) \cdot_Y C^+$ and $S(\sigma_1) \cdot_Y C^-$ respectively.
- The lines between the phases, that is, connecting the six large boxes, denote that there exist flop transitions between those linked phases.[12] The coloring of the charges is related these flops and will be discussed later.

[12] These are the flops that exist generically, as explained in [70]. This will be discussed later on.

In summary the charges for $\bar{\mathbf{5}}$ (and negative of these for the conjugate $\mathbf{5}$) that we find are:

$$U(1) \text{ charges of } \bar{\mathbf{5}} \text{ matter for } \begin{cases} I_5^{(01)} \in \{-3,-2,-1,0,+1,+2,+3\} \\ I_5^{(0|1)} \in \{-14,-9,-4,+1,+6,+11\} \\ I_5^{(0||1)} \in \{-13,-8,-3,+2,+7,+12\}\,. \end{cases} \tag{3.101}$$

This concludes the analysis of possible $U(1)$ charges for an $SU(5)$ gauge theory in F-theory with fundamental matter, for one additional abelian gauge factor. Note that all known charges from explicit realisations of the fiber in various toric tops as well as Tate models, including the individual $U(1)$ charges from models with multiple $U(1)$ factors, are a (strict) subset. We discuss the relation to the embedding into E_8, as discussed in [105], in appendix A.2.

3.4.7 $SU(n) \times U(1)$ with Fundamental Matter

In our discussion of fiber configurations in section 3.4.4 it was in fact of no particular importance that we started with an I_n fiber with $n = 5$. Indeed the situation is very similar and easily generalises, to $SU(n)$ with fundamental (i.e. the $\overline{\mathbf{n}}$ representation) matter, where the fiber enhances from an I_n to an I_{n+1}. Each section in codimension one intersects one of the rational curves F_i, $i = 0, 1, \cdots, n-1$, which intersect in an affine $SU(n)$ Dynkin diagram. In codimension two, one of the F_i splits, as shown in [70]. For an elliptic fibration with sections σ_0 and σ_1, we again use the notation

$$I_n^{(0|^m 1)}: \qquad \sigma_0 \cdot_Y F_0 = 1\,, \qquad \sigma_1 \cdot_Y F_m = 1\,. \tag{3.102}$$

Let F_p be the component that splits in codimension two. Then there are two cases to consider: either $\sigma \cdot_Y F_p = 0$ or 1, which are shown in figures 3.10 and 3.11, respectively. The reasoning is entirely as in section 3.4.4, with the only difference being the length of the chain of rational curves F_i that are located between C^+ and C^-. The distinct cases of intersections $(\sigma \cdot_Y C^+, \sigma \cdot_Y C^-)$ are also analogous to the $SU(5)$ case.

The Shioda map can be constructed for an $I_n^{(0|^m 1)}$ fiber and the $U(1)$ charges of a fibration with a specified wrapping configuration can be written in terms of m and n. The Shioda map for an I_n fiber with separation m between the sections is determined by the mth row of the inverse Cartan matrix associated to the codimension one singularity type [91]. The inverse Cartan matrix of $SU(n)$ is an $(n-1) \times (n-1)$ matrix with elements

$$C_{mc} = \frac{1}{n} \begin{cases} c(n-m) & c \le m \\ m(n-c) & m < c\,. \end{cases} \tag{3.103}$$

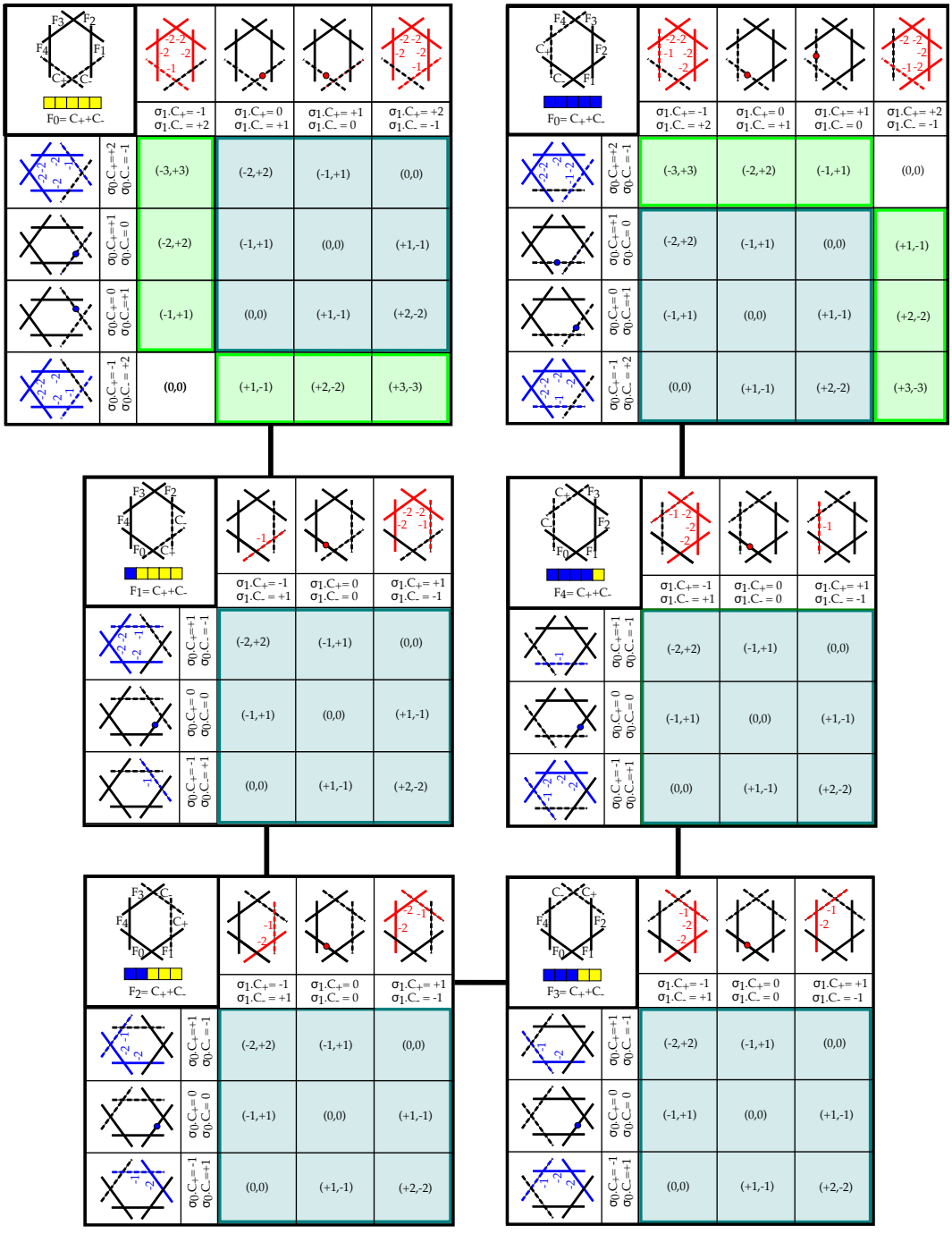

Figure 3.7: Codimension two fibers and charges for $\overline{\mathbf{5}}$ matter for $I_5^{(01)}$ models. For details see (3.100).

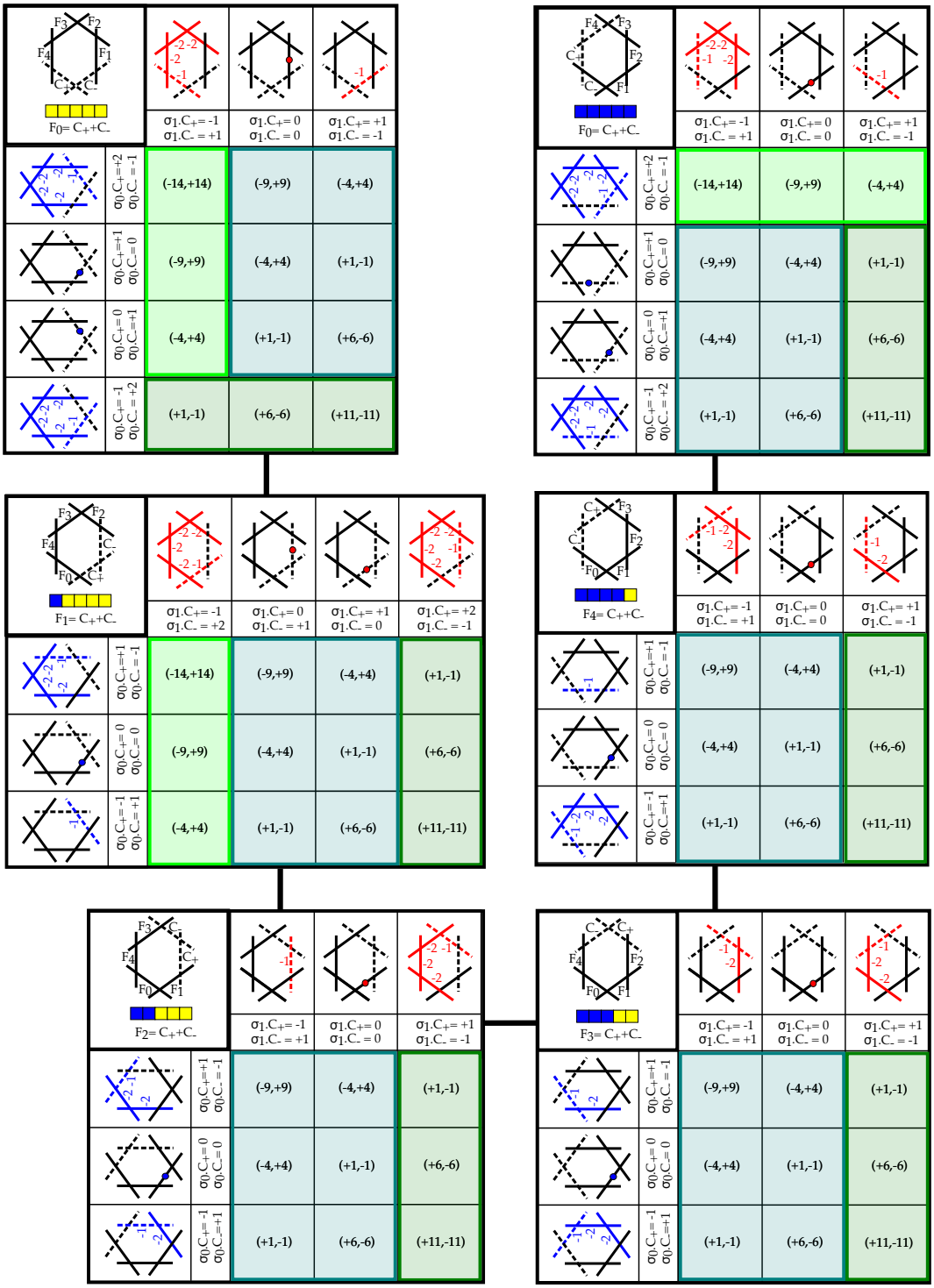

Figure 3.8: Codimension two fibers and charges for $\overline{\mathbf{5}}$ matter for $I_5^{(0|1)}$ models. For details see (3.100).

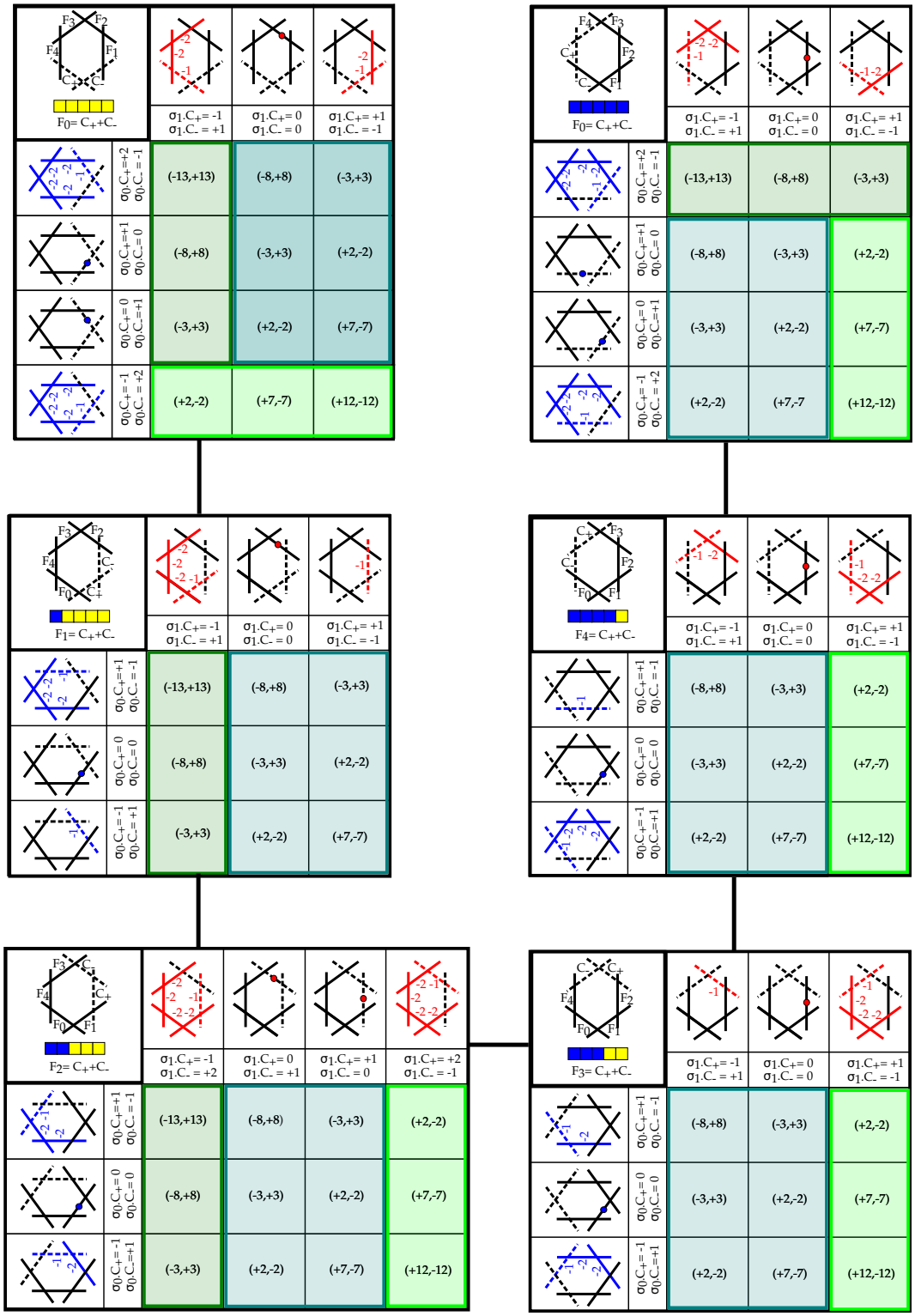

Figure 3.9: Codimension two fibers and charges for $\overline{\mathbf{5}}$ matter for $I_5^{(0||1)}$ models. For details see (3.100).

The Shioda map for an $I_n^{(0|^m 1)}$ fiber is then of the form

$$S(\sigma_1) = n(\sigma_1 - \sigma_0) + \sum_{i=1}^{n-1} C_{mi} D_{F_i}\,, \tag{3.104}$$

ignoring contributions from the base. For ease of notation we will allow c_p to denote the coefficient of the term D_{F_p} in the Shioda map, that is C_{mp}. The Shioda map excepting the term $n(\sigma_1 - \sigma_0)$ will be denoted by S_f as before. The conjugate $U(1)$ charges are obtained from the intersection numbers

$$S(\sigma_1) \cdot_Y C^{\pm}\,. \tag{3.105}$$

Such an intersection can be broken into two parts, contributions from $(\sigma_1 - \sigma_0) \cdot_Y C^{\pm}$, which were enumerated for each section in (3.96, 3.97), and contributions from $S_f \cdot_Y C^{\pm}$, which are determined here. Let us consider the phase where $F_p \to C^+ + C^-$, and we shall content ourselves with only obtaining the $U(1)$ charge of C^+, as the charge for C^- is simply its negative. From the resulting fiber it is observed that the only contributions from $S_f \cdot_Y C^+$ come from c_p and c_{p-1}, as these are the coefficients in the Shioda map of the divisors D_{F_i}, which C^+ intersects, i.e.

$$S_f \cdot_Y C^+ = c_{p-1} - c_p\,. \tag{3.106}$$

Given (3.103) this can be expanded explicitly in terms of m and n (importantly the dependence on the phase is minimal)

$$S_f \cdot_Y C^+ = \begin{cases} (m-n) & p \le m \\ m & m < p\,. \end{cases} \tag{3.107}$$

In the above we considered only the so-called $SU(n)$-phases, where $p = 1, \cdots, n-1$. What remains is to consider the phases with an additional $U(1)$, where $F_0 \to C^+ + C^-$. In this case the only contribution to $S_f \cdot_Y C^+$ comes from c_{n-1}, which is m. In the previous section the possible values of $\sigma \cdot_Y C^+$ were determined from the possible consistent wrapping scenarios to be such that

$$\sigma \cdot_Y C^+ \in \{-1, 0, 1, 2\}\,. \tag{3.108}$$

Combining this information with (3.107) tables can be constructed for all possible charges in each phase. The two tables which cover all the phases for $I_n^{(0|^m 1)}$ are given in table 3.3. It can be seen that the possible charges are

$$S(\sigma_1) \cdot_Y C^+ = m - 3n\,,\ m - 2n\,,\ \cdots\,,\ m + 2n\,. \tag{3.109}$$

The subset of charges that exist in *every* phase is

$$S(\sigma_1) \cdot_Y C^+ = m - 2n\,,\ m - n\,,\ \cdots\,,\ m + n\,. \tag{3.110}$$

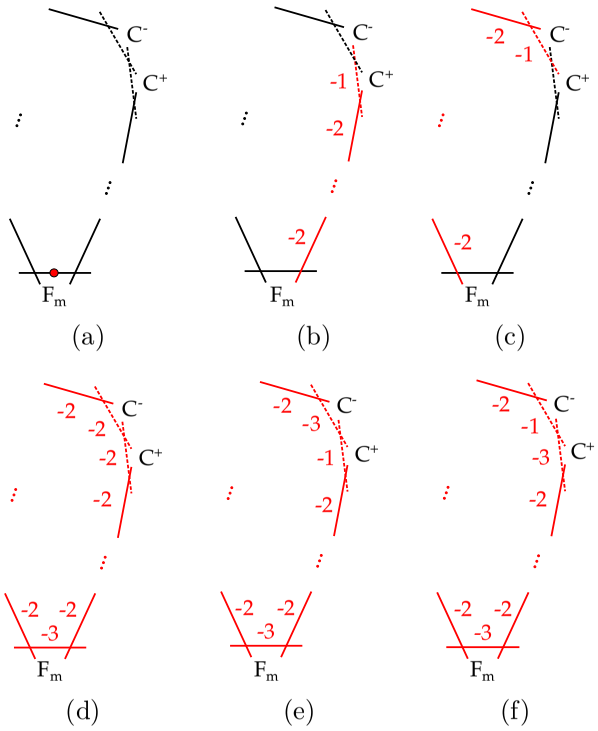

Figure 3.10: The six consistent wrapping configurations for $I_n \to I_{n+1}$ in the phases where the component F_p, which the section intersects in codimension one, does not split. Components which are coloured red are wrapped by the section, and the red numbers indicate the normal bundle degree of that curve inside the divisor σ. A red node indicates that the section intersects that component transversally.

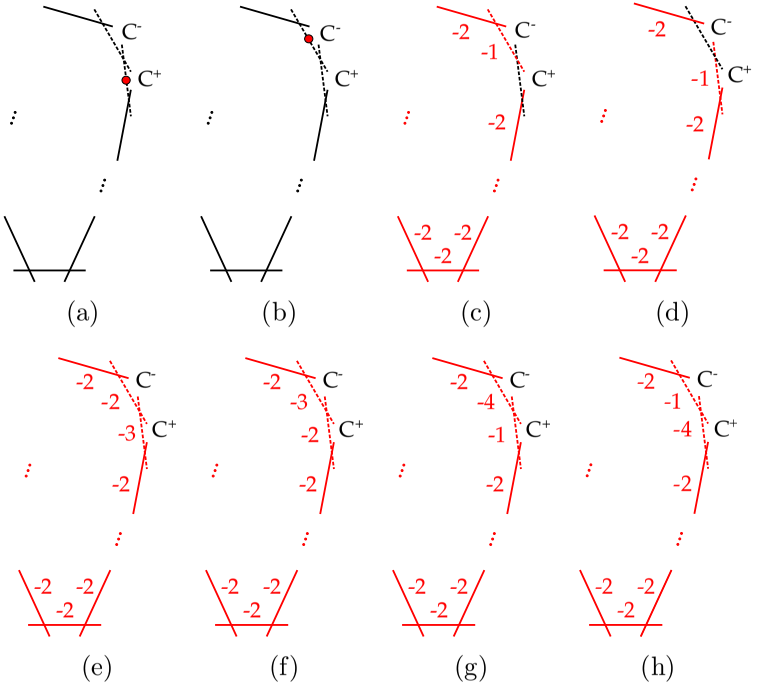

Figure 3.11: The eight consistent wrapping configurations for $I_n \to I_{n+1}$ in the phases where the component F_p which the section intersects in codimension one, $\sigma \cdot_Y F_p = 1$, splits: $F_p \to C^+ + C^-$. Components which are coloured red are wrapped by the section, and the red numbers indicate the normal bundle degree of that curves inside the divisor σ. A red node indicates that the section intersects that component transversally.

		$\sigma_1 \cdot_Y C^+$			
		-1	0	1	2
$\sigma_0 \cdot_Y C^+$	-1	$m-n$	m	$m+n$	$m+2n$
	0	$m-2n$	$m-n$	m	$m+n$
	1	$m-3n$	$m-2n$	$m-n$	m

		$\sigma_1 \cdot_Y C^+$		
		-1	0	1
$\sigma_0 \cdot_Y C^+$	-1	m	$m+n$	$m+2n$
	0	$m-n$	m	$m+n$
	1	$m-2n$	$m-n$	m
	2	$m-3n$	$m-2n$	$m-n$

Table 3.3: The $U(1)$ charges of all the possible wrapping combinations of the codimension one $I_n^{(0|^m 1)}$ fiber enhancing to an I_{n+1} fiber. On the left are the charges in phase where F_p splits for $p = 1, \cdots, m$, and on the right are the charges for the phases where $p = m+1, \cdots, n-1$ or $p = 0$. In each configuration, the cases $\sigma \cdot_Y C^+ = 2$ only appear in the $p = m$ or $p = 0$ phases.

While these are the charges that appear in every phase for every m, there are some special end-point values of m for which extra charges appear in all phases. When $m = 1$ or $m = n-1$ then charges $m+2n$ and $m-3n$ respectively appear in all phases. In addition, when $m = 0$ the tables degenerate on top of each other and the charge $m+2n$ appears in all phases. In the phase where F_0 splits there is a new charge $m+3n$ from $\sigma_1 \cdot_Y C^+ = 2$ and $\sigma_0 \cdot_Y C^+ = -1$.

There are charges, which do not appear in every phase within the framework of fibers satisfying the setup outlined in section 3.4.1. This has in particular to do with the flops of configurations of the type shown in (iii) and (iv) of figure 3.11, which we will elaborate on in section 3.6.

3.5 $SU(5) \times U(1)$ with 10 Matter

In this section we find the possible charges for **10** matter by analysing how the sections can behave under an I_5 to I_1^* enhancement. The codimension one I_5 fibers and Shioda maps are the same as those given in section 3.4.2.

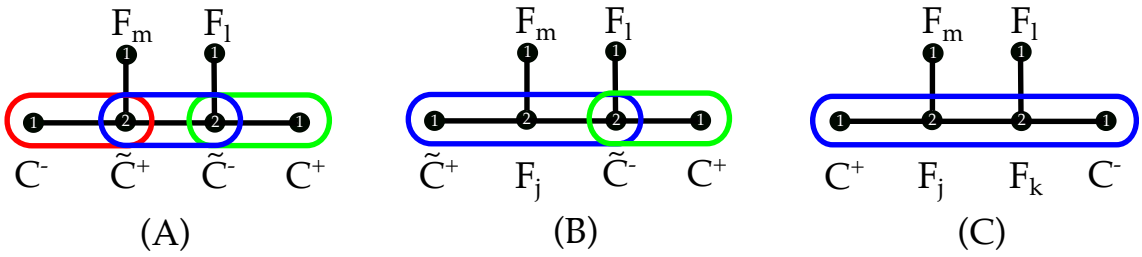

Figure 3.12: The three abstract splittings for I_5 to I_1^* enhancements. The colored loops indicate that there exists a root that splits into the encircled curves in codimension two.

3.5.1 Codimension two Fibers with Rational Sections

The fibers of the **10** representation are obtained from the box graphs in tables A.1 and A.2 in appendix A.1. The resulting fibers are all I_1^*, consistent with the local enhancement to $\mathfrak{so}(10)$, with the correct multiplicities. To find the charges of the **10** representation we employ the same method as before, solving for the possible configurations under the constraints of consistency with codimension one, $\sigma \cdot_Y \text{Fiber} = 1$. The multiplicity of each component in the I_1^* fiber must be taken into account when imposing the latter condition.

There are three classes of splitting types that can occur in the enhancement to I_1^*, shown in figure 3.12. They are one of the following,

(A) $F_i \to C^+ + \tilde{C}^-$, $F_j \to \tilde{C}^+ + \tilde{C}^-$, $F_k \to \tilde{C}^+ + C^-$

(B) $F_i \to \tilde{C}^\pm + F_j + \tilde{C}^\mp$, $F_k \to C^\pm + \tilde{C}^\mp$

(C) $F_i \to C^+ + F_j + F_k + C^-$, $j \neq k$ and $j, k \neq i$.

In each of the three cases there are different subcases to consider depending on which of the components of the fiber the section intersects in codimension one. There are five different options corresponding to the number of components in codimension one, however the reflection symmetry of the intersection graphs allows one to consider only eleven different configurations, instead of fifteen. The configurations will be termed the "splitting types" and will be denoted as

A.1: $\sigma \cdot_Y F_l = 1$
A.2: $\sigma \cdot_Y F_i = 1$
A.3: $\sigma \cdot_Y F_j = 1$

B.1: $\sigma \cdot_Y F_l = 1$
B.2: $\sigma \cdot_Y F_k = 1$
B.3: $\sigma \cdot_Y F_j = 1$
B.4: $\sigma \cdot_Y F_m = 1$
B.5: $\sigma \cdot_Y F_i = 1$

C.1: $\sigma \cdot_Y F_l = 1$
C.2: $\sigma \cdot_Y F_k = 1$
C.3: $\sigma \cdot_Y F_i = 1$.

For each splitting type one can determine the values of the intersection numbers, from the intersection of the section with the split curves, that are consistent with the constraints from codimension one and the requirement that the normal bundles of subspaces embed

as subbundles of the total normal bundle. Each possible set of intersection numbers may have multiple realisations in terms of configurations of the curves inside the section. The intersection numbers with σ are all that is necessary to determine $U(1)$ charges via the Shioda map. In this section splitting type A.2 will be detailed explicitly and the tables of results for all the other ten splitting types will be relegated to appendix A.1.

Consider then splitting type A.2, defined as the splitting

$$\begin{aligned} F_i &\to \tilde{C}^+ + C^- \\ F_j &\to \tilde{C}^+ + \tilde{C}^- \\ F_k &\to C^+ + \tilde{C}^- \,, \end{aligned} \tag{3.111}$$

with $\sigma \cdot_Y F_i = 1$, and the intersection of the section with all other codimension one fiber components being zero. As such the constraints from the split curves become

$$\begin{aligned} \sigma \cdot_Y (\tilde{C}^+ + C^-) &= 1 \\ \sigma \cdot_Y (\tilde{C}^+ + \tilde{C}^-) &= 0 \\ \sigma \cdot_Y (C^+ + \tilde{C}^-) &= 0 \,. \end{aligned} \tag{3.112}$$

Any one of the intersection numbers $\sigma \cdot_Y C$ for any curve C determines all the other intersection numbers with the Cs. As the normal bundle to the curves C that come from the splitting of the curves F_i in codimension two is $\mathcal{O}(-1) \oplus \mathcal{O}(-1)$ for three-folds and $\mathcal{O} \oplus \mathcal{O}(-1) \oplus \mathcal{O}(-1)$ for four-folds it is known by Theorems 3.3.5 and 3.3.8 that $\sigma \cdot_Y C \geq -1$ for all such C. Solving the constraints (3.112) subject to these inequalities leads to the three solutions

$$\begin{aligned} &(i) \quad \sigma \cdot_Y C^- = 2 \,, \quad \sigma \cdot_Y \tilde{C}^+ = \sigma \cdot_Y C^+ = -1 \,, \quad \sigma \cdot_Y \tilde{C}^- = 1 \\ &(ii) \quad \sigma \cdot_Y C^- = 1 \,, \quad \sigma \cdot_Y \tilde{C}^+ = \sigma \cdot_Y \tilde{C}^- = \sigma \cdot_Y C^+ = 0 \\ &(iii) \quad \sigma \cdot_Y C^- = 0 \,, \quad \sigma \cdot_Y \tilde{C}^+ = \sigma \cdot_Y C^+ = 1 \,, \quad \sigma \cdot_Y \tilde{C}^- = -1 \,. \end{aligned} \tag{3.113}$$

Each of these solutions has in addition that $\sigma \cdot_Y F_l = \sigma \cdot_Y F_m = 0$ from consistency of the curves which do not split with codimension one. It remains to ask whether there are any possible realisations of these intersection numbers. All the configurations realising each of these three solutions are shown in figure 3.13. If a curve is such that $\sigma \cdot_Y C = -1$ then it must be contained in σ with $\deg(N_{C/\sigma}) = -1$, else if a curve is such that $\sigma \cdot_Y C = k \geq 0$ then the curve is either not contained in σ and has k transverse intersections with σ, or it is contained in σ with $\deg(N_{C/\sigma}) = -k - 2$. In this way configurations of curves inside the section with particular intersection numbers can be constructed.

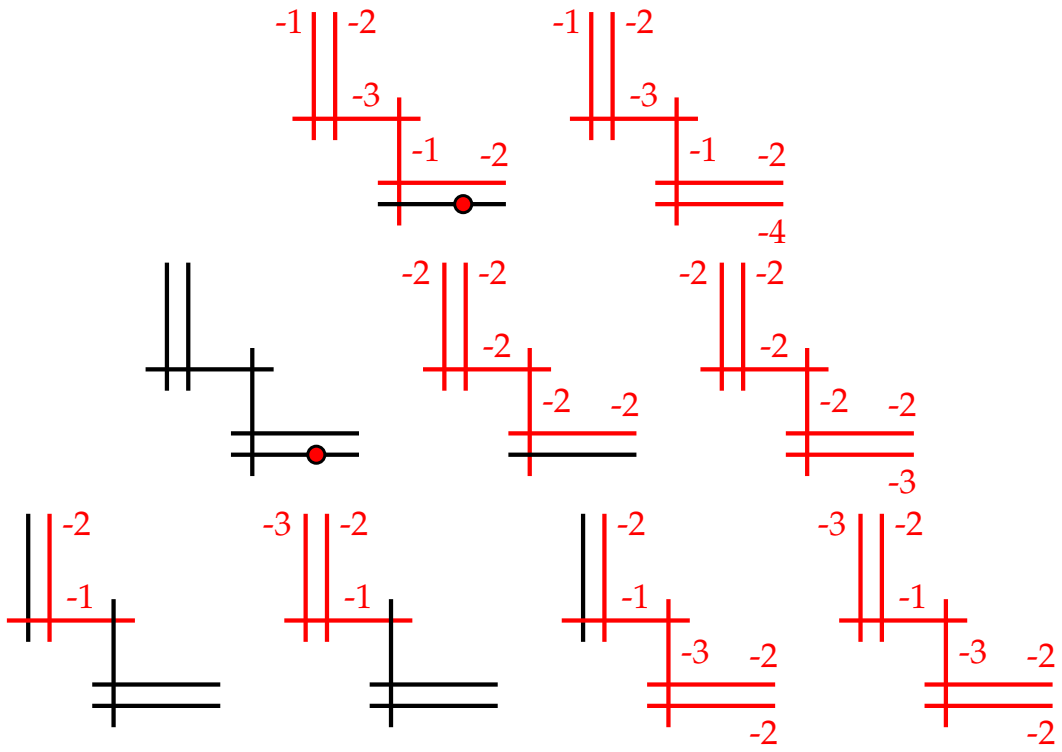

Figure 3.13: The different realisations of the intersection number solutions (*i*) (top row), (*ii*) (middle row), and (*iii*) (bottom row) for splitting type A.2. The red integers are the degree of the normal bundles of each curve inside the section.

Phase	$I_5^{(01)}$ charges	$I_5^{(0\|1)}$ charges	$I_5^{(0\|\|1)}$ charges
1	$-3,-2,-1,0,+1,+2,+3$	$-12,-7,-2,+3,+8,+13$	$-9,-4,+1,+6,+11$
2	$-2,-1,0,+1,+2$	$-12,-7,-2,+3,+8$	$-9,-4,+1,+6$
3	$-2,-1,0,+1,+2$	$-12,-7,-2,+3,+8$	$-9,-4,+1,+6$
4	$-2,-1,0,+1,+2$	$-12,-7,-2,+3,+8$	$-9,-4,+1,+6,+11$
5	$-2,-1,0,+1,+2$	$-12,-7,-2,+3,+8$	$-9,-4,+1,+6$
6	$-2,-1,0,+1,+2$	$-7,-2,+3,+8$	$-9,-4,+1,+6$
7	$-2,-1,0,+1,+2$	$-12,-7,-2,+3,+8$	$-9,-4,+1,+6,+11$
8	$-2,-1,0,+1,+2$	$-7,-2,+3,+8$	$-9,-4,+1,+6,+11$
9	$-2,-1,0,+1,+2$	$-12,-7,-2,+3,+8$	$-9,-4,+1,+6,+11$
10	$-2,-1,0,+1,+2$	$-7,-2,+3,+8$	$-9,-4,+1,+6,+11$
11	$-2,-1,0,+1,+2$	$-12,-7,-2,+3,+8,+13$	$-9,-4,+1,+6,+11$
12	$-2,-1,0,+1,+2$	$-7,-2,+3,+8,+13$	$-9,-4,+1,+6,+11$
13	$-2,-1,0,+1,+2$	$-7,-2,+3,+8$	$-9,-4,+1,+6,+11$
14	$-2,-1,0,+1,+2$	$-7,-2,+3,+8,+13$	$-9,-4,+1,+6,+11$
15	$-2,-1,0,+1,+2$	$-7,-2,+3,+8,+13$	$-9,-4,+1,+6,+11$
16	$-3,-2,-1,0,+1,+2,+3$	$-12,-7,-2,+3,+8,+13$	$-9,-4,+1,+6,+11$

Table 3.4: The range of possible $U(1)$ charges for each codimension one fiber type. The phases are those listed in tables A.1 and A.2 in appendix A.1.

3.5.2 $U(1)$ charges

The possible codimension two fibers are obtained by combining the σ_0 and σ_1 configurations appearing in the same phase. The $U(1)$ charges of the **10** representation for each such combined configuration are determined from the C^+/C^- intersections with the sections listed in the figures and the appropriate Shioda map (3.98). The results are shown in table 3.4. Each entry in the table lists the possible charges in each phase for a particular codimension one fiber type, and is summarised in terms of the following set of possible charges:

$$U(1) \text{ charges of } \mathbf{10} \text{ matter for } \begin{cases} I_5^{(01)} \in \{-15,-10,-5,0,+5,+10,+15\} \\ I_5^{(0|1)} \in \{-12,-7,-2,+3,+8,+13\} \\ I_5^{(0||1)} \in \{-9,-4,+1,+6,+11\}\ . \end{cases} \tag{3.114}$$

Again, like for the case of fundamental matter, the known charges that occur in concrete realisations of elliptic fibrations of $SU(5)$ GUTs are a strict subset of these. The comparison to the embedding into E_8 can be found in appendix A.2.

3.6 Flops and Rational Sections

Flops between distinct resolutions of singular elliptic Calabi–Yau fibrations have been discussed in terms of the Coulomb phases, or box graphs, in [70], and realised in terms of explicit elliptic fibrations (based on Tate models) in [65, 126–128]. In this section, we will study the flops for codimension two fibers with sections wrapping fiber components. For simplicity we consider here three-folds, however we expect all of the flops to generalise quite straightforwardly to four-fold flops, e.g. as discussed in [129, 130].

3.6.1 Flops and Intersections

The small resolutions of the singular fibers are related by flops along curves in the fiber in codimension two. To determine how the flops change the normal bundle degrees of $C \subset D$, which in the three-fold case is given by the self-intersections of the curves in D, it is useful to recapitulate some of the mathematical results on this for three-folds. The first important notion is that of a (-2)-curve as introduced in Theorem 3.3.6 (see [124] for more details). Recall that the normal bundle of the curves F_i, which remain irreducible in codimension two, are

$$N_{F_i/Y} = \mathcal{O} \oplus \mathcal{O}(-2)\,, \tag{3.115}$$

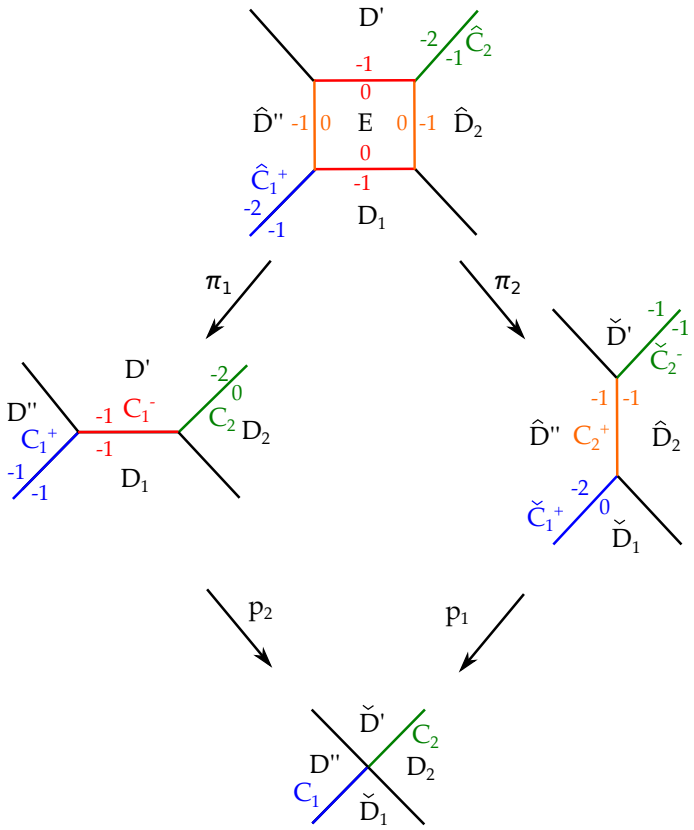

Figure 3.14: Flop of the curve C_1^- into C_2^+. D's are divisors, C the curves at their intersections, and the small numbers indicate the degree of the normal bundles of the curves inside the divisors. The exceptional divisor, $E = \mathbb{P}^1 \times \mathbb{P}^1$, is introduced in the blow-up as an intermediate stage. Alternatively one can blow down to the singular configuration at the bottom of the picture.

whereas if $F_p \to C^+ + C^-$ becomes reducible in codimension two, then each of the irreducible components $C^\pm$ have normal bundle in Y

$$N_{C^\pm/Y} = \mathcal{O}(-1) \oplus \mathcal{O}(-1)\,. \tag{3.116}$$

Consider the situation shown in figure 3.14, starting with the configuration in the lower left hand side. The curves $C_1^\pm$ both have normal bundles of degree $(-1,-1)$, the curve C_2 has normal bundle $(-2,0)$ (i.e. it is, in our standard notation, one of the F_i). Consider blowing up along the curve C_1^-.

Let D and $\hat{D}$ be divisors and $\pi_1 : \hat{D} \to D$ the blow-up of a curve C. The canonical class changes as

$$K_{\hat{D}} = \pi_1^* K_D + C\,. \tag{3.117}$$

Here the blow-up affects the two divisors D_2 and D'', in particular under $\pi_1 : \hat{D}_2 \to D_2$

the canonical class changes by the new curve, C_2^+,

$$K_{\hat{D}_2} = \pi_1^* K_{D_2} + C_2^+ \,, \qquad K_{\hat{D}''} = \pi_1^* K_{D''} + C_2^+ \,. \tag{3.118}$$

The curves C_2 and C_1^+, are contained within these two divisors, and their normal bundles change in the blow-up. Denoting their images under the blow-up by $\hat{C}$, the normal bundle degrees are (using adjunction that $K_D \cdot_D C = -(C)_D^2 - 2$)

$$\begin{aligned} \deg(N_{\hat{C}_2/\hat{D}_2}) &= (\hat{C}_2)^2_{\hat{D}_2} = -K_{\hat{D}_2} \cdot_{\hat{D}_2} \hat{C}_2 - 2 \\ &= -(\pi_1^* K_{D_2} + \hat{C}_2^+) \cdot_{\hat{D}_2} \hat{C}_2 - 2 = -(-2+1) - 2 = -1 \\ \deg(N_{\hat{C}_1^+/\hat{D}''}) &= (\hat{C}_1^+)^2_{\hat{D}''} = -K_{\hat{D}''} \cdot_{\hat{D}''} \hat{C}_1^+ - 2 \\ &= -(\pi_1^* K_{D''} + \hat{C}_2^+) \cdot_{\hat{D}''} \hat{C}_1^+ - 2 = -(-1+1) - 2 = -2 \,. \end{aligned} \tag{3.119}$$

The normal bundles of $\hat{C}_2^-$, $\hat{C}_1^+$ in the divisors D', D_1 respectively, are unchanged as the canonical class of these divisors remains the same under the blow-up. The resulting configuration is shown on the top of figure 3.14.

The flop is completed by blowing down the curve $\hat{C}_1^-$. The canonical classes change again as in (3.117) for the two divisors, which contain this curve, i.e. D_1 and D' under the blow down $\pi_2 : D \to \check{D}$

$$K_{D_1} = \pi_2^* K_{\check{D}_1} + \hat{C}_1^- \,, \qquad K_{D'} = \pi_2^* K_{\check{D}'} + \hat{C}_1^- \,. \tag{3.120}$$

After the blow down, denote the curve corresponding to $\hat{C}_2$ and $\hat{C}_1^+$ by $\check{C}_2^-$ and $\check{C}_1$, respectively. Then the normal bundles change as follows

$$\begin{aligned} \deg(N_{\check{C}_2^-/\check{D}_1}) &= (\check{C}_2^-)^2_{\check{D}'} = -K_{\check{D}'} \cdot_{\check{D}'} \check{C}_2^- - 2 \\ &= -(K_{D'} - \hat{C}_1^-) \cdot_{D'} \hat{C}_2 - 2 = -(0-1) - 2 = -1 \\ \deg(N_{\check{C}_1/\check{D}_1}) &= (\check{C}_1)^2_{\check{D}_1} = -K_{\check{D}_1} \cdot_{\check{D}_1} \check{C}_1 - 2 \\ &= -(K_{D_1} - \hat{C}_1^-) \cdot_{D_1} \hat{C}_1^+ - 2 = -(-1-1) - 2 = 0 \,. \end{aligned} \tag{3.121}$$

On the other hand, $\hat{C}_1^-$ is not in $\hat{D}_2$ or $\hat{D}''$, so the blow down does not affect the normal bundle of $\check{C}_2^-$ in $\hat{D}_2$ or of $\check{C}_1^+$ in $\hat{D}''$. Thus the flop of C_1^-, which was previously the intersection of D' and D_1, produces a new curve $\hat{C}_2^+$ which is no longer contained inside either D' or D_1 but instead intersects them in a point.

Alternatively, one can consider first blowing down with p_2 in figure 3.14, and then blowing up. The advantage of the process we described here, is that the geometry in every step is smooth, whereas the lower, singular configuration would require particular care in applying the intersection calculus.

The prior analysis can now be applied to the case of $SU(5)$ models with e.g. fundamental matter. Taking one of the divisors D' or D_1 above to be one of the rational sections we see

that, under a flop, a curve contained inside the section is flopped to one that intersects the section in a point and vice versa. Consider a configuration in figure 3.6, for example where $\sigma \cdot_Y F_1 = 1$ in codimension one, then the generic flops for fibers studied in [70] dictate how the configurations flop into each other. However for fibers with rational sections, not every configuration appears to have a flop image in the category of fiber configurations that satisfy our initial setup. This is indicated in the shading of the charges in figures 3.7−3.9, showing which charges flop into each other. The charges in blue appear in every phase whereas the charges highlighted in green only appear in certain phases. The flop of the configurations, which do not appear in all phases will be discussed in section 3.6.3.

3.6.2 An I_1^* Flop

Consider the flop of the curve $C^+_{3,4}$ depicted in figure 3.15. In this case it is simpler to consider first blowing down this curve, and then blowing up. The starting configuration, shown on the left of figure 3.15, appears in phase 6 of table A.4 where the section intersects F_1 in codimension one. The splitting in this phase is given by,

$$F_4 \to C^+_{3,4} + F_1 + F_2 + C^-_{1,5} \tag{3.122}$$

These curves have the following self-intersections, i.e. normal bundle degrees, inside D_{F_4},

$$\begin{aligned} (C^+_{3,4})^2_{D_{F_4}} &= -1 \\ (C^-_{1,5})^2_{D_{F_4}} &= -1 \\ (F_1)^2_{D_{F_4}} &= -2 \\ (F_2)^2_{D_{F_4}} &= -2\,, \end{aligned} \tag{3.123}$$

determined by the box graph for this phase. For the curves F_i do not split,

$$(F_i)^2_{D_{F_i}} = 0\,. \tag{3.124}$$

In the configuration shown $F_2, C^+_{3,4}, F_3 \subset \sigma_1$ and the self intersections in σ_1 are given by the red numbers appearing next to these curves in the figure. Now consider the blow down of the curve $C^+_{3,4}$ which changes the canonical class of D_{F_4} and σ_1,

$$K_{\sigma_1} = \pi_1^* K_{\check{\sigma}_1} + C^+_{3,4}, \qquad K_{D_{F_4}} = \pi_1^* K_{\check{D}_{F_4}} + C^+_{3,4}\,. \tag{3.125}$$

Under the blow-up π_2 of the singular geometry we reach the I_1^* fiber obtained by the splitting,

$$\begin{aligned} F_4 &\to C^+_{2,4} + F_1 + C^-_{1,5} \\ F_2 &\to C^+_{2,4} + C^-_{3,4} \end{aligned} \tag{3.126}$$

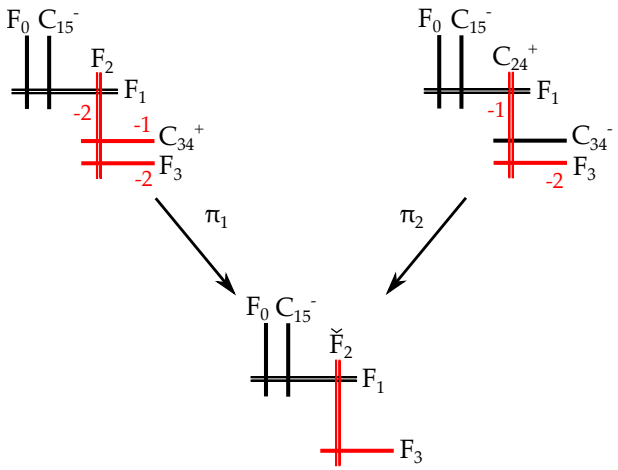

Figure 3.15: Flop of a σ_1 wrapping configuration from phase 6 (left) to phase 8 (right) where $\sigma_1 \cdot_Y F_1 = 1$. The red numbers denote the self intersections of the curves inside σ_1.

The configuration in this phase, phase 8, is shown on the right in figure 3.15, where the flopped curve $C^-_{3,4} \not\subset \sigma_1$ and the canonical class of the divisor $\check{D}_{F_2}$ is

$$K_{\hat{D}_{F_2}} = \pi_2^* K_{\check{D}_{F_2}} + C^-_{3,4}\,. \tag{3.127}$$

Only the normal bundle of the curve F_2, which becomes $C^+_{2,4}$, is altered by this flop as no other curve intersected $C^+_{3,4}$ in the original configuration. As the intermediate stage in this description of the flop is singular the self intersection of the curve $C^+_{2,4}$ in the divisors $\hat{D}_{F_4}$, $\hat{\sigma}_1$ and $\hat{D}_{F_2}$ in phase 8 is computed by always pulling back to one of the resolved geometries,

$$\begin{aligned}(C^+_{2,4})^2_{\hat{\sigma}_1/\hat{D}_{F_4}} &= -\,K_{\hat{\sigma}_1/\hat{D}_{F_4}} \cdot_{\hat{\sigma}_1/\hat{D}_{F_4}} C^+_{2,4} - 2\\ &= -\,K_{\check{\sigma}_1/\check{D}_{F_4}} \cdot_{\check{\sigma}_1/\check{D}_{F_4}} \check{F}_2 - 2\\ &= -\,(K_{\sigma_1/D_{F_4}} - C^+_{3,4}) \cdot_{\sigma_1/D_{F_4}} F_2 - 2\\ &= -\,(0-1) - 2 = -1\,.\end{aligned} \tag{3.128}$$

In the above, the second equality sign holds as the canonical class of $\check{D}_{F_4}$ and $\check{\sigma}_1$ is unchanged by the blow-up π_2.

$$\begin{aligned}(C^+_{2,4})^2_{\hat{D}_{F_2}} &= -\,K_{\hat{D}_{F_2}} \cdot_{\check{D}_{F_2}} C^+_{2,4} - 2\\ &= -\,(\pi_2^* K_{\check{D}_{F_2}} + C^-_{3,4}) \cdot_{\hat{D}_{F_2}} C^+_{2,4} - 2\\ &= -\,(\pi_2^* K_{D_{F_2}} + C^-_{3,4}) \cdot_{\hat{D}_{F_2}} C^+_{2,4} - 2\\ &= -\,(-2+1) - 2 = -1\,.\end{aligned} \tag{3.129}$$

Thus the curve $C^+_{2,4}$ has normal bundle degree $(-1,-1)$ in the flopped geometry which is exactly what we expect from the splitting in phase 8. The flop discussed here exactly reproduces what was claimed in the previous section: a curve contained inside the section is flopped to one which intersects it at a point.

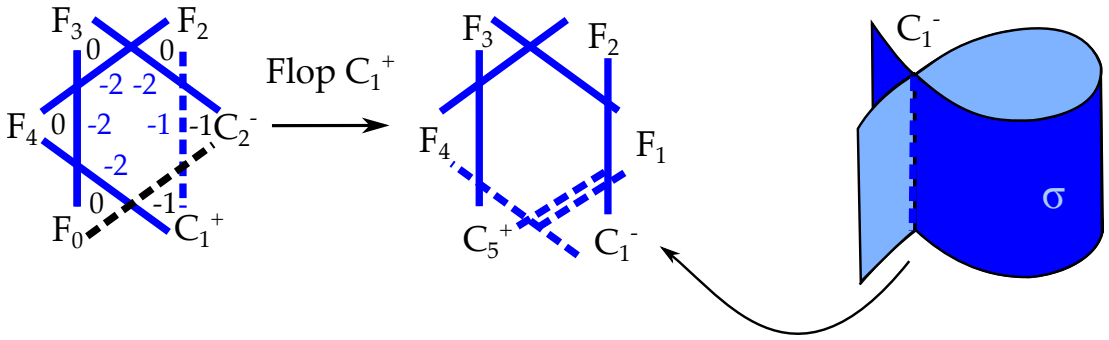

Figure 3.16: The almost fully wrapped fiber (the rational curves contained in the section σ are shown in blue) shown on the left flops via C_1^+ to the fiber, which is fully contained in the section. However the section is now singular along the curve C_1^-, along which it self-intersects as shown on the far right. The numbers in black and blue denote the degree of the normal bundle of the curves inside the divisors D_{F_i} and the section σ, respectively.

3.6.3 Flops to Singular Sections

It was mentioned in section 3.6.1 that certain configurations do not flop into configurations within the class of fibers that we considered here. All such fibers are of the type that the entire fiber except for one curve is contained inside the section. We now briefly comment on this. Consider for instance flopping the curve C_1^+ on the left hand side of figure 3.16. In this configuration the splitting is given by $F_1 \to C_1^+ + C_2^-$ and the curve C_1^+ has normal bundle $(-1,-1)$ inside of D_{F_1}.

Proceeding as described above, we blow-up every point along C_1^+ and in doing so we obtain the exceptional divisor E. The two points at which C_1^+ intersected the section become two curves contained inside the section. Under the contraction of the C_1^+ ruling of the exceptional divisor E, the two curves contained in the section are identified. Thus we obtain a curve which is contained inside the section twice. The section is now singular as it meets itself along this curve[13]. This configuration is shown on the right hand side of figure 3.16. In our analysis we assumed throughout that the section is a smooth divisor in the Calabi–Yau. Clearly, after this flop this condition ceases to hold, and it would be interesting to study such configurations, and to determine whether or not the singular section is consistent from the point of view of the F-theory compactification. We will comment on this further in the discussion section 3.10.

[13] We thank Dave Morrison for discussions on this point.

3.7 Singlets

As a final application of our method, we now turn to discuss $U(1)$-charged GUT singlets. Mathematically, this corresponds to analyzing the codimension two fibers with rational section for an I_1 to I_2 enhancement. Apart from the interest in the types of singlet charges that are possible, this has wide-ranging implications for Higgsing the $U(1)$ symmetries to a discrete gauge symmetry, as in e.g. [79–81]. Other phenomenologically interesting implications, in particular when applied to four-folds, concern the possible Yukawa couplings of the type $\mathbf{R\overline{R}1}$ as well as non-renormalisable couplings, which e.g. could regenerate proton decay operators. After some general properties of singlets, we first discuss the situation in three-folds in section 3.7.2, and for four-folds in section 3.7.3.

3.7.1 Constraints on Singlet Curves

Consider a smooth Calabi–Yau three- or four-fold Y. An I_1 fiber consists of a single nodal rational curve F_0, with arithmetic genus $p_a(F_0) = 1$, such that

$$D_{F_0} \cdot_Y F_0 = 0 \tag{3.130}$$

Above a codimension two locus, the node splits

$$F_0 \to C^+ + C^- \,, \tag{3.131}$$

where $C^\pm$ are smooth rational curves, which intersect in an I_2 Kodaira fiber. Consistency with codimension one requires that

$$D_{F_0} \cdot_Y C^+ = -D_{F_0} \cdot_Y C^- \,, . \tag{3.132}$$

As both $C^\pm$ are smooth rational curves contained inside D_{F_0}, it follows by Corollary 3.3.4 that

$$\deg(N_{C^+/D_{F_0}}) + \deg(N_{C^-/D_{F_0}}) = -4 \,. \tag{3.133}$$

However, as these curves do not arise as complete intersections, their normal bundles in Y are not fixed by the degrees of $N_{C^\pm/D_{F_0}}$. We require one of the curves in the I_2 fiber to be contractible. Without loss of generality, we take C^- to be the contractible curve. In Calabi–Yau three-folds this condition is known to have three solutions, as summarised in Theorem 3.3.6, which will be discussed in the next section. For four-folds we are not aware of a similar result, and we will therefore conduct a survey without imposing the additional contractibility condition in section 3.7.3.

3.7.2 Singlets in Three-folds

In this section, let Y be a smooth Calabi–Yau three-fold. We will first determine the possible section configurations that are consistent from the point of view of normal bundle degrees in a three-fold. Following this, we determine the possible singlet charges and fiber types.

Normal Bundle Constraints

We start by considering the possible normal bundle degrees for rational curves in an I_2 fiber. We assume C^- to be contractible. Theorem 3.3.6 implies that a contractible rational curve can have the following normal bundles in Y:

A) $N_{C^-/Y} = \mathcal{O}(-1) \oplus \mathcal{O}(-1)$

B) $N_{C^-/Y} = \mathcal{O} \oplus \mathcal{O}(-2)$

C) $N_{C^-/Y} = \mathcal{O}(1) \oplus \mathcal{O}(-3)$.

We do not constrain C^+ to be contractible therefore its normal bundle takes the general form

$$N_{C^+/Y} = \mathcal{O}(p) \oplus \mathcal{O}(-2-p), \quad p \geq -1\,. \tag{3.134}$$

We consider a fibration with two rational sections, σ_0 and σ_1. In codimension one both sections intersect F_0, therefore it is sufficient to just consider one of the sections to find the possible configurations for the fiber in codimension two. For an I_1 local enhancement to I_2 the constraint from codimension one is,

$$\sigma \cdot_Y (C^+ + C^-) = 1\,. \tag{3.135}$$

For each case A−C there always exists the solution, where the section intersects transversally either C^+ or C^- and does not contain any curves in the fiber. The two cases will differ in the possible wrapping configurations.

As the normal bundle of C^+ is the same for cases A−C we can first derive some general statements irrespective of the normal bundle of C^-. Consider $C^+ \subset \sigma$, using Theorem 3.3.5 (iii), there exists an embedding

$$N_{C^+/\sigma} \;\hookrightarrow\; N_{C^+/Y} = \mathcal{O}(p) \oplus \mathcal{O}(-2-p)\,, \qquad p \geq -1\,, \tag{3.136}$$

in the following two cases:

(i) $\deg(N_{C^+/\sigma}) = p$

(ii) $\deg(N_{C^+/\sigma}) \leq -p-2$.

Using Corollary 3.3.4 one finds that for (i)

$$\sigma \cdot_Y C^+ = -p-2\,. \tag{3.137}$$

Combining (3.137) with (3.135), one obtains the intersection of C^- with σ,

$$\sigma \cdot_Y C^- = p+3\,. \tag{3.138}$$

The intersections of σ with C^+ (resp. C^-) will be bounded from below (resp. above) by (3.137) (resp. (3.138)).

Now let us consider case A where C^- has normal bundle degree $(-1,-1)$. If $C^- \subset \sigma$ then in order for $N_{C^-/\sigma}$ to embed inside $N_{C^-/Y}$ we must have,

$$\deg(N_{C^-/\sigma}) \leq -1\,. \tag{3.139}$$

This is a consequence of Theorem 3.3.5 part (ii) and as a result the intersections of σ with $C^\pm$ are

$$(\sigma \cdot_Y C^+, \sigma \cdot_Y C^-) = (2,-1),\ (1,0),\ (0,1),\ (-p-2, p+3)\,. \tag{3.140}$$

The codimension one constraint (3.135) then specifies the upper bound for the intersection of σ with C^+. The possible configurations which realise these intersections are:

A.1) $\sigma \cdot_Y C^+ = 2$, $\sigma \cdot_Y C^- = -1$

The lower bound on $\sigma \cdot_Y C^-$ is achieved by $C^- \subset \sigma$, with $\deg(N_{C^-/\sigma}) = -1$. To obtain the correct intersection for C^+ with the section there are two possibilities:

(i) $C^+ \not\subset \sigma$

The correct intersections are automatic in this case as in any I_2 fiber the curves $C^\pm$ intersect each other in two points, and C^- is contained inside the section.

(ii) $C^+ \subset \sigma$

The degree of $N_{C^+/\sigma}$ is determined using Corollary 3.3.4, requiring $\sigma \cdot_Y C^+ = 2$ implies $\deg(N_{C^+/\sigma}) = -4$. This solution is only valid when $N_{C^+/Y} = \mathcal{O}(-4)$ can be embedded non-trivially into $N_{C^+/Y}$ which is true for

$$-1 \leq p \leq 2\,. \tag{3.141}$$

A.2) $\sigma \cdot_Y C^+ = 1$, $\sigma \cdot_Y C^- = 0$

There are two configurations, which realise the above intersections. The first is given by $C^+ \not\subset \sigma$, but σ intersects C^+ transversally. In this case the section does not contain any components of the fiber. The second solution is given by $C^+, C^- \subset \sigma$

and $\deg(N_{C^+/\sigma}) = -3$ and $\deg(N_{C^-/\sigma}) = -2$. One can check using Corollary 3.3.4 that these values give the correct intersection values for $\sigma \cdot_Y C^{\pm}$. The latter configuration can only be realised for

$$-1 \leq p \leq 1 \tag{3.142}$$

A.3) $\sigma \cdot_Y C^+ = 0$, $\sigma \cdot_Y C^- = 1$

The solutions in this case can be obtained from the solutions in A.2 by exchanging $C^{\pm}$. The configuration where the entire fiber is contained inside the section is a solution for

$$p = -1 \quad \text{or} \quad 0\,. \tag{3.143}$$

A.4) $\sigma \cdot_Y C^+ = -p-2$, $\sigma \cdot_Y C^- = p+3$

As was detailed above, to achieve a negative intersection with the section, C^+ must be contained inside it with $\deg(N_{C^+/\sigma}) = p$. There are two possibilities for C^-:

(i) $C^- \not\subset \sigma$

The section, from the containment of C^+, intersects C^- in two points necessarily. In order to satisfy (3.135) C^- requires $p+1$ additional intersections with the section.

(ii) $C^- \subset \sigma$

In this case we require $\deg(N_{C^-/\sigma}) = -p-5$ to satisfy $\sigma \cdot_Y C^- = p+3$. This solution is valid for $p \geq -1$ as for these values of p the following embedding always exists

$$\mathcal{O}(-p-5) \;\hookrightarrow\; \mathcal{O}(-1) \oplus \mathcal{O}(-1)\,. \tag{3.144}$$

The full set of configurations for A are summarised below. The configurations which have been marked $(*)$ are only valid when p falls within the ranges specified in (3.141), (3.142) and (3.143), respectively.

$\sigma \cdot_Y C^+$	$\sigma \cdot_Y C^-$	C^+configuration	C^-configuration
2	-1	$C^+ \not\subset \sigma, \sigma \cdot_Y C^+ = 2$	$C^- \subset \sigma, \deg(N_{C^-/\sigma}) = -1$
		$C^+ \subset \sigma, \deg(N_{C^+/\sigma}) = -4$	$C^- \subset \sigma, \deg(N_{C^-/\sigma}) = -1$ $(*)$
1	0	$C^+ \not\subset \sigma, \sigma \cdot_Y C^+ = 1$	$C^- \not\subset \sigma, \sigma \cdot_Y C^- = 0$
		$C^+ \subset \sigma, \deg(N_{C^+/\sigma}) = -3$	$C^- \subset \sigma, \deg(N_{C^-/\sigma}) = -2$ $(*)$
0	1	$C^+ \not\subset \sigma, \sigma \cdot_Y C^+ = 0$	$C^- \not\subset \sigma, \sigma \cdot_Y C^- = 1$
		$C^+ \subset \sigma, \deg(N_{C^+/\sigma}) = -2$	$C^- \subset \sigma, \deg(N_{C^-/\sigma}) = -3$ $(*)$
$-p-2$	$p+3$	$C^+ \subset \sigma, \deg(N_{C^+/\sigma}) = p$	$C^- \not\subset \sigma, \sigma \cdot_Y C^- = p+3$
		$C^+ \subset \sigma, \deg(N_{C^+/\sigma}) = p$	$C^- \subset \sigma, \deg(N_{C^-/\sigma}) = -p-5$

(3.145)

For case B the curve C^- has normal bundle degree $(0,-2)$. To find the lower bound for the intersection of C^- with the section we need to consider $C^- \subset \sigma$. Requiring $N_{C^-/\sigma}$ to embed inside $N_{C^-/Y}$ gives the constraint

$$\deg(N_{C^-/\sigma}) \leq 0\,, \tag{3.146}$$

where $\deg(N_{C^-/\sigma}) \neq -1$. This bounds the intersection of C^- with the section from below,

$$\sigma \cdot_Y C^- \geq -2 \;\Rightarrow\; \sigma \cdot_Y C^+ \leq 3\,. \tag{3.147}$$

The possible intersections are given by

$$(\sigma \cdot_Y C^+, \sigma \cdot_Y C^-) = (3,-2),\ (1,0),\ (0,1),\ (-p-2, p+3)\,. \tag{3.148}$$

The intersection of C^+ with σ can not take the value -1 due to the constraint $\deg(N_{C^-/\sigma}) \neq -1$. The solutions for the last three intersection sets are the same as those given for case A therefore we shall only detail the solutions for the first set here.

B.1) $\sigma \cdot_Y C^+ = 3, \sigma \cdot_Y C^- = -2$

The two configurations for this set of intersections must have $C^- \subset \sigma, \deg(N_{C^-/\sigma}) = 0$. This is mandated by the intersection of the section with C^-. There are two possibilities for C^+:

(i) $C^+ \not\subset \sigma$

The containment of C^- inside the section means that C^+ intersects the section twice through the intersection of C^- and C^+ in the fiber. Consistency with codimension one requires an additional transverse intersection between σ and C^+.

(ii) $C^+ \subset \sigma$

Requiring $\sigma \cdot_Y C^+ = 3$ means that $\deg(N_{C^+/\sigma}) = -5$. This configuration is a valid solution for

$$-1 \leq p \leq 3\,. \tag{3.149}$$

The configurations for case B are (p is constrained in the (*)'ed configurations as in (3.149), (3.142) and (3.143), respectively)

$\sigma \cdot_Y C^+$	$\sigma \cdot_Y C^-$	C^+configuration	C^-configuration
3	-2	$C^+ \not\subset \sigma, \sigma \cdot_Y C^+ = 3$	$C^- \subset \sigma, \deg(N_{C^-/\sigma}) = 0$
		$C^+ \subset \sigma, \deg(N_{C^+/\sigma}) = -5$	$C^- \subset \sigma, \deg(N_{C^-/\sigma}) = 0$ $(*)$
1	0	$C^+ \not\subset \sigma, \sigma \cdot_Y C^+ = 1$	$C^- \not\subset \sigma, \sigma \cdot_Y C^- \sigma = 0$
		$C^+ \subset \sigma, \deg(N_{C^+/\sigma}) = -3$	$C^- \subset \sigma, \deg(N_{C^-/\sigma}) = -2$ $(*)$
0	1	$C^+ \not\subset \sigma, \sigma \cdot_Y C^+ = 0$	$C^- \not\subset \sigma, \sigma \cdot_Y C^- = 1$
		$C^+ \subset \sigma, \deg(N_{C^+/\sigma}) = -2$	$C^- \subset \sigma, \deg(N_{C^-/\sigma}) = -3$ $(*)$
$-p-2$	$p+3$	$C^+ \subset \sigma, \deg(N_{C^+/\sigma}) = p$	$C^- \not\subset \sigma, \sigma \cdot_Y C^- = p+3$
		$C^+ \subset \sigma, \deg(N_{C^+/\sigma}) = p$	$C^- \subset \sigma, \deg(N_{C^-/\sigma}) = -p-5$

(3.150)

Finally, in case C, the curve C^- has normal bundle $(1,-3)$. If $C^- \subset \sigma$ then the only wrapped configuration which gives negative intersections with the section is

$$\deg(N_{C^-/\sigma}) = 1 \;\Rightarrow\; C^- \cdot_Y \sigma = -3\,. \tag{3.151}$$

This generates the upper bound $\sigma \cdot_Y C^+ \leq 4$. The set of possible intersections are

$$(\sigma \cdot_Y C^+, \sigma \cdot_Y C^-) = (4,-3),\ (1,0),\ (0,1),\ (-p-2, p+3)\,. \tag{3.152}$$

Once again, the solutions for second and fourth set of intersections are the same as those given in A. Though the third set of intersections has appeared previously the solutions for this normal bundle case are more restricted and we will find only one solution.

C.1) $\sigma \cdot_Y C^+ = 4, \sigma \cdot_Y C^- = -3$

The two solutions to this set of intersection numbers both require $C^- \subset \sigma$ and $\deg(N_{C^-/\sigma}) = 1$. To obtain the correct intersection for C^+ with the section there are two possibilities:

(i) $C^+ \not\subset \sigma$

In addition to the two intersections C^+ has with the section through the intersection of C^+ and C^- two further intersections are required to satisfy the codimension one constraint (3.135).

(ii) $C^+ \subset \sigma$

The degree of the normal bundle $N_{C^+/\sigma}$ is fixed by the intersection $\sigma \cdot_Y C^+ = 4$ to be $\deg(N_{C^+/\sigma}) = -6$. This is a valid solution for

$$-1 \leq p \leq 4\,. \tag{3.153}$$

C.3) $\sigma \cdot_Y C^+ = 0, \sigma \cdot_Y C^- = 1$

This set of intersections has appeared in A and B however the configuration given by $C^+, C^- \subset \sigma$ and $\deg(N_{C^+/\sigma}) = -3, \deg(N_{C^-/\sigma}) = -2$ is not a valid solution here as $N_{C^-/\sigma}$ does not embed into $N_{C^-/Y} = \mathcal{O}(1) \oplus \mathcal{O}(-3)$. The only solution is given by $C^+, C^- \not\subset \sigma$ and $\sigma \cdot_Y C^- = 1$.

The full set of solutions for case C are (with ranges of p in the (*)'ed configurations constrained as in (3.153) and (3.143))

$\sigma \cdot_Y C^+$	$\sigma \cdot_Y C^-$	C^+configuration	C^-configuration
4	-3	$C^+ \not\subset \sigma, \sigma \cdot_Y C^+ = 4$	$C^- \subset \sigma, \deg(N_{C^-/\sigma}) = 1$
		$C^+ \subset \sigma, \deg(N_{C^+/\sigma}) = -6$	$C^- \subset \sigma, \deg(N_{C^-/\sigma}) = 1$ $(*)$
1	0	$C^+ \not\subset \sigma, \sigma \cdot_Y C^+ = 1$	$C^- \not\subset \sigma, \sigma \cdot_Y C^- = 0$
0	1	$C^+ \not\subset \sigma, \sigma \cdot_Y C^+ = 0$	$C^- \not\subset \sigma, \sigma \cdot_Y C^- = 1$
		$C^+ \subset \sigma, \deg(N_{C^+/\sigma}) = -2$	$C^- \subset \sigma, \deg(N_{C^-/\sigma}) = -3$ $(*)$
$-p-2$	$p+3$	$C^+ \subset \sigma, \deg(N_{C^+/\sigma}) = p$	$C^- \not\subset \sigma, \sigma \cdot_Y C^- = p+3$
		$C^+ \subset \sigma, \deg(N_{C^+/\sigma}) = p$	$C^- \subset \sigma, \deg(N_{C^-/\sigma}) = -p-5$

(3.154)

Compilation of Fibers and $U(1)$ Charges

The solutions for each case A−C are presented in table 3.5 where the intersection sets appear along the horizontal axis and the different normal bundles run along vertically. The I_2 fibers are labeled as follows:

- The components of the fiber coloured in red are those contained inside the section and the red numbers appearing next to these components denote the degree of the normal bundle of those components inside σ.
- Red dots on unwrapped fiber components correspond to transverse singlet intersections with σ. The red numbers next to a sequence of such dots denote the number of such transverse intersection points.

Not every set of $\sigma \cdot_Y C^\pm$ intersections can be realised in each case A−C. Where an intersection column has been left blank there is no configuration corresponding to that set of intersections with σ.

The $U(1)$ charges of singlets can be determined by combining configurations for σ_0 and σ_1 in each case A−C. As both sections intersect F_0 in codimension one the Shioda map,

C^+C^-	$\sigma\cdot C^+=-p-2$ $\sigma\cdot C^-=p+3$	$\sigma\cdot C^+=0$ $\sigma\cdot C^-=1$	$\sigma\cdot C^+=1$ $\sigma\cdot C^-=0$	$\sigma\cdot C^+=+2$ $\sigma\cdot C^-=-1$	$\sigma\cdot C^+=+3$ $\sigma\cdot C^-=-2$	$\sigma\cdot C^+=+4$ $\sigma\cdot C^-=-3$
A	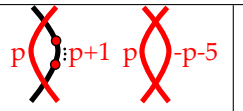	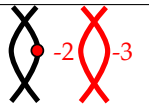	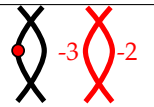	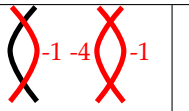		
B	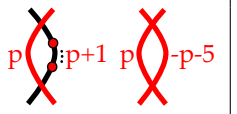	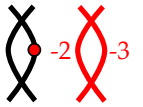	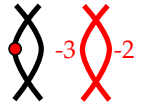		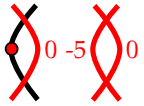	
C	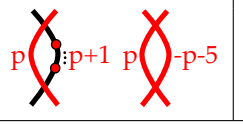	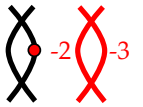				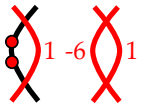

Table 3.5: Consistent wrapping configurations for $I_1 \to I_2$ for normal bundle cases A−C. The components in red are those contained inside the section with their normal bundle degrees in σ indicated by the red numbers adjacent to the component. Configurations where both components of the I_2 fiber are contained inside the section (excluding those appearing in the first column) are only valid for certain ranges of p, see main text for more details.

$S(\sigma_1)$, is given by

$$S(\sigma_1) = \sigma_1 - \sigma_0\,. \tag{3.155}$$

Singlet charges are obtained by computing $S(\sigma_1)\cdot_Y C^{\pm}$. The set of possible singlet charges and the associated I_2 fibers are shown in figure 3.17. The fibers along the horizontal (resp. vertical) axis, coloured in red (resp. blue), are for σ_1 (resp. σ_0). The entries $(a,-a)$ are the $U(1)$ charges obtained by combining configurations for σ_1 and σ_0. Only one representative has been chosen for each distinct set of intersections $\sigma\cdot_Y C^{\pm}$, wherefore there are more realisations of each charge than shown in the figure. The singlet charges which appear in each normal bundle pairing are:

$$U(1)\text{ charges of singlets in }\begin{cases} \text{A}\in\{0,\pm1,\pm2,\pm(p+2),\pm(p+3),\pm(p+4)\} \\ \text{B}\in\{0,\pm1,\pm2,\pm3,\pm(p+2),\pm(p+3),\pm(p+5)\} \\ \text{C}\in\{0,\pm1,\pm3,\pm4,\pm(p+2),\pm(p+3),\pm(p+6)\}\,. \end{cases} \tag{3.156}$$

The charges are dependent on p, appearing in (3.134), which defines the normal bundle of C^+.

Singlet configurations (I_2 fibers in the presence of an one additional rational section) with charges

$$S(\sigma_1)\cdot_Y C^- = \{-1,+1,+2\}\,, \tag{3.157}$$

have appeared in [91, 103, 97]. The zero-section in these configurations is holomorphic i.e. σ_0 does not contain curves in the fiber over codimension two. The range of possible

A	p:p+1			-1
C^+ C^-	$\sigma_1.C^+$=-p-2 $\sigma_1.C^-$=p+3	$\sigma_1.C^+$= 0 $\sigma_1.C^-$= +1	$\sigma_1.C^+$= +1 $\sigma_1.C^-$= 0	$\sigma_1.C^+$= +2 $\sigma_1.C^-$= -1
-1 $\sigma_0.C^+$= +2 $\sigma_0.C^-$= -1	(-p-4,p+4)	(-2,+2)	(-1,+1)	(0,0)
$\sigma_0.C^+$= +1 $\sigma_0.C^-$= 0	(-p-3,p+3)	(-1,+1)	(0,0)	(+1,-1)
$\sigma_0.C^+$= 0 $\sigma_0.C^-$= +1	(-p-2,p+2)	(0,0)	(+1,-1)	(+2,-2)
p:p+1 $\sigma_0.C^+$=-p-2 $\sigma_0.C^-$=p+3	(0,0)	(p+2,-p-2)	(p+3,-p-3)	(p+4,-p-4)

B	p:p+1			0
C^+ C^-	$\sigma_1.C^+$=-p-2 $\sigma_1.C^-$=p+3	$\sigma_1.C^+$= 0 $\sigma_1.C^-$= +1	$\sigma_1.C^+$= +1 $\sigma_1.C^-$= 0	$\sigma_1.C^+$= +3 $\sigma_1.C^-$= -2
0 $\sigma_0.C^+$= +3 $\sigma_0.C^-$= -2	(-p-5,p+5)	(-3,+3)	(-2,+2)	(0,0)
$\sigma_0.C^+$= +1 $\sigma_0.C^-$= 0	(-p-3,p+3)	(-1,+1)	(0,0)	(+2,-2)
$\sigma_0.C^+$= 0 $\sigma_0.C^-$= +1	(-p-2,p+2)	(0,0)	(+1,-1)	(+3,-3)
p:p+1 $\sigma_0.C^+$=-p-2 $\sigma_0.C^-$=p+3	(0,0)	(p+2,-p-2)	(p+3,-p-3)	(p+5,-p-5)

C	p:p+1			1
C^+ C^-	$\sigma_1.C^+$=-p-2 $\sigma_1.C^-$=p+3	$\sigma_1.C^+$= 0 $\sigma_1.C^-$= +1	$\sigma_1.C^+$= +1 $\sigma_1.C^-$= 0	$\sigma_1.C^+$= +4 $\sigma_1.C^-$= -3
1 $\sigma_0.C^+$= +4 $\sigma_0.C^-$= -3	(-p-6,p+6)	(-4,+4)	(-3,+3)	(0,0)
$\sigma_0.C^+$= +1 $\sigma_0.C^-$= 0	(-p-3,p+3)	(-1,+1)	(0,0)	(+3,-3)
$\sigma_0.C^+$= 0 $\sigma_0.C^-$= +1	(-p-2,p+2)	(0,0)	(+1,-1)	(+4,-4)
p:p+1 $\sigma_0.C^+$=-p-2 $\sigma_0.C^-$=p+3	(0,0)	(p+2,-p-2)	(p+3,-p-3)	(p+6,-p-6)

Figure 3.17: $U(1)$ charges of singlets for normal bundles cases A−C. Configurations for σ_1 (σ_0) are along the horizontal (vertical) axis and the charges are the pairs $(a, -a)$ in the grid. Only one representative has been chosen for each distinct set of intersections $\sigma \cdot_Y C^{\pm}$ therefore there are more realisations of each charge than shown.

singlet charges was extended in [100] where a singlet configuration with charge +3 was found. Comparing these fibers to those in figure 3.17, we find the same configurations in the following normal bundle cases:

Charge $S(\sigma_1)\cdot_Y C^-$	I_2 fiber	Realisation
-1		A
$+1$		A-C
$+2$		A-C when $p=-1$
$+3$		A when $p=-1$

(3.158)

Finally, we compare the singlet charges found above with those required for every $\bar{\mathbf{5}}_{q_1}$ and $\mathbf{5}_{q_2}$ in (3.101) to form a Yukawa coupling

$$\mathbf{5}_{q_1}\bar{\mathbf{5}}_{q_2}\mathbf{1}_{-q_1-q_2}\,. \tag{3.159}$$

Generically, in the geometry all such couplings will be present for base varieties of dimension ≥ 3 and correspond to codimension three enhancements to $SU(7)$, which will be discussed in detail in section 3.8. Using the set of $\bar{\mathbf{5}}$ charges in (3.101), the set of singlets, $\mathbf{1}_{-q_1-q_2}$, for each codimension one fiber in (3.60) is

$$U(1)\text{ charges of GUT singlets in }\begin{cases} I_5^{(01)} \in \{0,\pm1,\pm2,\pm3,\pm4,\pm5,\pm6\} \\ I_5^{(0|1)} \in \{0,\pm5,\pm10,\pm15,\pm20,\pm25\} \\ I_5^{(0||1)} \in \{0,\pm5,\pm10,\pm15,\pm20,\pm25\}\,. \end{cases} \tag{3.160}$$

Comparison (after multiplication by five) yields, that the singlet charges in (3.160) fall within the charges derived from analysing $I_1 \to I_2$ enhancements in (3.156). It would be interesting to analyse this further from the point of view of four-fold normal bundle consistencies at the Yukawa points.

3.7.3 Singlets in Four-folds

One of the criteria for the codimension two I_2 fiber is that one of the curves needs to be contractible. In the case of three-folds discussed in the last section, the relevant criterion goes back to Theorem 3.3.6. A similar result, which constrains the normal bundle of contractible curves in four-folds, to our knowledge, is not known. Nevertheless, we can consider a general types of I_2 fiber, and without imposing contractibility, determine the consistent section configurations and corresponding charges.

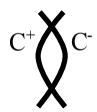 $\sigma_0, \sigma_1 \cdot_Y (C^+, C^-)$	 $(1,0)$	 $(0,1)$	 $(-r-2, r+3)$	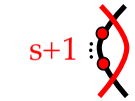 $(s+3, -s-2)$	 $(-r-2, r+3)$
 $(1,0)$	$(0,0)$	$(-1,+1)$	$(-r-3, r+3)$	$(s+2, -s-2)$	$(-r-3, r+3)$
 $(0,1)$	$(+1,-1)$	$(0,0)$	$(-r-2, r+2)$	$(s+3, -s-3)$	$(-r-2, r+2)$
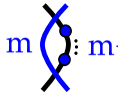 $(-m-2, m+3)$	$(m+3, -m-3)$	$(m+2, -m-2)$	$(-r+m, r-m)$	$(s+m+5, -s-m-5)$	$(-r+m, r-m)$
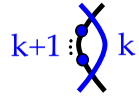 $(k+3, -k-2)$	$(-k-2, k+2)$	$(-k-3, k+3)$	$(-r-k-5, r+k+5)$	$(s-k, -s+k)$	$(-r-k-5, r+k+5)$
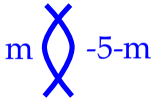 $(-m-2, m+3)$	$(m+3, -m-3)$	$(m+2, -m-2)$	$(-r+m, r-m)$	$(s+m+5, -s-m-5)$	$(-r+m, r-m)$

Table 3.6: Consistent wrapping configurations for $I_1 \to I_2$ in four-folds and $U(1)$ charges. Configurations for σ_1 (σ_0) are along the horizontal (vertical) axis and the charges are the pairs $(a, -a)$ in the grid. The components in red (blue) are those contained inside σ_1 (σ_0) with their normal bundle degrees in σ indicated by the red (blue) numbers adjacent to the component.

The result of this analysis is summarised in table 3.6. The normal bundle degrees $\deg(N_{C^\pm/\sigma})$ of curves $C^\pm$ that are wrapped by the sections in the I_2 fiber, represented by r, s, m and k in the table, have been left un-constrained, i.e. we do not impose that one of the curves in the I_2 fiber is contractible. The intersections of $C^\pm$ with the section are calculated using Corollary 3.3.4, the only input being the values of r, s, m and k. In the table, these intersections with σ_0 and σ_1 are shown below each fiber type, and the $U(1)$ charge is again computed using the Shioda map $S(\sigma_1) = \sigma_1 - \sigma_0$. It would be interesting to generalise the results of [124, 125] to four-folds in order to further constrain the normal bundles and thereby the $U(1)$ charge values in four-folds.

3.8 Codimension three Fibers and Yukawa Couplings

In elliptic Calabi–Yau four-folds there are codimension three points in the base of the fibration, above which the codimension two fibers can enhance further, i.e. again some of the rational curves become reducible. From an F-theory point of view, the fibers above such points in the base are of interest as they give rise to coupling of matter fields in Yukawa interactions.

3.8.1 Codimension three Fibers and Phases

The codimension three fibers for $SU(5)$ with $\overline{\mathbf{5}}$ and $\mathbf{10}$ matter were determined from the box graphs using mutual compatibility of the relative cones of effective curves in [70]. The Yukawa couplings $\mathbf{10} \times \mathbf{10} \times \mathbf{5}$ and $\overline{\mathbf{5}} \times \overline{\mathbf{5}} \times \mathbf{10}$ occur at codimension three loci, where the fiber enhances from the I_6 and I_1^* fibers, that realise the fundamental and anti-symmetric matter, to monodromy-reduced IV^* or I_2^* fibers, which correspond to a local enhancement of the symmetry to E_6 and $SO(12)$, respectively. Physically, the Yukawas can be thought of as generated by the splitting of matter curves into other matter curves, plus, potentially, roots [69].

Here we will focus on the coupling between singlets and two fundamentals: $\mathbf{5} \times \bar{\mathbf{5}} \times \mathbf{1}$. These are realised above codimension three loci with an $SU(7)$ enhancement. This is the simplest instance in which the fibers (without the presence of additional sections) are not standard Kodaira fibers in codimension three, but are monodromy-reduced, i.e. the fiber is not I_7, but remains I_6. However, if there is a suitable additional section, there is an enhancement to a full I_7 fiber [131, 71].

We will now explain how the box graphs can be used to determine the consistent codimension three fibers. The analysis works for general types of fibers, but we will concentrate

here on $SU(5)$ with $\overline{\mathbf{5}}$ matter, i.e. the phases and fibers shown in figure 3.4. As before, F_i are the rational curves associated to the simple roots of $SU(5)$. First consider two codimension two I_6 fibers, which are characterised by the splitting

$$F_i \to C_i^{T+} + C_i^{T-}\,, \qquad F_j \to C_j^{B+} + C_j^{B-}\,. \tag{3.161}$$

The superscripts Top and Bottom label the curves in the two I_6 fibers in codimension two. The combined phase is obtained by stacking the box graphs for each I_6 fiber on top of each other. Representation theoretically we are looking at the decomposition

$$\mathfrak{su}(7) \quad \to \quad \mathfrak{su}(5) \oplus \mathfrak{su}(2) \oplus \mathfrak{u}(1)\,. \tag{3.162}$$

Denote by $\widetilde{F}$ the curve associated to the simple root $\widetilde{\alpha}$ of the $\mathfrak{su}(2)$. Then in the combined box graph this acts between the two layers, from the bottom to the top layer, e.g.

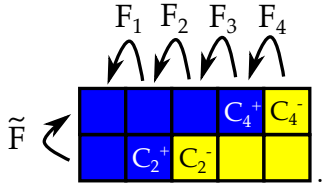

(3.163)

The combined box graphs need to satisfy both the flow rules for the $SU(5)$, as well as compatibility with the action of this additional root.

Let us first assume $i \neq j$. In this case, e.g. shown in figure 3.18, both F_i and F_j are reducible, and the extremal generators of the relative cone of curves are

$$C_i^{T+},\ C_i^{T-},\ C_j^{B+},\ C_j^{B-},\ F_k,\ k \neq i,j\,. \tag{3.164}$$

In particular $\widetilde{F}$ is not extremal. The resulting fiber is obtained applying similar rules to the standard box graph analysis, summarised in section 3.2 (for more details on how the fiber is determined from the graph we refer the reader to [70, 126, 128]) and exemplified in part (i) of figure 3.18.

For $i = j$, the phases of the two I_6 fibers agree, and the extremal generators are

$$C_i^{T-},\ C_j^{B+},\ \widetilde{F},\ F_k,\ k \neq i,j\,, \tag{3.165}$$

where $\widetilde{F}$ remains irreducible, and the curves in the I_6 fibers, which became reducible, split as follows

$$\begin{aligned} C_i^{T+} \quad &\to \quad C_i^{B+} + \widetilde{F} \\ C_j^{B-} \quad &\to \quad C_j^{T-} + \widetilde{F}\,. \end{aligned} \tag{3.166}$$

Note that this is the splitting from the I_6 Top and Bottom codimension two fibers respectively. The rational curves in the fiber in codimension three intersect again in an I_7 fiber, which is shown in part (ii) of figure 3.18.

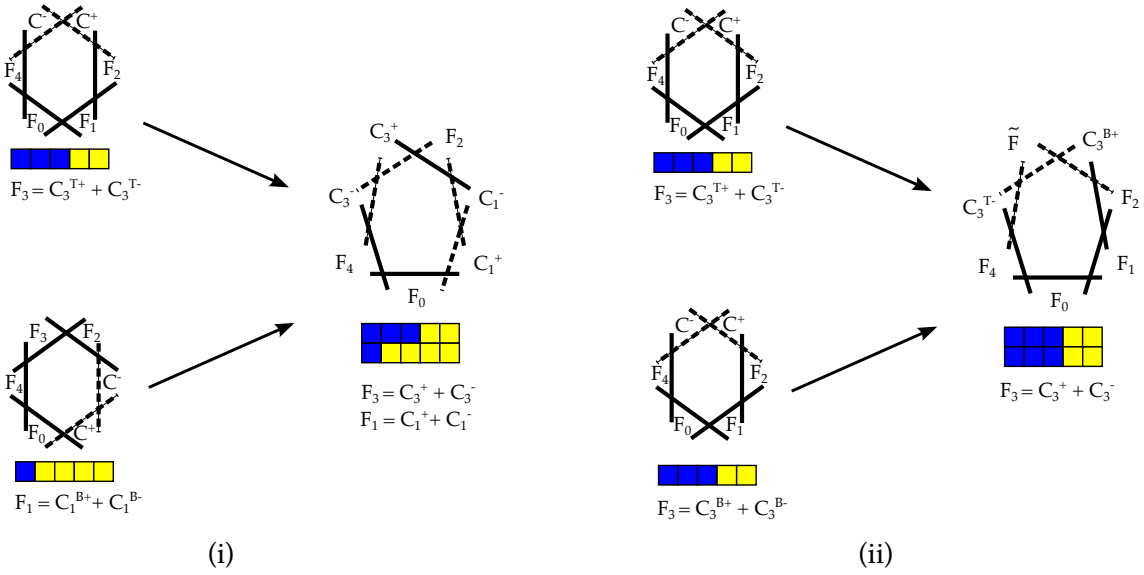

Figure 3.18: Construction of the fiber in codimension three, where two codimension two I_6 fibers in the phases/box graphs shown on the left, collide to give a fiber of type I_7 in codimension three. The box graph for the I_7 is shown on the right of each figure. Figure (i) shows the codimension three enhancement when the two I_6 fibers are in different phases/box graphs, whereas in (ii) they are in the same phase. Note that for each of these enhancements it is necessary to have at least one extra rational section.

Let us re-emphasise that in both these cases, it is paramount that the fiber has an additional rational section, as otherwise there is a monodromy reduction from I_7 to I_6.

3.8.2 Codimension three Fibers with Rational Sections

Like in the splitting from codimension one to two that we analysed in section 3.4.4, we require various conditions on the intersection numbers of the section σ with the fiber components to be retained, when passing from codimension two to three:

1. The section σ intersects the fiber as $\sigma \cdot_Y \text{Fiber} = 1$.

2. Let C be a rational curve in the fiber, which remains irreducible when passing from codimension two to codimension three, and let $S_C \not\subset \sigma$, i.e. matter surface obtained by fibering C over the matter locus is not contained in the section, but let C be contained in σ in codimension three. Then $\sigma \cdot_Y C$ needs to be preserved in codimension three.

3. If $S_C \subset \sigma$ in codimension two, and $C \to C^+ + C^-$ then by Corollary 3.3.4

$$\sigma \cdot_Y C = -4 - \deg(N_{C^+/\sigma}) - \deg(N_{C^-/\sigma})\,. \tag{3.167}$$

Note that, obviously, a curve that is contained in the codimension two fiber continues to be contained in the codimension three fiber to which the codimension two fiber degenerates. The compatibility between codimension two and three has to be imposed for *every* codimension two fiber whose codimension two locus in the base passes through the codimension three point in question (i.e. all the codimension two fibers that correspond to matter that participates in the Yukawa coupling).

Note also, that the constraints on the normal bundle derived for four-folds Y in section 3.3.3 need to be respected. The normal bundle of the rational curves in the fiber have to be such that they embed into the normal bundle $N_{C/Y}$. From Theorem 3.3.7 observe that the normal bundles of F_i in the four-fold Y are

$$N_{F_i/Y} = \mathcal{O} \oplus \mathcal{O} \oplus \mathcal{O}(-2)\,, \tag{3.168}$$

and the normal bundles of the curves $C_i^{\pm}$, obtained from the splitting $F_i \to C_i^+ + C_i^-$, which correspond to weights of the fundamental representation, are

$$N_{C_i^{\pm}/Y} = \mathcal{O} \oplus \mathcal{O}(-1) \oplus \mathcal{O}(-1)\,. \tag{3.169}$$

3.8.3 Charged Singlet Yukawas

We now consider the Yukawa couplings that are realised by codimension three enhancements to I_7 involving charged singlets, i.e. $\overline{\mathbf{5}} \times \mathbf{5} \times \mathbf{1}$ couplings. First consider the case of the two I_6 fibers in different phases. An example is shown in figure 3.19. Starting with an $I_5^{(0|1)}$ model at the far left in codimension one, the next two entries correspond to the codimension two fibers. The blue/red colored fibers indicate the rational curves that are contained in the sections σ_0 and σ_1, respectively. From figure 3.8 the configurations in codimension two, labeled (1) and (2), correspond to fundamental matter with $U(1)$ charges

$$q(\overline{\mathbf{5}}^{(1)}) = +11\,, \qquad q(\overline{\mathbf{5}}^{(2)}) = +1\,. \tag{3.170}$$

The codimension three fiber when these two collide can be determined by imposing the requirements in section 3.8.2. The compatibility conditions have to be satisfied for both of the two I_6 fibers enhancing to the I_7 fiber. For instance, consider the I_6 fiber (1). We can characterise the configuration by For instance, the configurations of the I_6 fibers (1)

and (2) can be characterised by

$$\begin{aligned}
(1): \quad & F_1, F_2, F_3 \subset \sigma_0 && \deg(N_{F_i/\sigma_0}) = -2 \\
& C_4^+ \subset \sigma_0 && \deg(N_{C_4^+/\sigma_0}) = -1 \\
& C_4^-, F_0 \not\subset \sigma_0 && \sigma_0 \cdot_Y C_4^- = \sigma_0 \cdot_Y F_0 = 1 \\
& F_0 \subset \sigma_1 && \deg(N_{F_0/\sigma_1}) = -2 \\
& C_4^- \subset \sigma_1 && \deg(N_{C_4^-/\sigma_1}) = -1 \\
& C_4^+, F_1 \not\subset \sigma_1 && \sigma_1 \cdot_Y C_4^+ = \sigma_1 \cdot_Y F_1 = 1 \\
(2): \quad & F_1 \subset \sigma_0 && \deg(N_{F_1/\sigma_0}) = -2 \\
& C_2^+ \subset \sigma_0 && \deg(N_{C_2^+/\sigma_0}) = -1 \\
& C_2^-, F_0 \not\subset \sigma_0 && \sigma_0 \cdot_Y C_2^- = \sigma_0 \cdot_Y F_0 = 1 \\
& C_2^+ \subset \sigma_1 && \deg(N_{C_2^+/\sigma_1}) = -1 \\
& C_2^-, F_1 \not\subset \sigma_1 && \sigma_1 \cdot_Y C_2^- = \sigma_1 \cdot_Y F_1 = 1\,.
\end{aligned} \tag{3.171}$$

The fibers split as determined by the box graphs, and applying the compatibility conditions on the sections in codimension three determines the fibers [14], e.g. it is clear that all the components that are contained in either of the codimension two fibers have to continue to be contained in the sections. Furthermore, imposing that the intersection numbers and normal bundles are consistent, results in the configuration shown in figure 3.19.

From the I_7 we can obtain the I_2 fiber and thereby the singlet that participates in the Yukawa coupling. As we consider two I_6 fibers in different phases $\widetilde{F}$ is not extremal, see (3.164) for the configuration in figure 3.19, but is given in terms of

$$\widetilde{F} \quad \to \quad C_4^+ + F_3 + C_2^-\,, \tag{3.172}$$

which can be read off from the box graph or directly from the fiber. In figure 3.164 the component $\widetilde{F}$ is shown, separated from its conjugate component, by the green cut through the I_7 fiber. The combination in equation (3.172) are uncharged under the GUT group $SU(5)$, i.e. geometrically

$$D_{F_i} \cdot_Y \widetilde{F} = 0\,, \qquad i = 0, \cdots, 4\,, \tag{3.173}$$

as required for a singlet, but intersects the sections as

$$\begin{aligned}
\sigma_0 \cdot_Y \widetilde{F} &= \sigma_0 \cdot_Y (C_4^+ + F_3 + C_2^-) = -1 + 0 + 1 = 0 \\
\sigma_1 \cdot_Y \widetilde{F} &= \sigma_1 \cdot_Y (C_4^+ + F_3 + C_2^-) = 1 + 0 + 1 = 2\,.
\end{aligned} \tag{3.174}$$

[14] Note that the codimension three fiber is not unique, but only unique in terms of the intersection numbers. This is similar to the codimension two fibers, where, for example, $\sigma \cdot_Y F = 1$ can be either realised in terms of a transverse intersection, or in terms of $F \subset \sigma$ with $\deg(N_{F/\sigma}) = -3$. These ambiguities however do not change the charges or, in the case of codimension three, the possible Yukawa couplings.

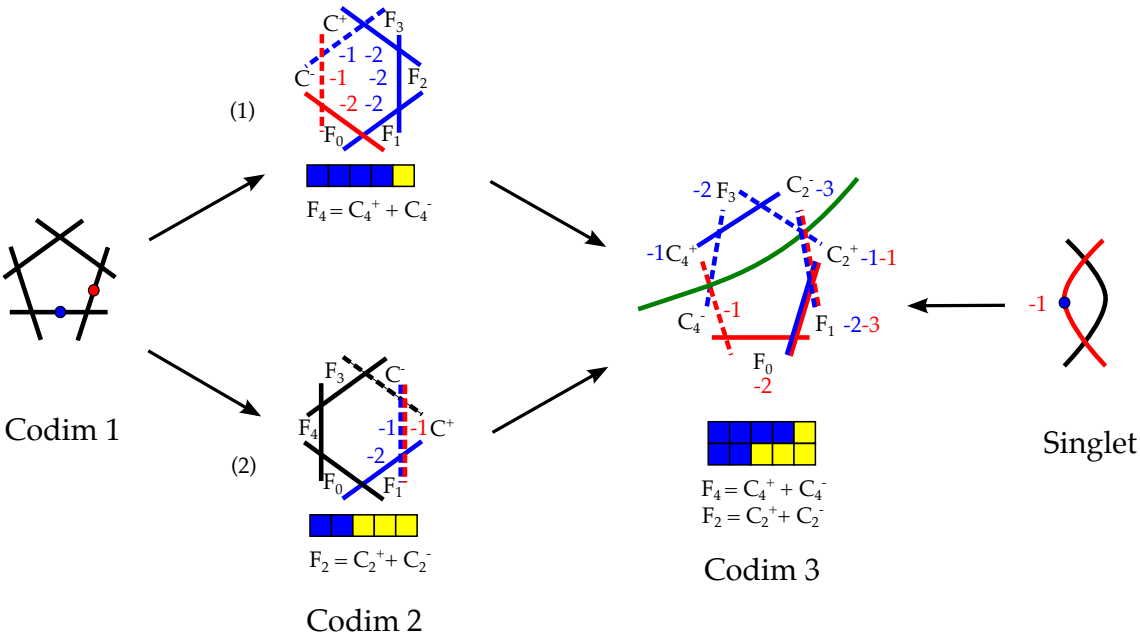

Figure 3.19: Example of a codimension three fiber with one additional rational section where the codimension two fibers are in different phases. Codimension one: I_5 fiber with two sections, σ_0 (blue) and σ_1 (red). Codimension two: I_6 fiber with sections as indicated (the configuration is described in (3.171)), corresponding to $\overline{\mathbf{5}}$ matter, with charge 11 and charge 1, respectively. Here the two I_6 fibers are in *different* phases. The curves, $C^{\pm}$, into which the F_i that become reducible in codimension two have split are shown by dotted lines. Colored fiber components correspond to rational curves that are contained in the respective sections. The numbers next to these indicate the degree of the normal bundle of these curves in the section. Codimension three: I_7 fiber with sections, as well as the corresponding box graph, obtained by stacking the box graphs associated to the codimension two fibers. Again, fiber components that are contained in the sections $\sigma_{0/1}$ are colored accordingly. The green line indicates where the I_7 fiber needs to be "cut" to determine the singlet that couples to the two fundamental matter multiplets. On the far right the I_2 fiber that realises this singlet is shown.

Likewise we can consider the conjugate field, given by the curve (so to speak the other half of the cut I_7 fiber)

$$\overline{\widetilde{F}} \quad \to \quad C_4^- + F_0 + F_1 + C_2^+ \,, \tag{3.175}$$

which intersects the sections as

$$\begin{aligned} \sigma_0 \cdot_Y \overline{\widetilde{F}} &= \sigma_0 \cdot_Y (C_4^- + F_0 + F_1 + C_2^+) = 1 + 1 + 0 - 1 = 1 \\ \sigma_1 \cdot_Y \overline{\widetilde{F}} &= \sigma_1 \cdot_Y (C_4^- + F_0 + F_1 + C_2^+) = -1 + 0 + 1 + -1 = -1 \,. \end{aligned} \tag{3.176}$$

Applying Shioda (and multiplying by 5 for the $SU(5)$ normalisation) we obtain that the charges of these singlets are indeed ∓ 10, as required for the coupling to the matter of charge ± 11 and ∓ 1, i.e. $\overline{\mathbf{5}}_{11} \times \mathbf{5}_{-1} \times \mathbf{1}_{-10}$.

Finally, let us briefly comment on the case when the two I_6 fibers are in the same phase, an example is shown in figure 3.20. The charges are

$$q(\overline{\mathbf{5}}^T) = +11 \qquad q(\overline{\mathbf{5}}^B) = -9 \,. \tag{3.177}$$

The splitting from codimension two to codimension three of the fiber components is that in (3.166) and part (ii) in figure 3.18, and $\tilde{F}$ is an irreducible, new fiber component. Again we impose ompatibility with the section configurations in codimensions two and three, as well as consistent normal bundle configurations. The resulting codimension three fiber is shown in figure 3.20. The singlet charge is obtained by intersecting $\widetilde{F}$ with the sections. Note, that $\widetilde{F} \cdot_Y D_{F_i} = 0$, which is consistent with this being the singlet, and

$$\begin{aligned} \sigma_0 \cdot_Y \widetilde{F} &= -2 \\ \sigma_1 \cdot_Y \widetilde{F} &= 2 \,. \end{aligned} \tag{3.178}$$

Likewise, the conjugate field is

$$\overline{\widetilde{F}} \quad \to \quad C_4^{B+} + F_3 + F_2 + F_1 + F_0 + C_4^{T-} \tag{3.179}$$

and

$$\begin{aligned} \sigma_0 \cdot_Y \overline{\widetilde{F}} &= 3 \\ \sigma_1 \cdot_Y \overline{\widetilde{F}} &= -1 \,. \end{aligned} \tag{3.180}$$

The associated I_2 fiber, which realises these intersections, is shown in figure 3.20, and matches the required charge of 20 from (3.177), such that the coupling $\overline{\mathbf{5}}_{-9}\mathbf{5}_{-11}\mathbf{1}_{20}$ is uncharged.

3.9 Multiple $U(1)$s and Higgsing

The analysis shown in the preceding sections has been for a single additional rational section of the elliptic fibration, which generates one $U(1)$ symmetry. This can be extended

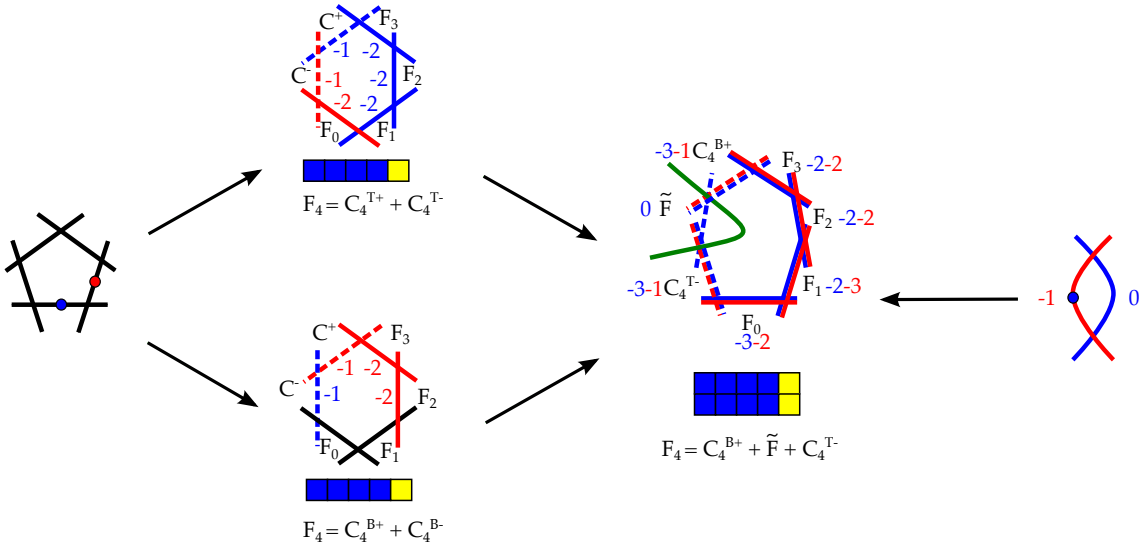

Figure 3.20: Example of a codimension three fiber with one additional rational section, where the codimension two fibers are in the same phase. The matter corresponds to charge $+11$ (T) and charge -9 (B) $\overline{\mathbf{5}}$ matter and a singlet of charge 20. The notation is as in figure 3.19.

to the case of elliptic fibrations with multiple rational sections, which generates multiple $U(1)$ symmetries. Furthermore, based on the classification of singlets, we can consider the possible Higgsings of the abelian symmetry to discrete subgroups. The case of partial Higgsing of multiple $U(1)$s is left for future work.

3.9.1 Multiple $U(1)$s and Rational Sections

The set of rational sections, σ_α, in an elliptic fibration generate the Mordell–Weil group, which is a finitely generated abelian group

$$\mathbb{Z}^r \oplus \Gamma\,, \tag{3.181}$$

where r is the number of rational sections in the fibration and Γ is the discrete part of the Mordell–Weil group, which we do not consider here. The zero-section σ_0 is the origin of the Mordell–Weil group, and σ_α, $\alpha = 1, \cdots, r$, are the generators of the free part.

The key point to note is that our analysis for one rational section applies independently to each generator of the free part of the Mordell–Weil group. The set of configurations for each section in an $I_k \to I_{k+1}$ enhancement is therefore just given by those in figures 3.10 and 3.11, where the section, σ_α, is taken to intersect F_{i_α} in codimension one. One can then construct the Shioda map, $S(\sigma_\alpha)$ for each section, which defines the generator of the abelian gauge factor $U(1)_\alpha$. Let us consider an example with two additional rational sections, σ_1 and σ_2, where the codimension one fiber type is $I_5^{(0|1||2)}$, as depicted in figure

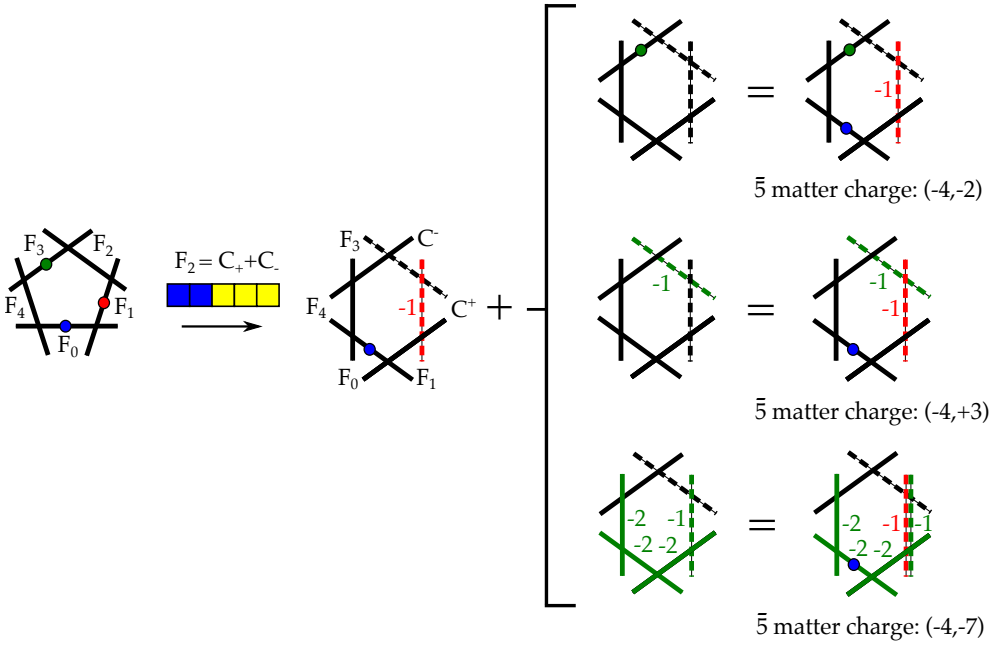

Figure 3.21: Example set of $\bar{\mathbf{5}}$ charges for an $I_5^{(0|1||2)}$ model in the phase where F_2 splits. The sections $\sigma_0/\sigma_1/\sigma_2$ are colored blue/red/green. The configurations for σ_0 and σ_1 are fixed to give charge -4 under $U(1)_1$. Combining this with the possible configurations for σ_2 gives the set of charges under $U(1)_2$.

3.21. For each phase, the possible charges for $\bar{\mathbf{5}}$ matter under $U(1)_1$, are given in figure 3.8 (modulo the fully wrapped configurations). To each of these one can overlay a configuration for σ_2 in the same phase and compute the charge under $U(1)_2$ by intersection $C^{\pm}$ with

$$S(\sigma_2) = 5\sigma_2 - 5\sigma_0 + 2D_{F_1} + 4D_{F_2} + 6D_{F_3} + 3D_{F_4}\,. \tag{3.182}$$

Further, consider σ_1 such that $q_{\bar{\mathbf{5}}} = -4$ in the phase where F_2 splits. This is shown in figure 3.21. This configuration can be combined with any one of the three possible configurations for σ_2, each of which gives a different charge under $U(1)_2$. Repeating this for every configuration in all phases gives the full set of charges for this codimension one fiber. Following this procedure we determine all possible combinations, and it can be shown that all known explicit realisations of models with multiple $U(1)$ factors form a subclass of the models obtained here.

3.9.2 Higgsing and Discrete Symmetries

In section 3.7 the set of possible codimension two I_2 fibers with rational sections were determined along with the corresponding singlet charges. One application of this result is to use such $U(1)$ charged singlets to Higgs the $U(1)$ symmetry to a discrete subgroup

$\mathbb{Z}_q$. Examples of such Higgsing have recently been considered in [79–81][15] for $q = 2, 3$. Though Higgsing different singlet configurations of the same charge leads to the same discrete symmetry in the F-theory compactification, this was shown not to be the case upon the circle reduction to M-theory. This can be seen field theoretically by reducing F-theory in 6d along an S^1 to M-theory in 5d [77–81]. Turning on a vacuum expectation value for the Higgs field, S_q, of charge q breaks the $U(1)$ in F-theory to $\mathbb{Z}_q$. Starting in 6d, and compactifying to 5d on a circle, the masses of the Kaluza–Klein modes are labeled by the charge q, the mode number (or KK-charge) n and the Wilson line ξ along the circle

$$m_n^q = |q\xi + n| \,. \tag{3.183}$$

The massless spectrum depends on the value of ξ and for $\xi = k/q$ with integral k the KK-charge $n = -k$ becomes massless. There are q distinct values for the Wilson line, modulo the action of $SL_2\mathbb{Z}$, which correspond to distinct M-theory vacua, between which the Tate-Shafarevich group acts [75].

Equipped with the set of I_2 fibers and their corresponding charges, given in figure 3.17, we can now consider the Higgsing with more general singlet configurations, with charges beyond $q = 2, 3$. Furthermore, it is possible to determine for a fixed singlet charge q, the fibers which realise the q different choices of 5d Higgs fields. Note that the KK-charge n is computed by intersecting with the zero-section

$$\sigma_0 \cdot_Y C^{\pm} = n^{\pm} \,. \tag{3.184}$$

That is, we look for configurations where C^+, or C^-, has intersections with σ_0 within the set

$$n^{\pm} = \sigma_0 \cdot_Y C^{\pm} \in \{0, \cdots, q-1\} \bmod q \,. \tag{3.185}$$

The result is that for charges up to $q = 9$ it is always possible, by tuning the degree of the normal bundle of the curve C^+ in (3.134), to obtain curves in the I_2 fiber with the desired intersections with σ_0. It would be interesting to study how these configurations are related via flop transitions such as in the case of $q = 3$ studied in [81]. For charges $q \geq 10$ the set of KK-charges, which do not have a realisation grows with q and it would be interesting to explore how the other configurations could be realised.

3.10 Discussion and Outlook

In this chapter we determined the possible $U(1)$ charges of matter in F-theory compactifications to four and six dimensions, by classifying the possible configurations of rational

[15] Other discussions of discrete symmetries in F-theory compactifications without section (i.e. genus one fibrations) have appeared in [100, 75–78]

sections in codimension two fibers. Our analysis for charged matter in the fundamental and anti-symmetric representations of $SU(n)$ in sections 3.4 and 3.5 holds for both Calabi–Yau three- and four-folds. The main inputs were the classification result of codimension two fibers in [70] as well as constraints on rational curves and their normal bundles in Calabi–Yau varieties, as discussed in section 3.3. There are various exciting directions for future research.

- Building complete models:
  In our analysis we did not discuss constraints from charged matter Yukawa couplings, only couplings between fundamental matter and singlets. It would be interesting to see whether codimension three constraints will provide further conditions as to how various codimension two fiber types can co-exist in a given model. The codimension three fibers and possible Coulomb phases without additional sections were derived already in [65, 70] and it would be interesting to generalise this to models with rational sections. Clearly further constraints that would select subsets of compatible codimension two fibers would also be of interest for model building, and could play an important role for a systematic study of the phenomenology similar to [104,106,132].

- Explicit realisations:
  The charges and fibers in explicitly known fibrations with various numbers of abelian factors [91–103, 76, 107, 108], as well as the matter charges in the singlet-extended E_8 model [105], form a strict subset of the fibers that we have found in the present thesis. It would be extremely interesting to determine realisations for the new fiber types, including the singlets that we classified in section 3.7.

- Flops:
  Our classification assumes that the section, which is a divisor in the Calabi–Yau variety, is smooth. We have observed in section 3.6 that, by flopping codimension two fibers with certain section configurations, the resulting fiber has a section which self-intersects in a curve in the fiber, and is thus no longer smooth. It would be very interesting to study such flops concretely, to determine the complete flop chain when the allowed configurations include such singular sections. It would also be interesting to study the flops for the I_2 fibers realising different KK-charges for the singlets, generalizing the analysis for charge 3 singlets in [81].

- Singlets:
  Unlike the charged matter, the analysis for the classification of singlets in section 3.7 is comprehensive only for Calabi–Yau three-folds, as we impose that one of the curves in the I_2 fiber should be contractible. A similar criterion for contractibility

for higher-dimensional Calabi–Yau varieties is not known to us, however we have determined all possible codimension two I_2 fibers with rational section, without necessarily requiring contractibility of the curves, in table 3.6. It would be interesting to determine a contractibility criterion on the normal bundle of rational curves in four-folds and to thereby constrain the singlet configurations in table 3.6 to the allowed set in four-folds. Note that no such disclaimer holds for the charged matter in sections 3.4 and 3.5, which do not rely on imposing any contractibility on the curves, and our results hold for codimension two in three- and four-folds alike.

- Higgsing and discrete groups:
  We determined the singlet fibers for $U(1)$ charges up until $q = 9$, including realisations for each KK-charge. This allows a comprehensive study of discrete symmetries by giving vacuum expectation values to these singlets, and it would be interesting to determine the effects on the low energy theories, for instance like in [74].

Chapter 4

Froggatt–Nielsen meets Mordell–Weil: A Phenomenological Survey of Global F-theory GUTs with $U(1)$s

4.1 Introduction

Remarkable progress in the construction of global F-theory compactifications in recent years has resulted in both conceptual and technical advances. After the initial surge in particle physics explorations of local F-theory Grand Unified Theories, the study of phenomenological implications was somewhat side-stepped in recent advances in global model building.

Global models have in particular seen much progress in view of a comprehensive understanding of F-theory vacua – both in terms of the base as well as the fiber geometry. In view of this, it is timely to conduct a survey of 4d F-theory vacua and their phenomenological viability. The goal of this chapter is to provide such an analysis, by imposing the most stringent phenomenological requirements upon the F-theory compactifications with additional $U(1)$ symmetries and their 4d effective theories, in particular an exotic-free Minimal Supersymmetric Standard Model (MSSM) spectrum, absence of dangerous couplings, such as proton decay operators, as well as consistent flavour physics generated by a Froggatt–Nielsen mechanism.

Central to both guaranteeing the absence of dangerous couplings and the applicability of a Froggatt–Nielsen mechanism is the presence abelian gauge symmetries. One of the string theoretic inputs in our analysis is the classification of $U(1)$ charges in $SU(5)$ F-theory GUTs, which was recently performed in [32]. This classification result utilises general

insights from codimension two fibers in [70], which realise the matter fields, and consistency of rational sections, which give rise to $U(1)$ gauge potentials. The one assumption in this classification is that the rational sections are smooth. The resulting analysis does not provide a constructive way of obtaining the elliptic fibrations, but gives a classification of all consistent fibers with rational sections, which in turn determines the set of matter $U(1)$ charges. It reproduces all charges known to exist in explicit geometric constructions based on hypersurfaces and complete intersections [101–103, 91–98, 107, 108, 99, 100, 76, 105, 133], but the set of possible charges from this classification is strictly larger than the ones arising from known geometries. This über-set obtained in [32] contains all charges that can potentially arise in global F-theory compactifications, under the assumption of smooth rational sections, and will be referred to as *F-theoretic* $U(1)$ *charges*.

A second constraining factor in F-theory GUT model building is the requirement of cancellation of anomalies that arise in the context of GUT breaking via hypercharge flux [87, 84, 45], which to date is the only known mechanism to break the GUT group in F-theory without immediately introducing exotics, such as is the case for Wilson line breaking [84, 85]. In the presence of additional $U(1)$ symmetries, hypercharge flux induces a chiral spectrum, which can be anomalous. The MSSM-$U(1)$ mixed anomalies were determined in [134, 135, 104, 136] and form a stringent constraint on the matter spectra and associated $U(1)$ charges. It is worth noting, that none of the models with charges in known geometric constructions solve these anomaly constraints without introducing exotics or dangerous proton decay operators[1]. However in the F-theory charge set obtained in [32] we do find solutions, including models with realistic flavour physics. One of the goals of this chapter is to identify these phenomenologically sound models, provide the corresponding charge patterns as well as fiber types, and thereby give guidance towards their geometric construction.

Before diving into a summary of the results of our analysis, we begin with a brief overview of F-theory phenomenology, in particular in view of flavour physics, which will play a key role in our analysis. The most promising particle physics results were thus far obtained in local F-theory GUTs and their associated spectral cover models, i.e. 4d supersymmetric GUTs obtained from compactifications of the 7-brane effective theory on a 4-cycle, that is embedded in a Calabi–Yau four-fold. Proton decay was studied in the context of local spectral cover models in [137, 138, 134, 139, 104, 106]. The anomalies of [134, 135, 104, 136] in conjunction with constraints on proton decay operators were surveyed in [104, 106] and in particular it was shown that in local spectral cover models, the anomalies were in conflict

[1] We will determine a new class of elliptic fibrations, which do in fact solve the anomalies and suppress the couplings of dangerous operators. This will be discussed in section 4.7.2. However these models are not amenable for an FN-type generation of flavour textures.

with $U(1)$ symmetries required for suppression of dimension five proton decay operators. The only way to consistently combine these two effects was to allow for exotics.

Flavour in local F-theory models has a long history starting with the initial exciting insight that the top Yukawa coupling is generated at order one at a local E_6 enhancement point [30, 31, 45, 140] and furthermore refined developments regarding corrections to the leading order Yukawa matrices [141–156], see [157, 158] for reviews of various particle physics implications of F-theory models. Local flavour models have undergone various stages of accurateness. The present status is that world-volume gauge fluxes do not lead to any corrections at all, but non-commutative fluxes in combination with non-perturbative effects can potentially give rise to suitable corrections. Froggatt–Nielsen models in local F-theory models were studied comprehensively in [159], however it was shown that unless one imposes by hand an R-parity, the local models universally suffer from regeneration of dangerous couplings. Clearly, global constraints, such as the type of $U(1)$ charges, fluxes and most likely the base geometry provide an additional set of constraints. The local models, by now are understood to be incomplete in that they do not seem to give rise to all possible $U(1)$ symmetries that can be constructed globally – this holds true for the geometrically realised charges, and even more so for the charge classification in [32]. This leads then to the question whether global models can more successfully implement these phenomenological constraints, and whether there are any distinct features in such models.

Phenomenological studies of global models have been rather scarce. The toric top-models were shown not to give rise to appealing flavour models and a stable proton [132]. As an alternative to GUTs, recent work has considered direct construction of the MSSM in F-theory [160–162], which however requires further careful analysis of the phenomenology. In this chapter we will assess the question of phenomenological implications of the $U(1)$ symmetries in F-theory based on the über-set obtained in [32], in conjunction with consistency requirements such as anomalies, and provide some insights into how to construct the relevant geometries.

Overview of Results and Search Strategy

To give the reader an overview of the results, we now summarise our framework and constraints, and provide pointers to where these are found in the main text of the chapter. The setups we consider are $SU(5)$ GUTs with hypercharge flux GUT breaking in F-theory compactification on an elliptically fibered Calabi–Yau four-fold. In addition, the following consistency requirements are imposed:

1. Exact MSSM spectrum and absence of anomalies (A1.)−(A5.) listed in (4.3)−(4.8).

2. $U(1)$ charges within the classification of [32] as summarised in (4.34).
3. $U(1)$ symmetries forbid all couplings (C1.)−(C7.) listed in (4.9)−(4.15).
4. $U(1)$ symmetries are compatible with one generation top Yukawa coupling.
5. Froggatt–Nielsen (FN) mechanism to generate remaining Yukawa textures for both quarks and leptons, by giving vevs to $U(1)$-charged GUT singlets without getting in conflict with the constraints (C1.)−(C7.).

A more detailed exposition of these conditions can be found in section 4.2. The survey is organised by number of $U(1)$ symmetries, number of $\mathbf{10}$ and $\bar{\mathbf{5}}$ representations, $\mathcal{N}_{\mathbf{10}}$ and $\mathcal{N}_{\bar{\mathbf{5}}}$, respectively. The models with a single $U(1)$ generically do not allow for very interesting flavour physics, without further input, such as non-perturbative effects, going beyond an FN-type mechanism. For $\mathcal{N}_{\mathbf{10}} = 1$ there is exactly one solution, which satisfies all anomaly and (C1.)–(C7.) constraints, given by I.1.4.a in table 4.1. All other models for any $\mathcal{N}_{\bar{\mathbf{5}}}$ regenerate dangerous couplings at the same order as Yukawa couplings, or include exotics (for high enough number of matter multiplets).

Models with two additional $U(1)$ symmetries allow for a more interesting solution space. We find a large set of solutions to the constraints, and focus on two subclasses: either the models satisfy conditions 1.−5., or they satisfy 1.−4., but have a geometric realisation. The models satisfying 1.−5., which will be referred to as *F-theoretic FN-models*, are discussed in section 4.5, and their spectra are summarised in tables 4.4 and 4.5. These models generate known Yukawa textures for the quarks, and furthermore provide realistic lepton and neutrino sectors. The matter charges of these solutions are within the set of F-theory $U(1)$ charges, however we do not yet know of an explicit construction. Nevertheless, to guide such geometric endeavours, we summarise the fiber types of these models in section 4.7.3.

The second subclass of two $U(1)$ models satisfy 1.−4., but not 5., i.e. do not allow for a realistic FN-mechanism. However, they have the advantage that we can construct the corresponding geometries:

$\widetilde{5}$. Geometric construction in terms explicit realisation of the elliptic fiber.

The existence of such global solutions to the anomalies and constraints on couplings is in stark contrast to local models, where there are no solutions satisfying all the conditions 1.−4. (with 2. modified to mean local spectral cover $U(1)$s). This class of global models are discussed in section 4.4 and their geometric realisation is given in section 4.7.2.

4.2 Constraints

This section provides an overview of all the constraints, and outlines the scope and strategy of our search. The setup in the following will be $SU(5)$ supersymmetric GUTs, with additional $U(1)$ symmetries with a realisation in F-theory compactifications on Calabi–Yau four-folds.

The first type of conditions arise from basic consistency of the 4d effective theories, namely an *exotic-free* MSSM spectrum and superpotential couplings, as well as absence of dangerous couplings that render the models inconsistent, which arise for instance through proton decay and R-parity violation. Throughout this chapter we will impose that suppressions of couplings will be administered through additional $U(1)$ symmetries, which will be one of the F-theoretic inputs into the models. Additional phenomenological requirements arise from flavour constraints. There is somewhat more flexibility in how the flavour hierarchies are engineered, and we will do a systematic analysis including flavour considerations using Froggatt–Nielsen type models in section 4.5.

The second type of constraints are specific to the class of theories, namely GUTs with a UV completion within F-theory. Here, one class of constraints arise from the GUT breaking, which in F-theory can be realised in terms of hypercharge flux breaking, i.e. non-trivial flux in the direction of the $U(1)_Y$ [84, 45]. In addition to imposing geometric conditions on the class of this background flux[2], if the model has in addition abelian symmetries, the mixed MSSM-$U(1)$ anomalies need to be cancelled [134, 135, 104, 136]. The second class of F-theoretic constraints is the type of $U(1)$ symmetries. In the recent work [32], constraints on these have been determined. The combination of F-theoretic $U(1)$ charges and the hypercharge flux induced anomalies result in additional constraints on the possible $U(1)$ charges and distributions of the matter fields. In the following we will discuss both classes of constraints in detail.

4.2.1 MSSM Spectrum and Anomalies

We consider $\mathcal{N} = 1$ supersymmetric GUTs with $SU(5)$ gauge group and matter in the $\mathbf{10}$ and $\bar{\mathbf{5}}$ representation. The Higgs doublets of the MSSM arise from fundamental and anti-fundamental representations of the $SU(5)$. In F-theory the GUT multiplets are geometrically localised on complex curves, so-called matter curves inside a 4-cycle S_{GUT},

[2]The requirement is that it is topologically trivial as a two-form in the Calabi–Yau, but non-trivial on the 4-cycle that realises the GUT theory. Examples of geometries realising such classes are known see e.g. [163, 164]. However constructions of the hypercharge flux in terms of an M-theory G_4 flux is thus far been elusive, although recent progress was made in [165] for the $U(1)$-restricted Weierstrass model of [101]. Extending this work to models with rational sections would be of vital importance.

which is wrapped by 7-branes in F-theory. The low energy theory on the 7-brane realises the gauge degrees of freedom. Chirality is induced by G_4-flux, and will be labeled by M_a and M_i for **10** and $\bar{\mathbf{5}}$ matter. GUT breaking is achieved by non-trivial flux in the $U(1)_Y$ direction, $\langle F_Y \rangle$. This lifts both the XY bosons of the gauge group $SU(5)$, as well as ensures that the Higgs triplets are massive. The restrictions of the hypercharge flux on the **10** and $\bar{\mathbf{5}}$ matter curves will be referred to in terms of integers N_a and N_i, respectively.

In summary the matter content of the $SU(5)$ GUT, with M chiral generations and restriction of hypercharge flux N is parametrised as follows:

$SU(5)$ representation	MSSM representation	Particle	Chirality
$\mathbf{10}_a$	$(\mathbf{3},\mathbf{2})_{1/6}$	Q	M_a
	$(\bar{\mathbf{3}},\mathbf{1})_{-2/3}$	$\bar{u}$	$M_a - N_a$
	$(\mathbf{1},\mathbf{1})_{1}$	$\bar{e}$	$M_a + N_a$
$\bar{\mathbf{5}}_i$	$(\bar{\mathbf{3}},\mathbf{1})_{1/3}$	$\bar{d}$	M_i
	$(\bar{\mathbf{1}},\mathbf{2})_{-1/2}$	L	$M_i + N_i$

(4.1)

The integers M and N have to satisfy basic requirements of realising the exact MSSM spectrum. In this chapter we will in particular impose that the spectra are free from exotics. In addition to placing constraints on the values of M and N, the absence of exotics places a bound on the number $\mathcal{N}$ of distinctly charged **10** and $\bar{\mathbf{5}}$,

$$\begin{aligned} \mathcal{N}_{\mathbf{10}} &\leq 3 \\ \mathcal{N}_{\bar{\mathbf{5}}} &\leq 8\,. \end{aligned} \tag{4.2}$$

To derive these bounds, note that if we were to consider more than three **10**s then some of these must have $M_a = 0$ as there are only three generations of left-handed quarks. Allowing a non-zero restriction of hypercharge flux over these allows the presence of either a right-handed quark or lepton with the wrong chirality for the MSSM spectrum, which results in the presence of exotics. Likewise, the maximum number of $\bar{\mathbf{5}}$s is given by the sum of three generations of left-handed leptons and right-handed quarks, in addition to H_u and H_d.

In addition to the GUT gauge symmetry, we require additional abelian gauge factors, $U(1)_\alpha$, $\alpha = 1, \ldots, r$, under which the $SU(5)$ representations $\mathbf{10}_a$ and $\bar{\mathbf{5}}_i$ carry charges q_a^α and q_i^α, respectively. The type of $U(1)$ charges are determined in terms of the F-theory geometry and will be the subject of section 4.2.4. The combined system of F_Y hypercharge flux breaking and additional $U(1)$ symmetries implies that there can potentially be mixed MSSM-$U(1)$ anomalies.

Anomaly cancellation and the requirement of three generations imply the following set of constraints on the chiralities M, hypercharge flux restriction N and charges q^α – all sums

$\sum_{a=1}^{\mathcal{N}_{\mathbf{10}}}$ are over **10** representations, $\sum_{i=1}^{\mathcal{N}_{\bar{\mathbf{5}}}}$ over $\bar{\mathbf{5}}$s, with $\mathcal{N}_{\mathbf{R}}$ corresponding to the number of matter multiplets in the representation $\mathbf{R}$ with distinct $U(1)$ charge:

(A1.) MSSM anomalies

$$\sum_i M_i = \sum_a M_a \,. \tag{4.3}$$

(A2.) Mixed $U(1)_Y$-MSSM anomalies [134, 135, 104]

$$\sum_i q_i^\alpha N_i + \sum_a q_a^\alpha N_a = 0 \,, \qquad \alpha = 1, \ldots, r \,. \tag{4.4}$$

(A3.) Mixed $U(1)_Y$-$U(1)_\alpha$-$U(1)_\beta$ anomalies [136]

$$3\sum_a q_a^\alpha q_a^\beta N_a + \sum_i q_i^\alpha q_i^\beta N_i = 0 \,, \qquad \alpha, \beta = 1, \ldots, r \,. \tag{4.5}$$

(A4.) Three generations of quarks and leptons:

$$\sum_a M_a = \sum_i M_i = 3 \,. \tag{4.6}$$

(A5.) Absence of exotics:

$$\sum_a N_a = \sum_i N_i = 0 \,. \tag{4.7}$$

(A5.) One pair of Higgs doublets:

$$\sum_i |M_i + N_i| = 5 \,. \tag{4.8}$$

The set of constraints (A1.)−(A5.) will be strictly imposed on each model, as a minimal requirement for realistic 4d physics. Note that we have not as yet imposed any Yukawa couplings – which Yukawas will be required to be compatible with the $U(1)$ charges will be discussed in section 4.2.3. We now turn to additional conditions on the $U(1)$ charges, on top of the anomaly constraints, which will ensure absence of dangerous couplings, such as proton decay.

4.2.2 Proton Decay, μ-Term and R-parity Violation

Rapid proton decay and R-parity violation (RPV) can cause supersymmetric GUTs to become phenomenologically unfit. In this thesis we will utilise $U(1)$ symmetries to forbid these couplings. The $U(1)$ symmetries are broken, at a higher scale and for some of these couplings we will require that they are not regenerated, e.g. by giving vevs to $U(1)$-charged singlets.

Summary of Dangerous Couplings

Let us first summarise the various problematic couplings and then discuss the bounds on their suppression – $i, j, \cdots$ and $a, b, \cdots$ label matter representations, whereas $I, J, \cdots = 1, 2, 3$ and $A, B, \cdots = 1, 2, 3$ label generations:

(C1.) μ-term:

$$\mu \mathbf{5}_{H_u} \bar{\mathbf{5}}_{H_d} \tag{4.9}$$

(C2.) Dimension five proton decay:

$$\delta^{(5)}_{abci} \mathbf{10}_a \mathbf{10}_b \mathbf{10}_c \bar{\mathbf{5}}_i \tag{4.10}$$

(C3.) Bilinear lepton number violating superpotential coupling:

$$\beta_i \bar{\mathbf{5}}_i \mathbf{5}_{H_u} \supset \beta_I L_I H_u \tag{4.11}$$

(C4.) Dimension four proton decay:

$$\lambda^{(4)}_{ija} \bar{\mathbf{5}}_i \bar{\mathbf{5}}_j \mathbf{10}_a \tag{4.12}$$

(C5.) Tri-linear lepton number violating Kähler potential couplings:

$$\kappa_{abi} \mathbf{10}_a \mathbf{10}_b \bar{\mathbf{5}}^\dagger_i \supset \kappa_{ABI} Q_A \bar{u}_B L^\dagger_I \tag{4.13}$$

(C6.) Dimension five lepton violating superpotential coupling:

$$\gamma_i \bar{\mathbf{5}}_i \bar{\mathbf{5}}_{H_d} \mathbf{5}_{H_u} \mathbf{5}_{H_u} \supset \gamma_I L_I H_d H_u H_u \tag{4.14}$$

(C7.) Dimension five lepton violating Kähler potential coupling:

$$\rho_a \bar{\mathbf{5}}_{H_d} \mathbf{5}^\dagger_{H_u} \mathbf{10}_a \supset \rho_A H_d H^\dagger_u \bar{e}_A \tag{4.15}$$

We require these couplings to be absent at leading order. Furthermore, if a Yukawa matrix element is generated by a singlet vev, we require that these operators do not re-appear with the same singlet suppression. In the case that multiple singlet vevs are required to generate a certain forbidden coupling, we study in detail whether the suppression is within the bounds that we summarise below. This occurs frequently in our analysis for dimension four and five proton decay operators.

Note that, if the top and bottom Yukawas are generated for all generations, then compatibility of the $U(1)$ symmetries with the Yukawas as well as absence of the μ-term (C1.)

implies (C2.) with opposite sign. However, this needs to be checked in addition, if not all Yukawas are generated perturbatively, as in most of the following models.

Imposing one top Yukawa coupling (for at least one generation, see (4.25)), as well as the absence of (C5.) implies that there cannot be $\bar{\mathbf{5}}$ matter on the same curve as H_u i.e.

$$Y^t,\ (C5.) \qquad \Rightarrow \qquad M_i = 0\,, \quad N_i = -1 \qquad i = H_u\,. \tag{4.16}$$

Likewise, imposing that the bottom Yukawa couplings are realised (either at leading order or regenerated by singlet vevs, see (4.26)), as well as the absence of the coupling (C4.) implies that there cannot be $\bar{\mathbf{5}}$ matter on the same curve as H_d, i.e.

$$Y^b,\ (C4.) \qquad \Rightarrow \qquad M_i = 0\,, \quad N_i = 1 \qquad i = H_d\,. \tag{4.17}$$

μ-Term

The μ-term is a supersymmetric Higgsino mass term. Radiative electroweak supersymmetry without much tuning in the MSSM requires μ to be around $O(100)$GeV. If this coupling is generated at tree-level, this cannot be achieved without a fair amount of fine-tuning and low-energy supersymmetry does not address the hierarchy problem. One way to avoid this problem is to forbid the μ-term at the high scale with a $U(1)$ symmetry – a so-called PQ $U(1)$ symmetry, i.e. the charge of the H_u and H_d do not add up to zero. The μ-term can then be generated by a coupling to a charged singlet S (or products of singlets) either via the superpotential or the Kähler potential. Concretely the μ-term can for instance be generated as follows

$$\frac{S^\dagger}{\Lambda} H_u H_d\,, \tag{4.18}$$

where the $\frac{\langle F_S\rangle}{\Lambda}$ then generically sets the scale of the μ-term, which is the Giudice-Masiero mechanism [166]. This type of μ-term has wide application in gravity [167,166] but also in gauge mediated supersymmetry breaking models, see for instance also in F-theory [168]. We shall not discuss the specific mechanisms of supersymmetry breaking in this thesis, as these are highly model dependent, thus deviating from the goal that we set out here, to be as comprehensive and general as possible. For our purposes we will impose that the coupling (C1.) is absent at tree-level.

Dimension 4 Proton Decay Operators

Dimensions four and five proton decay operators are highly constrained in GUT models, and one of the requirements in our search is the compatibility of the models with the

bound on the lifetime of the proton given by $\tau_p \geq 10^{34}$ years [15]. The dimension four proton decay operators originate in the coupling

$$\lambda^{(4)}_{ija}\overline{\mathbf{5}}_i\overline{\mathbf{5}}_j\mathbf{10}_a, \tag{4.19}$$

where the $\overline{\mathbf{5}}_i$ and $\mathbf{10}_a$ denote matter representations. This operator results in the following couplings,

$$\lambda^0_{IJA}L_IL_J\bar{e}_A + \lambda^1_{IJA}\bar{d}_IL_JQ_A + \lambda^2_{IJA}\bar{d}_I\bar{d}_J\bar{u}_A\,, \tag{4.20}$$

where I, J, A label the generation index. Dimension four proton decay occurs via interactions involving products of λ^i, the main decay channel being $p \to \pi^0 e^+$ [169] which involves the product $\lambda^1\lambda^2$. If both operators with couplings λ^1 and λ^2 are present this results in very fast proton decay. Proton lifetime results in the following bounds on the coupling constants for the lightest generation [170]

$$\sqrt{\lambda^1\lambda^2} \leq \left(\frac{M_{SUSY}}{\text{TeV}}\right)10^{-12}\,. \tag{4.21}$$

Here M_{SUSY} is the mass scale of the supersymmetric particles entering the process, and will be taken of $O(1)$ TeV. Bounds on the other generation couplings for GUT models are discussed in [171] and an up to date summary of all bounds can be found in section 6.5 of [172] from indirect searches, and section 7 from direct searches. In particular for λ^0 there are bounds which are much weaker $\sim 10^{-5}$, cf. (6.100), and for the other components of $\lambda^1\lambda^2$ see (6.110) in [172]. These operators violate baryon or lepton number and thereby R-parity. In this analysis we require the $U(1)$ symmetry forbid all operators of this type, and furthermore that singlets do not regenerate them outside of the bounds listed above.

Dimension 5 Proton Decay Operators

The main contribution to proton decay from dimension five operators occurs through the coupling

$$\delta^{(5)}_{abci}\mathbf{10}_a\mathbf{10}_b\mathbf{10}_c\overline{\mathbf{5}}_i\,, \tag{4.22}$$

which gives rise to the operators

$$\delta^1_{ABCI}Q_AQ_BQ_CL_I + \delta^2_{ABCI}\bar{u}_A\bar{u}_B\bar{e}_C\bar{d}_I + \delta^3_{ABCI}Q_A\bar{u}_B\bar{e}_CL_I. \tag{4.23}$$

The bound on the coupling constant due to the interaction involving δ^1 is [170]

$$\delta^1_{112I} \leq 16\pi^2\left(\frac{M_{SUSY}}{M^2_{GUT}}\right) \qquad I = 1, 2, 3\,, \tag{4.24}$$

where the relevant diagram is shown in figure 4.1. The mass M_{SUSY} is set by the mass of the sfermions contributing to the loop diagram. The operators involving other (s)quark

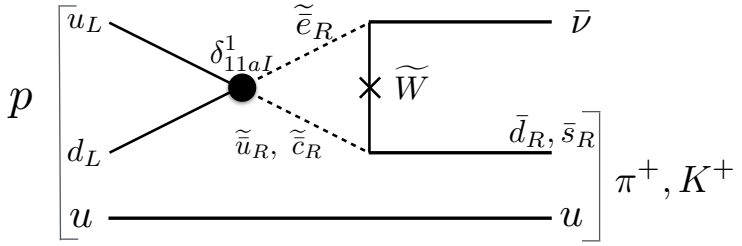

Figure 4.1: Process giving rise to dimension five proton decay parametrised by δ^1_{11aI}.

generations are suppressed with appropriate flavour insertions, i.e. at least the appropriate CKM elements have to be inserted. This ameliorates the bounds, in particular for operators involving the third generation.

Remaining B/L violating operators

The remaining couplings are also constrained in particular from limits on flavour changing processes, see [74] and for a review [172] . The bilinear coupling (C3.) violates lepton number and leads to a mixing between the Higgs and lepton sectors. At tree-level we will forbid this coupling, however in section 4.6 use it to generate neutrino masses. The couplings (C5.), (C6.) and (C7.) violate either lepton or baryon number, and thus contribute to proton decay in combination with the other B/L violating operators.

4.2.3 Flavour Constraints and FN-models

The assignment of the $U(1)$ charges of matter must be such that it allows for a top Yukawa coupling for the third generation, which amounts to requiring at least one charge neutral coupling of the form

$$Y^t_{ab}: \qquad \lambda^t_{ab}\mathbf{10}_a\mathbf{10}_b\mathbf{5}_{H_u} \supset Y^u_{AB}Q_A\bar{u}_BH_u\,, \tag{4.25}$$

where A, B label the quark generations. As the mass of the bottom quark is suppressed with respect to the mass of the top, a bottom Yukawa coupling

$$Y^b_{ai}: \qquad \lambda^b_{ai}\mathbf{10}_a\bar{\mathbf{5}}_i\bar{\mathbf{5}}_{H_d} \supset Y^d_{AI}Q_A\bar{d}_IH_d + Y^L_{IA}L_I\bar{e}_AH_d\,, \tag{4.26}$$

is not necessarily imposed at leading order. Both cases of rank 0 and rank 1 bottom Yukawa matrices at first order are studied. The up-type and down-type Yukawa matrices, Y^u and Y^d are the matrices formed from the couplings Y^u_{AB} and Y^d_{AI}, respectively after the distribution of MSSM matter has been assigned to the $\mathbf{10}$ and $\bar{\mathbf{5}}$ representations.

In the present context we will apply a FN-type mechanism [173] to generate the remaining Yukawa matrix entries, i.e. the $U(1)$-charged couplings are generated by giving suitably charged singlets a vev. In a generic F-theory models, the couplings between conjugate fields are always geometrically generated, i.e. the singlets required for all possible couplings of the form

$$\begin{aligned} &\mathbf{1}\,\overline{\mathbf{5}}_i\mathbf{5}_j \\ &\mathbf{1}\,\overline{\mathbf{10}}_m\mathbf{10}_n\,, \end{aligned} \tag{4.27}$$

are always present. Giving these singlets a vacuum expectation value breaks the $U(1)$ symmetry under which the singlet is charged, and generates the remaining Yukawa couplings. Whether or not such a vacuum expectation value can indeed be obtained, is a question of moduli stabilisation, which is beyond the scope of this thesis. For a singlet S of charge q a coupling, with charge nq, is regenerated with suppression

$$s^n = \left(\frac{\langle S\rangle}{M_{GUT}}\right)^n . \tag{4.28}$$

Experimentally masses, mixing angles and CP violation are measured at low energies compared to the UV scale at which we are calculating (see PDG flavour reviews [15] for the latest experimental summary). To compare UV models of Yukawa couplings to low-energy data, one needs to appropriately renormalise the couplings via the RG equations. This evolution allows for additional effects that can explain the flavour structure at low energies. For example flavour-violating effects from soft supersymmetry breaking can give large contributions to flavour observables, in fact they could even generate the entire flavour structure [174, 175].

However, the question here is different, namely, can the pattern that we can obtain from the additional $U(1)$s account for the entire flavour physics, i.e. with minimal RG evolution effects. This limit can be achieved when large flavour violating effects are absent in the soft-terms and canonical kinetic terms are present. In this context the RG evolution of quark and lepton masses as well as mixing parameters to high energies, e.g. the GUT scale at around 10^{16} GeV, has been performed (see for instance [176]). Roughly speaking one observes with the above assumptions that the quark mixing parameters and masses do not run very much. To first approximation, we hence aim at obtaining the following mass ratios and mixing angles in the quark and lepton sector [177, 178]:

$$\begin{aligned} m_t : m_c : m_u &\sim 1 : \epsilon^4 : \epsilon^8 \\ m_b : m_s : m_d &\sim 1 : \epsilon^2 : \epsilon^4 \\ m_\tau : m_\mu : m_e &\sim 1 : \epsilon^2 : \epsilon^{4,5}\,, \end{aligned} \tag{4.29}$$

and quark mixing angles

$$\theta_{12} \sim \epsilon\,, \quad \theta_{23} \sim \epsilon^2\,, \quad \theta_{31} \sim \epsilon^3\,, \tag{4.30}$$

where $\epsilon \approx 0.22$ is the Wolfenstein parameter [179]. We do not determine the ratio $\frac{m_b}{m_t} = \epsilon^x \tan^{-1}\beta$ as this is part of a full-fledged supersymmetry breaking model, which is not part of our analysis. Furthermore, we do not discuss CP violation here as the $U(1)$ symmetries used for obtaining the hierarchical scaling do not constrain the complex phases of the singlet insertions.

This experimentally constrained structure of masses and flavour mixings does not fix the entire structure in the Yukawa matrices. There are various popular models for this such as [177, 180, 181]. More systematically, by focusing on generating all hierarchies with one singlet, one can classify all viable textures for the quark masses [181]. In the present context, the only model in this classification, which is consistent with $SU(5)$, is the following hierarchical scaling of the Yukawa matrices first obtained by Haba in [182]

$$Y^u_{\text{Haba}} \sim \begin{pmatrix} \epsilon^8 & \epsilon^6 & \epsilon^4 \\ \epsilon^6 & \epsilon^4 & \epsilon^2 \\ \epsilon^4 & \epsilon^2 & 1 \end{pmatrix}, \qquad Y^d_{\text{Haba}} \sim \begin{pmatrix} \epsilon^4 & \epsilon^4 & \epsilon^4 \\ \epsilon^2 & \epsilon^2 & \epsilon^2 \\ 1 & 1 & 1 \end{pmatrix}. \tag{4.31}$$

Another texture which will be shown to be consistent with the F-theoretic setup was already obtained by Babu, Enkhbat and Gogoladze (BaEnGo) in [183] and is given by

$$Y^u_{\text{BaEnGo}} \sim \begin{pmatrix} \epsilon^8 & \epsilon^6 & \epsilon^4 \\ \epsilon^6 & \epsilon^4 & \epsilon^2 \\ \epsilon^4 & \epsilon^2 & 1 \end{pmatrix}, \qquad Y^d_{\text{BaEnGo}} \sim \begin{pmatrix} \epsilon^5 & \epsilon^4 & \epsilon^4 \\ \epsilon^3 & \epsilon^2 & \epsilon^2 \\ \epsilon & 1 & 1 \end{pmatrix}. \tag{4.32}$$

The $U(1)$ symmetries and associated singlet vevs generate these hierarchies in the couplings, but do not predict the exact values for the masses. These are obtained by $O(1)$ numbers in front of each coupling, whose string theoretic origin can for instance be non-canonical contributions to the kinetic terms. The couplings do not only depend on the singlets but also on uncharged complex structure moduli. In practice we will determine $O(1)$ numbers which generate the experimentally favoured values, in particular for the lepton sectors, which will be discussed in section 4.6.

A detailed analysis of the flavour constraints in the context of Froggatt–Nielsen models will be done in section 4.5. We find F-theoretic models consistent with the above two hierarchies as in [182] and [183]. In appendix B.4 we consider other known textures [176, 159] and show that it is not possible to find F-theoretic charges, which solve the anomaly cancellation conditions and generate the required quark Yukawa matrices.

4.2.4 F-theory $U(1)$s and the Mordell–Weil group

The key input from F-theory – apart from the anomalies – is the set of possible $U(1)$ charges for matter fields as determined in [32]. Much recent progress in F-theory model

building has resulted in constructions of examples of global elliptic Calabi–Yau four-folds, which realise both, GUT gauge groups in terms of singularities in the elliptic fiber, as well as additional abelian gauge symmetries (see introduction for a list of references). Abelian gauge symmetries are constructed in terms of so-called rational sections, which are maps from the base of the fibration back to the fiber [38]. None of the explicit algebraic realisations, however, resulted in a complete classification of the possible $U(1)$ symmetries. The collection of rational sections form a finitely generated abelian group (under the elliptic curve group law), called the Mordell–Weil group, which is isomorphic to $\mathbb{Z}^r \oplus \Gamma$, where Γ is the torsional part, which will not play a role in the current discussion. If the Mordell–Weil group has rank r, then the resulting compactification will have r additional $U(1)$ symmetries. Realising elliptic fibrations with multiple matter curves of distinct $U(1)$ charges is technically a highly challenging enterprise. Therefore an alternative approach that would yield the charges, without necessarily constructing the corresponding geometries is highly desirable.

Models with one $U(1)$

Such a full classification of possible $U(1)$ symmetries for $SU(5)$ was obtained in [32][3]. There the starting point is not a concrete realisation of the elliptic fiber, but a more abstract approach pursued by studying the constraints on the possible $U(1)$ charges in terms of general consistency requirements between the rational sections and codimension two fibers from the classification in [70]. This approach has the great advantage of giving rise to a super-set of $U(1)$ charges, that can be realised in F-theory, without however providing a direct geometric construction. We take this set of charges as an input for our analysis and show that certain charges in this set are phenomenologically favoured, as they satisfy all constraints and provide realistic flavour physics. In this way, we provide a pointer towards which geometric constructions can yield globally consistent compactifications. We shall give some details on geometries of this type later in the chapter in section 4.7.

The input from the classification result in [32] for F-theory compactifications to 4d with r $U(1)$ symmetries, and matter in the **10** and $\bar{\mathbf{5}}$ of $SU(5)$ is the set of possible charges. For a single $U(1)$, there are three types of distinct distributions of sections in the codimension one fiber[4] – for the reader interested solely in the model building aspects, it is sufficient

[3]There is an assumption, that the section is a smooth divisor in the resolved Calabi–Yau four-fold. A discussion of this particular point and potential extensions beyond that can be found in [32].

[4]Recall that sections can be thought of as marked points on the elliptic curve. A model that realises an $SU(5)$ gauge theory has special, so-called singular I_5 fibers above a codimension one locus in the base of the fibrations. Geometrically these are a ring of five rational curves, i.e. two-sphere, which intersect in the affine $SU(5)$ Dynkin diagram – as shown in figure 4.2. To describe a model with a single $U(1)$ there is a zero-section (origin of the elliptic curve) and the additional rational section, which generates the

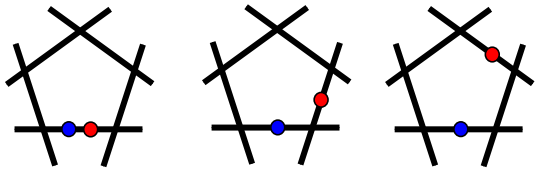

Figure 4.2: The configurations of fibers for an $SU(5)$ model with one $U(1)$ symmetry. The I_5 fiber, realised by the five black lines (corresponding to $\mathbb{P}^1$s in the fiber) gives rise to the $SU(5)$ gauge bosons, and the sections, shown as colored dots corresponding to the zero-section (blue) and the additional section (red), give rise to the additional abelian gauge factor.

to understand that there are three set of charges, labeled by

$$I_5^{(01)}\,, \qquad I_5^{(0|1)}\,, \qquad I_5^{(0||1)}\,. \tag{4.33}$$

and are shown in figure 4.2. For a given codimension one distribution of sections labeled by I_5 with the superindex indicating the separation between the zero-section (0) and the extra section (1), it was found in [32] that, for smooth rational sections, the possible charges for $\mathbf{10}$ and $\bar{\mathbf{5}}$ matter that can arise in $SU(5)$ F-theory models are as follows[5]:

$$\begin{aligned}
I_5^{(01)}\,: &\begin{cases} q_{\mathbf{10}} \in \{-3,-2,-1,0,+1,+2,+3\} \\ q_{\bar{\mathbf{5}}} \in \{-3,-2,-1,0,+1,+2,+3\} \end{cases} \\
I_5^{(0|1)}\,: &\begin{cases} q_{\mathbf{10}} \in \{-12,-7,-2,+3,+8,+13\} \\ q_{\bar{\mathbf{5}}} \in \{-14,-9,-4,+1,+6,+11\} \end{cases} \\
I_5^{(0||1)}\,: &\begin{cases} q_{\mathbf{10}} \in \{-9,-4,+1,+6,+11\} \\ q_{\bar{\mathbf{5}}} \in \{-13,-8,-3,+2,+7,+12\}\,. \end{cases}
\end{aligned} \tag{4.34}$$

A natural question is then to determine, whether there are integral solutions for the Ms and Ns, such that the resulting charge assignments solve anomaly conditions (A1.)−(A5.) and do not give rise to proton decay.

Finally we should comment on the $U(1)$ charges of GUT singlets, which will play a role later on in the Froggatt–Nielsen inspired flavour construction. In F-theory $SU(5)$ GUTs, the singlets arise at the intersection of any two $\bar{\mathbf{5}}$ curves (as well as two $\mathbf{10}$s). Hence, we can read off the singlet charges from the difference of charges

$$q_{\mathbf{1}_{ij}} = q_{\bar{\mathbf{5}}_\mathbf{i}} - q_{\bar{\mathbf{5}}_\mathbf{j}}\,, \qquad i \neq j\,, \tag{4.35}$$

for each of the three codimension one models.

Mordell–Weil group. The codimension one fibers with rational sections are thus decorations of the affine $SU(5)$ Dynkin diagram with two marked points, modulo trivial relabelling. These are shown in figure 4.2.

[5]For some studies it will be useful to rescale the models in $I_5^{(01)}$ by 5, so that a uniform treatment is possible, i.e. that the unit charges is "normalised" to 5.

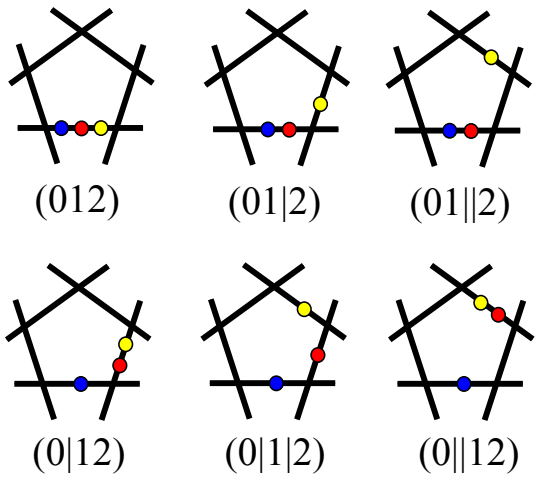

Figure 4.3: The configurations of fibers for an $SU(5)$ model with two $U(1)$ symmetries. The I_5 fiber, realised by the five black lines (corresponding to $\mathbb{P}^1$s in the fiber) gives rise to the $SU(5)$ gauge bosons, and the sections, shown as colored dots corresponding to the zero-section (blue) and the two additional sections (red, yellow), give rise to the additional abelian gauge factors.

Throughout the main text we will consider only these F-theory charges (4.34). In certain cases it is possible to use methods from solutions of Diophantine equations to solve the anomalies in general and we will provide these in appendix B.3.

Models with two $U(1)$s

As we will see in section 4.3, there are only very few viable solutions with one $U(1)$ symmetry. To construct models with two additional $U(1)$s we need two additional rational sections, σ_1 and σ_2 in the elliptic fibration, in addition to the zero-section, σ_0. There are nine possible codimension one fiber types in this case, up to a reordering of the simple roots and exchanging the two rational sections. These are given by,

$$I_5^{(012)},\quad I_5^{(01|2)},\quad I_5^{(01||2)},\quad I_5^{(0|12)},\quad I_5^{(0|1|2)},\quad I_5^{(0|1||2)},\quad I_5^{(0|1|||2)},\quad I_5^{(0||12)},\quad I_5^{(0||1|2)}, \tag{4.36}$$

where $i = 0, 1, 2$ denotes the position of the section σ_i. For each codimension one fiber there is a collection of codimension two fibers, and thus charge-sets.

The charges that appear in each of these codimension one fibers can be obtained from the charges in (4.34) by noting that the charges in an $I_5^{(0|||1)}$ model are simply the negative of those in $I_5^{(0||1)}$. The same statement holds for $I_5^{(0||||1)}$ and $I_5^{(0|1)}$. The two codimension one fibers, $I_5^{(0|||1)}$ and $I_5^{(0||||1)}$, were not considered in the case of a single additional rational section as they are equivalent, under a reordering of the simple roots to $I_5^{(0||1)}$ and $I_5^{(0|1)}$, respectively. In the case of two rational sections it is not always possible to bring both of

the sections into one of these forms.

From what is stated above, it is clear that not all of the codimension one fibers in (4.36) are distinct. For example, the charges in $I_5^{(0|12)}$ are the same as those in $I_5^{(0|1|||2)}$ if the charges under the second $U(1)$ are multiplied by -1. The anomaly cancellation conditions (A2.) and (A3.) are invariant under such re-scalings of the $U(1)$ charges therefore these two fibers will give rise to the same set of solutions up to the normalisation of one of the $U(1)$s. In this analysis we will consider the reduced set of codimension one fibers which give rise to distinct $U(1)$ charges given by

$$I_5^{(012)}, \quad I_5^{(01|2)}, \quad I_5^{(01||2)}, \quad I_5^{(0|12)}, \quad I_5^{(0|1|2)}, \quad I_5^{(0||12)}. \tag{4.37}$$

These configurations are also shown in figure 4.3. For these fibers, each additional rational section with the zero-section will generate a $U(1)$ with charges equal to those in (4.34). By taking all possible pairings between these two sets of charges one obtains the charges for a model with two additional $U(1)$ symmetries.

4.3 Single $U(1)$ Models

We begin our analysis by considering $SU(5)$ models with one additional $U(1)$ symmetry, and varying $\mathcal{N}_{\mathbf{10}}$ and $\mathcal{N}_{\bar{\mathbf{5}}}$. In summary: a single phenomenologically good model is found for $\mathcal{N}_{\mathbf{10}} = 1$ and $\mathcal{N}_{\bar{\mathbf{5}}} = 4$, denoted I.1.4.a in table 4.1, where the unwanted operators are not regenerated at the same order as the remaining charged Yukawa couplings. For $\mathcal{N}_{\mathbf{10}} = 1$ and $\mathcal{N}_{\bar{\mathbf{5}}} = 5$ as well as $\mathcal{N}_{\mathbf{10}} > 1$ (see appendix B.1) solutions are found, which however regenerate some dimension five proton decay operators along-side the charged Yukawas. This in itself is not problematic, as long as the suppression is high enough. However, single $U(1)$ models suffer generically from a poor flavour structure as generated by a FN-type mechanism. Nevertheless it is interesting to note that there are solutions to the constraints within the F-theoretic $U(1)$ charges, which could be augmented with other mechanisms for generating flavour such as [156], to produce a phenomenologically consistent F-theory model.

Contrary to this, models with two $U(1)$s can satisfy the constraints from anomalies and couplings, and in addition will generate successful flavour physics via an FN-mechanism as will be discussed in section 4.5.

4.3.1 $\mathcal{N}_{\mathbf{10}} = 1$

We start the analysis with one **10** representation. Requiring one top Yukawa coupling implies that not all **10** charges listed in (4.34) can be used. The charges, in each codimension one configuration, which have a top Yukawa coupling with one of the possible **5** charges are

$$U(1) \text{ charges of } \mathbf{10} \text{ with } \mathbf{10}_q\mathbf{10}_q\mathbf{5}_{-2q}\text{:} \quad \begin{cases} I_5^{(01)} & q_{\mathbf{10}} \in \{-1, 0, +1\} \\ I_5^{(0|1)} & q_{\mathbf{10}} \in \{-7, -2, +3\} \\ I_5^{(0||1)} & q_{\mathbf{10}} \in \{-4, +1, +6\}\ . \end{cases} \tag{4.38}$$

For the case of one **10** representations the solutions to the anomaly equations can be parametrised as follows[6]

$\mathbf{R}$	$q(\mathbf{R})$	M	N
$\bar{\mathbf{5}}_{H_u}$	$-q_{H_u}$	0	-1
$\bar{\mathbf{5}}_{H_d}$	$-q_{H_u} + 5w_{H_d}$	0	1
$\bar{\mathbf{5}}_i$	$-q_{H_u} + 5w_{\bar{5}_i}$	M_i	N_i
$\mathbf{10}$	$q_{\mathbf{10}}$	3	0

(4.39)

where $i = 1, \ldots, \mathcal{N}_{\bar{\mathbf{5}}} - 2$, where $\mathcal{N}_{\bar{\mathbf{5}}}$ is the number of $\bar{\mathbf{5}}$ representations. The integer parameters w_{H_d} and $w_{\bar{5}_i}$ denote the separation between the charges of H_d and $\overline{\mathbf{5}}$ matter from the charge of H_u [7]. The charges for the **10** and $\overline{\mathbf{5}}$ representations take values in (4.38) and (4.34), respectively.

$\mathcal{N}_{\bar{\mathbf{5}}} = 3$

In view of the arguments in (4.16) and (4.17), the minimal number of $\bar{\mathbf{5}}$ representations is three. However this case always allows the μ-term, which disfavours these models. To see this, parametrise the models as in (4.39) with one $\bar{\mathbf{5}}_1$ curve, which has $M = 3$ and $N = 0$. The anomaly condition (A2.) implies $w_{H_d} = 0$, which exactly generates the μ-term.

[6] Note that we give the charge of the conjugate of the up-type Higgs, i.e. q_{H_u} is the charge of **5**, whereas $-q_{H_u}$ is the charge for $\bar{\mathbf{5}}$.

[7] In this analysis we have multiplied the charges of the fiber type $I_5^{(01)}$ by 5 so that all fiber types can be analysed with the same parametrisation.

	I.1.4.a	I.1.4.b	I.1.4.c	I.1.4.d	I.1.4.e	I.1.4.f
M	1	3	2/3	3	0	3
N	2	-3	-2	-3	3	-3
q_{10}	-1	-1	-7	0	-7	6
q_{H_u}	2	2	14	0	14	-12
q_{H_d}	2	1	6	-3	1	-3
$q_{\bar{5}_1}$	-1	0	1	-2	-9	2
$q_{\bar{5}_2}$	1	-1	-9	-1	-4	7
Y_1^b	0	0	0	-5	-15	5
Y_2^b	2	-1	-10	-4	-10	10
μ	4	3	20	-3	15	-15
C2	$\{-4,-2\}$	$\{-3,-4\}$	$\{-20,-30\}$	$\{-2,-1\}$	$\{-30,-25\}$	$\{20,25\}$
C3	$\{1,3\}$	$\{1,2\}$	$\{15,5\}$	$\{-2,-1\}$	$\{5,10\}$	$\{-10,-15\}$
C4	$\{-3,-1,1\}$	$\{-3,-2,-1\}$	$\{-25,-15,-5\}$	$\{-4,-3,-2\}$	$\{-25,-10,-15\}$	$\{10,15,20\}$
C5	$\{-3,-1\}$	$\{-2,-1\}$	$\{-15,-5\}$	$\{2,1\}$	$\{-5,-10\}$	$\{10,5\}$
C6	$\{5,7\}$	$\{4,5\}$	$\{35,25\}$	$\{-5,-4\}$	$\{20,25\}$	$\{-25,-20\}$
C7	-1	-2	-15	-3	-20	15

Table 4.1: Solutions for $\mathcal{N}_{\mathbf{10}} = 1$ and $\mathcal{N}_{\overline{\mathbf{5}}} = 4$, which do not generate (C1.)$-$(C7.). The charges of the bottom Yukawa couplings are shown in the row Y_i^b, where $i = 1, 2$ labels the which $\overline{\mathbf{5}}_i$ is involved in the coupling. The charges of the couplings (C2.)$-$(C7.) are shown in the corresponding rows. The model I.1.4.a is such that the bottom Yukawa coupling does not bring back any of the dangerous couplings and is phenomenologically preferred. The model I.1.4.c brings back dimension five proton decay operators. The remaining models are disfavoured as they regenerate dimension four proton decay operators at the same level as the bottom Yukawas.

$\mathcal{N}_{\bar{\mathbf{5}}} = 4$

For four $\overline{\mathbf{5}}$ representations, the anomaly conditions can be solved exactly, and we will find one model, which is phenomenologically viable. Consider again the parametrisation

$\mathbf{R}$	$q(\mathbf{R})$	M	N
$\bar{\mathbf{5}}_{H_u}$	$-q_{H_u}$	0	-1
$\bar{\mathbf{5}}_{H_d}$	$-q_{H_u}+5w_{H_d}$	0	1
$\bar{\mathbf{5}}_1$	$-q_{H_u}+5w_{\bar{5}_1}$	M	N
$\bar{\mathbf{5}}_2$	$-q_{H_u}+5w_{\bar{5}_2}$	$3-M$	$-N$
$\mathbf{10}$	$-\frac{1}{2}q_{H_u}$	3	0

(4.40)

where $M, N \in \mathbb{Z}^+$. In the analysis of four and more[8] $\overline{\mathbf{5}}$s we do not allow solutions where $M_i = N_i = 0$ for any of the $\overline{\mathbf{5}}$s. The above parametrisation already satisfies (A1.), (A4.) and (A5.) by construction. Constraint (A2.) and (A3.) imply

$$w_{H_d} = N(w_{\bar{5}_2} - w_{\bar{5}_1})\,, \qquad N(w_{\bar{5}_1} - w_{\bar{5}_2})(w_{\bar{5}_1} + Nw_{\bar{5}_1} + w_{\bar{5}_2} - Nw_{\bar{5}_2}) = 0\,, \tag{4.41}$$

where we exclude cases $N = 0$ as well as $w_{\bar{5}_1} = w_{\bar{5}_2}$ as they imply $q_{H_u} = -q_{H_d}$. If we do not require a bottom Yukawa coupling q_{H_u} is left unconstrained and the charges are given by

$$q_{H_d} = -q_{H_u} + \frac{10w_{\bar{5}_2}N}{1+N} \qquad q_{\bar{5}_1} = -q_{H_u} + \frac{5w_{\bar{5}_2}(N-1)}{1+N} \qquad q_{\bar{5}_2} = -q_{H_u} + 5w_{\bar{5}_2}\,. \tag{4.42}$$

Requiring a bottom Yukawa with $\overline{\mathbf{5}}_1$ gives the additional constraint

$$q_{H_u} = \frac{6N-2}{N+1} w_{\bar{5}_2}\,. \tag{4.43}$$

This results in the following set of charges

$$q_{10} = \frac{-3N+1}{N+1} w_{\bar{5}_2}\,, \quad q_{H_d} = \frac{4N+2}{N+1} w_{\bar{5}_2} \quad q_{\bar{5}_1} = -\frac{N+3}{N+1} w_{\bar{5}_2}\,, \quad q_{\bar{5}_2} = \frac{-N+7}{N+1} w_{\bar{5}_2}\,, \tag{4.44}$$

where $w_{\bar{5}_2}$ is unconstrained. In this case we do not consider the case $M = 0$ as we want a bottom Yukawa coupling with $q_{\bar{5}_1}$, which must then contain a down-type quark.

To exemplify our solution process, in this case we summarise all solutions in table 4.1, which fall within (4.34) and (4.38). This corresponds to picking a specific value for $w_{\bar{5}_2}$, and q_{H_u} in the case without a leading order bottom Yukawa coupling. The table also displays the charges of the forbidden couplings (C1.)−(C7.) as well as the charged Yukawa couplings, Y_i^b. The solutions can be summarised as follows:

[8] This is to avoid repetition of solutions and in all sections that follow each $\overline{\mathbf{5}}$ will have a non-zero net flux restriction.

- Model I.1.4a is the only phenomenologically viable solution for a single $U(1)$ solving all constraints, without bringing back any of the dangerous operators, when generating the remaining Yukawa couplings. It does regenerate the μ-term with two singlet insertions. As noted already in general, the flavour physics of this model is however quite limited, which is a matter that will be improved upon in the multiple $U(1)$ case.
- Model I.1.4.c regenerates both dimension five proton decay operators with two and three singlet insertions and all other remaining models regenerate the dimension four proton decay operators (C4.).

$\mathcal{N}_{\bar{\mathbf{5}}} = 5, 6, 7$

For $\mathcal{N}_{\bar{\mathbf{5}}} > 4$ solving the anomaly cancellation conditions for general charges is difficult, however we provide a method for solving these in general in appendix B.3. In practice given the finite set of charges, one can simply scan over all possibilities. For each **10** charge in (4.38), one can require the top Yukawa coupling, which fixes the charge of $\mathbf{5}_{H_u}$. Solving (A1.)−(A5.) and requiring absence of (C1.)−(C7.), we find very few solutions, where *every* single one regenerates dimension 5 or dimension 4 proton decay operators at the same order as the remaining Yukawa couplings (with exactly the same singlet suppression). Thus all models are disfavoured.

For $\mathcal{N}_{\bar{\mathbf{5}}} \geq 6$ there are no solutions. The case of six $\bar{\mathbf{5}}$ is maximal for two of the charge sets in (4.34). For these sets the only freedom comes in selecting the charge of the **10** representation which will fix q_{H_u}. As there are seven possible charges for fundamental matter in the case of $I_5^{(01)}$ we need to consider all possible subsets of six once the charge of the **10** has been fixed.

One can go further and allow for seven distinctly charged $\bar{\mathbf{5}}$ representations in the case of the $I_5^{(01)}$ models. One finds two solutions to the anomaly cancellation conditions for $q_{\mathbf{10}} = \pm 1$, however, these solutions do not forbid (C2.) and are therefore excluded.

4.3.2 $\mathcal{N}_{\mathbf{10}} \geq 2$

The case of multiple **10** representations for a single $U(1)$ symmetry does not yield any interesting solutions to the constraints. In particular for a single $U(1)$ the flavour physics is very constrained. The analysis is provided in appendix B.1 for completeness. In summary we find the following:

- There are two solutions for $\mathcal{N}_{\mathbf{10}} = 2$ and $\mathcal{N}_{\overline{\mathbf{5}}} = 4$, shown in table B.1. Both these models regenerate dimension five operators at the same order as the charged Yukawas. In terms of the flavour physics of these models, with only two **10** representations and four $\overline{\mathbf{5}}$s one can not satisfy the mass hierarchies for the up-type and down-type quarks simultaneously.
- For $\mathcal{N}_{\mathbf{10}} = 3$ there is one model, which has realistic flavour structure for the quark sector. In fact it generates the Haba textures (4.31), albeit it does regenerate dimension four proton decay operators at the same order as the Yukawas.
- No other solution exists with two or three **10**s, which solve the anomaly cancellation conditions and forbid the dangerous operators.

It is clear from the analysis carried out in this section that in order to construct feasible models, that might give rise to interesting flavour structure, it is necessary to extend to multiple $U(1)$s.

4.4 Two $U(1)$ Models with Hypersurface Realisation

For two additional $U(1)$ symmetries, the phenomenological properties of the models become much more favourable. Allowing models with up to three **10** and eight $\overline{\mathbf{5}}$ representations in the survey, one finds a large number of solutions to the anomaly cancellation conditions with no exotics, which furthermore forbid the unwanted operators. In view of this, it is then useful to focus on two subclasses of solutions:

1. Models with charges that have a known geometric realisation.
2. Models, where the $U(1)$ symmetries can be used to construct realistic flavour textures. This is detailed in section 4.5.

We now turn to point 1. and find solutions, which have charges that are closest to known geometric models. We will find in this section that there are no solutions, which are within the charges obtained in the literature. However, there are solutions, summarised in tables 4.2 and 4.3, for which we determine new geometric models, that give rise to these charges in section 4.7.

	II.1.6.a	**II.1.6.b**
M_1	1	1
M_2	1	1
M_3	0	0
N_1	1	1
N_2	-1	-1
N_3	1	1
q_{10}	$(-2, 3)$	$(-2, 1)$
q_{H_u}	$(4, -6)$	$(4, -2)$
q_{H_d}	$(6, -4)$	$(6, 2)$
$q_{\bar{5}_1}$	$(-4, 1)$	$(-4, -3)$
$q_{\bar{5}_2}$	$(1, -4)$	$(1, -3)$
$q_{\bar{5}_3}$	$(1, 6)$	$(1, 7)$
$q_{\bar{5}_4}$	$(6, 1)$	$(6, 7)$
Y_1^b	(0,0)	(0,0)
Y_2^b	$(5, -5)$	$(5, 0)$
Y_3^b	$(5, 5)$	$(5, 10)$
Y_4^b	$(10, 0)$	$(10, 10)$
μ	$(10, -10)$	$(10, 0)$
C2	$\{(-10, 10), (-5, 5), (-5, 15), (0, 10)\}$	$\{(-10, 0), (-5, 0), (-5, 10), (0, 10)\}$
C3	$\{(0, -5), (5, -10), (5, 0), (10, -5)\}$	$\{(0, -5), (5, -5), (5, 5), (10, 5)\}$
C4	$\{(-10, 5), (-5, 0), (-5, 10), (0, 5),$ $(0, -5), (5, 0), (0, 15), (5, 10),$ $(10, 5)\}$	$\{(-10, -5), (-5, -5), (-5, 5), (0, 5),$ $(0, -5), (5, 5), (0, 15), (5, 15),$ $(0, 15)\}$
C5	$\{(0, 5), (-5, 10), (-5, 0), (-10, 5)\}$	$\{(0, 5), (-5, 5), (-5, -5), (-10, -5)\}$
C6	$\{(10, -15), (15, -20), (15, -10), (20, -15)\}$	$\{(10, -5), (15, -5), (15, 5), (20, 5)\}$
C7	$(0, 5)$	$(0, 5)$

Table 4.2: Solutions for $\mathcal{N}_{\mathbf{10}} = 1$ and $\mathcal{N}_{\bar{\mathbf{5}}} = 6$ with 2 $U(1)$s. The charges of the bottom Yukawa couplings are shown in the row Y_i^b, where $i = 1, 2, 3, 4$ labels the $\overline{\mathbf{5}}_i$ involved in the coupling. The charges of the couplings (C1.)$-$(C7.) are shown in the corresponding rows.

	II.1.6.c	II.1.6.d
M_1	1	1/2
M_2	1	1/2
M_3	1	0/1
N_1	1	-1
N_2	-1	-1
N_3	-1	1
q_{10}	(3, 1)	(3, 1)
q_{H_u}	$(-6,-2)$	$(-6,-2)$
q_{H_d}	$(-4,2)$	$(-4,2)$
$q_{\bar{5}_1}$	$(1,-3)$	$(1,-3)$
$q_{\bar{5}_2}$	$(-4,-3)$	$(-4,7)$
$q_{\bar{5}_3}$	(1, 7)	(1, 7)
$q_{\bar{5}_4}$	(6,7)	(6, -3)
Y_1^b	(0,0)	(0,0)
Y_2^b	$(-5,0)$	$(-5,10)$
Y_3^b	(0, 10)	(0, 10)
Y_4^b	(5, 10)	(5,0)
μ	$(-10,0)$	$(-10,0)$
C2	$\{(10,0),(5,0),(10,10),(15,10)\}$	$\{(10,0),(5,10),(10,10),(15,0)\}$
C3	$\{(-5,-5),(-10,-5),(-5,5),(0,5)\}$	$\{(-5,-5),(-10,5),(-5,5),(0,-5)\}$
C4	$\{(5,-5),(0,-5),(5,5),(10,5),$ $(-5,-5),(0,5),(5,5),(5,15),(10,15),$ $(15,15)\}$	$\{(5,-5),(0,5),(5,5),(10,-5),$ $(-5,15),(0,15),(5,15),(10,5),$ $(15,-5)\}$
C5	$\{(5,5),(10,5),(5,-5),(0,-5)\}$	$\{(5,5),(10,-5),(5,-5),(0,5)\}$
C6	$\{(-15,-5),(-20,-5),(-15,5),(-10,5)\}$	$\{(-15,-5),(-20,5),(-15,5),(-10,-5)\}$
C7	(5, 5)	(5, 5)

Table 4.3: Solutions for $\mathcal{N}_{\mathbf{10}} = 1$ and $\mathcal{N}_{\bar{\mathbf{5}}} = 6$ with 2 $U(1)$s. The model II.1.6.d regenerates dimension five proton decay operators with multiple insertions of the singlets regenerating the charged Yukawas.

In the following we restrict to the set of $U(1)$ charges which have appeared in explicit realisations of two U(1) models [92–95, 108]. These charges are given by[9]

$$I_5^{(01)}: \begin{cases} q_{\mathbf{10}} \in \{0,+1\} \\ q_{\overline{\mathbf{5}}} \in \{-1,0,+1\} \end{cases} \quad I_5^{(0|1)}: \begin{cases} q_{\mathbf{10}} \in \{-2,+3\} \\ q_{\overline{\mathbf{5}}} \in \{-4,+1,+6\} \end{cases} \quad I_5^{(0||1)}: \begin{cases} q_{\mathbf{10}} \in \{-4,+1\} \\ q_{\overline{\mathbf{5}}} \in \{-3,+2,+7\} \end{cases} \tag{4.45}$$

Taking this reduced set of charges we look for subsets, which solve the anomaly cancellation conditions, allowing up to $\mathcal{N}_{\mathbf{10}} = 3$ and $\mathcal{N}_{\overline{\mathbf{5}}} = 8$. The set of models, which solve the conditions (A1.)−(A5.) are then further filtered down to those which forbid the dangerous couplings (C1.)−(C7.) at leading order. These dangerous couplings should also not be regenerated with the same singlet insertion, that regenerates the charged Yukawa couplings.

The phenomenologically good solutions are given in tables 4.2 and 4.3. These models all feature $\mathcal{N}_{\mathbf{10}} = 1$ and $\overline{\mathbf{5}} = 6$ and have a top and bottom Yukawa coupling at leading order. The model II.1.6.d regenerates dimension five proton decay operators with multiple insertions of the singlets, that generate the charged Yukawas. The remaining three models all give rise to the μ-term with two singlet insertions. Interesting flavour textures for these models, which have only a single **10**, cannot be generated through the $U(1)$ symmetries, however these models have the advantage of having a concrete geometric realisation: none of the geometries in the literature [92–95, 108] generate this particular combination of charges, however we will determine elliptic fibrations for these models in section 4.7.

4.5 F-theoretic Froggatt–Nielsen Models with two $U(1)$s

The constructions passing all anomaly and coupling constraints with charges seen in known geometric constructions have not revealed an interesting flavour structure from the $U(1)$s, as we only found solutions with a single **10** curve. We now turn our discussion to the question whether we can find models with two $U(1)$s and three **10** curves with the more general, F-theoretic set of charges in (4.34). This increase in complexity improves the models, which as we will see, allow for realistic flavour physics. In short, we identify models that lead to a realisation of the FN mechanism. Note that we will match the quark Yukawas to several known flavour hierarchies. It certainly would be very interesting to scan through all the possibilities in the solution space, and possibly determine new textures. Concretely, we find two classes of flavour models, which appeared in [182, 183],

[9] Note that not all combinations of these charges are realised in geometric models in the literature – for instance the models we find in tables 4.2 and 4.3 are of this type. However in section 4.7, we will determine new geometries (based on the generalised cubic model of [133]), which give a concrete realisation of these models.

for the quark sector that can be realised. This will be the topic of the current section, and the resulting new lepton flavour structure is discussed in section 4.6. There are several popular flavour models, that we cannot realise in our class of models, which are detailed in appendix B.4.

4.5.1 Models with $\mathcal{N}_{\mathbf{10}} = 3$

We now analyse F-theoretic $U(1)$ models with two $U(1)$s for their potential to solve all the constraints as well as induce realistic flavour hierarchies by a Froggatt–Nielsen type mechanism. Each entry in the Yukawa matrix for the up-type quarks, Y^u, is given by the couplings

$$Y^u_{ij}\, Q_i \bar{u}_j H_u\,, \quad i,j = 1,2,3\,. \tag{4.46}$$

The $U(1)$ charges of **10** representations within which these quarks reside will determine the charges of the singlets required to regenerate these couplings and therefore their suppression. If we require that Y^u is rank one at leading order so that only $Y^u_{3,3}$, for the third generation, is uncharged under the additional $U(1)$s and that $Y^u_{1,1}$ and $Y^u_{2,2}$ appear with different suppressions, to match with a large class of known textures, we are required to consider models with three **10** representations.

A leading order rank one up-type Yukawa matrix is achieved most easily by having Q_3 and $\bar{u}_3$ residing on the same **10** representation, $\mathbf{10}_3$, with $U(1)$ charges satisfying

$$2q_{10_3} + q_{H_u} = 0\,. \tag{4.47}$$

In order for the top Yukawa coupling involving $\mathbf{10}_3$ to only generate a leading order mass for the top quark we require

$$M_{10_3} = 1 \text{ and } N_{10_3} = 0, \tag{4.48}$$

so that only the third generation of left- and right-handed quarks lie within this **10** representation. It is crucial that only the third generation is present on $\mathbf{10}_3$ otherwise off diagonal terms in the Yukawa matrix will also be regenerated at first order.

Between the remaining two **10** representations, $\mathbf{10}_1$ and $\mathbf{10}_2$, one can have the following distribution of the remaining quarks:

T.1: $M_{10_1} = M_{10_2} = 1$, $N_{10_1} = N_{10_2} = 0$
For these configurations one has

$$\mathbf{10}_A \supset Q_A + \bar{u}_A + \bar{e}_A, \quad A = 1,2,3\,, \tag{4.49}$$

and the resulting Yukawa matrix is symmetric. These textures could potentially agree with those in [182, 176, 183, 159].

T.2: $M_{10_1} = M_{10_2} = 1$, $N_{10_1} = -1$, $M_{10_2} = 1$
Here, both the remaining right-handed up-type quarks, $\bar{u}_1$ and $\bar{u}_2$, originate from $\mathbf{10}_1$,

$$\begin{aligned} \mathbf{10}_1 &\supset Q_1 + \bar{u}_1 + \bar{u}_2 \\ \mathbf{10}_2 &\supset Q_2 + \bar{e}_1 + \bar{e}_2 \,. \end{aligned} \tag{4.50}$$

The resulting Y^u, denoting the singlet insertion which regenerates the top Yukawa coupling between $\mathbf{10}_A$ and $\mathbf{10}_B$ as s_{AB}, has the following form

$$Y^u \sim \begin{pmatrix} s_{11} & s_{11} & s_{13} \\ s_{12} & s_{12} & s_{23} \\ s_{13} & s_{13} & 1 \end{pmatrix} , \tag{4.51}$$

where two columns have identical singlet insertions, as the charges for the couplings involving $\bar{u}_A$, $A = 1, 2$ are the same. This does not match known textures, where off diagonal terms have a greater suppression compared to their nearest diagonal terms.

T.3: $M_{10_1} = 2, M_{10_2} = 0$, $N_{10_1} = 0$, $M_{10_2} = 0$
We do not consider this case as $\mathbf{10}_2$ has no net chirality and therefore this case reduces to two $\mathbf{10}$ representations.

The case T.2 can be shown to not give rise to good flavour textures. In the following section we focus on case T.1, where each differently charged $\mathbf{10}$ representation contains a different generation of Q_A and u_A, and match to known textures in the literature. We show in appendix B.4 that the flavour hierarchies in [176, 159] cannot be realised within our global F-theoretic charge framework. Note that the textures in [181], which do not have a symmetric Y^u, cannot be realised. The two flavour models that can be realised in our framework are those in Haba [182] as well as Babu, Enkhbat, and Gogoladze [183], which we now discuss in turn.

4.5.2 F-theoretic FN-models (Haba1) and (Haba2)

In this section we determine solutions to our constraints, which furthermore generate the Yukawa textures in Haba [182]

$$Y^u_{\text{Haba}} \sim \begin{pmatrix} \epsilon^8 & \epsilon^6 & \epsilon^4 \\ \epsilon^6 & \epsilon^4 & \epsilon^2 \\ \epsilon^4 & \epsilon^2 & 1 \end{pmatrix} , \qquad Y^d_{\text{Haba}} \sim \begin{pmatrix} \epsilon^4 & \epsilon^4 & \epsilon^4 \\ \epsilon^2 & \epsilon^2 & \epsilon^2 \\ 1 & 1 & 1 \end{pmatrix} \tag{4.52}$$

from a Froggatt–Nielsen type mechanism. Let

$$M_{10_A} = 1, \quad N_{10_A} = 0, \quad A = 1, 2, 3\,. \tag{4.53}$$

The charges of the **10** representations therefore do not contribute to the anomaly cancellation conditions, as $N_{10_A} = 0$. We consider $\mathcal{N}_{\overline{\mathbf{5}}} = 4$ in the following. The sets of $\overline{\mathbf{5}}$ charges, which solve the conditions were determined in appendix B.2 and are given in (B.16), (B.17) and (B.18).

In order to match to this texture we need to impose that all $\bar{d}_i$ are from the same $\overline{\mathbf{5}}$ representation, which is achieved by

$$\begin{aligned} M_{\bar{5}_1} &= 0, \quad N_{\bar{5}_1} = 1, 2 \text{ or } 3 \\ M_{\bar{5}_2} &= 3, \quad N_{\bar{5}_2} = -N_{\bar{5}_1}\,. \end{aligned} \tag{4.54}$$

The cases $N_{\bar{5}_1} = 1, 3$ give phenomenologically disfavourable models as the solutions either allow the μ-term or regenerate dimension four proton decay with the remaining charged Yukawas. This leaves only $N = 2$, the solutions of which are given in table B.2. Imposing the presence of a bottom Yukawa coupling of the form

$$\mathbf{10}_3\overline{\mathbf{5}}_2 H_d\,, \tag{4.55}$$

restricts the set of solutions further. The set of charges with

$$\begin{aligned} M_{5_1} &= 0, \quad N_{5_1} = 2 \\ M_{5_2} &= 3, \quad N_{5_2} = -2\,, \end{aligned} \tag{4.56}$$

which furthermore allow for a bottom Yukawa coupling are as follows:

	$\mathbf{10}_3$	$\mathbf{5}_{H_u}$	$\overline{\mathbf{5}}_{H_d}$	$\overline{\mathbf{5}}_1$	$\overline{\mathbf{5}}_2$
$q(\mathbf{R})^1$	$-q^1_{H_u}/2$	$q^1_{H_u}$	$3q^1_{H_u}/7$	$-9q^1_{H_u}/14$	$q^1_{H_u}/14$
$q(\mathbf{R})^2$	$-q^2_{H_u}/2$	$q^2_{H_u}$	$3q^2_{H_u}/7$	$-9q^2_{H_u}/14$	$q^2_{H_u}/14$

(4.57)

where we have imposed the top Yukawa coupling for $\mathbf{10}_3$. The charges of $\mathbf{10}_1$ and $\mathbf{10}_2$ are given by[10]

$$\left(q^1_{10_A}, q^2_{10_A}\right) = \left(-\frac{1}{2}q^1_{H_u}, -\frac{1}{2}q^2_{H_u}\right) + 5\left(w^1_{10_A}, w^2_{10_A}\right)\,, \tag{4.58}$$

where q^α denotes the charges under $U(1)_\alpha$ and $A = 1, 2$. The charges of matter under these two $U(1)$s will therefore be almost identical, the only difference being in the charge of $\mathbf{10}_1$ and $\mathbf{10}_2$, which should be chosen so that no dangerous couplings are allowed at

[10] In order to uniformly study all F-theoretic charges we rescaled for convenience the models of type $I_5^{(01)}$ by a factor of 5. This allows us to study all the models where the unit charges is now set to be 5 (rather than 1).

leading order. Restricting these general charges to the F-theory charges one finds that there are only two choices for the charge of the Higgs up given by

$$(q^1_{H_u}, q^2_{H_u}) = (14, 14) \quad \text{or} \quad (0, 14)\,. \tag{4.59}$$

The integer separations, parametrised by $w^\alpha_{10_A}$, satisfy the constraint

$$w^1_{10_A} \neq w^2_{10_A}, \quad A = 1, 2\,, \tag{4.60}$$

as there were no two **10** models for a single $U(1)$ which were phenomenologically viable. Violating the above constraint for either $\mathbf{10}_1$ or $\mathbf{10}_2$ will either bring back dangerous operators or regenerate them with the charged Yukawas. This implies the following distribution:

Representation	Charge	M	N	Matter
$\mathbf{10}_1$	$\left(-\frac{1}{2}q^1_{H_u} + 5w^1_{10_1}, -\frac{1}{2}q^2_{H_u} + 5w^2_{10_1}\right)$	1	0	$Q_1, \bar{u}_1, \bar{e}_A,\ A = 1, 2$
$\mathbf{10}_2$	$\left(-\frac{1}{2}q^1_{H_u} + 5w^1_{10_2}, -\frac{1}{2}q^2_{H_u} + 5w^2_{10_2}\right)$	1	0	$Q_2, \bar{u}_2, \bar{e}_B,\ B \neq A,\ B = 1, 2$
$\mathbf{10}_3$	$\left(-\frac{1}{2}q^1_{H_u}, -\frac{1}{2}q^2_{H_u}\right)$	1	0	$Q_3, \bar{u}_3, \bar{e}_3$
$\bar{\mathbf{5}}_{H_u}$	$(-q^1_{H_u}, -q^2_{H_u})$	0	-1	H_u
$\bar{\mathbf{5}}_{H_d}$	$(\frac{3}{7}q^1_{H_u}, \frac{3}{7}q^2_{H_u})$	0	1	H_d
$\bar{\mathbf{5}}_1$	$(-\frac{9}{14}q^1_{H_u}, -\frac{9}{14}q^2_{H_u})$	0	2	$L_I, I = 1, 2$
$\bar{\mathbf{5}}_2$	$(\frac{1}{14}q^1_{H_u}, \frac{1}{14}q^2_{H_u})$	3	-2	$L_3, \bar{d}_I, I = 1, 2, 3$

(4.61)

The necessary singlet insertions to regenerate the full up and down-type Yukawa matrices can be determined to be

$$Y^u \sim \begin{pmatrix} s_1^2 & s_1 s_2 & s_1 \\ s_1 s_2 & s_2^2 & s_2 \\ s_1 & s_2 & 1 \end{pmatrix}, \quad Y^d \sim \begin{pmatrix} s_1 & s_1 & s_1 \\ s_2 & s_2 & s_2 \\ 1 & 1 & 1 \end{pmatrix}, \tag{4.62}$$

where $s_i = \frac{\langle S_i \rangle}{M_{GUT}}$. The charges of the singlets, S_1 and S_2 are given by

$$\begin{aligned} (q^1_{S_1}, q^2_{S_1}) &= -5(w^1_{10_1}, w^2_{10_1}) \\ (q^1_{S_2}, q^2_{S_2}) &= -5(w^1_{10_2}, w^2_{10_2})\,. \end{aligned} \tag{4.63}$$

These singlets exactly correspond to those which are present in $\overline{\mathbf{10}}_3\mathbf{10}_A\mathbf{1}$ couplings, where $A = 1, 2$, as can be seen from their charges.

Choosing $s_1 = \epsilon^2$ and $s_2 = \epsilon^4$ one obtains the Haba texture in (4.31). When the charges of the two singlets are not coprime we have the following relation

$$(q^1_{S_1}, q^2_{S_1}) = n(q^1_{S_2}, q^2_{S_2})\,, \tag{4.64}$$

for some integer n. In (4.62) s_1 can be replaced with s_2^n, and from this we see that in order to match to the texture in (4.31) we must have $n = 2$. In this case we can generate the entire Yukawa matrix by giving a vev to only one singlet.

One choice of $w^{\alpha}_{10_A}$ which avoids all dangerous operators is given by[11]

$$\begin{aligned}(w^1_{10_1}, w^2_{10_1}) &= (2,0)\\ (w^1_{10_2}, w^2_{10_2}) &= (1,0)\,.\end{aligned} \tag{4.65}$$

Within this setup there are two choices for the charge of the up-type Higgs:

$$\begin{aligned}\text{(Haba1)}: &\qquad (q^1_{H_u}, q^2_{H_u}) = (14,14)\\ \text{(Haba2)}: &\qquad (q^1_{H_u}, q^2_{H_u}) = (0,14)\,.\end{aligned} \tag{4.66}$$

The full set of charges for these models are as follows[12]

GUT	Charges for (Haba1)	Charges for (Haba2)	M	N	MSSM Matter
$\mathbf{10}_1$	$(3,-7)$	$(10,-7)$	1	0	$Q_1, \bar{u}_1, \bar{e}_A,\ A=1,2$
$\mathbf{10}_2$	$(-2,-7)$	$(5,-7)$	1	0	$Q_2, \bar{u}_2, \bar{e}_B,\ B\neq A,\ B=1,2$
$\mathbf{10}_3$	$(-7,-7)$	$(0,-7)$	1	0	$Q_3, \bar{u}_3, \bar{e}_3$
$\bar{\mathbf{5}}_{H_u}$	$(-14,-14)$	$(0,-14)$	0	-1	H_u
$\bar{\mathbf{5}}_{H_d}$	$(6,6)$	$(0,6)$	0	1	H_d
$\bar{\mathbf{5}}_1$	$(-9,-9)$	$(0,-9)$	0	2	$L_I, I=1,2$
$\bar{\mathbf{5}}_2$	$(1,1)$	$(0,1)$	3	-2	$L_3, \bar{d}_I, I=1,2,3$

(4.67)

The models are summarised in table 4.4, including the charges for all the couplings (C1.)−(C7.). Both models have up- and down-type Yukawas with the same singlet insertion structure

$$\text{(Haba1,2)}: \qquad Y^u \sim \begin{pmatrix} \omega_1^4 & \omega_1^3 & \omega_1^2 \\ \omega_1^3 & \omega_1^2 & \omega_1 \\ \omega_1^2 & \omega_1 & 1 \end{pmatrix}, \quad Y^d \sim \begin{pmatrix} \omega_1^2 & \omega_1^2 & \omega_1^2 \\ \omega_1 & \omega_1 & \omega_1 \\ 1 & 1 & 1 \end{pmatrix}, \tag{4.68}$$

where $\omega_1 = \frac{\langle W_1\rangle}{M_{GUT}}$, where the charge of the singlet W_1 is

$$(q^1_{W_1}, q^2_{W_1}) = (-5,0)\,. \tag{4.69}$$

By choosing $\omega_1 = \epsilon^2$ one recovers the Haba flavour texture in (4.31). The lepton Yukawa matrices, from the above sets of charges, have the following singlet structure

$$\text{(Haba1,2)}: \qquad Y^L \sim \begin{pmatrix} \omega_1^2\omega_2 & \omega_1\omega_2 & \omega_2 \\ \omega_1^2\omega_2 & \omega_1\omega_2 & \omega_2 \\ \omega_1^2 & \omega_1 & 1 \end{pmatrix} \qquad \text{with } \mathbf{10}_A \supset \bar{e}_A, \text{ where } A=1,2\,. \tag{4.70}$$

[11] The charge of the $\mathbf{10}_{1,2}$ are not fixed so far, even when including the constraint of suppressing all dangerous couplings. Here they are chosen to bring them closest to the known geometric models.

[12] Note, that as mentioned earlier we rescaled the charges of the class of models $I_5^{(01)}$ by 5, to allow for a uniform treatment of all models. This means, that instead of the **10** charges (2,1,0) we write (10, 5, 0).

	(Haba1)	**(Haba2)**
M	0	0
N	2	2
M_{10_A}	1	1
N_{10_A}	0	0
q_{10_1}	$(3,-7)$	$(10,-7)$
q_{10_2}	$(-2,-7)$	$(5,-7)$
q_{10_3}	$(-7,-7)$	$(0,-7)$
q_{H_u}	$(14,14)$	$(0,14)$
q_{H_d}	$(6,6)$	$(0,6)$
$q_{\bar{5}_1}$	$(-9,-9)$	$(0,-9)$
$q_{\bar{5}_2}$	$(1,1)$	$(0,1)$
μ	$(20,20)$	$(0,20)$
C2	$\{(0,-30),(10,-20),(-5,-30),$ $(5,-20),(-10,-30),(0,-20),$ $(-15,-30),(-5,-20),(-20,-30),$ $(-10,-20),(-25,-30),(-15,-20),$ $(-30,-30),(-20,-20)\}$	$\{(30,-30),(30,-20),(25,-30),$ $(25,-20),(20,-30),(20,-20),$ $(15,-30),(15,-20),(10,-30),$ $(10,-20),(5,-30),(5,-20),$ $(0,-30),(0,-20)\}$
C3	$\{(5,5),(15,15)\}$	$\{(0,5),(0,15)\}$
C4	$\{(-15,-25),(-5,-15),(-20,-25),$ $(-10,-15),(-25,-25),(-15,-15),$ $(5,-5),(0,-5),(-5,-5)\}$	$\{(10,-25),(10,-15),(5,-25),$ $(5,-15),(0,-25),(0,-15),$ $(10,-5),(5,-5),(0,-5)\}$
C5	$\{(15,-5),(5,-15),(10,-5),(0,-15),$ $(5,-5),(-5,-15),(0,-5),(-10,-15),$ $(-5,-5),(-15,-15)\}$	$\{(20,-5),(20,-15),(15,-5),(15,-15),$ $(10,-5),(10,-15),(5,-5),(5,-15),$ $(0,-5),(0,-15)\}$
C6	$\{(25,25),(35,35)\}$	$\{(0,25),(0,35)\}$
C7	$\{(-5,-15),(-10,-15),(-15,-15)\}$	$\{(10,-15),(5,-15),(0,-15)\}$

Table 4.4: F-theoretic FN-models (Haba1) and (Haba2): these models have two $U(1)$s and $\mathcal{N}_{\mathbf{10}} = 3$ and $\mathcal{N}_{\bar{\mathbf{5}}} = 4$ and have realistic flavour textures, which for the quark sector match those by Haba in [182].

Here again the second singlet vev is $\omega_2 = \frac{\langle W_2 \rangle}{M_{GUT}}$. The choice for how the e_A are distributed on the $\mathbf{10}_B$ matter loci is made to get the standard hierarchy between first and second generation. To regenerate the entries in these matrices the following charged singlets must gain a vacuum expectation value

$$\begin{aligned} &\text{(Haba1)}: && (q^1_{W_2}, q^2_{W_2}) = (10, 10) \\ &\text{(Haba2)}: && (q^1_{W_2}, q^2_{W_2}) = (0, 10)\,. \end{aligned} \tag{4.71}$$

As one can see from the charges of the (C2.) couplings in table 4.4, regenerating the lepton Yukawas regenerates all the dimension five operators in both models. The dangerous dimension five couplings with coupling constant δ^1_{112I} that are regenerated with certain singlet insertions are shown below for both models, where we take $\omega_2 = O(1)$:

Model	Coupling	Charge	Singlet insertions	ϵ suppression
(Haba1)	$\mathbf{10}_1\mathbf{10}_1\mathbf{10}_2\overline{\mathbf{5}}_1$	$(-5,-30)$	$\omega_1^5\omega_2^3$	$\leq \epsilon^{10}$
	$\mathbf{10}_1\mathbf{10}_1\mathbf{10}_2\overline{\mathbf{5}}_2$	$(5,-20)$	$\omega_1^5\omega_2^2$	$\leq \epsilon^{10}$
(Haba2)	$\mathbf{10}_1\mathbf{10}_1\mathbf{10}_2\overline{\mathbf{5}}_1$	$(25,-30)$	$\omega_1^5\omega_2^3$	$\leq \epsilon^{10}$
	$\mathbf{10}_1\mathbf{10}_1\mathbf{10}_2\overline{\mathbf{5}}_2$	$(25,-20)$	$\omega_1^5\omega_2^2$	$\leq \epsilon^{10}$

(4.72)

For both models, in order for the

$$\frac{\epsilon^{10}}{M_{GUT}} \approx \frac{10^{-7}}{M_{GUT}} \leq 16\pi^2 \frac{M_{SUSY}}{M^2_{GUT}}\,, \tag{4.73}$$

where the Wolfenstein parameter is $\epsilon \approx 0.22$. This translates into the following relation

$$M_{SUSY} \geq 10^{-9} M_{GUT}\,, \tag{4.74}$$

where as before $\omega_1 = \epsilon^2$ and $\omega_2 = O(1)$. The latter can be improved upon by considering lepton flavour, where the most constraining factor, for both the models, is the mass ratio between the second and third generation, which is of order ϵ^2. This is discussed in section 4.6.

Other dimension five operators of type Q^3L are also regenerated with suppressions of ϵ^2 and higher. For example, in this case one also gets the coupling

$$\mathbf{10}_3\mathbf{10}_3\mathbf{10}_3\overline{\mathbf{5}}_2 \supset Q_3Q_3Q_3L_3\,, \tag{4.75}$$

which can be compared to the bound on δ^1_{112I} by inserting suppression factors from the CKM between the third generation and the first and second. One finds that this coupling, which has ϵ^2 suppression from the singlets, picks up at least an additional ϵ^{10} once we take into account the mixing between the quark generations. This coupling does not pose a greater threat than those considered above and the lower bound of M_{SUSY} from this

model is unchanged. In section 4.6 we consider the lepton and neutrino flavour physics of these models in more detail.

We extended this analysis to $\mathcal{N}_{\overline{\mathbf{5}}} = 5$ and 6, which are all possible choices, however there are no further solutions. Extending the number of $\overline{\mathbf{5}}$ beyond that results in exotics. Thus the presently analysed case of $\mathcal{N}_{\overline{\mathbf{5}}} = 4$ presents a sort of sweetspot.

4.5.3 F-theoretic FN-models (BaEnGo1)–(BaEnGo3)

Below we consider solutions which allow for a symmetric up-type Yukawa matrix paired with a down-type Yukawa matrix, which has only two distinct columns. These textures (4.32), as we shall show give rise to a realistic CKM structure. This has appeared in the literature before in [183], and will be referred to as the BaEnGo texture

$$Y^u_{\text{BaEnGo}} \sim \begin{pmatrix} \epsilon^8 & \epsilon^6 & \epsilon^4 \\ \epsilon^6 & \epsilon^4 & \epsilon^2 \\ \epsilon^4 & \epsilon^2 & 1 \end{pmatrix}, \qquad Y^d_{\text{BaEnGo}} \sim \begin{pmatrix} \epsilon^5 & \epsilon^4 & \epsilon^4 \\ \epsilon^3 & \epsilon^2 & \epsilon^2 \\ \epsilon & 1 & 1 \end{pmatrix}. \tag{4.76}$$

In this case the structure of singlet insertions is of the form

$$Y^u \sim \begin{pmatrix} s_1^2 & s_1 s_2 & s_1 \\ s_1 s_2 & s_2^2 & s_2 \\ s_1 & s_2 & 1 \end{pmatrix}, \quad Y^d \sim \begin{pmatrix} s_1 s_3 & s_1 & s_1 \\ s_2 s_3 & s_2 & s_2 \\ s_3 & 1 & 1 \end{pmatrix}, \tag{4.77}$$

where $s_i = \frac{\langle S_i \rangle}{M_{GUT}}$. The charges of the singlets, S_1, S_2 and S_3 are given by

$$\begin{aligned} (q^1_{S_1}, q^2_{S_1}) &= -5(w^1_{10_1}, w^2_{10_1}) \\ (q^1_{S_2}, q^2_{S_2}) &= -5(w^1_{10_2}, w^2_{10_2}) \\ (q^1_{S_3}, q^2_{S_3}) &= -5(w^1_{\overline{5}_n} - w^1_{\overline{5}_2}, w^2_{\overline{5}_n} - w^2_{\overline{5}_2}), \end{aligned} \tag{4.78}$$

where one of the $\overline{\mathbf{5}}$s, in this case $\overline{\mathbf{5}}_2$, is the one taken to have a leading order bottom Yukawa coupling and must contain two down-type quarks. One other $\overline{\mathbf{5}}$, in the above, labelled $\overline{\mathbf{5}}_n$, must contain the last down-type quark. Assuming the dominant contribution to the masses comes from the diagonal elements, we choose

$$s_1 = \epsilon^4, \quad s_2 = \epsilon^2, \tag{4.79}$$

to satisfy the up-type ratios in (4.29). Taking $s_3 = 1$ we recover a down-type Yukawa matrix in section 4.5.2, here we take the third singlet insertion to be

$$s_3 = \epsilon. \tag{4.80}$$

Using the formulas for the three mixing angles derived in [184, 185] the CKM, neglecting the CP phase, can be calculated to take the form

$$V_{CKM} \sim \begin{pmatrix} 1 & \epsilon^2 & \epsilon^4 \\ \epsilon^2 & 1 & \epsilon^2 \\ \epsilon^4 & \epsilon^2 & 1 \end{pmatrix} , \tag{4.81}$$

to leading order in ϵ. The corresponding Yukawas are those shown in (4.32). Below we study the models, which realise these textures with four and five $\overline{\mathbf{5}}$s. These models share the same up-type and down-type Yukawas, which have the structure in (4.77), however, they differ on the texture of the lepton Yukawa matrix.

$\mathcal{N}_{\overline{\mathbf{5}}} = 4$

One class of such solutions can be obtained by altering the M, Ns in (4.56) to

$$\begin{aligned} M_{5_1} &= 1, \quad N_{5_1} = 2 \\ M_{5_2} &= 2, \quad N_{5_2} = -2\,, \end{aligned} \tag{4.82}$$

which gives rise to models with the same set of possible charges, but the down-type Yukawa matrix now has the structure in (4.77). In this distribution of M, Ns all three generations of leptons reside in $\overline{\mathbf{5}}_1$ which produces lepton Yukawas of the form

$$\text{(BaEnGo1,2)}: \qquad Y^L \sim \begin{pmatrix} s_1 s_3 & s_2 s_3 & s_3 \\ s_1 s_3 & s_2 s_3 & s_3 \\ s_1 s_3 & s_2 s_3 & s_3 \end{pmatrix} , \tag{4.83}$$

where we have chosen the following distribution of right-handed leptons $\mathbf{10}_A \supset \bar{e}_A$, where $A = 1, 2, 3$ for both models. These choices ensure that the singlet suppressions generate the correct hierarchy in lepton masses.

Restricting to the charges in (4.67), where the singlets s_i are not coprime, the up- and down-type Yukawa matrices take the form

$$\text{(BaEnGo1,2)}: \qquad Y^u \sim \begin{pmatrix} \omega_1^4 & \omega_1^3 & \omega_1^2 \\ \omega_1^3 & \omega_1^2 & \omega_1 \\ \omega_1^2 & \omega_1 & 1 \end{pmatrix} , \quad Y^d \sim \begin{pmatrix} \omega_1^2\omega_2 & \omega_1^2 & \omega_1^2 \\ \omega_1\omega_2 & \omega_1 & \omega_1 \\ \omega_2 & 1 & 1 \end{pmatrix} , \tag{4.84}$$

where $\omega_i = \frac{\langle W_i \rangle}{M_{GUT}}$. The lepton Yukawa matrix for both sets of charges takes the form

$$Y^L \sim \begin{pmatrix} \omega_1^2\omega_2 & \omega_1\omega_2 & \omega_2 \\ \omega_1^2\omega_2 & \omega_1\omega_2 & \omega_2 \\ \omega_1^2\omega_2 & \omega_1\omega_2 & \omega_2 \end{pmatrix} , \tag{4.85}$$

where the singlets W_i have the following charges

$$\begin{aligned} (\text{BaEnGo1}): \quad & (q^1_{W_1}, q^2_{W_1}) = (-5, 0) \\ & (q^1_{W_2}, q^2_{W_2}) = (10, 10) \\ (\text{BaEnGo2}): \quad & (q^1_{W_1}, q^2_{W_1}) = (-5, 0) \\ & (q^1_{W_2}, q^2_{W_2}) = (0, 10)\,. \end{aligned} \tag{4.86}$$

The singlet suppressions, in terms of the Wolfenstein parameter ϵ, are given by

$$w_1 = \epsilon^2, \qquad w_2 = \epsilon\,, \tag{4.87}$$

to match the suppression of the singlets s_i in the general texture.

The charges of the unwanted operators are shown in table 4.5, in this case one regenerates dimension five proton decay operators with the down-type Yukawas. For the couplings involving δ^1_{112I} one finds the following suppression:

Model	Coupling	Charge	Singlet insertions	ϵ suppression
(BaEnGo1)	$\mathbf{10}_1\mathbf{10}_1\mathbf{10}_2\overline{\mathbf{5}}_1$	$(-5, -30)$	$\omega_1^5\omega_2^3$	$\leq \epsilon^{13}$
(BaEnGo2)	$\mathbf{10}_1\mathbf{10}_1\mathbf{10}_2\overline{\mathbf{5}}_1$	$(25, -30)$	$\omega_1^5\omega_2^3$	$\leq \epsilon^{13}$

(4.88)

The suppression of these dimension five couplings are bounded as

$$\frac{\epsilon^{13}}{M_{GUT}} \approx \frac{10^{-9}}{M_{GUT}} \leq 16\pi^2 \frac{M_{SUSY}}{M^2_{GUT}}\,, \tag{4.89}$$

which results in the following bound on the mass of the sparticles participating in the process:

$$M_{SUSY} \geq 10^{-11} M_{GUT}\,. \tag{4.90}$$

As in the earlier case of the Haba textures, the other operators are further suppressed compared to δ^1_{112I} and thus not threatening to the consistency of the model.

$\mathcal{N}_{\overline{\mathbf{5}}} = 5$

Finally, we discuss a solution, which has a distinct lepton flavour structure, by extending the solution in section 4.5.2 to five $\overline{\mathbf{5}}$s with

$$\begin{aligned} M_{5_1} &= 0, \quad & N_{5_1} &= 2 \\ M_{5_2} &= 2, \quad & N_{5_2} &= -2 \\ M_{5_3} &= 1, \quad & N_{5_3} &= 0\,. \end{aligned} \tag{4.91}$$

In this case the charges of the three $\mathbf{10}$s, $\overline{\mathbf{5}}_1$ and $\overline{\mathbf{5}}_2$ are as in (4.57) and (4.58). However the charge of $\overline{\mathbf{5}}_3$ is constrained not by the anomaly cancellation conditions, but by the

	(BaEnGo1)	**(BaEnGo2)**
M	1	1
N	2	2
M_{10_A}	1	1
N_{10_A}	0	0
q_{10_1}	$(3,-7)$	$(10,-7)$
q_{10_2}	$(-2,-7)$	$(5,-7)$
q_{10_3}	$(-7,-7)$	$(0,-7)$
q_{H_u}	$(14,14)$	$(0,14)$
q_{H_d}	$(6,6)$	$(0,6)$
$q_{\bar{5}_1}$	$(-9,-9)$	$(0,-9)$
$q_{\bar{5}_2}$	$(1,1)$	$(0,1)$
μ	$(20,20)$	$(0,20)$
C2	$\{(0,-30),(10,-20),(-5,-30),$ $(5,-20),(-10,-30),(0,-20),$ $(-15,-30),(-5,-20),(-20,-30),$ $(-10,-20),(-25,-30),(-15,-20),$ $(-30,-30),(-20,-20)\}$	$\{(30,-30),(30,-20),(25,-30),$ $(25,-20),(20,-30),(20,-20),$ $(10,-30),(10,-20),(5,-30),$ $(5,-20),(15,-30),(15,-20),$ $(0,-30),(0,-20)\}$
C3	$\{(5,5)\}$	$\{(0,5)\}$
C4	$\{(-15,-25),(-5,-15),(-20,-25),$ $(-10,-15),(-25,-25),(-15,-15),$ $(5,-5),(0,-5),(-5,-5)\}$	$\{(10,-25),(10,-15),(5,-25),$ $(5,-15),(0,-25),(0,-15),$ $(10,-5),(5,-5),(0,-5)\}$
C5	$\{(15,-5),(10,-5),(5,-5),(0,-5),$ $(-5,-5)\}$	$\{(20,-5),(15,-5),(10,-5),(5,-5),$ $(0,-5)\}$
C6	$\{(25,25)\}$	$\{(0,25)\}$
C7	$\{(-5,-15),(-10,-15),(-15,-15)\}$	$\{(10,-15),(5,-15),(0,-15)\}$

Table 4.5: F-theoretic FN-models (BaEnGo1) and (BaEnGo2): these models have two $U(1)$s and $\mathcal{N}_{\mathbf{10}} = 3$ and $\mathcal{N}_{\overline{\mathbf{5}}} = 4$ and have realistic flavour textures, which for the quark sector match those by BaEnGo in (4.32).

requirement of suppressing the unwanted operators. The distribution of MSSM matter is

Representation	Charge	M	N	Matter
$\mathbf{10}_1$	$(q^1_{10_1}, q^2_{10_1})$	1	0	$Q_1, \bar{u}_1, \bar{e}_3$
$\mathbf{10}_2$	$(q^1_{10_2}, q^2_{10_2})$	1	0	$Q_2, \bar{u}_2, \bar{e}_2,$
$\mathbf{10}_3$	$(-7, -7)$	1	0	$Q_3, \bar{u}_3, \bar{e}_1$
$\bar{\mathbf{5}}_{H_u}$	$(-14, -14)$	0	-1	H_u
$\bar{\mathbf{5}}_{H_d}$	$(6, 6)$	0	1	H_d
$\bar{\mathbf{5}}_1$	$(-9, -9)$	0	2	$L_I, L_J, I, J = 1, 2, 3$
$\bar{\mathbf{5}}_2$	$(1, 1)$	2	-2	$\bar{d}_2, \bar{d}_3$
$\bar{\mathbf{5}}_3$	$(q^1_{5_3}, q^2_{5_3})$	1	0	$L_K, \bar{d}_1$

(4.92)

where there is a choice in how the different generations of leptons are distributed, which is unfixed by the anomaly cancellation conditions. The general structure of the lepton Yukawas is given by

$$Y^L \sim \begin{pmatrix} s_4 s_1 & s_4 s_2 & s_4 \\ s_4 s_1 & s_4 s_2 & s_4 \\ s_3 s_1 & s_3 s_2 & s_3 \end{pmatrix}, \tag{4.93}$$

where the singlets have charges

$$\begin{aligned} (q^1_{S_3}, q^2_{S_3}) &= -5(w^1_{5_3} - w^1_{5_2}, w^2_{5_3} - w^2_{5_2}) \\ (q^1_{S_4}, q^2_{S_4}) &= -5(w^1_{5_1} - w^1_{5_2}, w^2_{5_1} - w^2_{5_2})\,. \end{aligned} \tag{4.94}$$

The up-type and down-type Yukawa textures are given in (4.77). One choice of charges, which we will denote as model (BaEnGo3), that does not allow unwanted operators at leading order is given by:

(BaEnGo3) :

Representation	Charge	M	N	Matter
$\mathbf{10}_1$	$(-12, 13)$	1	0	$Q_1, \bar{u}_1, \bar{e}_3$
$\mathbf{10}_2$	$(-7, 3)$	1	0	$Q_2, \bar{u}_2, \bar{e}_2,$
$\mathbf{10}_3$	$(-7, -7)$	1	0	$Q_3, \bar{u}_3, \bar{e}_1$
$\bar{\mathbf{5}}_{H_u}$	$(-14, -14)$	0	-1	H_u
$\bar{\mathbf{5}}_{H_d}$	$(6, 6)$	0	1	H_d
$\bar{\mathbf{5}}_1$	$(-9, -9)$	0	2	L_1, L_2
$\bar{\mathbf{5}}_2$	$(1, 1)$	2	-2	$\bar{d}_2, \bar{d}_3$
$\bar{\mathbf{5}}_3$	$(-4, -9)$	1	0	$L_3, \bar{d}_1$

(4.95)

A scan yields that there are no models, which give a lower bound on M_{SUSY} than that derived in the case for four $\bar{\mathbf{5}}$s. This model has been chosen as it produces the same bound for M_{SUSY} as in (4.90) and does not regenerate any dimension four operators with any number of singlet insertions.

In this case the charges of the singlets required to regenerate the up-type, W_1 and W_2, down-type, W_3, and lepton Yukawa matrices, W_4, have charges

$$\begin{aligned}(q^1_{W_1}, q^2_{W_1}) &= (5, -20)\\ (q^1_{W_2}, q^2_{W_2}) &= (0, -10)\\ (q^1_{W_3}, q^2_{W_3}) &= (5, 10)\\ (q^1_{W_4}, q^2_{W_4}) &= (10, 10)\,,\end{aligned} \tag{4.96}$$

where the Yukawa matrices take the general forms (4.77) and (4.93). The singlet insertions, ω_1 and ω_2, expressed in terms of the Wolfenstein parameter, ϵ, are

$$\omega_1 = \epsilon^4, \quad \omega_2 = \epsilon^2, \quad \omega_3 = \epsilon\,. \tag{4.97}$$

As was the case in the previous textures, regenerating the lepton Yukawas also regenerates dimension five operators. The dangerous couplings with coupling constant δ^1_{112I} are given below where we have written the singlet insertions which give rise to the lowest suppression

Model	Coupling	Charge	Singlet insertions	ϵ suppression
(BaEnGo3)	$\mathbf{10}_1\mathbf{10}_1\mathbf{10}_2\overline{\mathbf{5}}_1$	$(-40, 20)$	$\omega_1^2\omega_2\omega_4^3$	ϵ^{13}
	$\mathbf{10}_1\mathbf{10}_1\mathbf{10}_2\overline{\mathbf{5}}_3$	$(-35, 20)$	$\omega_1\omega_2^3\omega_4^3 + \omega_1^2\omega_2\omega_4^2\omega_3$	$\leq \epsilon^{13}$

(4.98)

In the coupling involving $\overline{\mathbf{5}}_3$ we have taken $\omega_4 = \epsilon$, which is consistent with the lepton mass hierarchies, in the estimation of the suppression. These suppression levels are the same as those derived in the previous section and give rise to the bound on M_{SUSY} in (4.90). In the next section we examine model (BaEnGo1-3), as well as the models (Haba1) and (Haba2) of section 4.5.2 under the constraints of lepton and neutrino flavour.

Finally, we should note, extending the current analysis to more $\overline{\mathbf{5}}$ matter we find, for $\mathcal{N}_{\overline{\mathbf{5}}} = 6$ there no solutions with suitable flavour structure. It would be interesting to extend this to $\mathcal{N}_{\overline{\mathbf{5}}} = 7$ (which is the largest for this type of model without introducing exotics), however increasing the number of $\overline{\mathbf{5}}$s usually brings back proton decay operators.

4.6 Lepton and Neutrino Flavour

Let us now turn to the lepton and neutrino flavour properties of the F-theoretic FN-models of the last section. Unlike the quark sector and the lepton masses (4.29), the neutrino sector is far less experimentally constrained. Nevertheless let us state the respective ex-

perimental bounds on the masses[13]

$$\begin{aligned} \Delta m^2_{12}\left[10^{-5}\text{eV}^2\right] &= 7.54^{+0.64}_{-0.56} \\ \Delta m^2_{23}\left[10^{-3}\text{eV}^2\right] &= 2.43^{+0.18}_{-0.20} \\ \sum m_{\nu_j} &< 0.66 \text{ eV} \end{aligned} \tag{4.99}$$

and mixing angles

$$\theta_{12} = 0.59^{+0.05}_{-0.06}\,, \quad \theta_{23} = 0.72^{+0.19}_{-0.06}\,, \quad \theta_{13} = 0.15^{+0.02}_{-0.02}\,. \tag{4.100}$$

The absolute masses for the neutrinos are not known and various different hierarchies could be accommodated within these constraints. Furthermore the mixing angles are not hierarchical. Nevertheless, we show that our F-theoretic FN-models from above can accommodate the mixing angles.

The neutrino masses can arise from a so-called standard type I seesaw mechanism, for which we introduce three right-handed neutrinos that are $SU(5)$ singlets but are charged under the additional $U(1)$s. The couplings needed are

$$(Y_\nu)_{IJ}\mathbf{5}_{L_I}\mathbf{5}_{H_u}\mathbf{1}_{\nu_R^J}, \quad M_{IJ}\mathbf{1}_{\nu_R^I}\mathbf{1}_{\nu_R^J}\,, \tag{4.101}$$

where M_{IJ} is generated by singlets with a vev. Below the mass scale of the right-handed neutrinos Λ this leads to an effective neutrino mass via the Weinberg operator

$$\frac{1}{\Lambda} L_I L_J H_u H_u\,. \tag{4.102}$$

Again this operator can be forbidden by the additional $U(1)$ symmetries, but regenerated by appropriate singlet insertions. Note that the charges of the right-handed neutrinos do not enter the effective Weinberg operator and are not relevant for the discussion of neutrino mixing. For the flavour models in section 4.5, the three distinct phenomenological scenarios are studied in turn in the following.

[13] These are best-fit values and 3σ allowed ranges for neutrino masses with a normal hierarchy ($m_1 < m_2 < m_3$). The sum of neutrino masses and the other values can be found in the Neutrino mass, mixing and oscillations chapter of [15].

4.6.1 Models (Haba1) and (Haba2)

Including the structure of the neutrino Yukawa matrix arising from the Weinberg operators, the models from section 4.5.2 have the following Yukawa structures

$$\begin{aligned} Y^u_{\text{Haba}} &\sim \begin{pmatrix} \epsilon^8 & \epsilon^6 & \epsilon^4 \\ \epsilon^6 & \epsilon^4 & \epsilon^2 \\ \epsilon^4 & \epsilon^2 & 1 \end{pmatrix} \qquad Y^d_{\text{Haba}} \sim \begin{pmatrix} \epsilon^4 & \epsilon^4 & \epsilon^4 \\ \epsilon^2 & \epsilon^2 & \epsilon^2 \\ 1 & 1 & 1 \end{pmatrix} \\ Y^L &\sim \begin{pmatrix} \epsilon^{4+a} & \epsilon^{2+a} & \epsilon^a \\ \epsilon^{4+a} & \epsilon^{2+a} & \epsilon^a \\ \epsilon^4 & \epsilon^2 & 1 \end{pmatrix} \qquad M_\nu \sim \begin{pmatrix} \kappa_1 & \kappa_1 & \kappa_2 \\ \kappa_1 & \kappa_1 & \kappa_2 \\ \kappa_2 & \kappa_2 & \kappa_1\kappa_2 + \kappa_1^3 \end{pmatrix}, \end{aligned} \tag{4.103}$$

where the charges of singlets regenerating entries in the neutrino Yukawa matrices are given by

$$\begin{aligned} &\text{(Haba1)}: \qquad q_{K_1} = (-10,-10),\ q_{K_2} = (-20,-20) \\ &\text{(Haba2)}: \qquad q_{K_1} = (0,-10),\ q_{K_2} = (0,-20)\,. \end{aligned} \tag{4.104}$$

Note also that despite the fact that the quark mixing are those in Haba [182] (and BaEnGo [183] in section 4.6.2) the lepton and neutrino textures are distinct from the models in the literature.

For each choice of hierarchical singlet scalings, we scan over the $O(1)$ coefficients in front of each coupling and identify experimentally viable masses and mixings using the `Mathematica` package `Mixing Parameter Tools` [186]. For each of the three different scalings we find consistent mixing angles with suitable choices for the $O(1)$ coefficients and mass hierarchies that are consistent with (4.29). We allow the $O(1)$ coefficients, z, for the Yukawa matrices to be within the range

$$0.8 < |z| < 1.2\,, \tag{4.105}$$

where in the case of the lepton Yukawa matrices z is complex.

For models (Haba1), (Haba2) with $a = 0.05, \kappa_1 = 0.1$ and $\kappa_2 = 0.3$ one choice of $O(1)$ coefficients for the lepton and neutrino Yukawa matrices which give consistent mixing angles is given by

$$\begin{aligned} Y^L &\sim \begin{pmatrix} 1.00\epsilon^{4.05} & -(0.68+0.97i)\epsilon^{2.05} & (0.30-0.78i)\epsilon^{0.05} \\ (-0.89+0.54i)\epsilon^{4.05} & -(0.14+1.13i)\epsilon^{2.05} & -(0.43+1.10i)\epsilon^{0.05} \\ (0.64+0.63i)\epsilon^4 & -(0.12+0.97i)\epsilon^2 & -0.81-0.10i \end{pmatrix} \\ M_\nu &\sim \begin{pmatrix} 1.17\kappa_1 & 1.13\kappa_1 & 0.92\kappa_2 \\ 1.13\kappa_1 & 0.92\kappa_1 & 0.83\kappa_2 \\ 0.92\kappa_2 & 0.83\kappa_2 & 0.96(\kappa_1\kappa_2+\kappa_1^3) \end{pmatrix}. \end{aligned} \tag{4.106}$$

This choice for a means that s_2 in these models is a $O(1)$ number as was assumed in the calculation of the bound for M_{SUSY} in section 4.5.2. This set of matrices gives the following mass ratios and mixing angles

$$\begin{aligned} \theta_{12} = 0.60, \quad \theta_{13} = 0.20, \quad \theta_{23} = 0.72 \\ m_\tau : m_\mu : m_e = 1 : 0.88\epsilon^2 : 0.63\epsilon^4 \,, \end{aligned} \tag{4.107}$$

which are consistent with the constraints in (4.29) and (4.100).

More interestingly, one can take $a = 1$ and still find $O(1)$ coefficients which give rise to good mixing angles and lepton mass hierarchies. This choice for a improves the bound on M_{SUSY} in (4.74) to

$$M_{SUSY} \geq 10^{-10} M_{GUT} \,, \tag{4.108}$$

as now $s_2 = 0.22$. In this case the other singlets take values $\kappa_1 = 0.7, \kappa_2 = 0.7$ and the Yukawa matrices are given by

$$\begin{aligned} Y^L &\sim \begin{pmatrix} 1.00\epsilon^5 & (-0.79+0.27i)\epsilon^3 & (0.72-0.61i)\epsilon \\ -(0.70+0.87i)\epsilon^5 & (-0.86+0.57i)\epsilon^3 & (0.99+0.01i)\epsilon \\ (0.98-0.30i)\epsilon^4 & (0.32-1.08i)\epsilon^2 & 0.34-0.80i \end{pmatrix} \\ M_\nu &\sim \begin{pmatrix} 0.90\kappa_1 & 0.98\kappa_1 & 1.07\kappa_2 \\ 0.98\kappa_1 & 1.16\kappa_1 & 0.89\kappa_2 \\ 1.07\kappa_2 & 0.89\kappa_2 & 1.00(\kappa_1\kappa_2+\kappa_1^3) \end{pmatrix} . \end{aligned} \tag{4.109}$$

The mixing angles and mass hierarchies are in very good agreement with those in (4.100) and (4.29)

$$\begin{aligned} \theta_{12} = 0.56, \quad \theta_{13} = 0.14, \quad \theta_{23} = 0.71 \\ m_\tau : m_\mu : m_e = 1 : 0.68\epsilon^2 : 1.02\epsilon^5 \,. \end{aligned} \tag{4.110}$$

4.6.2 Models (BaEnGo1)–(BaEnGo3)

For the matter distributions in the F-theoretic FN-models (BaEnGo1) and (BaEnGo2) of section 4.5.3 we find that the leptons and neutrinos are different from the models in [183], and are given by

$$\begin{aligned} Y^u_{\text{BaEnGo}} &\sim \begin{pmatrix} \epsilon^8 & \epsilon^6 & \epsilon^4 \\ \epsilon^6 & \epsilon^4 & \epsilon^2 \\ \epsilon^4 & \epsilon^2 & 1 \end{pmatrix} \quad Y^d_{\text{BaEnGo}} \sim \begin{pmatrix} \epsilon^5 & \epsilon^4 & \epsilon^4 \\ \epsilon^3 & \epsilon^2 & \epsilon^2 \\ \epsilon & 1 & 1 \end{pmatrix} \\ Y^L &\sim \begin{pmatrix} \epsilon^5 & \epsilon^3 & \epsilon^1 \\ \epsilon^5 & \epsilon^3 & \epsilon^1 \\ \epsilon^5 & \epsilon^3 & \epsilon^1 \end{pmatrix} \qquad M_\nu \sim \begin{pmatrix} \kappa_1 & \kappa_1 & \kappa_1 \\ \kappa_1 & \kappa_1 & \kappa_1 \\ \kappa_1 & \kappa_1 & \kappa_1 \end{pmatrix} , \end{aligned} \tag{4.111}$$

where the singlets have charges

$$(\text{BaEnGo1}):\ q_{K_2}=(-10,-10),\quad (\text{BaEnGo2}):q_{K_2}=(0,-10)\,. \tag{4.112}$$

Likewise for model (BaEnGo3) we get

$$\begin{aligned} Y^u_{\text{BaEnGo}} &\sim \begin{pmatrix} \epsilon^8 & \epsilon^6 & \epsilon^4 \\ \epsilon^6 & \epsilon^4 & \epsilon^2 \\ \epsilon^4 & \epsilon^2 & 1 \end{pmatrix} \qquad Y^d_{\text{BaEnGo}} \sim \begin{pmatrix} \epsilon^5 & \epsilon^4 & \epsilon^4 \\ \epsilon^3 & \epsilon^2 & \epsilon^2 \\ \epsilon & 1 & 1 \end{pmatrix} \\ Y^L &\sim \begin{pmatrix} \epsilon^{4+c} & \epsilon^{2+c} & \epsilon^c \\ \epsilon^{4+c} & \epsilon^{2+c} & \epsilon^c \\ \epsilon^5 & \epsilon^3 & \epsilon \end{pmatrix} \qquad M_\nu \sim \begin{pmatrix} \kappa_1 & \kappa_1 & \kappa_1\kappa_2 \\ \kappa_1 & \kappa_1 & \kappa_1\kappa_2 \\ \kappa_1\kappa_2 & \kappa_1\kappa_2 & \kappa_1\kappa_2^2 \end{pmatrix}, \end{aligned} \tag{4.113}$$

where

$$q_{K_1}=(-10,-10)\,,\quad q_{K_2}=(-5,0)\,. \tag{4.114}$$

For (BaEnGo1) and (BaEnGo2) the following $O(1)$ coefficients in the lepton and neutrino Yukawa matrices

$$\begin{aligned} Y^L &\sim \begin{pmatrix} (1.09-0.04i)\epsilon^5 & (-1.11+0.42i)\epsilon^3 & (-0.13-0.91i)\epsilon \\ (0.19+1.05i)\epsilon^5 & (-0.88+0.31i)\epsilon^3 & (1.04-0.52i)\epsilon \\ (-0.21+0.93i)\epsilon^5 & (-0.24+1.00i)\epsilon^3 & 0.97+0.10i\epsilon \end{pmatrix} \\ M_\nu &\sim \begin{pmatrix} 0.81\kappa_1 & 1.10\kappa_1 & 1.03\kappa_1 \\ 1.10\kappa_1 & 1.11\kappa_1 & 1.05\kappa_1 \\ 1.03\kappa_1 & 1.05\kappa_1 & 1.01\kappa_1 \end{pmatrix} \end{aligned} \tag{4.115}$$

with $\kappa_1 = 0.22$ result in PMNS mixing angles and lepton mass hierarchies, which are consistent with the phenomenological constraints (4.29) and (4.100)

$$\begin{aligned} \theta_{12}=0.60,\quad \theta_{13}=0.18,\quad \theta_{23}=0.69 \\ m_\tau : m_\mu : m_e = 1 : 0.92\epsilon^2 : 0.59\epsilon^5\,. \end{aligned} \tag{4.116}$$

This model fits precisely the anarchy models in [187].

Finally, consider FN-model (BaEnGo3), where in addition to the quark Yukawa matrices in (4.113) one finds the following set of lepton and neutrino Yukawa matrices for $c = 1, \kappa_1 = 0.2$ and $\kappa_2 = 0.4$

$$\begin{aligned} Y^L &\sim \begin{pmatrix} (-0.92+0.08i)\epsilon^5 & (1.06+0.36i)\epsilon^3 & (0.69-0.57i)\epsilon \\ (0.89-0.33i)\epsilon^5 & (1.00+0.10i)\epsilon^3 & (0.30-0.77i)\epsilon \\ (0.38+0.82i)\epsilon^5 & (1.02+0.19i)\epsilon^3 & (0.53+0.61i)\epsilon \end{pmatrix} \\ M_\nu &\sim \begin{pmatrix} 0.82\kappa_1 & 0.88\kappa_1 & 0.85\kappa_1\kappa_2 \\ 0.88\kappa_1 & 0.94\kappa_1 & 1.10\kappa_1\kappa_2 \\ 0.85\kappa_1\kappa_2 & 1.10\kappa_1\kappa_2 & 0.93\kappa_1\kappa_2^2 \end{pmatrix}. \end{aligned} \tag{4.117}$$

The resulting mixing angles and lepton mass ratios are

$$\begin{aligned} \theta_{12} = 0.61, \quad \theta_{13} = 0.16, \quad \theta_{23} = 0.71 \\ m_\tau : m_\mu : m_e = 1 : 0.92\epsilon^2 : 0.97\epsilon^4 \,, \end{aligned} \tag{4.118}$$

which again are phenomenologically sound.

4.7 Geometric Realisation

In this section we discuss how some of the phenomenologically viable models can be realised geometrically. For the case of the two $U(1)$ models, some of the solutions in section 4.4 can be realised in terms of a general cubic in $\mathbb{P}^2$. For the F-theoretic FN-models, we have not determined a geometric construction, however we provide the necessary fiber types, that realise the charge patterns underlying these flavour models.

4.7.1 Single $U(1)$ Models

For one $U(1)$ there is exactly one model that is consistent, denoted by I.1.4.a in table 4.1. All other models bring back in one way or another the dimension four or five proton decay operators. In addition the single $U(1)$ models have very limited scope with respect to flavour. Nevertheless to geometrically engineer the solution I.1.4.a one has to consider the codimension one fiber type $I_5^{(01)}$. As one can see however, the charges in the model are wider separated than in known constructions. We will focus our attention on the phenomenologically more interesting multiple $U(1)$ models.

4.7.2 Two $U(1)$ Models

In section 4.4, the charge spectrum of the four models, with two $U(1)$ symmetries, which solved the anomaly cancellation conditions and forbid dangerous proton decay operators were detailed. In this section we show how three of these models can be constructed by considering elliptic fibrations with two additional rational sections, described by enhancing the singularity type of the general cubic in $\mathbb{P}^2$. The elliptically fibered Calabi–Yau four-fold, as a hypersurface in an ambient five-fold, is given by the following cubic equation [133]

$$w(s_1 w^2 + s_2 wx + s_3 x^2 + s_5 wy + s_6 xy + s_8 y^2) + \prod_{i=1}^{3}(a_i x + b_i y) = 0 \,, \tag{4.119}$$

where $[w : x : y]$ are projective coordinates in $\mathbb{P}^2$. This fibration has three rational sections given by

$$\sigma_0 : [0 : -b_1 : a_1], \qquad \sigma_1 : [0 : -b_2 : a_2], \qquad \sigma_2 : [0 : -b_3 : a_3] \,. \tag{4.120}$$

Section	Line bundle
$s_{1,j}$	$\mathcal{O}(-6K_B - 2[a_1] - 2[a_2] - 2[a_3] - 3[s_8] - jS_G)$
$s_{2,j}$	$\mathcal{O}(-4K_B - [a_1] - [a_2] - [a_3] - 2[s_8] - jS_G)$
$s_{3,j}$	$\mathcal{O}(-2K_B - [s_8] - jS_G)$
$s_{5,j}$	$\mathcal{O}(-3K_B - [a_1] - [a_2] - [a_3] - [s_8] - jS_G)$
$s_{6,j}$	$\mathcal{O}(-K_B - jS_G)$
$s_{8,j}$	$\mathcal{O}([s_8] - jS_G)$
$a_{1,j}$	$\mathcal{O}([a_1] - jS_G)$
$a_{2,j}$	$\mathcal{O}([a_2] - jS_G)$
$a_{3,j}$	$\mathcal{O}([a_3] - jS_G)$
$b_{1,j}$	$\mathcal{O}(K_B + [a_1] + [s_8] - jS_G)$
$b_{2,j}$	$\mathcal{O}(K_B + [a_2] + [s_8] - jS_G)$
$b_{3,j}$	$\mathcal{O}(K_B + [a_3] + [s_8] - jS_G)$

Table 4.6: Classes of the sections for the elliptic fibration realised in terms of a general cubic in $\mathbb{P}^2$.

By expanding the coefficients above, which we denote generally as c_i, along a coordinate in the base, z, as

$$c_i = \sum_{j=1}^{\infty} c_{i,j} z^j \,, \tag{4.121}$$

singularities can be tuned along the locus $z = 0$. The coefficients $s_{i,j}, a_{i,j}$ and $b_{i,j}$ are sections of the following holomorphic line bundles over the base shown in table 4.6, where K_B is the pullback of the canonical class of the base, B, and S_G is the class of z.

As we are interested in $SU(5)$ GUTs we will only consider models which realise I_5 singularities. To determine this, we apply Tate's algorithm to the general cubic. Resolving the I_5 singularities introduces four exceptional curves F_m, where $m = 1, \cdots, 4$, into the fiber. The fibration of each F_m over the singular locus z gives a divisor D_{F_m}. With each rational section, in addition to the zero-section σ_0, we can define the Shioda map, $S(\sigma_\alpha)$ such that

$$S(\sigma_\alpha) \cdot_Y F_i = 0 \,, \qquad i = (0, m) \,, \tag{4.122}$$

Here $\cdot_Y$ denotes that the intersection is taken in the four-fold Y. The Shioda map constructs from each rational section a divisor which corresponds to the generator of the $U(1)$ symmetry. The $U(1)$ charges of matter are found by intersecting $S(\sigma_\alpha)$ with the matter curves obtained from the splitting of the F_i in codimension two. The resolutions and intersections carried out in this thesis are computed using the `Mathematica` package `Smooth` [66].

Here, we label our models as in [108], where the vanishing orders, n_{c_i}, are given in the

order

$$(n_{s_1}, n_{s_2}, n_{s_3}, n_{s_5}, n_{s_6}, n_{s_8}, n_{a_1}, n_{b_1}, n_{a_2}, n_{b_2}, n_{a_3}, n_{b_3})\,. \tag{4.123}$$

Furthermore it will be necessary to consider so-called non-canonical models, where the enhancement of the discriminant to $O(z^5)$, occurs not by simply specifying the vanishing order of the coefficients, but by subtle cancellations between the coefficients, which are non-trivially related see e.g. [64,107,108]. In the models we consider here the enhancement to I_5 requires solving

$$AB - CD = 0\,, \tag{4.124}$$

in terms of the coefficients of the hypersurface equation. This has to be solved over the coordinate ring of the base of the elliptic fibration, which is a unique factorisation domain. Applying the standard Tate's algorithm in this context [64, 107, 108] the enhancement is obtained as a so-called non-canonical solution in terms of sections ξ_i

$$A = \xi_1\xi_2, \quad B = \xi_3\xi_4, \quad C = \xi_1\xi_3, \quad D = \xi_2\xi_4\,. \tag{4.125}$$

In addition to specifying the vanishing order, the labelling of the non-canonical models also includes the specialisation of the coefficients in terms of ξ_i, which is given underneath the vanishing orders.

The models which realise the solutions in section 4.4 are given in table 4.7. For each model the fiber type, vanishing orders and non-canonical specialisation is given along with the charges of the **10** and $\bar{\mathbf{5}}$ matter in the model. The equations for the matter loci referred to in the table are given below:

$$\xi_2\xi_3\xi_4^2 s_{3,0} + \xi_1\xi_4(\xi_3^2 a_{3,1} + \xi_2^2 a_{1,0} b_{2,0} s_{5,0} - \xi_2\xi_3 s_{6,1}) - \xi_1^2(\xi_3^2 b_{3,1} + \xi_2^2 b_{1,0} b_{2,0} s_{5,0} - \xi_2\xi_3 s_{8,1}) = 0 \tag{4.126}$$

$$a_{1,0}^2 b_{2,0} b_{3,0} s_{5,0} + b_{1,0} s_{6,0}^2 - a_{1,0} s_{6,0} s_{8,0} = 0 \tag{4.127}$$

$$\begin{aligned}\xi_4^2(\xi_3^2 s_{1,1} - \xi_2\xi_3 s_{2,1} + \xi_2^2 s_{3,0}) - \xi_1\xi_4(\xi_2^2 a_{1,0} a_{3,0} b_{2,0} + \xi_3^2 s_{5,1} - \xi_2\xi_3 s_{6,1}) \\ + \xi_1^2\xi_3(-\xi_2 a_{1,0} b_{2,0} b_{3,0} + \xi_3 s_{8,0}) = 0\end{aligned} \tag{4.128}$$

These models provide new charge configurations that have thus far not been obtained in the literature.

Each of the models in table 4.7 have additional charged matter, which is not present in the corresponding solutions given in section 4.4, which can be forbidden in the base. As an aside: the charges for the non-canonical model $(3, 2, 1, 1, 0, 0, 0, 0, 1, 0, 0, 0)$ under the first $U(1)$ is reversed to those in solution II.1.6.a. This can be further seen by the fact that the fiber type of this model is not one considered in the analysis in section 4.4, as was noted earlier. This is justified as the charges in an $I_5^{(i|j|k)}$ model are the same as those

in $I_5^{(i|jk)}$ except with the sign of one of the $U(1)$s reversed. As the anomaly cancellation conditions are unaffected by global rescalings of the $U(1)$ charges, the model in the table solves the anomaly cancellation condition as in solution II.1.6.a.

4.7.3 Fibers for Models (Haba1) and (Haba2)

The F-theoretic FN-models in section 4.5.2 have particularly nice phenomenology in addition to satisfying all anomaly constraints and absence of dangerous couplings. The charges for those models are within the classification of the F-theory charges [32], however so far no concrete geometric realisation is known. To guide the construction of these geometries, we now provide the possible fiber types necessary for these models in the following for the models in table 4.4.

The models are based on $I_5^{(02|1)}$, where the two additional sections σ_1 and σ_2 generate the two extra $U(1)$ symmetries. For simplicity we discuss the model (Haba2) in table 4.4 – for model (Haba1) the only change is that the two extra sections have the same charges, for the $\bar{\mathbf{5}}$ matter loci, and thus have the same configurations. The fibers in codimension two, including the configuration of the sections is shown in figure 4.4. We shall refrain from providing the details of this result and refer the reader to [32], where a comprehensive discussion of these fibers was obtained.

The main difficulty in constructing this class of models is that the charges are separated, e.g. the $\bar{\mathbf{5}}$ charges have a range from $q_2 = -14$ to 6, i.e. $q_{\bar{\mathbf{5}}}^{max} - q_{\bar{\mathbf{5}}}^{min} = 20$, which is in current algebraic constructions not observed. Generically the charge differences are $q_{\bar{\mathbf{5}}}^{max} - q_{\bar{\mathbf{5}}}^{min} = 10$, with the only example, known to us, with this difference given by 15 is a toric construction obtained in [97]. It would be very interesting to systematically search for models with wider separation of charges. One complication is of course, that the codimension two fibers will have to be more and more wrapped, i.e. there will be components in the codimension two fibers that are contained within the section, as shown in figure 4.4.

4.8 Discussion and Outlook

We have shown that there are viable models in the class of F-theory charge configurations from the classification in [32], which satisfy all consistency requirements (A1.)−(A5.) and (C1.)−(C7.), and have realistic flavour physics, however these are very scarce.

We considered one or two $U(1)$ symmetries, although our analysis can be easily extended

Solution	Fiber	Vanishing Orders	Matter Locus	Matter
II.1.6.a (Sign of charges under first $U(1)$ is reversed)	$I_{5,nc}^{(1\|0\|2)}$	(3,2,1,1,0,0,0,0,1,0,0,0) $[-,-,-,-,\xi_1\xi_3,\xi_3\xi_4,-,-,-,-,\xi_1\xi_2,\xi_2\xi_4]$	ξ_1 ξ_3 ξ_2 $a_{1,0}$ $b_{2,0}$ $\xi_4 a_{1,0}-\xi_1 b_{1,0}$ $\xi_1\xi_3 a_{2,0}-b_{2,0}s_{3,0}$ $\xi_1^2\xi_3^2 s_{1,0}-\xi_1\xi_3 s_{2,0}s_{5,0}+s_{3,0}s_{5,0}^2$ (4.126)	$\mathbf{10}_{2,-2}\oplus\overline{\mathbf{10}}_{-2,2}$ $\mathbf{10}_{2,3}\oplus\overline{\mathbf{10}}_{-2,-3}$ $\mathbf{5}_{6,-1}\oplus\overline{\mathbf{5}}_{-6,1}$ $\mathbf{5}_{-4,-6}\oplus\overline{\mathbf{5}}_{4,6}$ $\mathbf{5}_{1,-6}\oplus\overline{\mathbf{5}}_{-1,6}$ $\mathbf{5}_{6,4}\oplus\overline{\mathbf{5}}_{-6,-4}$ $\mathbf{5}_{1,4}\oplus\overline{\mathbf{5}}_{-1,-4}$ $\mathbf{5}_{1,-1}\oplus\overline{\mathbf{5}}_{-1,1}$ $\mathbf{5}_{-4,-1}\oplus\overline{\mathbf{5}}_{4,1}$
II.1.6.b	$I_5^{(0\|2\|1)}$	(3,2,1,1,0,1,0,1,1,0,0,0)	$s_{6,0}$ $a_{1,0}$ $a_{3,0}$ $b_{2,0}$ $b_{3,0}$ $b_{2,0}s_{3,0}-a_{2,0}s_{6,0}$ $s_{3,0}s_{5,0}^2-s_{6,0}s_{2,0}s_{5,0}+s_{1,0}s_{6,0}^2$ (4.127)	$\mathbf{10}_{-2,1}\oplus\overline{\mathbf{10}}_{2,-1}$ $\mathbf{5}_{-6,-7}\oplus\overline{\mathbf{5}}_{6,7}$ $\mathbf{5}_{4,-2}\oplus\overline{\mathbf{5}}_{-4,2}$ $\mathbf{5}_{-1,-7}\oplus\overline{\mathbf{5}}_{1,7}$ $\mathbf{5}_{-6,-2}\oplus\overline{\mathbf{5}}_{6,2}$ $\mathbf{5}_{-1,3}\oplus\overline{\mathbf{5}}_{1,-3}$ $\mathbf{5}_{-1,-2}\oplus\overline{\mathbf{5}}_{1,2}$ $\mathbf{5}_{4,3}\oplus\overline{\mathbf{5}}_{-4,-3}$
II.1.6.c	$I_{5,nc}^{(0\|2\|1)}$	(2,1,1,1,0,1,0,1,1,0,0,0) $[\xi_1\xi_2,\xi_1\xi_3,-,\xi_2\xi_4,\xi_3\xi_4,-,-,-,-,-,-,-]$	ξ_3 ξ_4 $a_{1,0}$ $a_{3,0}$ $b_{2,0}$ $b_{3,0}$ $\xi_3\xi_4^2 a_{2,0}-b_{2,0}\xi_4 s_{3,0}+\xi_1 a_{1,0}a_{3,0}b_{2,0}^2)$ $\xi_3^2\xi_4 b_{1,0}+\xi_2 a_{1,0}^2 b_{2,0}b_{3,0}-\xi_3 a_{1,0}s_{8,0}$ (4.128)	$\mathbf{10}_{-2,1}\oplus\overline{\mathbf{10}}_{2,-1}$ $\mathbf{10}_{3,1}\oplus\overline{\mathbf{10}}_{-3,-1}$ $\mathbf{5}_{-6,-7}\oplus\overline{\mathbf{5}}_{6,7}$ $\mathbf{5}_{4,-2}\oplus\overline{\mathbf{5}}_{-4,2}$ $\mathbf{5}_{-1,-7}\oplus\overline{\mathbf{5}}_{1,7}$ $\mathbf{5}_{-6,-2}\oplus\overline{\mathbf{5}}_{6,2}$ $\mathbf{5}_{-1,3}\oplus\overline{\mathbf{5}}_{1,-3}$ $\mathbf{5}_{4,3}\oplus\overline{\mathbf{5}}_{-4,-3}$ $\mathbf{5}_{-1,-2}\oplus\overline{\mathbf{5}}_{1,2}$

Table 4.7: Geometric realisations of the models with two $U(1)$s corresponding to the solutions II.1.6.a, II.1.6.b and II.1.6.c. The charges under the first $U(1)$ in solution II.1.6.a are reversed with respect to those in the model.

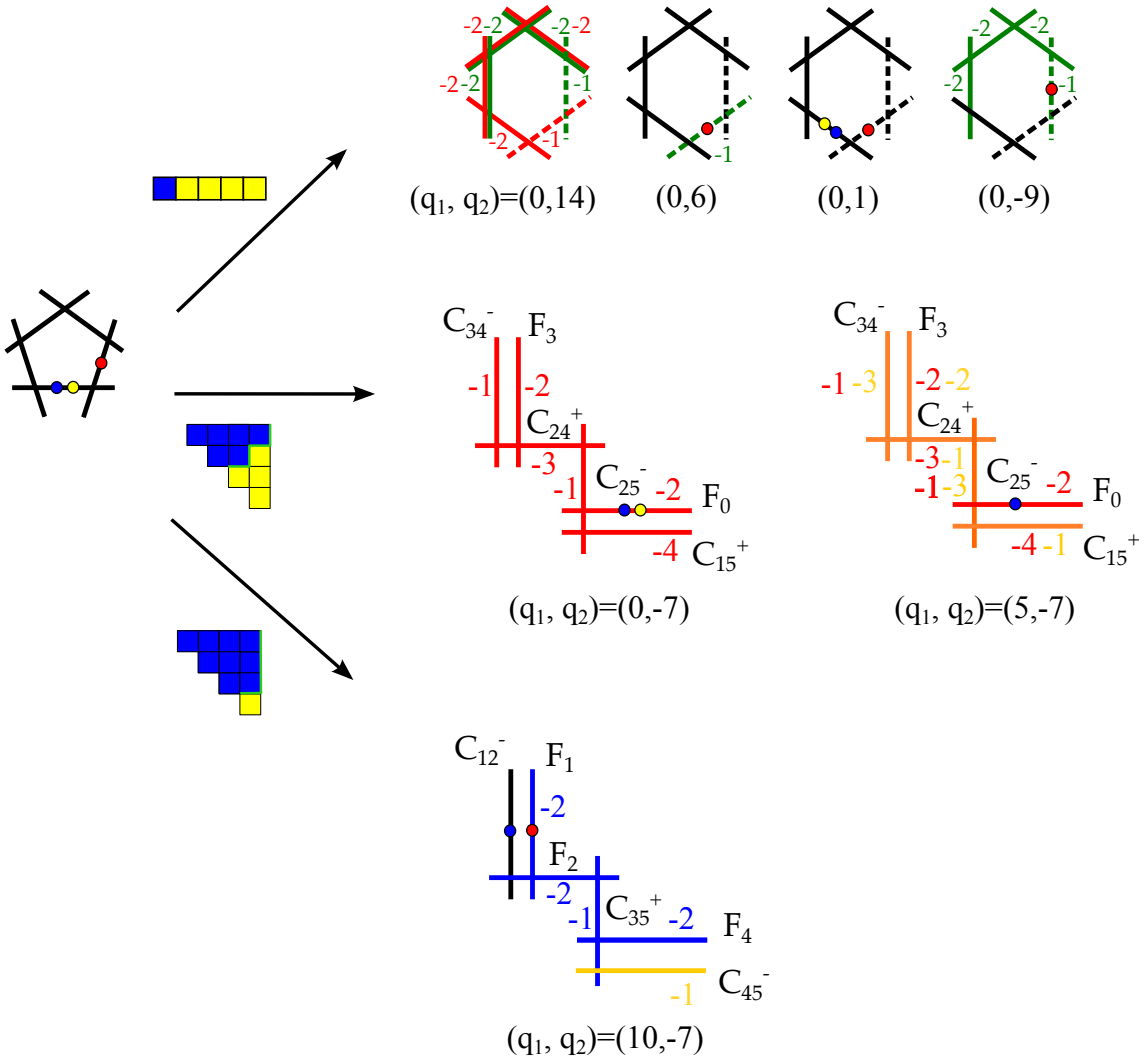

Figure 4.4: Fibers for the F-theoretic FN-model (Haba2) of table 4.4. The codimension one type $I_5^{(02|1)}$ is as in figure 4.3 (up to permutation of the two extra sections), with the zero-section shown in blue. The nomenclature is as in [32]: The codimension two fibers realising the $\bar{\mathbf{5}}$ matter (I_6) as well as $\mathbf{10}$ matter (I_1^* fibers) are shown together with their charges. The coloring correspond to the wrapping of the fibers, and the labels along the wrapped components correspond to the degrees of the normal bundle, which in turn determine the charges. For the $\bar{\mathbf{5}}$ matter, the blue and yellow sections have to have the same configurations, as the charge is zero. These are shown in terms of green coloring. The blue/yellow colored representation graphs (box graphs) indicate the phases of the respective resolution type, see [70].

to three or more $U(1)$s. For single $U(1)$ models there is one solution, which does not regenerate any of the dangerous couplings at the same order as the Yukawa couplings, however single $U(1)$ models have very limited scope with regards to FN-type modeling. For two $U(1)$s we studied two sets of solutions: one which solves all the constraints and has an explicit geometric construction – albeit coming short on the flavour physics. The second class of solutions have realistic flavour textures generated by an FN-mechanism, which we studied in both quark and lepton sectors, however their geometric construction is unknown – these were denoted by (Haba1)-(Haba2) and (BaEnGo1)-(BaEnGo3), according to the Yukawa textures for the quarks. We provided the required fiber types for (Haba1) and (Haba2) and hope that our result gives a guidance to the geometric efforts to construct more elaborate F-theory compactifications. It would be very exciting to find a geometric construction of these models summarised in table 4.4. This includes the construction of the elliptic fibration with two rational sections as well as the G-flux, in particular also the hypercharge flux, that induces the necessary matter distributions as detailed by the M and N values. Furthermore, combining our general insights from the structure of the elliptic fiber with recent advances on the understanding of the base of the fibration of four-folds [188,189] would lead to a very powerful way to constrain the set of phenomenologically viable F-theory vacua.

Chapter 5

M5-branes and Compactifications

In the latter part of this thesis the focal point shifts to the non-perturbative limit of type IIA string theory, M-theory. The absence of a dimensionless coupling constant in M-theory has greatly hindered progress in understanding the eleven-dimensional description as one can not make use of perturbation theory. This is associated with the fact that the fundamental object in M-theory is not the string but instead an object of one greater space-time dimension; a membrane. In this chapter we introduce both the membrane (M2-brane) and its magnetic dual, the M5-brane, however the latter shall be the centerpiece.

The low energy effective theory of M-theory is eleven-dimensional supergravity whose bosonic field content is the metric g and a three-form potential C_3. The eleven-dimensional supersymmetry algebra with a Majorana spinor Q_α, which has 32 real components, is given by [190]

$$\{Q_\alpha, Q_\beta\} = (\gamma^m)_{\alpha\beta} P_m + (\gamma^{mn})_{\alpha\beta} Z_{mn} + (\Gamma^{mnpqr})_{\alpha\beta} Z_{mnpqr}\,, \quad m, n = 1, \cdots, 11\,, \quad (5.1)$$

where P_m is the generator of translations and Z_{mn}, Z_{mnpqr} are central charges. The presence of central charges in the supersymmetry algebra means the theory can contain topological BPS solitons. In order to preserve Lorentz invariance of the index structure these states must extend two or five spatial dimensions [191]. These solitons are called the M2-brane and M5-brane, which couple to the potential C_3.

Before discussing these M-branes directly let us recall that M-theory reduced on a circle is type IIA string theory. As a result the fundamental string and branes in type IIA all have an origin in eleven dimensions which were determined in [192,193]. Here we summarise the simplest cases arising from the reduction of the M2-brane and M5-brane to ten dimensions and refer to [194,7] for a more complete discussion. An M2-brane wrapped on the M-theory circle is reduced to an object spanning two space-time dimensions which corresponds to the fundamental string. In the alternative scenario, an unwrapped M2-brane descends to

a D2-brane in type IIA. For the M5-branes the wrapped and unwrapped configurations reduce to D4-branes and NS5-branes, respectively.

The M2-brane couples electrically to the three-form potential in M-theory and the action for a single M2-brane is given by [11]

$$S_{M_2} = T_{M_2} \int d^3\xi \sqrt{|G_{IJ}|} + T_{M_2} \int C_{IJK} \,, \tag{5.2}$$

where T_{M_2} is the M2-brane tension and G_{IJ} is the induced metric on the world-volume of the brane and C_{IJK} is the pull-back of the three-form flux onto the brane world-volume. The M2-brane is maximally supersymmetric in three-dimensions and so preserves $\mathcal{N} = 8$ supersymmetry, i.e. 16 supercharges. The theory of multiple M2-branes, whose bosonic field content consists of a gauge field and eight scalars transforming in the fundamental of the $SO(8)$ R-symmetry of the theory, remained largely mysterious for a long time. However, in the last decade two actions have been proposed for multiple M2-branes. The first action determined by Bagger–Lambert and Gustavsson (BLG) [195, 196] made use of 3-algebras and accurately describes the interacting theory of two M2-branes. This was subsequently followed by a proposal from Aharony–Bergman–Jafferis–Maldacena (ABJM) [197] for an arbitrary number of M2-branes in an orbifold background.

The object which couples magnetically to the three-form potential is the M5-brane [198]. Due to many reasons, which will be mentioned in section 5.1, the theory for multiple M5-branes has evaded discovery. It is an interacting superconformal theory which preserves two chiral supercharges [199, 9], whose abelian equations of motion are known. Despite our limited access to the interacting theory many interesting correspondences have arisen from studying the compactifications of the six-dimensional theory to lower dimensions. In this chapter we give an introduction to known M5-brane compactifications and the related correspondences as motivations for the work carried out in chapter 6.

5.1 The Mysterious Theory of M5-branes

The superconformal algebras were classified by Nahm in [200]. He found that only in six dimensions and lower can the supersymmetry algebra be extended to a superconformal algebra. From Nahm's classification in six dimensions one can preserve maximal supersymmetry and half maximal, these correspond to 16 and 8 supercharges, respectively. Furthermore, the supercharges must be of the same chirality so the possible superconformal field theories preserve $\mathcal{N} = (2,0)$ or $\mathcal{N} = (1,0)$ supersymmetry. The 6d $\mathcal{N} = (2,0)$ theories are classified by a simply laced compact Lie algebra $\mathfrak{g}$ i.e. of ADE-type [9]. A clas-

sification of the 6d $\mathcal{N} = (1,0)$ SCFTs was recently determined in [46,47] based on F-theory compactifications. In this thesis we shall only discuss the maximally supersymmetric case.

The interacting theory of multiple M5-branes is a 6d $\mathcal{N} = (2,0)$ SCFT, where the Lie algebra associated to a stack of k M5-branes is A_{k-1}. The equations of motion for a single M5-brane were determined in [201, 202]. The theory consists of a two-form $\mathcal{B}_{\underline{AB}}$ with self-dual field strength H, five scalars $\Phi^{\widehat{A}}$ and a symplectic-Majorana fermion $\rho^{\widehat{m}}$. The supersymmetry variations, using the index notation in appendix C, are given by

$$\begin{aligned} \delta\mathcal{B}_{\underline{AB}} &= -\epsilon^{\widehat{m}}\Gamma_{\underline{AB}}\rho_{\widehat{m}} \\ \delta\Phi^{\widehat{m}\widehat{n}} &= -4\epsilon^{[\widehat{m}}\rho^{\widehat{n}]} - \Omega^{\widehat{m}\widehat{n}}\epsilon^{\widehat{r}}\,\rho_{\widehat{r}} \\ \delta\rho^{\widehat{m}} &= \frac{1}{48}H^{+}_{\underline{\mu\nu\sigma}}\Gamma^{\underline{\mu\nu\sigma}}\epsilon^{\widehat{m}} + \frac{1}{4}\partial\!\!\!/\Phi^{\widehat{m}\widehat{n}}\epsilon_{\widehat{n}}\,, \end{aligned} \tag{5.3}$$

where $H^{\pm} = \frac{1}{2}(1 \pm *)H$. The supersymmetry algebra closes on the equations motion for the free fields.

The presence of the self-dual field strength has made constructing an action for a single M5-brane a difficult task as the natural coupling

$$\int H \wedge *H\,, \tag{5.4}$$

vanishes. However, a Dirac–Born–Infield type action for the abelian self-dual three-form was constructed in [203] by sacrificing manifest 6d Lorentz invariance, which was later covariantised in [204]. Building on this progress a complete action for the single M5-brane was later obtained in [205, 206]. More recently an alternative action for the single M5-brane was proposed in [207, 208] employing the 3-algebra construction of the BLG action for multiple M2-branes.

Despite this progress, the non-abelian theory for multiple M5-branes is still unknown. The non-abelianisation of Maxwell theory and matter was first introduced in [209], who first developed the notion of gauge theory using Lie groups. The procedure for non-abelianising, which involves introducing a covariant derivative containing the gauge field as the connection for the gauge bundle, has now become standard. When supersymmetry is included this procedure produces SYM theories with couplings between the gauge field and matter, which all transform in the adjoint representation of the gauge group. However, the M5-brane theory does not contain a gauge field but instead a two-form potential. The non-abelian theory requires this two-form to take values in the Lie algebra and one is required to consider non-abelian gerbe theories. This framework was considered in [210], where the 3-algebra construction for the M2-brane was applied to obtain the non-abelian supersymmetry variations for multiple M5-branes and the corresponding equations of motion.

Understanding the interacting 6d $\mathcal{N} = (2, 0)$ theory remains an active area of research and greater understanding of this elusive theory will certainly lead to a deeper appreciation of M-theory. For a review of the developments in this direction see [211]. Despite not knowing the interacting theory in six dimensions it can be fruitful to study the compactification of the M5-brane theory to lower dimensions where we can get access to a non-abelian description.

5.2 Compactifications and Dualities

The simplest reduction one can perform is the one originally considered in Kaluza–Klein theory where the internal manifold is a circle. From the reduction of M-theory to type IIA string theory we know that an M5-brane wrapped on the M-theory circle descends to a D4-brane in the limit of vanishing circle radius [192]. As a result the 6d $\mathcal{N} = (2, 0)$ theory on an S^1 reduces to 5d $\mathcal{N} = 2$ SYM [212, 213], the theory describing multiple D4-branes. The Yang–Mills coupling is related to the radius of the circle, R as

$$\frac{1}{g^2_{\text{YM}}} = \frac{1}{R}\,, \tag{5.5}$$

and an alternative viewpoint was conjectured in [213, 214] that the 6d $\mathcal{N} = (2, 0)$ theory compactified on an S^1 is exactly 5d $\mathcal{N} = 2$ SYM for any value of the coupling. The Kaluza–Klein modes with momentum along the S^1 are captured by instantons in the five-dimensional theory.

One can consider a further reduction on another S^1 which corresponds to the 6d $\mathcal{N} = (2, 0)$ theory on the torus $T^2 = S^1 \times S^1$. This preserves all 16 supercharges and we obtain 4d $\mathcal{N} = 4$ SYM, the world-volume theory of D3-branes in type IIB string theory. The complex structure of the torus τ descends to the four-dimensional complexified coupling

$$\tau = \frac{\theta}{2\pi} + i\frac{4\pi}{g^2_{YM}}\,, \tag{5.6}$$

where θ is the θ-angle. From this construction the S-duality symmetry of 4d $\mathcal{N} = 4$ SYM has a six-dimensional origin as the $SL(2, \mathbb{Z})$ modular transformation of the complex structure [215]. This set-up was generalised in [216] by considering the M5-brane theory on an elliptic three-fold. The dimensional reduction produces 4d $\mathcal{N} = 4$ SYM with varying coupling constant and singularities in the elliptic fibration give rise to codimension one and two defects in the 4d theory.

Compactifications down to four dimensions preserving less supersymmetry were considered in [217]. Gaiotto studied a class of 4d $\mathcal{N} = 2$ superconformal field theories of A_{k-1}

type which arise from the compactification of k M5-branes on a Riemann surface with n punctures, $\Sigma_{n,g}$, where g is the genus of the Riemann surface. These theories are often referred to as class $\mathcal{S}$ theories in the literature. The world-volume of the M5-branes lies along $\mathbb{R}^{1,3} \times \Sigma_{n,g}$ and in order to preserve supersymmetry on the Riemann surface one needs to perform a topological twist.

In the introduction the conditions for supersymmetry preserving compactifications were formulated in terms of the existence of covariantly constant spinors, which require the compactification manifold X to have reduced holonomy. The covariantly constant spinors transform as singlets under the holonomy group of the manifold. For manifolds with general holonomy no such spinors exist, however one can preserve some supersymmetry by performing a topological twist [218]. This involves turning on a gauge field for the R-symmetry, or a subgroup of it, along the internal manifold which modifies the covariant derivative of the spinors to

$$\nabla_X \to \tilde{\nabla}_X = \partial_X + \omega_X + V_X \,, \tag{5.7}$$

where ω_X is the spin-connection and V_X is the R-symmetry gauge field. Using the R-symmetry gauge field to cancel the spin-connection piece in the covariant derivative, the condition for covariantly constant spinors reduces to simply constant spinors on X. These spinors transform as scalars under the twisting of the holonomy group and the R-symmetry.

The topological twist required to preserve supersymmetry on the Riemann surface involves twisting the holonomy of the Riemann surface with an $SO(2)_R$ subgroup inside the $SO(5)_R$ R-symmetry of the 6d theory. The Lorentz and R-symmetry groups of the 6d theory are decomposed as

$$\begin{aligned} SO(1,5)_L &\to SO(1,3)_L \times SO(2)_L \\ SO(5)_R &\to SO(3)_R \times SO(2)_R \,. \end{aligned} \tag{5.8}$$

The transformation of the supercharges under the new space-time symmetries is given by

$$\begin{aligned} SO(1,5)_L \oplus SO(5)_R \quad &\to \quad SO(1,3)_L \times SO(2)_L \times SO(3)_R \times SO(2)_R \\ (\mathbf{4},\overline{\mathbf{4}}) \quad &\to \quad ((\mathbf{2},\mathbf{1})_{-\frac{1}{2}} \oplus (\mathbf{1},\mathbf{2})_{\frac{1}{2}}, \mathbf{2}_{+\frac{1}{2}} \oplus \mathbf{2}_{-\frac{1}{2}}) \,, \end{aligned} \tag{5.9}$$

and the topological twist is defined as $SO(2)_{\text{twist}} = \text{diag}(SO(2)_L \times SO(2)_R)$. Under the twisted holonomy the supercharges transform as

$$\begin{aligned} SO(5,1)_L \oplus SO(5)_R \quad &\to \quad SO(3,1)_L \times SO(3)_R \times SO(2)_{\text{twist}} \\ (\mathbf{4},\overline{\mathbf{4}}) \quad &\to \quad (\mathbf{2},\mathbf{1},\mathbf{2})_{\mathbf{0}} \oplus (\mathbf{2},\mathbf{1},\mathbf{2})_{\mathbf{-1}} \oplus (\mathbf{1},\mathbf{2},\mathbf{2})_{\mathbf{+1}} \oplus (\mathbf{1},\mathbf{2},\mathbf{2})_{\mathbf{0}} \,. \end{aligned} \tag{5.10}$$

From this twist we obtain a right- and left-moving spinor in four dimensions which are doublets of the $SO(3)_R$ R-symmetry compatible with $\mathcal{N} = 2$ supersymmetry in four

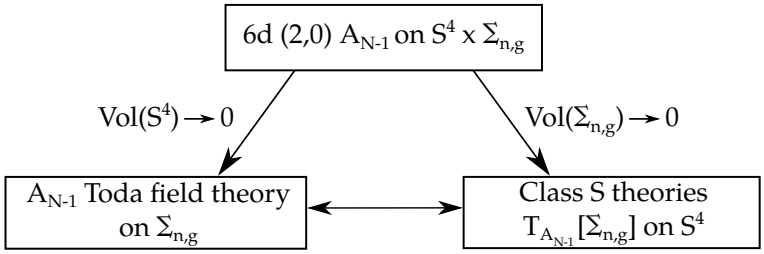

Figure 5.1: Schematic diagram depicting the two theories related by the AGT correspondence and how they arise from compactifications of the M5-brane theory.

dimensions. These supercharges, which transform in the representations $(\mathbf{2},\mathbf{1},\mathbf{2})_{\mathbf{0}}$ and $(\mathbf{1},\mathbf{2},\mathbf{2})_{\mathbf{0}}$, are now uncharged under $SO(2)_{\text{twist}}$ and therefore transform as scalars on the Riemann surface.

From the compactification of N M5-branes on $\Sigma_{n,g}$ we obtain a class of 4d $\mathcal{N}=2$ superconformal field theories, $T_{A_{N-1}}[\Sigma_{n,g}]$, labelled by the Riemann surface. It materialised that viewing the four-dimensional theories as reductions of the 6d $\mathcal{N}=(2,0)$ theory on the Riemann surface allowed an identification between components of the gauge theory and the geometry of the Riemann surface. This correspondence was studied further by Alday, Gaiotto and Tachikawa in [219], where a relation was made between the Nekrasov partition function [220,221] of $T_{A_1}[\Sigma_{n,g}]$ on a four-sphere and the Liouville correlation function on $\Sigma_{n,g}$. This correspondence was later generalised to $SU(N)$ gauge groups in [222] using the fact that Liouville theory is the simplest case of A_{N-1} Toda theory. Both sides of this correspondence can be obtained by considering the 6d $\mathcal{N}=(2,0)$ theory of A_{N-1} type on the background $S^4\times\Sigma_{n,g}$. Toda theory of type A_{N-1} and the 4d theories $T_{A_{N-1}}[\Sigma_{n,g}]$ can then be obtained as the lower dimensional theories arising from taking the volume of the S^4 and the Riemann surface, respectively, to zero. This correspondence is depicted in figure 5.1.

Shortly after the proposal of the AGT correspondence a 3d-3d correspondence between 3d $\mathcal{N}=2$ SCFTs on S^3, denoted $T_{\mathfrak{g}}[M_3]$ where $\mathfrak{g}$ is of ADE-type, and 3d Chern-Simons theory with complexified gauge group on a three-manifold M_3 was conjectured in [223,224]. The dictionary between the two theories relates symmetries and parameters of $T_{\mathfrak{g}}[M_3]$ to the geometry of the three-manifold as well as the partition functions on both sides

$$Z_{T_{\mathfrak{g}}[M_3]} \text{ on } S^3 = Z_{\text{CS}_{\mathfrak{g}_{\mathbb{C}}}} \text{ on } M_3\,. \tag{5.11}$$

This correspondence can also be seen to arise from the 6d $\mathcal{N}=(2,0)$ theory on $S^3\times M_3$, where the theories on each side of the correspondence is obtained by taking the volume of either the three-sphere or M_3 to zero.

In light of the discussion above a natural question now arises regarding the 6d theory

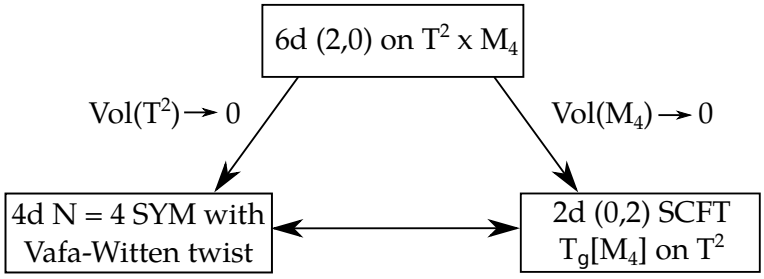

Figure 5.2: A correspondence between 2d SCFTs with two chiral supercharges and 4d $\mathcal{N} = 4$ SYM with the Vafa-Witten twist arising from reductions of the 6d $\mathcal{N} = (2,0)$ theory on $T^2 \times M_4$.

on $S^2 \times M_4$, which would lead to a 4d-2d correspondence. In order to make progress in exploring this possible correspondence one first needs to identify the two theories which arise from the reduction on the S^2 and M_4. Similarly to the two known correspondences the 6d $\mathcal{N} = (2,0)$ theory needs to be topologically twisted in order for some supersymmetry to be preserved on a general four-manifold. In chapter 6 we discuss the possible topological twists and carry out the reduction of the 6d $\mathcal{N} = (2,0)$ theory of type A_{N-1} on the two-sphere with a particular twist, the Vafa-Witten twist [225], as a step towards providing answers to the question posed above.

A related set-up was considered in [226] where the authors studied the 6d $\mathcal{N} = (2,0)$ theory on $T^2 \times M_4$. This scenario is depicted in figure 5.2, where as discussed earlier the compactification on the torus gives rise to 4d $\mathcal{N} = 4$ SYM on $\mathbb{R}^{1,3}$. In order to preserve supersymmetry on a general four-manifold the 4d theory needs to be topologically twisted and the type of supersymmetry preserved in the two-dimensional theory depends on the choice of topological twist. In [226] they considered the Vafa-Witten twist where the Lorentz symmetry and R-symmetry of the 6d theory is decomposed as in (5.8) and $SO(3)_R$ subgroup of the R-symmetry is twisted with an $SO(3)$ subgroup of the holonomy of the four-manifold. This twist, which will be discussed in detail in chapter 6, produces two chiral supercharges i.e. $\mathcal{N} = (0,2)$ supersymmetry in two dimensions.

The dictionary of the correspondence matches basic operations on four-manifolds with dualities in the 2d $\mathcal{N} = (0,2)$ theory. At the level of observables in the two theories the Vafa-Witten partition function is matched with the elliptic genus, the T^2 partition function, of $T_{\mathfrak{g}}[M_4]$. More recent work [227] proposes a method of obtaining invariants of four-manifolds from the correlation functions of the half-twisted 2d theory[1].

[1]The topological half-twist [228] involves twisting the $U(1)_L$ Lorentz symmetry with the $U(1)_R$ R-symmetry of the 2d $\mathcal{N} = (0,2)$ theory. As the two supercharges transform with opposite charges under $U(1)_R$ the topological half-twist preserves one scalar supercharge.

5.3 Derivation of Correspondences

AGT and the 3d-3d correspondence can be associated with the 6d $\mathcal{N} = (2, 0)$ theory on the product space $S^d \times M_{6-d}$, where $d = 3, 4$. Employing this relation, both correspondences were derived in a series of papers by Cordova and Jafferis [229,230], where they considered the reduction of the 6d $\mathcal{N} = (2, 0)$ theory on the three-sphere and four-sphere to arrive at Chern-Simons theory and Toda theory, respectively. This provided proof for the existence of these correspondences, which were previously only well-substantiated conjectures.

In this section we will briefly recall the salient points in their reduction relevant for the determining the theory on the S^2.

- Coupling to Supergravity
  Firstly, we note that the three-sphere and four-sphere are backgrounds which preserve supersymmetry as they admit Killing spinors [231], therefore the reduction can be performed on $S^d \times \mathbb{R}^{6-d}$ without a topological twist.[2] In order to keep track of the additional curvature couplings on S^d Cordova and Jafferis considered the abelian 6d $\mathcal{N} = (2, 0)$ theory, a free tensor multiplet, coupled to six-dimensional $\mathcal{N} = (2, 0)$ off-shell conformal supergravity [232,233]. The supergravity background fields are then determined by solving the Killing spinor equations for the background $S^d \times \mathbb{R}^{6-d}$. For more general backgrounds this procedure ensures that supersymmetry is preserved.

- Non-abelianisation in 5d
  In order to obtain a non-abelian theory the dimensional reduction is carried out via five dimensions. This requires the background to contain a circle direction along which one can reduce to 5d. For the S^3 the circle is the Hopf fiber in the smooth Hopf fibration over S^2. The reduction on the four-sphere was carried out by viewing it as an S^3-fibration over an interval and the circle direction was therefore also the Hopf fiber inside the three-sphere. The 5d theory obtained after the circle reduction is given by the action for Maxwell theory, five free scalars and a fermion coupled to the background supergravity fields. The non-abelianisation of this action was determined in [234, 235] and the theory obtained was 5d $\mathcal{N} = 2$ SYM coupled to background supergravity.

The remaining details of the reductions depend on the specific geometry and will therefore be omitted. However, the above two points are key to obtaining a supersymmetric and non-abelian theory more generally. Armed with this machinery we now consider the reduction

[2] The topological twist can be performed after the reduction on S^d to obtain a topological theory on a general manifold M_{6-d}.

on $S^2 \times M_4$ in the next chapter.

Chapter 6

M5-branes on $S^2 \times M_4$: Nahm's Equations and 4d Topological Sigma-models

6.1 Introduction

The six-dimensional $\mathcal{N} = (2,0)$ superconformal theory with an ADE type gauge group is believed to describe the theory on multiple M5-branes. The equations of motion in six dimensions are known only for the abelian theory [201,202], and a Lagrangian formulation of this theory is believed to not exist. However, in the last few years, much progress has been made in uncovering properties of this elusive theory by considering compactifications to lower dimensions. Compactification of the 6d theory on a product $S^d \times M_{6-d}$ has resulted in correspondences between supersymmetric gauge theories on d-dimensional spheres S^d and conformal/topological field theories on a $6-d$- dimensional manifold M_{6-d}. The goal of this chapter is to consider the compactification of the 6d theory on a four-manifold M_4 times a two-sphere S^2 and to determine the topological theory on M_4. The particular background that we consider is a half-topological twist along the S^2, together with a Vafa-Witten-like twist on M_4, and we will find that the theory on M_4 is a twisted version of a sigma-model into the moduli space of $SU(2)$ monopoles with k centers, where k is the number of M5-branes, or equivalently, the moduli space of Nahm's equations [236] with certain singular boundary conditions. This suggests the existence of a correspondence between this topological sigma-model on M_4 and a two-dimensional $\mathcal{N} = (0,2)$ theory, with a half-twist. This fits into the correspondences studied in the last years, which we shall now briefly summarise.

For $d = 4$, the Alday-Gaiotto-Tachikawa (AGT) correspondence [219] connects 4d $\mathcal{N} = 2$ supersymmetric gauge theories on S^4 with Liouville or Toda theories on Riemann surfaces

M_2. Correlation functions in Toda theories are equal to the partition function of an $\mathcal{N} = 2$ supersymmetric gauge theory, which depends on the Riemann surface M_2. Such 4d $\mathcal{N} = 2$ gauge theories obtained by dimensional reduction of the 6d $\mathcal{N} = (2, 0)$ theories were first studied by Gaiotto in [217], generalizing the Seiberg-Witten construction [237]. For $d = 3$, a correspondence between 3d supersymmetric gauge theories, labelled by three-manifolds M_3, and complex Chern-Simons theory on M_3 was proposed in [224, 223], also referred to as the 3d-3d correspondence. This correspondence has a direct connection to the AGT correspondence by considering three-manifolds, which are a Riemann surface M_2 times an interval I, $M_3 = M_2 \times_\varphi I$, whose endpoints are identified modulo the action of an element φ of the mapping class group of M_2. On the dual gauge theory side, the mapping class group action translates into a generalised S-duality, and the three-dimensional gauge theories, dual to complex Chern-Simons theory are obtained on duality defects in the 4d $\mathcal{N} = 2$ Gaiotto theory. The 3d-3d correspondence was ultimately derived from a direct dimensional reduction of the 6d $\mathcal{N} = (2, 0)$ theory on a three-sphere via 5d by Cordova and Jafferis [235, 229].

Both the AGT and 3d-3d correspondences uncovered very deep and surprising relations between supersymmetric gauge theories and two/three-manifolds, their geometry and moduli spaces. In view of this a very natural question is to ask, whether we can obtain insights into four-manifolds, as well as the dual two-dimensional gauge theories obtained by dimensional reduction of the 6d $\mathcal{N} = (2, 0)$ theory. Here, unlike the AGT case, the theory on the four-manifold is a topological theory, and the gauge theory lives in the remaining two dimensions and has (half-twisted) $\mathcal{N} = (0, 2)$ supersymmetry. A schematic depiction of this is given in figure 6.1. More precisely, we propose a correspondence between a 4d topological sigma-model and a 2d half-twisted $\mathcal{N} = (0, 2)$ gauge theory. In particular we expect that topological observables in the 4d theory can be mapped to the partition function and other supersymmetric observables of the 2d theory. Note that the S^2 partition function defined with the topological half-twist [238] is ambiguous as explained in [239]. However the analysis of counter-terms (and therefore ambiguities) must be revisited in the context of the embedding in 6d conformal supergravity, which is our set-up. In particular, the 2d counter-terms should originate from 6d counter-terms. Recent results on localisation in 2d $\mathcal{N} = (0, 2)$ theories have appeared in [240], albeit only for theories that have $\mathcal{N} = (2, 2)$ loci. The theories obtained from the reduction in this chapter do not necessarily have such a $\mathcal{N} = (2, 2)$ locus.

From a brane picture, the theory we consider can be obtained by compactifying k M5-branes on a co-associave four-cycle in G_2 [241, 242]. The two-dimensional theory that is transverse to the co-associative cycle has $\mathcal{N} = (0, 2)$ supersymmetry, and we consider this

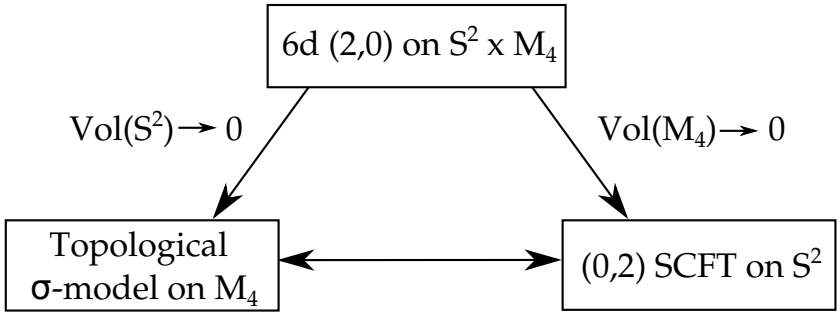

Figure 6.1: 4d-2d correspondence between the reduction of the 6d $\mathcal{N} = (2,0)$ theory on M_4 to a 2d $\mathcal{N} = (0,2)$ SCFT on S^2, and the 'dual' 4d topological sigma-model from M_4 into the Nahm or monopole moduli space, which is obtained in this thesis by reducing the 6d theory on a two-sphere.

on a two-sphere, with an additional topological half-twist.

The first question in view of this proposal is to determine what the topological theory on M_4 is. There are various ways to approach this question. The simplest case is the abelian theory, which on $S^2 \times \mathbb{R}^{1,3}$ gives rise to a 4d free $\mathcal{N} = 2$ hyper-multiplet [243], which we shall view as a sigma-model into the one-monopole moduli space. On a general four-manifold M_4, we will show that in the topologically twisted reduction, the abelian theory integrates indeed to a "twisted version" of a hyper-multiplet, where the fields are a compact scalar and self-dual two-form on M_4.

For the general, non-abelian case, this 4d-2d correspondence can in principle be connected to the 3d-3d correspondence by considering the special case of $M_4 = M_3 \times_\varphi I$, where I is an interval, similar to the derivation of the 3d-3d correspondence from AGT. In this chapter we will refrain from considering this approach, and study instead the reduction via 5d $\mathcal{N} = 2$ SYM, in the same spirit as [235, 229].

We first consider the dimensional reduction on flat M_4, and then topologically twist the resulting 4d $\mathcal{N} = 2$ theory. We restrict to the $U(k)$ gauge groups, but in principle the analysis holds also for the D and E type. To determine the flat space reduction, we view the S^2 in terms of a circle fibration over an interval, where the circle fiber shrinks to zero radius at the two endpoints. We determine the 6d supergravity background which corresponds to the 6d theory on $S^2 \times \mathbb{R}^4$. After dimensional reduction on S^1 the resulting theory is 5d $\mathcal{N} = 2$ SYM on an interval, where the scalars satisfy Nahm pole boundary conditions [244,245]. Further dimensional reduction to 4d requires to consider scalars, that satisfy Nahm's equations. The resulting theory is a 4d sigma-model into the moduli space of solutions of Nahm's equations, which is isomorphic to the moduli space of k-centered monopoles [246] and has a natural Hyper-Kähler structure. Much of the geometry of the

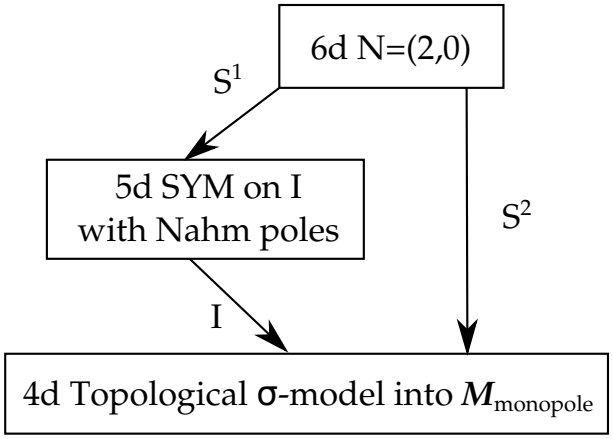

Figure 6.2: The dimensional reduction of the 6d $\mathcal{N} = (2,0)$ theory on an S^2, viewed as a circle-fibration along an interval I, is determined by dimensional reduction via 5d $\mathcal{N} = 2$ SYM. The scalars of the 5d theory satisfy the Nahm equations, with Nahm pole boundary conditions at the endpoints of the interval. The 4d theory is a topological sigma-model into the moduli space of solutions to these Nahm equations, or equivalently the moduli space of monopoles.

moduli space is known, in particular for one- or two-monopoles [247], and a more algebraic formulation in terms of Slodowy-slices exists following [248–250]. The latter description is particularly amenable for the characterisation of $\mathcal{N} = 2$ Gaiotto theories with finite area for the Riemann surface as studied in [245]. Figure 6.2 summarises our dimensional reduction procedure.

The 4d $\mathcal{N} = 2$ supersymmetric sigma-model for flat M_4 falls into the class of models obtained in [251, 252]. We find that the coupling constant of the 4d sigma-model is given in terms of the area of the two-sphere. To define this sigma-model on a general four-manifold requires topologically twisting the theory with the R-symmetry of the 4d theory. One of the complications is that the $SU(2)$ R-symmetry of the 4d theory gets identified with an $SU(2)$ isometry of the Hyper-Kähler target. The twisting requires thus a precise knowledge of how the coordinates of the monopole moduli space transform under the $SU(2)$ symmetry. This is known only in the case of one- and two-monopoles, where a metric has been determined explicitly [247]. In these cases, we shall describe in section 6.6 the topological sigma-models, which have both scalars and self-dual two-form fields on M_4. The sigma-model into the one-monopole moduli space $S^1 \times \mathbb{R}^3$, corresponding to the reduction of the abelian theory to a free 4d hypermultiplet, gives rise upon twisting to a (free) theory on M_4 with a compact scalar and a self-dual two-form, and belongs to the class of 4d A-models of [253]. The sigma-model into the two-monopole moduli space, which is closely related to the Atiyah-Hitchin manifold, gives rise to an exotic sigma-model of scalars and self-dual two-forms obeying constraints. Sigma-models in 4d

are non-renormalisable and infrared free, however, the observables of the topologically twisted theory are independent of the RG flow and can in principle be computed in the weak coupling regime.

In the case of M_4 a Hyper-Kähler manifold, the holonomy is reduced and the twisting does not require knowledge of the R-symmetry transformations of the coordinate fields. This is discussed in section 6.5.1, and the topological sigma-model that we find upon twisting is the one studied in [254] by Anselmi and Frè for almost quaternionic target spaces.

In this thesis we focus on the reduction of the 6d $\mathcal{N} = (2,0)$ theory on a two-sphere, however, as we emphasise in section 6.3, the reduction would proceed in the same way with the addition of two arbitrary 'punctures' on the two-sphere, characterizing BPS defects of the 6d non-abelian theory. In the intermediate 5d theory, it would result in different Nahm-pole boundary conditions for scalar fields at the two ends of the interval and the final flat space four-dimensional theory would be a sigma-model into the moduli space of solutions of Nahm's equations with these modified Nahm-pole boundary conditions.

We should also remark upon the connection of our results to the paper by Gadde, Gukov and Putrov [226], who consider the torus reduction of the M5-brane theory. The topological twist along M_4 is the same in their setup as in our construction. Thus, the dictionary to the data of the 2d theory as developed in [226], such as its dependence on the topological/geometric data of M_4, should hold in our case as well. For instance, the rank of the 2d gauge group is determined by $b^2(M_4)$. The key difference is however, that we consider this 2d theory on S^2, and topologically twist the chiral supersymmetry. Interestingly, the reduction of the 6d theory on either T^2 or S^2 with half-twist gives rather distinct 4d topological theories: in the former, the 4d $\mathcal{N} = 4$ SYM theory with Vafa-Witten twist, in the latter, we find a four-dimensional topological sigma-model into the monopole moduli space, which for general M_4 has both scalars as well as self-dual two-forms. The appearance of self-dual two-forms is indeed not surprising in this context, as the topological twist along M_4 is precisely realised in terms of M5-branes wrapping a co-associative cycle in G_2, which locally is given in terms of the bundle of self-dual two-forms $\Omega^{2+}(M_4)$ [255].

The plan of the chapter is as follows. We begin in section 6.2 by setting up the various topological twists of the 6d $\mathcal{N} = (2,0)$ theory on $S^2 \times M_4$, and provide the supergravity background and Killing spinors, for the S^2 reduction with the half-twist. In section 6.3 we dimensionally reduce the 6d theory to 5d $\mathcal{N} = 2$ SYM on an interval times $\mathbb{R}^4$, with Nahm pole boundary conditions for the scalar fields. In particular we study this with a generic squashed metric on S^2 and in a special 'cylinder' limit. The reduction to 4d is then performed in section 6.4, where we show that the fields have to take values in the moduli

space of Nahm's equations, and determine the $\mathcal{N} = 2$ supersymmetric sigma-model on $\mathbb{R}^4$. The action can be found in (6.110), as well as in the form of the models of [251, 252] in (6.115). In sections 6.5 and 6.6 we study the associated topological sigma-models: in section 6.5 we consider the case of M_4 a Hyper-Kähler manifold, and show that this gives rise to the topological sigma-model in [254]. The action can be found in (6.130). We furthermore connect this to the dimensional reduction of the topologically twisted 5d $\mathcal{N} = 2$ SYM theory and show that both approaches yield the same 4d sigma-model in appendix C.6. In section 6.6, we let M_4 be a general four-manifold, but specialise to the case of one- or two- monopole moduli spaces, and use the explicit metrics to determine the topological field theory. In this case, the bosonic fields are scalars and self-dual two-forms on M_4. The action for $k = 1$ is (6.153) and for $k = 2$ we obtain (6.176). We close with some open questions in section 6.7, and provide details on our conventions and computational intricacies in the appendices.

6.2 Topological Twists and Supergravity Backgrounds

This section serves two purposes: firstly, to explain the possible twists of the 6d $\mathcal{N} = (2, 0)$ theory on a two-sphere S^2, and secondly, to determine the supergravity background associated to the topological half-twist on S^2.

6.2.1 Twists of the M5-brane on M_4

We consider the compactification of the M5-brane theory, i.e. the six-dimensional $\mathcal{N} = (2, 0)$ theory, on $M_4 \times S^2$, where M_4 is a four-dimensional manifold. More generally, we can consider the twists for reductions on general Riemann surfaces Σ instead of S^2. We will determine the 4d theory that is obtained upon dimensional reduction on the S^2, and consider this theory on a general four-manifold M_4. Supersymmetry of this theory requires that certain background fields are switched on, which correspond to twisting the theory – both along M_4 as well as along S^2. The twisting procedure requires to identify part of the Lorentz algebra of the flat space theory with a subalgebra of the R-symmetry. The R-symmetry and Lorentz algebra of the M5-brane theory on $\mathbb{R}^6$ are[1]

$$\mathfrak{sp}(4)_R \oplus \mathfrak{so}(6)_L \,. \tag{6.1}$$

The supercharges transform in the $(\mathbf{4}, \bar{\mathbf{4}})$ spinor representation (the same representation as the fermions in the theory, see appendix C.1). The product structure of the space-time

[1] In the dimensional reduction via 5d $\mathcal{N} = 2$ SYM, we will in fact consider the Lorentzian theory to derive the theory on $\mathbb{R}^{1,3}$. As we have in mind a compactification on a compact four-manifold M_4, we will discuss here the Euclidean version.

implies that we decompose the Lorentz algebra as

$$\mathfrak{so}(6)_L \quad \to \quad \mathfrak{so}(4)_L \oplus \mathfrak{so}(2)_L \cong \mathfrak{su}(2)_\ell \oplus \mathfrak{su}(2)_r \oplus \mathfrak{so}(2)_L \,. \tag{6.2}$$

We can consider the following twists of the theory along M_4. Either we identify an $\mathfrak{su}(2)$ subalgebra of both Lorentz and R-symmetry, or we twist with the full $\mathfrak{so}(4)$.

On M_4 there are two $\mathfrak{su}(2)$ twists that we can consider. In the first instance consider the decomposition of the R-symmetry as

$$\mathfrak{sp}(4)_R \quad \to \quad \mathfrak{su}(2)_R \oplus \mathfrak{so}(2)_R \tag{6.3}$$

and the $\mathfrak{su}(2)_\ell$ is twisted by $\mathfrak{su}(2)_R$. That is we replace $\mathfrak{su}(2)_\ell$ by the diagonal $\mathfrak{su}(2)_{\text{twist}} \subset \mathfrak{su}(2)_\ell \oplus \mathfrak{su}(2)_R$ and define the twisted $\mathfrak{su}(2)$ generators by

$$T^a_{\text{twist}} = \frac{1}{2}\left(T^a_\ell + T^a_R\right) \,, \tag{6.4}$$

so that the twisted theory has the following symmetries

$$\text{Twist 1}: \qquad \mathfrak{sp}(4)_R \oplus \mathfrak{so}(6)_L \quad \to \quad \mathfrak{su}(2)_{\text{twist}} \oplus \mathfrak{su}(2)_r \oplus \mathfrak{so}(2)_R \oplus \mathfrak{so}(2)_L \,. \tag{6.5}$$

This twist is reminiscent of the Vafa-Witten twist of 4d $\mathcal{N} = 4$ SYM [225]. The supercharges decompose under (6.2) and (6.3) as

$$\begin{aligned} \mathfrak{sp}(4)_R \oplus \mathfrak{so}(6)_L \quad &\to \quad \mathfrak{su}(2)_R \oplus \mathfrak{so}(2)_R \oplus \mathfrak{su}(2)_\ell \oplus \mathfrak{su}(2)_r \oplus \mathfrak{so}(2)_L \\ (\mathbf{4}, \overline{\mathbf{4}}) \quad &\to \quad (\mathbf{2}_{+\mathbf{1}} \oplus \mathbf{2}_{-\mathbf{1}}, (\mathbf{2},\mathbf{1})_{-\mathbf{1}} \oplus (\mathbf{1},\mathbf{2})_{\mathbf{1}}) \,, \end{aligned} \tag{6.6}$$

which after the twist becomes

$$\begin{aligned} \mathfrak{sp}(4)_R \oplus \mathfrak{so}(6)_L \quad &\to \quad \mathfrak{su}(2)_{\text{twist}} \oplus \mathfrak{su}(2)_r \oplus \mathfrak{so}(2)_R \oplus \mathfrak{so}(2)_L \\ (\mathbf{4}, \bar{\mathbf{4}}) \quad &\to \quad (\mathbf{1} \oplus \mathbf{3}, \mathbf{1})_{+-} \oplus (\mathbf{1} \oplus \mathbf{3}, \mathbf{1})_{--} \oplus (\mathbf{2},\mathbf{2})_{++} \oplus (\mathbf{2},\mathbf{2})_{-+} \,. \end{aligned} \tag{6.7}$$

This yields two scalar supercharges on M_4, which are of the same negative 2d chirality under $\mathfrak{so}(2)_L$

$$(\mathbf{1},\mathbf{1})_{+-} \oplus (\mathbf{1},\mathbf{1})_{--} \,. \tag{6.8}$$

Upon reduction on M_4, this twist leads to a 2d theory with $\mathcal{N} = (0,2)$ supersymmetry. In this thesis we are not concerned with the reduction on M_4, but focus on the reverse, namely the theory on M_4. This twist is compatible with a further twist along S^2 or more generally an arbitrary Riemann surface Σ, which identifies $\mathfrak{so}(2)_L$ with the remaining R-symmetry $\mathfrak{so}(2)_R$. This is the setup that we will study in this chapter. In the following we will first perform the reduction (and topological twisting) along the S^2, and then further twist the resulting four-dimensional theory on M_4.

Finally, let us briefly discuss alternative twists. We can use a different $\mathfrak{su}(2)$ R-symmetry factor to twist the theory along M_4, namely we can use $\mathfrak{su}(2)_1 \subset \mathfrak{su}(2)_1 \oplus \mathfrak{su}(2)_2 \simeq \mathfrak{so}(4)_R \subset \mathfrak{sp}(4)_R$ decomposed as

$$\mathfrak{sp}(4)_R \quad \to \quad \mathfrak{su}(2)_1 \oplus \mathfrak{su}(2)_2 \,. \tag{6.9}$$

This twist leads upon reduction on M_4 to a 2d theory with $\mathcal{N} = (0,1)$ supersymmetry.

$$\begin{aligned} \text{Twist 2}: \qquad \mathfrak{sp}(4)_R \oplus \mathfrak{so}(6)_L \quad &\to \quad \mathfrak{su}(2)_{\text{twist}} \oplus \mathfrak{su}(2)_2 \oplus \mathfrak{su}(2)_r \oplus \mathfrak{so}(2)_L \\ (\mathbf{4}, \bar{\mathbf{4}}) \quad &\to \quad (\mathbf{3} \oplus \mathbf{1}, \mathbf{1}, \mathbf{1})_- \oplus (\mathbf{2}, \mathbf{1}, \mathbf{2})_+ \oplus (\mathbf{2}, \mathbf{2}, \mathbf{1})_- \oplus (\mathbf{1}, \mathbf{2}, \mathbf{2})_+ \,. \end{aligned} \tag{6.10}$$

We can in fact further twist the $\mathfrak{su}(2)_2$ with the remaining $\mathfrak{su}(2)_r$ Lorentz symmetry on M_4. This corresponds to a total twist of the full $\mathfrak{so}(4)_R$ with $\mathfrak{so}(4)_L$ and is analogous to the geometric Langlands (or Marcus) twist of 4d $\mathcal{N} = 4$ SYM theory on M_4 [256, 257]

$$\begin{aligned} \text{Twist 3}: \qquad \mathfrak{sp}(4)_R \oplus \mathfrak{so}(6)_L \quad &\to \quad \mathfrak{so}(4)_{\text{twist}} \oplus \mathfrak{so}(2)_L \\ (\mathbf{4}, \bar{\mathbf{4}}) \quad &\to \quad (\mathbf{3} \oplus \mathbf{1}, \mathbf{1})_- \oplus (\mathbf{2}, \mathbf{2})_+ \oplus (\mathbf{2}, \mathbf{2})_- \oplus (\mathbf{1}, \mathbf{1} \oplus \mathbf{3})_+ \,, \end{aligned} \tag{6.11}$$

which has two scalar supercharges of opposite 2d chiralities

$$(\mathbf{1}, \mathbf{1})_+ \;\oplus\; (\mathbf{1}, \mathbf{1})_- \,, \tag{6.12}$$

so that this twist leads upon reduction on M_4 to a 2d theory with $\mathcal{N} = (1,1)$ supersymmetry. It is not compatible with a further topological twist on S^2. Interestingly it was found in [258] that supersymmetry can be preserved by turning on suitable background supergravity fields on M_4. We will not study this background in this thesis, but will return to this in the future.

We will now consider the setup of twist 1 and carry out the reduction of the 6d $\mathcal{N} = (2,0)$ theory on $S^2 \times M_4$. As explained in the introduction our strategy is to find the 6d supergravity background corresponding to the twisted theory along S^2, taking $M_4 = \mathbb{R}^4$ to begin with, and carry out the reduction to 4d, where we will finally twist the theory along an arbitrary M_4.

6.2.2 Twisting on S^2

For our analysis we first consider the theory on $S^2 \times \mathbb{R}^4$ and the twist along S^2. The Lorentz and R-symmetry groups reduce again as in (6.2) and (6.3). The twist is implemented by identifying $\mathfrak{so}(2)_R$ with $\mathfrak{so}(2)_L$ and we denote it $\mathfrak{so}(2)_{\text{twist}} \simeq \mathfrak{u}(1)_{\text{twist}}$, whose generators are given by

$$U_{\text{twist}} = U_L + U_R \,. \tag{6.13}$$

As we have seen this is compatible with the twist 1, discussed in the last subsection.

$$S^2 \text{ Twist}: \qquad \mathfrak{so}(6)_L \oplus \mathfrak{sp}(4)_R \quad \to \quad \mathfrak{g}_{res} \cong \mathfrak{su}(2)_\ell \oplus \mathfrak{su}(2)_r \oplus \mathfrak{su}(2)_R \oplus \mathfrak{u}(1)_{\text{twist}} \,. \tag{6.14}$$

The residual symmetry group and decomposition of the supercharges and fermions is then

$$\begin{aligned} \mathfrak{so}(6)_L \oplus \mathfrak{sp}(4)_R \quad &\to \quad \mathfrak{g}_{res} \cong \mathfrak{su}(2)_\ell \oplus \mathfrak{su}(2)_r \oplus \mathfrak{su}(2)_R \oplus \mathfrak{u}(1)_{\text{twist}} \\ (\overline{\mathbf{4}}, \mathbf{4}) \quad &\to \quad (\mathbf{2},\mathbf{1},\mathbf{2})_0 \oplus (\mathbf{2},\mathbf{1},\mathbf{2})_{-2} \oplus (\mathbf{1},\mathbf{2},\mathbf{2})_2 \oplus (\mathbf{1},\mathbf{2},\mathbf{2})_0 \,. \end{aligned} \tag{6.15}$$

There are eight supercharges transforming as singlets on S^2 and transforming as Weyl spinors of opposite chirality on M_4 and doublets under the remaining R-symmetry. The fields of the 6d $\mathcal{N} = (2,0)$ theory decompose as follows

$$\begin{aligned} \mathfrak{so}(6)_L \oplus \mathfrak{sp}(4)_R \quad &\to \quad \mathfrak{su}(2)_\ell \oplus \mathfrak{su}(2)_r \oplus \mathfrak{su}(2)_R \oplus \mathfrak{u}(1)_L \oplus \mathfrak{u}(1)_R \\ \Phi^{\widehat{m}\widehat{n}} = (\mathbf{1},\mathbf{5}) \quad &\to \quad (\mathbf{1},\mathbf{1},\mathbf{1})_{0,2} \oplus (\mathbf{1},\mathbf{1},\mathbf{1})_{0,-2} \oplus (\mathbf{1},\mathbf{1},\mathbf{3})_{0,0} \\ \rho^{\widehat{m}}_{\underline{m}} = (\overline{\mathbf{4}},\mathbf{4}) \quad &\to \quad (\mathbf{1},\mathbf{2},\mathbf{2})_{+1,-1} \oplus (\mathbf{1},\mathbf{2},\mathbf{2})_{+1,+1} \oplus (\mathbf{2},\mathbf{1},\mathbf{2})_{-1,-1} \oplus (\mathbf{2},\mathbf{1},\mathbf{2})_{-1,+1} \\ \mathcal{B}_{\underline{AB}} = (\mathbf{15},\mathbf{1}) \quad &\to \quad (\mathbf{1},\mathbf{1},\mathbf{1})_{0,0} \oplus (\mathbf{3},\mathbf{1},\mathbf{1})_{0,0} \oplus (\mathbf{1},\mathbf{3},\mathbf{1})_{0,0} \oplus (\mathbf{2},\mathbf{2},\mathbf{1})_{2,0} \oplus (\mathbf{2},\mathbf{2},\mathbf{1})_{-2,0} \,. \end{aligned} \tag{6.16}$$

Note from the point of view of the 4d $\mathcal{N} = 2$ superalgebra, some of these fields transform in hyper-multiplets, however with a non-standard transformation under the R-symmetry, under which some of the scalars form a triplet. The standard transformation of the hyper-multiplet can be obtained using an additional $SU(2)$ symmetry [259]. However, in the present situation, we have to use the R-symmetry as given in the above decomposition. Twisting with the $\mathfrak{su}(2)_\ell$ Lorentz with the remaining $\mathfrak{su}(2)_R$, i.e.

$$\mathfrak{su}(2)_{\text{twist}} \cong \text{diag}(\mathfrak{su}(2)_\ell \oplus \mathfrak{su}(2)_R) \tag{6.17}$$

the resulting topological theory has the following matter content

$$\begin{aligned} \mathfrak{so}(6)_L \oplus \mathfrak{sp}(4)_R \quad &\to \quad \tilde{\mathfrak{g}} \cong \mathfrak{su}(2)_{\text{twist}} \oplus \mathfrak{su}(2)_r \oplus \mathfrak{u}(1)_{\text{twist}} \\ \Phi^{\widehat{m}\widehat{n}} = (\mathbf{1},\mathbf{5}) \quad &\to \quad (\mathbf{1},\mathbf{1})_2 \oplus (\mathbf{1},\mathbf{1})_{-2} \oplus (\mathbf{3},\mathbf{1})_0 \\ \rho^{\widehat{m}}_{\underline{m}} = (\overline{\mathbf{4}},\mathbf{4}) \quad &\to \quad (\mathbf{2},\mathbf{2})_0 \oplus (\mathbf{2},\mathbf{2})_2 \oplus (\mathbf{1}\oplus\mathbf{3},\mathbf{1})_{-2} \oplus (\mathbf{1}\oplus\mathbf{3},\mathbf{1})_0 \\ \mathcal{B}_{\underline{AB}} = (\mathbf{15},\mathbf{1}) \quad &\to \quad (\mathbf{1},\mathbf{1})_0 \oplus (\mathbf{3},\mathbf{1})_0 \oplus (\mathbf{1},\mathbf{3})_0 \oplus (\mathbf{2},\mathbf{2})_2 \oplus (\mathbf{2},\mathbf{2})_{-2} \,. \end{aligned} \tag{6.18}$$

In the following it will be clear that the 6d scalars Φ give rise to scalars and a self-dual two-form on M_4. The fermions give rise to either vectors, or scalars and self-dual two-forms as well. The fields appearing in the decomposition of the two-form $\mathcal{B}$ are not all independent due to the constraint of self-duality of $H = d\mathcal{B}$. They will give rise to a vector field and a scalar on M_4. This matter content will be visible in the intermediate 5d description that we reach later in section 6.3, however, after reducing the theory to 4d and integrating out massive fields, the matter content of the final 4d theories will be different.

6.2.3 Supergravity Background Fields

Before describing the details of the reduction, we should summarise our strategy. Our goal is to determine the dimensional reduction of the 6d $\mathcal{N} = (2,0)$ theory with non-abelian $\mathfrak{u}(k)$ gauge algebra. For the abelian theory, the dimensional reduction is possible, using the equations of motions in 6d [201,202]. However, for the non-abelian case, due to absence of a 6d formulation of the theory, we have to follow an alternative strategy. Our strategy is much alike to the derivation of complex Chern-Simons theory as the dimensional reduction on an S^3 in [229]. First note, that the 6d theory on S^1 gives rise to 5d $\mathcal{N} = 2$ SYM theory. More generally, the dimensional reduction of the 6d theory on a circle fibration gives rise to a 5d $\mathcal{N} = 2$ SYM theory in a supergravity background [235] (for earlier references see [260,234]). This theory has a non-abelian extension, consistent with gauge invariance and supersymmetry, which is then conjectured to be the dimensional reduction of the non-abelian 6d theory.

More precisely, this approach requires first to determine the background of the 6d abelian theory as described in terms of the $\mathcal{N} = (2,0)$ conformal supergravity theory [232,233]. The 5d background is determined by reduction on the circle fiber, and is then non-abelianised. We can further reduce the theory along the remaining compact directions to determine the theory in 4d. For S^3, there is the Hopf-fibration, used in [229] to derive the Chern-Simons theory in this two-step reduction process. In the present case of the two-sphere, we will fiber the S^1 over an interval I, and necessarily, the fibers will have to become singular at the end-points.

In the following we will prepare the analysis of the supergravity background. By requiring invariance under the residual group of symmetries $\mathfrak{g}_{res}$ preserved by the topological twist on S^2, we derive ansätze for the background fields in 6d $\mathcal{N} = (2,0)$ off-shell conformal supergravity fields. In the next section we will consider the Killing spinor equations and fix the background fields completely.

To begin with, the 6d metric on $S^2 \times \mathbb{R}^4$ is given by

$$ds^2 \;=\; ds^2_{\mathbb{R}^4} + r^2 d\theta^2 + \ell(\theta)^2\, d\phi^2\,, \tag{6.19}$$

with $\ell(\theta) = r\sin(\theta)$ for the round two-sphere and $\theta \in I = [0,\pi]$. More generally, $\ell(\theta)$ can be a function, which is smooth and interpolates between

$$\frac{\ell(\theta)}{r} \sim \theta\,, \quad \text{for} \quad \theta \to 0\,, \qquad \frac{\ell(\theta)}{r} \sim \pi - \theta\,, \quad \text{for} \quad \theta \to \pi\,. \tag{6.20}$$

We choose the frame

$$e^A = dx^A\,, \qquad e^5 = r\, d\theta\,, \qquad e^6 = \ell(\theta)\, d\phi\,. \tag{6.21}$$

Label	Field	$\mathfrak{sp}(4)_R$	Properties
$e_{\underline{\mu}}^{\underline{A}}$	Frame	**1**	
$V_{\underline{A}}^{\widehat{B}\widehat{C}}$	R-symmetry gauge field	**10**	$V_{\underline{A}}^{\widehat{B}\widehat{C}} = -V_{\underline{A}}^{\widehat{C}\widehat{B}}$
$T^{\widehat{A}}_{[\underline{BCD}]}$	Auxiliary 3-form	**5**	$T^{\widehat{A}} = - \star T^{\widehat{A}}$
$D_{(\widehat{A}\widehat{B})}$	Auxiliary scalar	**14**	$D_{\widehat{A}\widehat{B}} = D_{\widehat{B}\widehat{A}}$, $D^{\widehat{A}}_{\widehat{A}} = 0$
$b_{\underline{A}}$	Dilatation gauge field	**1**	

Table 6.1: The bosonic background fields for the 6d $\mathcal{N} = (2,0)$ conformal supergravity.

The corresponding non-vanishing components of the spin connection are

$$\omega^{56} = -\omega^{65} = -\frac{\ell'(\theta)}{r}\, d\phi\,. \tag{6.22}$$

In the following the index conventions are such that all hatted indices refer to the R-symmetry, all unhatted ones are Lorentz indices. The background fields for the off-shell gravity multiplet are summarised in table 6.1. Underlined Roman capital letters are flat 6d coordinates, underlined Greek are curved space indices in 6d, and middle Roman alphabet underlined indices are 6d spinors. All our conventions are summarised in appendix C.1.

Before making the ansätze for the background fields, we note the following decompositions of representations that these background fields transform under, first for the Lorentz symmetry,

$$\begin{aligned}
\mathfrak{so}(6)_L &\to \mathfrak{su}(2)_\ell \oplus \mathfrak{su}(2)_r \oplus \mathfrak{u}(1)_L \\
\underline{A}: \quad \mathbf{6} &\to (\mathbf{2},\mathbf{2})_{\mathbf{0}} \oplus (\mathbf{1},\mathbf{1})_{\mathbf{2}} \oplus (\mathbf{1},\mathbf{1})_{\mathbf{-2}} \\
[\underline{BCD}]^{(+)}: \quad \mathbf{10} &\to (\mathbf{2},\mathbf{2})_{\mathbf{0}} \oplus (\mathbf{3},\mathbf{1})_{\mathbf{2}} \oplus (\mathbf{1},\mathbf{3})_{\mathbf{-2}} \\
[\underline{BC}]: \quad \mathbf{15} &\to (\mathbf{2},\mathbf{2})_{\mathbf{2}} \oplus (\mathbf{2},\mathbf{2})_{\mathbf{-2}} \oplus (\mathbf{3},\mathbf{1})_{\mathbf{0}} \oplus (\mathbf{1},\mathbf{3})_{\mathbf{0}} \oplus (\mathbf{1},\mathbf{1})_{\mathbf{0}}
\end{aligned} \tag{6.23}$$

and also for the R-symmetry

$$\begin{aligned}
\mathfrak{so}(5)_R &\to \mathfrak{su}(2)_R \oplus \mathfrak{u}(1)_R \\
\widehat{A}: \quad \mathbf{5} &\to \mathbf{3_0} \oplus \mathbf{1_2} \oplus \mathbf{1_{-2}} \\
[\widehat{B}\widehat{C}]: \quad \mathbf{10} &\to \mathbf{3_0} \oplus \mathbf{3_2} \oplus \mathbf{3_{-2}} \oplus \mathbf{1_0} \\
(\widehat{B}\widehat{C}): \quad \mathbf{14} &\to \mathbf{5_0} \oplus \mathbf{3_2} \oplus \mathbf{3_{-2}} \oplus \mathbf{1_2} \oplus \mathbf{1_{-2}} \oplus \mathbf{1_0}\,.
\end{aligned} \tag{6.24}$$

The bosonic supergravity fields of 6d off-shell conformal maximal supergravity were determined in [232, 233, 261, 260, 235]. They are the frame $e_{\underline{\mu}}^{\underline{A}}$ and

$$T_{[\underline{BCD}]\widehat{A}}\,, \qquad V_{\underline{A}\,[\widehat{B}\widehat{C}]} \to (dV)_{[\underline{AB}]\,[\widehat{C}\widehat{D}]}\,, \qquad D_{(\widehat{A}\widehat{B})}\,, \qquad b_{\underline{A}} \to (db)_{[\underline{AB}]}\,, \tag{6.25}$$

where dV and db denote the field strength of the R-symmetry and dilatation gauge fields, respectively. Furthermore $T_{[\underline{BCD}]\widehat{A}}$ is anti-self-dual[2] and $D_{(\widehat{A}\widehat{B})}$ is traceless

$$T_{[\underline{BCD}]\widehat{A}} = T_{[\underline{BCD}]^{(+)}\widehat{A}}\,, \qquad \delta^{\widehat{A}\widehat{B}} D_{\widehat{A}\widehat{B}} = 0\,. \tag{6.26}$$

We shall now decompose these in turn under the residual symmetry group $\mathfrak{g}_{res} \cong \mathfrak{su}(2)_\ell \oplus \mathfrak{su}(2)_r \oplus \mathfrak{su}(2)_R \oplus \mathfrak{u}(1)_{\text{twist}}$ and determine the components that transform trivially, and thus can take non-trivial background values.

1. $T_{[\underline{BCD}]\widehat{A}}$: The decomposition under $\mathfrak{g}_{res}$ is given by

$$\begin{aligned}(\mathbf{10},\mathbf{5}) \to &(\mathbf{2},\mathbf{2},\mathbf{3})_{(\mathbf{2})} \oplus (\mathbf{3},\mathbf{1},\mathbf{3})_{(\mathbf{2})} \oplus (\mathbf{1},\mathbf{3},\mathbf{3})_{(-\mathbf{2})} \oplus (\mathbf{2},\mathbf{2},\mathbf{1})_{(\pm\mathbf{2})} \oplus (\mathbf{3},\mathbf{1},\mathbf{1})_{(\mathbf{4})} \\ &\oplus (\mathbf{3},\mathbf{1},\mathbf{1})_{(\mathbf{0})} \oplus (\mathbf{1},\mathbf{3},\mathbf{1})_{(\mathbf{0})} \oplus (\mathbf{1},\mathbf{3},\mathbf{1})_{(-\mathbf{4})}\,.\end{aligned} \tag{6.27}$$

   This tensor product does not contain any singlet under $\mathfrak{g}_{res}$, so the backgrounds we consider have $T_{[\underline{BCD}]\widehat{A}} = 0$.

2. $V_{\underline{A}[\widehat{B}\widehat{C}]}$: We are looking for components of the field strength $(dV)_{[\underline{AB}]\,[\widehat{C}\widehat{D}]}$ invariant under $\mathfrak{g}_{res}$. The decomposition of $(dV)_{[\underline{AB}]\,[\widehat{C}\widehat{D}]}$ is:

$$\begin{aligned}(\mathbf{15},\mathbf{10}) \to &(\mathbf{2},\mathbf{2},\mathbf{3})_{(\pm\mathbf{2})} \oplus (\mathbf{3},\mathbf{1},\mathbf{3})_{(\mathbf{0})} \oplus (\mathbf{1},\mathbf{3},\mathbf{3})_{(\mathbf{0})} \oplus (\mathbf{1},\mathbf{1},\mathbf{3})_{(\mathbf{0})} \oplus (\mathbf{2},\mathbf{2},\mathbf{3})_{(\pm\mathbf{4})} \\ &\oplus 2\times(\mathbf{2},\mathbf{2},\mathbf{3})_{(\mathbf{0})} \oplus (\mathbf{3},\mathbf{1},\mathbf{3})_{(\pm\mathbf{2})} \oplus (\mathbf{1},\mathbf{3},\mathbf{3})_{(\pm\mathbf{2})} \oplus (\mathbf{1},\mathbf{1},\mathbf{3})_{(\pm\mathbf{2})} \\ &\oplus (\mathbf{2},\mathbf{2},\mathbf{1})_{(\pm\mathbf{2})} \oplus (\mathbf{3},\mathbf{1},\mathbf{1})_{(\mathbf{0})} \oplus (\mathbf{1},\mathbf{3},\mathbf{1})_{(\mathbf{0})} \oplus (\mathbf{1},\mathbf{1},\mathbf{1})_{(\mathbf{0})}\,.\end{aligned} \tag{6.28}$$

   We see that we have a singlet that corresponds to turning on a flux on the S^2 and an ansatz for V is given by

$$V_{\phi\,\widehat{x}\widehat{y}} = \frac{1}{2}\, v(\theta)\, \epsilon_{\widehat{x}\widehat{y}}\,, \tag{6.29}$$

   where $\widehat{x}, \widehat{y}$ run over the components $\widehat{B}, \widehat{C} = 4, 5$, and the other components of V vanish.

3. $b_{\underline{A}}$: The field strength $(db)_{[\underline{AB}]}$ decomposes under $\mathfrak{g}_{res}$ as

$$(\mathbf{15},\mathbf{1}) \to (\mathbf{2},\mathbf{2},\mathbf{1})_{(\pm\mathbf{2})} \oplus (\mathbf{3},\mathbf{1},\mathbf{1})_{(\mathbf{0})} \oplus (\mathbf{1},\mathbf{3},\mathbf{1})_{(\mathbf{0})} \oplus (\mathbf{1},\mathbf{1},\mathbf{1})_{(\mathbf{0})}\,. \tag{6.30}$$

   There is a singlet, which corresponds to turning on a field strength on the S^2. In the following we will not consider this possibility. Note that any other choice can always be obtained by a conformal transformation with K, which shifts $b_{\underline{A}}$ [233]. In the following we thus set

$$b_{\underline{A}} = 0\,. \tag{6.31}$$

[2] In Euclidean signature, $T_{[\underline{BCD}]\widehat{A}}$ can be complexified and taken to satify $T = i \star T$.

4. $D_{(\widehat{A}\widehat{B})}$: The decomposition under $\mathfrak{g}_{res}$ is given by

$$(\mathbf{1},\mathbf{14}) \to (\mathbf{1},\mathbf{1},\mathbf{5})_{(\mathbf{0})} \oplus (\mathbf{1},\mathbf{1},\mathbf{3})_{(\pm\mathbf{2})} \oplus (\mathbf{1},\mathbf{1},\mathbf{1})_{(\pm\mathbf{2})} \oplus (\mathbf{1},\mathbf{1},\mathbf{1})_{(\mathbf{0})} \,. \tag{6.32}$$

There is one singlet corresponding to the ansatz

$$D_{\widehat{a}\widehat{b}} = d\,\delta_{\widehat{a}\widehat{b}} \quad , \quad D_{\widehat{x}\widehat{y}} = -\frac{3}{2}\,d\,\delta_{\widehat{x}\widehat{y}}\,, \tag{6.33}$$

with other components vanishing. The relative coefficients are fixed by the tracelessness condition on $D_{(\widehat{A}\widehat{B})}$.

6.2.4 Killing spinors

With the ansätze for the supergravity background fields we can now determine the conditions on the coefficients v and d, to preserve supersymmetry. The background of the 6d supergravity is summarised in section 6.2.3 and the Killing spinor equations (C.23) and (C.29) are solved in appendix C.2. In summary the background with $T_{[\underline{BCD}]\widehat{A}} = b_{\underline{A}} = 0$ preserves half the supersymmetries if

$$\begin{aligned} v(\theta) &= -\frac{\ell'(\theta)}{r} \\ d(\theta) &= \frac{3}{2}\frac{\ell''(\theta)}{r^2\ell(\theta)}\,, \end{aligned} \tag{6.34}$$

where for the round two-sphere $\ell(\theta) = r\sin(\theta)$, and the Killing spinor ϵ is constant and satisfies the following constraint

$$(\Gamma^{\widehat{45}})^{\widehat{m}}{}_{\widehat{n}}\epsilon^{\widehat{n}} - \Gamma^{56}\epsilon^{\widehat{m}} = 0\,. \tag{6.35}$$

The value of the R-symmetry gauge field $V^{56} = -\frac{\ell'(\theta)}{r}d\phi = \omega^{56}$ and the fact that the preserved supersymmetries are generated by constant spinors indicates that this supergravity background realises the topological twist on S^2, as expected.

Finally, recall that we chose a gauge for which $b_{\underline{A}} = 0$. Note that the background field $b_{\underline{A}}$ can be fixed to an arbitrary other value by a special conformal transformation (see [233]). The special conformal transformation does not act on the other background fields (they transform as scalars under these transformations), nor on the spinor $\epsilon^{\widehat{m}}$, however it changes the spinor $\eta^{\widehat{m}}$ parametrizing conformal supersymmetry transformations. Indeed one can show that the Killing spinor equations (C.23) and (C.29) are solved for an arbitrary $b_{\underline{A}}$ by the same solution $\epsilon^{\widehat{m}}$ together with

$$\eta^{\widehat{m}} \;=\; -\frac{1}{2}b_{\underline{A}}\Gamma^{\underline{A}}\epsilon^{\widehat{m}}\,. \tag{6.36}$$

In this way one can recover the gauge choice $b_{\underline{\mu}} = \alpha^{-1}\partial_{\underline{\mu}}\alpha$ (with $\alpha = 1/\ell$ in our conventions) of [235], although we will keep our more convenient choice $b_{\underline{\mu}} = 0$. For our gauge choice, the dimensional reduction to 5d is rederived in appendix C.3.

6.3 From 6d $\mathcal{N} = (2,0)$ on S^2 to 5d $\mathcal{N} = 2$ SYM

We now proceed with the dimensional reduction of the six-dimensional $\mathcal{N} = (2,0)$ theory on S^1 to obtain 5d maximally supersymmetric Yang–Mills theory, as in [260, 235]. The main distinction in our case arises in subtle boundary conditions, which will have to be imposed on the fields along the 5d interval. All our conventions are summarised in appendix C.1.

We should remark on an important point in the signature conventions: the reduction to the 5d $\mathcal{N} = 2$ SYM theory is accomplished in Lorentzian signature, $\mathbb{R}^4 \to \mathbb{R}^{1,3}$, where fields admit 6d reality conditions, however it would go through in Euclidean signature upon complexifying the fields in 6d and then imposing reality conditions in 5d. This amounts to Wick-rotating the Lorentzian 5d theory. In later sections, when we study the 5d theory on a generic M_4, we adopt the Euclidean signature, which is compatible with the twist on M_4.

6.3.1 The 6d $\mathcal{N} = (2,0)$ Theory

The abelian 6d $\mathcal{N} = (2,0)$ theory contains a tensor multiplet, which is comprised of a two-form $\mathcal{B}$ with field strength $H = d\mathcal{B}$, five scalars $\Phi_{\widehat{m}\widehat{n}}$, and four Weyl spinors $\rho^{\widehat{m}}_{\underline{m}}$ of negative chirality, which are symplectic Majorana. The scalars satisfy $\Phi_{\widehat{m}\widehat{n}} = -\Phi_{\widehat{n}\widehat{m}}$ and $\Omega^{\widehat{m}\widehat{n}}\Phi_{\widehat{m}\widehat{n}} = 0$. The equations of motion are (we will use the conventions of [233])

$$\begin{aligned} H^-_{\underline{\mu\nu\sigma}} - \frac{1}{2}\Phi_{\widehat{m}\widehat{n}} T^{\widehat{m}\widehat{n}}_{\underline{\mu\nu\sigma}} &= 0 \\ D^2\Phi_{\widehat{m}\widehat{n}} - \frac{1}{15} D^{\widehat{r}\widehat{s}}_{\widehat{m}\widehat{n}}\Phi_{\widehat{r}\widehat{s}} + \frac{1}{3} H^+_{\underline{\mu\nu\sigma}} T^{\underline{\mu\nu\sigma}}_{\widehat{m}\widehat{n}} &= 0 \\ \not{D}\rho^{\widehat{m}} - \frac{1}{12} T^{\widehat{m}\widehat{n}}_{\underline{\mu\nu\sigma}} \Gamma^{\underline{\mu\nu\sigma}} \rho_{\widehat{n}} &= 0\,. \end{aligned} \tag{6.37}$$

Here $H^\pm = 1/2(H \pm \star H)$ and the R-symmetry indices of the background fields have been transformed from $\widehat{A} \to \widehat{m}\widehat{n}$ using the Gamma-matrices as in (C.25). The covariant derivatives are defined as follows

$$\begin{aligned} D_{\underline{\mu}}\rho^{\widehat{m}} &= \left(\partial_{\underline{\mu}} - \frac{5}{2} b_{\underline{\mu}} + \frac{1}{4}\omega_{\underline{\mu}}^{\underline{AB}}\Gamma_{\underline{AB}}\right)\rho^{\widehat{m}} - \frac{1}{2} V^{\widehat{m}}_{\underline{\mu}\widehat{n}}\rho^{\widehat{n}} \\ D_{\underline{\mu}}\Phi^{\widehat{m}\widehat{n}} &= (\partial_{\underline{\mu}} - 2b_{\underline{\mu}})\Phi^{\widehat{m}\widehat{n}} + V^{[\widehat{m}}_{\underline{\mu}\widehat{r}}\Phi^{\widehat{n}]\widehat{r}} \\ D^2\Phi^{\widehat{m}\widehat{n}} &= \left(\partial^{\underline{A}} - 3b^{\underline{A}} + \omega^{\underline{BA}}_{\underline{B}}\right) D_{\underline{A}}\Phi^{\widehat{m}\widehat{n}} + V^{\underline{A}[\widehat{m}}_{\widehat{r}} D_{\underline{A}}\Phi^{\widehat{n}]\widehat{r}} - \frac{R_{6d}}{5}\Phi^{\widehat{m}\widehat{n}}\,. \end{aligned} \tag{6.38}$$

Here R_{6d} is the 6d Ricci scalar. These equations are invariant under the following supersymmetry transformations

$$\begin{aligned}\delta\mathcal{B}_{\underline{\mu\nu}} &= -\epsilon^{\widehat{m}}\Gamma_{\underline{\mu\nu}}\rho_{\widehat{m}}\\ \delta\Phi^{\widehat{m}\widehat{n}} &= -4\epsilon^{[\widehat{m}}\rho^{\widehat{n}]} - \Omega^{\widehat{m}\widehat{n}}\epsilon^{\widehat{r}}\,\rho_{\widehat{r}}\\ \delta\rho^{\widehat{m}} &= \frac{1}{48}H^{+}_{\underline{\mu\nu\sigma}}\Gamma^{\underline{\mu\nu\sigma}}\epsilon^{\widehat{m}} + \frac{1}{4}\not{D}\Phi^{\widehat{m}\widehat{n}}\epsilon_{\widehat{n}} - \Phi^{\widehat{m}\widehat{n}}\eta_{\widehat{n}}\,.\end{aligned} \tag{6.39}$$

The dimensional reduction of these equations yields abelian 5d $\mathcal{N}=2$ SYM in a general supergravity background. We will perform this reduction in a gauge choice where $b_{\underline{A}}=0$, which is for instance different from the choice in [235]. The details of this general reduction are given in appendix C.3. The 6d supergravity fields decompose as follows

$$\begin{aligned} e^{\underline{\mu}}_{\underline{A}} \;&\to\; \begin{pmatrix} e^{\mu'}_{A'} & e^{\phi}_{A'}\equiv C_{A'} \\ e^{\mu'}_{6}\equiv 0 & e^{\phi}_{6}\equiv\alpha \end{pmatrix} \qquad & H \;&\to\; F=dA\\ & & \rho^{\underline{m}\widehat{m}} \;&\to\; \begin{pmatrix} 0 \\ i\rho^{m'\widehat{m}} \end{pmatrix}\\ & & \Phi^{\widehat{m}\widehat{n}} \;&\to\; \Phi^{\widehat{m}\widehat{n}}\,, \end{aligned} \tag{6.40}$$

where we used again the index conventions in appendix C.1. The action of abelian 5d $\mathcal{N}=2$ SYM theory in a general background is

$$S_{5d} = S_F + S_{\text{scalar}} + S_\rho\,, \tag{6.41}$$

where

$$\begin{aligned} S_F &= -\int [\alpha\tilde{F}\wedge\star_{5d}\tilde{F} + C\wedge F\wedge F]\\ S_{\text{scalar}} &= -\int d^5x\,\sqrt{|g|}\,\alpha^{-1}\left(D_{A'}\Phi^{\widehat{m}\widehat{n}}D^{A'}\Phi_{\widehat{m}\widehat{n}} + 4\Phi^{\widehat{m}\widehat{n}}F_{A'B'}T^{A'B'}_{\widehat{m}\widehat{n}} - \Phi_{\widehat{m}\widehat{n}}(M_\Phi)^{\widehat{m}\widehat{n}}_{\widehat{r}\widehat{s}}\Phi^{\widehat{r}\widehat{s}}\right)\\ S_\rho &= -\int d^5x\sqrt{|g|}\,\alpha^{-1}\rho_{m'\widehat{m}}\left(i\not{D}^{m'}_{n'}\rho^{n'\widehat{m}} + (M_\rho)^{m'\widehat{m}}_{n'\widehat{n}}\rho^{n'\widehat{n}}\right)\,, \end{aligned} \tag{6.42}$$

with all mass matrices defined in appendix C.3 and $\tilde{F}$ is defined as

$$\tilde{F} = F - \frac{1}{\alpha}\Phi_{\widehat{m}\widehat{n}}T^{\widehat{m}\widehat{n}}\,. \tag{6.43}$$

6.3.2 5d $\mathcal{N}=2$ SYM in the Supergravity Background

We can now specialise to the 6d background $\mathbb{R}^4\times S^2$, including the background supergravity fields of section 6.2 and determine the 5d $\mathcal{N}=2$ SYM theory in the background, which corresponds to the 6d $\mathcal{N}=(2,0)$ theory on S^2, by performing the dimensional reduction along the circle fiber. As shown in section 6.2.3, the only background fields for the 5d $\mathcal{N}=2$ SYM theory, which are compatible with the residual symmetry group, are $D^{\widehat{m}\widehat{n}}_{\widehat{r}\widehat{s}}$ and $V^{\widehat{m}\widehat{n}}_{\phi}\equiv S^{\widehat{m}\widehat{n}}$. With these background fields, and the action of the 5d $\mathcal{N}=2$ SYM

theory in a general background, that we derived in appendix C.3 in the gauge $b_{\underline{A}} = 0$, we can now determine the non-abelian 5d action in our background.

For our background the metric, graviphoton, $C_{A'}$, and the dilaton, α, are given by

$$ds_5^2 = ds^2_{\mathbb{R}^4} + r^2 d\theta^2\,, \quad C_{A'} = 0\,, \quad \alpha = \frac{1}{\ell(\theta)}\,, \quad 0 \leq \theta \leq \pi\,, \tag{6.44}$$

which means that $G = dC = 0$. Imposing these conditions and turning on only the background fields $D^{\widehat{m}\widehat{n}}_{rs}$ and $S^{\widehat{m}\widehat{n}}$ the full action is given by[3]

$$S = S_F + S_{\text{scalar}} + S_\rho + S_{\text{int}}\,, \tag{6.45}$$

where

$$\begin{aligned}
S_F &= -\frac{1}{4}\int \frac{1}{\ell(\theta)}\ \text{Tr}(F \wedge \star_{5d} F)\\
S_{\text{scalar}} &= \frac{1}{16}\int d^5x\ \sqrt{|g|}\,\ell(\theta)\,\text{Tr}\left(\Phi^{\widehat{m}\widehat{n}} D^2 \Phi_{\widehat{m}\widehat{n}} + \Phi^{\widehat{m}\widehat{n}} (M_\Phi)^{\widehat{r}\widehat{s}}_{\widehat{m}\widehat{n}} \Phi_{\widehat{r}\widehat{s}}\right)\\
S_\rho &= -\int d^5x\ \sqrt{|g|}\,\ell(\theta)\,\text{Tr}\left(i\rho_{m'\widehat{m}} \not{D}^{m'}_{n'}\rho^{n'\widehat{m}} + \rho_{m'\widehat{m}} (M_\rho)^{\widehat{m}\widehat{n}m'}_{\quad n'} \rho^{n'}_{\widehat{n}}\right)\,.
\end{aligned} \tag{6.46}$$

Here, we non-abelianised the theory, and the covariant derivatives and mass matrices

$$\begin{aligned}
D_{\mu'}\Phi^{\widehat{m}\widehat{n}} &= \partial_{\mu'} + [A_{\mu'}, \Phi^{\widehat{m}\widehat{n}}]\\
D^2\Phi^{\widehat{m}\widehat{n}} &= \partial^{\mu'} D_{\mu'}\Phi^{\widehat{m}\widehat{n}} + \frac{\ell'(\theta)}{r^2\ell(\theta)}\, D_\theta \Phi^{\widehat{m}\widehat{n}} + [A_{\mu'}, \partial^{\mu'}\Phi^{\widehat{m}\widehat{n}}] + [A_{\mu'}, [A^{\mu'}, \Phi^{\widehat{m}\widehat{n}}]]\\
D_{\mu'}\rho^{\widehat{m}} &= \partial_{\mu'}\rho^{\widehat{m}} + [A_{\mu'}, \rho^{\widehat{m}}]\\
(M_\Phi)^{\widehat{m}\widehat{n}}_{\widehat{r}\widehat{s}} &= \frac{2\ell''(\theta)}{5r^2\ell(\theta)}\,\delta^{\widehat{m}}_{[\widehat{r}}\delta^{\widehat{n}}_{\widehat{s}]} + \frac{1}{2\ell(\theta)^2}\left(S^{\widehat{m}}_{[\widehat{r}} S^{\widehat{n}}_{\widehat{s}]} - S^{\widehat{n}}_{\widehat{t}} S^{\widehat{t}}_{[\widehat{r}}\delta^{\widehat{m}}_{\widehat{s}]}\right) - \frac{1}{15} D^{\widehat{m}\widehat{n}}_{\widehat{r}\widehat{s}}\\
(M_\rho)^{\widehat{m}\widehat{n}m'}_{\quad n'} &= \frac{1}{\ell(\theta)}\left(\frac{1}{2} S^{\widehat{m}\widehat{n}}\delta^{m'}_{n'} + \frac{i\ell'(\theta)}{2r}\,\Omega^{\widehat{m}\widehat{n}}(\gamma_5)^{m'}_{n'}\right)\,,
\end{aligned} \tag{6.47}$$

where the five-dimensional Ricci scalar vanishes, because we have a flat metric on the interval. In the non-abelian case we can add the following interaction terms

$$S_{\text{int}} = \int d^5x\sqrt{|g|}\text{Tr}\left(\frac{\ell(\theta)^3}{64}[\Phi_{\widehat{m}\widehat{n}}, \Phi^{\widehat{n}\widehat{r}}][\Phi_{\widehat{r}\widehat{s}}, \Phi^{\widehat{s}\widehat{m}}] + \frac{\ell(\theta)}{24} S_{\widehat{m}\widehat{n}}\Phi^{\widehat{m}\widehat{r}}[\Phi^{\widehat{n}\widehat{s}}, \Phi_{\widehat{r}\widehat{s}}] - \ell(\theta)^2\rho_{m'\widehat{m}}[\Phi^{\widehat{m}\widehat{n}}, \rho^{m'}_{\widehat{n}}]\right)\,, \tag{6.48}$$

where the non-vanishing background fields are

$$\begin{aligned}
S^{\widehat{m}}_{\widehat{n}} &= -\frac{\ell'(\theta)}{r}(\Gamma^{\widehat{4}\widehat{5}})^{\widehat{m}}_{\widehat{n}}\\
D^{\widehat{m}\widehat{n}}_{\widehat{r}\widehat{s}} &= \frac{3\ell''(\theta)}{2r^2\ell(\theta)}\left[5(\Gamma^{\widehat{4}\widehat{5}})^{[\widehat{m}}_{\widehat{r}}(\Gamma^{\widehat{4}\widehat{5}})^{\widehat{n}]}_{\widehat{s}} - \delta^{[\widehat{m}}_{\widehat{r}}\delta^{\widehat{n}]}_{\widehat{s}} - \Omega^{\widehat{m}\widehat{n}}\Omega_{\widehat{r}\widehat{s}}\right]\,,
\end{aligned} \tag{6.49}$$

[3]The ratios of numerical prefactors are determined by supersymmetry. Note that our convention for the scalar fields and gauge fields is that they are anti-hermitian.

where ℓ' and ℓ'' denote first and second derivatives of ℓ with respect to θ. The action is invariant under the following supersymmetry transformations

$$\begin{aligned}
\delta A_{\mu'} &= \ell(\theta)\, \epsilon_{\widehat{m}} \gamma_{\mu'} \rho^{\widehat{m}} \\
\delta \Phi^{\widehat{m}\widehat{n}} &= -4i\epsilon^{[\widehat{m}} \rho^{\widehat{n}]} - i\Omega^{\widehat{m}\widehat{n}} \epsilon^{\widehat{r}}\, \rho_{\widehat{r}} \\
\delta \rho^{\widehat{m}} &= \frac{i}{8\ell(\theta)} F_{\mu'\nu'} \gamma^{\mu'\nu'} \epsilon^{\widehat{m}} + \frac{1}{4} \not{D} \Phi^{\widehat{m}\widehat{n}} \epsilon_{\widehat{n}} + \frac{i}{4\ell(\theta)} S^{[\widehat{m}}_{\widehat{r}} \Phi^{\widehat{n}]\widehat{r}} \epsilon_{\widehat{n}} - \frac{i}{8} \ell(\theta) \Omega_{\widehat{n}\widehat{r}} [\Phi^{\widehat{m}\widehat{n}}, \Phi^{\widehat{r}\widehat{s}}] \epsilon_{\widehat{s}}\,.
\end{aligned} \tag{6.50}$$

Note that the Killing spinor $\epsilon^{m'}_{\widehat{m}}$ satisfies the relation (6.35) which now reads

$$(\Gamma^{\widehat{45}})^{\widehat{m}\widehat{n}} \epsilon^{m'}_{\widehat{n}} = -i(\gamma_5)^{m'}_{n'} \epsilon^{n'\widehat{m}}\,. \tag{6.51}$$

So far we have kept the $\mathfrak{sp}(4)_R$ R-symmetry indices explicit. However the background breaks the R-symmetry to $\mathfrak{su}(2)_R \oplus \mathfrak{so}(2)_R$. To make the symmetry of the theory manifest, we decompose the scalar fields $\Phi^{\widehat{m}\widehat{n}}$ into a triplet of scalars $\varphi^{\widehat{a}}$, transforming in the $\mathbf{3_0}$ of $\mathfrak{su}(2)_R \oplus \mathfrak{so}(2)_R$, and the complex field φ, which is a singlet $\mathbf{1_1}$. This can be achieved as follows

$$\begin{aligned}
\varphi^{\widehat{a}} &= \frac{1}{4} (\Gamma^{\widehat{a}})_{\widehat{m}\widehat{n}} \Phi^{\widehat{m}\widehat{n}}\,, \quad \widehat{a} = 1,2,3 \\
\varphi = \varphi^4 + i\varphi^5 &= \frac{1}{4} \left(\Gamma^4 + i\Gamma^5\right)_{\widehat{m}\widehat{n}} \Phi^{\widehat{m}\widehat{n}}\,.
\end{aligned} \tag{6.52}$$

The spinors $\rho_{\widehat{m}}$ decompose into the two doublets $\rho^{(1)}_{\widehat{p}}$, $\rho^{(2)}_{\widehat{p}}$, transforming in $(\mathbf{2})_{\mathbf{1}} \oplus (\mathbf{2})_{\mathbf{-1}}$, as detailed in appendix C.1.3. We also split the gauge field (singlet of the R-symmetry) into the components A_μ along $\mathbb{R}^4$ and the component A_θ along the interval.

The spinor $\epsilon_{\widehat{n}}$ parametrizing supersymmetry transformations decomposes under the R-symmetry subalgebra $\mathfrak{su}(2)_R \oplus \mathfrak{so}(2)_R$ into two $\mathfrak{su}(2)_R$ doublets of opposite $\mathfrak{so}(2)_R$ charge: $\epsilon_{\widehat{m}} \to \epsilon^{(1)}_{\widehat{p}}, \epsilon^{(2)}_{\widehat{p}}$ (see appendix C.1.3). The projection condition (6.51) becomes

$$\epsilon^{(1)}_{\widehat{p}} - \gamma^5 \epsilon^{(1)}_{\widehat{p}} = 0\,, \quad \epsilon^{(2)}_{\widehat{p}} + \gamma^5 \epsilon^{(2)}_{\widehat{p}} = 0\,. \tag{6.53}$$

For any 5d spinor χ we define

$$\chi_\pm = \frac{1}{2}(\chi \pm \gamma^5 \chi)\,, \tag{6.54}$$

as the four-dimensional chirality. The action for the gauge field is

$$S_F = -\frac{1}{8} \int d^5x \sqrt{|g|}\, \frac{1}{\ell(\theta)} \operatorname{Tr} \left(F_{\mu\nu} F^{\mu\nu} + 2 F_{\mu\theta} F^{\mu\theta} \right)\,, \tag{6.55}$$

and for the scalars we find

$$\begin{aligned}
&S_{\text{scalar}} \\
&= -\frac{1}{4} \int d^5x \sqrt{|g|} \ell(\theta) \operatorname{Tr} \left(D^\mu \varphi^{\widehat{a}} D_\mu \varphi_{\widehat{a}} + D^\mu \varphi D_\mu \bar{\varphi} + \frac{1}{r^2} D_\theta \varphi^{\widehat{a}} D_\theta \varphi_{\widehat{a}} + \frac{1}{r^2} D_\theta \varphi D_\theta \bar{\varphi} + m_\varphi^2 \varphi \bar{\varphi} \right)\,,
\end{aligned} \tag{6.56}$$

with the mass term

$$m_\varphi(\theta)^2 = \frac{\ell'(\theta)^2 - \ell(\theta)\ell''(\theta)}{r^2 \ell(\theta)^2}\,, \tag{6.57}$$

which for the round sphere is $m_\varphi^2 = \cot(\theta)^2/r^2$ and diverges at the endpoints of the interval. We will return to this matter when discussing the boundary conditions. The action for the fermions is

$$S_\rho = -2i \int d^5x \sqrt{|g|}\; \ell(\theta)\, \mathrm{Tr}\left(\rho^{(1)}_{\widehat{p}+}\gamma^\mu D_\mu \rho^{(2)\widehat{p}}_{-} + \rho^{(1)}_{\widehat{p}-}\gamma^\mu D_\mu \rho^{(2)\widehat{p}}_{+} + \frac{1}{r}\rho^{(1)}_{\widehat{p}+} D_\theta \rho^{(2)\widehat{p}}_{+} - \frac{1}{r}\rho^{(2)}_{\widehat{p}-} D_\theta \rho^{(1)\widehat{p}}_{-}\right)\,. \tag{6.58}$$

Finally, the interaction terms in this decomposition read as follows

$$\begin{aligned}
S_{\text{Yukawa}} = -\int d^5x \sqrt{|g|}\, \ell(\theta)^2\, \mathrm{Tr}\Big[&2(\sigma^{\widehat{a}})^{\widehat{p}\widehat{q}}\rho^{(2)}_{\widehat{p}-}\left[\varphi_{\widehat{a}}, \rho^{(1)}_{\widehat{q}-}\right] + 2(\sigma^{\widehat{a}})^{\widehat{p}\widehat{q}}\rho^{(2)}_{\widehat{p}+}\left[\varphi_{\widehat{a}}, \rho^{(1)}_{\widehat{q}+}\right] \\
&+ i\left(\rho^{(1)}_{\widehat{p}-}\left[\bar{\varphi}, \rho^{\widehat{p}(1)}_{-}\right] + \rho^{(1)}_{\widehat{p}+}\left[\bar{\varphi}, \rho^{\widehat{p}(1)}_{+}\right] - \rho^{(2)}_{\widehat{p}-}\left[\varphi, \rho^{\widehat{p}(2)}_{-}\right] - \rho^{(2)}_{\widehat{p}+}\left[\varphi, \rho^{\widehat{p}(2)}_{+}\right]\right)\Big] \\
S_{\text{quartic}} = -\frac{1}{4}\int d^5x \sqrt{|g|}\, \ell(\theta)^3\, \mathrm{Tr}&\left([\varphi_{\widehat{a}}, \varphi][\varphi^{\widehat{a}}, \bar{\varphi}] + \frac{1}{2}[\varphi_{\widehat{a}}, \varphi_{\widehat{b}}][\varphi^{\widehat{a}}, \varphi^{\widehat{b}}] - \frac{1}{4}[\varphi, \bar{\varphi}][\varphi, \bar{\varphi}]\right) \\
S_{\text{cubic}} = -\frac{1}{6}\int d^5x \sqrt{|g|}\, &\frac{\ell(\theta)\ell'(\theta)}{r}\, \epsilon^{\widehat{a}\widehat{b}\widehat{c}}\, \mathrm{Tr}\left(\varphi_{\widehat{a}}[\varphi_{\widehat{b}}, \varphi_{\widehat{c}}]\right)\,.
\end{aligned} \tag{6.59}$$

The complete 5d action is

$$S_{5d} = S_F + S_{\text{scalar}} + S_\rho + S_{\text{Yukawa}} + S_{\text{quartic}} + S_{\text{cubic}}\,, \tag{6.60}$$

and the supersymmetry variations for this action, decomposed with regards to the R-symmetry, are summarised in appendix C.4. The action above should be supplemented with appropriate boundary terms, which ensure that supersymmetry is preserved and that the action is finite. This will be addressed subsequently.

We need to determine the boundary conditions of the 5d fields at the endpoints of the θ interval. To proceed we first notice that the complex scalar φ has a mass term $m(\theta)^2$ which diverges at the boundaries $\theta = 0, \pi$ [4]

$$m(\theta)^2 \simeq \begin{cases} \frac{1}{\theta^2} & , \quad \theta \to 0\,, \\ \frac{1}{(\pi-\theta)^2} & , \quad \theta \to \pi\,. \end{cases} \tag{6.61}$$

Finiteness of the action requires that φ behaves as

$$\varphi = \begin{cases} O(\theta) & , \quad \theta \to 0\,, \\ O(\pi-\theta) & , \quad \theta \to \pi\,. \end{cases} \tag{6.62}$$

The boundary conditions on the other fields are most easily determined by the requirement of preserving supersymmetry under the transformations generated by $\epsilon^{(1)}_{\widehat{p}}$ and $\epsilon^{(2)}_{\widehat{p}}$ presented in appendix C.4. We obtain at $\theta = 0$:

$$\rho^{(1)}_{\widehat{p}+} = O(\theta)\,, \quad \rho^{(2)}_{\widehat{p}-} = O(\theta)\,, \quad A_\mu = O(\theta^2)\,, \tag{6.63}$$

[4] This follows from the regularity conditions (6.20) on ℓ.

and the counterpart at $\theta = \pi$.

The fields $\varphi^{\widehat{a}}, A_\theta$ are constrained by supersymmetry to obey modified Nahm's equations as they approach the boundaries, given by

$$D_\theta \varphi^{\widehat{a}} - \frac{1}{2} r \ell(\theta) \epsilon^{\widehat{a}}{}_{\widehat{b}\widehat{c}} [\varphi^{\widehat{b}}, \varphi^{\widehat{c}}] = 0 \,. \tag{6.64}$$

These equations are compatible with a singular boundary behaviour of the fields at the endpoints of the θ-interval. For simplicity let us assume the gauge $A_\theta = 0$ in a neighborhood of $\theta = 0$, then the above modified Nahm's equations are compatible with the polar behavior at $\theta = 0$

$$\varphi^{\widehat{a}} = \frac{2\varrho(\tau^{\widehat{a}})}{r^2 \theta^2} + O(1) \,, \tag{6.65}$$

where

$$\varrho : \quad \mathfrak{su}(2) \to \mathfrak{u}(k) \tag{6.66}$$

denotes a Lie algebra homomorphism from $\mathfrak{su}(2)$ to $\mathfrak{u}(k)$, see e.g. in [244, 245] and $\tau^{\widehat{a}}$ are related to the Pauli matrices $\sigma^{\widehat{a}}$ as follows

$$\tau^{\widehat{a}} = \frac{i}{2} \sigma^{\widehat{a}} \,. \tag{6.67}$$

Moreover the $O(1)$ term is constrained to be in the commutant of ϱ in $\mathfrak{u}(k)$. The reduction that we study, from a smooth two-sphere to the interval, corresponds to ϱ being an irreducible embedding [245].

More generally the Nahm pole boundary condition (6.64) is compatible with any homomorphism ϱ and is associated with the presence of 'punctures' – or field singularities – at the poles of the two-sphere in the 6d non-abelian theory [217]. An embedding ϱ can be associated to a decomposition of the fundamental representation $\mathbf{k}$ under $\mathfrak{su}(2)$ and can be recast into a partition $[n_1, n_2, \cdots]$ of k. The irreducible embedding is associated to the partition $\varrho = [k]$ and corresponds to the absence of punctures in 6d, and is therefore the sphere reduction that we consider here. The boundary conditions at $\theta = \pi$ are symmetric to the ones at $\theta = 0$ and are also characterised by Nahm pole behaviour with irreducible embedding $\varrho = [k]$.

The remaining fermions $\rho_-^{(1)}, \rho_+^{(2)}$ appear in the supersymmetry variations of $\varphi^{\widehat{a}}$ and hence are of order $O(1)$ at $\theta = 0$

$$\rho^{(1)}_{\widehat{p}\,-} = O(1) \,, \qquad \rho^{(2)}_{\widehat{p}\,+} = O(1) \,, \tag{6.68}$$

and similarly at $\theta = \pi$.

The boundary condition (6.65) for the scalars $\varphi^{\widehat{a}}$ introduces two difficulties: the supersymmetry variation of the action results in a non-vanishing boundary term and the poles

of the scalar fields make the action diverge. These two problems are cured by the addition of the following boundary term

$$\begin{aligned} S_{\text{bdry}} &= \left[\frac{\ell(\theta)^2}{12}\int d^4x\sqrt{|g_4|}\,\text{Tr}\left(\epsilon^{\widehat{a}\widehat{b}\widehat{c}}\varphi_{\widehat{a}}[\varphi_{\widehat{b}},\varphi_{\widehat{c}}]\right)\right]_0^\pi \\ &= \int d\theta\,\partial_\theta\left[\frac{\ell(\theta)^2}{12}\int d^4x\sqrt{|g_4|}\,\text{Tr}\left(\epsilon^{\widehat{a}\widehat{b}\widehat{c}}\varphi_{\widehat{a}}[\varphi_{\widehat{b}},\varphi_{\widehat{c}}]\right)\right], \end{aligned} \tag{6.69}$$

The second line gives S_{bdry} as a total θ-derivative and we shall take this as the definition of the boundary term. This additional term ensures supersymmetry and makes the 5d action finite. In particular, taking the derivative along θ we find,

$$S_{\text{bdry}} = \int d^5x\sqrt{|g|}\left[\frac{\ell(\theta)\ell'(\theta)}{6r}\epsilon^{\widehat{a}\widehat{b}\widehat{c}}\,\text{Tr}\left(\varphi_{\widehat{a}}[\varphi_{\widehat{b}},\varphi_{\widehat{c}}]\right)+\frac{\ell(\theta)^2}{4r}\epsilon^{\widehat{a}\widehat{b}\widehat{c}}\,\text{Tr}\left(\partial_\theta\varphi_{\widehat{a}}[\varphi_{\widehat{b}},\varphi_{\widehat{c}}]\right)\right], \tag{6.70}$$

where the first piece cancels the cubic scalar interaction in the 5d action and the second term combines to give

$$\begin{aligned} &-\frac{1}{4r^2}\int d^5x\sqrt{|g|}\ell(\theta)\,\text{Tr}\left(D_\theta\varphi^{\widehat{a}}D_\theta\varphi_{\widehat{a}}+r^2\ell(\theta)^2\frac{1}{2}[\varphi_{\widehat{a}},\varphi_{\widehat{b}}][\varphi^{\widehat{a}},\varphi^{\widehat{b}}]-r\ell(\theta)\epsilon^{\widehat{a}\widehat{b}\widehat{c}}\partial_\theta\varphi_{\widehat{a}}[\varphi_{\widehat{b}},\varphi_{\widehat{c}}]\right) \\ &\qquad = -\frac{1}{4r^2}\int d^5x\sqrt{|g|}\,\text{Tr}\left(D_\theta\varphi_{\widehat{a}}-\frac{1}{2}r\ell(\theta)\epsilon_{\widehat{a}\widehat{b}\widehat{c}}[\varphi^{\widehat{b}},\varphi^{\widehat{c}}]\right)^2, \end{aligned} \tag{6.71}$$

which is the square of modified Nahm's equations. The 5d action is finite since the scalar fields $\varphi^{\widehat{a}}$ obey modified Nahm's equations at the boundaries.

We notice that the modified Nahm's equations (6.64) can be recast into the form of standard Nahm's equations by a change of coordinate to

$$\widetilde{\theta} = \frac{1}{r}\int_0^\theta dx\,\ell(x)\,. \tag{6.72}$$

One obtains

$$\begin{aligned} &D_{\widetilde{\theta}}\varphi^{\widehat{a}}-\frac{1}{2}r^2\epsilon^{\widehat{a}}{}_{\widehat{b}\widehat{c}}[\varphi^{\widehat{b}},\varphi^{\widehat{c}}]=0\,, \\ &r^2\varphi^{\widehat{a}}=\frac{\varrho(\tau^{\widehat{a}})}{\widetilde{\theta}}+O(\widetilde{\theta}^0)\,, \end{aligned} \tag{6.73}$$

and a similar Nahm pole behavior at the other end of the $\widetilde{\theta}$ interval. We conclude then that the moduli space of solutions of the modified Nahm's equations is the same as the moduli space of solution of the standard Nahm's equations.

6.3.3 Cylinder Limit

For general hyperbolic Riemann surfaces, with a half-topological twist, the dimensional reduction depends only on the complex structure moduli [217]. The two-sphere has no complex structure moduli, however, there will be a metric-dependence in terms of the area

of the sphere, which enters as the coupling constant of the 4d sigma-model [245]. We do not expect the reduction to depend on the function $\ell(\theta)$, except through the area of the sphere. This can be checked explicitly by performing the reduction keeping $\ell(\theta)$ arbitrary. However, for simplicity we consider here the special singular limiting case, when the two-sphere is deformed to a thin cylinder. This is achieved by taking the metric factor $\ell(\theta)$ as follows

$$\begin{aligned} &\ell(\theta) = \ell = \text{constant} \qquad \text{for} \quad \epsilon < \theta < \pi - \epsilon\,, \\ &\ell(\theta) \to \text{ smooth caps} \quad \text{for} \quad \theta < \epsilon\,,\ \pi - \epsilon < \theta\,, \end{aligned}$$

and then taking the limit $\epsilon \to 0$. The limit is singular at the endpoints of the θ-interval, since at finite ϵ, the two-sphere has smooth caps, $\ell(\theta) \sim r\theta$, while at $\epsilon = 0$, $\ell(\theta) = \ell$ is constant on the whole θ interval and describes the metric on a cylinder, or a sphere with two punctures. One may worry that such a singular limit is too strong and would change the theory itself. We will argue below in section 6.3.4 that the reduction of the theory with ℓ constant leads to the same four-dimensional sigma model as for arbitrary $\ell(\theta)$. The reason for choosing ℓ constant is only to simplify the derivation.

We rescale the fields as follows

$$\varphi^{\widehat{a}} \to \frac{1}{r\ell}\varphi^{\widehat{a}}\,, \quad \varphi \to \frac{1}{r\ell}\varphi\,, \quad \rho^{(1)}_{\pm} \to \frac{1}{r\ell}\rho^{(1)}_{\pm}\,, \quad \rho^{(2)}_{\pm} \to \frac{1}{r\ell}\rho^{(2)}_{\pm}\,. \tag{6.74}$$

The action in this limit simplifies to

$$\begin{aligned} S_F &= -\frac{r}{8\ell}\int d\theta d^4x\sqrt{|g_4|}\,\mathrm{Tr}\left(F_{\mu\nu}F^{\mu\nu} + \frac{2}{r^2}(\partial_\mu A_\theta - \partial_\theta A_\mu + [A_\mu, A_\theta])^2\right) \\ S_{\text{scalar}} &= -\frac{1}{4r\ell}\int d\theta d^4x\sqrt{|g_4|}\,\mathrm{Tr}\left(D^\mu\varphi^{\widehat{a}}D_\mu\varphi_{\widehat{a}} + D^\mu\varphi D_\mu\bar{\varphi} + \frac{1}{r^2}D_\theta\varphi^{\widehat{a}}D_\theta\varphi_{\widehat{a}} + \frac{1}{r^2}D_\theta\varphi D_\theta\bar{\varphi}\right) \\ S_\rho &= -\frac{2i}{r\ell}\int d\theta d^4x\sqrt{|g_4|}\,\mathrm{Tr}\left(\rho^{(1)}_{\widehat{p}+}\gamma^\mu D_\mu\rho^{(2)\widehat{p}}_{-} + \rho^{(1)}_{\widehat{p}-}\gamma^\mu D_\mu\rho^{(2)\widehat{p}}_{+} + \frac{1}{r}\rho^{(1)}_{\widehat{p}+}D_\theta\rho^{(2)\widehat{p}}_{+}\right. \\ &\qquad\left. -\frac{1}{r}\rho^{(1)}_{\widehat{p}-}D_\theta\rho^{(2)\widehat{p}}_{-}\right) \\ S_{\text{Yukawa}} &= -\frac{1}{r^2\ell}\int d\theta d^4x\sqrt{|g_4|}\,\mathrm{Tr}\left(2\rho^{(2)}_{\widehat{p}-}\left[\varphi^{\widehat{p}\widehat{q}}, \rho^{(1)}_{\widehat{q}-}\right] + 2\rho^{(2)}_{\widehat{p}+}\left[\varphi^{\widehat{p}\widehat{q}}, \rho^{(1)}_{\widehat{q}+}\right]\right. \\ &\qquad\left. +i\left(\rho^{(1)}_{\widehat{p}-}\left[\bar{\varphi}, \rho^{\widehat{p}(1)}_{-}\right] + \rho^{(1)}_{\widehat{p}+}\left[\bar{\varphi}, \rho^{\widehat{p}(1)}_{+}\right] - \rho^{(2)}_{\widehat{p}-}\left[\varphi, \rho^{\widehat{p}(2)}_{-}\right] - \rho^{(2)}_{\widehat{p}+}\left[\varphi, \rho^{\widehat{p}(2)}_{+}\right]\right)\right) \\ S_{\text{quartic}} &= -\frac{1}{4r^3\ell}\int d\theta d^4x\sqrt{|g_4|}\,\mathrm{Tr}\left(\frac{1}{2}[\varphi_{\widehat{a}}, \varphi_{\widehat{b}}][\varphi^{\widehat{a}}, \varphi^{\widehat{b}}] + [\varphi_{\widehat{a}}, \varphi][\varphi^{\widehat{a}}, \bar{\varphi}] - \frac{1}{4}[\varphi, \bar{\varphi}][\varphi, \bar{\varphi}]\right) \\ S_{\text{bdry}} &= \frac{1}{6r^3\ell}\int d\theta d^4x\sqrt{|g_4|}\partial_\theta\,\mathrm{Tr}\left(\epsilon^{\widehat{a}\widehat{b}\widehat{c}}\varphi^{\widehat{a}}\varphi^{\widehat{b}}\varphi^{\widehat{c}}\right)\,. \end{aligned} \tag{6.75}$$

The supersymmetry variations of the 5d action summarised in appendix C.4 simplify in

the cylinder limit and for the bosonic fields are

$$\begin{aligned}
\delta A_\mu &= -\frac{1}{r}\left(\epsilon^{(1)\widehat{p}}\gamma_\mu \rho^{(2)}_{\widehat{p}-} + \epsilon^{(2)\widehat{p}}\gamma_\mu \rho^{(1)}_{\widehat{p}+}\right) \\
\delta A_\theta &= -\left(\epsilon^{(1)\widehat{p}}\rho^{(2)}_{\widehat{p}+} - \epsilon^{(2)\widehat{p}}\rho^{(1)}_{\widehat{p}-}\right) \\
\delta\varphi^{\widehat{a}} &= i\left(\epsilon^{(1)}{}_{\widehat{p}}(\sigma^{\widehat{a}})^{\widehat{p}\widehat{q}}\rho^{(2)}_{\widehat{q}+} - \epsilon^{(2)}{}_{\widehat{p}}(\sigma^{\widehat{a}})^{\widehat{p}\widehat{q}}\rho^{(1)}_{\widehat{q}-}\right) \\
\delta\varphi &= -2\epsilon^{(1)\widehat{p}}\rho^{(1)}_{\widehat{p}+} \\
\delta\bar{\varphi} &= +2\epsilon^{(2)\widehat{p}}\rho^{(2)}_{\widehat{p}-}
\end{aligned} \tag{6.76}$$

and for the fermions

$$\begin{aligned}
\delta\rho^{(1)}_{\widehat{p}+} &= \frac{ir}{8}F_{\mu\nu}\gamma^{\mu\nu}\epsilon^{(1)}_{\widehat{p}} - \frac{i}{4}D_\mu\varphi\gamma^\mu\epsilon^{(2)}_{\widehat{p}} + \frac{1}{4r}D_\theta\varphi^{\widehat{q}}_{\widehat{p}}\epsilon^{(1)}_{\widehat{q}} - \frac{1}{8r}\left(\epsilon^{\widehat{a}\widehat{b}\widehat{c}}[\varphi_{\widehat{a}},\varphi_{\widehat{b}}](\sigma_{\widehat{c}})^{\widehat{q}}_{\widehat{p}}\epsilon^{(1)}_{\widehat{q}} - i[\varphi,\bar{\varphi}]\epsilon^{(1)}_{\widehat{p}}\right) \\
\delta\rho^{(1)}_{\widehat{p}-} &= \frac{i}{4}F_{\mu\theta}\gamma^\mu\epsilon^{(1)}_{\widehat{p}} + \frac{1}{4}D_\mu\varphi^{\widehat{q}}_{\widehat{p}}\gamma^\mu\epsilon^{(1)}_{\widehat{q}} + \frac{i}{4r}D_\theta\varphi\epsilon^{(2)}_{\widehat{p}} - \frac{1}{4r}[\varphi,\varphi^{\widehat{q}}_{\widehat{p}}]\epsilon^{(2)}_{\widehat{q}} \\
\delta\rho^{(2)}_{\widehat{p}+} &= -\frac{i}{4}F_{\mu\theta}\gamma^\mu\epsilon^{(2)}_{\widehat{p}} - \frac{1}{4}D_\mu\varphi^{\widehat{q}}_{\widehat{p}}\gamma^\mu\epsilon^{(2)}_{\widehat{q}} + \frac{i}{4r}D_\theta\bar{\varphi}\epsilon^{(1)}_{\widehat{p}} - \frac{1}{4r}[\bar{\varphi},\varphi^{\widehat{q}}_{\widehat{p}}]\epsilon^{(1)}_{\widehat{q}} \\
\delta\rho^{(2)}_{\widehat{p}-} &= \frac{ir}{8}F_{\mu\nu}\gamma^{\mu\nu}\epsilon^{(2)}_{\widehat{p}} + \frac{i}{4}D_\mu\bar{\varphi}\gamma^\mu\epsilon^{(1)}_{\widehat{p}} + \frac{1}{4r}D_\theta\varphi^{\widehat{q}}_{\widehat{p}}\epsilon^{(2)}_{\widehat{q}} - \frac{1}{8r}\left(\epsilon^{\widehat{a}\widehat{b}\widehat{c}}[\varphi_{\widehat{a}},\varphi_{\widehat{b}}](\sigma_{\widehat{c}})^{\widehat{q}}_{\widehat{p}}\epsilon^{(2)}_{\widehat{q}} + i[\varphi,\bar{\varphi}]\epsilon^{(2)}_{\widehat{p}}\right).
\end{aligned} \tag{6.77}$$

The theory we obtain is nothing else than the maximally supersymmetric SYM in 5d. A similar reduction of the 6d $\mathcal{N} = (2,0)$ theory on a cigar geometry was considered in [244]. This five-dimensional $\mathcal{N} = 2$ SYM theory is defined on a manifold with boundaries, which are at the end-points of the θ-interval and half of the supersymmetries are broken by the boundary conditions. It is key to study the boundary terms and boundary conditions in detail, which will be done in the next subsection.

6.3.4 Nahm's Equations and Boundary Considerations

The boundary conditions at the two ends of the θ interval are affected by the singular cylinder limit. They can be worked out in the same way as in section 6.3.2 by enforcing supersymmetry at the boundaries. In the cylinder limit of the two-sphere $\ell(\theta) \to \ell$ the mass term $m(\theta)^2$ goes to zero everywhere along the θ-interval except at the endpoints $\theta = 0, \pi$ where it diverges, forcing the scalar φ to vanish at the boundary, as before. The other boundary conditions are found by requiring supersymmetry under the eight supercharges. This requires that the scalars $\varphi^{\widehat{a}}$ obey the standard Nahm's equations close to the boundaries

$$D_\theta\varphi^{\widehat{a}} - \frac{1}{2}\epsilon^{\widehat{a}}{}_{\widehat{b}\widehat{c}}[\varphi^{\widehat{b}},\varphi^{\widehat{c}}] = 0\,. \tag{6.78}$$

Furthermore, the boundary behavior of the fields in the gauge $A_\theta = 0$ around $\theta = 0$ are (although this is not the gauge we will choose later)

$$\begin{aligned} &\varphi = O(\theta)\,, \quad A_\mu = O(\theta)\,, \quad \varphi^{\widehat{a}} = \frac{\varrho(\tau^{\widehat{a}})}{\theta} + \varphi^{\widehat{a}}_{(0)} + O(\theta)\,, \\ &\rho^{(1)}_{\widehat{p}\,-} = O(1)\,, \quad \rho^{(2)}_{\widehat{p}\,+} = O(1)\,, \quad \rho^{(1)}_{\widehat{p}\,+} = O(\theta)\,, \quad \rho^{(2)}_{\widehat{p}\,-} = O(\theta)\,, \end{aligned} \tag{6.79}$$

where $\varrho : \mathfrak{su}(2) \to \mathfrak{u}(k)$ is an irreducible embedding of $\mathfrak{su}(2)$ into $\mathfrak{u}(k)$, with τ as in (6.67) . There are similar boundary conditions at $\theta = \pi$. The constant term $\varphi^{\widehat{a}}_{(0)}$ in the $\varphi^{\widehat{a}}$-expansion is constrained to be in the commutant of embedding ϱ. With $\varrho = [k]$ the irreducible embedding, this commutant is simply the diagonal $\mathfrak{u}(1) \subset \mathfrak{u}(k)$, so $\varphi^{\widehat{a}}_{(0)}$ is a constant diagonal matrix. This condition propagates by supersymmetry to the other fields.

The maximally supersymmetric configurations are vacua of the theory preserving eight supercharges and are given by solutions to the BPS equations

$$\begin{aligned} D_\theta \varphi^{\widehat{a}} - \frac{1}{2}\epsilon^{\widehat{a}}{}_{\widehat{b}\widehat{c}}[\varphi^{\widehat{b}}, \varphi^{\widehat{c}}] = 0 \\ \varphi = \bar{\varphi} = F_{\mu\nu} = F_{\mu\theta} = 0 \\ D_\mu \varphi_{\widehat{a}} = 0\,, \end{aligned} \tag{6.80}$$

with all fermions vanishing. The 5d action is minimised and vanishes for supersymmetric field configurations (6.80). Moreover there is the additional constraint that the scalars $\varphi^{\widehat{a}}$ have poles at $\theta = 0, \pi$ both characterised by the partition/embedding $\varrho = [k]$. The first equation in (6.80) is Nahm's equation for the fields $(\varphi^{\widehat{a}}, A_\theta)$ and the boundary behaviour of $\varphi^{\widehat{a}}$ are standard Nahm poles.

We can now address the validity of the singular cylinder limit $\ell(\theta) = \ell$ constant. In the following we will reduce the theory on the interval and find that the dominant field configurations are given by solutions of Nahm's equations. The resulting four-dimensional theory will be a sigma model into the moduli space of solutions of Nahm's equations. It is easy to see that for arbitrary $\ell(\theta)$ describing a smooth two-sphere metric, the same dimensional reduction will be dominated by field configurations satisfying the modified Nahm's equations (6.64). We can then reasonably expect that the reduction will lead to a four-dimensional sigma model into the moduli space of the modified Nahm's equations. However we argued at the end of section 6.3.2 that this moduli space is the same as the moduli space of standard Nahm's equations, so the reduction for arbitrary $\ell(\theta)$ would lead to the same sigma model.

Finally, let us comment on generalisations of the Nahm pole boundary conditions with two arbitrary partitions ϱ_0 and ϱ_π for the scalar fields at the two boundaries $\theta = 0, \pi$,

respectively, as described in [245]. The polar boundary behavior at $\theta = 0$ is given by (6.79) with $\varrho \to \varrho_0$ and the subleading constant piece $\varphi^{\widehat{a}}_{(0)}$ takes values in the commutant of ϱ_0 (i.e. matrices commuting with the image of ϱ_0). These boundary conditions preserve the same amount of supersymmetry and admit global symmetry groups $H_0 \times H_\pi \subset SU(k) \times SU(k)$ acting by gauge transformations at the end-points of the θ-interval. H_0 and H_π are the groups, whose algebras $\mathfrak{h}_0$, $\mathfrak{h}_\pi$ are respectively the commutants of ϱ_0 and ϱ_π in $\mathfrak{su}(k)$. These global transformations leave the ϱ_0 and ϱ_π boundary conditions invariant. In the reduction to 4d, only a subgroup of $H_0 \times H_\pi$ can be preserved (see the discussion in section 2 of [245]).

The general (ϱ_0, ϱ_π) boundary conditions correspond to inserting singularities or 'punctures' of the type ϱ_0 at one pole of the two-sphere and of the type ϱ_π at the other pole in the 6d $\mathcal{N} = (2,0)$ theory. All our results can be directly generalised to having general (ϱ_0, ϱ_π) Nahm poles at the boundaries of the θ-interval. In this case we would obtain sigma-models into a different moduli space: the moduli space of Nahm's equations with (ϱ_0, ϱ_π) boundary conditions.

For the sphere with two punctures labeled by two arbitrary partitions ϱ_0, ϱ_π, it is very natural to consider the metric describing a cylinder, since this is the topology of a sphere with two punctures, and the reduction, whether with the sphere or the cylinder metric, is expected to lead to the same four-dimensional theory. From this point of view, the sphere without punctures, or "trivial punctures", is simply a subcase corresponding to the specific partitions $\varrho_0 = \varrho_\pi = [k]$, and we may take the cylinder metric, as for any other choice of punctures.

6.4 Nahm's Equations and 4d Sigma-Model

In the last section we have seen that the 5d $\mathcal{N} = 2$ SYM in the background corresponding to the S^2 reduction of the 6d $\mathcal{N} = (2,0)$ theory requires the scalars $\varphi^{\widehat{a}}$ to satisfy Nahm's equations, and the supersymmetric boundary conditions require them to have Nahm poles (6.79) at the boundary of the interval. The four-dimensional theory is therefore dependent on solutions to Nahm's equations. To dimensionally reduce the theory, we pass to a description in terms of coordinates on the moduli space $\mathcal{M}_k$ of solutions to Nahm's equations and find the theory to be a four-dimensional sigma-model into $\mathcal{M}_k$ with the action

$$S_{4d} = \frac{1}{4r\ell} \int d^4x \sqrt{|g_4|} \Big[G_{IJ} \left(\partial_\mu X^I \partial^\mu X^J - 2i \xi^{(1)I\widehat{p}} \sigma^\mu \mathcal{D}_\mu \xi^{(2)J}_{\widehat{p}} \right) - \frac{1}{2} R_{IJKL} \xi^{(1)I\widehat{p}} \xi^{(1)J}_{\widehat{p}} \xi^{(2)K\widehat{q}} \xi^{(2)L}_{\widehat{q}} \Big] \tag{6.81}$$

with X^I the coordinates on the moduli space

$$X : \qquad M_4 \ \to \ \mathcal{M}_k \,, \tag{6.82}$$

and $\xi^{(i)}$, where $i = 1, 2$, Grassmann-valued sections of the pull-back of the tangent bundle to $\mathcal{M}_k$

$$\xi^{(1,2)} \in \Gamma(X^* T\mathcal{M}_k \otimes \mathcal{S}^{\pm}) \,, \tag{6.83}$$

where $\mathcal{S}^{\pm}$ is the spin bundle of $\pm$ chirality on M_4. The sigma-model for $M_4 = \mathbb{R}^4$ is supersymmetric, with $\mathcal{N} = 2$ supersymmetry in 4d. The coupling constant for the sigma-model is proportional to the area of the two-sphere, which is $\sim r\ell$, as anticipated.

6.4.1 Poles and Monopoles

Before studying the dimensional reduction to 4d, we summarise a few well-known useful properties of the moduli space $\mathcal{M}_k$. The moduli space $\mathcal{M}_k$ of solutions to Nahm's equations, on an interval with Nahm pole boundary conditions given by the irreducible embedding $\varrho = [k]$, is well-known to be isomorphic to the moduli space of (framed) $SU(2)$ magnetic monopoles of charge k [262, 263, 246, 247], which is $4k$-dimensional and has a Hyper-Kähler structure. The metric of the spaces $\mathcal{M}_k$ is not known in explicit form, other than for the cases $\mathcal{M}_1 \simeq \mathbb{R}^3 \times S^1$ (which is the position of the monopole in $\mathbb{R}^3$ and the large gauge transformations parametrised by S^1) and for the case

$$\mathcal{M}_2 \simeq \mathbb{R}^3 \times \frac{S^1 \times \mathcal{M}_{\rm AH}}{\mathbb{Z}_2} \,, \tag{6.84}$$

where $\mathcal{M}_{\rm AH}$ is the Atiyah-Hitchin manifold [247]. A detailed description of the metric in the latter case will be given in section 6.6.2. Hitchin showed the equivalence of $SU(2)$ monopoles of charge k with solutions of Nahm's equations [263]

$$\frac{dT_i}{d\theta} - \frac{1}{2}\epsilon_{ijk}[T_j, T_k] = 0 \,, \qquad i = 1, 2, 3 \,, \tag{6.85}$$

where T_i are matrix-valued, depending on $\theta \in [0, \pi]$ and have poles at the endpoints of the interval, the residues of which define representations of $\mathfrak{su}(2)$. Furthermore, Donaldson [246] identified Nahm's equations in terms of the anti-self-duality equation $F_A = - \star F_A$ of a connection

$$A = T_\theta d\theta + \sum_i T_i dx_i \,, \tag{6.86}$$

on $\mathbb{R}^4$, where T_θ, the gauge field along the interval, can be gauged away and the T_i are taken independent of the x^i coordinates. The metric of the solution-space (modulo gauge transformations) has a Hyper-Kähler structure [264, 265].

This Nahm moduli space (or monopole moduli space) takes the form [247]

$$\mathcal{M}_k \simeq \mathbb{R}^3 \times \frac{S^1 \times \mathcal{M}_k^0}{\mathbb{Z}_k}\,, \tag{6.87}$$

where $\mathbb{R}^3$ parameterises the center of mass of the k-centered monopole. A particularly useful characterisation of the reduced Nahm moduli space $\mathcal{M}_k^0$ is in terms of Slodowy-slices. Kronheimer has shown that the solutions of Nahm's equations with no poles at the boundaries have a moduli space given by the cotangent bundle of the complexified gauge group, $T^*G_{\mathbb{C}} \equiv \mathfrak{g}_{\mathbb{C}} \times G_{\mathbb{C}}$, which has a natural Hyper-Kähler structure. Furthermore, Bielawski showed in [249,250], that the moduli space of solutions with Nahm pole boundary conditions for k-centered $SU(2)$ monopoles is given in terms of

$$\mathcal{M}_k^0 \cong \{(g, X) \in SU(N)_{\mathbb{C}} \times \mathfrak{su}(N)_{\mathbb{C}};\ X \in S_{[k]} \cap g^{-1} S_{[k]} g\} \subset T^* SU(k)_{\mathbb{C}}\,, \tag{6.88}$$

where the Slodowy slice for an embedding $\rho : \mathfrak{su}(2) \to \mathfrak{u}(k)$ is

$$S_\rho = \{\rho(\tau^+) + x \in \mathfrak{su}(k)_{\mathbb{C}};\ [\rho(\tau^-), x] = 0\}\,. \tag{6.89}$$

Here $\tau^\pm \equiv \tau^1 \pm i\tau^2$ are the raising/lowering operators of $\mathfrak{su}(2)$. The Hyper-Kähler metric on $\mathcal{M}_k$ will play a particularly important role in section 6.6, where this will be discussed in more detail.

6.4.2 Reduction to the 4d Sigma-Model

To proceed with the reduction on the θ-interval to four dimensions, we take the limit where the size of the interval, r, is small.[5] The terms in the action (6.75) are organised in powers of r, and in the limit, the divergent terms which are of order r^{-n}, $n = 2, 3$, must vanish separately. The terms of order r^{-1} contain the four-dimensional kinetic terms and lead to the 4d action. The terms of order r^n, $n \geq 0$ are subleading and can be set to zero. To perform this reduction we must expand the fields in powers of r, $\Phi = \Phi_0 + \Phi_1 r + \Phi_2 r^2 + \cdots$, and compute the contribution at each order. We find that only the leading term Φ_0 contributes to the final 4d action for each field, except for the 'massive' scalars $\varphi, \bar{\varphi}$ and spinors $\rho^{(1)}_{+\widehat{p}}, \rho^{(2)}_{-\widehat{p}}$, whose leading contribution arise at order r. The final 4d action will arise with the overall coupling $\frac{1}{r\ell}$.

Let us now proceed with detailing the dimensional reduction. At order r^{-3} we find the

[5] By r small, we mean that we consider the effective theory at energies small compared to $\frac{1}{r}$.

term

$$S = -\frac{1}{4r^3\ell}\int d\theta d^4x\sqrt{|g_4|} \\ \mathrm{Tr}\left[\left(D_\theta\varphi^{\widehat{a}} - \frac{1}{2}\epsilon^{\widehat{a}}{}_{\widehat{b}\widehat{c}}[\varphi^{\widehat{b}},\varphi^{\widehat{c}}]\right)^2 + [\varphi_{\widehat{a}},\varphi][\varphi^{\widehat{a}},\bar{\varphi}] + D_\theta\varphi D_\theta\bar{\varphi} - \frac{1}{4}[\varphi,\bar{\varphi}][\varphi,\bar{\varphi}]\right]. \tag{6.90}$$

This term is minimised (and actually vanishes)[6], up to order $O(r^{-1})$ corrections, upon imposing the following constraints: $\varphi, \bar{\varphi}$ vanish at order r^0,

$$\varphi = \bar{\varphi} = O(r)\,, \tag{6.91}$$

and the fields $\varphi^{\widehat{a}}$ and A_θ obey Nahm's equations, up to order $O(r)$ corrections,

$$D_\theta\varphi^{\widehat{a}} - \frac{\epsilon^{\widehat{a}}{}_{\widehat{b}\widehat{c}}}{2}[\varphi^{\widehat{b}},\varphi^{\widehat{c}}] = 0\,, \tag{6.92}$$

with Nahm pole behaviour $\varrho = [k]$ at the two ends of the interval. The four-dimensional theory then localises onto maps $X : \mathbb{R}^4 \to \mathcal{M}_k$, where $\mathcal{M}_k$ is the moduli space of $\mathfrak{u}(k)$ valued solutions of Nahm's equations on the interval with ϱ-poles at the boundaries, or equivalently the moduli space of k-centered $SU(2)$ monopoles, as reviewed in section 6.4.1. The fields satisfying Nahm's equations can be written in terms of an explicit dependence on the point X^I in the moduli space $\mathcal{M}_k$

$$\varphi^{\widehat{a}}(\theta, x^\mu) = \varphi^{\widehat{a}}(\theta, X(x^\mu))\,, \quad A_\theta(\theta, x^\mu) = A_\theta(\theta, X(x^\mu))\,. \tag{6.93}$$

Furthermore, we choose the gauge fixing

$$\partial_\theta A_\theta = 0\,. \tag{6.94}$$

The terms at $O(r^{-2})$ vanish by imposing the spinors $\rho^{(1)}_{\widehat{p}+}, \rho^{(2)}_{\widehat{p}-}$ to have no $O(r^0)$ term

$$\rho^{(1)}_{\widehat{p}+} = O(r)\,, \quad \rho^{(2)}_{\widehat{p}-} = O(r)\,. \tag{6.95}$$

The kinetic term of these spinors becomes of order r and can be dropped in the small r limit. The fermions $\rho^{(1)}_{\widehat{p}+}, \rho^{(2)}_{\widehat{p}-}$ become Lagrange multipliers and can then be integrated out, leading to the constraints on the fermions $\rho^{(1)}_{\widehat{p}-}, \rho^{(2)}_{\widehat{p}+}$

$$\begin{aligned} D_\theta\rho^{(2)}_{+\widehat{p}} + i[\varphi^{\widehat{p}}_{\widehat{q}}, \rho^{(2)}_{+\widehat{q}}] = 0 \\ D_\theta\rho^{(1)}_{-\widehat{p}} + i[\varphi^{\widehat{p}}_{\widehat{q}}, \rho^{(1)}_{-\widehat{q}}] = 0\,, \end{aligned} \tag{6.96}$$

which are supersymmetric counterparts to Nahm's equations (6.78). We will use these localizing equations below to expand the fermionic fields in terms of vectors in the tangent space to the moduli space of Nahm's equations, $\mathcal{M}_k$.

[6] To avoid possible confusions about the positivity of the action, we remind that our conventions are such that the fields are anti-hermitian.

Finally we drop the order r kinetic terms of the 4d gauge field and scalars $\varphi, \bar{\varphi}$ (which contribute only at order r), and we are left with the terms of order $\frac{1}{r}$ which describe the 4d action. The remaining task is to express this action in terms of the fields $X = \{X^I\}$ and the massless fermionic degrees of freedom, and to integrate out the 4d components of the gauge field A_μ and the scalars $\varphi, \bar{\varphi}$, which appear as auxiliary fields in the 4d action. The subleading terms (at order r) in the $\varphi^{\widehat{a}}$ expansion can similarly be integrated out without producing any term in the final 4d action, so we ignore these contributions in the rest of the derivation.

In addition one should integrate over the one-loop fluctuations of the fields around their saddle point configurations. We will assume here that the bosonic and fermionic one-loop determinants cancel, as is frequently the case in similar computations [266], and now turn to deriving the 4d action. Some of the technical details have been relegated to appendix C.5.

Scalars

We will now describe the 4d theory in terms of 'collective coordinates' X^I, similar to the approach taken in e.g. [266] for the dimensional reduction of 4d SYM theories on a Riemann surface resulting in a 2d sigma-model into the Hitchin moduli space. Related work can also be found in [267, 268]. The resulting theory is a (supersymmetric) sigma-model (6.82), where for this part of the chapter we will consider $M_4 = \mathbb{R}^4$. The three scalar fields $\varphi_{\widehat{a}}$ and A_θ are expanded in the collective coordinates as follows

$$\begin{aligned} \delta\varphi^{\widehat{a}} &= \Upsilon^{\widehat{a}}_I \delta X^I \\ \delta A_\theta &= \Upsilon^\theta_I \delta X^I \,, \end{aligned} \tag{6.97}$$

where $I = 1, \ldots, 4k$. Here, the basis of the cotangent bundle of $\mathcal{M}_k$ is given by

$$\begin{aligned} \Upsilon^{\widehat{a}}_I &= \frac{\partial \varphi^{\widehat{a}}}{\partial X^I} + [E_I, \varphi^{\widehat{a}}] \\ \Upsilon^\theta_I &= \frac{\partial A_\theta}{\partial X^I} - D_\theta E_I \,, \end{aligned} \tag{6.98}$$

where E_I defines a $\mathfrak{u}(k)$ connection $\nabla_I \equiv \partial_I + [E_I, .]$ on $\mathcal{M}_k$. The $\Upsilon^{\widehat{a}}_I, \Upsilon^\theta_I$ satisfy linearised Nahm's equations

$$D_\theta \Upsilon^{\widehat{a}}_I + \left[\Upsilon^\theta_I, \varphi^{\widehat{a}}\right] = \epsilon^{\widehat{a}\widehat{b}\widehat{c}} \left[\Upsilon_{I\widehat{b}}, \varphi_{\widehat{c}}\right] \,. \tag{6.99}$$

The metric on $\mathcal{M}_k$ can be expressed in terms of these one-forms as

$$G_{IJ} = -\int d\theta \, \mathrm{Tr}(\Upsilon^{\widehat{a}}_I \Upsilon_{J\widehat{a}} + \Upsilon^\theta_I \Upsilon^\theta_J) \,. \tag{6.100}$$

The Hyper-Kähler structure on $\mathcal{M}_k$ can be made manifest in this formulation, by defining the three symplectic forms (see for instance [269])

$$\omega^{\widehat{a}}_{IJ} = \int d\theta \, \mathrm{Tr}(\epsilon^{\widehat{a}\widehat{b}\widehat{c}} \Upsilon_{I\widehat{b}} \Upsilon_{J\widehat{c}} + \Upsilon^{\widehat{a}}_I \Upsilon^{\theta}_J - \Upsilon^{\theta}_I \Upsilon^{\widehat{a}}_J) \,. \tag{6.101}$$

Some useful properties of these are summarised in appendix C.5.1. Using the expansion (6.98) we obtain

$$S_{\text{scalars}} = -\frac{1}{4r\ell} \int d\theta d^4x \sqrt{|g_4|} \, \mathrm{Tr} \left(\partial_I A_\theta \partial_J A_\theta + \partial_I \varphi^{\widehat{a}} \partial_J \varphi_{\widehat{a}} \right) \partial_\mu X^I \, \partial^\mu X^J \,. \tag{6.102}$$

This will combine with terms arising from integrating out the gauge field to give the usual sigma-model kinetic term.

Fermions

The fermions satisfy the equation (6.96), which is the supersymmetry variation of Nahm's equations. The spinors therefore take values in the cotangent bundle to the moduli space $\mathcal{M}_k$ and we can expand them in the basis that we defined in (6.98)

$$\begin{aligned} \rho^{(1)}_{-\widehat{p}} &= \Upsilon^{\widehat{a}}_I (\sigma_{\widehat{a}})^{\widehat{q}}_{\widehat{p}} \lambda^{(1)I}_{\widehat{q}} + i \Upsilon^{(\theta)}_I \lambda^{(1)I}_{\widehat{p}} \\ \rho^{(2)}_{+\widehat{p}} &= \Upsilon^{\widehat{a}}_I (\sigma_{\widehat{a}})^{\widehat{q}}_{\widehat{p}} \lambda^{(2)I}_{\widehat{q}} + i \Upsilon^{(\theta)}_I \lambda^{(2)I}_{\widehat{p}} \,, \end{aligned} \tag{6.103}$$

where $\lambda^{(1)I}_{\widehat{p}}, \lambda^{(2)I}_{\widehat{p}}$ are spacetime spinors, valued in $T\mathcal{M}_k$. The identities (C.58) imply that the fermionic fields obey the constraints

$$\omega^{\widehat{a}I}{}_J \lambda^{(i)J}_{\widehat{p}} = i (\sigma^{\widehat{a}})^{\widehat{q}}_{\widehat{p}} \lambda^{(i)I}_{\widehat{q}} \,. \tag{6.104}$$

The expansion in (6.103) can be seen to satisfy the equation of motion for the spinors (6.96) by making use of (6.99) and the gauge fixing condition (C.62). Then substituting in the kinetic term for the spinors and making use of the expression for the metric on $\mathcal{M}_k$ (6.100), the symplectic forms $\omega^{\widehat{a}}_{IJ}$ and the constraint (6.104), we find

$$\begin{aligned} S_{\rho_{\text{kin}}} = \frac{8i}{rl} \int d^4x \sqrt{|g_4|} \Big[& G_{IJ} \lambda^{(1)I\widehat{p}} \gamma^\mu \partial_\mu \lambda^{(2)J}_{\widehat{p}} \\ & - \int d\theta \, \mathrm{Tr} \Big(\Upsilon^{\widehat{a}}_I \partial_J \Upsilon_{K\widehat{a}} + \Upsilon^{(\theta)}_I \partial_J \Upsilon^{(\theta)}_K \Big) \lambda^{(1)I\widehat{p}} \gamma^\mu \lambda^{(2)K}_{\widehat{p}} \partial_\mu X^J \Big] \,. \end{aligned} \tag{6.105}$$

6.4.3 4d Sigma-Model into the Nahm Moduli Space

Finally, we need to integrate out the gauge field and the scalars $\varphi, \bar{\varphi}$, which is done in appendix C.5.2. The conclusion is that, in addition to giving the standard kinetic term for

the scalars, this covariantises the fermion action and results in a quartic fermion interaction that depends on the Riemann tensor of the moduli space. In summary we find the action

$$S = \frac{1}{r\ell}\int d^4x\sqrt{|g_4|}\left[\frac{1}{4}G_{IJ}\partial_\mu X^I\partial^\mu X^J + 8iG_{IJ}\lambda^{(1)I\widehat{p}}\gamma^\mu\mathcal{D}_\mu\lambda^{(2)J}_{\widehat{p}} \right. \\ \left. -32R_{IJKL}\left(\lambda^{(1)I\widehat{p}}\lambda^{(1)J}_{\widehat{p}}\right)\left(\lambda^{(2)K\widehat{q}}\lambda^{(2)L}_{\widehat{q}}\right)\right], \tag{6.106}$$

where $\mathcal{D}_\mu\lambda^{(2)I}_{\widehat{p}} = \partial_\mu\lambda^{(2)I}_{\widehat{p}} + \lambda^{(2)J}_{\widehat{p}}\Gamma^I_{JK}\partial_\mu X^K$. The final step is to decompose the spinors $\lambda^{(i)}$, as explained in appendix C.1.2, into 4d Weyl spinors

$$\lambda^{(1)I}_{\widehat{p}} = \frac{1}{4}\begin{pmatrix}\xi^{(1)I}_{\widehat{p}}\\ 0\end{pmatrix}, \quad \lambda^{(2)I}_{\widehat{p}} = \frac{1}{4}\begin{pmatrix}0\\ \xi^{(2)I}_{\widehat{p}}\end{pmatrix}, \tag{6.107}$$

obeying the reality conditions

$$(\xi^{(1)p})^* = \xi^{(2)}_{\dot{p}}, \quad (\xi^{(2)\dot{p}})^* = \xi^{(1)}_p, \tag{6.108}$$

and the constraint

$$\omega^{\widehat{a}I}{}_J\xi^{(i)J}_{\widehat{p}} = i(\sigma^{\widehat{a}})^{\widehat{q}}_{\widehat{p}}\xi^{(i)I}_{\widehat{q}}. \tag{6.109}$$

The 4d sigma-model action from flat M_4 into the monopole moduli space $\mathcal{M}_k$ is then given by

$$S_{4d} = \frac{1}{4r\ell}\int d^4x\sqrt{|g_4|}\left[G_{IJ}\left(\partial_\mu X^I\partial^\mu X^J - 2i\xi^{(1)I\widehat{p}}\sigma^\mu\mathcal{D}_\mu\xi^{(2)J}_{\widehat{p}}\right) \right. \\ \left. -\frac{1}{2}R_{IJKL}\xi^{(1)I\widehat{p}}\xi^{(1)J}_{\widehat{p}}\xi^{(2)K\widehat{q}}\xi^{(2)L}_{\widehat{q}}\right]. \tag{6.110}$$

The supersymmetry transformations are

$$\begin{aligned}\delta X^I &= -i\left(\epsilon^{(2)\widehat{p}}\xi^{(1)I}_{\widehat{p}} + \epsilon^{(1)\widehat{p}}\xi^{(2)I}_{\widehat{p}}\right)\\ \delta\xi^{(1)I}_{\widehat{p}} &= \frac{1}{4}\left(\partial_\mu X^I\sigma^\mu\epsilon^{(1)}_{\widehat{p}} - i\omega^{\widehat{a}I}{}_J(\sigma_{\widehat{a}})^{\widehat{q}}_{\widehat{p}}\partial_\mu X^J\sigma^\mu\epsilon^{(1)}_{\widehat{q}}\right) - \Gamma^I_{JK}\delta X^J\xi^{(1)K}_{\widehat{p}}\\ \delta\xi^{(2)I}_{\widehat{p}} &= -\frac{1}{4}\left(\partial_\mu X^I\bar{\sigma}^\mu\epsilon^{(2)}_{\widehat{p}} - i\omega^{\widehat{a}I}{}_J(\sigma_{\widehat{a}})^{\widehat{q}}_{\widehat{p}}\partial_\mu X^J\bar{\sigma}^\mu\epsilon^{(2)}_{\widehat{q}}\right) - \Gamma^I_{JK}\delta X^J\xi^{(2)K}_{\widehat{p}}.\end{aligned} \tag{6.111}$$

We have thus shown, that the M5-brane theory reduced on an S^2 gives rise to a four-dimensional sigma-model with $\mathcal{N} = 2$ supersymmetry, based on maps from $\mathbb{R}^4$ into the moduli space $\mathcal{M}_k$ of Nahm's equations (with $\varrho = [k]$ boundary conditions).

6.4.4 Relation to the Bagger-Witten Model

There is an equivalent description of the sigma-model in (6.110), which relates it to the models in [251,252]. In this alternative description we make use of the reduced holonomy of the Hyper-Kähler target $\mathcal{M}_k$. We will consider an $(Sp(k)\times Sp(1))/\mathbb{Z}_2$ subgroup of $SO(4k)$,

under which the complexified tangent bundle of a Hyper-Kähler space decomposes into a rank $2k$ vector bundle V and a rank 2 trivial bundle S. The index I decomposes under this into $i\widehat{p}$, where $i = 1, \cdots, 2k$ labels the $2k$-dimensional representation of $\mathfrak{sp}(k)$ and $\widehat{p} = 1, 2$ is the doublet index of $\mathfrak{sp}(1) = \mathfrak{su}(2)_R$. The map $I \to i\widehat{p}$ is realised by the invariant tensors $f^{i\widehat{p}}{}_I$ [270], which satisfy

$$f^{i\widehat{p}}{}_I f^J{}_{i\widehat{p}} = \delta^I_J\,, \quad f^{i\widehat{p}}{}_I\, f^I{}_{j\widehat{q}} = \delta^i_j \delta^{\widehat{p}}_{\widehat{q}}\,, \quad 2 f^{i\widehat{p}}{}_I\, f^J{}_{i\widehat{q}} = \delta^I_J \delta^{\widehat{p}}_{\widehat{q}} + i\omega^{\widehat{a}J}_I (\sigma_{\widehat{a}})^{\widehat{p}}_{\widehat{q}}\,. \tag{6.112}$$

The alternative description of the sigma-model is obtained by defining the fields

$$\xi^{(1)i} \equiv \frac{1}{2} f^{i\widehat{p}}{}_I\, \xi^{(1)I}_{\widehat{p}}\,, \qquad \xi^{(2)i} \equiv \frac{1}{2} f^{i\widehat{p}}{}_I\, \xi^{(2)I}_{\widehat{p}}\,. \tag{6.113}$$

which can be inverted, by using the constraint on the fermions (6.109)

$$\xi^{(1)I}_{\widehat{p}} = f^I{}_{i\widehat{p}}\, \xi^{(1)i}\,, \qquad \xi^{(2)I}_{\widehat{p}} = f^I{}_{i\widehat{p}}\, \xi^{(2)i}\,. \tag{6.114}$$

Using this decomposition the 4d untwisted sigma-model action into the monopole moduli space $\mathcal{M}_k$ can be re-expressed in terms of the fermionic fields (6.113)

$$S = \frac{1}{r\ell} \int d^4x \sqrt{|g_4|}\, \left[\frac{1}{4} G_{IJ} \partial_\mu X^I\, \partial^\mu X^J - i g_{ij} \xi^{(1)i} \sigma^\mu D_\mu \xi^{(2)j} - \frac{1}{4} W_{ijkl} (\xi^{(1)i} \xi^{(1)j})(\xi^{(2)k} \xi^{(2)l}) \right]\,, \tag{6.115}$$

where the covariant derivative is

$$D_\mu \xi^{(2)i} = \partial_\mu \xi^{(2)i} + \xi^{(2)j} w_{Ij}{}^i \partial_\mu X^I\,. \tag{6.116}$$

The tensors $w_{Ij}{}^i$ and W_{ijkl} are the $Sp(k)$ connection on V and the totally symmetric curvature tensor, respectively. These are expressed in terms of the Christoffel connection and Riemann tensor as

$$\begin{aligned} w_{Ii}{}^j &= \frac{1}{2} f^{j\widehat{p}}{}_J \left(\partial_I f^J{}_{i\widehat{p}} + \Gamma^J_{IK} f^K{}_{i\widehat{p}} \right) \\ W_{ijkl} &= \frac{1}{2} f^{I\widehat{p}}{}_i f^J{}_{\widehat{p}j} f^{K\widehat{q}}{}_k f^L{}_{\widehat{q}l} R_{IJKL}\,. \end{aligned} \tag{6.117}$$

The supersymmetry transformations are

$$\begin{aligned} \delta X^I &= -i\epsilon^{(2)\widehat{p}} f^I{}_{i\widehat{p}} \xi^{(1)i} - i\epsilon^{(1)\widehat{p}} f^I{}_{i\widehat{p}} \xi^{(2)i} \\ \delta \xi^{(1)i} &= \frac{1}{2} f^{i\widehat{p}}{}_I \partial_\mu X^I \sigma^\mu \epsilon^{(1)}_{\widehat{p}} - w_{Ij}{}^i \delta X^I \xi^{(1)j} \\ \delta \xi^{(2)i} &= -\frac{1}{2} f^{i\widehat{p}}{}_I \partial_\mu X^I \bar{\sigma}^\mu \epsilon^{(2)}_{\widehat{p}} - w_{Ij}{}^i \delta X^I \xi^{(2)j}\,. \end{aligned} \tag{6.118}$$

It is natural to ask how this sigma-model can be extended to general, oriented four-manifolds M_4. Using the topological twist 1 in section 6.2.1, we will now consider this generalisation.

6.5 4d Topological Sigma-Models: Hyper-Kähler M_4

So far we have discussed the five-dimensional theory on flat $I \times \mathbb{R}^4$, where I is the θ interval, reducing it to a sigma-model in four-dimensional flat space. The goal in the following is to define a 4d topological sigma-model on a general four-manifold. We first describe the twist in terms of the 4d theory in section 6.5.1.

As we shall see, for the target space a Hyper-Kähler manifold, as is the case for the Nahm moduli space, and general gauge group, we determine a general form of the sigma-model for the case of Hyper-Kähler M_4. For compact M_4, this comprises T^4 and $K3$ varieties. We will discuss the special reductions for the abelian case and the two-monopole case for general M_4 later on.

6.5.1 Topological Twist

Twist 1 in section 6.2.1 was formulated for the 6d theory. We now briefly summarise how this twist acts in 4d. From now on we switch to Euclidean signature [7].

Recall, that in 6d, we twist the $\mathfrak{su}(2)_\ell \subset \mathfrak{su}(2)_\ell \oplus \mathfrak{su}(2)_r$ of the 4d Lorentz algebra with the $\mathfrak{su}(2)_R \subset \mathfrak{su}(2)_R \oplus \mathfrak{so}(2)_R \subset \mathfrak{sp}(4)_R$. From the point of view of the 4d theory, we start with the R-symmetry $\mathfrak{su}(2)_R$ and twist this with the Lorentz symmetry of M_4, which generically is $\mathfrak{so}(4)_L \cong \mathfrak{su}(2)_\ell \oplus \mathfrak{su}(2)_r$, resulting in

$$\mathfrak{g}_{4d} = \mathfrak{su}(2)_R \oplus \mathfrak{so}(4)_L \quad \to \quad \mathfrak{g}_{\text{twist}} \;=\; \mathfrak{su}(2)_{\text{twist}} \oplus \mathfrak{su}(2)_r \,. \tag{6.119}$$

In terms of 4d representations, $\epsilon^{(1)}_{\widehat{p}}$ and $\epsilon^{(2)}_{\widehat{p}}$ are Weyl spinors of positive and negative chirality respectively. We adopt the convention that negative/positive chirality spinors correspond to doublets of $\mathfrak{su}(2)_\ell / \mathfrak{su}(2)_r$ respectively. After the twisting, $\epsilon^{(2)}_{\widehat{p}}$ has one scalar component under $\mathfrak{su}(2)_{\text{twist}} \oplus \mathfrak{su}(2)_r$, which is selected by the projections

$$(\gamma_{0a}\delta^{\widehat{q}}_{\widehat{p}} + i(\sigma_{\widehat{a}})^{\widehat{q}}_{\widehat{p}})\epsilon^{(2)}_{\widehat{q}} = 0\,, \quad a \simeq \widehat{a} = 1,2,3\,, \tag{6.120}$$

where the indices a and $\widehat{a}$ are identified in the twisted theory. The spinor $\epsilon^{(2)\widehat{p}}$ parametrises the preserved supercharge and can be decomposed as

$$\epsilon^{(2)\widehat{p}} = u\,\tilde{\epsilon}^{\widehat{p}}\,, \tag{6.121}$$

where u is a complex Grassmann-odd parameter and $\tilde{\epsilon}^{\widehat{p}}$ is a Grassmann-even spinor normalised so that

$$\tilde{\epsilon}^{\widehat{p}}\tilde{\epsilon}_{\widehat{p}} = 1\,. \tag{6.122}$$

[7] For this twist we change from Lorentzian to Euclidean signature. In what follows γ_0 as defined in appendix C.1.2 is replaced with $\gamma_{0'} = i\gamma_0$, where the prime will be omitted.

We can associate the $\mathfrak{u}(1)_R$ charge -1 to the parameter u and consider $\widetilde{\epsilon^{\widehat{p}}}$ as uncharged.

The $\mathfrak{su}(2)_R$ R-symmetry with which we twist rotates the complex structures of the target and therefore is identified with the $\mathfrak{sp}(1) \subset \mathfrak{so}(4k)$ of the Hyper-Kähler target. This means that $SU(2)_R/\mathbb{Z}_2$ is mapped to an $SO(3)$ isometry of the metric on $\mathcal{M}_k$. In order to do the twist one needs to know how the coordinates X^I transform under this $\mathfrak{sp}(1) \equiv \mathfrak{su}(2)_R$. For the monopole moduli space with charge 1 and 2, $\mathcal{M}_1$ and $\mathcal{M}_2$, where the explicit metric on the moduli space is known, the coordinates split into two sets transforming respectively in the trivial and adjoint representation of $\mathfrak{su}(2)_R$. This suggests that this property could hold for moduli spaces $\mathcal{M}_k$, with $k > 2$. Under the twist, the coordinates transforming in the adjoint of $\mathfrak{su}(2)_R$ become self-dual two forms on M_4 and the resulting theory is a sigma-model, whose bosonic fields are maps into a reduced target space and self-dual two-forms. We shall study the $\mathcal{M}_1$ and $\mathcal{M}_2$ cases in section 6.6.

A simplification occurs when the bundle of self-dual two-forms on M_4 is trivial i.e. when M_4 is Hyper-Kähler. In this case, all the coordinates transform as scalars on M_4 after the twist and therefore the twist can be performed without knowledge of the metric on $\mathcal{M}_k$. In this situation, the twisting procedure is simply a re-writing of the theory, making manifest the transformation of the fields under the new Lorentz group. This is done in the next section and gives a topological sigma-model on Hyper-Kähler M_4.

6.5.2 Topological Sigma-Model for Hyper-Kähler M_4

The 4d sigma-model into the Nahm moduli space (6.110) can be topologically twisted for Hyper-Kähler M_4. We now show that this reduces to the 4d topological theory by Anselmi and Frè [254], for the special target space given by the moduli space of Nahm's equations. This topological theory describes *tri-holomorphic maps* from M_4 into $\mathcal{M}_k$

$$X = \{X^I\} : \qquad M_4 \ \to \ \mathcal{M}_k \,, \tag{6.123}$$

which satisfy the triholomorphicity constraint

$$\partial_\mu X^I - (j^a)_\mu{}^\nu \partial_\nu X^J \omega^a{}_J{}^I = 0 \,, \tag{6.124}$$

where the index $a = 1, 2, 3$ is summed over and j^a and ω^a are triplets of complex structures on M_4 and $\mathcal{M}_k$ respectively, which define the Hyper-Kähler structures. We will also comment in section 6.5.3 on how this can be obtained by first topologically twisting the 5d $\mathcal{N} = 2$ SYM theory, and then dimensionally reducing this to 4d. This alternative derivation from the twisted 5d $\mathcal{N} = 2$ SYM theory can be found in appendix C.6.

We now turn to the topological twisting of the 4d sigma-model into the Nahm moduli space (6.110), by the twist of section 6.5.1. The fields of the 4d sigma-model become forms on M_4, with the degree depending on their transformations under $\mathfrak{g}_{\text{twist}}$

Field	$\mathfrak{g}_{4d}$	$\mathfrak{g}_{\text{twist}}$	Twisted Field
X^I	$(\mathbf{1},\mathbf{1},\mathbf{1})$	$(\mathbf{1},\mathbf{1})$	X^I
$\xi^{(1)Ip}_{\widehat{p}}$	$(\mathbf{2},\mathbf{2},\mathbf{1})$	$(\mathbf{1}\oplus\mathbf{3},\mathbf{1})$	$\lambda^I, \chi^I_{\mu\nu}$
$\xi^{(2)I\dot{p}}_{\widehat{p}}$	$(\mathbf{2},\mathbf{1},\mathbf{2})$	$(\mathbf{2},\mathbf{2})$	κ^I_μ

(6.125)

Despite the fact that the index I transforms non-trivially under the R-symmetry $SO(3)_R$, this will not play a role in the twist for the Hyper-Kähler four-manifold M_4: the holonomy is reduced to $\mathfrak{su}(2)_r$ and the $\mathfrak{su}(2)_\ell$ connection that we twist with vanishes. To be even more concrete, the covariant derivatives acting on fields with an index I will not pick up any $\mathfrak{su}(2)_{\text{twist}}$ connection because the connection vanishes, so we may treat I as an external index. This is of course not true for non-Hyper-Kähler M_4.

The most general decomposition of the spinors into twisted fields is given by

$$\begin{aligned}\xi^{(1)I}_{\widehat{p}} &= \left(\lambda^I + \frac{1}{4}\sigma^{\mu\nu}\chi^I_{\mu\nu}\right)\tilde{\epsilon}_{\widehat{p}}\\ \xi^{(2)I}_{\widehat{p}} &= \bar{\sigma}^\mu \kappa^I_\mu \tilde{\epsilon}_{\widehat{p}}\,,\end{aligned} \tag{6.126}$$

where the Grassmann-odd fields $\lambda^I, \chi^I_{\mu\nu}, \kappa^I_\mu$ are respectively a scalar, a self-dual two-form and a one-form, valued in the pull-back of the tangent bundle of the target space $X^*T\mathcal{M}_k$. However the components of $\xi^{(i)I}_{\widehat{p}}$ are not all independent as they satisfy the constraint (6.109). This constraint on the components of $\xi^{(i)I}_{\widehat{p}}$ translates into

$$\begin{aligned}\omega_{\mu\nu}{}^I{}_J\lambda^J &= \chi^I_{\mu\nu}\,,\\ \omega_{\mu\nu}{}^I{}_J\kappa^{\nu J} &= -3\kappa^I_\mu\,,\end{aligned} \tag{6.127}$$

where $\omega_{\mu\nu}{}^I{}_J \equiv -(j^{\widehat{a}})_{\mu\nu}\omega^{\widehat{a}I}{}_J$. As the self-dual two-form $\chi^I_{\mu\nu}$ is not an independent degree of freedom we shall consider the decomposition of $\xi^{(1)I}_{\widehat{p}}$ just in terms of the fermionic scalar λ^I, with a convenient normalisation,

$$\begin{aligned}\xi^{(1)I}_{\widehat{p}} &= i\left(\lambda^I + \frac{1}{4}\sigma^{\mu\nu}\omega_{\mu\nu}{}^I{}_J\lambda^J\right)\tilde{\epsilon}_{\widehat{p}}\\ \xi^{(2)I}_{\widehat{p}} &= -\frac{1}{4}\bar{\sigma}^\mu\kappa^I_\mu\tilde{\epsilon}_{\widehat{p}}\,.\end{aligned} \tag{6.128}$$

Note that this decomposition of $\xi^{(1)I}_{\widehat{p}}$ solves the constraint (6.109) automatically, and thus all components of λ^I are independent. However, this is not the case for $\xi^{(2)I}_{\widehat{p}}$ and we need to impose upon the fermionic one-form κ^I_μ the constraint (6.127), which can be re-expressed as

$$\kappa^I_\mu + \frac{1}{3}(j^a)_\mu{}^\nu\kappa^J_\nu(\omega^a)_J{}^I = 0\,. \tag{6.129}$$

The action in terms of the twisted fields takes the form

$$S_{HK} = \frac{1}{4r\ell} \int d^4x \sqrt{|g_4|} \left[G_{IJ} \partial_\mu X^I \partial^\mu X^J - 2 G_{IJ} g^{\mu\nu} \lambda^I \mathcal{D}_\mu \kappa_\nu^J + \frac{1}{8} R_{IJKL} \kappa_\mu^I \kappa_\nu^J \lambda^K \lambda^L \right] , \tag{6.130}$$

and is invariant under the supersymmetry transformations

$$\begin{aligned} \delta X^I &= u \lambda^I \\ \delta \lambda^I &= 0 \\ \delta \kappa_\mu^I &= u \left(\partial_\mu X^I - \omega_{\mu\nu}{}^I{}_J \partial^\nu X^J \right) - \Gamma^I_{JK} \delta X^J \kappa_\mu^K . \end{aligned} \tag{6.131}$$

This is precisely the form of the topological sigma-model of [254] for Hyper-Kähler M_4. The action takes a simpler form than in the model presented in [254] since the target space $\mathcal{M}_k$ is also Hyper-Kähler (i.e. has a covariantly constant quaternionic structure).

The topological BRST transformation Q (with $\delta_u = uQ$) squares to zero $Q^2 = 0$ on-shell. To make the algebra close off-shell, we can introduce an auxiliary one-form b_μ^I valued in the pull-back of the tangent space to $\mathcal{M}_k$, $b \in \Gamma(X^* T\mathcal{M} \otimes \Omega^1)$ and satisfying the constraint

$$b_\mu^I + \frac{1}{3} (j^a)_\mu{}^\nu b_\nu^J (\omega^a)_J{}^I = 0 . \tag{6.132}$$

We then define the BRST transformation to be

$$\begin{aligned} Q X^I &= \lambda^I \\ Q \lambda^I &= 0 \\ Q \kappa_\mu^I &= b_\mu^I - \Gamma^I_{JK} \lambda^J \kappa_\mu^K \\ Q b_\mu^I &= \frac{1}{2} R_{JK}{}^I{}_L \lambda^J \lambda^K \kappa_\mu^L - \Gamma^I_{JK} \lambda^J b_\mu^K . \end{aligned} \tag{6.133}$$

The action (6.130) can then be recast in the form

$$S_{HK}^{\text{off-shell}} = S' - S_T . \tag{6.134}$$

where S' and S_T are Q-exact and topological, respectively, given by

$$\begin{aligned} S' &= Q \left(\frac{1}{2r\ell} \int d^4x \sqrt{|g_4|}\, G_{IJ} g^{\mu\nu} \kappa_\mu^I \left(\partial_\nu X^J - \frac{1}{8} b_\nu^J \right) \right) \\ S_T &= \frac{1}{4r\ell} \int d^4x \sqrt{|g_4|}\, (j^a)^{\mu\nu} \omega^a_{IJ} \partial_\mu X^I \partial_\nu X^J . \end{aligned} \tag{6.135}$$

Integrating out b_μ^I

$$b_\mu^I = \partial_\mu X^I - (j^a)_\mu{}^\nu \partial_\nu X^J \omega^a{}_J{}^I , \tag{6.136}$$

we recover the on-shell action (6.130). The term S_T is 'topological', in the sense that it is invariant under Hyper-Kähler deformations, and can be written as

$$S_T = \frac{1}{2r\ell} \int_{M_4} j^a \wedge X^* \omega^a , \tag{6.137}$$

where $X^*\omega^a$ is the pull-back of the Kähler forms on $\mathcal{M}_k$, and for Hyper-Kähler M_4, j^a are the Kähler forms. From this form it is clear that the term is invariant under Hyper-Kähler deformations, but not deformations, that break the Hyper-Kählerity.

Finally, to show that the theory is topological, meaning independent of continuous deformations of the metric (which preserve the Hyper-Kähler structure), we must check that the energy-momentum tensor $T_{\mu\nu}$ associated with S' part of the action is Q-exact. We find

$$T_{\mu\nu} \equiv \frac{2}{\sqrt{g}} \frac{\delta S'}{\delta g^{\mu\nu}} = G_{IJ} b^I_\mu (\partial_\nu X^J - \frac{1}{8} b^J_\nu) + G_{IJ} b^I_\nu (\partial_\mu X^J - \frac{1}{8} b^J_\mu) - g_{\mu\nu} \mathcal{L}' \,, \tag{6.138}$$

where $\mathcal{L}$ is the Lagrangian density in (6.135). This can be expressed as

$$T_{\mu\nu} = Q \left\{ G_{IJ} \kappa^I_\mu \left(\partial_\nu X^J - \frac{1}{8} b^J_\nu \right) + G_{IJ} \kappa^I_\nu \left(\partial_\mu X^J - \frac{1}{8} b^J_\mu \right) - g_{\mu\nu} G_{IJ} \kappa^{I\rho} \left(\partial_\rho X^J - \frac{1}{8} b^J_\rho \right) \right\} . \tag{6.139}$$

Clearly it is of interest to study further properties of these theories, in particular observables, which will be postponed to future work. Some preliminary results for sigma-models that localise on tri-holomorphic maps have appeared in [254], however only in terms of simplified setups, where the target is the same as M_4.

6.5.3 Relation to topologically twisted 5d $\mathcal{N} = 2$ SYM

The topological sigma-model (6.130) for the Hyper-Kähler case, can also be obtained by first topologically twisting the 5d $\mathcal{N} = 2$ SYM theory on an interval obtained in section 6.3, with the twist described in section 6.5.1. The derivation is quite similar to the analysis in section 6.4, and we summarise the salient points here. The details are provided for the interested reader in appendix C.6. There, we also discuss the topological twist 1 in the context of the 5d $\mathcal{N} = 2$ SYM theory. The action for the bosonic fields, and some analysis of the boundary conditions in terms of Nahm data, has appeared in [244]. The supersymmetric version has appeared in [271], albeit without the supersymmetric boundary conditions.

The topologically twisted 5d $\mathcal{N} = 2$ SYM theory can be written in terms of the fields $B_{\mu\nu}$, which is a self-dual two-form defined in (C.80), a complex scalar field φ, the gauge field A_μ and fermions, which in terms of the twisted fields have the following decomposition

$$\begin{aligned} \rho^{(1)}_{+\widehat{p}} &= \gamma^\mu \psi^{(1)}_\mu \tilde{\epsilon}_{\widehat{p}} & \rho^{(2)}_{+\widehat{p}} &= \gamma^\mu \psi^{(2)}_\mu \tilde{\epsilon}_{\widehat{p}} \\ \rho^{(1)}_{-\widehat{p}} &= \left(\eta^{(1)} + \frac{1}{4} \gamma^{\mu\nu} \chi^{(1)}_{\mu\nu} \right) \tilde{\epsilon}_{\widehat{p}} & \rho^{(2)}_{-\widehat{p}} &= \left(\eta^{(2)} + \frac{1}{4} \gamma^{\mu\nu} \chi^{(2)}_{\mu\nu} \right) \tilde{\epsilon}_{\widehat{p}} \,. \end{aligned} \tag{6.140}$$

Nahm's equations in terms of the self-dual two-forms are

$$D_\theta B_{\mu\nu} - \frac{1}{2}[B_{\mu\rho}, B_\nu{}^\rho] = 0\,. \tag{6.141}$$

The supersymmetric vacuum configurations which satisfy this, are again characterised in terms of maps into the moduli space of solutions to the equations (6.141), which is the k-centered monopole moduli space, when M_4 is Hyper-Kähler. The 4d topological theory is obtained by expanding the fields $B_{\mu\nu}$, A_θ and the fermions in terms of coordinates on the moduli space, much like in section 6.4, and the resulting 4d topological sigma-model is precisely the one we obtained by twisting the flat space sigma-model in (6.130).

6.6 Sigma-models with Self-dual Two-forms

Having understood the Hyper-Kähler M_4 case, we can finally turn to the case of general M_4. The reduction proceeds in the same way as for the Hyper-Kähler case, but the situation is somewhat complicated by the fact that part of the coordinates X^I become sections of $\Omega_2^+(M_4)$, namely self-dual two-forms. We consider in detail the abelian case with target space $\mathcal{M}_1 \simeq \mathbb{R}^3 \times S^1$ and the first non-trivial case, corresponding to the reduction of the 5d $U(2)$ theory, with target space $\mathcal{M}_2 \simeq \mathbb{R}^3 \times \frac{S^1 \times \mathcal{M}_2^0}{\mathbb{Z}_2}$, where $\mathcal{M}_2^0$ is the Atiyah-Hitchin manifold.

In the case of an arbitrary (oriented) four-manifold M_4, there is no Hyper-Kähler structure, only an almost quaternionic structure [272]. One could anticipate dimensionally reducing the twisted 5d SYM theory, as discussed in section 6.5.3 and appendix C.6.1. However, this requires that Nahm's equations for the self-dual two-forms $B_{\mu\nu}$

$$D_\theta B_{\mu\nu} - \frac{1}{2}[B_{\mu\rho}, B_\nu{}^\rho] = 0\,, \tag{6.142}$$

to be solved locally on patches in M_4 and the patching must be defined globally, according to the transformation of B on overlaps. Generically this means that part of the mapping coordinates X^I will transform from one patch to the other and therefore belong to non-trivial $SU(2)_\ell$ bundles over M_4. A similar situation appears in [266] appendix B, when twisting the sigma-model into the Hitchin moduli space. To understand precisely, which coordinates X^I become sections of $SU(2)_\ell$ bundles on M_4, we require a detailed understanding of the metric on $\mathcal{M}_k$ and the action of the $SU(2)_\ell$ isometries. In the following, we will address this in the case of $k = 1, 2$, where the metrics are known.

We provide here the analysis in the case of the reduction of the abelian theory, as a warm-up, and then the reduction of the $U(2)$ theory, which is the first non-trivial case. In these

cases we find that the four-dimensional theory is a topological sigma-model with part of the coordinates X^I on the target space transforming as self-dual two-forms on M_4.

6.6.1 Abelian Theory

Recall that the dimensional reduction on S^2 of the untwisted single M5-brane theory gives a free hyper-multiplet in $\mathbb{R}^{1,3}$. We shall now discuss this in the context of the topologically twisted theory on $S^2 \times M_4$ and determine the sigma-model into the one-monopole moduli space $\mathcal{M}_{k=1} \cong \mathbb{R}^3 \times S^1$, with $\mathbb{R}^3$ the position of the center and S^1 parametrizing a phase angle. As the metric is known, we can identity the coordinates parametrising the position of the center as those which transform under the $\mathfrak{su}(2)_R$ and the twist gives a topological model for general M_4. In fact, we find the abelian version of a model in [253] in the context of 4d topological A-models. The 4d field content is the self-dual two-form $B_{\mu\nu}$, the scalar ϕ and (twisted) for the fermions, a scalar η, a vector ψ_μ, and a self-dual two-form $\chi_{\mu\nu}$.

We begin by decomposing the target space index $I \to (a, \phi)$, with $a = 1, 2, 3$. Under this decomposition the constraints on the spinors $\xi^{(i)I}_{\widehat{p}}$ can be solved as

$$\xi^{(i)\widehat{a}}_{\widehat{p}} = i(\sigma^a)^{\widehat{q}}_{\widehat{p}}\, \xi^{(i)\phi}_{\widehat{q}}\,, \tag{6.143}$$

leaving only $\xi^{(i)\phi}_{\widehat{q}}$ as the unconstrained fermions in the theory. Under the twist the fields become

Field	$\mathfrak{g}_{4d}$	$\mathfrak{g}_{\text{twist}}$	Twisted Field
X^ϕ	$(\mathbf{1},\mathbf{1},\mathbf{1})$	$(\mathbf{1},\mathbf{1})$	ϕ
X^a	$(\mathbf{3},\mathbf{1},\mathbf{1})$	$(\mathbf{3},\mathbf{1})$	$B_{\mu\nu}$
$\xi^{(1)\phi}_{\widehat{p}}$	$(\mathbf{2},\mathbf{2},\mathbf{1})$	$(\mathbf{1}\oplus\mathbf{3},\mathbf{1})$	$\eta, \chi_{\mu\nu}$
$\xi^{(2)\phi}_{\widehat{p}}$	$(\mathbf{2},\mathbf{1},\mathbf{2})$	$(\mathbf{2},\mathbf{2})$	ψ_μ

(6.144)

where the twisted fermions are obtained from the decompositions

$$\begin{aligned} \xi^{(1)\phi}_{\widehat{p}} &= i\left(\eta + \frac{1}{4}\sigma^{\mu\nu}\chi_{\mu\nu}\right)\tilde{\epsilon}_{\widehat{p}} \\ \xi^{(2)\phi}_{\widehat{p}} &= -\frac{1}{4}\bar{\sigma}^\mu\psi_\mu\tilde{\epsilon}_{\widehat{p}}\,. \end{aligned} \tag{6.145}$$

The scalars X^a are decomposed in terms of the self-dual two-form $B_{\mu\nu}$ by making use of the invariant tensors $j^a_{\mu\nu}$

$$B_{\mu\nu} = -j^a_{\mu\nu}X^a\,. \tag{6.146}$$

The action for the $k = 1$ topological sigma-model from flat space into the monopole moduli space $\mathcal{M}_1$ is then

$$S_{\mathcal{M}_1} = \frac{1}{4r\ell}\int d^4x\sqrt{|g_4|}(\partial_\mu\phi\partial^\mu\phi + \frac{1}{4}\partial_\mu B_{\rho\sigma}\partial^\mu B^{\rho\sigma} - 2\psi^\mu\partial_\mu\eta + 2\psi_\mu\partial_\nu\chi^{\mu\nu})\,, \tag{6.147}$$

and it is invariant the supersymmetry transformations

$$\begin{aligned} \delta\phi &= u\eta \\ \delta B_{\mu\nu} &= u\chi_{\mu\nu} \\ \delta\eta = \delta\chi &= 0 \\ \delta\psi_\mu &= u(\partial_\mu\phi + \partial^\nu B_{\nu\mu})\,. \end{aligned} \tag{6.148}$$

To show that this action is topological we introduce the auxiliary field

$$P_\mu = \partial_\mu\phi + \partial^\nu B_{\nu\mu}\,, \tag{6.149}$$

so that $\delta P_\mu = 0$ and $\delta\psi_\mu = uP_\mu$. The action can be written as the sum of a Q-exact term and a topological term by noting that $\delta_u = uQ$

$$S_{\mathcal{M}_1} = Q\mathcal{V} + \frac{1}{2r\ell}\int_{M_4} d\phi \wedge dB\,, \tag{6.150}$$

where

$$\mathcal{V} = \frac{1}{4r\ell}\int_{M_4} d^4x\sqrt{|g_4|}\,(-\psi^\mu P_\mu + 2\psi^\mu(\partial_\mu\phi + \partial^\nu B_{\nu\mu}))\ . \tag{6.151}$$

For M_4 without boundary, the second term in (6.150) vanishes upon integrating by parts. This action can then be generalised to arbitrary M_4 by covariantising the derivatives, and add curvature terms

$$\mathcal{R}_{\mu\nu\rho\sigma}B^{\mu\nu}B^{\rho\sigma}\,, \quad \mathcal{R}B_{\mu\nu}B^{\mu\nu}. \tag{6.152}$$

The resulting theory is a (free) topological sigma-model based on the map $\phi : M_4 \to U(1)$, together with a self-dual two-form B and fermionic fields and is given by

$$S_{\mathcal{M}_1} = \frac{1}{4r\ell}\int (\star d\phi \wedge d\phi + \star dB \wedge dB + 2\psi \wedge (\star d\eta - d\chi))\ . \tag{6.153}$$

The supersymmetric vacua, which are the saddle points of the action, satisfy

$$d\phi + \star dB = 0\,, \tag{6.154}$$

which implies that ϕ and B are harmonic, and in particular then $d\phi = 0$ and $dB = 0$. Thus, ϕ is a constant scalar, and B is a self-dual 2-form in a cohomology class of $H^{2,+}(M_4)$.

Note, likewise one can obtain the same abelian theory starting with the 5d twisted theory for curved M_4 as discussed in section 6.5.3 and appendix C.6.1. The reduction can be done straight forwardly, integrating out the fields $\psi^{(1)}$, $\chi^{(2)}$ and $\eta^{(2)}$, and taking the leading $1/r$ terms in the action. The match to the action in (6.153) can be found by defining the fields in the 4d reduction as

$$A_\theta \equiv \phi\,, \quad \eta \equiv \eta^{(1)}\,, \quad \psi_\mu \equiv 4i\psi^{(2)}_\mu\,, \quad \chi_{\mu\nu} \equiv \chi^{(1)}_{\mu\nu}\,. \tag{6.155}$$

The scalar ϕ is actually defined in a gauge invariant way as $\phi = \int_0^\pi d\theta A_\theta$. Moreover it takes values in $i\mathbb{R}/\mathbb{Z} = U(1)$ [8], where the $\mathbb{Z}$-quotient is due to the large gauge transformations $\delta(\int A_\theta) = 2\pi i n$, $n \in \mathbb{Z}$ [9].

6.6.2 $U(2)$ Theory and Atiyah-Hitchin Manifold

In this section we study the simplest non-abelian case, corresponding to two M5-branes wrapped on S^2, or equivalently we study the reduction of the 5d $U(2)$ theory to 4d on an interval with Nahm pole boundary conditions. The flat 4d theory is given by a map into the 2-monopole moduli space $\mathcal{M}_2$, with the action given in (6.110). For the curved space theory we find a description in terms of a sigma-model into $S^1 \times \mathbb{R}_{\geq 0}$ supplemented by self-dual two-forms obeying some constraints. We provide a detailed analysis of the geometrical data entering the sigma-model and we give the bosonic part of the topological sigma-model on an arbitrary four-manifold M_4.

The 2-monopole moduli space has been studied extensively in the literature (see for instance [247, 273–276]), starting with the work of Atiyah and Hitchin [247]. It has the product structure

$$\mathcal{M}_2 = \mathbb{R}^3 \times \frac{S^1 \times \mathcal{M}_{\text{AH}}}{\mathbb{Z}_2}\,, \tag{6.156}$$

where $\mathbb{R}^3$ parametrises the position of the center of mass of the 2-monopole system, and $\mathcal{M}_{\text{AH}}$ is the Atiyah-Hitchin manifold, which is a four-dimensional Hyper-Kähler manifold. The metric on $\mathbb{R}^3 \times S^1$ is flat, it is associated to the abelian part of the theory $U(1) \subset U(2)$. The non-trivial geometry is carried by the Atiyah-Hitchin (AH) manifold [247], whose Hyper-Kähler metric (AH metric) is given by

$$ds^2_{\text{AH}} = f(r)^2 dr^2 + a(r)^2\sigma_1^2 + b(r)^2\sigma_2^2 + c(r)^2\sigma_3^2\,, \tag{6.157}$$

where f, a, b, c are functions of $r \in \mathbb{R}_{\geq 0}$ and σ_i are $SO(3)$ left invariant one-forms

$$\begin{aligned}
\sigma^1 &= -\sin\psi d\theta + \cos(\psi)\sin(\theta)d\phi \\
\sigma^2 &= \cos\psi d\theta + \sin(\psi)\sin(\theta)d\phi \\
\sigma^2 &= \cos(\theta)d\phi + d\psi\,,
\end{aligned} \tag{6.158}$$

with $0 \leq \theta \leq \pi$, $0 \leq \phi \leq 2\pi$ and $0 \leq \psi < 2\pi$, with $\psi \sim \psi + 2\pi$. In addition the coordinates are subject to the following identifications [273],

$$(\theta, \phi, \psi) \sim (\pi - \theta, \phi + \pi, -\psi)\,, \quad (\beta, \psi) \sim (\beta + \pi, \psi + \pi)\,, \tag{6.159}$$

[8] The factor i is due to our conventions in which A_θ is purely imaginary.

[9] These transformations correspond to gauge group elements $g = e^{i\alpha(\theta)}$ with $\alpha(0) = 0$ and $\alpha(\pi) = 2\pi n$. The quantisation of n is required for g to be trivial at the endpoints of the θ interval.

where the second identification accounts for the $\mathbb{Z}_2$ quotient in (6.156), $\beta \in [0, 2\pi]$ being the angle coordinate on the S^1. The one-forms obey

$$d\sigma^1 = \sigma^2 \wedge \sigma^3 \,, \tag{6.160}$$

and cyclic permutations of $1, 2, 3$. The metric has an $SO(3) \equiv SO(3)_{\rm AH}$ isometry (leaving the one-form $\sigma^{1,2,3}$ invariant). The function f can be fixed to any desirable value by a reparametrisation of r (usual choices are $f = abc$ or $f = -b/r$). The functions a, b, c obey the differential equation

$$\frac{da}{dr} = \frac{f}{2bc}\left(b^2 + c^2 - a^2 - 2bc\right) \,, \tag{6.161}$$

and cyclic permutations of a, b, c. More details on the geometry of $\mathcal{M}_{\rm AH}$, including the explicit Riemann tensor, can be found in [275].

The geometry is Hyper-Kähler and therefore possesses three complex structures J^a, $a = 1, 2, 3$. These three complex structures transform as a triplet of the $SO(3)_{\rm AH}$ isometry. They extend naturally to complex structures on the full $\mathcal{M}_2$ geometry and then transform as a triplet of $SO(3)_{\mathcal{M}_2}$ =diag$(SO(3)_{\rm AH} \times SO(3)_{\rm abel})$, where $SO(3)_{\rm abel}$ is the rotation group of $\mathbb{R}^3$. In the untwisted sigma-model (6.110), this $SO(3)_{\mathcal{M}_2}$ isometry is identified with the $SO(3)_R$ R-symmetry of the 4d theory,

$$\underline{\text{Untwisted theory:}} \quad SO(3)_{\mathcal{M}_2} \simeq SO(3)_R \,. \tag{6.162}$$

In the twisted sigma-model $SO(3)_{\mathcal{M}_2}$ gets identified with the $SO(3)_\ell$ left Lorentz rotations on the base manifold M_4,

$$\underline{\text{Twisted theory:}} \quad SO(3)_{\mathcal{M}_2} \simeq SO(3)_\ell \,. \tag{6.163}$$

Because of this identification, some coordinates on $\mathcal{M}_2$ acquire $SO(3)_\ell$ Lorentz indices and become forms on M_4. To make the action of $SO(3)_\ell$ on the $\mathcal{M}_2$ coordinates explicit and manageable, we need to choose appropriate coordinates.

The treatment of the $\mathbb{R}^3 \times S^1$ coordinates is identical to the abelian case. We have coordinates ϕ^a, $a = 1, 2, 3$, parametrizing $\mathbb{R}^3$, transforming as a triplet of $SO(3)_{\mathcal{M}_2}$, and β parametrizing S^1, scalar under $SO(3)_{\mathcal{M}_2}$. Here and in the rest of the section we identify the indices $\widehat{a}$ and a, namely we implement the 4d twisting which identifies $SO(3)_R$ and $SO(3)_\ell$.

The treatment of the coordinates on $\mathcal{M}_{\rm AH}$ is more involved. Here we propose to introduce the coordinates $y^{i,a} \equiv y^a{}_i$, with $a, i = 1, 2, 3$, forming an $SO(3)$ matrix $(y^a{}_i) \in SO(3)$

$$(y^a{}_i) = \begin{pmatrix} -\sin\psi\sin\phi + \cos\theta\cos\phi\cos\psi & -\cos\psi\sin\phi - \cos\theta\cos\phi\sin\psi & \cos\phi\sin\theta \\ -\sin\psi\cos\phi - \cos\theta\sin\phi\cos\psi & -\cos\psi\cos\phi + \cos\theta\sin\phi\sin\psi & -\sin\phi\sin\theta \\ \cos\psi\sin\theta & -\sin\theta\sin\psi & -\cos\theta \end{pmatrix} . \tag{6.164}$$

The $SO(3)_{\mathcal{M}_2}$ isometries act on the matrix $(y^a{}_i)$ by left matrix multiplication, so that the three vectors $y^{1,a}, y^{2,a}, y^{3,a}$ transform as three triplets of $SO(3)_{\mathcal{M}_2}$. The identifications (6.159) become

$$(\beta, y^{1,a}, y^{2,a}, y^{3,a}) \sim (\beta, y^{1,a}, -y^{2,a}, -y^{3,a}) \,, \quad (\beta, y^{1,a}, y^{2,a}, y^{3,a}) \sim (\beta+\pi, -y^{1,a}, -y^{2,a}, y^{3,a}) \,. \tag{6.165}$$

We can express the AH metric in terms of the $y^{i,a}$ coordinates by using the relations

$$\begin{aligned} (\sigma_1)^2 &= \frac{1}{2}(-dy^{1,a}dy^{1,a} + dy^{2,a}dy^{2,a} + dy^{3,a}dy^{3,a}) \\ (\sigma_2)^2 &= \frac{1}{2}(dy^{1,a}dy^{1,a} - dy^{2,a}dy^{2,a} + dy^{3,a}dy^{3,a}) \\ (\sigma_3)^2 &= \frac{1}{2}(dy^{1,a}dy^{1,a} + dy^{2,a}dy^{2,a} - dy^{3,a}dy^{3,a}) \,, \end{aligned} \tag{6.166}$$

where the index a is summed over. The AH metric (6.157) is then understood as the pull-back of the metric

$$\widetilde{ds}^2_{\rm AH} = f^2 dr^2 + v_1 dy^{1,a}dy^{1,a} + v_2 dy^{2,a}dy^{2,a} + v_3 dy^{3,a}dy^{3,a} \,, \tag{6.167}$$

where

$$v_1 = \frac{1}{2}(-a^2+b^2+c^2) \,, \; v_2 = \frac{1}{2}(a^2-b^2+c^2) \,, \; v_3 = \frac{1}{2}(a^2+b^2-c^2) \,. \tag{6.168}$$

As already mentioned the AH manifold $\mathcal{M}_{\rm AH}$ admits three complex structures J^a, $a = 1,2,3$, preserved by the above metric, and satisfying the quaternionic relations

$$(J^a)^I{}_J (J^b)^J{}_K = -\delta^{ab}\delta^I_K + \epsilon^{abc}(J^c)^I{}_K \,, \tag{6.169}$$

where the indices I, J, K run over the four coordinates of the AH metric [10]. Lowering an index with the AH metric G_{IJ} (6.157), we define the three Kähler forms $(\Omega^a)_{IJ} = G_{IK}(J^a)^K{}_J$. These forms can be nicely expressed as the pull-back of the forms $\widetilde{\Omega}^a$ on the space parametrised by the $r, y^{i,a}$ coordinates:[11]

$$\begin{aligned} \widetilde{\Omega}^a = \frac{1}{2}\epsilon^a{}_{bc}\Big[&(-a+b+c) f y^{1,b} dr \wedge dy^{1,c} + (a-b+c) f y^{2,b} dr \wedge dy^{2,c} + (a+b-c) f y^{3,b} dr \wedge dy^{3,c} \\ &- bc\, dy^{1,b} \wedge dy^{1,c} - ac\, dy^{2,b} \wedge dy^{2,c} - ab\, dy^{3,b} \wedge dy^{3,c}\Big] \,. \end{aligned} \tag{6.170}$$

These forms can be further simplified by using the functions $w_1 = bc$, $w_2 = ca$, $w_3 = ab$, which obey

$$\frac{dw_1}{dr} = -f\,(-a+b+c) \,, \quad \frac{dw_2}{dr} = -f\,(c+a-b) \,, \quad \frac{dw_3}{dr} = -f\,(b-c+a) \,. \tag{6.171}$$

[10] This is a small abuse of notation compared to the convention of previous sections where I, J, K run over all the coordinates on $\mathcal{M}_k$.

[11] We found the expression of one complex structure in [274] in terms of the Euler angles θ, ϕ, ψ and worked out the re-writing in terms of $y^{i,a}$. The other two complex structures were easily obtained by cyclic permutation of the $y^{i,a}$ coordinates.

We obtain the nice expression

$$\widetilde{\Omega}^a = -\frac{1}{2}\epsilon^a{}_{bc} \sum_{i=1,2,3} d(w_i y^{i,b}) \wedge dy^{i,c} \,. \tag{6.172}$$

The pull-backs Ω^a are complex structures on $\mathcal{M}_{\rm AH}$, hence they obey $d\Omega^a = 0$. This description of the complex structures is convenient, because it is much simpler than the expression in terms of the Euler angles θ, ϕ, ψ, but more importantly because it makes manifest the fact that the three Kähler forms Ω^a, or the three complex structures J^a, transform as a triplet under the $SO(3)_{\mathcal{M}_2}$ isometry.

After this preliminary work we can express the bosonic part of the flat space sigma-model action (6.110) in terms of the new coordinates $\beta, \phi^a, r, y^{i,a}$, describing the maps $M_4 \to \mathcal{M}_2$. Fixing $f(r) = 1$ for simplicity, we obtain

$$S_{\mathcal{M}_2,\rm bos} = \frac{1}{4r\ell} \int d^4x \sqrt{|g_4|} \left(\partial^\mu \beta \partial_\mu \beta + \delta_{ab} \partial^\mu \phi^a \partial_\mu \phi^b + \partial^\mu r \partial_\mu r + \sum_{i=1}^{3} v_i(r) \delta_{ab} \partial^\mu y^{i,a} \partial_\mu y^{i,b} \right) , \tag{6.173}$$

where the sigma-model coordinates $y^{i,a}$ are constrained to form an $SO(3)$ matrix (6.164) and to obey (6.165). These constraints can be stated explicitly

$$\delta_{ab} y^{i,a} y^{j,b} = \delta^{ij} \,, \qquad \epsilon_{abc} y^{1,a} y^{2,b} y^{3,c} = 1 \,. \tag{6.174}$$

The coordinate r is also constrained to be positive $r \geq 0$.

Having described the (bosonic) action of the twisted theory on flat space we can easily derive the (bosonic) action on an arbitrary M_4. The fields β, r are scalars on M_4, so their kinetic term is unchanged. The fields $\phi^a, y^{i,a}$ are triplets of $SO(3)_\ell$. They are mapped to self-dual two-forms

$$b_{\mu\nu} = -j^a_{\mu\nu} \phi^a \,, \quad y^i_{\mu\nu} = -j^a_{\mu\nu} y^{i,a} \,. \tag{6.175}$$

Their kinetic term gets covariantised by adding suitable curvature terms and we obtain

$$S_{\mathcal{M}_2,\rm bos} = -\frac{1}{4r\ell} \int d\beta \wedge \star d\beta + db \wedge \star db + dr \wedge \star dr + \sum_{i=1}^{3} v_i(r) dy^i \wedge \star dy^i \,. \tag{6.176}$$

The constraints (6.174) become $y^i_{\mu\nu} y^{j\,\mu\nu} = 4\delta^{ij}$ and $y^1{}_\mu{}^\nu y^2{}_\nu{}^\rho y^3{}_\rho{}^\mu = 4$.

The fermionic part of the action $S_{\mathcal{M}_2,\rm ferm}$ that is obtained from the untwisted action (6.110), is somewhat more involved, due to the presence of the four-Fermi interaction and the constraint (6.109) on the fields $\xi^{(i)I}$. From the abelian part of the $U(2)$ theory we obtain the fermionic field content of the abelian model (6.153). In the following we describe only the fermions related to $\mathcal{M}_{AH}$. Explicitly we can define the push-forward of the fermionic fields

$$\xi^{(1)\widetilde{I}p}_{\widehat{q}} = \partial_I y^{\widetilde{I}} \xi^{(1)Ip}_{\widehat{q}} \,, \qquad \xi^{(2)\widetilde{I}\dot{p}}_{\widehat{q}} = \partial_I y^{\widetilde{I}} \xi^{(2)I\dot{p}}_{\widehat{q}} \,, \tag{6.177}$$

where the index $\widetilde{I}$ runs over $r, (i,a)$. In the twisted theory we identify the $\mathfrak{su}(2)_\ell$ and $\mathfrak{su}(2)_R$ doublet indices q and $\widehat{q}$ and the fermionic fields of the resulting sigma model are a vector κ_μ, a scalar η and self-dual two-forms $\eta^{i,a} \sim \eta^i_{\mu\nu}$ satisfying the constraints

$$\delta_{ab} y^{i,a} \eta^{j,b} = -\delta_{ab} y^{j,a} \eta^{i,b} , \qquad \sum_j y^{j,a} \eta^{j,b} = -\sum_j y^{j,b} \eta^{j,a} . \tag{6.178}$$

The other fields appearing after the twisting are expect to be expressed in terms the above fields by solving the constraints (6.109). However the computation is rather involved and we do not provide an explicit expression here.

The sigma-model we obtain seems to be different from the sigma-models studied in the literature so far. It is a sigma-model with target $S^1 \times \mathbb{R}_{\geq 0}$ with constrained self-dual two-forms. To study this sigma-model, and in particular to show that it defines a topological theory, one would need to work out the details of the fermionic part of the Lagrangian and the action of the preserved supersymmetry (or BRST) transformation on the fields. We leave this for future work.

To conclude we can see how the bosonic action (6.176) compares with the bosonic action of the topological model that we obtained for Hyper-Kähler M_4 (6.130). More precisely we would like to know how the action (6.176) decomposes into Q-exact plus topological terms as in (6.135). For this we simply evaluate S_T for the sigma-model into $\mathcal{M}_2$, using the explicit form of the Ω^a (6.172). The terms involving the fields ϕ and b vanish upon integration by parts as in the abelian case, assuming M_4 has no boundary. When the theory is defined on an generic four-manifold $\mathcal{M}_4$, the remaining contribution is

$$S_T = \frac{1}{2r\ell} \int j^a \wedge X^*(\Omega^a) = \frac{1}{4r\ell} \int j^a \wedge dx^\mu \wedge dx^\nu (\Omega^a)_{IJ} D_\mu X^I D_\nu X^J + \text{curv.} , \tag{6.179}$$

where D_μ is covariant with respect to the Christoffel connection and $SU(2)_\ell$ Lorentz rotations (in the tangent space), and "+curv." denotes extra curvature terms, which appear when we consider a general curved M_4 and covariantise S_T. Replacing $X^I \to r, y^{i,a}$ we obtain

$$\begin{aligned}
S_T &= -\sum_{i=1}^3 \frac{1}{16r\ell} \int dx^\mu \wedge dx^\nu \wedge dx^\rho \wedge dx^\sigma \epsilon^{abc} (j^a)_{\rho\sigma} D_\mu (w_i y^{b,i}) D_\nu y^{c,i} + \text{curv.} \\
&= -\sum_{i=1}^3 \frac{1}{16r\ell} \int d^4x \sqrt{g} \epsilon^{\mu\nu\rho\sigma} (j^b)_\rho{}^\tau (j^c)_{\tau\sigma} D_\mu (w_i y^{b,i}) D_\nu y^{c,i} + \text{curv.} \\
&= -\sum_{i=1}^3 \frac{1}{16r\ell} \int d^4x \sqrt{g} \epsilon^{\mu\nu\rho\sigma} D_\mu (w_i y^{i\,\tau}_\rho) D_\nu y^i_{\tau\sigma} + \text{curv.} \\
&= \sum_{i=1}^3 \frac{1}{16r\ell} \int d^4x \sqrt{g} \epsilon^{\mu\nu\rho\sigma} (w_i y^{i\,\tau}_\rho) D_{[\mu} D_{\nu]} y^i_{\tau\sigma} + \text{curv.} \\
&= 0 .
\end{aligned} \tag{6.180}$$

From the third to the fourth line we have integrated by parts assuming M_4 has no boundary. The result on the fourth line can be recognised as containing only curvature terms (no derivatives on the fields $r, y^i_{\mu\nu}$) which must cancel each-other. This is necessary for supersymmetry to be preserved (since this term must be supersymmetric by itself). We conclude that the sigma-model action (6.176) must be Q-exact, without an extra topological term. Clearly, studying topological observables and further properties of this model are interesting directions for future investigations.

6.7 Discussion and Outlook

In this chapter we determined the dimensional reduction of the 6d $\mathcal{N} = (2,0)$ theory on S^2, and found this to be a 4d sigma-model into the moduli space $\mathcal{M}_k$ of k-centered $SU(2)$ monopoles. There are several exciting follow-up questions to consider:

1. 4d-2d Correspondence:
   Let us comment now on the proposed correspondence between 2d $\mathcal{N} = (0,2)$ theories with a half-topological twist, and four-dimensional topological sigma-models into $\mathcal{M}_k$. The setup we considered, much like the AGT and 3d-3d correspondences, implies a dependence of the 2d theory on the geometric properties of the four-manifold. In [226] such a dictionary was setup in the context of the torus-reduction, which leads to the Vafa-Witten topological field theory in 4d. It would be very important to develop such a dictionary in the present case. From the point of view of the 2d theory, the twist along M_4 is the same, and thus the dictionary developed between the topological data of M_4 and matter content of the 2d theory will apply here as well. The key difference is that we consider this theory on a two-sphere, and the corresponding 'dual' is not the Vafa-Witten theory, but the topological sigma-model into the Nahm moduli space.

2. Observables in 2d $\mathcal{N} = (0,2)$ theories:
   Recently much progress has been made in 2d $\mathcal{N} = (0,2)$ theories, both in constructing new classes of such theories [226, 277, 49, 50] as well as studying anomalies [278] and computing correlation functions using localisation [240]. In particular, the localisation results are based on deformations of $\mathcal{N} = (2,2)$ theories and the associated localisation computations in [279, 280]. The theories obtained in this thesis from the compactification of the M5-brane theory do not necessarily have such a $(2,2)$ locus and thus extending the results on localisation beyond the models studied in [240] would be most interesting.

3. Observables in the 4d topological sigma-model:
   An equally pressing question is to develop the theory on M_4, determine the cohomology of the twisted supercharges, and compute topological observables. For the case of Hyper-Kähler M_4, with the target also given by M_4, some observables of the topological sigma-model were discussed in [254]. However, we find ourselves in a more general situation, where the target is a specific $4k$-dimensional Hyper-Kähler manifold. For the general M_4 case we clearly get a new class of theories, which have scalars and self-dual two-forms. The only place where a similar theory has thus far appeared that we are aware of, is in [253] in the context of 4d topological A-models. We have studied the topological sigma-models for $k = 1, 2$, and the explicit topological sigma-models for $k \geq 3$ remain unknown. It would certainly be one of the most interesting directions to study these.

4. Generalisation to spheres with punctures:
   The analysis in this thesis for the sphere reduction can be easily generalised to spheres with two (general) punctures, i.e. with different boundary conditions for the scalars in the 5d $\mathcal{N} = 2$ SYM theory. We expect the 4d theory to be again a topological sigma-model, however, now into the moduli space of Nahm's equations with modified boundary conditions. Studying this case may provide further interesting examples of 4d topological field theories, which seem to be an interesting class of models to study in the future.

5. Reduction to three-dimensions and 3d duality:
   The four-dimensional sigma-model that we found by compactification of the 6d $\mathcal{N} = (2, 0)$ theory on a two-sphere, can be further reduced on a circle S^1 to give rise to a three-dimensional sigma-model into the same $\mathcal{M}_k$ target space. Similarly the twisted sigma-model on a manifold $S^1 \times M_3$ reduces along S^1 to a twisted sigma-model on M_3. On the other hand the compactification of the twisted 6d $\mathcal{N} = (2, 0)$ A_k theory on $S^2 \times S^1 \times M_3$ can be performed by reducing first on S^1, obtaining 5d $\mathcal{N} = 2$ SYM theory on $S^2 \times M_3$, and then reducing on S^2. We expect this reduction to yield a different three-dimensional theory, which would be dual to the 3d sigma model into $\mathcal{M}_k$, for $M_3 = \mathbb{R}^3$, or twisted sigma model, for general M_3, that we studied in this thesis. This new duality would be understood as an extension of 3d mirror symmetry [281] to topological theories. To our knowledge the reduction of 5d $\mathcal{N} = 2$ SYM on the topologically twisted S^2 has not been studied [12]. It would be very interesting to study it and to further investigate these ideas in the future.

[12] Note that the reduction of 5d $\mathcal{N} = 2$ SYM on a two-sphere, but in a different supersymmetric background, has been considered in [282, 283], in relation with the 3d-3d correspondence [223, 284], and leads to an $SL(k, \mathbb{C})$ Chern-Simons theory on M_3 with a complex Chern-Simons coupling.

Chapter 7

Conclusion

In this thesis aspects of gauge theories derived from higher dimensional compactifications were studied in the framework of M-theory and F-theory. Many key features of the lower dimensional theory are encoded in intricate aspects of the compactification manifold, which is one of the reasons why the study of this subject is so fascinating. We shall briefly review the material presented in this thesis.

As a natural consequence of string theory living in dimensions greater than the four space-time dimensions which we observe compactifications are central in the study of string phenomenology. Requiring some supersymmetry to be preserved in the reduction requires the compact dimensions to admit covariantly constant spinors. M-theory reductions to four dimensions preserving $\mathcal{N} = 1$ supersymmetry requires the compactification manifold to have G_2 holonomy[1], which has recently received considerable attention. Four-dimensional reductions of F-theory preserving minimal supersymmetry singles out elliptically fibered Calabi–Yau four-folds, and part of this thesis has focussed on exploring one particular aspect of these manifolds.

This thesis began with an exploration of additional $U(1)$ symmetries in $SU(5)$ GUT models engineered in F-theory. In chapter 3 the possible $U(1)$ charges for $\overline{\mathbf{5}}$ and $\mathbf{10}$ representations of $SU(5)$ were determined by studying elliptically fibered Calabi–Yau manifolds with additional rational sections. One important ingredient in this analysis is the possible splittings of the fibral curves over codimension two loci over which matter is localised, which was determined in [70]. Together with the geometric constraints on the rational sections the possible intersections of the section with matter curves in the fiber were ascertained and the realisable $U(1)$ charges computed.

[1] The other known seven-dimensional manifold which can be considered is one with Calabi–Yau three-fold boundary [14].

In chapter 4 a phenomenological survey of the $U(1)$ charges determined in chapter 3 was conducted with the objective of establishing whether these abelian gauge symmetries would be effective at forbidding couplings which result in fast proton decay, common to $SU(5)$ GUT models. To engineer a matter spectrum consistent with the minimal supersymmetric Standard Model one needs to incorporate fluxes. The fluxes are constrained by requiring the absence of exotics and also by the cancellation of mixed anomalies between the additional $U(1)$ symmetries and the Standard Model gauge group. Despite the abundance of constraining factors phenomenologically favourable models were discovered and could be extended, in the case of two additional $U(1)$ symmetries, to also generate known Yukawa textures through the Froggatt–Nielsen mechanism.

In the context of gauge theories compactifications have a long history of yielding interesting equations on lower dimensional spaces. One well-known example is the reduction of the instanton equations, which arise as the minimal energy configurations in pure Yang–Mills theory in four dimensions. The dimensional reduction of the self-dual Yang–Mills equations yield the monopole equations in three dimensions and Hitchin's equations in two dimensions [285]. The study of Hitchin's equations on Riemann surfaces, or flat holomorphic vector bundles, has remarkable connections to other areas of mathematics.

In the final chapter of this thesis the focal point changes to the 6d $\mathcal{N} = (2, 0)$ superconformal field theory describing the interacting theory of multiple M5-branes. The dimensional reduction of the 6d theory on the two-sphere is carried out in chapter 6. The S^2 is expressed as a circle fibration over an interval and the reduction proceeds via 5d $\mathcal{N} = 2$ SYM. The reduction of the 5d theory on an interval with supersymmetric boundary conditions require the fields to solve Nahm's equations and the resulting 4d theory, after topological twisting, is a topological sigma-model into the moduli space of Nahm's equations. Supersymmetric observables in this theory should have a counterpart in the 2d $\mathcal{N} = (0, 2)$ superconformal field theory which arises from the compactification of M5-branes on a general four-manifold with the Vafa–Witten twist. It would be very interesting to explore this further in the future.

Appendix A

Appendices for Chapter 3

A.1 Details for Anti-Symmetric Matter

In this appendix the various details of the enhancements from I_5 to I_1^*, which gives rise to matter in the **10** representation of $SU(5)$, are collected. Tables A.1 and A.2 list the sixteen different enhancements that can occur, as determined in [70], and represented by the appropriate box graph. The possible $U(1)$ charges listed in section 3.5 are determined by studying each of these sixteen enhancements and asking in what ways fiber curves, or collections of fiber curves, can be contained inside the section, whilst remaining consistent with the intersection data in codimension one. There are eleven qualitatively different "splitting types", which were previously listed in section 3.5, and for each of these it is determined what the possible configurations of curves in any rational section for that particular splitting type are.

A.1.1 Codimension two I_1^* Fibers

For the purpose of this appendix a new notation will need to be introduced to concisely summarise all of the different configurations as there are many configurations that realise the same intersection numbers of the curves with the section. Each fiber will be displayed as in figure A.1a. As such there is an obvious choice of ordering $C_1, \cdots, C_6$, where these curves can be curves associated to either roots or weights. If a curve C_i is contained within the section it is such that $\deg(N_{C_i/\sigma}) \leq -1$ by Theorems 3.3.5 and 3.3.8, and by the analysis it is also known that this value always happens to be in the (negative) single digits. The notation is then given by the string $(n_1 n_2 n_3 n_4 n_5 n_6)$ where the n_i are

(i) If C_i is contained inside the section then $n_i = -\deg(N_{C_i/\sigma})$.

(ii) If C_i is uncontained in the section and has an additional transverse intersection with

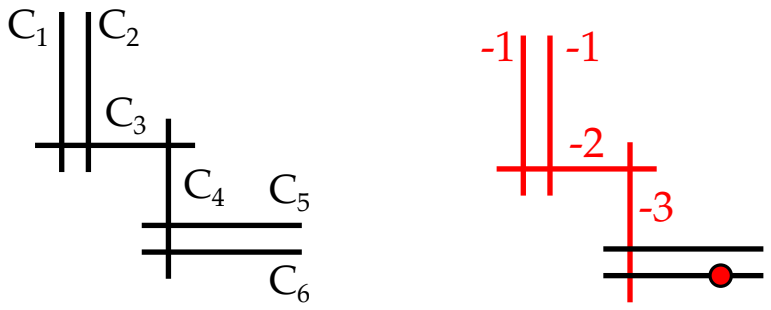

(a) (b)

Figure A.1: (i) is a schematic depiction of an I_1^* fiber and (ii) is this I_1^* fiber in the configuration (1123–x). As usual if a component is colored red then it is contained inside the section, and the red integer adjacent to the component is the degree of the normal bundle to that component in the section. A red node indicates an additional transverse intersection with the section.

the section then the n_i is replaced by an "x". Additional here means that there is a transverse intersection that does not come from the intersection(s) of C_i with another curve C_j which is contained inside the section.

(iii) If the curve C_i is otherwise then the n_i is replaced with an en-dash "–".

Such a string completely determines the configuration, for example consider the configuration (1123–x) on the fiber presented in figure A.1a. Such a configuration is represented in figure A.1b. The string fixes that

- $C_1, C_2, C_3, C_4 \subset \sigma$ with $\deg(N_{C_1/\sigma}) = \deg(N_{C_2/\sigma}) = -1$, $\deg(N_{C_3/\sigma}) = -2$, and $\deg(N_{C_4/\sigma}) = -3$.
- $C_5 \not\subset \sigma$ and $\sigma \cdot_Y C_5 = 1$ from the single intersection point between C_5 and the contained curve C_4.
- $C_6 \not\subset \sigma$ and $\sigma \cdot_Y C_6 = 2$ with one contribution from the intersection point of C_6 and C_4, and an additional contribution from the extra transverse intersection of the section with C_6.

A.1.2 Compilation of Codimension two Fibers

In this section the different sets of intersection numbers and the possible realisations as configurations of the fiber curves contained within the section are enumerated for each splitting type introduced in section 3.5.1. Figure A.2 demonstrates the ordering of the fiber components for each of the three major types, and fixes the ordering of the notation $(n_1 \cdots n_6)$. All the configurations, determined by a similar procedure to that used in

#	Box Graph	Splitting	Intersections	$I_5^{(0\|1)}$ S_f values	$I_5^{(0\|\|1)}$ S_f values
1	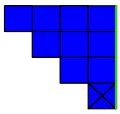	$F_0 \to C^+_{4,5} + F_2 + F_3 + \tilde{F}_0$ $\tilde{F}_0 = C^-_{1,2}$	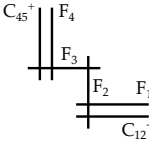	$S_f \cdot_Y C^+_{4,5} = +2$ $S_f \cdot_Y C^-_{1,2} = +3$	$S_f \cdot_Y C^+_{4,5} = +4$ $S_f \cdot_Y C^-_{1,2} = +6$
2	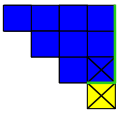	$F_3 \to C^+_{3,5} + C^-_{4,5}$ $F_0 \to C^+_{3,5} + F_2 + \tilde{F}_0$ $\tilde{F}_0 = C^-_{12}$	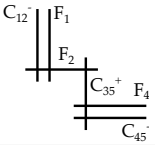	$S_f \cdot_Y C^+_{3,5} = +2$ $S_f \cdot_Y C^-_{4,5} = -2$ $S_f \cdot_Y C^-_{1,2} = +3$	$S_f \cdot_Y C^+_{3,5} = +4$ $S_f \cdot_Y C^-_{4,5} = -4$ $S_f \cdot_Y C^-_{1,2} = +6$
3	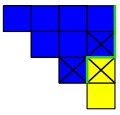	$F_2 \to C^+_{2,5} + C^-_{3,5}$ $F_4 \to C^+_{3,4} + C^-_{3,5}$ $F_0 \to C^+_{2,5} + \tilde{F}_0$ $\tilde{F}_0 = C^-_{1,2}$	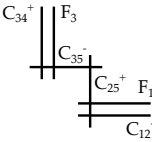	$S_f \cdot_Y C^+_{2,5} = +2$ $S_f \cdot_Y C^-_{3,5} = -2$ $S_f \cdot_Y C^+_{3,4} = +2$ $S_f \cdot_Y C^-_{1,2} = +3$	$S_f \cdot_Y C^+_{2,5} = -1$ $S_f \cdot_Y C^-_{3,5} = -4$ $S_f \cdot_Y C^+_{3,4} = +4$ $S_f \cdot_Y C^-_{1,2} = +6$
4	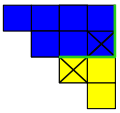	$F_2 \to C^+_{2,5} + C^-_{3,4} + F_4$ $F_0 \to C^+_{2,5} + \tilde{F}_0$ $\tilde{F}_0 = C^-_{12}$	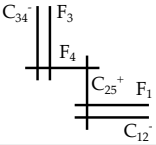	$S_f \cdot_Y C^+_{2,5} = +2$ $S_f \cdot_Y C^-_{3,4} = -2$	$S_f \cdot_Y C^+_{2,5} = -1$ $S_f \cdot_Y C^-_{3,4} = -4$
5	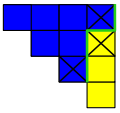	$F_1 \to C^+_{1,5} + C^-_{2,5}$ $F_4 \to C^+_{3,4} + F_2 + C^-_{2,5}$	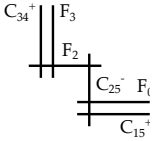	$S_f \cdot_Y C^+_{1,5} = -3$ $S_f \cdot_Y C^-_{2,5} = -2$ $S_f \cdot_Y C^+_{3,4} = +2$	$S_f \cdot_Y C^+_{1,5} = -1$ $S_f \cdot_Y C^-_{2,5} = +1$ $S_f \cdot_Y C^+_{3,4} = +4$
6	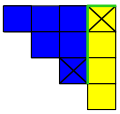	$F_4 \to C^+_{3,4} + F_1 + F_2 + C^-_{1,5}$	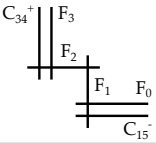	$S_f \cdot_Y C^+_{3,4} = +2$ $S_f \cdot_Y C^-_{1,5} = +3$	$S_f \cdot_Y C^+_{3,4} = +4$ $S_f \cdot_Y C^-_{1,5} = +1$
7	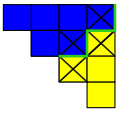	$F_1 \to C^+_{1,5} + C^-_{2,5}$ $F_2 \to C^+_{2,4} + C^-_{3,4}$ $F_4 \to C^+_{2,4} + C^-_{2,5}$	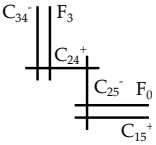	$S_f \cdot_Y C^+_{1,5} = -3$ $S_f \cdot_Y C^-_{2,5} = -2$ $S_f \cdot_Y C^+_{2,4} = +2$ $S_f \cdot_Y C^-_{3,4} = -2$	$S_f \cdot_Y C^+_{1,5} = -1$ $S_f \cdot_Y C^-_{2,5} = +1$ $S_f \cdot_Y C^+_{2,4} = -1$ $S_f \cdot_Y C^-_{3,4} = -4$
8	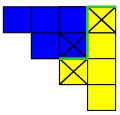	$F_2 \to C^+_{2,4} + C^-_{3,5}$ $F_4 \to C^+_{2,4} + F_1 + C^-_{1,5}$	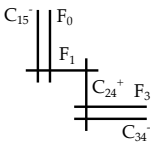	$S_f \cdot_Y C^+_{2,4} = +2$ $S_f \cdot_Y C^-_{3,4} = -2$ $S_f \cdot_Y C^-_{1,5} = +3$	$S_f \cdot_Y C^+_{2,4} = -1$ $S_f \cdot_Y C^-_{3,4} = -4$ $S_f \cdot_Y C^-_{1,5} = +1$

Table A.1: Splitting rules for $SU(5) \times U(1)$ with **10** and Shioda map details S_f for $I_5^{(0|1)}$ and $I_5^{(0||1)}$ for phases $1-8$.

#	Box Graph	Splitting	Intersections	$I_5^{(0\|1)}$ S_f values	$I_5^{(0\|\|1)}$ S_f values
9	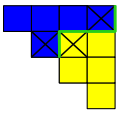	$F_1 \to C^+_{1,5} + F_4 + C^-_{2,4}$ $F_3 \to C^+_{2,3} + C^-_{2,4}$	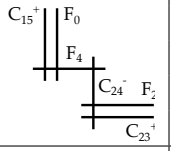	$S_f \cdot_Y C^+_{1,5} = -3$ $S_f \cdot_Y C^-_{2,4} = -2$ $S_f \cdot_Y C^+_{2,3} = +2$	$S_f \cdot_Y C^+_{1,5} = -1$ $S_f \cdot_Y C^-_{2,4} = +1$ $S_f \cdot_Y C^+_{2,3} = -1$
10	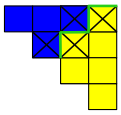	$F_1 \to C^+_{1,4} + C^-_{2,4}$ $F_3 \to C^+_{2,3} + C^-_{2,4}$ $F_4 \to C^+_{1,4} + C^-_{1,5}$	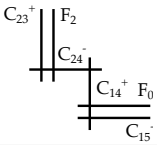	$S_f \cdot_Y C^+_{1,4} = -3$ $S_f \cdot_Y C^-_{2,4} = -2$ $S_f \cdot_Y C^+_{2,3} = +2$ $S_f \cdot_Y C^-_{1,5} = +3$	$S_f \cdot_Y C^+_{1,4} = -1$ $S_f \cdot_Y C^-_{2,4} = +1$ $S_f \cdot_Y C^+_{2,3} = -1$ $S_f \cdot_Y C^-_{1,5} = +1$
11	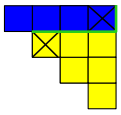	$F_1 \to C^+_{1,5} + F_4 + F_3 + C^-_{2,3}$	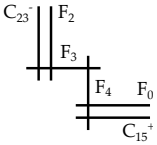	$S_f \cdot_Y C^+_{1,5} = -3$ $S_f \cdot_Y C^-_{2,3} = -2$	$S_f \cdot_Y C^+_{1,5} = -1$ $S_f \cdot_Y C^-_{2,3} = +1$
12	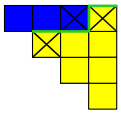	$F_1 \to C^+_{1,4} + F_3 + C^-_{2,3}$ $F_4 \to C^+_{1,4} + C^-_{1,5}$	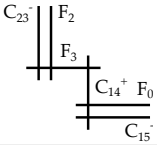	$S_f \cdot_Y C^+_{1,4} = -3$ $S_f \cdot_Y C^-_{2,3} = -2$ $S_f \cdot_Y C^-_{1,5} = +3$	$S_f \cdot_Y C^+_{1,4} = -1$ $S_f \cdot_Y C^-_{2,3} = +1$ $S_f \cdot_Y C^-_{1,5} = +1$
13	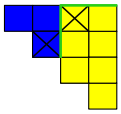	$F_3 \to C^+_{2,3} + F_1 + C^-_{1,4}$ $F_0 \to C^-_{1,4} + \tilde{F}_0$ $\tilde{F}_0 = C^+_{4,5}$	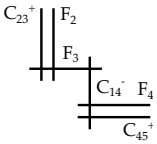	$S_f \cdot_Y C^+_{2,3} = +2$ $S_f \cdot_Y C^-_{1,4} = +3$ $S_f \cdot_Y C^+_{4,5} = +2$	$S_f \cdot_Y C^+_{2,3} = -1$ $S_f \cdot_Y C^-_{1,4} = +1$ $S_f \cdot_Y C^+_{4,5} = -4$
14	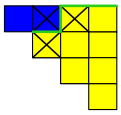	$F_1 \to C^+_{1,3} + C^-_{2,3}$ $F_3 \to C^+_{1,3} + C^-_{1,4}$ $F_0 \to C^-_{1,4} + \tilde{F}_0$ $\tilde{F}_0 = C^+_{4,5}$	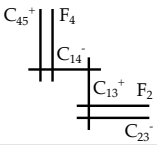	$S_f \cdot_Y C^+_{1,3} = -3$ $S_f \cdot_Y C^-_{2,3} = -2$ $S_f \cdot_Y C^-_{1,4} = +3$ $S_f \cdot_Y C^+_{4,5} = +2$	$S_f \cdot_Y C^+_{1,3} = -1$ $S_f \cdot_Y C^-_{2,3} = +1$ $S_f \cdot_Y C^-_{1,4} = +1$ $S_f \cdot_Y C^+_{4,5} = +4$
15	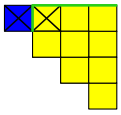	$F_2 \to C^+_{1,2} + C^-_{1,3}$ $F_0 \to \tilde{F}_0 + F_3 + C^-_{1,3}$ $F_0 = C^+_{4,5}$	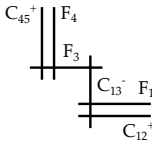	$S_f \cdot_Y C^+_{1,2} = -3$ $S_f \cdot_Y C^-_{1,3} = +3$	$S_f \cdot_Y C^+_{1,2} = -6$ $S_f \cdot_Y C^-_{1,3} = +1$
16	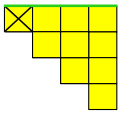	$F_0 \to C^-_{1,2} + F_2 + F_3 + \tilde{F}_0$ $F_0 = C^+_{4,5}$	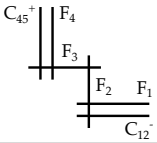	$S_f \cdot_Y C^+_{4,5} = +2$ $S_f \cdot_Y C^-_{1,2} = +3$	$S_f \cdot_Y C^+_{4,5} = +4$ $S_f \cdot_Y C^-_{1,2} = +6$

Table A.2: Splitting rules for $SU(5) \times U(1)$ with **10** and Shioda map details S_f for $I_5^{(0|1)}$ and $I_5^{(0||1)}$ for phases $9 - 16$.

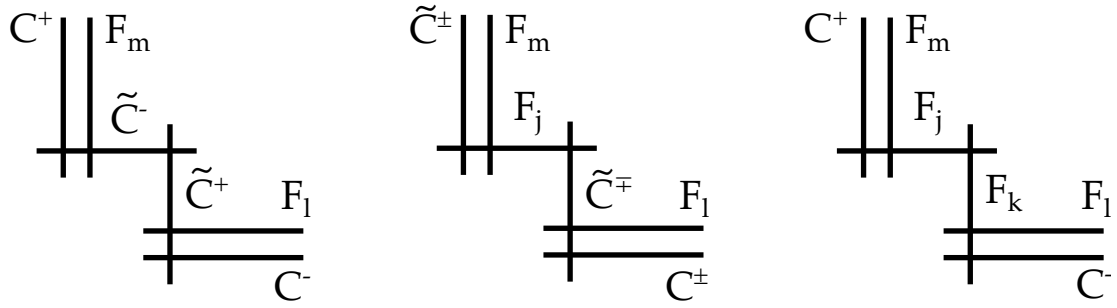

Figure A.2: The structure and ordering of the I_1^* fibers of A-type, B-type, and C-type, respectively.

section 3.5 for the A.2 splitting types, are listed in table A.3.

For each splitting type there are many more configurations than there are possible sets of intersections numbers between the split curves and the section. Multiple configurations correspond to the same intersection numbers, the same $U(1)$ charges. In table A.3 the intersection numbers are listed for each set of configurations with common intersection numbers. The intersection numbers $\sigma \cdot_Y C$ are given as a tuple of integers in the same ordering as the strings describing the configurations. The intersections of the section with curves that do not split are not included in such a listing as they are always determined by codimension one: they are either zero or one depending on whether the section intersects that component in codimension one.

Each of the concrete enhancements from the I_5 fiber into an I_1^* fiber, listed in tables A.1 and A.2, are realisations of one of the splitting types just analysed. Determining the splitting type depends on the phase (which fixes whether it is of type A, B, or C), and the codimension one configuration, which determines the subcase. The configurations of I_1^* curves in the section can then be determined for each phase and codimension one configuration of the section. All of the configurations for each of the sixteen phases are listed in tables A.4 and A.5.

A.2 Charge Comparison to Singlet-Extended E_8

In [105] $U(1)$ charges for $SU(5)$ models that come from a Higgsing of E_8, extended by non-E_8 singlets, are determined. What is considered is the decomposition of the adjoint of $E_8 \to SU(5) \times U(1)^4$, which is then augmented by additional singlets carrying different charge under the abelian $U(1)^4$ such that for every pair of $\mathbf{5}$ and $\overline{\mathbf{5}}$ representations of $SU(5)$ coming from the decomposition of E_8 there exists a singlet such that the coupling $\mathbf{15}\overline{\mathbf{5}}$ is uncharged under the $U(1)^4$. Various singlets can be Higgsed to produce models with fewer

Splitting type	Intersection numbers	Configurations
A.1	(-1,1,-1,1)	(1231– –), (1231–3), (12313–), (123133)
	(0,0,0,0)	(– – – –x–), (2222–2), (222232)
	(1,-1,1,-1)	(–213–1), (3213–1), (–21331), (321331)
A.2	(-1,1,-1,2)	(12312x), (123124)
	(0,0,0,1)	(– – – – –x), (22222–), (222223)
	(1,-1,1,0)	(–21– – –), (321– – –), (–21322), (321322)
A.3	(-1,1,0,0)	(1– – – – –), (123222)
	(0,0,1,-1)	(– – – – –1), (222321)
B.1	(-1,1,-1)	(1223–1), (122331)
	(0,0,0)	(– – – –x–), (2222–2), (222232)
	(1,-1,1)	(–221– –), (3221– –), (–2213–), (–221–3), (32213–), (3221–3), (–22133), (322133)
B.2	(-1,1,0)	(122– – –), (122322)
	(0,0,1)	(– – – – –x), (22222–), (222223)
	(1,-1,2)	(–2212x), (32212x), (–22124), (322124)
B.3	(-1,0,0)	(1– – – – –), (123222)
	(0,-1,1)	(– – –12–), (22312–), (– – –123), (223123)
B.4	(-1,1,-1)	(1–2321), (132321)
	(0,0,0)	(–x– – – –), (2–2222), (232222)
	(1,-1,1)	(– –212–), (3–212–), (–3212–), (– –2123) (33212–), (3–2123), (–32123), (332123)
B.5	(0,1,-1)	(– – – – –1), (222321)
	(1,0,0)	(x– – – – –), (–22222), (322222)
	(2,-1,1)	(x2212–), (x22123), (42212–), (422123)
C.1	(1,-1)	(–222–1), (3222–1), (–22231), (322231)
	(0,0)	(– – – –x–), (2222–2), (222232)
	(-1,1)	(1222– –), (12223–), (1222–3), (122233)
C.2	(-1,0)	(122– – –), (122322)
	(0,-1)	(– – – – –1), (222321)
C.3	(2,-1)	(x22221), (422221)
	(1,0)	(x– – – – –), (–22222), (322222)
	(0,1)	(– – – – –x), (22222–), (222223)
	(-1,2)	(12222x), (122224)

Table A.3: For each of the different splitting types, listed in section 3.5.1, for the enhancements from an I_5 fiber to an I_1^*, including the information of which fiber component the section intersects in codimension one, all the possible consistent configurations of the I_1^* fiber components with the section are listed in the third column, using the notation described in section A.1.1. There are multiple configurations of the curves inside the section where all of the fiber curves have the same intersection numbers with the section, these are collected and the intersection numbers particular to those configurations are listed in the second column. These intersection numbers are the relevant datum for the computation of the $U(1)$ charges. The tuples of intersection numbers do not include the curves which do not split as their intersection numbers are always uniquely fixed by codimension one.

Phase	Configurations		
	$\sigma \cdot_Y F_0 = 1$	$\sigma \cdot_Y F_1 = 1$	$\sigma \cdot_Y F_2 = 1$
1	(x22221), (422221)	(–222–1), (3222–1), (–22231), (322231)	(122– – –), (122322)
	(x– – – – –), (–22222), (322222)	(– – – –x–), (2222–2), (222232)	(– – – – –1), (222321)
	(– – – – –x), (22222–), (222223)	(1222– –), (12223–), (1222–3), (122233)	
	(12222x), (122224)		
2	(– – – – –1), (222321)	(1–2321), (132321)	(1– – – – –), (123222)
	(x– – – – –), (–22222), (322222)	(–x– – – –), (2–2222), (232222)	(– – –12–), (22312–), (– – –123), (223123)
	(x2212–), (x22123), (42212–), (422123)	(– –212–), (3–212–), (–3212–), (– –2123) (33212–), (3–2123), (–32123), (332123)	
3	(12312x), (123124)	(1231– –), (12313–), (1231–3), (123133)	(1– – – – –), (123222)
	(– – – – –x), (22222–), (222223)	(– – – –x–), (2222–2), (222232)	(– – – – –1), (222321)
	(–21– – –), (321– – –), (–21322), (321322)	(–213–1), (3213–1), (–21331), (321331)	
4	(122– – –), (122322)	(1223–1), (122331)	(– – – – –1), (222321)
	(– – – – –x), (22222–), (222223)	(– – – –x–), (2222–2), (222232)	(x– – – – –), (–22222), (322222)
	(–2212x), (32212x), (–22124), (322124)	(–221– –), (3221– –), (–2213–), (–221–3) (32213–), (3221–3), (–22133), (322133)	(x2212–), (x22123), (42212–), (422123)
5	(1223–1), (122331)	(122– – –), (122322)	(1– – – – –), (123222)
	(– – – –x–), (2222–2), (222232)	(– – – – –x), (22222–), (222223)	(– – –12–), (22312–), (– – –123), (223123)
	(–221– –), (3221– –), (–2213–), (–221–3) (32213–), (3221–3), (–22133), (322133)	(–2212x), (32212x), (–22124), (322124)	
6	(–222–1), (3222–1), (–22231), (322231)	(122– – –), (122322)	(– – –221), (232221)
	(– – – –x–), (2222–2), (222232)	(– – – – –1), (222321)	(1– – – – –), (123222)
	(1222– –), (12223–), (1222–3), (122233)		
7	(1231– –), (12313–), (1231–3), (123133)	(12312x), (123124)	(x21321), (421321)
	(– – – –x–), (2222–2), (222232)	(– – – – –x), (22222–), (222223)	(x– – – – –), (–22222), (322222)
	(–213–1), (3213–1), (–21331), (321331)	(–21– – –), (321– – –), (–21322), (321322)	(– – –12–), (– – –123), (22312–), (223123)
8	(1–2321), (132321)	(1– – – – –), (123222)	(122– – –), (122322)
	(–x– – – –), (2–2222), (232222)	(– – –12–), (22312–), (– – –123), (223123)	(– – – – –x), (22222–), (222223)
	(– –212–), (3–212–), (–3212–), (– –2123) (33212–), (3–2123), (–32123), (332123)		(–2212x), (32212x), (–22124), (322124)

Table A.4: For each of the three configurations of a section, σ, with the codimension one components it is listed for the phases 1 – 8, which are the distinct enhancements from I_5 to I_1^* listed in table A.1, the possible consistent configurations of the curves of the I_1^* fiber with the section, in the notation of section A.1.1. Configurations of the same phase and codimension one configuration that are not separated by a horizontal divider have the same intersection numbers between all the curves of the I_1^* fiber and the section.

Phase	Configurations		
	$\sigma \cdot_Y F_0 = 1$	$\sigma \cdot_Y F_1 = 1$	$\sigma \cdot_Y F_2 = 1$
9	(1–2321), (132321)	(– – – – –1), (222321)	(1223–1), (122331)
	(–x– – – –), (2–2222), (232222)	(x– – – – –), (–22222), (322222)	(– – – –x–), (2222–2), (222232)
	(– –212–), (3–212–), (–3212–), (– –2123) (3–2123), (33212–), (–32123), (332123)	(x2212–), (x22123), (42212–), (422123)	(–221– –), (3221– –), (–2213–), (–221–3) (32213–), (3221–3), (–22133), (322133)
10	(1231– –), (12313–), (1231–3), (123133)	(1– – – – –), (123222)	(– –1321), (3–1321), (–31231), 331321)
	(– – – –x–), (2222–2), (222232)	(– – – – –1), (222321)	(–x– – – –), (2–2222), (232222)
	(–213–1), (3213–1), (–21331), (321331)		(1–312–), (13312–), (1–3123), (133123)
11	(–222–1), (3222–1), (–22231), (322231)	(x22221), (422221)	(1–222–), (13222–), (1–2223), (132223)
	(– – – –x–), (2222–2), (222232)	(x– – – – –), (–22222), (322222)	(–x– – – –), (2–2222), (232222)
	(1222– –), (12223–), (1222–3), (122233)	(– – – – –x), (22222–), (222223)	(– –2221), (3–2221), (–32221), (332221)
		(12222x), (122224)	
12	(1223–1), (122331)	(– – – – –1), (222321)	(1–2321), (132321)
	(– – – –x–), (2222–2), (222232)	(x– – – – –), (–22222), (322222)	(–x– – – –), (2–2222), (232222)
	(–221– –), (3221– –), (–2213–), (–221–3) (32213–), (3221–3), (–22133), (322133)	(x22212–), (x22123), (42212–), (422123)	(– –212–), (3–212–), (–3212–), (– –2123) (33212–), (3–2123), (–32123), (332123)
13	(122– – –), (122322)	(1– – – – –), (123222)	(1–2321), (132321)
	(– – – – –x), (22222–), (222223)	(– – –12–), (22312–), (– – –123), (223123)	(–x– – – –), (2–2222), (232222)
	(–2212x), (32212x), (–22124), (322124)		(– –212–), (3–212–), (–3212–), (– –2123) (33212–), (3–2123), (–32123), (332123)
14	(x21321), (421321)	(12312x), (123124)	(1231– –), (12313–), (1231–3), (123133)
	(x– – – – –), (–22222), (322222)	(– – – – –x), (22222–), (222223)	(– – – –x–), (2222–2), (222232)
	(– – –12–), (22312–), (– – –123), (223123)	(–21– – –), (321– – –), (–21322), (321322)	(–213–1), (3213–1), (–21331), (321331)
15	(– – – – –1), (222321)	(1223–1), (122331)	(122– – –), (122322)
	(x– – – – –), (–22222), (322222)	(– – – –x–), (2222–2), (222232)	(– – – – –x), (22222–), (222223)
	(x2212–), (x22123), (42212–), (422123)	(–221– –), (3221– –), (–2213–), (–221–3) (32213–), (3221–3), (–22133), (322133)	(–2212x), (32212x), (–22124), (322124)
16	(x22221), (422221)	(–222–1), (3222–1), (–22231), (322231)	(122– – –), (122322)
	(x– – – – –), (–22222), (322222)	(– – – –x–), (2222–2), (222232)	(– – – – –1), (222321)
	(– – – – –x), (22222–), (222223)	(1222– –), (12223–), (1222–3), (122233)	
	(12222x), (122224)		

Table A.5: Similar to table A.4, all the configurations of the curves of the I_1^* fiber with the section σ are listed for the codimension one configurations of the section and the phases 9 – 16, which were listed previously in table A.2. The configurations are again listed with the notation of section A.1.1. There can be multiple configurations of the curves with the section which have the same intersection numbers, and thus the same $U(1)$ charges, and these are collected together inside each phase and codimension one configuration.

abelian symmetries, and determine the tree of possible theories arising from this singlet-extension of E_8. In this appendix the charges found from this analysis, listed in tables 2.1 and 2.2 of [105], are compared to the possible $U(1)$ charges determined in the main body of this thesis. In summary, it is found that the charges appearing in descendants of the singlet-extended E_8 form a strict subset of the charges found herein.

Consider first the single $U(1)$ models from the singlet-extended E_8. There are eleven such models listed in [105], which all have $U(1)$ charges[1] that are subsets of one of the following three classes of charges

$$\begin{array}{lll} & \mathbf{10} & \overline{\mathbf{5}} \\ (1): & \{-2,-1,0,1,2\} & \{-3,-2,-1,0,1,2,3\} \\ (2): & \{-8,-3,2,7\} & \{-11,-6,-1,4,9\} \\ (3): & \{-4,1,6\} & \{-8,-3,2,7\}\,. \end{array} \tag{A.1}$$

For each of the three classes there is at least one model which realises matter representations with all of the charges in that class. These three classes have charges which are subsets of the charges[2] from the three codimension one fiber types, $I_5^{(01)}$, $I_5^{(0|1)}$, and $I_5^{(0||1)}$ respectively, as determined in sections 3.4 and 3.5 for the $\overline{\mathbf{5}}$ and $\mathbf{10}$ matter. There are some $U(1)$ charges which come from the analysis of configurations of the fiber curves with the section which do not appear to arise from the singlet-extended E_8. The missing charges are

- In class (1) the charges ± 3 for the $\mathbf{10}$ representation.
- In class (2) the charges -13 and $+12$ for the $\mathbf{10}$ and 14 for the $\overline{\mathbf{5}}$.
- In class (3) the charges -9 and $+11$ for the $\mathbf{10}$ and -13 and $+12$ for the $\overline{\mathbf{5}}$.

The significance of E_8 is not entirely clear so that this mismatch in the charges of the $\mathbf{10}$ and $\overline{\mathbf{5}}$ matter is perhaps not too surprising. However all the single $U(1)$ models from the singlet-extended E_8 have charges which come from the analysis of the possible configurations of the section in the present thesis, as expected. This includes also the singlet charges which appear in [105] as, from the analysis in section 3.7, the range of singlet charges depends on an integer p, which specifies the normal bundle of one of the curves in the I_2 fiber. As we do not know of any constraint on the possible values of p it is possible to tune p such that one realises the charges in the singlet-extended E_8 analysis.

Moving on to the models with two or more remaining $U(1)$ symmetries after the further

[1] Some models have an additional discrete symmetry from the Higgsing of the $U(1)$. This is not relevant for this comparison and will be ignored at this point.

[2] There is an overall sign between the charges of class (2) and the $I_5^{(0|1)}$ codimension one configurations which were listed in figure 3.8.

Higgsing of the $U(1)^4$ it appears that there are models which have charges that are not neatly pairs of charges that would be possible for single $U(1)$s. As discussed in section 3.9, when there are multiple $U(1)$s one can consider any linear combination of the $U(1)$ generators and thus produce another $U(1)$ generator, under which the matter will have different charges. To be concrete, consider the model labelled $\{4, 6, 8\}$ from table 2.1 of [105]. This model has $\overline{\mathbf{5}}$ matter with $U(1)$ charges $(-4, -4)$ and $(-2, -1)$, among other $\overline{\mathbf{5}}$ matter. Recall that for a single $U(1)$ it was only possible to realise a $\overline{\mathbf{5}}$ matter curve with charge -4 in an $I_5^{(0|1)}$ model, and thus all the $\overline{\mathbf{5}}$ matter should have charge, under that $U(1)$, which take values in -14, -9, -4, 1, 6, and 11. The model in question also has $\overline{\mathbf{5}}$ matter with charge -2 (or -1 if one studies the second $U(1)$) which is not one of the possible charges. However, if one designates the two $U(1)$ generators as U_1 and U_2 respectively then one can define two new $U(1)$s by linear combinations of these, as

$$\begin{aligned} U_1' &= U_1 - U_2 \\ U_2' &= 2U_1 - 3U_2 \,. \end{aligned} \tag{A.2}$$

Under this new pair of $U(1)$ generators the charges of the $\mathbf{10}$ and $\overline{\mathbf{5}}$ curves in the model $\{4, 6, 8\}$ transform as

$\mathbf{10}$	$\overline{\mathbf{5}}$		$\mathbf{10}$	$\overline{\mathbf{5}}$
$(-2, -2)$	$(-4, -4)$		$(2, 0)$	$(4, 0)$
$(0, 1)$	$(-2, -1)$		$(-3, -1)$	$(-1, -1)$
$(1, 0)$	$(-1, -2)$	$\leftrightarrow$	$(2, 1)$	$(4, 1)$
$(3, 3)$	$(1, 1)$		$(-3, 0)$	$(-1, 0)$
	$(3, 4)$			$(-6, -1)$
	$(4, 3)$			$(-1, 1)$.

(A.3)

Now it can be seen that the sets of charges are consistent with the charges listed in the main text for each additional $U(1)$. Indeed with respect to the first new generator U_1' the section σ_2 to which it is associated seems to be an $I_5^{(0|2)}$ fiber in codimension one, and the section of the second generator, σ_1, seems to intersect the codimension one fiber as $I_5^{(01)}$. The $\{4, 6, 8\}$ model can be seen to come from an enhancement of an $I_5^{(01|2)}$ model.

The remaining multiple $U(1)$ models in table 2.1 of [105] which have charges that do not immediately match the charges found in the main body of this thesis can all be brought into the form listed here by taking the appropriate linear combination of the $U(1)$ generators, and thus all the $U(1)$ charges found therein can be seen to be $U(1)$ charges that also come from the analysis of how the section can contain curves in the codimension two fiber that has been the focus of this thesis.

Appendix B

Appendices for Chapter 4

B.1 Multiple 10 curves for single $U(1)$ Models

In this appendix we provide details on multiple **10** representations for single $U(1)$ models, completing the analysis in section 4.3. We find only models with $\mathcal{N}_{\mathbf{10}} = 2$ and $\mathcal{N}_{\bar{\mathbf{5}}} = 4$ solve the anomaly cancellation conditions and forbid the unwanted operators at leading order. These models regenerate dimension five proton decay operators with the remaining charged Yukawas, which if sufficiently suppressed, could still leave these models phenomenologically viable. However their flavour physics is highly constrained and does not yield phenomenologically interesting textures.

B.1.1 $\mathcal{N}_{\mathbf{10}} = 2$

For the case of multiple **10** representations with one $U(1)$ symmetries it is possible to have top Yukawa couplings of the form,

$$\mathbf{10}_{q_1}\mathbf{10}_{q_2}\mathbf{5}_{-q_1-q_2}\,, \tag{B.1}$$

where the two **10** representations do not have the same charge under the $U(1)$. This means we can make use of the full set of charges in (4.34) and, in particular, we do not require one of the **10** representations to have a U(1) charge within the set given in (4.38).

In this case the general parametrisation will be of the form,

$\mathbf{R}$	$q(\mathbf{R})$	M	N
$\bar{\mathbf{5}}_{H_u}$	$-q_{H_u}$	0	-1
$\bar{\mathbf{5}}_{H_d}$	q_{H_d}	0	1
$\bar{\mathbf{5}}_i$	$q_{\bar{5}_i}$	M_i	N_i
$\mathbf{10}_1$	q_{10_1}	M_{10}	N_{10}
$\mathbf{10}_2$	q_{10_2}	$3 - M_{10}$	$-N_{10}$

(B.2)

where $i = 1, \ldots, \mathcal{N}_{\bar{\mathbf{5}}}$, the latter being the number of $\bar{\mathbf{5}}$ representations.

$\mathcal{N}_{\bar{\mathbf{5}}} = 3$

Here the anomaly cancellation conditions can be solved for general charges. There are two possible parametrisations, which differ in the structure of the top Yukawa coupling.

$\mathbf{R}$	$q(\mathbf{R})$	M	N
$\bar{\mathbf{5}}_{H_u}$	$-q_{H_u}$	0	-1
$\bar{\mathbf{5}}_{H_d}$	$-q_{H_u} + 5w_{H_d}$	0	1
$\bar{\mathbf{5}}_1$	$-q_{H_u} + 5w_{\bar{5}_1}$	3	0
$\mathbf{10}_1$	$-\frac{1}{2}q_{H_u}$	M_{10}	N_{10}
$\mathbf{10}_2$	$-\frac{1}{2}q_{H_u} + 5w_{10}$	$3 - M_{10}$	$-N_{10}$

(a)

$\mathbf{R}$	$q(\mathbf{R})$	M	N
$\bar{\mathbf{5}}_{H_u}$	$-q_{H_u}$	0	-1
$\bar{\mathbf{5}}_{H_d}$	$-q_{H_u} + 5w_{H_d}$	0	1
$\bar{\mathbf{5}}_1$	$-q_{H_u} + 5w_{\bar{5}_1}$	3	0
$\mathbf{10}_1$	q_{10}	M_{10}	N_{10}
$\mathbf{10}_2$	$-q_{10} - q_{H_u}$	$3 - M_{10}$	$-N_{10}$

(b)

(B.3)

In the above parametrisation, $N_{10} = 0, \pm 1$, this is to ensure the absence of exotics. However setting $N_{10} = 0$ only gives solutions where the μ-term is allowed at leading order, therefore we neglect this case and focus on $N_{10} = \pm 1$. For parametrisation (a) the top Yukawa coupling is of the standard form,

$$\mathbf{10}_{q_1}\mathbf{10}_{q_1}H_u\,, \tag{B.4}$$

where the two **10**s have the same charge under the $U(1)$. In (b) the top Yukawa coupling is of the form given in (B.1). Below we outline the solution for (a) but a very similar analysis can be done for (b).

The anomaly condition (A2.) imposes $w_{H_d} = w_{10}N_{10}$, which upon imposing (A3.) yields

$$w_{10}N_{10}(q_{H_u} + 5w_{10}(N_{10} - 3)) = 0\,. \tag{B.5}$$

As we require the two **10**s to be different charged and $w_{H_d} \neq 0$ to avoid the μ-term thus $w_{10}, N_{10} \neq 0$, the only allowed solution to (B.5) is given by $q_{H_u} = -5w_{10}(N_{10} - 3)$. The charges, which satisfy the anomaly conditions are

$\mathbf{R}$	$q(\mathbf{R})$	M	N
$\bar{\mathbf{5}}_{H_u}$	$5w_{10}(N_{10} - 3)$	0	-1
$\bar{\mathbf{5}}_{H_d}$	$5w_{10}(2N_{10} - 3)$	0	1
$\bar{\mathbf{5}}_1$	$5(w_{\bar{5}_1} + w_{10}(N_{10} - 3))$	3	0
$\mathbf{10}_1$	$\frac{5}{2}w_{10}(N_{10} - 3)$	M_{10}	N_{10}
$\mathbf{10}_2$	$\frac{5}{2}w_{10}(N_{10} - 1)$	$3 - M_{10}$	$-N_{10}$

(B.6)

Imposing a bottom Yukawa coupling with $\mathbf{10}_1$ gives the additional constraint,

$$w_{\bar{5}_1} = \frac{w_{10}}{2}(15 - 7N_{10})\,. \tag{B.7}$$

	I.2.3.a	I.2.3.b
M_{10}	$1/2$	$1/2$
N_{10}	1	1
q_{10_1}	-1	0
q_{10_2}	0	-1
q_{H_u}	2	1
q_{H_d}	-1	-2
$q_{\bar{5}_1}$	$w_{\bar{5}_1} - 2$	$w_{\bar{5}_1} - 1$
Y^t_{ab}	$\{\{0,1\},\{1,2\}\}$	$\{\{1,0\},\{0,-1\}\}$
Y^b_a	$\{w_{\bar{5}_1}-4, w_{\bar{5}_1}-3\}$	$\{w_{\bar{5}_1}-3, w_{\bar{5}_1}-4\}$
μ	1	-1
C2	$\{w_{\bar{5}_1}-5, w_{\bar{5}_1}-4,$ $w_{\bar{5}_1}-3, w_{\bar{5}_1}-2\}$	$\{w_{\bar{5}_1}-1, w_{\bar{5}_1}-2$ $w_{\bar{5}_1}-3, w_{\bar{5}_1}-4\}$
C3	$w_{\bar{5}_1}$	$w_{\bar{5}_1}$
C4	$2w_{\bar{5}_1}-5$ $2w_{\bar{5}_1}-4$	$2w_{\bar{5}_1}-2$ $2w_{\bar{5}_1}-3$
C5	$\{-w_{\bar{5}_1}, 1-w_{\bar{5}_1},$ $2-w_{\bar{5}_1}\}$	$\{1-w_{\bar{5}_1}, -w_{\bar{5}_1},$ $-1-w_{\bar{5}_1}\}$
C6	$w_{\bar{5}_1}+1$	$w_{\bar{5}_1}-1$
C7	$\{-4,-3\}$	$\{-3,-4\}$

	I.2.4.a	I.2.4.b
M_1	0	$0/1$
N_1	3	2
M_{10}	$1/2$	$1/2$
N_{10}	-1	0
q_{10_1}	-3	-3
q_{10_2}	-1	-1
q_{H_u}	2	2
q_{H_d}	2	2
$q_{\bar{5}_1}$	-3	-1
$q_{\bar{5}_2}$	-1	1
$Y^t_{a,b}$	$\{\{-4,-2\},\{-2,0\}\}$	$\{\{-4,-2\},\{-2,0\}\}$
$Y^b_{a,j}$	$\{\{-4,-2\},\{-2,0\}\}$	$\{\{-2,0\},\{0,2\}\}$
μ	4	20
C2	$\{-12,-10,-8,-6,-4\}$	$\{-10,-8,-6,-4,-2\}$
C3	$\{-1,1\}$	$\{1,3\}$
C4	$\{-9,-7,-5,-3\}$	$\{-5,-3,-1,1\}$
C5	$\{-3,-5,1,-1\}$	$\{-5,-7,-1,-3\}$
C6	$\{3,5\}$	$\{5,7\}$
C7	$\{-3,-1\}$	$\{-3,-1\}$

Table B.1: Solutions for one $U(1)$, $\mathcal{N}_{\mathbf{10}} = 2$ and $\mathcal{N}_{\bar{\mathbf{5}}} = 3$ (LHS) and 4 (RHS). The charges of the Yukawa couplings are labelled by Y^t_{ab} and Y^b_{aj}, where $a = 1, 2$ ($j = 1, 2$) specifies the $\mathbf{10}$ ($\bar{\mathbf{5}}$). All models regenerate either dimension four or five proton decay operators, although in the latter case the operators are less problematic as will be discussed in the main text.

There are solutions to the above set of charges, which satisfy the F-theory charge pattern, which we summarise in table B.1. Here we have not imposed the presence of the bottom Yukawa coupling explicitly as these solutions correspond to one particular choice for $w_{\bar{5}_1}$. Restricting to the F-theory charge range, (4.38) and (4.34), we are constrained to take $w_{10} \pm 1$, and, without loss of generality, we take $w_{10} = 1$ as the two choices differ by an overall factor of -1 in normalisation of the $U(1)$ charges. Likewise we have taken $q_{H_u} = 5$ in case (b). All the possible choices for $w_{\bar{5}_1}$, which are within the F-theory charge range, are given by,

$$w_{\bar{5}_1} \text{ for } \begin{cases} \text{I.2.3.a} \in \{-1, 2, 3, 4, 5\} \\ \text{I.2.3.b} \in \{-2, 1, 2, 3, 4\} \, . \end{cases} \tag{B.8}$$

As one can see from the general solutions, all but one of these allow either the dimension five proton decay operators (C2.) or (C6.) and are therefore excluded. The case which forbids the unwanted operators at leading order is given by $w_{\bar{5}_1} = -2$ in I.2.3.b however in this model dimension four proton decay operators are regenerated with bottom Yukawa couplings and therefore is also not a viable model.

$\mathcal{N}_{\bar{\mathbf{5}}} = 4$

For $N_{\bar{\mathbf{5}}} \geq 4$, the strategy for finding solutions to the anomaly conditions is to take all possible sets of $\mathbf{10}$ and $\bar{\mathbf{5}}$ charges, selected from (4.34) and find those, which can solve (A1.)$-$(A5.) for allowed M, Ns. The two solutions shown in table B.1 solve the anomaly cancellation conditions, forbid operators (C1.)$-$(C7.) and do not regenerate dimension four proton decay operators with the charged Yukawas. They do, however, regenerate dimension five proton decay operators, which, if sufficiently suppressed, could still give viable models.

The matter in the MSSM can be allocated to the $U(1)$ charged $\mathbf{10}$ and $\bar{\mathbf{5}}$ representations in model I.2.4.a as follows:

Representation	Charge	M	N	Matter
$\mathbf{10}_1$	-3	1	-1	$Q_1, \bar{u}_1, \bar{u}_2,$
$\mathbf{10}_2$	-1	2	1	$Q_2, Q_3, \bar{u}_3, \bar{e}_A, A = 1, 2, 3$
$\bar{\mathbf{5}}_{H_u}$	-2	0	-1	H_u
$\bar{\mathbf{5}}_{H_d}$	2	0	1	H_d
$\bar{\mathbf{5}}_1$	-3	0	3	$L_I, I = 1, 2, 3$
$\bar{\mathbf{5}}_2$	-1	3	-3	$\bar{d}_I, I = 1, 2, 3$

(B.9)

In this spectrum the following couplings are allowed by the additional $U(1)$ symmetry

$$\begin{aligned} Y^t_{22}\mathbf{10}_2\mathbf{10}_2\mathbf{5}_{H_u} &\supset Q_3\bar{u}_3H_u \\ Y^b_{24}\mathbf{10}_2\bar{\mathbf{5}}_{H_d}\bar{\mathbf{5}}_2 &\supset Q_3\bar{d}_3H_d + Q_2\bar{d}_2H_d \, . \end{aligned} \tag{B.10}$$

In order to regenerate the remaining Yukawa couplings one needs the singlet of charge 2 to acquire a vev, which however, also regenerates all dimension five operator, with various suppressions. This model may still be viable from the point of view of proton decay, with sufficient suppression, however, the flavour physics based on an FN-type model is not very realistic, and we therefore discard these solutions.

For model I.2.4.b the spectrum is given by

Representation	Charge	M	N	Matter
$\mathbf{10}_1$	-3	2	0	$Q_1, Q_2, \bar{u}_1, \bar{u}_2, \bar{e}_1, \bar{e}_2$
$\mathbf{10}_2$	-1	1	0	$Q_3, \bar{u}_3, \bar{e}_3$
$\bar{\mathbf{5}}_{H_u}$	-2	0	-1	H_u
$\bar{\mathbf{5}}_{H_d}$	2	0	1	H_d
$\bar{\mathbf{5}}_1$	-1	1	2	$\bar{d}_3, L_I, I = 1, 2, 3$
$\bar{\mathbf{5}}_2$	1	2	-2	$\bar{d}_1, \bar{d}_2$

(B.11)

For this model there were two sets of M, Ns which solved the anomaly cancellation conditions, the values displayed in (B.11) are the ones compatible with having rank one top and bottom Yukawa matrices at tree level. In order to regenerate the top Yukawa coupling involving the two differently charged **10**s a singlet of charge 2 is required, and the same remarks as for I.2.4.a apply.

$\mathcal{N}_{\bar{\mathbf{5}}} \geq 5$

All but one of the models, for $N_{\bar{\mathbf{5}}} = 5$,regenerate the dimension four operator (C4.) with the missing Yukawa couplings. The remaining model however is inconsistent with the hierarchy of Yukawa couplings. For the cases of six and seven $\bar{\mathbf{5}}$ representations there are no solutions, which both solve the anomaly cancellation conditions and forbid the unwanted operators, in agreement with what was found for a single **10** representation.

B.1.2 $\mathcal{N}_{\mathbf{10}} = 3$

This case is maximal for the number of **10** representations and has the greatest potential for generating a Yukawa texture with good quark mass ratios. However, by increasing the number of **10**s one increases the chance of generating forbidden couplings, in particular the operator (C5.) becomes unavoidable in most models. There is only one solution to the anomaly cancellation conditions which forbids the unwanted couplings at leading order.

This solution, I.3.4.a

Representation	Charge	M	N
$\mathbf{10}_1$	-3	1	0
$\mathbf{10}_2$	-2	1	0
$\mathbf{10}_3$	-1	1	0
$\overline{\mathbf{5}}_{H_u}$	-2	0	-1
$\overline{\mathbf{5}}_{H_d}$	1	0	1
$\overline{\mathbf{5}}_1$	-1	0	3
$\overline{\mathbf{5}}_2$	0	3	-3

(B.12)

A full rank Yukawa matrix can be generated by giving a vev to the singlet of charge 1. This model interestingly generates the Haba textures (4.31), however one also regenerates dimension four proton decay operators with a singlet insertion of the singlet, which is phenomenologically unacceptable.

In conclusion we see that for a single $U(1)$ the solution space is very limited – even disregarding flavour problems – and for solutions to the anomalies and constraints on couplings, generically the Yukawas bring back the unwanted couplings at subleading order.

B.2 General Solution for $\mathcal{N}_{\mathbf{10}} = 1$ and $\mathcal{N}_{\overline{\mathbf{5}}} = 4$ with multiple $U(1)$s

B.2.1 Two $U(1)$s

In this appendix the general solution for the case of one **10** and four $\overline{\mathbf{5}}$s is derived for two $U(1)$s. This class of solutions, which give rise to good phenomenological models, is given in table B.2. The extension of the solutions for the case of two $U(1)$s to multiple $U(1)s$ is also discussed. Consider a model with two abelian factors, parametrised as

$\mathbf{R}$	$q(\mathbf{R})^\alpha$	M	N
$\overline{\mathbf{5}}_{H_u}$	$-q^\alpha_{H_u}$	0	-1
$\overline{\mathbf{5}}_{H_d}$	$-q^\alpha_{H_u} + 5w^\alpha_{H_d}$	0	1
$\overline{\mathbf{5}}_1$	$-q^\alpha_{H_u} + 5w^\alpha_{\overline{5}_1}$	M	N
$\overline{\mathbf{5}}_2$	$-q^\alpha_{H_u} + 5w^\alpha_{\overline{5}_2}$	$3-M$	$-N$
10	$q_{\mathbf{10}} = -\frac{1}{2}q^\alpha_{H_u}$	3	0

(B.13)

where q^α_i denotes the charges under $U(1)_\alpha$, $\alpha = 1, 2$. Without loss of generality, we take $N \geq 0$. The linear anomaly (A2.) for each abelian factor is of the form

$$w^\alpha_{H_d} + N(w^\alpha_{\overline{5}_1} - w^\alpha_{\overline{5}_2}) = 0\,, \tag{B.14}$$

which can be solved for $w^{\alpha}_{H_d}$. Inserting this equation into the quadratic set of anomalies (A3.), we have,

$$\begin{aligned} N(w^1_{\bar{5}_1} - w^1_{\bar{5}_2})(w^1_{\bar{5}_1} + w^1_{\bar{5}_2} + (w^1_{\bar{5}_1} - w^1_{\bar{5}_2})N) = 0 \\ N(w^2_{\bar{5}_1} - w^2_{\bar{5}_2})(w^2_{\bar{5}_1} + w^2_{\bar{5}_2} + (w^2_{\bar{5}_1} - w^2_{\bar{5}_2})N) = 0 \\ N(w^1_{\bar{5}_1} w^2_{\bar{5}_1} - w^1_{\bar{5}_2} w^2_{\bar{5}_2} + (w^1_{\bar{5}_1} - w^1_{\bar{5}_2})(w^2_{\bar{5}_1} - w^2_{\bar{5}_2})N) = 0\,. \end{aligned} \tag{B.15}$$

Setting $N = 0$ solves all the anomaly conditions simultaneously but from (B.14) we see that this results in the presence of the μ-term at tree-level, which is unfavourable. We therefore neglect this class of solutions. The first two quadratic anomalies can be solved in three distinct ways:

a) $w^1_{\bar{5}_1} = w^1_{\bar{5}_2}, w^2_{\bar{5}_1} = w^2_{\bar{5}_2}$

b) $w^1_{\bar{5}_1} = \frac{(N-1)}{N+1} w^1_{\bar{5}_2}, w^2_{\bar{5}_1} = \frac{(N-1)}{N+1} w^2_{\bar{5}_2}$

c) $w^1_{\bar{5}_1} = w^1_{\bar{5}_2}, w^2_{\bar{5}_1} = \frac{(N-1)}{N+1} w^2_{\bar{5}_2}$

The sets of charges from these three possibilities are given below.

a) Upon the insertion of $w^1_{\bar{5}_1} = w^1_{\bar{5}_2}, w^2_{\bar{5}_1} = w^2_{\bar{5}_2}$ into the third anomaly condition in (B.15) the mixed quadratic anomaly is automatically solved. The $U(1)$ charges in this case are

	$\mathbf{10}$	$\mathbf{5}_{H_u}$	$\overline{\mathbf{5}}_{H_d}$	$\overline{\mathbf{5}}_1$	$\overline{\mathbf{5}}_2$
$q^1(\mathbf{R})$	$-\frac{1}{2}q^1_{H_u}$	$q^1_{H_u}$	$-q^1_{H_u}$	$-q^1_{H_u} + 5w^1_{\bar{5}_2}$	$-q^1_{H_u} + 5w^1_{\bar{5}_2}$
$q^2(\mathbf{R})$	$-\frac{1}{2}q^2_{H_u}$	$q^2_{H_u}$	$-q^2_{H_u}$	$-q^2_{H_u} + 5w^2_{\bar{5}_2}$	$-q^2_{H_u} + 5w^2_{\bar{5}_2}$

(B.16)

This pair of $U(1)$s always gives rise to the μ-term at leading order and therefore does not give phenomenologically favourable models.

b) Here the solutions for $w^1_{\bar{5}_1}$ and $w^2_{\bar{5}_1}$ have the same form as in the single $U(1)$ case. The mixed anomaly in (B.15) is automatically solved and the charges for each $U(1)$ are

	$\mathbf{10}$	$\mathbf{5}_{H_u}$	$\overline{\mathbf{5}}_{H_d}$	$\overline{\mathbf{5}}_1$	$\overline{\mathbf{5}}_2$
$q^1(\mathbf{R})$	$-\frac{1}{2}q^1_{H_u}$	$q^1_{H_u}$	$-q^1_{H_u} + \frac{10N}{1+N} w^1_{\bar{5}_2}$	$-q^1_{H_u} + \frac{5(N-1)}{1+N} w^1_{\bar{5}_2}$	$-q^1_{H_u} + 5w^1_{\bar{5}_2}$
$q^2(\mathbf{R})$	$-\frac{1}{2}q^2_{H_u}$	$q^2_{H_u}$	$-q^2_{H_u} + \frac{10N}{1+N} w^2_{\bar{5}_2}$	$-q^2_{H_u} + \frac{5(N-1)}{1+N} w^2_{\bar{5}_2}$	$-q^2_{H_u} + 5w^2_{\bar{5}_2}$

(B.17)

c) The mixed anomaly in (B.15) is not automatically solved, but instead it reduces to

$$\frac{w^1_{\bar{5}_2} w^2_{\bar{5}_2} N}{1+N} = 0\,. \tag{B.18}$$

The charges for the two different solutions to (B.18) are:

	II.1.4.a	**II.1.4.b**
M	0/1	0/1
N	2	2
q_{10_1}	$(-\frac{1}{2}q^1_{H_u}, -\frac{1}{2}q^2_{H_u})$	$(-\frac{1}{2}q^1_{H_u}, -\frac{1}{2}q^2_{H_u})$
q_{H_u}	$(q^1_{H_u}, q^2_{H_u})$	$(q^1_{H_u}, q^2_{H_u})$
q_{H_d}	$(-q^1_{H_u} + \frac{20}{3}w^1_{5_2}, -q^2_{H_u} + \frac{20}{3}w^2_{5_2})$	$(-q^1_{H_u}, -q^2_{H_u} + \frac{20}{3}w^2_{5_2})$
$q_{\bar{5}_1}$	$(-q^1_{H_u} + \frac{5}{3}w^1_{5_2}, -q^2_{H_u} + \frac{5}{3}w^2_{5_2})$	$(-q^1_{H_u}, -q^2_{H_u} + \frac{5}{3}w^2_{5_2})$
$q_{\bar{5}_2}$	$(-q^1_{H_u} + 5w^1_{5_2}, -q^2_{H_u} + 5w^2_{5_2})$	$(-q^1_{H_u}, -q^2_{H_u} + 5w^2_{5_2})$
Y^b_1	$(-\frac{5}{2}q^1_{H_u} + \frac{25}{3}w^1_{5_2}, -\frac{5}{2}q^2_{H_u} + \frac{25}{3}w^2_{5_2})$	$(-\frac{5}{2}q^1_{H_u}, -\frac{5}{2}q^2_{H_u} + \frac{25}{3}w^2_{5_2})$
Y^b_2	$(-\frac{5}{2}q^1_{H_u} + \frac{35}{3}w^1_{5_2}, -\frac{5}{2}q^2_{H_u} + \frac{35}{3}w^2_{5_2})$	$(-\frac{5}{2}q^1_{H_u}, -\frac{5}{2}q^2_{H_u} + \frac{35}{3}w^2_{5_2})$

Table B.2: Solution for $\mathcal{N}_{\bar{\mathbf{5}}} = 4$, $\mathcal{N}_{\mathbf{10}} = 1$ for two $U(1)$s.

i) $w^1_{\bar{5}_2} = 0$

	$\mathbf{10}$	$\mathbf{5}_{H_u}$	$\overline{\mathbf{5}}_{H_d}$	$\overline{\mathbf{5}}_1$	$\overline{\mathbf{5}}_2$
$q^1(\mathbf{R})$	$-\frac{1}{2}q^1_{H_u}$	$q^1_{H_u}$	$-q^1_{H_u}$	$-q^1_{H_u}$	$-q^1_{H_u}$
$q^2(\mathbf{R})$	$-\frac{1}{2}q^2_{H_u}$	$q^2_{H_u}$	$-q^2_{H_u} + \frac{10N}{1+N}w^2_{5_2}$	$-q^2_{H_u} + \frac{5(N-1)}{1+N}w^2_{5_2}$	$-q^2_{H_u} + 5w^2_{5_2}$

(B.19)

ii) $w^2_{\bar{5}_2} = 0$

	$\mathbf{10}$	$\mathbf{5}_{H_u}$	$\overline{\mathbf{5}}_{H_d}$	$\overline{\mathbf{5}}_1$	$\overline{\mathbf{5}}_2$
$q^1(\mathbf{R})$	$-\frac{1}{2}q^1_{H_u}$	$q^1_{H_u}$	$-q^1_{H_u}$	$-q^1_{H_u} + 5w^1_{\bar{5}_2}$	$-q^1_{H_u} + 5w^1_{\bar{5}_2}$
$q^2(\mathbf{R})$	$-\frac{1}{2}q^2_{H_u}$	$q^2_{H_u}$	$-q^2_{H_u}$	$-q^2_{H_u}$	$-q^2_{H_u}$

(B.20)

This set of charges also does not forbid the μ-term at leading order and therefore is disfavoured.

Excluding the cases where the tree-level μ-term is not forbidden by the additional $U(1)$ symmetries we are left with only case b) and ci). In both cases setting $N = 1$ results in the separation between the charges of $\overline{\mathbf{5}}_1$ and $\overline{\mathbf{5}}_{H_u}$ becoming zero, this produces a leading order coupling of the form (C5.)

$$\mathbf{10}_1\mathbf{10}_1\mathbf{5}_1\,, \tag{B.21}$$

which is forbidden. Similarly, $N = 3$ can be excluded as these cases always regenerate dimension four proton decay operators with the remaining charged Yukawa couplings. This can be seen from the charge relation

$$q^\alpha_{H_d} + q^\alpha_{\bar{5}_1} = 2q^\alpha_{\bar{5}_2}\,, \quad \alpha = 1, 2\,, \tag{B.22}$$

which is true only when $N = 3$. This relation implies that the charge of the dimension four proton operator coupling $\mathbf{10}_1$ and $\overline{\mathbf{5}}_2$ will be the same as the bottom Yukawa couplings for $\overline{\mathbf{5}}_1$.

The charges for case (b) and (ci) for $N = 2$ are given in table B.2. If the charges are to remain within the F-theory charge set then $w^{\alpha}_{5_2} = \pm 3$, $\alpha = 1, 2$ and the charges of H_u are restricted to,

$$q^{\alpha}_{H_u} \quad \text{for} \quad \begin{cases} I_5^{(01)} \in \{-2, +2\} \\ I_5^{(0|1)} \in \{-14, +6\} \\ I_5^{(0||1)} \in \{-8, +12\} \ . \end{cases} \tag{B.23}$$

Each distinct pair of charges $(q^1_{H_u}, q^2_{H_u})$ gives a phenomenologically viable model, which forbids the unwanted operators at leading order.

Imposing the presence of a bottom Yukawa coupling further constrains the sets of possible $U(1)$ charges. For II.1.4.a the requirement of a bottom Yukawa coupling with either $\overline{\mathbf{5}}_1$ or $\overline{\mathbf{5}}_2$ gives solutions where all matter is charged the same under both $U(1)$s. In model II.1.4.b requiring a bottom Yukawa coupling forces all matter to be completely uncharged under one of the two $U(1)$s. Thus in both cases, the solutions reduce to the single $U(1)$ models I.1.4.a and I.1.4.c given in table 4.1. Extending to two additional $U(1)$ symmetries results in no new models, if one requires the presence of a bottom Yukawa coupling.

B.2.2 Extension to Multiple $U(1)$s

The pairs of matter charges for two $U(1)$s, determined above, can be combined to give models charged under multiple $U(1)$s. Every pair of $U(1)$s must solve the anomaly cancellation conditions in one of the cases a), b), ci) or cii). From examining the charges in each case one can rule out certain combinations of the four different pairs of $U(1)$ charges. One obtains four types of models with multiple $U(1)$s:

Type A: Charges from case a) and case cii) are combined in one model

Type B: Charges from case a) are combined in one model

Type C: Charges from case b) and case ci) are combined in one model

Type D: Charges from case b) are combined in one model

Models of type A and B are phenomenologically disfavoured as the μ-term is always present at leading order. This can be seen from the charges in (B.16) and (B.20). All models of type C and D can be obtained by combining the charges which arise in II1.4.a and II.1.4.b in table B.2, however none of these allow for a leading order bottom Yukawa coupling. This implies that all multiple $U(1)$ models in this case, with F-theory charges and a bottom Yukawa coupling at leading order, are trivial extensions of the single $U(1)$ solutions I.1.4.a and I.1.4.c in table 4.1.

B.3 General solutions to Anomaly Equations

Solving the anomaly constraints in generality for multiple matter curves can be quite difficult. Here we provide some systematic approach how to do so. The quadratic anomaly (A3.) is a diophantine equation in terms of the $U(1)$ charges and integer multiplicities M and N, and we will use some methods from Mordell's work in [72] to find general solutions. Note that for the case of the restricted F-theory charge range (as we can simply scan through all the possibilities), these methods are not necessary, however it provides an elegant approach to finding closed forms of the solutions.

We would like to stress that this approach can be used to classify all possible solutions allowed after imposing the constraints (A1.)-(A5.) and (C1.)-(C7.). This approach allows to classify all phenomenologically allowed solutions and can be used to survey all field-theoretically allowed FN models. It is similar to the approach taken in [74, 286] where anomaly free, flavour universal gauge symmetry extensions to the MSSM were classified.

B.3.1 Mordell's solution for Diophantine equations

Consider one $U(1)$ with $\mathcal{N}_{\mathbf{10}} = 1$ and $\mathcal{N}_{\bar{\mathbf{5}}} = n$. We will now solve the system of anomaly constraints using a method of Mordell. First let us set up the equations: the matter spectrum in this case takes the following form, where the top Yukawa coupling is already imposed

$\mathbf{R}$	$q(\mathbf{R})$	M	N
$\bar{\mathbf{5}}_{H_u}$	$-q_{H_u}$	0	-1
$\bar{\mathbf{5}}_{H_d}$	q_{H_d}	0	1
$\bar{\mathbf{5}}_{i\neq n}$	q_i	M_i	N_i
$\bar{\mathbf{5}}_n$	q_n	$3-\sum_{i=1}^{n-1} M_i$	$-\sum_{i=1}^{n-1} N_i$
$\mathbf{10}$	$q_{\mathbf{10}} = -\frac{1}{2}q_{H_u}$	3	0

(B.24)

The constraints on the integers M_i and N_i is

$$0 \leq M_i \leq 3\,, \qquad 0 \leq M_i + N_i \leq 3\,, \qquad \sum_{i=1}^{n-1} M_i \leq 3\,, \qquad (N_1,\ldots,N_n) \neq (0,\ldots,0)\,. \tag{B.25}$$

Imposing the anomaly constraint

$$\text{(A2.)} \quad \Rightarrow \quad q_{H_d} = -q_{H_u} + \sum_{i=1}^{n-1} N_i(q_n - q_i)\,. \tag{B.26}$$

This automatically implies that the charge of the μ-term is

$$q_\mu = q_{H_u} + q_{H_d} = \sum_{i=1}^{n-1} N_i(q_n - q_i)\,. \tag{B.27}$$

Next, impose the bottom Yukawa coupling, without loss of generality, for $\bar{\mathbf{5}}_1$

$$\begin{aligned}(\text{Y2.}): \quad q_1 + q_{H_d} + q_{\mathbf{10}} = 0 \quad \Rightarrow \quad q_{H_u} &= \frac{2}{3}\left(q_1 + \sum_{i=1}^{n-1} N_i(q_n - q_i)\right) \\ q_{H_d} &= \frac{1}{3}\left(-2q_1 + \sum_{i=1}^{n-1} N_i(q_n - q_i)\right) .\end{aligned} \tag{B.28}$$

Finally, we impose the anomaly (A3.), which results for a single $U(1)$ in a quadratic constraint

$$q_\mu\,(q_{H_d} - q_{H_u}) + \sum_{i=1}^{n-1} N_i(q_i^2 - q_n^2) = 0\,, \tag{B.29}$$

which after inserting the solution of the charges for the Higgs doublets takes the form of a Diophantine equation

$$\sum_{i,j=1}^{n-1} a_{ij} q_i q_j = 0\,, \tag{B.30}$$

where the integers a_{ij} depend on the multiplicities N_i. From the form (B.29) it is clear that each term in the anomaly is proportional to the difference of two charges, so that one initial seed solution is

$$q_i = q_0 \qquad i = 1, \ldots, n\,. \tag{B.31}$$

Starting from this solution, we can generate all solutions to this with the method from Mordell [72].

The theorem in Mordell [72] states, that if a non-zero integer solution to

$$aq_1^2 + bq_2^2 + cq_3^2 + 2fq_2q_3 + 2gq_1q_3 + 2hq_1q_2 = 0 \tag{B.32}$$

exists, then the general solution with all q_i coprime, i.e. $(q_1, q_2, q_3) = 1$, is given by expressions

$$q_i = a_i p^2 + b_i pq + c_i q^2\,, \qquad (p, q) = 1\,, \quad p, q \in \mathbb{Z}\,, \tag{B.33}$$

with $a_i, b_i, c_i \in \mathbb{Z}$ constants. In fact a constructive method is given: consider an initial seed solution (q_1^0, q_2^0, q_3^0). Then let

$$q_1 = rq_1^0 + p\,, \qquad q_2 = rq_2^0 + q\,, \qquad q_3 = rq_3^0\,. \tag{B.34}$$

Inserting this back into (B.32) results in a linear equation for r, which can be solved and thus one determines the expressions for q_i from (B.34).

This method can be applied more generally for $n > 2$. The ansätze are

$$\begin{aligned} q_i &= q_i^0 r + p_i\,, \text{ for } i = 1, \ldots, n-1 \\ q_n &= q_n^0 r\,. \end{aligned} \tag{B.35}$$

Again, the resulting equation (B.30) becomes lines in r, and can be solved in each case to yield the charges q_i for all i. In general this leaves $n-1$ charges unfixed by the constraints imposed thus far. For each case we will now consider in the following the charges of the unwanted couplings (C1.)−(C7.), in order to determine the phenomenological soundness of the models.

B.3.2 General Solutions for $\mathcal{N}_{\bar{\mathbf{5}}} = 5$

To exemplify the method in the last section, consider the case of three matter $\bar{\mathbf{5}}$ representations, in addition to the two Higgs ones, which will be parametrised as

$\mathbf{R}$	$q(\mathbf{R})$	M	N
$\bar{\mathbf{5}}_{H_u}$	$-q_{H_u}$	0	-1
$\bar{\mathbf{5}}_{H_d}$	q_{H_d}	0	1
$\bar{\mathbf{5}}_1$	q_1	M_1	N_1
$\bar{\mathbf{5}}_2$	q_2	M_2	N_2
$\bar{\mathbf{5}}_3$	q_3	$3-M_1-M_2$	$-N_1-N_2$
$\mathbf{10}$	$q_{\mathbf{10}} = -\frac{1}{2}q_{H_u}$	3	0

(B.36)

Note that for fewer, the equations always factor and can be solved easily. The first non-trivial case is $n = 5$. The constraints on the integers M_i and N_i is

$$0 \leq M_i \leq 3\,, \qquad 0 \leq M_i + N_i \leq 3\,, \qquad M_1 + M_2 \leq 3\,, \qquad (N_1, N_2) \neq (0,0)\,. \tag{B.37}$$

There are 90 solutions, however only 40 will be eventually of interest and distinct from earlier cases with fewer, distinctly charged matter.

Again, we first solve the anomaly constraint (A2.) which yields

$$\text{(A2.)} \quad \Rightarrow \quad q_{H_d} = q_3(N_1+N_2) - N_1 q_1 - N_2 q_2 - q_{H_u}\,. \tag{B.38}$$

Furthermore, without loss of generality, we impose the bottom Yukawa coupling for the $\bar{\mathbf{5}}_1$ matter, i.e.

$$\text{(Y2.)} \quad \Rightarrow \quad q_1 + q_{H_d} + q_{\mathbf{10}} = 0 \quad \Rightarrow \quad q_{H_u} = -\frac{2}{3}(N_1 q_1 - N_1 q_3 + N_2 q_2 - N_2 q_3 - q_1)\,, \tag{B.39}$$

where q_{H_d} from the anomaly was used. Furthermore as we impose the bottom Yukawa for $\bar{\mathbf{5}}_1$, we require $M_1 \neq 0$. Note that the μ-term has charge

$$q_\mu = q_{H_u} + q_{H_d} = (N_1+N_2)\,q_3 - N_1 q_1 - N_2 q_2 \neq 0\,. \tag{B.40}$$

This in particular implies

$$(N_1, N_2) \neq (0,0)\,. \tag{B.41}$$

The anomaly (A2.) constraint now reads

$$\begin{aligned}(A3.) \quad \Rightarrow \quad & (7-N_1)\,N_1 q_1^2 + (3-N_2)\,N_2 q_2^2 - (N_1+N_2)\,(N_1+N_2+3)\,q_3^2 \\ & + 2\,(N_1-2)\,(N_1+N_2)\,q_1 q_3 - 2\,(N_1-2)\,N_2 q_1 q_2 + 2N_2\,(N_1+N_2)\,q_2 q_3 = 0\,,\end{aligned} \tag{B.42}$$

which is a homogeneous quadratic equation in q_i with integer coefficients. We are searching for rational solutions, although by rescaling, we can consider integer solutions. Such Diophantine equations are for instance discussed in [72], which gives a systematic construction of its solution, starting with a seed solution.

Applying this to the anomaly constraint (B.42) with the seed solutions

$$q_1^0 = 4N_1N_2 - 3N_1 + 9N_2\,, \quad q_2^0 = 4N_1N_2 + 17N_1 - 11N_2\,, \quad q_3^0 = 4N_1N_2 - 3N_1 - 11N_2\,, \tag{B.43}$$

which is non-trivial as N_i cannot both vanish. We now need to choose these integers so that the seed solution satisfies $(q_1^0, q_2^0, q_3^0) = 1$. Examples of these are

$$(N_1, N_2, N_3) = (-1,-2,3),\ (1,-2,1),\ (-3,2,1),\ (-2,1,1),\ (2,-1,-1)\,. \tag{B.44}$$

The resulting charges from the Mordell argument are

$$\begin{aligned} q_1 &= p - \frac{(9N_2 + N_1\,(4N_2-3))\left((N_1-7)\,N_1 p^2 + 2\,(N_1-2)\,N_2 pq + (N_2-3)\,N_2 q^2\right)}{10\,(N_1\,(N_1\,(4N_2+3) - 25N_2)\,p + N_2\,(3N_2 + N_1\,(4N_2-9))\,q)} \\ q_2 &= q - \frac{(N_1\,(4N_2+17) - 11N_2)\left((N_1-7)\,N_1 p^2 + 2\,(N_1-2)\,N_2 pq + (N_2-3)\,N_2 q^2\right)}{10\,(N_1\,(N_1\,(4N_2+3) - 25N_2)\,p + N_2\,(3N_2 + N_1\,(4N_2-9))\,q)} \\ q_3 &= -\frac{(N_1\,(4N_2-3) - 11N_2)\left((N_1-7)\,N_1 p^2 + 2\,(N_1-2)\,N_2 pq + (N_2-3)\,N_2 q^2\right)}{10\,(N_1\,(N_1\,(4N_2+3) - 25N_2)\,p + N_2\,(3N_2 + N_1\,(4N_2-9))\,q)}\,. \end{aligned} \tag{B.45}$$

Here, $p, q \in \mathbb{Z}$ and coprime. The μ-term is

$$q_\mu = -\frac{3\,(N_1+N_2)\,(N_1 p - N_2 q)^{\,2}}{N_1\,(N_1\,(4N_2+3) - 25N_2)\,p + N_2\,(3N_2 + N_1\,(4N_2-9))\,q} \neq 0\,. \tag{B.46}$$

The remaining bottom Yukawa couplings have charge

$$\begin{aligned} q(\lambda_2^b) &= -\frac{(N_1+N_2)\,(N_1 p - N_2 q)\,((2N_1-11)\,p + (2N_2-3)\,q)}{N_1\,(N_1\,(4N_2+3) - 25N_2)\,p + N_2\,(3N_2 + N_1\,(4N_2-9))\,q} \\ q(\lambda_3^b) &= -\frac{(N_1 p - N_2 q)\,(-11N_2 p + N_1\,(2N_2+3)\,p + 2\,(N_2-3)\,N_2 q)}{N_1\,(N_1\,(4N_2+3) - 25N_2)\,p + N_2\,(3N_2 + N_1\,(4N_2-9))\,q}\,. \end{aligned} \tag{B.47}$$

Similarly one can solve for more $\bar{\mathbf{5}}$ curves using this Mordell approach. In the main text we will constrain ourselves to the F-theoretic charges, which comprise a finite set, and thus do not necessarily need to use this method.

B.4 Search for Other Known Textures

In section 4.5 we saw that the case of four $\overline{\mathbf{5}}$ representations produced Yukawa textures matching (4.31) and (4.32). Extending the analysis to five and six $\overline{\mathbf{5}}$s we find that there are no solutions to the anomaly cancellation conditions, which produce the same Yukawa hierarchies. Here we consider whether other known flavour models can be realised within our F-theory framework. We find no fits to other known flavour textures.

B.4.1 Symmetric Textures

Consider first the Yukawa hierarchies in [176] given by

$$Y^u \sim \begin{pmatrix} \epsilon^4 & \epsilon^3 & \epsilon^3 \\ \epsilon^3 & \epsilon^2 & \epsilon^2 \\ \epsilon^3 & \epsilon^2 & 1 \end{pmatrix}, \quad Y^d \sim \begin{pmatrix} \epsilon^4 & \epsilon^3 & \epsilon^3 \\ \epsilon^3 & \epsilon^2 & \epsilon^2 \\ \epsilon^3 & \epsilon^2 & 1 \end{pmatrix}. \tag{B.48}$$

In this section we will show it is not possible to match to this texture in our framework, due to the form of the down-type Yukawa matrix. To see this, note that we need at least five $\overline{\mathbf{5}}$s so that each down-type quark resides within a differently charged $\overline{\mathbf{5}}$. Consider the parametrisation

$\mathbf{R}$	$q^1(\mathbf{R})$	$q^2(\mathbf{R})$	M	N
$\overline{\mathbf{5}}_{H_u}$	$-q^1_{H_u}$	$-q^2_{H_u}$	0	-1
$\overline{\mathbf{5}}_{H_d}$	$\frac{3}{2}q^1_{H_u} - 5w^1_{5_3}$	$\frac{3}{2}q^2_{H_u} - 5w^2_{5_3}$	0	1
$\overline{\mathbf{5}}_1$	$-q^1_{H_u} + 5w^1_{5_1}$	$-q^2_{H_u} + 5w^2_{5_1}$	1	N_1
$\overline{\mathbf{5}}_2$	$-q^1_{H_u} + 5w^1_{5_2}$	$-q^2_{H_u} + 5w^2_{5_2}$	1	N_2
$\overline{\mathbf{5}}_3$	$-q^1_{H_u} + 5w^1_{5_3}$	$-q^2_{H_u} + 5w^2_{5_3}$	1	$-N_1 - N_2$
$\mathbf{10}_1$	$-\frac{1}{2}q^1_{H_u} + 5w^1_{10_1}$	$-\frac{1}{2}q^2_{H_u} + 5w^2_{10_1}$	1	0
$\mathbf{10}_2$	$-\frac{1}{2}q^1_{H_u} + 5w^1_{10_2}$	$-\frac{1}{2}q^2_{H_u} + 5w^2_{10_2}$	10	
$\mathbf{10}_3$	$-\frac{1}{2}q^1_{H_u}$	$-\frac{1}{2}q^2_{H_u}$	1	0

(B.49)

where the charge of H_d has been chosen to allow an order one bottom Yukawa coupling (which we choose to be $\overline{\mathbf{5}}_3$) at leading order. This set of charges gives rise to the following Yukawa textures written in terms of the singlet insertions required to regenerate each entry

$$Y^u \sim \begin{pmatrix} s_1^2 & s_1 s_2 & s_1 \\ s_1 s_2 & s_2^2 & s_2 \\ s_1 & s_2 & 1 \end{pmatrix}, \quad Y^d \sim \begin{pmatrix} s_4 s_1 & s_1 s_3 & s_1 \\ s_4 s_2 & s_2 s_3 & s_2 \\ s_4 & s_3 & 1 \end{pmatrix}. \tag{B.50}$$

where $s_i = \frac{\langle S_i \rangle}{M_{GUT}}$ and the charges of the singlets S_i are

$$\begin{aligned}
(q^1_{S_1}, q^2_{S_1}) &= -5(w^1_{10_1}, w^2_{10_1}) \\
(q^1_{S_2}, q^2_{S_2}) &= -5(w^1_{10_2}, w^2_{10_2}) \\
(q^1_{S_3}, q^2_{S_3}) &= -5(w^1_{\overline{5}_2} - w^1_{\overline{5}_3}, w^2_{\overline{5}_2} - w^2_{\overline{5}_3}) \\
(q^1_{S_4}, q^2_{S_4}) &= -5(w^1_{\overline{5}_1} - w^1_{\overline{5}_3}, w^2_{\overline{5}_1} - w^2_{\overline{5}_3})\,.
\end{aligned} \tag{B.51}$$

From the structure of the singlet insertions in the Yukawa matrices shown above one can see that it is not possible to match to the ϵ suppressions shown in (B.48). The problem lies in the texture of the down-type matrix in (B.50), if the singlet insertions in (2,3) and (3,2) are chosen to have ϵ^2 suppression then the (2,2) entry is automatically of order ϵ^4. This is in disagreement with (B.48) therefore it is not possible achieve the texture in [176].

B.4.2 E_8-model Textures

Consider the Yukawa hierarchies discussed in [159][1], which was discussed in the context of local models in F-theory in the context of models obtained by higgsing E_8,

$$Y^u \sim \begin{pmatrix} \epsilon^6 & \epsilon^5 & \epsilon^3 \\ \epsilon^5 & \epsilon^4 & \epsilon^2 \\ \epsilon^3 & \epsilon^2 & 1 \end{pmatrix}, \quad Y^d \sim \begin{pmatrix} \epsilon^6 & \epsilon^5 & \epsilon^3 \\ \epsilon^4 & \epsilon^3 & \epsilon \\ \epsilon^3 & \epsilon^2 & 1 \end{pmatrix}. \tag{B.52}$$

One finds that it is not possible to match to this set of textures either. It is not surprising that the local analysis in [159] is not consistent with the analysis here, as it relied on local $U(1)$ charges and does not consider the quadratic anomaly (A3.). To see that the global F-theory charges do not allow for these texture in (B.52), note that each down-type quark must originate from a differently charged $\overline{\mathbf{5}}$ representation which requires

$$\begin{aligned}
M_{5_i} &= 1, \\
N_{5_i} &= -1, 0, 1, 2, \quad i = 1, 2, 3\,,
\end{aligned} \tag{B.53}$$

where the restriction on N_{5_i} stems from imposing the absence of exotics. For general $\overline{\mathbf{5}}$ charges there are three distinct cases to consider

$$(N_{5_1}, N_{5_2}, N_{5_3}) = \{(0,0,0), (1,-1,0), (2,-1,-1)\}\,. \tag{B.54}$$

The first case is excluded as the cancellation of the linear anomaly (A2.) requires the presence of the μ-term at leading order which is unfavourable. We shall see in the following that we find no phenomenologically good models for the second and third cases either.

[1] The down-type Yukawa matrix has been transposed to match the convention defined in (4.26).

For the second case, the anomaly cancellation conditions can be solved exactly for the following parametrisation,

$\mathbf{R}$	$q^1(\mathbf{R})$	$q^2(\mathbf{R})$	M	N
$\bar{\mathbf{5}}_{H_u}$	$-q^1_{H_u}$	$-q^2_{H_u}$	0	-1
$\bar{\mathbf{5}}_{H_d}$	$-q^1_{H_u}+5w^1_{H_d}$	$-q^2_{H_u}+5w^2_{H_d}$	0	1
$\bar{\mathbf{5}}_1$	$-q^1_{H_u}+5w^1_{5_1}$	$-q^2_{H_u}+5w^2_{5_1}$	1	1
$\bar{\mathbf{5}}_2$	$-q^1_{H_u}+5w^1_{5_2}$	$-q^2_{H_u}+5w^2_{5_2}$	1	-1
$\bar{\mathbf{5}}_3$	$-q^1_{H_u}+5w^1_{5_3}$	$-q^2_{H_u}+5w^2_{5_3}$	1	0
$\mathbf{10}_1$	$-\frac{1}{2}q^1_{H_u}+5w^1_{10_1}$	$-\frac{1}{2}q^2_{H_u}+5w^2_{10_1}$	1	0
$\mathbf{10}_2$	$-\frac{1}{2}q^1_{H_u}+5w^1_{10_2}$	$-\frac{1}{2}q^2_{H_u}+5w^2_{10_2}$	1	0
$\mathbf{10}_3$	$-\frac{1}{2}q^1_{H_u}$	$-\frac{1}{2}q^2_{H_u}$	1	0

(B.55)

The third generation quarks are taken to reside within $\mathbf{10}_3$, the charge of which has been fixed to allow for a leading order top Yukawa coupling. Inserting this set of charges and M, Ns into the linear anomaly we obtain,

$$w^\alpha_{H_d}+w^\alpha_{5_1}-w^\alpha_{5_2}=0\,, \tag{B.56}$$

where $\alpha=1,2$. Solving for $w^\alpha_{H_d}$ and inserting into the quadratic anomaly (A3.) we obtain,

$$\begin{aligned} w^\alpha_{5_1}(w^\alpha_{5_1}-w^\alpha_{5_2})&=0,\\ 2w^1_{5_1}w^2_{5_1}-w^2_{5_1}w^1_{5_2}+w^1_{5_1}w^2_{5_2}&=0\,. \end{aligned} \tag{B.57}$$

This set of three equations has two distinct solutions however neither of them lead to phenomenologically good models

- $w^1_{5_1}=w^2_{5_1}=0$
  Substituting this into the charges in (B.55) we observe that,

  $$(q^1_{H_u},q^2_{H_u})=(q^1_{5_1},q^2_{5_1})\,, \tag{B.58}$$

  which means that the unwanted operator (C5.) is present at leading order through the coupling $\mathbf{10}_3\mathbf{10}_3\bar{\mathbf{5}}_1$. This set of solutions is therefore not viable.

- $w^1_{5_1}=w^1_{5_2}$ and $w^2_{5_1}=w^2_{5_2}$
  Substituting this solution into (B.56) one observes that $w^\alpha_{H_d}=0$, which results in a leading order μ-term which is unfavourable.

To find solutions for the last case, given by the choice, $N_{5_1}=2$, $N_{5_2}=N_{5_3}=-1$ we scan through the possible charges of $\mathbf{10}$ and $\bar{\mathbf{5}}$ matter under two $U(1)$s for the six codimension one fibers in (4.37). We find no sets of charges which solve the anomaly cancellation conditions for this set of N_{5_i}s. Therefore, in order to obtain a model that is consistent with the flavour texture in (B.52), anomaly cancellation and absence of dangerous operators

one must go to greater than five $\overline{\mathbf{5}}$ representations. However, on extending this analysis to six $\overline{\mathbf{5}}$ representations, there are again no solutions matching to flavour texture in (B.52). Possibly, by including more $U(1)$s these other textures become accessible in this class of models as well. We leave this for future investigations.

Appendix C

Appendices for Chapter 6

C.1 Conventions and Spinor Decompositions

C.1.1 Indices

Our index conventions, for Lorentz and R-symmetry representations, which are used throughout chapter 6 of the thesis are summarised in the following tables. Note that R-symmetry indices are always hatted. Furthermore, note that $\underline{m} = 1, \cdots, 8$, however only four components are independent for Weyl spinors in 6d.

Lorentz indices	6d	5d	4d	3d	2d
Curved vector	$\underline{\mu}, \underline{\nu}$	μ', ν'	μ, ν	.	.
Flat vector	$\underline{A}, \underline{B}$	A', B'	A, B	a, b	x, y
Spinors	$\underline{m}, \underline{n}$ ($\mathbf{4}$ of $\mathfrak{su}(4)_L$)	m', n' ($\mathbf{4}$ of $\mathfrak{sp}(4)_L$)	$p, q; \dot{p}, \dot{q}$ ($\mathbf{2}$ of $\mathfrak{su}(2)_\ell$; $\mathbf{2}$ of $\mathfrak{su}(2)_r$)	.	.

Table C.1: Spacetime indices in various dimensions.

	$\mathfrak{so}(5)_R$	$\mathfrak{sp}(4)_R$	$\mathfrak{so}(3)_R$	$\mathfrak{su}(2)_R$	$\mathfrak{so}(2)_R$
Index for the fundamental rep	$\widehat{A}, \widehat{B}$	$\widehat{m}, \widehat{n}$	$\widehat{a}, \widehat{b}$	$\widehat{p}, \widehat{q}$	$\widehat{x}, \widehat{y}$

Table C.2: R-symmetry indices.

C.1.2 Gamma-matrices and Spinors: 6d, 5d and 4d

We work with the mostly + signature $(-,+,\cdots,+)$. The gamma matrices $\Gamma^{\underline{A}}$ in 6d, $\gamma^{A'}$ in 5d and γ^{A} in 4d, respectively, are defined as follows:

$$\begin{aligned}
\Gamma_1 &= i\sigma_2\otimes\mathbf{1}_2\otimes\sigma_1 \equiv \gamma_1\otimes\sigma_1\\
\Gamma_2 &= \sigma_1\otimes\sigma_1\otimes\sigma_1 \equiv \gamma_2\otimes\sigma_1\\
\Gamma_3 &= \sigma_1\otimes\sigma_2\otimes\sigma_1 \equiv \gamma_3\otimes\sigma_1\\
\Gamma_4 &= \sigma_1\otimes\sigma_3\otimes\sigma_1 \equiv \gamma_4\otimes\sigma_1\\
\Gamma_5 &= -\sigma_3\otimes\mathbf{1}_2\otimes\sigma_1 \equiv \gamma_5\otimes\sigma_1\\
\Gamma_6 &= \mathbf{1}_2\otimes\mathbf{1}_2\otimes\sigma_2\,,
\end{aligned} \tag{C.1}$$

with the Pauli matrices

$$\sigma_1=\begin{pmatrix}0&1\\1&0\end{pmatrix},\qquad \sigma_2=\begin{pmatrix}0&-i\\i&0\end{pmatrix},\qquad \sigma_3=\begin{pmatrix}1&0\\0&-1\end{pmatrix}. \tag{C.2}$$

The 6d gamma matrices satisfy the Clifford algebra

$$\{\Gamma_{\underline{A}},\Gamma_{\underline{B}}\}=2\eta_{\underline{AB}}\,, \tag{C.3}$$

and similarly for the 5d and 4d gamma matrices.

Futhermore we define

$$\Gamma^{\underline{A}_1\underline{A}_2\cdots\underline{A}_n}\equiv\Gamma^{[\underline{A}_1\underline{A}_2\cdots\underline{A}_n]}=\frac{1}{n!}\sum_{w\in\mathcal{S}_n}(-1)^w\Gamma^{\underline{A}_{w(1)}}\,\Gamma^{\underline{A}_{w(2)}}\ldots\Gamma^{\underline{A}_{w(n)}}\,, \tag{C.4}$$

and similarly for all types of gamma matrices.

The chirality matrix in 4d is $\gamma_5=-\sigma_3\otimes\mathbf{1}_2$ and in 6d is defined by

$$\Gamma_7=\Gamma^1\Gamma^2\cdots\Gamma^6 \;=\; \mathbf{1}_2\otimes\mathbf{1}_2\otimes\sigma_3\,. \tag{C.5}$$

The charge conjugation matrices in 6d, 5d and 4d are defined by

$$\begin{aligned}
C_{(6\mathrm{d})} &= \sigma_3\otimes\sigma_2\otimes\sigma_2 \quad \equiv\underline{C}\\
C_{(5\mathrm{d})} &= C_{(4\mathrm{d})} \;=\; -i\,\sigma_3\otimes\sigma_2 \quad \equiv C\,.
\end{aligned} \tag{C.6}$$

They obey the identities

$$\begin{aligned}
\left(\Gamma^{\underline{A}}\right)^T &= -\underline{C}\Gamma^{\underline{A}}\underline{C}^{-1}\,,\quad \underline{A}=1,\cdots,6.\\
\left(\gamma^{A'}\right)^T &= C\gamma^{A'}C^{-1}\,,\quad A'=1,\cdots,5.\\
\left(\gamma^{A}\right)^T &= C\gamma^{A}C^{-1}\,,\quad A=1,\cdots,4.
\end{aligned} \tag{C.7}$$

To define irreducible spinors we also introduce the B-matrices

$$\begin{aligned} B_{(6\mathrm{d})} &= i\sigma_1 \otimes \sigma_2 \otimes \sigma_3 \\ B_{(5\mathrm{d})} &= B_{(4\mathrm{d})} = i\,\sigma_1 \otimes \sigma_2\,, \end{aligned} \tag{C.8}$$

which satisfy

$$\begin{aligned} \left(\Gamma^{\underline{A}}\right)^* &= B_{(6\mathrm{d})}\Gamma^{\underline{A}}B^{-1}_{(6\mathrm{d})}\,, \quad \underline{A} = 1, \cdots, 6. \\ \left(\gamma^{A'}\right)^* &= -B_{(5\mathrm{d})}\gamma^{A'}B^{-1}_{(5\mathrm{d})}\,, \quad A' = 1, \cdots, 5. \\ \left(\gamma^{A}\right)^* &= -B_{(4\mathrm{d})}\gamma^{A}B^{-1}_{(4\mathrm{d})}\,, \quad A = 1, \cdots, 4. \end{aligned} \tag{C.9}$$

The 6d Dirac spinors have eight complex components. Irreducible spinors have a definite chirality and have only four complex components. For instance a spinor ρ of positive chirality satisfies $\Gamma_7\rho = \rho$. Similarly Dirac spinors in 4d have four complex components and Weyl spinors obey a chirality projection, for instance $\gamma_5\psi = \psi$ for positive chirality, and have two complex components. The components of positive and negative, chirality spinors in 4d are denoted with the index $\dot{p} = 1, 2$ and $p = 1, 2$, respectively.

The indices of Weyl spinors in 6d can be raised and lowered using the SW/NE (South-West/North-East) convention:

$$\rho^{\underline{m}} = \rho_{\underline{n}}\underline{C}^{\underline{n}\underline{m}}\,, \quad \rho_{\underline{m}} = \underline{C}_{\underline{m}\underline{n}}\rho^{\underline{n}}\,, \tag{C.10}$$

with $(\underline{C}^{\underline{m}\underline{n}}) = (\underline{C}_{\underline{m}\underline{n}}) = \underline{C}$. There is a slight abuse of notation here: the indices $\underline{m}, \underline{n}$ go from 1 to 8 here (instead of 1 to 4), but half of the spinor components are zero due to the chirality condition. When indices are omitted the contraction is implicitly SW/NE. For instance

$$\rho\widetilde{\rho} = \rho_{\underline{m}}\widetilde{\rho}^{\underline{m}}\,, \quad \rho\Gamma^{\underline{A}}\widetilde{\rho} = \rho_{\underline{n}}(\Gamma^{\underline{A}})^{\underline{n}}{}_{\underline{m}}\widetilde{\rho}^{\underline{m}}\,, \tag{C.11}$$

with $(\Gamma^{\underline{A}})^{\underline{n}}{}_{\underline{m}}$ the components of $\Gamma^{\underline{A}}$ as given above.

The conventions on 5d and 4d spinors are analogous: indices are raised and lowered using the SW/NE convention with $(C^{m'n'}) = (C_{m'n'}) = C$ in 5d and with the epsilon matrices $\epsilon^{pq} = \epsilon_{pq} = \epsilon^{\dot{p}\dot{q}} = \epsilon_{\dot{p}\dot{q}}$, with $\epsilon^{12} = 1$. They are contracted using the SW/NE convention.

We also introduce gamma matrices $\Gamma^{\widehat{A}}$ for the $\mathfrak{sp}(4)_R = \mathfrak{so}(5)_R$ R-symmetry

$$\Gamma^{\hat{1}} = \sigma_1 \otimes \sigma_3 \quad , \; \Gamma^{\hat{2}} = \sigma_2 \otimes \sigma_3 \quad , \; \Gamma^{\hat{3}} = \sigma_3 \otimes \sigma_3 \quad , \; \Gamma^{\hat{4}} = \mathbf{1}_2 \otimes \sigma_2 \quad , \; \Gamma^{\hat{5}} = \mathbf{1}_2 \otimes \sigma_1 \quad . \tag{C.12}$$

For the R-symmetry indices we use the opposite convention compared to the Lorentz indices, namely indices are raised and lowered with the NW/SE convention:

$$\rho_{\widehat{m}} = \rho^{\widehat{n}}\Omega_{\widehat{n}\widehat{m}}\,, \quad \rho^{\widehat{m}} = \Omega^{\widehat{m}\widehat{n}}\rho_{\widehat{n}}\,, \tag{C.13}$$

with $(\Omega_{\widehat{m}\widehat{n}}) = (\Omega^{\widehat{m}\widehat{n}}) = i\sigma_2 \otimes \sigma_1$. When unspecified, R-symmetry indices are contracted with the NW/SE convention, so that we have for instance $\rho\widetilde{\rho} = \rho^{\widehat{m}}_{m}\widetilde{\rho}^{m}_{\widehat{m}}$.

A collection of Weyl spinors $\rho_{\widehat{m}}$ in 6d transforming in the **4** of $\mathfrak{sp}(4)_R$ can further satisfy a Symplectic-Majorana condition (which exists in Lorentzian signature, but not in Euclidean signature)

$$(\rho_{\widehat{m}})^* = B_{(6\mathrm{d})}\rho^{\widehat{m}}\,. \tag{C.14}$$

In 5d the Symplectic-Majorana condition on spinors is similarly

$$(\rho_{\widehat{m}})^* = B_{(5\mathrm{d})}\rho^{\widehat{m}}\,. \tag{C.15}$$

In 4d the Weyl spinors are irreducible, however 4d Dirac spinor can obey a Symplectic-Majorana condition identical to (C.15).

Let us finally comment on the conventions for the supersymmetries and their chiralities in 6d. The fermions and supercharges have the same chirality, which we will chose to be $\overline{\mathbf{4}}$ of $\mathfrak{so}(6)_L$, and we consider an $\mathcal{N} = (2,0)$ theory in 6d. Subsequently, from the invariant contraction of spinors (C.11) and (C.10), it follows since $\{\Gamma_7, \underline{C}\} = 0$ and $\underline{C}^T = \underline{C}$, that the supersymmetry transformation parameters are of opposite chirality, i.e. left chiral spinors transforming in **4**.

C.1.3 Spinor Decompositions

6d to 5d :

A Dirac spinor in 6d decomposes into two 5d spinors. A 6d spinor $\underline{\rho} = (\underline{\rho^m})$ (eight components) of positive chirality reduces to a single 5d spinor $\rho = (\rho^{m'})$, with the embedding

$$\underline{\rho} = \rho \otimes \begin{pmatrix} 1 \\ 0 \end{pmatrix}. \tag{C.16}$$

For a 6d spinor of negative chirality, the 5d spinor is embedded in the complementary four spinor components. The 6d Symplectic-Majorana condition (C.14) on $\underline{\rho}_{\widehat{m}}$ reduces to the 5d Symplectic-Majorana condition (C.15) on $\rho_{\widehat{m}}$ if $\underline{\rho}_{\widehat{m}}$ has positive chirality, or reduces to the opposite reality condition (extra minus sign on the right hand side of (C.15)), if $\underline{\rho}_{\widehat{m}}$ has negative chirality.

5d to 4d :

A 5d spinor $\rho = (\rho^{m'})$ decomposes into two 4d Weyl spinors ψ_+, ψ_- of opposite chiralities, with the embedding

$$\rho = \begin{pmatrix}0\\1\end{pmatrix} \otimes \psi_+ + \begin{pmatrix}1\\0\end{pmatrix} \otimes \psi_- \;=\; \begin{pmatrix}\psi_-\\ \psi_+\end{pmatrix}. \tag{C.17}$$

If $\rho^{\widehat{m}}$ obeys the 5d Symplectic-Majorana condition (C.15), the spinors $\psi_+^{\widehat{m}}, \psi_-^{\widehat{m}}$ are not independent. They form four-component spinors which obey a 4d Symplectic-Majorana condition:

$$\begin{pmatrix}\psi_{-\widehat{m}}\\ \psi_{+\widehat{m}}\end{pmatrix}^* = B_{(4\mathrm{d})} \begin{pmatrix}\psi_-{}^{\widehat{m}}\\ \psi_+{}^{\widehat{m}}\end{pmatrix}. \tag{C.18}$$

With these conventions, we obtain for two 5d spinors $\rho, \widetilde{\rho}$ the decomposition of bilinears

$$\begin{aligned}
&\rho\widetilde{\rho} = \rho_{m'}\widetilde{\rho}^{m'} = \psi_{+p}\widetilde{\psi}_+^p - \psi_{-\dot{p}}\widetilde{\psi}_-^{\dot{p}} = \psi_+\widetilde{\psi}_+ - \psi_-\widetilde{\psi}_-\,,\\
&\rho\gamma^5\widetilde{\rho} = \rho_{m'}(\gamma^5)^{m'}{}_{n'}\widetilde{\rho}^{n'} = \psi_{+p}\widetilde{\psi}_+^p + \psi_{-\dot{p}}\widetilde{\psi}_-^{\dot{p}} = \psi_+\widetilde{\psi}_+ + \psi_-\widetilde{\psi}_-\\
&\rho\gamma^\mu\widetilde{\rho} = \psi_{+p}(\tau^\mu)^p{}_{\dot{p}}\widetilde{\psi}_-^{\dot{p}} + \psi_{-\dot{p}}(\bar{\tau}^\mu)^{\dot{p}}{}_p\widetilde{\psi}_+^p = \psi_+\tau^\mu\widetilde{\psi}_- + \psi_-\bar{\tau}^\mu\widetilde{\psi}_+\,,
\end{aligned} \tag{C.19}$$

with $(\tau_1,\tau_2,\tau_3,\tau_4) = (-\mathbf{1}_2,\sigma_1,\sigma_2,\sigma_3)$ and $(\bar{\tau}_1,\bar{\tau}_2,\bar{\tau}_3,\bar{\tau}_4) = (-\mathbf{1}_2,-\sigma_1,-\sigma_2,-\sigma_3)$.

R-symmetry reduction :

In this thesis we consider the reduction of the R-symmetry group

$$\mathfrak{sp}(4)_R \;\to\; \mathfrak{su}(2)_R \oplus \mathfrak{so}(2)_R\,. \tag{C.20}$$

The fundamental index $\widehat{m}$ of $\mathfrak{sp}(4)_R$ decomposes into the index $(\widehat{p},\widehat{x})$ of $\mathfrak{su}(2)_R \oplus \mathfrak{so}(2)_R$. A (collection of) spinors $\rho_{\widehat{m}}$ in any spacetime dimension can be gathered in a column four-vector ρ with each component being a full spinor. The decomposition is then

$$\rho = \;\rho^{(1)} \otimes \begin{pmatrix}1\\0\end{pmatrix} + \rho^{(2)} \otimes \begin{pmatrix}0\\1\end{pmatrix}, \tag{C.21}$$

with $\rho^{(1)} = (\rho^{(1)}{}_{\widehat{p}})$ transforming in the $(\mathbf{2})_{+1}$ of $\mathfrak{su}(2)_R \oplus \mathfrak{so}(2)_R$ and $\rho^{(2)} = (\rho^{(2)}{}_{\widehat{p}})$ transforming in the $(\mathbf{2})_{-1}$. So the four spinors $\rho_{\widehat{m}}$ get replaced by the four spinors $\rho^{(1)}{}_{\widehat{p}}, \rho^{(2)}{}_{\widehat{p}}$. From the $\mathfrak{sp}(4)_R$ invariant tensor $\Omega_{\widehat{m}\widehat{n}}$, with $\Omega = \epsilon \otimes \sigma_1$, and the explicit gamma matrices (C.12) we find the bilinear decompositions. For instance

$$\begin{aligned}
\rho^{\widehat{m}}\widetilde{\rho}_{\widehat{m}} &= \rho^{(1)\widehat{p}}\widetilde{\rho}^{(2)}_{\widehat{p}} + \rho^{(2)\widehat{p}}\widetilde{\rho}^{(1)}_{\widehat{p}}\\
\rho\Gamma^{\widehat{a}}\widetilde{\rho} \equiv \rho^{\widehat{m}}(\Gamma^{\widehat{a}})_{\widehat{m}}{}^{\widehat{n}}\widetilde{\rho}_{\widehat{n}} \;&=\; \rho^{(2)\widehat{p}}(\sigma^{\widehat{a}})_{\widehat{p}}{}^{\widehat{q}}\widetilde{\rho}^{(1)}_{\widehat{q}} - \rho^{(1)\widehat{p}}(\sigma^{\widehat{a}})_{\widehat{p}}{}^{\widehat{q}}\widetilde{\rho}^{(2)}_{\widehat{q}}\\
&\equiv\; \rho^{(2)}\sigma^{\widehat{a}}\widetilde{\rho}^{(1)} - \rho^{(1)}\sigma^{\widehat{a}}\widetilde{\rho}^{(2)}\,, \quad \widehat{a} = 1,2,3\,.
\end{aligned}$$

Another useful identity is

$$(\Gamma^{\widehat{A}})^{\widehat{m}\widehat{n}}(\Gamma_{\widehat{A}})_{\widehat{r}\widehat{s}} = 4\delta^{[\widehat{m}}{}_{\widehat{r}}\delta^{\widehat{n}]}{}_{\widehat{s}} - \Omega^{\widehat{m}\widehat{n}}\Omega_{\widehat{r}\widehat{s}}\,. \tag{C.22}$$

C.2 Killing Spinors for the S^2 Background

In this appendix we determine the solutions to the Killing spinor equations for the S^2 background of section 6.2.3.

C.2.1 $\delta\psi_A^{\widehat{m}} = 0$

The supersymmetry transformations of conformal supergravity are parametrised by two complex eight-component spinors $\epsilon^{\widehat{m}}, \eta^{\widehat{m}}$, of positive chirality and negative chirality, respectively,[1] with an index $\widehat{m}$ transforming in the **4** of $\mathfrak{sp}(4)_R$. The first Killing spinor equation is

$$0 = \delta\psi_{\underline{A}}^{\widehat{m}} = \mathcal{D}_{\underline{A}}\epsilon^{\widehat{m}} + \frac{1}{24}(T^{\widehat{m}\widehat{n}})^{\underline{BCD}}\Gamma_{\underline{BCD}}\Gamma_{\underline{A}}\epsilon_{\widehat{n}} + \Gamma_{\underline{A}}\eta^{\widehat{m}} \tag{C.23}$$

with

$$\begin{aligned} \mathcal{D}_{\underline{\mu}}\epsilon^{\widehat{m}} &= \partial_{\underline{\mu}}\epsilon^{\widehat{m}} + \frac{1}{2}b_{\underline{\mu}}\epsilon^{\widehat{m}} + \frac{1}{4}\widetilde{\omega}_{\underline{\mu}}^{\underline{BC}}\Gamma_{\underline{BC}}\epsilon^{\widehat{m}} - \frac{1}{2}V_{\underline{\mu}}^{\widehat{m}}{}_{\widehat{n}}\epsilon^{\widehat{n}} \\ \widetilde{\omega}_{\underline{\mu}}^{\underline{AB}} &= 2e^{\underline{\nu}[\underline{A}}\partial_{[\underline{\mu}}e_{\underline{\nu}]}^{\underline{B}]} - e^{\underline{\rho}[\underline{A}}e^{\underline{B}]\underline{\sigma}}e_{\underline{\mu}}^{\underline{C}}\partial_{\underline{\rho}}e_{\underline{\sigma C}} + 2e_{\underline{\mu}}^{[\underline{A}}b^{\underline{B}]} \;=\; \omega_{\underline{\mu}}^{\underline{AB}} + 2e_{\underline{\mu}}^{[\underline{A}}b^{\underline{B}]}\;, \end{aligned} \tag{C.24}$$

where the background fields have been converted to $\mathfrak{sp}(4)_R$ representations with

$$V_{\underline{A}}^{\widehat{m}}{}_{\widehat{n}} = V_{\underline{A}\widehat{B}\widehat{C}}(\Gamma^{\widehat{B}\widehat{C}})^{\widehat{m}}{}_{\widehat{n}} \quad , \quad T_{\underline{BCD}}^{\widehat{m}\widehat{n}} = T_{\widehat{A}\underline{BCD}}(\Gamma^{\widehat{A}})^{\widehat{m}\widehat{n}} \quad , \quad D^{\widehat{m}\widehat{n}}{}_{\widehat{r}\widehat{s}} = D_{\widehat{A}\widehat{B}}(\Gamma^{\widehat{A}})^{\widehat{m}\widehat{n}}(\Gamma^{\widehat{B}})_{\widehat{r}\widehat{s}}\,. \tag{C.25}$$

We choose to set $\eta = 0$. After inserting our ansatz, in particular $T_{\underline{BCD}}^{\widehat{m}\widehat{n}} = b_{\underline{A}} = 0$, we obtain

$$\begin{aligned} 0 &= \partial_\phi\epsilon^{\widehat{m}} - \frac{1}{2r}\ell'(\theta)\,\Gamma^{56}\epsilon^{\widehat{m}} - \frac{1}{2}\,v(\theta)\,(\Gamma^{\widehat{45}})^{\widehat{m}}{}_{\widehat{n}}\epsilon^{\widehat{n}} \\ 0 &= \partial_{\mu'}\epsilon^{\widehat{m}} \quad , \quad \mu' = x^1, x^2, x^3, x^4, \theta\;, \end{aligned} \tag{C.26}$$

We find solutions for constant spinors $\epsilon^{\widehat{m}}$ subject to the constraint

$$0 \;=\; -\Gamma^{56}\epsilon^{\widehat{m}} + (\Gamma^{\widehat{45}})^{\widehat{m}}{}_{\widehat{n}}\epsilon^{\widehat{n}}\,, \tag{C.27}$$

with

$$v(\theta) = -\frac{\ell'(\theta)}{r}\,. \tag{C.28}$$

The condition (C.27) projects out half of the components of a constant spinor, leaving eight real supercharges in Lorentzian signature, or eight complex supercharges in Euclidean signature.

[1] In Lorentzian signature these spinors obey a Symplectic-Majorana condition, leaving 16+16 real supercharges.

C.2.2 $\delta\chi^{\widehat{m}\widehat{n}}_{\widehat{r}} = 0$

The second Killing spinor equation is given by

$$\begin{aligned} 0 &= \delta\chi^{\widehat{m}\widehat{n}}_{\widehat{r}} \\ &= \frac{5}{32}\left(\mathcal{D}_{\underline{A}} T^{\widehat{m}\widehat{n}}_{\underline{BCD}}\right)\Gamma^{\underline{BCD}}\Gamma^{\underline{A}}\epsilon_{\widehat{r}} - \frac{15}{16}\Gamma^{\underline{BC}} R^{[\widehat{m}}_{\underline{BC}\,\widehat{r}}\epsilon^{\widehat{n}]} - \frac{1}{4} D^{\widehat{m}\widehat{n}}{}_{\widehat{r}\widehat{s}}\epsilon^{\widehat{s}} + \frac{5}{8} T^{\widehat{m}\widehat{n}}_{\underline{BCD}}\Gamma^{\underline{BCD}}\eta_{\widehat{r}} - \text{traces}\,, \end{aligned} \tag{C.29}$$

with

$$\begin{aligned} \mathcal{D}_{\underline{\mu}} T^{\widehat{m}\widehat{n}}_{\underline{BCD}} &= \partial_{\underline{\mu}} T^{\widehat{m}\widehat{n}}_{\underline{BCD}} + 3\widetilde{\omega}^{\underline{E}}_{\underline{\mu}[\underline{B}} T^{\widehat{m}\widehat{n}}_{\underline{CD}]\underline{E}} - b_{\underline{\mu}}\, T^{\widehat{m}\widehat{n}}_{\underline{BCD}} + V^{[\widehat{m}}_{\underline{\mu}\widehat{r}} T^{\widehat{n}]\widehat{r}}_{\underline{BCD}} \\ R^{\widehat{m}\widehat{n}}_{\underline{\mu}\underline{\nu}} &= 2\partial_{[\underline{\mu}} V^{\widehat{m}\widehat{n}}_{\underline{\nu}]} + V^{\widehat{r}(\widehat{m}}_{[\underline{\mu}} V^{\widehat{n})}_{\underline{\nu}]\widehat{r}}\,. \end{aligned} \tag{C.30}$$

Here, 'traces' indicates terms proportional to invariant tensors $\Omega^{\widehat{m}\widehat{n}}, \delta^{\widehat{m}}_{\widehat{r}}, \delta^{\widehat{n}}_{\widehat{r}}$. Again the background fields are converted to $\mathfrak{sp}(4)_R$ representations using (C.25).

With $T^{\widehat{m}\widehat{n}}_{\underline{BCD}} = 0$, we obtain the simpler conditions

$$0 = -\frac{15}{4}\Gamma^{\underline{BC}} R^{[\widehat{m}}_{\underline{BC}\,\widehat{r}}\epsilon^{\widehat{n}]} - D^{\widehat{m}\widehat{n}}{}_{\widehat{r}\widehat{s}}\epsilon^{\widehat{s}} - \text{traces}\,. \tag{C.31}$$

The R-symmetry field strength has a single non-vanishing component, corresponding to a flux on S^2

$$R^{\widehat{m}\widehat{n}}_{\theta\phi} = -R^{\widehat{m}\widehat{n}}_{\phi\theta} = -\frac{\ell''(\theta)}{r}\,(\Gamma^{\widehat{45}})^{\widehat{m}\widehat{n}}\,. \tag{C.32}$$

In flat space indices this becomes

$$R^{\widehat{m}\widehat{n}}_{56} = -R^{\widehat{m}\widehat{n}}_{65} = -\frac{\ell''(\theta)}{r^2\ell(\theta)}\,(\Gamma^{\widehat{45}})^{\widehat{m}\widehat{n}}\,. \tag{C.33}$$

Moreover our ansätze for $D_{\widehat{A}\widehat{B}}$ (6.33) can be re-expressed in $\mathfrak{sp}(4)_R$ indices as:

$$D^{\widehat{m}\widehat{n}}{}_{\widehat{r}\widehat{s}} = d\Big[5(\Gamma^{\widehat{45}})^{[\widehat{m}}{}_{\widehat{r}}(\Gamma^{\widehat{45}})^{\widehat{n}]}{}_{\widehat{s}} - \delta^{[\widehat{m}}{}_{\widehat{r}}\delta^{\widehat{n}]}{}_{\widehat{s}} - \Omega^{\widehat{m}\widehat{n}}\Omega_{\widehat{r}\widehat{s}}\Big]\,, \tag{C.34}$$

where the two last terms lead only to "trace" contributions in (C.31) and hence drop from the equations. We obtain

$$0 = \frac{15}{2}\frac{\ell''(\theta)}{r^2\ell(\theta)}\,\Gamma^{56}(\Gamma^{\widehat{45}})^{[\widehat{m}}{}_{\widehat{r}}\epsilon^{\widehat{n}]} - 5d(\Gamma^{\widehat{45}})^{[\widehat{m}}{}_{\widehat{r}}(\Gamma^{\widehat{45}})^{\widehat{n}]}{}_{\widehat{s}}\epsilon^{\widehat{s}}\,. \tag{C.35}$$

Using (C.27), we solve the equations without further constraints on $\epsilon^{\widehat{m}}$ if

$$d = \frac{3}{2}\frac{\ell''(\theta)}{r^2\ell(\theta)}\,. \tag{C.36}$$

The background we found corresponds to the twisting $\mathfrak{u}(1)_L \oplus \mathfrak{u}(1)_R \to \mathfrak{u}(1)$ on S^2. It preserves half of the supersymmetries (and no conformal supersymmetries) of the flat space theory, and corresponds to the topological half-twist of the 2d theory.

C.3 6d to 5d Reduction for $b_\mu = 0$

In this appendix we detail the reduction of the six-dimensional equations of motion on an S^1. This is done following [260, 235] however we choose to gauge fix $b_{\underline{\mu}} = 0$, which is possible without loss of generality.

We start by decomposing the six-dimensional frame as

$$e_{\underline{A}}^{\underline{\mu}} = \begin{pmatrix} e_{A'}^{\mu'} & e_{A'}^{\phi} = -C_{A'} \\ e_6^{\mu'} = 0 & e_6^{\phi} = \alpha \end{pmatrix} \qquad e_{\underline{\mu}}^{\underline{A}} = \begin{pmatrix} e_{\mu'}^{A'} & e_{\mu'}^{6} = \alpha^{-1} C_{\mu'} \\ e_{\phi}^{A'} = 0 & e_{\phi}^{6} = \alpha^{-1} \end{pmatrix}, \tag{C.37}$$

where the 5d indices are primed. We work in the gauge $b_{\underline{\mu}} = 0$, which is achieved by fixing the special conformal generators, $K_{\underline{A}}$. Note that this choice is different from the gauge fixing of $b_{\underline{\mu}}$ in [260, 235], in particular α is not covariantly constant in our case. Furthermore, we fix the conformal supersymmetry generators to ensure $\psi_5 = 0$, which means that $e_6^{\underline{\mu}} = 0$ is invariant under supersymmetry transformations. For a general background the bosonic supergravity fields descend to 5d fields as

$$\begin{aligned} D_{\widehat{rs}}^{\widehat{mn}} &\to D_{\widehat{rs}}^{\widehat{mn}} \\ V_{\underline{A}}^{\widehat{mn}} &\to \begin{cases} V_{A'}^{\widehat{mn}} & \underline{A} \neq 6 \\ S^{\widehat{mn}} & \underline{A} = 6 \end{cases} \\ T_{\underline{ABC}}^{\widehat{mn}} &\to T_{A'B'6}^{\widehat{mn}} \equiv T_{A'B'}^{\widehat{mn}} \,. \end{aligned} \tag{C.38}$$

The components of the spin connection along the ϕ direction are given by

$$\omega_\phi^{A'6} = \frac{1}{\alpha^2} e^{\mu' A'} \partial_{\mu'} \alpha \,, \qquad \omega_\phi^{A'B'} = -\frac{1}{2\alpha^2} G^{A'B'} \,, \qquad \omega_{\mu'}^{A'6} = \frac{1}{2\alpha} e^{\nu' A'} G_{\mu'\nu'} + \frac{1}{\alpha^2} C_{\mu'} e_{\nu'}^{A'} \partial^{\nu'} \alpha \,, \tag{C.39}$$

where $G = dC$, and can be derived from the six-dimensional vielbein using

$$\omega_{\underline{\mu}}^{\underline{AB}} = 2 e^{\underline{\nu}[\underline{A}} \partial_{[\underline{\mu}} e_{\underline{\nu}]}^{\underline{B}]} - e^{\underline{\rho}[\underline{A}} e^{\underline{B}]\underline{\sigma}} e_{\underline{\mu}}^{\underline{C}} \partial_{\underline{\rho}} e_{\underline{\sigma C}} \,. \tag{C.40}$$

C.3.1 Equations of Motion for $\mathcal{B}$

The 6d equations of motion for the three-form H are given by

$$\begin{aligned} dH &= 0 \\ H_{\underline{ABC}}^{-} - \frac{1}{2} \Phi_{\widehat{mn}} T_{\underline{ABC}}^{\widehat{mn}} &= 0 \,. \end{aligned} \tag{C.41}$$

We decompose H into 5d components

$$H = \frac{1}{3!} H_{A'B'C'} e^{A'} \wedge e^{B'} \wedge^{C'} + \frac{1}{2} H_{D'E'6} e^{D'} \wedge e^{E'} \wedge e^6 \,. \tag{C.42}$$

We can solve the second equation of motion by setting

$$\begin{aligned} H_{A'B'6} &= \alpha F_{A'B'} \\ H_{A'B'C'} &= \frac{1}{2}\epsilon_{A'B'C'}{}^{D'E'}\left(\alpha F_{D'E'} - \Phi_{\widehat{m}\widehat{n}} T^{\widehat{m}\widehat{n}}_{D'E'}\right), \end{aligned} \tag{C.43}$$

where $F_{\mu'\nu'}$ is a two-form in five dimensions. Substituting this into the expansion of H and reducing to 5d we obtain

$$H = \alpha \star_{5d}\left(F - \frac{1}{\alpha}\Phi_{\widehat{m}\widehat{n}} T^{\widehat{m}\widehat{n}}\right) + F\wedge C + F\wedge d\varphi\,. \tag{C.44}$$

The equations of motion $dH = 0$ imply

$$dF = 0\,, \qquad F\wedge dC + d\left(\alpha\star_5 F - \Phi_{\widehat{m}\widehat{n}}\star_5 T^{\widehat{m}\widehat{n}}\right), \tag{C.45}$$

which can be integrated to the 5d action

$$S_F = -\int\left(\alpha\tilde{F}\wedge\star_{5d}\tilde{F} + C\wedge F\wedge F\right), \tag{C.46}$$

where

$$\tilde{F} = F - \frac{1}{\alpha}\Phi_{\widehat{m}\widehat{n}} T^{\widehat{m}\widehat{n}}\,. \tag{C.47}$$

Together with the constraint $dF = 0$, which identifies F with the field strength of a five-dimensional connection A, given by $F_{\mu'\nu'} = \partial_{\mu'}A_{\nu'} - \partial_{\nu'}A_{\mu'}$.

C.3.2 Equations of Motion for the Scalars

The dimensionally reduced 6d scalar equations of motion are

$$D^2\Phi^{\widehat{m}\widehat{n}} + 2F_{A'B'}T^{A'B'}_{\widehat{m}\widehat{n}} + (M_\Phi)^{\widehat{m}\widehat{n}}_{\widehat{r}\widehat{s}}\Phi^{\widehat{r}\widehat{s}} = 0\,, \tag{C.48}$$

where

$$\begin{aligned} D_{\mu'}\Phi^{\widehat{m}\widehat{n}} &= \partial_{\mu'} + V^{[\widehat{m}}_{\mu'\widehat{r}}\Phi^{\widehat{n}]\widehat{r}} \\ D^2\Phi^{\widehat{m}\widehat{n}} &= (\partial^{A'} + \omega_{B'}^{B'A'})D_{A'}\Phi^{\widehat{m}\widehat{n}} + V^{\widehat{[m}}_{\mu'\widehat{r}}D^{\mu'}\Phi^{\widehat{n}]\widehat{r}} \\ (M_\Phi)^{\widehat{m}\widehat{n}}_{\widehat{r}\widehat{s}} &= -\frac{R_{6d}}{5}\delta^{[\widehat{m}}_{\widehat{r}}\delta^{\widehat{n}]}_{\widehat{s}} + \frac{1}{\alpha}C^{\mu'}\partial_{\mu'}\alpha S^{[\widehat{m}}_{\widehat{r}}\Phi^{\widehat{n}]\widehat{r}} + \frac{1}{2}\alpha^2(S^{[\widehat{m}}_{\widehat{r}}S^{\widehat{n}]}_{\widehat{s}} - S^{\widehat{t}}_{\widehat{s}}S^{[\widehat{m}}_{\widehat{t}}\delta^{\widehat{n}]}_{\widehat{r}}) - \frac{1}{15}D^{\widehat{m}\widehat{n}}_{\widehat{r}\widehat{s}} - T^{A'B'}_{\widehat{r}\widehat{s}}T^{\widehat{m}\widehat{n}}_{A'B'}\,. \end{aligned} \tag{C.49}$$

The 6d Ricci scalar R_{6d} can be rewritten of course in terms of the 5d fields. This equation of motion can be integrated to the following action

$$\S_\Phi = -\int d^5x\,\sqrt{|g|}\,\alpha^{-1}\left(D_{A'}\Phi^{\widehat{m}\widehat{n}}D^{A'}\Phi_{\widehat{m}\widehat{n}} + 4\Phi^{\widehat{m}\widehat{n}}F_{A'B'}T^{A'B'}_{\widehat{m}\widehat{n}} - \Phi_{\widehat{m}\widehat{n}}(M_\Phi)^{\widehat{m}\widehat{n}}_{\widehat{r}\widehat{s}}\Phi^{\widehat{r}\widehat{s}}\right). \tag{C.50}$$

C.3.3 Equations of Motion for the Fermions

The 6d fermions are decomposed as follows

$$\rho^{\underline{m}\widehat{m}} \to \begin{pmatrix} 0 \\ i\rho^{m'\widehat{m}} \end{pmatrix} . \tag{C.51}$$

Then for a general background the six-dimensional equation of motion reduces to

$$i\not{D}\rho^{m'\widehat{m}} + (M_\rho)^{m'\widehat{m}}_{n'\widehat{n}}\rho^{n'\widehat{n}} = 0\,, \tag{C.52}$$

where

$$\begin{aligned} D_{\mu'}\rho^{m'\widehat{m}} &= \left(\partial_{\mu'} + \frac{1}{4}\omega_{\mu'}^{A'B'}\gamma_{A'B'}\right)\rho^{m'\widehat{m}} - \frac{1}{2}V^{\widehat{m}}_{\mu'\widehat{n}}\rho^{\widehat{n}} \\ (M_\rho)^{m'\widehat{m}}_{n'\widehat{n}} &= \alpha\left(-\frac{1}{2}S^{\widehat{m}}_{\widehat{n}}\delta^{m'}_{n'} + \frac{1}{8\alpha^2}G_{A'B'}(\gamma^{A'B'})^{m'}_{n'}\delta^{\widehat{m}}_{\widehat{n}} - \frac{i}{2\alpha^2}e^{\mu'A'}\partial_{\mu'}\alpha(\gamma_{A'})^{m'}_{n'}\delta^{\widehat{m}}_{\widehat{n}}\right) \\ &\quad + \frac{1}{2\alpha^2}(\gamma^{\mu'}\gamma^{\nu'})^{m'}_{n'}\delta^{\widehat{m}}_{\widehat{n}}C_{\mu'}\partial_{\nu'}\alpha + \frac{1}{2}T_{A'B'}{}^{\widehat{m}}{}_{\widehat{n}}(\gamma^{A'B'})^{m'}_{n'}\,. \end{aligned} \tag{C.53}$$

From this we obtain the action

$$S_\rho = -\int d^5x\sqrt{|g|}\,\alpha^{-1}\rho_{m\widehat{m}}\left(i\not{D}^m_n\rho^{n\widehat{m}} + (M_\rho)^{m\widehat{m}}_{n\widehat{n}}\rho^{n\widehat{n}}\right) . \tag{C.54}$$

C.4 Supersymmetry Variations of the 5d Action

The supersymmetry variations (6.50), which leave the 5d action (6.60) invariant, can be decomposed with respect to the R-symmetry, following appendix C.1.3. This decomposition will be useful in further proceeding to four dimensions. The scalar and gauge field variations are then

$$\begin{aligned} \delta A_\mu &= -\ell(\theta)\left(\epsilon^{(1)\widehat{p}}\gamma_\mu\rho^{(2)}_{\widehat{p}-} + \epsilon^{(2)\widehat{p}}\gamma_\mu\rho^{(1)}_{\widehat{p}+}\right) \\ \delta A_\theta &= -r\ell(\theta)\left(\epsilon^{(1)\widehat{p}}\rho^{(2)}_{\widehat{p}+} - \epsilon^{(2)\widehat{p}}\rho^{(1)}_{\widehat{p}-}\right) \\ \delta\varphi^{\widehat{a}} &= i\left(\epsilon^{(1)}{}_{\widehat{p}}(\sigma^{\widehat{a}})^{\widehat{p}\widehat{q}}\rho^{(2)}_{\widehat{q}+} - \epsilon^{(2)}{}_{\widehat{p}}(\sigma^{\widehat{a}})^{\widehat{p}\widehat{q}}\rho^{(1)}_{\widehat{q}-}\right) \\ \delta\varphi &= -2\epsilon^{(1)\widehat{p}}\rho^{(1)}_{\widehat{p}+}\,, \quad \delta\bar{\varphi} \;=\; 2\epsilon^{(2)\widehat{p}}\rho^{(2)}_{\widehat{p}-} \end{aligned} \tag{C.55}$$

and for the fermions we find

$$\begin{aligned} \delta\rho^{(1)}_{\widehat{p}+} &= \frac{i}{8\ell(\theta)}F_{\mu\nu}\gamma^{\mu\nu}\epsilon^{(1)}_{\widehat{p}} - \frac{i}{4}D_\mu\varphi\gamma^\mu\epsilon^{(2)}_{\widehat{p}} + \frac{1}{4r}D_\theta\varphi^{\widehat{q}}_{\widehat{p}}\epsilon^{(1)}_{\widehat{q}} - \frac{\ell(\theta)}{8}\left(\epsilon^{\widehat{a}\widehat{b}\widehat{c}}[\varphi_{\widehat{a}},\varphi_{\widehat{b}}](\sigma_{\widehat{c}})^{\widehat{q}}_{\widehat{p}}\epsilon^{(1)}_{\widehat{q}} - i[\varphi,\bar{\varphi}]\epsilon^{(1)}_{\widehat{p}}\right) \\ \delta\rho^{(1)}_{\widehat{p}-} &= \frac{i}{4r\ell(\theta)}F_{\mu\theta}\gamma^\mu\epsilon^{(1)}_{\widehat{p}} + \frac{1}{4}D_\mu\varphi^{\widehat{q}}_{\widehat{p}}\gamma^\mu\epsilon^{(1)}_{\widehat{q}} + \frac{i}{4r}\left(D_\theta\varphi + \frac{\ell'(\theta)}{\ell(\theta)}\varphi\right)\epsilon^{(2)}_{\widehat{p}} - \frac{\ell(\theta)}{4}[\varphi,\varphi^{\widehat{q}}_{\widehat{p}}]\epsilon^{(2)}_{\widehat{q}} \\ \delta\rho^{(2)}_{\widehat{p}+} &= -\frac{i}{4r\ell(\theta)}F_{\mu\theta}\gamma^\mu\epsilon^{(2)}_{\widehat{p}} - \frac{1}{4}D_\mu\varphi^{\widehat{q}}_{\widehat{p}}\gamma^\mu\epsilon^{(2)}_{\widehat{q}} + \frac{i}{4r}\left(D_\theta\bar{\varphi} + \frac{\ell'(\theta)}{\ell(\theta)}\bar{\varphi}\right)\epsilon^{(1)}_{\widehat{p}} - \frac{\ell(\theta)}{4}[\bar{\varphi},\varphi^{\widehat{q}}_{\widehat{p}}]\epsilon^{(1)}_{\widehat{q}} \\ \delta\rho^{(2)}_{\widehat{p}-} &= \frac{i}{8\ell(\theta)}F_{\mu\nu}\gamma^{\mu\nu}\epsilon^{(2)}_{\widehat{p}} + \frac{i}{4}D_\mu\bar{\varphi}\gamma^\mu\epsilon^{(1)}_{\widehat{p}} + \frac{1}{4r}D_\theta\varphi^{\widehat{q}}_{\widehat{p}}\epsilon^{(2)}_{\widehat{q}} - \frac{\ell(\theta)}{8}\left(\epsilon^{\widehat{a}\widehat{b}\widehat{c}}[\varphi_{\widehat{a}},\varphi_{\widehat{b}}](\sigma_{\widehat{c}})^{\widehat{q}}_{\widehat{p}}\epsilon^{(2)}_{\widehat{q}} + i[\varphi,\bar{\varphi}]\epsilon^{(2)}_{\widehat{p}}\right) , \end{aligned} \tag{C.56}$$

where $\varphi_{\widehat{p}}{}^{\widehat{q}} = \sum_{\widehat{a}}\varphi^{\widehat{a}}(\sigma^{\widehat{a}})_{\widehat{p}}{}^{\widehat{q}}$.

C.5 Aspects of the 4d Sigma-model

In this appendix we collect several useful relations for the sigma-model reduction, as well as give details on integrating out the gauge field and the scalars φ and $\bar{\varphi}$, which appear only algebraically in the $r \to 0$ limit of the 5d action.

C.5.1 Useful Relations

We now summarise properties of the sigma-model defined in section 6.4. The three symplectic structures (6.101) of the Hyper-Kähler target can be used to define the three complex structures $\omega_K^{\widehat{a}\ I} = \omega_{KJ}^{\widehat{a}} G^{JI}$, which satisfy

$$\omega_{\widehat{a}I}{}^{J}\omega_{\widehat{b}J}{}^{K} = -\delta_{\widehat{a}\widehat{b}}\delta_I^K + \epsilon_{\widehat{a}\widehat{b}\widehat{c}}\omega_I^{\widehat{c}K}\,. \tag{C.57}$$

The complex structures exchange the cotangent vectors $\Upsilon_I^{\widehat{a}}$ and Υ_I^{θ} in the following fashion

$$\begin{aligned}\omega_I^{\widehat{a}J}\Upsilon_J^{\theta} &= -\Upsilon_I^{\widehat{a}}\\ \omega_I^{\widehat{a}J}\Upsilon_J^{\widehat{b}} &= \delta^{\widehat{a}\widehat{b}}\Upsilon_I^{\theta} + \epsilon^{\widehat{a}\widehat{b}\widehat{c}}\Upsilon_{I\widehat{c}}\,.\end{aligned} \tag{C.58}$$

We introduce a complete set of functions, satisfying the completeness relations [268]

$$\begin{aligned}G^{IJ}\Upsilon_I^{\widehat{a}\alpha}(\theta)\Upsilon_J^{\widehat{b}\beta}(\tau) + \sum_i \Psi_i^{\widehat{a}\alpha}(\theta)\Psi_i^{\widehat{b}\beta}(\tau) &= \delta^{\widehat{a}\widehat{b}}\,\delta^{\alpha\beta}\,\delta(\theta-\tau)\\ G^{IJ}\Upsilon_I^{\theta\alpha}(\theta)\Upsilon_J^{\theta\beta}(\tau) + \sum_i \Psi_i^{\theta\alpha}(\theta)\Psi_i^{\theta\beta}(\tau) &= \delta^{\alpha\beta}\,\delta(\theta-\tau)\\ G^{IJ}\Upsilon_I^{\widehat{a}\alpha}(\theta)\Upsilon_J^{\theta\beta}(\tau) + \sum_i \Psi_i^{\widehat{a}\alpha}(\theta)\Psi_i^{\theta\beta}(\tau) &= 0\,.\end{aligned} \tag{C.59}$$

Here, α, β are indices labeling the generators of the gauge algebra. These functions satisfy the orthogonality relations

$$\int d\theta \Upsilon_I^{\widehat{a}\alpha}(\theta)\Psi_i^{\widehat{b}\beta}(\theta) = 0\,, \quad \int d\theta \Upsilon_I^{\theta\alpha}(\theta)\Psi_i^{\theta\beta}(\theta) = 0\,. \tag{C.60}$$

C.5.2 Integrating out Fields

In this appendix we discuss how the scalars $\varphi, \bar{\varphi}$ and the 4d gauge field A_μ are integrated out in the sigma-model reduction. The equation of motions for $\varphi, \bar{\varphi}$ and A_μ are

$$\begin{aligned}\mathcal{D}_\theta^2\varphi + \left[\varphi_{\widehat{a}}, \left[\varphi^{\widehat{a}}, \varphi\right]\right] &= -4ir[\rho_{-\widehat{p}}^{(1)}, \rho_+^{(1)\widehat{p}}]\\ \mathcal{D}_\theta^2\bar{\varphi} + \left[\varphi_{\widehat{a}}, \left[\varphi^{\widehat{a}}, \bar{\varphi}\right]\right] &= 4ir[\rho_{+\widehat{p}}^{(2)}, \rho_-^{(2)\widehat{p}}]\\ \mathcal{D}_\theta^2 A_\mu + \left[\varphi_{\widehat{a}}, \left[\varphi^{\widehat{a}}, A_\mu\right]\right] &= [A_\theta, \partial_I A_\theta]\,\partial_\mu X^I + \left[\varphi_{\widehat{a}}, \partial_I\varphi^{\widehat{a}}\right]\partial_\mu X^I - 4i[\rho_{-\widehat{p}}^{(1)}, \gamma_\mu\rho_+^{(2)\widehat{p}}]\,.\end{aligned} \tag{C.61}$$

We adopt a convenient gauge for the connection E_I

$$\mathcal{D}_\theta \Upsilon^\theta_I + [\varphi_{\widehat{a}}, \Upsilon^{\widehat{a}}_I] = 0\,, \tag{C.62}$$

which can be re-expressed as

$$\mathcal{D}^2_\theta E_I + [\varphi_{\widehat{a}}, [\varphi^{\widehat{a}}, E_I]] = [A_\theta, \partial_I A_\theta] + [\varphi_{\widehat{a}}, \partial_I \varphi^{\widehat{a}}]\,, \tag{C.63}$$

where we have used the gauge fixing condition $\partial_\theta A_\theta = 0$. Using the expansion for the spinors (6.103) and the constraints (6.104), we evaluate the spinor bilinears in (C.61) to give

$$\begin{aligned}
\left[\rho^{(1)}_{-\widehat{p}}, \rho^{(1)\widehat{p}}_{-}\right] &= -4\left(\left[\Upsilon^{\widehat{a}}_I, \Upsilon_{J\widehat{a}}\right] + \left[\Upsilon^\theta_I, \Upsilon^\theta_J\right]\right)\lambda^{(1)I}_{\widehat{p}}\lambda^{(1)J\widehat{p}} \\
\left[\rho^{(2)}_{+\widehat{p}}, \rho^{(2)\widehat{p}}_{+}\right] &= -4\left(\left[\Upsilon^{\widehat{a}}_I, \Upsilon_{J\widehat{a}}\right] + \left[\Upsilon^\theta_I, \Upsilon^\theta_J\right]\right)\lambda^{(2)I}_{\widehat{p}}\lambda^{(2)J\widehat{p}} \\
\left[\rho^{(1)}_{-\widehat{p}}, \gamma_\mu \rho^{(2)\widehat{p}}_{+}\right] &= -4\left(\left[\Upsilon^{\widehat{a}}_I, \Upsilon_{J\widehat{a}}\right] + \left[\Upsilon^\theta_I, \Upsilon^\theta_J\right]\right)\lambda^{(1)I}_{\widehat{p}}\gamma_\mu\lambda^{(2)J\widehat{p}}\,.
\end{aligned} \tag{C.64}$$

We note that the curvature

$$\Phi_{IJ} = [\nabla_I, \nabla_J]\,, \tag{C.65}$$

where $\nabla_I = \partial_I + [E_I, \cdot\,]$, satisfies the equation

$$\mathcal{D}^2_\theta \Phi_{IJ} + [\varphi_{\widehat{a}}, [\varphi^{\widehat{a}}, \Phi_{IJ}]] = 2\left([\Upsilon_{I\widehat{a}}, \Upsilon^{\widehat{a}}_J] + [\Upsilon^\theta_I, \Upsilon^\theta_J]\right). \tag{C.66}$$

It can be used to solve the equations of motion by

$$\begin{aligned}
\varphi &= 8ir\Phi_{IJ}\lambda^{(1)I}_{\widehat{p}}\lambda^{(1)J\widehat{p}} \\
\bar{\varphi} &= -8ir\Phi_{IJ}\lambda^{(2)I}_{\widehat{p}}\lambda^{(2)J\widehat{p}} \\
A_\mu &= E_I\partial_\mu X^I + 8i\Phi_{IJ}\lambda^{(1)I}_{\widehat{p}}\gamma_\mu\lambda^{(2)J\widehat{p}}\,.
\end{aligned} \tag{C.67}$$

Inserting this back in the action the terms with $\varphi, \bar{\varphi}$ results in

$$S_{\varphi,\bar{\varphi}} = \frac{16}{r\ell}\int d\theta d^4x\sqrt{|g_4|}\,\mathrm{Tr}\left(\mathcal{D}_\theta\Phi_{IJ}\mathcal{D}_\theta\Phi_{KL} + [\Phi_{IJ}, \varphi^{\widehat{a}}][\Phi_{KL}, \varphi_{\widehat{a}}]\right)\lambda^{(1)I\widehat{p}}\lambda^{(1)J}_{\widehat{p}}\lambda^{(2)K\widehat{q}}\lambda^{(2)L}_{\widehat{q}}\,. \tag{C.68}$$

The terms we obtain by integrating out A_μ will be grouped into three types of terms. The first type are such that X^I appear quadratically

$$\begin{aligned}
S_{A_\mu,\text{type 1}} = -\frac{1}{4r\ell}\int d\theta d^4x\sqrt{|g_4|}\,\mathrm{Tr}\Big(&\mathcal{D}_\theta E_I\mathcal{D}_\theta E_J - 2\partial_I A_\theta\mathcal{D}_\theta E_J + 2\partial_I\varphi^{\widehat{a}}[E_J, \varphi_{\widehat{a}}] \\
&+ [E_I, \varphi^{\widehat{a}}][E_J, \varphi_{\widehat{a}}]\Big)\partial_\mu X^I\partial^\mu X^J\,.
\end{aligned} \tag{C.69}$$

These terms combine with terms in the scalar action (6.102) to give the usual sigma-model kinetic term

$$S_{\text{scalars}} + S_{A_{\mu,\text{type 1}}} = \frac{1}{4r\ell}\int d^4x\sqrt{|g_4|}\,G_{IJ}\partial_\mu X^I\partial^\mu X^J\,. \tag{C.70}$$

Terms of type 2 are linear in X^I and covariantise the kinetic terms of the spinor

$$S_{A_\mu,\text{type 2}} = -\frac{4i}{r\ell}\int d\theta d^4x\sqrt{|g_4|}\,\mathrm{Tr}\left(2\Upsilon^{\widehat{a}}_I[E_J,\Upsilon_{K\widehat{a}}]+2\Upsilon^{\theta}_I[E_J,\Upsilon^{\theta}_K]\right)\lambda^{(1)I\widehat{p}}\gamma^\mu\lambda^{(2)K}_{\widehat{p}}\partial_\mu X^J\,. \tag{C.71}$$

The terms involving the connection E_I are promoted to covariant derivatives ∇_I when combined with the terms in the spinor action (6.105). Using the identities

$$\begin{aligned}\nabla_I\Upsilon^{\widehat{a}}_J &= \Gamma^K_{IJ}\Upsilon^{\widehat{a}}_K+\frac{1}{2}[\Phi_{IJ},\varphi^{\widehat{a}}]\\ \nabla_I\Upsilon^{\theta}_J &= \Gamma^K_{IJ}\Upsilon^{\theta}_K-\frac{1}{2}\mathcal{D}_\theta\Phi_{IJ}\,,\end{aligned} \tag{C.72}$$

where

$$\Gamma_{IJ,K} = -\int d\theta\,\mathrm{Tr}\left(\Upsilon^{\widehat{a}}_K\nabla_{(I}\Upsilon_{J)\widehat{a}}+\Upsilon^{\theta}_K\nabla_{(I}\Upsilon^{\theta}_{J)}\right), \tag{C.73}$$

the kinetic term in the spinor action is covariantised. Lastly, the terms of type 3 give rise to the quartic fermion interaction. Using (C.66) these terms simplify to

$$\begin{aligned}S_{A_\mu,\text{type 3}} = -\frac{16}{r\ell}\int d^4xd\theta\sqrt{|g_4|}\,\mathrm{Tr}\left(\mathcal{D}_\theta\Phi_{IJ}\mathcal{D}_\theta\Phi_{KL}+[\Phi_{IJ},\varphi^{\widehat{a}}][\Phi_{KL},\varphi_{\widehat{a}}]\right)\\ \times\lambda^{(1)I\widehat{p}}\gamma^\mu\lambda^{(2)J}_{\widehat{p}}\lambda^{(1)K\widehat{q}}\gamma_\mu\lambda^{(2)L}_{\widehat{q}}\,.\end{aligned} \tag{C.74}$$

Using various identities, including Fierz-type identities,

$$\begin{aligned}(\lambda^{(1)\widehat{p}[I}\lambda^{(1)J]}_{\widehat{p}})(\lambda^{(2)\widehat{q}[K}\lambda^{(2)L]}_{\widehat{q}}) &= 2(\lambda^{(1)\widehat{p}[I}\lambda^{(1)J]\widehat{q}})(\lambda^{(2)[K}_{\widehat{p}}\lambda^{(2)L]}_{\widehat{q}})\\ \omega^{\widehat{a}}{}_I{}^K\nabla_{[K}\Upsilon^{\theta}_{J]} &= \nabla_{[I}\Upsilon^{\widehat{a}}_{J]}\\ \nabla_{[I}\Upsilon^{\widehat{a}}_{J]}\lambda^{(i)J}_{\widehat{p}} &= i\nabla_{[I}\Upsilon^{\theta}_{J]}(\sigma^{\widehat{a}})^{\widehat{q}}_{\widehat{p}}\lambda^{(i)J}_{\widehat{q}}\\ \nabla_{[I}\Upsilon^{\widehat{a}}_{J]}\nabla_{[K}\Upsilon_{L]\widehat{a}}\lambda^{(i)J}_{\widehat{p}}\lambda^{(i)L}_{\widehat{q}} &= 3\nabla_{[I}\Upsilon^{\theta}_{J]}\nabla_{[K}\Upsilon^{\theta}_{L]}\lambda^{(i)[J}_{\widehat{p}}\lambda^{(i)L]}_{\widehat{q}}\,,\end{aligned} \tag{C.75}$$

it can be shown that this quartic fermion interaction combines with the term (C.68) to make the Riemann tensor of the target space appear

$$S_{A_\mu,\text{type 3}}+S_{\varphi,\bar{\varphi}} = -\frac{32}{r\ell}\int d^4x\sqrt{|g_4|}\,R_{IJKL}(\lambda^{(1)I\widehat{p}}\lambda^{(1)J}_{\widehat{p}})(\lambda^{(2)K\widehat{q}}\lambda^{(2)L}_{\widehat{q}})\,, \tag{C.76}$$

where the Riemann tensor is given by

$$\begin{aligned}R_{IJKL} &= -\int d\theta\,\mathrm{Tr}\Big(2\nabla_{[I}\Upsilon^{\widehat{a}}_{J]}\nabla_{[K}\Upsilon_{L]\widehat{a}}+\nabla_{[I}\Upsilon^{\widehat{a}}_{K]}\nabla_{[J}\Upsilon_{L]\widehat{a}}-\nabla_{[I}\Upsilon^{\widehat{a}}_{L]}\nabla_{[J}\Upsilon_{K]\widehat{a}}\\ &\qquad+2\nabla_{[I}\Upsilon^{\theta}_{J]}\nabla_{[K}\Upsilon^{\theta}_{L]}+\nabla_{[I}\Upsilon^{\theta}_{K]}\nabla_{[J}\Upsilon^{\theta}_{L]}-\nabla_{[I}\Upsilon^{\theta}_{L]}\nabla_{[J}\Upsilon^{\theta}_{K]}\Big)\\ &= -\frac{1}{4}\int d\theta\;\mathrm{Tr}\Big(2\mathcal{D}_\theta\Phi_{IJ}\mathcal{D}_\theta\Phi_{KL}+2[\Phi_{IJ},\varphi^{\widehat{a}}][\Phi_{KL},\varphi_{\widehat{a}}]\\ &\qquad+\mathcal{D}_\theta\Phi_{IK}\mathcal{D}_\theta\Phi_{JL}+[\Phi_{IK},\varphi^{\widehat{a}}][\Phi_{JL},\varphi_{\widehat{a}}]\\ &\qquad-\mathcal{D}_\theta\Phi_{IL}\mathcal{D}_\theta\Phi_{JK}-[\Phi_{IL},\varphi^{\widehat{a}}][\Phi_{JK},\varphi_{\widehat{a}}]\Big)\,.\end{aligned} \tag{C.77}$$

Combining all the terms we obtain the final sigma-model (6.106).

C.6 Sigma-model for Hyper-Kähler M_4 from 5d $\mathcal{N}=2$ SYM

In this appendix we provide a comprehensive discussion of the topological twist of the 5d $\mathcal{N}=2$ SYM on an interval with Nahm pole boundary conditions, and its dimensional reduction to 4d for M_4 a Hyper-Kähler manifold. This results in the same 4d topological sigma-model as we obtained in section 6.5.2, by twisting the 4d sigma-model on flat M_4.

C.6.1 Topological Twist

Let us first consider the topological twist 1 of section 6.2.1 applied to the 5d $\mathcal{N}=2$ SYM theory. From now on we switch to Euclidean signature [2]. The twisted 5d theory was already considered in [244, 271].

Twist 1 of the 6d $\mathcal{N}=(2,0)$ theory identifies $\mathfrak{su}(2)_\ell \subset \mathfrak{su}(2)_\ell \oplus \mathfrak{su}(2)_r$ of the 4d Lorentz algebra with the $\mathfrak{su}(2)_R \subset \mathfrak{su}(2)_R \oplus \mathfrak{so}(2)_R \subset \mathfrak{sp}(4)_R$. Under dimensional reduction to 5d the symmetries after the twist are

$$\mathfrak{sp}(4)_R \oplus \mathfrak{so}(5)_L \quad \to \quad \mathfrak{g}_{\text{twist}} \;=\; \mathfrak{su}(2)_{\text{twist}} \oplus \mathfrak{su}(2)_r \oplus \mathfrak{u}(1)_R \,. \tag{C.78}$$

The fields of the 5d theory become forms in the twisted theory, according to their transformations with respect to the $\mathfrak{g}_{\text{twist}}$, as summarised in the following table:

Field	$\mathfrak{g}_{\text{twist}}$ Representation	Twisted Field
A_μ	$(\mathbf{2},\mathbf{2})_0$	A_μ
φ	$(\mathbf{1},\mathbf{1})_2$	φ
$\bar\varphi$	$(\mathbf{1},\mathbf{1})_{-2}$	$\bar\varphi$
$\varphi^{\widehat{a}}$	$(\mathbf{3},\mathbf{1})_0$	$B_{\mu\nu}$
$\rho_+^{(1)}$	$(\mathbf{2},\mathbf{2})_1$	$\psi_\mu^{(1)}$
$\rho_+^{(2)}$	$(\mathbf{2},\mathbf{2})_{-1}$	$\psi_\mu^{(2)}$
$\rho_-^{(1)}$	$(\mathbf{1},\mathbf{1})_1 \oplus (\mathbf{3},\mathbf{1})_1$	$(\eta^{(1)}, \chi_{\mu\nu}^{(1)})$
$\rho_-^{(2)}$	$(\mathbf{1},\mathbf{1})_{-1} \oplus (\mathbf{3},\mathbf{1})_{-1}$	$(\eta^{(2)}, \chi_{\mu\nu}^{(2)})$

(C.79)

The fields $A_\mu, \varphi, \bar\varphi$ do not carry $\mathfrak{su}(2)_R$ charge and are thus unaffected. The scalars $\varphi^{\widehat{a}}$ transform as a triplet of $\mathfrak{su}(2)_R$. In the twisted theory they become a triplet φ^a of $\mathfrak{su}(2)_{\text{twist}}$, defining a self-dual two-form $B_{\mu\nu}$ on M_4:

$$B_{\mu\nu} = -(j^{\widehat{a}})_{\mu\nu}\varphi^{\widehat{a}} \,, \tag{C.80}$$

where the three local self-dual two-forms $j^{\widehat{a}}$ transforming as a triplet of $\mathfrak{su}(2)_{\text{twist}}$. They can be defined in a local frame e_μ^A as $(j^a)_{\mu\nu} = e_\mu^A e_\nu^B (j^a)^A{}_B$, $a=1,2,3$, with

$$(j^a)_{0b} = -\delta^a_b \,, \quad (j^a)_{bc} = -\epsilon^a{}_{bc} \,, \quad a,b,c = 1,2,3 \,. \tag{C.81}$$

[2] For this twist we change from Lorentzian to Euclidean signature. In what follows γ_0 as defined in appendix C.1.2 is replaced with $\gamma_{0'} = i\gamma_0$, where the prime will be omitted.

In this local frame we have

$$B_{0a} = \varphi^a, \quad B_{ab} = \epsilon_{abc}\varphi^c, \quad a, b, c = 1, 2, 3\,. \tag{C.82}$$

The self-dual tensors j^a are used to map the vector index a of $\mathfrak{so}(3)$ to the self-dual two-form index $[AB]^+$. The tensors $(j^a)^\mu{}_\nu$ define an almost quaternionic structure, since they satisfy

$$(j^a)^\mu{}_\rho (j^b)^\rho{}_\nu = -\delta^{ab}\delta^\mu_\nu + \epsilon^{ab}{}_c (j^c)^\mu{}_\nu\,. \tag{C.83}$$

The spinor fields transform as doublets of $\mathfrak{su}(2)_R$. They become scalar, self-dual two-forms and one-form fields on M_4 as indicated in the table. The explicit decomposition, is obtained using the Killing spinor associated to the scalar supercharge in the twisted theory. This Killing spinor can be found as follows. The spinor $\epsilon_{\widehat{m}}$ generating the preserved supersymmetry is a constant spinor and is invariant under the twisted Lorentz algebra $\mathfrak{su}(2)_{\text{twist}} \oplus \mathfrak{su}(2)_r$. As explained in section 6.3.2 and in appendix C.1.3 $\epsilon_{\widehat{m}}$ decomposes under $\mathfrak{sp}(4)_R \to \mathfrak{su}(2)_R \oplus \mathfrak{u}(1)_R$ into two spinors doublets of $\mathfrak{su}(2)_R$: $\epsilon_{\widehat{m}} \to \epsilon^{(1)}_{\widehat{p}}, \epsilon^{(2)}_{\widehat{p}}$, satisfying the projections (6.53)

$$\epsilon^{(1)}_{\widehat{p}} - \gamma^5 \epsilon^{(1)}_{\widehat{p}} = 0\,, \quad \epsilon^{(2)}_{\widehat{p}} + \gamma^5 \epsilon^{(2)}_{\widehat{p}} = 0\,. \tag{C.84}$$

As explained in section 6.5.1, $\epsilon^{(2)}_{\widehat{p}}$ has one scalar component under $\mathfrak{su}(2)_{\text{twist}} \oplus \mathfrak{su}(2)_r$ selected out by the projections

$$(\gamma_{0a}\delta^{\widehat{q}}_{\widehat{p}} + i(\sigma_{\widehat{a}})^{\widehat{q}}_{\widehat{p}})\epsilon^{(2)}_{\widehat{q}} = 0\,, \quad a \simeq \widehat{a} = 1, 2, 3\,, \tag{C.85}$$

where the indices a and $\widehat{a}$ gets identified in the twisted theory. The spinor $\epsilon^{(2)\widehat{p}}$ parametrizing the preserved supercharge is then decomposed as

$$\epsilon^{(2)\widehat{p}} = u\,\tilde{\epsilon}^{\widehat{p}}\,, \tag{C.86}$$

where u is complex Grassmann-odd parameter and $\tilde{\epsilon}^{\widehat{p}}$ is a Grassmann-even spinor with unit normalisation. The decomposition of the spinors into the twisted fields is then given by

$$\begin{aligned}
\rho^{(1)}_{+\widehat{p}} &= \gamma^\mu \psi^{(1)}_\mu \tilde{\epsilon}_{\widehat{p}} \\
\rho^{(2)}_{+\widehat{p}} &= \gamma^\mu \psi^{(2)}_\mu \tilde{\epsilon}_{\widehat{p}} \\
\rho^{(1)}_{-\widehat{p}} &= \left(\eta^{(1)} + \frac{1}{4}\gamma^{\mu\nu}\chi^{(1)}_{\mu\nu}\right)\tilde{\epsilon}_{\widehat{p}} \\
\rho^{(2)}_{-\widehat{p}} &= \left(\eta^{(2)} + \frac{1}{4}\gamma^{\mu\nu}\chi^{(2)}_{\mu\nu}\right)\tilde{\epsilon}_{\widehat{p}}\,.
\end{aligned} \tag{C.87}$$

C.6.2 Twisted 5d Action

We rewrite now the action in terms of the twisted fields and provide the preserved supersymmetry transformations. The bosonic part of this action has appeared in [244], and related considerations regarding the supersymmetric versions of the twisted model can be found in [271].

The action in (6.75) in terms of the twisted fields takes the form

$$\begin{aligned}
S_F &= -\frac{r}{8\ell}\int d\theta d^4x\sqrt{|g_4|}\,\mathrm{Tr}\left(F_{\mu\nu}F^{\mu\nu}+\frac{2}{r^2}(\partial_\mu A_\theta-\partial_\theta A_\mu+[A_\mu,A_\theta])^2\right)\\
S_{\text{scalars}} &= -\frac{1}{4r\ell}\int d\theta d^4x\sqrt{|g_4|}\,\mathrm{Tr}\left(\frac{1}{4}D^\mu B_{\rho\sigma}D_\mu B^{\rho\sigma}+\frac{1}{4r^2}D_\theta B_{\rho\sigma}D_\theta B^{\rho\sigma}\right.\\
&\qquad\left.+D^\mu\varphi D_\mu\bar\varphi+\frac{1}{r^2}D_\theta\varphi D_\theta\bar\varphi\right)\\
S_\rho &= \frac{2i}{r\ell}\int d\theta d^4x\sqrt{|g_4|}\,\mathrm{Tr}\Big[\eta^{(2)}D_\mu\psi^{(1)\mu}-\psi^{(1)}_\mu D_\nu\chi^{(2)\mu\nu}+\eta^{(1)}D_\mu\psi^{(2)\mu}-\psi^{(2)}_\mu D_\nu\chi^{(1)\mu\nu}\\
&\qquad+\frac{1}{r}\left(\psi^{(1)}_\mu D_\theta\psi^{(2)\mu}-\eta^{(1)}D_\theta\eta^{(2)}-\frac{1}{4}\chi^{(1)}_{\mu\nu}D_\theta\chi^{(2)\mu\nu}\right)\Big]\\
S_{\text{Yukawa}} &= -\frac{i}{r^2\ell}\int d\theta d^4x\sqrt{|g_4|}\,\mathrm{Tr}\left(-\frac{1}{2}B_{\mu\nu}\left[\eta^{(2)},\chi^{(1)\mu\nu}\right]+\frac{1}{2}B_{\mu\nu}\left[\eta^{(1)},\chi^{(2)\mu\nu}\right]\right.\\
&\qquad-\frac{1}{2}B_{\mu\nu}\left[\chi^{(2)\mu\tau},\chi^{(1)\nu}{}_\tau\right]-2B_{\mu\nu}\left[\psi^{(2)\mu},\psi^{(1)\nu}\right]\\
&\qquad+\bar\varphi\left[\eta^{(1)},\eta^{(1)}\right]+\frac{1}{4}\bar\varphi\left[\chi^{(1)}_{\mu\nu},\chi^{(1)\mu\nu}\right]+\bar\varphi\left[\psi^{(1)}_\mu,\psi^{(1)\mu}\right]\\
&\qquad\left.-\varphi\left[\eta^{(2)},\eta^{(2)}\right]-\frac{1}{4}\varphi\left[\chi^{(2)}_{\mu\nu},\chi^{(2)\mu\nu}\right]-\varphi\left[\psi^{(2)}_\mu,\psi^{(2)\mu}\right]\right)\\
S_{\text{quartic}} &= -\frac{1}{16r^3\ell}\int d\theta d^4x\sqrt{|g_4|}\,\mathrm{Tr}\left(\frac{1}{4}\left[B_{\mu\rho},B_\nu{}^\rho\right]\left[B^\mu{}_\sigma,B^{\nu\sigma}\right]+[B_{\mu\nu},\varphi][B^{\mu\nu},\bar\varphi]-[\varphi,\bar\varphi][\varphi,\bar\varphi]\right)\\
S_{\text{bdry}} &= \frac{1}{16r^3\ell}\int d\theta d^4x\sqrt{|g_4|}\,\mathrm{Tr}\left(\partial_\theta B_{\mu\nu}[B^{\mu\rho},B^\nu{}_\rho]\right)\,.
\end{aligned}\tag{C.88}$$

The supersymmetry transformations of this 5d topologically twisted SYM theory are

$$\begin{aligned}
\delta A_\mu &= -\frac{u}{r}\psi^{(1)}_\mu & \delta A_\theta &= u\eta^{(1)}\\
\delta B_{\mu\nu} &= u\chi^{(1)}_{\mu\nu}\\
\delta\varphi &= 0 & \delta\bar\varphi &= 2u\eta^{(2)}\\
\delta\psi^{(1)}_\mu &= -\frac{iu}{4}D_\mu\varphi & \delta\psi^{(2)}_\mu &= -\frac{iu}{4}F_{\mu\theta}-\frac{iu}{4}D^\nu B_{\nu\mu}\\
\delta\eta^{(1)} &= \frac{iu}{4r}D_\theta\varphi & \delta\eta^{(2)} &= -\frac{iu}{8r}[\varphi,\bar\varphi]\\
\delta\chi^{(1)}_{\mu\nu} &= -\frac{iu}{4r}[\varphi,B_{\mu\nu}] & \delta\chi^{(2)}_{\mu\nu} &= \frac{iur}{2}F^+_{\mu\nu}+\frac{iu}{4r}D_\theta B_{\mu\nu}-\frac{iu}{8r}[B_{\mu\tau},B_\nu{}^\tau]\,,
\end{aligned}\tag{C.89}$$

where the self-dual part of the gauge field is defined as

$$F^+ = \frac{1}{2}(1+*)F\,. \tag{C.90}$$

To define the twisted action for curved M_4, in addition to covariantising the derivatives, the curvature terms

$$\mathcal{R}B_{\mu\nu}B^{\mu\nu} \text{ and } \mathcal{R}_{\mu\nu\rho\sigma}B^{\mu\nu}B^{\rho\sigma}\,, \tag{C.91}$$

must be added to the action in order to preserve supersymmetry. These terms can be repackaged with the kinetic term for $B_{\mu\nu}$ changing the action for the scalars to

$$\begin{aligned} &S_{\text{scalars}} \\ &= -\frac{1}{4r\ell}\int d\theta d^4x\sqrt{|g|}\,\mathrm{Tr}\left(\mathcal{D}^\mu B_{\mu\rho}\mathcal{D}^\nu B_\nu{}^\rho - \frac{1}{2}F_{\mu\nu}B^\mu{}_\sigma B^{\nu\sigma} + \frac{1}{4r^2}D_\theta B_{\rho\sigma}D_\theta B^{\rho\sigma} + \mathcal{D}^{\mu'}\varphi\mathcal{D}_{\mu'}\bar\varphi\right)\,, \end{aligned} \tag{C.92}$$

where $\mathcal{D}$ is defined to be covariant with respect to the curvature connection on M_4 and the gauge connection. The 5d twisted action on curved M_4 can be written in the form

$$S_{5d} = QV + S_{5d,\text{top}}\,, \tag{C.93}$$

where the Q-exact and topological terms are given by

$$\begin{aligned} V = -\frac{1}{r\ell}\int d\theta d^4x\sqrt{|g|}\,\mathrm{Tr}\Bigg[&\chi^{(2)\mu\nu}\left(P_{\mu\nu} - i(rF_{\mu\nu} + \frac{1}{2r}(D_\theta B_{\mu\nu} - \frac{1}{2}[B_{\mu\tau}, B_\nu{}^\tau]))\right) \\ &+2\psi^{(2)\mu}\left(2P_\mu + i(F_{\mu\theta} + D^\nu B_{\nu\mu})\right) + i\psi^{(1)\mu}D_\mu\bar\varphi - \frac{i}{2r}\eta^{(2)}[\varphi,\bar\varphi] - \frac{i}{r}\eta^{(1)}D_\theta\bar\varphi \\ &+\frac{i}{4r}\chi^{(1)\mu\nu}[\bar\varphi, B_{\mu\nu}]\Bigg] \\ S_{5d,\text{top}} = \frac{r}{4\ell}\int_{M_4\times I}\mathrm{Tr}\,F\wedge *F - \frac{1}{2r\ell}&\left[\int_{M_4}\mathrm{Tr}\,F\wedge B\right]_{\theta=0}^{\theta=\pi}\,, \end{aligned} \tag{C.94}$$

where $P_{\mu\nu}$ and P_μ are auxiliary fields. The supersymmetry transformations are

$$\begin{aligned} QA_\mu &= -\frac{1}{r}\psi_\mu^{(1)} & QA_\theta &= \eta^{(1)} & QB_{\mu\nu} &= \chi_{\mu\nu}^{(1)} \\ Q\varphi &= 0 & Q\bar\varphi &= 2\eta^{(2)} & & \\ QP_\mu &= \frac{i}{4r}[\psi_\mu^{(2)},\varphi] & QP_{\mu\nu} &= \frac{i}{4r}[\chi_{\mu\nu}^{(2)},\varphi] & & \\ Q\eta^{(1)} &= \frac{i}{4r}D_\theta\varphi & Q\psi_\mu^{(1)} &= -\frac{i}{4}D_\mu\varphi & Q\chi_{\mu\nu}^{(1)} &= -\frac{iu}{4r}[\varphi, B_{\mu\nu}] \\ Q\eta^{(2)} &= -\frac{i}{8r}[\varphi,\bar\varphi] & Q\psi_\mu^{(2)} &= P_\mu\,, & Q\chi_{\mu\nu}^{(2)} &= P_{\mu\nu}\,. \end{aligned} \tag{C.95}$$

The auxiliary fields are integrated out by

$$\begin{aligned} P_\mu &= -\frac{i}{4}(F_{\mu\theta} + D^\nu B_{\nu\mu}) \\ P_{\mu\nu} &= \frac{ir}{2}F^+_{\mu\nu} + \frac{i}{4r}\left(D_\theta B_{\mu\nu} - \frac{1}{2}[B_{\mu\tau}, B_\nu{}^\tau]\right)\,. \end{aligned} \tag{C.96}$$

We can now proceed with the dimensional reduction to four-dimensions.

C.6.3 Triholomorphic Sigma-model with Hyper-Kähler M_4

We now reduce the twisted 5d SYM theory to 4d on Hyper-Kähler M_4. We proceed similar to the analysis in section 6.4.2 and in appendix C.5, and expand all fields in powers of r and demand that the leading order terms in $\frac{1}{r}$ in the action (C.88) vanish. This sets $\varphi = \bar{\varphi} = O(r)$ and leads to Nahm's equations for the self-dual two-forms

$$D_\theta B_{\mu\nu} - \frac{1}{2}[B_{\mu\rho}, B_\nu{}^\rho] = 0\,, \tag{C.97}$$

with $\varrho = [k]$ Nahm pole boundary condition. Locally this is the same situation as in the untwisted theory, but not globally. In the untwisted theory the scalars $\varphi^{\widehat{a}}$ were scalar fields on $\mathbb{R}_4$ and the solutions to the Nahm's equations are described by a map $\mathbb{R}^4 \to \mathcal{M}_k$. In the twisted theory B belongs to the bundle $\Omega^{2,+}(M_4)$ and the global solutions to (C.97) are generically more involved. However this complication does not happen when the bundle of self-dual two-forms $\Omega^{2,+}(M_4)$ is trivial, namely when B transforms as a scalar. In this case one can regard the components $B_{\mu\nu}$ as scalars on M_4 and the solutions to (C.97) are again given in terms of a map

$$X : M_4 \to \mathcal{M}_k\,, \tag{C.98}$$

where $\mathcal{M}_k$ is the moduli space of solutions to Nahm's equations with ϱ Nahm pole boundary conditions. As before we define coordinates $X = \{X^I\}$ on $\mathcal{M}_k$. The case when $\Omega^{2,+}(M_4)$ is trivial corresponds to M_4 having reduced holonomy $SU(2)_r \subset SU(2)_\ell \times SU(2)_r$, which is the definition of a Hyper-Kähler manifold.

The zero modes around a solution $B_{\mu\nu}(X^I)$ can be expressed as

$$\begin{aligned} \delta B_{\mu\nu} &= \Upsilon_{I,\mu\nu}\delta X^I \\ \delta A_\theta &= \Upsilon^\theta_I \delta X^I\,, \end{aligned} \tag{C.99}$$

where the expansion is in terms of the cotangent vectors Υ, which satisfy

$$\begin{aligned} \Upsilon_{I,\mu\nu} &= \partial_I B_{\mu\nu} + [E_I, B_{\mu\nu}] \\ \Upsilon^\theta_I &= \partial_I A_\theta - \partial_\theta E_I - [A_\theta, E_I]\,, \end{aligned} \tag{C.100}$$

with E_I defining a gauge connection on $\mathcal{M}_N$. We will choose the convenient 'gauge fixing condition'

$$D_\theta \Upsilon^\theta_I - \frac{1}{4}[\Upsilon_{I,\mu\nu}, B^{\mu\nu}] = 0\,. \tag{C.101}$$

The equations obeyed by the cotangent vectors $\Upsilon^{\mu\nu}_I$, Υ^θ_I are

$$D_\theta \Upsilon_{I,\mu\nu} + [\Upsilon^\theta_I, B_{\mu\nu}] - \frac{1}{2}\left([\Upsilon_{I,\mu\rho}, B_\nu{}^\rho] - [\Upsilon_{I,\nu\rho}, B_\mu{}^\rho]\right) = 0\,. \tag{C.102}$$

A natural metric on $\mathcal{M}_N$ can be defined as

$$G_{IJ} = -\int d\theta\, \mathrm{Tr}\left(\frac{1}{4}\Upsilon^{\mu\nu}_I \Upsilon_{J,\mu\nu} + \Upsilon^\theta_I \Upsilon^\theta_J\right)\,. \tag{C.103}$$

Similarly we can write down an expression for the three symplectic forms $\omega^a{}_{IJ}$ (see e.g. [269]), repackaged into $\omega_{\mu\nu,IJ} = -(j^a)_{\mu\nu}\omega^a{}_{IJ}$, as

$$\omega_{\mu\nu,IJ} = -\int d\theta\, \mathrm{Tr}\left(\frac{1}{2}\Upsilon_{I,\mu\rho}\Upsilon_J{}^{\rho}{}_{\nu} - \frac{1}{2}\Upsilon_{I,\nu\rho}\Upsilon_J{}^{\rho}{}_{\mu} - \Upsilon_{I,\mu\nu}\Upsilon^{\theta}_{J} + \Upsilon^{\theta}_{I}\Upsilon_{J,\mu\nu}\right). \tag{C.104}$$

These provide the Hyper-Kähler structure of the moduli space $\mathcal{M}_k$. The quaternionic relations on the three complex structures $\omega^{aI}{}_J$ becomes

$$\omega_{\mu\rho,I}{}^{J}\omega_{\nu}{}^{\rho}{}_{J}{}^{K} = 2\omega_{\mu\nu,I}{}^{K} - 3g_{\mu\nu}\delta^{K}_{I}\,. \tag{C.105}$$

Using the orthogonality of the $\Upsilon^{\mu\nu}_I$, Υ^{θ}_I modes we derive the relations

$$\begin{aligned}\omega_{\mu\nu,I}{}^{J}\Upsilon^{\theta}_{J} &= -\Upsilon_{I,\mu\nu}\\ \omega_{\mu\rho,I}{}^{J}\Upsilon^{\nu\rho}_{J} &= 2\Upsilon_{I,\mu}{}^{\nu} + 3\delta^{\nu}_{\mu}\Upsilon^{\theta}_{I}\,.\end{aligned} \tag{C.106}$$

At order r^{-2} in the 5d action we find terms involving fermions. They vanish upon imposing

$$\eta^{(2)} = O(r), \quad \psi^{(1)}_{\mu} = O(r), \quad \chi^{(2)}_{\mu\nu} = O(r)\,. \tag{C.107}$$

The 4d action arises with overall coupling $\frac{1}{4r\ell}$ and at this order in r the above fermions appear as Lagrange multipliers and can be integrated out to give the constraints

$$\begin{aligned}D_\theta\chi^{(1)}_{\mu\nu} + [\eta^{(1)}, B^{\mu\nu}] - \frac{1}{2}\left([\chi^{(1)}_{\mu\rho}, B_{\nu}{}^{\rho}] - [\chi^{(1)}_{\nu\rho}, B_{\mu}{}^{\rho}]\right) &= 0\\ D_\theta\eta^{(1)} - \frac{1}{4}[\chi^{(1)}_{\mu\nu}, B^{\mu\nu}] &= 0\\ D_\theta\psi^{(2)}_{\mu} - [\psi^{(2)}_{\nu}, B_{\mu}{}^{\nu}] &= 0\,.\end{aligned} \tag{C.108}$$

These equations are solved using the basis of the contangent bundle, which obey (C.102) and (C.101), with the following relations

$$\begin{aligned}\chi^{(1)}_{\mu\nu} &= \Upsilon_{I\,\mu\nu}\lambda^I + \Upsilon^{\theta}_{I}\zeta^{I}_{\mu\nu} + \Upsilon_{I\,\sigma[\mu}\zeta^{I\,\sigma}{}_{\nu]}\\ \eta^{(1)} &= \Upsilon^{\theta}_{I}\lambda^I - \frac{1}{4}\Upsilon_{I\,\mu\nu}\zeta^{I\,\mu\nu}\\ \psi^{(2)}_{\mu} &= \Upsilon_{I\,\mu}{}^{\nu}\kappa^I_{\nu} - \Upsilon^{\theta}_{I}\kappa^I_{\mu}\,,\end{aligned} \tag{C.109}$$

where the fields λ^I, κ^I_μ and $\zeta^I_{\mu\nu}$ are Grassmann-odd scalars, vectors and self-dual two-forms on M_4, respectively. The identities (C.106) imply that the fermionic fields obey the constraints

$$\begin{aligned}\omega_{\mu\nu}{}^{I}{}_{J}\lambda^J &= \xi^I_{\mu\nu}\\ \omega_{\mu\sigma}{}^{I}{}_{J}\xi^{J}{}_{\nu}{}^{\sigma} &= 2\xi^I_{\mu\nu} - 3\delta_{\mu\nu}\lambda^I\\ \omega_{\mu\nu}{}^{I}{}_{J}\kappa^{J\nu} &= -3\kappa^I_{\mu}\,.\end{aligned} \tag{C.110}$$

or more generally

$$\omega_{\mu\nu}{}^{I}{}_{J}\kappa^J_{\sigma} = g_{\mu\sigma}\kappa^I_{\nu} - g_{\nu\sigma}\kappa^I_{\mu} + \epsilon_{\mu\nu\sigma}{}^{\rho}\kappa^I_{\rho}\,. \tag{C.111}$$

This decomposition satisfies the fermion equtaions of motion, which can be seen by using the identity

$$\Omega_{\rho\mu}\tilde{\Omega}^{\rho}{}_{\nu} = \frac{1}{4}\Omega_{\rho\sigma}\tilde{\Omega}^{\rho\sigma}g_{\mu\nu} + \Omega_{\rho[\mu}\tilde{\Omega}^{\rho}{}_{\nu]}\,, \tag{C.112}$$

where $\Omega_{\mu\nu}, \tilde{\Omega}_{\mu\nu}$ are self-dual two-forms.

C.6.4 Dimensional Reduction to 4d Sigma-Model

After reduction to four dimensions the bosonic fields of the theory will be the collective coordinates X^I describing a map $M_4 \to \mathcal{M}_k$ and the fermionic fields will be the scalars λ^I, one-forms κ^I and self-dual two-forms $\zeta^I_{\mu\nu}$, which are valued in the pull-back of the tangent bundle to $\mathcal{M}_k$

$$\begin{aligned}\lambda &\in \Gamma(X^*T\mathcal{M}_k)\\ \kappa &\in \Gamma(X^*T\mathcal{M}_k \otimes \Omega^1)\\ \zeta &\in \Gamma(X^*T\mathcal{M}_k \otimes \Omega^2)\,.\end{aligned} \tag{C.113}$$

The bosonic and fermionic zero modes lead to a four-dimensional effective action with overall coupling constant $\frac{1}{r\ell}$ for the fields X^I, λ^I, κ^I_μ, $\zeta^I_{\mu\nu}$, A_μ and the scalars φ, $\bar{\varphi}$.

As mentioned previously the kinetic term for A_μ, namely $F^2_{\mu\nu}$ is of order r and drops from the action in the small r limit. The gauge field A_μ becomes an auxiliary field and can be integrated out using its equation of motion, and likewise for the scalars φ and $\bar{\varphi}$. Their equations of motion are

$$\begin{aligned}D^2_\theta\varphi + \frac{1}{4}[B_{\mu\nu},[B^{\mu\nu},\varphi]] =& 4ir\left([\eta^{(1)},\eta^{(1)}] + \frac{1}{4}[\chi^{(1)}_{\mu\nu},\chi^{(1)\mu\nu}]\right)\\ D^2_\theta\bar{\varphi} + \frac{1}{4}[B_{\mu\nu},[B^{\mu\nu},\bar{\varphi}]] =& -4ir\left([\psi^{(1)}_\mu,\psi^{(1)\mu}]\right)\\ D^2_\theta A_\mu + \frac{1}{4}\left[B_{\nu\rho},[B^{\nu\rho},A_\mu]\right] =& \left[A_\theta,\partial_I A_\theta\right]\partial_\mu X^I + \frac{1}{4}\left[B_{\nu\rho},\partial_I B^{\nu\rho}\right]\partial_\mu X^I\\ &+ 4i([\eta^{(1)},\psi^{(2)}_\mu] - [\chi^{(1)}_{\nu\mu},\psi^{(2)\nu}])\,.\end{aligned} \tag{C.114}$$

The spinor bilinears can be further simplified by applying the expansion for the spinors (C.109)

$$\begin{aligned}[\eta^{(1)},\eta^{(1)}] + \frac{1}{4}[\chi^{(1)}_{\mu\nu},\chi^{(1)\mu\nu}] &= 4([\Upsilon^\theta_I,\Upsilon^\theta_J] + \frac{1}{4}[\Upsilon_{I\mu\nu},\Upsilon^{\mu\nu}_J])(\lambda^I\lambda^J + \frac{1}{4}\zeta^I_{\sigma\rho}\zeta^{J\sigma\rho})\\ [\psi^{(1)}_\mu,\psi^{(1)\mu}] &= -4([\Upsilon^\theta_I,\Upsilon^\theta_J] + \frac{1}{4}[\Upsilon_{I\sigma\rho},\Upsilon^{\sigma\rho}_J])\kappa^I_\mu\kappa^{J\mu}\\ [\eta^{(1)},\psi^{(2)}_\mu] - [\chi^{(1)}_{\nu\mu},\psi^{(2)\nu}] &= -4([\Upsilon^\theta_I,\Upsilon^\theta_J] + \frac{1}{4}[\Upsilon_{I\nu\rho},\Upsilon^{\nu\rho}_J])\lambda^I\kappa^J_\mu\,.\end{aligned} \tag{C.115}$$

To solve these equations we note that the curvature

$$\Phi_{IJ} = [\nabla_I,\nabla_J]\,, \tag{C.116}$$

where $\nabla_I = \partial_I + [E_I, \cdot\,]$, satisfies the equation

$$D_\theta^2 \Phi_{IJ} + \frac{1}{4}[B_{\nu\rho}, [B^{\nu\rho}, \Phi_{IJ}]] = \frac{1}{2}[\Upsilon_{I\nu\rho}, \Upsilon_J^{\nu\rho}] + 2[\Upsilon_I^\theta, \Upsilon_J^\theta]\,. \tag{C.117}$$

Combining the information above the solutions are

$$\begin{aligned} \varphi &= 8ir\Phi_{IJ}\lambda^I\lambda^J + 2ir\Phi_{IJ}\zeta^I_{\mu\nu}\zeta^{J\mu\nu} \\ \bar\varphi &= -8ir\Phi_{IJ}\kappa^I_\mu\kappa^{\mu J} \\ A_\mu &= E_I\partial_\mu X^I - 8i\Phi_{IJ}(\lambda^I\kappa^J_\mu - \zeta^I_{\nu\mu}\kappa^{J\nu})\,. \end{aligned} \tag{C.118}$$

Replacing the fermionic and bosonic zero modes in the action one obtains

$$\begin{aligned} S_{\text{scalars}} &= -\frac{1}{4r\ell}\int d\theta d^4x\sqrt{|g_4|}\,\left[\mathrm{Tr}\left(\partial_I A_\theta \partial_J A_\theta + \frac{1}{4}\partial_I B_{\rho\sigma}\partial_J B^{\rho\sigma}\right)\partial_\mu X^I \partial^\mu X^J\right] \\ S_{\text{fermions}} &= +\frac{2i}{r\ell}\int d^4x\sqrt{|g_4|}\,\left[\left(G_{IJ}g^{\mu\nu} - \omega^{\mu\nu}_{IJ}\right)(\lambda^I\partial_\mu\kappa^J_\nu - \xi^I{}_\mu{}^\sigma\partial_\sigma\kappa^J_\nu)\right. \\ &\quad \left. -(\delta^K_I g^{\sigma\nu} - \omega^{\sigma\nu}{}_I{}^K)\mathrm{Tr}\left(\frac{1}{4}\Upsilon_{K\,\rho\tau}\partial_J\Upsilon_L^{\rho\tau} + \Upsilon^\theta_K\partial_J\Upsilon^\theta_L\right)\partial_\mu X^J(\delta^\mu_\sigma\lambda^I\kappa^L_\nu - \xi^I{}_\sigma{}^\mu\kappa^L_\nu)\right]\,. \end{aligned} \tag{C.119}$$

Substituting in the solution for the gauge field (C.118) we obtain three different types of terms, which we address in turn. Terms of type 1 are proportional to $\partial_\mu X^I\partial_\nu X^J$ and combine with the terms in the scalar action to give

$$S_{\text{scalars}} + S_{A_\mu,\text{type 1}} = \frac{1}{4r\ell}\int d^4x\sqrt{|g_4|}\,G_{IJ}g^{\mu\nu}\partial_\mu X^I\partial_\nu X^J\,. \tag{C.120}$$

Terms of type 2 combine with terms from the action of the fermions to give

$$\begin{aligned} S_{A_\mu,\text{type 2}} = -\frac{2i}{r\ell}\int d\theta d^4x\sqrt{|g_4|}\,(\delta^K_I g^{\sigma\nu} - \omega^{\sigma\nu}{}_I{}^K)\mathrm{Tr}\left(\frac{1}{4}\Upsilon_{K\,\rho\tau}\nabla_J\Upsilon_L^{\rho\tau} + \Upsilon^\theta_K\nabla_J\Upsilon^\theta_L\right)\partial_\mu X^J \\ \times(\delta^\mu_\sigma\lambda^I\kappa^L_\nu - \xi^I{}_\sigma{}^\mu\kappa^L_\nu)\,. \end{aligned} \tag{C.121}$$

Using the identities

$$\begin{aligned} \nabla_I\Upsilon^{\mu\nu}_J &= \Gamma^K_{IJ}\Upsilon^{\mu\nu}_K + \frac{1}{2}[\Phi_{IJ}, B^{\mu\nu}] \\ \nabla_I\Upsilon^\theta_J &= \Gamma^K_{IJ}\Upsilon^\theta_K - \frac{1}{2}D_\theta\Phi_{IJ}\,, \end{aligned} \tag{C.122}$$

where

$$\Gamma_{IJ,K} = -\int d\theta\,\mathrm{Tr}\left(\frac{1}{4}\Upsilon^{\mu\nu}_K\nabla_{(I}\Upsilon_{J)\mu\nu} + \Upsilon^\theta_K\nabla_{(I}\Upsilon^\theta_{J)}\right)\,, \tag{C.123}$$

these terms simplify to

$$S_{A_\mu,\text{type 2}} = \frac{2i}{r\ell}\int d\theta d^4x\sqrt{|g_4|}\,(G_{IJ}g^{\sigma\nu} - \omega^{\sigma\nu}{}_{IJ})\Gamma^J_{KL}\partial_\mu X^K(\delta^\mu_\sigma\lambda^I\kappa^L_\nu - \xi^I{}_\sigma{}^\mu\kappa^L_\nu)\,. \tag{C.124}$$

and covariantise the kinetic terms for the fermions. Lastly the terms of type three contribute towards quartic fermion interactions. These take the form

$$\begin{aligned} S_{A_\mu,\text{type}\,3} &= \frac{16}{r\ell}\int d\theta d^4x\sqrt{|g_4|}\,\mathrm{Tr}\left(D_\theta\Phi_{IK}D_\theta\Phi_{JL}+\frac{1}{4}[\Phi_{IK},B_{\mu\nu}][\Phi_{JL},B^{\mu\nu}]\right)\\ &\qquad\times(\lambda^I\lambda^J\kappa_\tau^K\kappa^{L\tau}+\frac{1}{4}\zeta^I_{\rho\sigma}\zeta^{J\rho\sigma}\kappa_\tau^K\kappa^{L\tau})\\ &= \frac{8}{r\ell}\int d\theta d^4x\sqrt{|g_4|}\,\mathrm{Tr}\Big(D_\theta\Phi_{IK}D_\theta\Phi_{JL}+\frac{1}{4}[\Phi_{IK},B_{\mu\nu}][\Phi_{JL},B^{\mu\nu}]\\ &\qquad-D_\theta\Phi_{IL}D_\theta\Phi_{JK}+\frac{1}{4}[\Phi_{IL},B_{\mu\nu}][\Phi_{JK},B^{\mu\nu}]\Big)\\ &\qquad\times\left(\lambda^I\lambda^J\kappa_\tau^K\kappa^{L\tau}+\frac{1}{4}\zeta^I_{\rho\sigma}\zeta^{J\rho\sigma}\kappa_\tau^K\kappa^{L\tau}\right), \end{aligned} \tag{C.125}$$

where we have made use of the identity

$$\omega^{\mu\nu}{}_M{}^I\nabla_{[I}\Upsilon^\theta_{J]}=-\omega^{\mu\nu}{}_J{}^I\nabla_{[I}\Upsilon^\theta_{M]}\,, \tag{C.126}$$

and the analogous relation for $\Upsilon^{\mu\nu}_I$, and antisymmetrised in KL indices. To obtain a quartic fermion interaction involving the Riemann tensor of the target we need to combine the terms in (C.125) with the term which arises from integrating out φ and $\bar\varphi$

$$\begin{aligned} S_{\varphi/\bar\varphi} &= \frac{16}{r\ell}\int d\theta d^4x\sqrt{|g_4|}\,\mathrm{Tr}\left(D_\theta\Phi_{IJ}D_\theta\Phi_{KL}+\frac{1}{4}[\Phi_{IJ},B_{\mu\nu}][\Phi_{KL},B^{\mu\nu}]\right)\\ &\qquad\times(\lambda^I\lambda^J\kappa_\tau^K\kappa^{L\tau}+\frac{1}{4}\zeta^I_{\rho\sigma}\zeta^{J\rho\sigma}\kappa_\tau^K\kappa^{L\tau})\,. \end{aligned} \tag{C.127}$$

Combining (C.127) and (C.125), as well as the fact that the Riemann tensor on the target is given by

$$\begin{aligned} R_{IJKL} = -\int d\theta\,\mathrm{Tr}\,\Big(&\frac{1}{2}\nabla_{[I}\Upsilon^{\mu\nu}_{J]}\nabla_{[K}\Upsilon_{L]\mu\nu}+\frac{1}{4}\nabla_{[I}\Upsilon^{\mu\nu}_{K]}\nabla_{[J}\Upsilon_{L]\mu\nu}-\frac{1}{4}\nabla_{[I}\Upsilon^{\mu\nu}_{L]}\nabla_{[J}\Upsilon_{K]\mu\nu}\\ &+2\nabla_{[I}\Upsilon^\theta_{J]}\nabla_{[K}\Upsilon^\theta_{L]}+\nabla_{[I}\Upsilon^\theta_{K]}\nabla_{[J}\Upsilon^\theta_{L]}-\nabla_{[I}\Upsilon^\theta_{L]}\nabla_{[J}\Upsilon^\theta_{K]}\Big)\,, \end{aligned} \tag{C.128}$$

we obtain the four fermi interaction

$$S_{\text{fermi}^4}=-\frac{32}{r\ell}\int d^4x\sqrt{|g_4|}\,R_{IJKL}\left(\lambda^I\lambda^J\kappa_\tau^K\kappa^{L\tau}+\frac{1}{4}\zeta^I_{\rho\sigma}\zeta^{J\rho\sigma}\kappa_\tau^K\kappa^{L\tau}\right). \tag{C.129}$$

The final action upon combining all the above terms is

$$\begin{aligned} S=\frac{1}{r\ell}\int d^4x\sqrt{|g_4|}\,\Big[&\frac{1}{4}G_{IJ}g^{\mu\nu}\partial_\mu X^I\partial^\nu X^J+2i\left(G_{IJ}g^{\mu\nu}-\omega^{\mu\nu}_{IJ}\right)(\lambda^I D_\mu\kappa^J_\nu-\zeta^I{}_\mu{}^\sigma\mathcal{D}_\sigma\kappa^J_\nu)\\ &-32R_{IJKL}\left(\lambda^I\lambda^J\kappa_\tau^K\kappa^{L\tau}+\frac{1}{4}\zeta^I_{\rho\sigma}\zeta^{J\rho\sigma}\kappa_\tau^K\kappa^{L\tau}\right)\Big]\,, \end{aligned} \tag{C.130}$$

where

$$D_\mu\kappa^I_\nu=\partial_\mu\kappa^I_\nu+\Gamma^I_{JK}\partial_\mu X^J\kappa^K_\nu\,. \tag{C.131}$$

The action can be further simplified by using relations between the complex structures $\omega_{\mu\nu}{}^I{}_J$ and the fermions (C.110) to eliminate the self-dual two-form $\zeta^I_{\mu\nu}$. In addition we know that the target space $\mathcal{M}_k$ is Hyper-Kähler, which means that the three complex structures $\omega_{\mu\nu}{}^I{}_J$ define covariantly constant on $\mathcal{M}_k$

$$D_I \omega_{\mu\nu}{}^J{}_K = 0\,. \tag{C.132}$$

This in turn implies the relations with the Riemann tensor on $\mathcal{M}_k$

$$R_{IJK}{}^M \omega_{\mu\nu,ML} = R_{IJL}{}^M \omega_{\mu\nu,MK}\,, \tag{C.133}$$

and other relations obtained using the standard symmetries of the Riemann tensor. With (C.110) and (C.133), and after rescaling $\lambda \to \frac{1}{4}\lambda^I$ and $\kappa_\mu \to \frac{i}{16}\kappa_\mu$, the action simplifies to

$$S_{HK} = \frac{1}{4r\ell}\int d^4x\sqrt{|g_4|}\left(G_{IJ}g^{\mu\nu}\partial_\mu X^I \partial_\nu X^J - 2G_{IJ}g^{\mu\nu}\kappa^I_\mu D_\nu \lambda^J + \frac{1}{8}g^{\mu\nu}R_{IJKL}\kappa^I_\mu \kappa^J_\nu \lambda^K \lambda^L\right). \tag{C.134}$$

The constraint on the fermions κ^I_μ can be re-expressed as

$$\kappa^I_\mu + \frac{1}{3}(j^a)_\mu{}^\nu \kappa^J_\nu \omega^a{}_J{}^I = 0\,, \tag{C.135}$$

The supersymmetry transformations are

$$\begin{aligned} \delta X^I &= u\lambda^I \\ \delta\lambda^I &= 0 \\ \delta\kappa^I_\mu &= u\left(\partial_\mu X^I - (j^a)_\mu{}^\nu \partial_\nu X^J \omega^a{}_J{}^I\right) - u\Gamma^I_{JK}\lambda^J\kappa^K_\mu\,. \end{aligned} \tag{C.136}$$

This dimensional reduction of the 5d topologically twisted SYM theory, thus gives precisely the same action we obtained in (6.130), by topologically twisting the 4d sigma-model for Hyper-Kähler M_4.

Bibliography

[1] T. Kaluza, *On the Problem of Unity in Physics*, *Sitzungsber. Preuss. Akad. Wiss. Berlin (Math. Phys.)* **1921** (1921) 966–972. 1

[2] O. Klein, *Quantum Theory and Five-Dimensional Theory of Relativity. (In German and English)*, *Z. Phys.* **37** (1926) 895–906. [Surveys High Energ. Phys.5,241(1986)]. 1

[3] G. Veneziano, *Construction of a crossing - symmetric, Regge behaved amplitude for linearly rising trajectories*, *Nuovo Cim.* **A57** (1968) 190–197. 1

[4] M. B. Green and J. H. Schwarz, *Anomaly Cancellation in Supersymmetric D=10 Gauge Theory and Superstring Theory*, *Phys. Lett.* **B149** (1984) 117–122. 1.1

[5] M. B. Green and J. H. Schwarz, *Supersymmetrical String Theories*, *Phys. Lett.* **B109** (1982) 444–448. 1.1, 1, 2.1

[6] D. J. Gross, J. A. Harvey, E. J. Martinec, and R. Rohm, *The Heterotic String*, *Phys. Rev. Lett.* **54** (1985) 502–505. 1.1, 1

[7] J. Polchinski, *String theory. Vol. 2: Superstring theory and beyond.* Cambridge University Press, 2007. 1, 5

[8] J. Polchinski, *Dirichlet Branes and Ramond-Ramond charges*, *Phys. Rev. Lett.* **75** (1995) 4724–4727, [hep-th/9510017]. 1.1

[9] E. Witten, *Some comments on string dynamics*, in *Future perspectives in string theory. Proceedings, Conference, Strings'95, Los Angeles, USA, March 13-18, 1995*, pp. 501–523, 1995. hep-th/9507121. 1.1, 5, 5.1

[10] C. V. Johnson, *D-branes.* 2003. 1.1

[11] E. Bergshoeff, E. Sezgin, and P. Townsend, *Supermembranes and Eleven-Dimensional Supergravity*, *Phys.Lett.* **B189** (1987) 75–78. 1.1, 5

[12] E. Witten, *String theory dynamics in various dimensions*, *Nucl. Phys.* **B443** (1995) 85–126, [hep-th/9503124]. 1.1

[13] C. M. Hull and P. K. Townsend, *Unity of superstring dualities*, *Nucl. Phys.* **B438** (1995) 109–137, [hep-th/9410167]. 1.1

[14] P. Horava and E. Witten, *Eleven-dimensional supergravity on a manifold with boundary*, *Nucl. Phys.* **B475** (1996) 94–114, [hep-th/9603142]. 1.1, 1

[15] **Particle Data Group** Collaboration, K. Olive et al., *Review of Particle Physics*, *Chin.Phys.* **C38** (2014) 090001. 1.2, 1.2, 4.2.2, 4.2.3, 13

[16] E. Witten, *Dynamical Breaking of Supersymmetry*, *Nucl. Phys.* **B188** (1981) 513. 1.2

[17] S. Dimopoulos and H. Georgi, *Softly Broken Supersymmetry and SU(5)*, *Nucl. Phys.* **B193** (1981) 150–162. 1.2

[18] N. Sakai, *Naturalness in Supersymmetric Guts*, *Z. Phys.* **C11** (1981) 153. 1.2

[19] R. K. Kaul and P. Majumdar, *Cancellation of Quadratically Divergent Mass Corrections in Globally Supersymmetric Spontaneously Broken Gauge Theories*, *Nucl. Phys.* **B199** (1982) 36. 1.2

[20] **ATLAS** Collaboration, G. Aad et al., *Observation of a new particle in the search for the Standard Model Higgs boson with the ATLAS detector at the LHC*, *Phys. Lett.* **B716** (2012) 1–29, [arXiv:1207.7214]. 1.2

[21] **CMS** Collaboration, S. Chatrchyan et al., *Observation of a new boson at a mass of 125 GeV with the CMS experiment at the LHC*, *Phys. Lett.* **B716** (2012) 30–61, [arXiv:1207.7235]. 1.2

[22] **Particle Data Group** Collaboration, C. Patrignani et al., *Review of Particle Physics*, *Chin. Phys.* **C40** (2016), no. 10 100001. 1.2

[23] O. Buchmuller and P. de Jong, *Supersymmetry, Part II (Experiment)*, 2015. http://pdg.lbl.gov/2016/reviews/rpp2016-rev-susy-2-experiment.pdf. 1.2

[24] E. Calabi, *On Kähler Manifolds with Vanishing Canonical Class*, pp. 78–89. Princeton University Press, 1957. 1.2

[25] S.-T. Yau, *On the ricci curvature of a compact kähler manifold and the complex monge-ampre equation, i*, *Communications on Pure and Applied Mathematics* **31** (1978), no. 3 339–411. 1.2

[26] P. Candelas, G. T. Horowitz, A. Strominger, and E. Witten, *Vacuum Configurations for Superstrings*, *Nucl. Phys.* **B258** (1985) 46–74. 1.2

[27] P. Fayet, *Supergauge Invariant Extension of the Higgs Mechanism and a Model for the electron and Its Neutrino*, *Nucl. Phys.* **B90** (1975) 104–124. 1.2

[28] J. F. Gunion and H. E. Haber, *Higgs Bosons in Supersymmetric Models. 1.*, *Nucl. Phys.* **B272** (1986) 1. [Erratum: Nucl. Phys.B402,567(1993)]. 1.2

[29] **Particle Data Group** Collaboration, C. Amsler et al., *Review of particle physics*, *Phys. Lett.* **B667** (2008) 1. 1.2

[30] R. Donagi and M. Wijnholt, *Model Building with F-Theory*, arXiv:0802.2969. 1.2, 2, 2.4, 2.4, 2.4, 3.1, 4.1

[31] C. Beasley, J. J. Heckman, and C. Vafa, *GUTs and Exceptional Branes in F-theory - I*, *JHEP* **01** (2009) 058, [arXiv:0802.3391]. 1.2, 2, 2.4, 3.1, 4.1

[32] C. Lawrie, S. Schafer-Nameki, and J.-M. Wong, *F-theory and All Things Rational: Surveying U(1) Symmetries with Rational Sections*, *JHEP* **09** (2015) 144, [arXiv:1504.0559]. 1.3, 4.1, 4.1, 4.2, 4.2.4, 4.2.4, 3, 4.2.4, 4.7.3, 4.8, 4.4

[33] S. Krippendorf, S. Schafer-Nameki, and J.-M. Wong, *Froggatt-Nielsen meets Mordell-Weil: A Phenomenological Survey of Global F-theory GUTs with U(1)s*, *JHEP* **11** (2015) 008, [arXiv:1507.0596]. 1.3

[34] B. Assel, S. Schafer-Nameki, and J.-M. Wong, *M5-branes on S^2 M_4: Nahms equations and 4d topological sigma-models*, *JHEP* **09** (2016) 120, [arXiv:1604.0360]. 1.3

[35] C. Couzens, C. Lawrie, D. Martelli, S. Schafer-Nameki, and J.-M. Wong, *F-theory and AdS_3/CFT_2*, arXiv:1705.0467. 1.3

[36] C. Vafa, *Evidence for F-Theory*, *Nucl. Phys.* **B469** (1996) 403–418, [hep-th/9602022]. 2, 2.1, 3.1

[37] D. R. Morrison and C. Vafa, *Compactifications of F-Theory on Calabi–Yau Threefolds – I*, *Nucl. Phys.* **B473** (1996) 74–92, [hep-th/9602114]. 2, 2.2, 2.2.3, 2.3

[38] D. R. Morrison and C. Vafa, *Compactifications of F-Theory on Calabi–Yau Threefolds – II*, *Nucl. Phys.* **B476** (1996) 437–469, [hep-th/9603161]. 2, 2.3, 2.3, 3.1, 4.2.4

[39] P. Candelas, E. Perevalov, and G. Rajesh, *F theory duals of nonperturbative heterotic E(8) x E(8) vacua in six-dimensions*, *Nucl. Phys.* **B502** (1997) 613–628, [hep-th/9606133]. 2

[40] G. Lopes Cardoso, G. Curio, D. Lust, and T. Mohaupt, *On the duality between the heterotic string and F theory in eight-dimensions*, *Phys. Lett.* **B389** (1996) 479–484, [hep-th/9609111]. 2

[41] R. Friedman, J. Morgan, and E. Witten, *Vector bundles and F theory*, *Commun.Math.Phys.* **187** (1997) 679–743, [hep-th/9701162]. 2

[42] P. Candelas, E. Perevalov, and G. Rajesh, *Toric geometry and enhanced gauge symmetry of F theory / heterotic vacua*, *Nucl. Phys.* **B507** (1997) 445–474, [hep-th/9704097]. 2

[43] G. Curio and R. Y. Donagi, *Moduli in N=1 heterotic / F theory duality*, *Nucl. Phys.* **B518** (1998) 603–631, [hep-th/9801057]. 2

[44] Z. Kakushadze, G. Shiu, and S. H. H. Tye, *Type IIB orientifolds, F theory, type I strings on orbifolds and type I - Heterotic duality*, *Nucl. Phys.* **B533** (1998) 25–87, [hep-th/9804092]. 2

[45] C. Beasley, J. J. Heckman, and C. Vafa, *GUTs and Exceptional Branes in F-theory - II: Experimental Predictions*, *JHEP* **01** (2009) 059, [arXiv:0806.0102]. 2, 2.4, 2.4, 2.4, 3.1, 4.1, 4.2

[46] J. J. Heckman, D. R. Morrison, and C. Vafa, *On the Classification of 6D SCFTs and Generalized ADE Orbifolds*, *JHEP* **05** (2014) 028, [arXiv:1312.5746]. [Erratum: JHEP06,017(2015)]. 2, 5.1

[47] J. J. Heckman, D. R. Morrison, T. Rudelius, and C. Vafa, *Atomic Classification of 6D SCFTs*, *Fortsch. Phys.* **63** (2015) 468–530, [arXiv:1502.0540]. 2, 5.1

[48] I. Garca-Etxebarria and D. Regalado, $\mathcal{N} = 3$ *four dimensional field theories*, *JHEP* **03** (2016) 083, [arXiv:1512.0643]. 2

[49] S. Schafer-Nameki and T. Weigand, *F-theory and 2d* $(0, 2)$ *theories*, *JHEP* **05** (2016) 059, [arXiv:1601.0201]. 3, 2

[50] F. Apruzzi, F. Hassler, J. J. Heckman, and I. V. Melnikov, *UV Completions for Non-Critical Strings*, arXiv:1602.0422. 3, 2

[51] C. Lawrie, S. Schafer-Nameki, and T. Weigand, *The Gravitational Sector of 2d (0,2) F-theory Vacua*, *JHEP* **05** (2017) 103, [arXiv:1612.0639]. 3

[52] P. Deligne, *Courbes elliptiques: formulaire d'aprés J.Tate*, in *Modular functions of one variable, IV (Proc. Internat. Summer School, Univ. Antwerp, Antwerp, 1972)*, vol. 476 of *Lecture Notes in Math.*, pp. 53–73. Springer, Berlin, 1975. 2.2

[53] J. H. Silverman, *The arithmetic of elliptic curves*, vol. 106 of *Graduate Texts in Mathematics*, pp. xx+513. Springer, Dordrecht, second ed., 2009. 2.2

[54] O. Debarre, *Higher-dimensional algebraic geometry*. Universitext. Springer-Verlag, New York, 2001. 4, 3.2.2

[55] J. Kollár, *Lectures on Resolution of Singularities*. Princeton University Press, 2007. 2.2.1

[56] S. Ishii, *Introduction to Singularities*. Springer, Japan, 2014. 2.2.1

[57] Y. Kawamata, *Flops connect minimal models*, *Publ. Res. Inst. Math. Sci.* **44** (2008) 419–423. 2.2.1

[58] J. Kollár, *Flip and flop*, *In: Proc. of the ICM, Kyoto 1990. Mathematical Soc. of Japan* (1991) 709–714. 2.2.1

[59] K. Kodaira, *On the structure of compact complex analytic surfaces. II, III*, vol. 88 of *Amer. J. Math.*, pp. 682–721. 1966. 2.2.2, 2.2.2, 3.1, 3.2.1

[60] K. Kodaira, *On the structure of compact complex analytic surfaces. I*, vol. 86 of *Amer. J. Math.*, pp. 751–798. 1964. 2.2.2, 2.2.2, 3.1, 3.2.1

[61] A. Néron, *Modèles minimaux des variétés abéliennes sur les corps locaux et globaux*, *Inst. Hautes Études Sci. Publ.Math. No.* **21** (1964) 128. 2.2.2, 2.2.2, 3.1, 3.2.1

[62] J. Tate, *Algorithm for determining the type of a singular fiber in an elliptic pencil*, *Modular functions of one variable, IV (Proc. Internat. Summer School, Univ. Antwerp, Antwerp, 1972), Lecture Notes in Math.* **476** (1975) 33–52. 2.2.2, 2.2.2

[63] M. Bershadsky, K. A. Intriligator, S. Kachru, D. R. Morrison, V. Sadov, et al., *Geometric singularities and enhanced gauge symmetries*, *Nucl.Phys.* **B481** (1996) 215–252, [hep-th/9605200]. 2.2.2, 2.2.3, 3.1

[64] S. Katz, D. R. Morrison, S. Schafer-Nameki, and J. Sully, *Tate's algorithm and F-theory*, *JHEP* **1108** (2011) 094, [arXiv:1106.3854]. 2.2.2, 2.2.3, 2.2.4, 3.1, 4.7.2, 4.7.2

[65] H. Hayashi, C. Lawrie, and S. Schafer-Nameki, *Phases, Flops and F-theory: SU(5) Gauge Theories*, *JHEP* **1310** (2013) 046, [arXiv:1304.1678]. 2.2.3, 2.3, 3.1, 3.2.1, 3.6, 3.10

[66] M. Kuntzler and C. Lawrie, *Smooth: A Mathematica package for studying resolutions of singular fibrations, Version 0.4*, . 2.2.3, 4.7.2

[67] E. Witten, *Nonperturbative superpotentials in string theory*, *Nucl.Phys.* **B474** (1996) 343–360, [hep-th/9604030]. 2.2.4

[68] S. H. Katz and C. Vafa, *Matter from geometry*, *Nucl.Phys.* **B497** (1997) 146–154, [hep-th/9606086]. 2.2.5

[69] J. Marsano and S. Schafer-Nameki, *Yukawas, G-flux, and Spectral Covers from Resolved Calabi-Yau's*, *JHEP* **1111** (2011) 098, [arXiv:1108.1794]. 2.3, 2.2.5, 3.8.1

[70] H. Hayashi, C. Lawrie, D. R. Morrison, and S. Schafer-Nameki, *Box Graphs and Singular Fibers*, *JHEP* **1405** (2014) 048, [arXiv:1402.2653]. 2.2.5, 3.1, 3.1, 3.2, 3.2.1, 3.2.1, 3.2.1, 3.2.1, 3.2.1, 3.2.2, 6, 3.2.3, 3.2.3, 12, 3.4.7, 3.6, 3.6.1, 3.8.1, 3.8.1, 3.10, 4.1, 4.2.4, 4.4, 7, A.1

[71] C. Lawrie and S. Schafer-Nameki, *The Tate Form on Steroids: Resolution and Higher Codimension Fibers*, *JHEP* **1304** (2013) 061, [arXiv:1212.2949]. 2.2.5, 3.8.1

[72] L. J. Mordell, *Diophantine equations*. Pure and Applied Mathematics, Vol. 30. Academic Press, London-New York, 1969. 2.3, B.3, B.3.1, B.3.2

[73] A. Weil, *L'arithmétique sur les courbes algébriques*, vol. 52 of *Acta Math.*, pp. 281–315. 1929. 2.3

[74] L. E. Ibanez and G. G. Ross, *Discrete gauge symmetries and the origin of baryon and lepton number conservation in supersymmetric versions of the standard model*, *Nucl.Phys.* **B368** (1992) 3–37. 2.3, 3.10, 4.2.2, B.3

[75] V. Braun and D. R. Morrison, *F-theory on Genus-One Fibrations*, *JHEP* **1408** (2014) 132, [arXiv:1401.7844]. 2.3, 3.9.2, 15

[76] D. R. Morrison and W. Taylor, *Sections, multisections, and U(1) fields in F-theory*, arXiv:1404.1527. 2.3, 3.1, 15, 3.10, 4.1

[77] L. B. Anderson, I. Garca-Etxebarria, T. W. Grimm, and J. Keitel, *Physics of F-theory compactifications without section*, *JHEP* **1412** (2014) 156, [arXiv:1406.5180]. 2.3, 3.9.2, 15

[78] I. Garca-Etxebarria, T. W. Grimm, and J. Keitel, *Yukawas and discrete symmetries in F-theory compactifications without section*, *JHEP* **1411** (2014) 125, [arXiv:1408.6448]. 2.3, 3.9.2, 15

[79] C. Mayrhofer, E. Palti, O. Till, and T. Weigand, *Discrete Gauge Symmetries by Higgsing in four-dimensional F-Theory Compactifications*, *JHEP* **1412** (2014) 068, [arXiv:1408.6831]. 2.3, 3.1, 3.7, 3.9.2

[80] C. Mayrhofer, E. Palti, O. Till, and T. Weigand, *On Discrete Symmetries and Torsion Homology in F-Theory*, arXiv:1410.7814. 2.3, 3.1, 3.7, 3.9.2

[81] M. Cvetic, R. Donagi, D. Klevers, H. Piragua, and M. Poretschkin, *F-Theory Vacua with Z_3 Gauge Symmetry*, arXiv:1502.0695. 2.3, 3.1, 3.7, 3.9.2, 3.9.2, 3.10

[82] M. Cvetic, A. Grassi, and M. Poretschkin, *Discrete Symmetries in Heterotic/F-theory Duality and Mirror Symmetry*, arXiv:1607.0317. 2.3

[83] H. Hayashi, R. Tatar, Y. Toda, T. Watari, and M. Yamazaki, *New Aspects of Heterotic–F Theory Duality*, *Nucl. Phys.* **B806** (2009) 224–299, [arXiv:0805.1057]. 2.4

[84] R. Donagi and M. Wijnholt, *Breaking GUT Groups in F-Theory*, arXiv:0808.2223. 2.4, 2.4, 2.4, 4.1, 4.2

[85] J. Marsano, H. Clemens, T. Pantev, S. Raby, and H.-H. Tseng, *A Global SU(5) F-theory model with Wilson line breaking*, *JHEP* **01** (2013) 150, [arXiv:1206.6132]. 2.4, 4.1

[86] R. Tatar and T. Watari, *GUT Relations from String Theory Compactifications*, *Nucl. Phys.* **B810** (2009) 316–353, [arXiv:0806.0634]. 2.4

[87] M. Buican, D. Malyshev, D. R. Morrison, H. Verlinde, and M. Wijnholt, *D-branes at singularities, compactification, and hypercharge*, *JHEP* **01** (2007) 107, [hep-th/0610007]. 2.4, 4.1

[88] E. Witten, *On flux quantization in M-theory and the effective action*, *J. Geom. Phys.* **22** (1997) 1–13, [hep-th/9609122]. 2.4

[89] R. Friedman, *On threefolds with trivial canonical bundle*, in *Complex geometry and Lie theory (Sundance, UT, 1989)*, vol. 53 of *Proc. Sympos. Pure Math.*, pp. 103–134. Amer. Math. Soc., Providence, RI, 1991. 2.4

[90] A. Kanazawa and P. M. H. Wilson, *Trilinear forms and Chern classes of Calabi-Yau threefolds*, *Osaka J. Math.* **51** (2014), no. 1 203–213. 2.4

[91] D. R. Morrison and D. S. Park, *F-Theory and the Mordell-Weil Group of Elliptically-Fibered Calabi-Yau Threefolds*, *JHEP* **1210** (2012) 128, [arXiv:1208.2695]. 3.1, 3.4.2, 3.4.7, 3.7.2, 3.10, 4.1

[92] J. Borchmann, C. Mayrhofer, E. Palti, and T. Weigand, *Elliptic fibrations for SU(5) x U(1) x U(1) F-theory vacua*, *Phys.Rev.* **D88** (2013) 046005, [arXiv:1303.5054]. 3.1, 3.10, 4.1, 4.4, 4.4

[93] M. Cvetic, D. Klevers, and H. Piragua, *F-Theory Compactifications with Multiple U(1)-Factors: Constructing Elliptic Fibrations with Rational Sections*, *JHEP* **1306** (2013) 067, [arXiv:1303.6970]. 3.1, 3.4.3, 3.10, 4.1, 4.4, 4.4

[94] J. Borchmann, C. Mayrhofer, E. Palti, and T. Weigand, *SU(5) Tops with Multiple U(1)s in F-theory*, *Nucl.Phys.* **B882** (2014) 1–69, [arXiv:1307.2902]. 3.1, 3.10, 4.1, 4.4, 4.4

[95] M. Cvetic, D. Klevers, and H. Piragua, *F-Theory Compactifications with Multiple U(1)-Factors: Addendum*, *JHEP* **1312** (2013) 056, [arXiv:1307.6425]. 3.1, 3.10, 4.1, 4.4, 4.4

[96] M. Cvetic, D. Klevers, H. Piragua, and P. Song, *Elliptic Fibrations with Rank Three Mordell-Weil Group: F-theory with U(1) x U(1) x U(1) Gauge Symmetry*, arXiv:1310.0463. 3.1, 3.10, 4.1

[97] V. Braun, T. W. Grimm, and J. Keitel, *New Global F-theory GUTs with U(1) symmetries*, *JHEP* **1309** (2013) 154, [arXiv:1302.1854]. 3.1, 3.4.3, 3.7.2, 3.10, 4.1, 4.7.3

[98] V. Braun, T. W. Grimm, and J. Keitel, *Geometric Engineering in Toric F-Theory and GUTs with U(1) Gauge Factors*, *JHEP* **1312** (2013) 069, [arXiv:1306.0577]. 3.1, 3.10, 4.1

[99] V. Braun, T. W. Grimm, and J. Keitel, *Complete Intersection Fibers in F-Theory*, *JHEP* **1503** (2015) 125, [arXiv:1411.2615]. 3.1, 3.10, 4.1

[100] D. Klevers, D. K. Mayorga Pena, P.-K. Oehlmann, H. Piragua, and J. Reuter, *F-Theory on all Toric Hypersurface Fibrations and its Higgs Branches*, *JHEP* **1501** (2015) 142, [arXiv:1408.4808]. 3.1, 3.7.2, 15, 3.10, 4.1

[101] T. W. Grimm and T. Weigand, *On Abelian Gauge Symmetries and Proton Decay in Global F-theory GUTs*, *Phys.Rev.* **D82** (2010) 086009, [arXiv:1006.0226]. 3.1, 3.10, 4.1, 2

[102] A. P. Braun, A. Collinucci, and R. Valandro, *G-flux in F-theory and algebraic cycles*, *Nucl.Phys.* **B856** (2012) 129–179, [arXiv:1107.5337]. 3.1, 3.10, 4.1

[103] C. Mayrhofer, E. Palti, and T. Weigand, *U(1) symmetries in F-theory GUTs with multiple sections*, *JHEP* **1303** (2013) 098, [arXiv:1211.6742]. 3.1, 3.7.2, 3.10, 4.1

[104] M. J. Dolan, J. Marsano, N. Saulina, and S. Schafer-Nameki, *F-theory GUTs with U(1) Symmetries: Generalities and Survey*, arXiv:1102.0290. 3.1, 3.10, 4.1, 4.2, 4.2.1

[105] F. Baume, E. Palti, and S. Schwieger, *On E_8 and F-Theory GUTs*, arXiv:1502.0387. 3.1, 3.1, 3.4.6, 3.10, 4.1, A.2, A.2, A.2

[106] M. J. Dolan, J. Marsano, and S. Schafer-Nameki, *Unification and Phenomenology of F-Theory GUTs with $U(1)_{PQ}$*, *JHEP* **1112** (2011) 032, [arXiv:1109.4958]. 3.1, 3.10, 4.1

[107] M. Kuntzler and S. Schafer-Nameki, *Tate Trees for Elliptic Fibrations with Rank one Mordell-Weil group*, arXiv:1406.5174. 3.1, 3.4.2, 3.10, 4.1, 4.7.2, 4.7.2

[108] C. Lawrie and D. Sacco, *Tates algorithm for F-theory GUTs with two U(1)s*, *JHEP* **1503** (2015) 055, [arXiv:1412.4125]. 3.1, 3.10, 4.1, 4.4, 4.4, 4.7.2, 4.7.2, 4.7.2

[109] K. A. Intriligator, D. R. Morrison, and N. Seiberg, *Five-dimensional supersymmetric gauge theories and degenerations of Calabi-Yau spaces*, *Nucl.Phys.* **B497** (1997) 56–100, [hep-th/9702198]. 3.1, 3.2.1

[110] O. Aharony, A. Hanany, K. A. Intriligator, N. Seiberg, and M. Strassler, *Aspects of N=2 supersymmetric gauge theories in three-dimensions*, *Nucl.Phys.* **B499** (1997) 67–99, [hep-th/9703110]. 3.1, 3.2.1

[111] J. de Boer, K. Hori, and Y. Oz, *Dynamics of N=2 supersymmetric gauge theories in three-dimensions*, *Nucl.Phys.* **B500** (1997) 163–191, [hep-th/9703100]. 3.1, 3.2.1

[112] D.-E. Diaconescu and S. Gukov, *Three-dimensional N=2 gauge theories and degenerations of Calabi-Yau four folds*, *Nucl.Phys.* **B535** (1998) 171–196, [hep-th/9804059]. 3.1, 3.2.1

[113] T. W. Grimm and H. Hayashi, *F-theory fluxes, Chirality and Chern-Simons theories*, *JHEP* **1203** (2012) 027, [arXiv:1111.1232]. 3.1, 3.2.1

[114] T. Shioda, *Mordell-Weil lattices and Galois representation. I*, *Proc. Japan Acad. Ser. A Math. Sci.* **65** (1989), no. 7 268–271. 3.1

[115] N. Nakayama, *On Weierstrass models*, in *Algebraic geometry and commutative algebra, Vol. II*, pp. 405–431. Kinokuniya, Tokyo, 1988. 3.2.2

[116] C. Lawrie and S. Schafer-Nameki, *In progress*, . 3.2.2

[117] T. W. Grimm, A. Kapfer, and J. Keitel, *Effective action of 6D F-Theory with U(1) factors: Rational sections make Chern-Simons terms jump*, *JHEP* **1307** (2013) 115, [arXiv:1305.1929]. 7

[118] T. W. Grimm and A. Kapfer, *Anomaly Cancelation in Field Theory and F-theory on a Circle*, arXiv:1502.0539. 7

[119] S. Katz, *Rational curves on Calabi-Yau threefolds*, in *Essays on mirror manifolds*, pp. 168–180. Int. Press, Hong Kong, 1992. 3.3.1

[120] A. Grothendieck, *Sur la classification des fibrés holomorphes sur la sphère de Riemann*, *Amer. J. Math.* **79** (1957) 121–138. 3.3.1

[121] A. Grothendieck, *Éléments de géométrie algébrique. IV. Étude locale des schémas et des morphismes de schémas. I*, *Inst. Hautes Études Sci. Publ. Math.* (1964), no. 20 259. 3.3.1, 3.3.3

[122] D. Eisenbud and J. Harris, *3264 & All That Intersection Theory in Algebraic Geometry*, . 3.3.1

[123] R. Miranda, *The basic theory of elliptic surfaces*. Dottorato di Ricerca in Matematica. ETS Editrice, Pisa, 1989. 3.3.2

[124] M. Reid, *Minimal models of canonical 3-folds*, in *Algebraic varieties and analytic varieties (Tokyo, 1981)*, vol. 1 of *Adv. Stud. Pure Math.*, pp. 131–180. North-Holland, Amsterdam, 1983. 3.3.2, 3.6.1, 3.7.3

[125] H. B. Laufer, *On* $\mathbf{C}P^1$ *as an exceptional set*, in *Recent developments in several complex variables (Proc. Conf., Princeton Univ., Princeton, N. J., 1979)*, vol. 100 of *Ann. of Math. Stud.*, pp. 261–275. Princeton Univ. Press, Princeton, N.J., 1981. 3.3.2, 3.7.3

[126] A. P. Braun and S. Schafer-Nameki, *Box Graphs and Resolutions I*, *Nucl. Phys.* **B905** (2016) 447–479, [arXiv:1407.3520]. 3.6, 3.8.1

[127] M. Esole, S.-H. Shao, and S.-T. Yau, *Singularities and Gauge Theory Phases II*, arXiv:1407.1867. 3.6

[128] A. P. Braun and S. Schafer-Nameki, *Box Graphs and Resolutions II: From Coulomb Phases to Fiber Faces*, *Nucl. Phys.* **B905** (2016) 480–530, [arXiv:1511.0180]. 3.6, 3.8.1

[129] K. Matsuki, *Introduction to the Mori program*. Universitext. Springer-Verlag, New York, 2002. 3.6

[130] K. Matsuki, *Weyl groups and birational transformations among minimal models*, *Mem. Amer. Math. Soc.* **116** (1995), no. 557 vi+133. 3.6

[131] M. Esole and S.-T. Yau, *Small resolutions of SU(5)-models in F-theory*, arXiv:1107.0733. 3.8.1

[132] S. Krippendorf, D. K. M. Pena, P.-K. Oehlmann, and F. Ruehle, *Rational F-Theory GUTs without exotics*, arXiv:1401.5084. 3.10, 4.1

[133] M. Cvetic, D. Klevers, H. Piragua, and W. Taylor, *General U(1)U(1) F-theory compactifications and beyond: geometry of unHiggsings and novel matter structure*, *JHEP* **11** (2015) 204, [arXiv:1507.0595]. 4.1, 9, 4.7.2

[134] E. Dudas and E. Palti, *On hypercharge flux and exotics in F-theory GUTs*, *JHEP* **09** (2010) 013, [arXiv:1007.1297]. 4.1, 4.2, 4.2.1

[135] J. Marsano, *Hypercharge Flux, Exotics, and Anomaly Cancellation in F-theory GUTs*, *Phys.Rev.Lett.* **106** (2011) 081601, [arXiv:1011.2212]. 4.1, 4.2, 4.2.1

[136] E. Palti, *A Note on Hypercharge Flux, Anomalies, and U(1)s in F-theory GUTs*, *Phys.Rev.* **D87** (2013), no. 8 085036, [arXiv:1209.4421]. 4.1, 4.2, 4.2.1

[137] J. Marsano, N. Saulina, and S. Schafer-Nameki, *Monodromies, Fluxes, and Compact Three-Generation F-theory GUTs*, *JHEP* **08** (2009) 046, [arXiv:0906.4672]. 4.1

[138] J. Marsano, N. Saulina, and S. Schafer-Nameki, *Compact F-theory GUTs with $U(1)_{PQ}$*, *JHEP* **04** (2010) 095, [arXiv:0912.0272]. 4.1

[139] H. Hayashi, T. Kawano, Y. Tsuchiya, and T. Watari, *More on Dimension-4 Proton Decay Problem in F-theory – Spectral Surface, Discriminant Locus and Monodromy*, *Nucl.Phys.* **B840** (2010) 304–348, [arXiv:1004.3870]. 4.1

[140] H. Hayashi, T. Kawano, R. Tatar, and T. Watari, *Codimension-3 Singularities and Yukawa Couplings in F-theory*, *Nucl.Phys.* **B823** (2009) 47–115, [arXiv:0901.4941]. 4.1

[141] J. J. Heckman and C. Vafa, *Flavor Hierarchy From F-theory*, *Nucl.Phys.* **B837** (2010) 137–151, [arXiv:0811.2417]. 4.1

[142] A. Font and L. E. Ibanez, *Yukawa Structure from U(1) Fluxes in F-theory Grand Unification*, *JHEP* **02** (2009) 016, [arXiv:0811.2157]. 4.1

[143] R. Tatar, Y. Tsuchiya, and T. Watari, *Right-handed Neutrinos in F-theory Compactifications*, *Nucl.Phys.* **B823** (2009) 1–46, [arXiv:0905.2289]. 4.1

[144] V. Bouchard, J. J. Heckman, J. Seo, and C. Vafa, *F-theory and Neutrinos: Kaluza-Klein Dilution of Flavor Hierarchy*, *JHEP* **1001** (2010) 061, [arXiv:0904.1419]. 4.1

[145] F. Marchesano and L. Martucci, *Non-perturbative effects on seven-brane Yukawa couplings*, *Phys. Rev. Lett.* **104** (2010) 231601, [arXiv:0910.5496]. 4.1

[146] H. Hayashi, T. Kawano, Y. Tsuchiya, and T. Watari, *Flavor Structure in F-theory Compactifications*, arXiv:0910.2762. 4.1

[147] J. P. Conlon and E. Palti, *Aspects of Flavour and Supersymmetry in F-theory GUTs*, arXiv:0910.2413. 4.1

[148] S. Cecotti, M. C. N. Cheng, J. J. Heckman, and C. Vafa, *Yukawa Couplings in F-theory and Non-Commutative Geometry*, arXiv:0910.0477. 4.1

[149] S. F. King, G. K. Leontaris, and G. G. Ross, *Family symmetries in F-theory GUTs*, *Nucl. Phys.* **B838** (2010) 119–135, [arXiv:1005.1025]. 4.1

[150] G. K. Leontaris and G. G. Ross, *Yukawa couplings and fermion mass structure in F-theory GUTs*, *JHEP* **02** (2011) 108, [arXiv:1009.6000]. 4.1

[151] P. G. Camara, E. Dudas, and E. Palti, *Massive wavefunctions, proton decay and FCNCs in local F-theory GUTs*, *JHEP* **12** (2011) 112, [arXiv:1110.2206]. 4.1

[152] C. Ludeling, H. P. Nilles, and C. C. Stephan, *The Potential Fate of Local Model Building*, *Phys.Rev.* **D83** (2011) 086008, [arXiv:1101.3346]. 4.1

[153] L. Aparicio, A. Font, L. E. Ibanez, and F. Marchesano, *Flux and Instanton Effects in Local F-theory Models and Hierarchical Fermion Masses*, *JHEP* **08** (2011) 152, [arXiv:1104.2609]. 4.1

[154] A. Font, L. E. Ibanez, F. Marchesano, and D. Regalado, *Non-perturbative effects and Yukawa hierarchies in F-theory SU(5) Unification*, *JHEP* **1303** (2013) 140, [arXiv:1211.6529]. 4.1

[155] A. Font, F. Marchesano, D. Regalado, and G. Zoccarato, *Up-type quark masses in SU(5) F-theory models*, *JHEP* **1311** (2013) 125, [arXiv:1307.8089]. 4.1

[156] F. Marchesano, D. Regalado, and G. Zoccarato, *Yukawa hierarchies at the point of E_8 in F-theory*, *JHEP* **04** (2015) 179, [arXiv:1503.0268]. 4.1, 4.3

[157] J. J. Heckman, *Particle Physics Implications of F-theory*, *Ann. Rev. Nucl. Part. Sci.* **60** (2010) 237–265, [arXiv:1001.0577]. 4.1

[158] A. Maharana and E. Palti, *Models of Particle Physics from Type IIB String Theory and F-theory: A Review*, *Int.J.Mod.Phys.* **A28** (2013) 1330005, [arXiv:1212.0555]. 4.1

[159] E. Dudas and E. Palti, *Froggatt-Nielsen models from E(8) in F-theory GUTs*, *JHEP* **1001** (2010) 127, [arXiv:0912.0853]. 4.1, 4.2.3, 4.5.1, 4.5.1, B.4.2, B.4.2

[160] L. Lin and T. Weigand, *Towards the Standard Model in F-theory*, *Fortsch. Phys.* **63** (2015), no. 2 55–104, [arXiv:1406.6071]. 4.1

[161] A. Grassi, J. Halverson, J. Shaneson, and W. Taylor, *Non-Higgsable QCD and the Standard Model Spectrum in F-theory*, *JHEP* **01** (2015) 086, [arXiv:1409.8295]. 4.1

[162] M. Cvetic, D. Klevers, D. K. M. Pena, P.-K. Oehlmann, and J. Reuter, *Three-Family Particle Physics Models from Global F-theory Compactifications*, *JHEP* **08** (2015) 087, [arXiv:1503.0206]. 4.1

[163] J. Marsano, N. Saulina, and S. Schafer-Nameki, *F-theory Compactifications for Supersymmetric GUTs*, *JHEP* **08** (2009) 030, [arXiv:0904.3932]. 2

[164] R. Blumenhagen, T. W. Grimm, B. Jurke, and T. Weigand, *Global F-theory GUTs*, *Nucl.Phys.* **B829** (2010) 325–369, [arXiv:0908.1784]. 2

[165] A. P. Braun, A. Collinucci, and R. Valandro, *Hypercharge flux in F-theory and the stable Sen limit*, *JHEP* **07** (2014) 121, [arXiv:1402.4096]. 2

[166] G. Giudice and A. Masiero, *A Natural Solution to the mu Problem in Supergravity Theories*, *Phys.Lett.* **B206** (1988) 480–484. 4.2.2

[167] J. E. Kim and H. P. Nilles, *The mu Problem and the Strong CP Problem*, *Phys.Lett.* **B138** (1984) 150. 4.2.2

[168] J. Marsano, N. Saulina, and S. Schafer-Nameki, *Gauge Mediation in F-Theory GUT Models*, *Phys. Rev.* **D80** (2009) 046006, [arXiv:0808.1571]. 4.2.2

[169] H. Baer and X. Tata, *Weak Scale Supersymmetry*. Cambridge University Press, Cambridge, 1996. 4.2.2

[170] I. Hinchliffe and T. Kaeding, *B+L violating couplings in the minimal supersymmetric Standard Model*, *Phys.Rev.* **D47** (1993) 279–284. 4.2.2, 4.2.2

[171] A. Y. Smirnov and F. Vissani, *Large R-parity violating couplings and grand unification*, *Nucl.Phys.* **B460** (1996) 37–56, [hep-ph/9506416]. 4.2.2

[172] R. Barbier, C. Berat, M. Besancon, M. Chemtob, A. Deandrea, et al., *R-parity violating supersymmetry*, *Phys.Rept.* **420** (2005) 1–202, [hep-ph/0406039]. 4.2.2, 4.2.2

[173] C. D. Froggatt and H. B. Nielsen, *Hierarchy of Quark Masses, Cabibbo Angles and CP Violation*, *Nucl. Phys.* **B147** (1979) 277. 4.2.3

[174] S. Weinberg, *Electromagnetic and weak masses*, *Phys.Rev.Lett.* **29** (1972) 388–392. 4.2.3

[175] A. Lahanas and D. Wyler, *Radiative Fermion Masses and Supersymmetry*, *Phys.Lett.* **B122** (1983) 258. 4.2.3

[176] G. Ross and M. Serna, *Unification and fermion mass structure*, *Phys.Lett.* **B664** (2008) 97–102, [arXiv:0704.1248]. 4.2.3, 4.2.3, 4.5.1, 4.5.1, B.4.1, B.4.1

[177] P. Ramond, R. Roberts, and G. G. Ross, *Stitching the Yukawa quilt*, *Nucl.Phys.* **B406** (1993) 19–42, [hep-ph/9303320]. 4.2.3, 4.2.3

[178] Y. Nir, *Gauge unification, Yukawa hierarchy and the mu problem*, *Phys.Lett.* **B354** (1995) 107–110, [hep-ph/9504312]. 4.2.3

[179] L. Wolfenstein, *Parametrization of the Kobayashi-Maskawa Matrix*, *Phys.Rev.Lett.* **51** (1983) 1945. 4.2.3

[180] L. E. Ibanez and G. G. Ross, *Fermion masses and mixing angles from gauge symmetries*, *Phys.Lett.* **B332** (1994) 100–110, [hep-ph/9403338]. 4.2.3

[181] H. K. Dreiner and M. Thormeier, *Supersymmetric Froggatt-Nielsen models with baryon and lepton number violation*, *Phys.Rev.* **D69** (2004) 053002, [hep-ph/0305270]. 4.2.3, 4.5.1

[182] N. Haba, *Composite model with neutrino large mixing*, *Phys. Rev.* **D59** (1999) 035011, [hep-ph/9807552]. 4.2.3, 4.2.3, 4.5, 4.5.1, 4.5.1, 4.5.2, 4.4, 4.6.1

[183] K. S. Babu, T. Enkhbat, and I. Gogoladze, *Anomalous U(1) symmetry and lepton flavor violation*, *Nucl. Phys.* **B678** (2004) 233–257, [hep-ph/0308093]. 4.2.3, 4.2.3, 4.5, 4.5.1, 4.5.1, 4.5.3, 4.6.1, 4.6.2

[184] L. J. Hall and A. Rasin, *On the generality of certain predictions for quark mixing*, *Phys.Lett.* **B315** (1993) 164–169, [hep-ph/9303303]. 4.5.3

[185] E. Dudas, S. Pokorski, and C. A. Savoy, *Yukawa matrices from a spontaneously broken Abelian symmetry*, *Phys.Lett.* **B356** (1995) 45–55, [hep-ph/9504292]. 4.5.3

[186] S. Antusch, J. Kersten, M. Lindner, M. Ratz, and M. A. Schmidt, *Running neutrino mass parameters in see-saw scenarios*, *JHEP* **03** (2005) 024, [hep-ph/0501272]. 4.6.1

[187] N. Haba and H. Murayama, *Anarchy and hierarchy*, *Phys.Rev.* **D63** (2001) 053010, [hep-ph/0009174]. 4.6.2

[188] D. R. Morrison and W. Taylor, *Non-Higgsable clusters for 4D F-theory models*, *JHEP* **05** (2015) 080, [arXiv:1412.6112]. 4.8

[189] J. Halverson and W. Taylor, $\mathbb{P}^1$*-bundle bases and the prevalence of non-Higgsable structure in 4D F-theory models*, arXiv:1506.0320. 4.8

[190] J. W. van Holten and A. Van Proeyen, *N=1 Supersymmetry Algebras in D=2, D=3, D=4 MOD-8*, *J. Phys.* **A15** (1982) 3763. 5

[191] J. Labastida and M. Marino, *Topological quantum field theory and four manifolds*. 2005. 5

[192] P. K. Townsend, *The eleven-dimensional supermembrane revisited*, *Phys. Lett.* **B350** (1995) 184–187, [hep-th/9501068]. 5, 5.2

[193] P. K. Townsend, *D-branes from M-branes*, *Phys. Lett.* **B373** (1996) 68–75, [hep-th/9512062]. 5

[194] J. H. Schwarz, *Lectures on superstring and M theory dualities: Given at ICTP Spring School and at TASI Summer School*, *Nucl. Phys. Proc. Suppl.* **55B** (1997) 1–32, [hep-th/9607201]. 5

[195] J. Bagger and N. Lambert, *Gauge symmetry and supersymmetry of multiple M2-branes*, *Phys. Rev.* **D77** (2008) 065008, [arXiv:0711.0955]. 5

[196] A. Gustavsson, *Algebraic structures on parallel M2-branes*, *Nucl. Phys.* **B811** (2009) 66–76, [arXiv:0709.1260]. 5

[197] O. Aharony, O. Bergman, D. L. Jafferis, and J. Maldacena, *N=6 superconformal Chern-Simons-matter theories, M2-branes and their gravity duals*, *JHEP* **0810** (2008) 091, [arXiv:0806.1218]. 5

[198] R. Gueven, *Black p-brane solutions of D = 11 supergravity theory*, *Phys. Lett.* **B276** (1992) 49–55. 5

[199] C. G. Callan, Jr., J. A. Harvey, and A. Strominger, *Worldbrane actions for string solitons*, *Nucl. Phys.* **B367** (1991) 60–82. 5

[200] W. Nahm, *Supersymmetries and their Representations*, *Nucl. Phys.* **B135** (1978) 149. 5.1

[201] P. S. Howe and E. Sezgin, *D = 11, p = 5*, *Phys. Lett.* **B394** (1997) 62–66, [hep-th/9611008]. 5.1, 6.1, 6.2.3

[202] P. S. Howe, E. Sezgin, and P. C. West, *Covariant field equations of the M theory five-brane*, *Phys. Lett.* **B399** (1997) 49–59, [hep-th/9702008]. 5.1, 6.1, 6.2.3

[203] M. Perry and J. H. Schwarz, *Interacting chiral gauge fields in six-dimensions and Born-Infeld theory*, *Nucl. Phys.* **B489** (1997) 47–64, [hep-th/9611065]. 5.1

[204] P. Pasti, D. P. Sorokin, and M. Tonin, *Covariant action for a D = 11 five-brane with the chiral field*, *Phys. Lett.* **B398** (1997) 41–46, [hep-th/9701037]. 5.1

[205] M. Aganagic, J. Park, C. Popescu, and J. H. Schwarz, *World volume action of the M theory five-brane*, *Nucl. Phys.* **B496** (1997) 191–214, [hep-th/9701166]. 5.1

[206] I. A. Bandos, K. Lechner, A. Nurmagambetov, P. Pasti, D. P. Sorokin, and M. Tonin, *Covariant action for the superfive-brane of M theory*, *Phys. Rev. Lett.* **78** (1997) 4332–4334, [hep-th/9701149]. 5.1

[207] P.-M. Ho and Y. Matsuo, *M5 from M2*, *JHEP* **06** (2008) 105, [arXiv:0804.3629]. 5.1

[208] P.-M. Ho, Y. Imamura, Y. Matsuo, and S. Shiba, *M5-brane in three-form flux and multiple M2-branes*, *JHEP* **08** (2008) 014, [arXiv:0805.2898]. 5.1

[209] C.-N. Yang and R. L. Mills, *Conservation of Isotopic Spin and Isotopic Gauge Invariance*, *Phys. Rev.* **96** (1954) 191–195. 5.1

[210] N. Lambert and C. Papageorgakis, *Nonabelian (2,0) Tensor Multiplets and 3-algebras*, *JHEP* **08** (2010) 083, [arXiv:1007.2982]. 5.1

[211] D. S. Berman, *M-theory branes and their interactions*, *Phys. Rept.* **456** (2008) 89–126, [arXiv:0710.1707]. 5.1

[212] N. Seiberg, *Notes on theories with 16 supercharges*, *Nucl. Phys. Proc. Suppl.* **67** (1998) 158–171, [hep-th/9705117]. 5.2

[213] M. R. Douglas, *On D=5 super Yang-Mills theory and (2,0) theory*, *JHEP* **02** (2011) 011, [arXiv:1012.2880]. 5.2, 5.2

[214] N. Lambert, C. Papageorgakis, and M. Schmidt-Sommerfeld, *M5-Branes, D4-Branes and Quantum 5D super-Yang-Mills*, *JHEP* **01** (2011) 083, [arXiv:1012.2882]. 5.2

[215] E. Witten, *Geometric Langlands From Six Dimensions*, arXiv:0905.2720. 5.2

[216] B. Assel and S. Schfer-Nameki, *Six-dimensional origin of $\mathcal{N} = 4$ SYM with duality defects*, *JHEP* **12** (2016) 058, [arXiv:1610.0366]. 5.2

[217] D. Gaiotto, *N=2 dualities*, *JHEP* **08** (2012) 034, [arXiv:0904.2715]. 5.2, 6.1, 6.3.2, 6.3.3

[218] E. Witten, *Topological Quantum Field Theory*, *Commun.Math.Phys.* **117** (1988) 353. 5.2

[219] L. F. Alday, D. Gaiotto, and Y. Tachikawa, *Liouville Correlation Functions from Four-dimensional Gauge Theories*, *Lett. Math. Phys.* **91** (2010) 167–197, [arXiv:0906.3219]. 5.2, 6.1

[220] N. A. Nekrasov, *Seiberg-Witten prepotential from instanton counting*, *Adv. Theor. Math. Phys.* **7** (2003), no. 5 831–864, [hep-th/0206161]. 5.2

[221] N. Nekrasov and A. Okounkov, *Seiberg-Witten theory and random partitions*, *Prog. Math.* **244** (2006) 525–596, [hep-th/0306238]. 5.2

[222] N. Wyllard, *A(N-1) conformal Toda field theory correlation functions from conformal $N = 2$ SU(N) quiver gauge theories*, *JHEP* **11** (2009) 002, [arXiv:0907.2189]. 5.2

[223] T. Dimofte, D. Gaiotto, and S. Gukov, *Gauge Theories Labelled by Three-Manifolds*, *Commun. Math. Phys.* **325** (2014) 367–419, [arXiv:1108.4389]. 5.2, 6.1, 12

[224] Y. Terashima and M. Yamazaki, *SL(2,R) Chern-Simons, Liouville, and Gauge Theory on Duality Walls*, *JHEP* **08** (2011) 135, [arXiv:1103.5748]. 5.2, 6.1

[225] C. Vafa and E. Witten, *A Strong coupling test of S duality*, *Nucl.Phys.* **B431** (1994) 3–77, [hep-th/9408074]. 5.2, 6.2.1

[226] A. Gadde, S. Gukov, and P. Putrov, *Fivebranes and 4-manifolds*, arXiv:1306.4320. 5.2, 6.1, 1, 2

[227] M. Dedushenko, S. Gukov, and P. Putrov, *Vertex algebras and 4-manifold invariants*, arXiv:1705.0164. 5.2

[228] E. Witten, *Mirror manifolds and topological field theory*, hep-th/9112056. [AMS/IP Stud. Adv. Math.9,121(1998)]. 1

[229] C. Cordova and D. L. Jafferis, *Complex Chern-Simons from M5-branes on the Squashed Three-Sphere*, arXiv:1305.2891. 5.3, 6.1, 6.1, 6.2.3

[230] C. Cordova and D. L. Jafferis, *Toda Theory From Six Dimensions*, arXiv:1605.0399. 5.3

[231] H. Lu, C. N. Pope, and J. Rahmfeld, *A Construction of Killing spinors on S**n*, *J. Math. Phys.* **40** (1999) 4518–4526, [hep-th/9805151]. 5.3

[232] E. Bergshoeff, E. Sezgin, and A. Van Proeyen, *Superconformal Tensor Calculus and Matter Couplings in Six-dimensions*, *Nucl. Phys.* **B264** (1986) 653. 5.3, 6.2.3, 6.2.3

[233] E. Bergshoeff, E. Sezgin, and A. Van Proeyen, *(2,0) tensor multiplets and conformal supergravity in D = 6*, *Class.Quant.Grav.* **16** (1999) 3193–3206, [hep-th/9904085]. 5.3, 6.2.3, 6.2.3, 3, 6.2.4, 6.3.1

[234] T. Kugo and K. Ohashi, *Off-shell D = 5 supergravity coupled to matter Yang-Mills system*, *Prog. Theor. Phys.* **105** (2001) 323–353, [hep-ph/0010288]. 5.3, 6.2.3

[235] C. Cordova and D. L. Jafferis, *Five-Dimensional Maximally Supersymmetric Yang-Mills in Supergravity Backgrounds*, arXiv:1305.2886. 5.3, 6.1, 6.1, 6.2.3, 6.2.3, 6.2.4, 6.3, 6.3.1, C.3, C.3

[236] W. Nahm, *A Simple Formalism for the BPS Monopole*, *Phys. Lett.* **B90** (1980) 413. 6.1

[237] N. Seiberg and E. Witten, *Monopoles, duality and chiral symmetry breaking in N=2 supersymmetric QCD*, *Nucl. Phys.* **B431** (1994) 484–550, [hep-th/9408099]. 6.1

[238] E. Witten, *Phases of N=2 theories in two-dimensions*, *Nucl. Phys.* **B403** (1993) 159–222, [hep-th/9301042]. 6.1

[239] J. Gomis, Z. Komargodski, P.-S. Hsin, A. Schwimmer, N. Seiberg, and S. Theisen, *Anomalies, Conformal Manifolds, and Spheres*, arXiv:1509.0851. 6.1

[240] C. Closset, W. Gu, B. Jia, and E. Sharpe, *Localization of twisted $\mathcal{N} = (0,\ 2)$ gauged linear sigma models in two dimensions*, *JHEP* **03** (2016) 070, [arXiv:1512.0805]. 6.1, 2

[241] M. Bershadsky, C. Vafa, and V. Sadov, *D-branes and topological field theories*, *Nucl. Phys.* **B463** (1996) 420–434, [hep-th/9511222]. 6.1

[242] J. P. Gauntlett, N. Kim, and D. Waldram, *M Five-branes wrapped on supersymmetric cycles*, *Phys. Rev.* **D63** (2001) 126001, [hep-th/0012195]. 6.1

[243] J. M. Maldacena and C. Nunez, *Supergravity description of field theories on curved manifolds and a no go theorem*, *Int. J. Mod. Phys.* **A16** (2001) 822–855, [hep-th/0007018]. 6.1

[244] E. Witten, *Fivebranes and Knots*, arXiv:1101.3216. 6.1, 6.3.2, 6.3.3, 6.5.3, C.6.1, C.6.2

[245] D. Gaiotto, G. W. Moore, and Y. Tachikawa, *On 6d N=(2,0) theory compactified on a Riemann surface with finite area*, *Prog. Theor. Exp. Phys.* **2013** (2013) 013B03, [arXiv:1110.2657]. 6.1, 6.3.2, 6.3.2, 6.3.3, 6.3.4

[246] S. K. Donaldson, *Nahm's equations and the classification of monopoles*, *Comm. Math. Phys.* **96** (1984), no. 3 387–407. 6.1, 6.4.1, 6.4.1

[247] M. Atiyah and N. Hitchin, *The geometry and dynamics of magnetic monopoles*. M. B. Porter Lectures. Princeton University Press, Princeton, NJ, 1988. 6.1, 6.4.1, 6.4.1, 6.4.1, 6.6.2, 6.6.2

[248] P. B. Kronheimer, *A hyper-Kählerian structure on coadjoint orbits of a semisimple complex group*, *J. London Math. Soc. (2)* **42** (1990), no. 2 193–208. 6.1

[249] R. Bielawski, *Lie groups, Nahm's equations and hyperkähler manifolds*, in *Algebraic groups*, pp. 1–17. Universitätsverlag Göttingen, Göttingen, 2007. 6.1, 6.4.1

[250] R. Bielawski, *Hyper-Kähler structures and group actions*, *J. London Math. Soc. (2)* **55** (1997), no. 2 400–414. 6.1, 6.4.1

[251] L. Alvarez-Gaume and D. Z. Freedman, *Geometrical Structure and Ultraviolet Finiteness in the Supersymmetric Sigma Model*, *Commun. Math. Phys.* **80** (1981) 443. 6.1, 6.4.4

[252] J. Bagger and E. Witten, *Matter Couplings in N=2 Supergravity*, *Nucl. Phys.* **B222** (1983) 1. 6.1, 6.4.4

[253] A. Kapustin and K. Vyas, *A-Models in Three and Four Dimensions*, arXiv:1002.4241. 6.1, 6.6.1, 3

[254] D. Anselmi and P. Fre, *Topological sigma models in four-dimensions and triholomorphic maps*, *Nucl. Phys.* **B416** (1994) 255–300, [hep-th/9306080]. 6.1, 6.5.2, 6.5.2, 6.5.2, 3

[255] D. Joyce, *Compact Manifolds with Special Holonomy*. Oxford mathematical monographs. Oxford University Press, 2000. 6.1

[256] N. Marcus, *The Other topological twisting of N=4 Yang-Mills*, *Nucl.Phys.* **B452** (1995) 331–345, [hep-th/9506002]. 6.2.1

[257] A. Kapustin and E. Witten, *Electric-Magnetic Duality And The Geometric Langlands Program*, *Commun. Num. Theor. Phys.* **1** (2007) 1–236, [hep-th/0604151]. 6.2.1

[258] D. Bak and A. Gustavsson, *Partially twisted superconformal M5 brane in R-symmetry gauge field backgrounds*, arXiv:1508.0449. 6.2.1

[259] A. S. Galperin, E. A. Ivanov, V. I. Ogievetsky, and E. S. Sokatchev, *Harmonic superspace*. Cambridge Monographs on Mathematical Physics. Cambridge University Press, Cambridge, 2007. 6.2.2

[260] T. Kugo and K. Ohashi, *Supergravity tensor calculus in 5-D from 6-D*, *Prog. Theor. Phys.* **104** (2000) 835–865, [hep-ph/0006231]. 6.2.3, 6.2.3, 6.3, C.3, C.3

[261] F. Riccioni, *Tensor multiplets in six-dimensional (2,0) supergravity*, *Phys. Lett.* **B422** (1998) 126–134, [hep-th/9712176]. 6.2.3

[262] N. J. Hitchin, *Monopoles and geodesics*, *Comm. Math. Phys.* **83** (1982), no. 4 579–602. 6.4.1

[263] N. J. Hitchin, *On the construction of monopoles*, *Comm. Math. Phys.* **89** (1983), no. 2 145–190. 6.4.1, 6.4.1

[264] N. J. Hitchin, A. Karlhede, U. Lindstrom, and M. Rocek, *Hyperkähler Metrics and Supersymmetry*, *Commun. Math. Phys.* **108** (1987) 535. 6.4.1

[265] A. S. Dancer, *Nahm's equations and hyper-Kähler geometry*, *Comm. Math. Phys.* **158** (1993), no. 3 545–568. 6.4.1

[266] M. Bershadsky, A. Johansen, V. Sadov, and C. Vafa, *Topological reduction of 4-d SYM to 2-d sigma models*, *Nucl. Phys.* **B448** (1995) 166–186, [hep-th/9501096]. 6.4.2, 6.4.2, 6.6

[267] J. A. Harvey and A. Strominger, *String theory and the Donaldson polynomial*, *Commun. Math. Phys.* **151** (1993) 221–232, [hep-th/9108020]. 6.4.2

[268] J. P. Gauntlett, *Low-energy dynamics of N=2 supersymmetric monopoles*, *Nucl. Phys.* **B411** (1994) 443–460, [hep-th/9305068]. 6.4.2, C.5.1

[269] D. Gaiotto and E. Witten, *Supersymmetric Boundary Conditions in N=4 Super Yang-Mills Theory*, arXiv:0804.2902. 6.4.2, C.6.3

[270] D. Z. Freedman and A. Van Proeyen, *Supergravity*. Cambridge University Press, Cambridge, 2012. 6.4.4

[271] L. Anderson, *Five-dimensional topologically twisted maximally supersymmetric Yang-Mills theory*, *JHEP* **02** (2013) 131, [arXiv:1212.5019]. 6.5.3, C.6.1, C.6.2

[272] S. Salamon, *Riemannian geometry and holonomy groups*, vol. 201 of *Pitman Research Notes in Mathematics Series*. Longman Scientific & Technical, Harlow; copublished in the United States with John Wiley & Sons, Inc., New York, 1989. 6.6

[273] G. W. Gibbons and N. S. Manton, *Classical and Quantum Dynamics of BPS Monopoles*, *Nucl. Phys.* **B274** (1986) 183. 6.6.2, 6.6.2

[274] I. T. Ivanov and M. Rocek, *Supersymmetric sigma models, twistors, and the Atiyah-Hitchin metric*, *Commun. Math. Phys.* **182** (1996) 291–302, [hep-th/9512075]. 6.6.2, 11

[275] N. Dorey, V. V. Khoze, M. P. Mattis, D. Tong, and S. Vandoren, *Instantons, three-dimensional gauge theory, and the Atiyah-Hitchin manifold*, *Nucl. Phys.* **B502** (1997) 59–93, [hep-th/9703228]. 6.6.2, 6.6.2

[276] A. Hanany and B. Pioline, *(Anti-)instantons and the Atiyah-Hitchin manifold*, *JHEP* **07** (2000) 001, [hep-th/0005160]. 6.6.2

[277] S. Franco, D. Ghim, S. Lee, R.-K. Seong, and D. Yokoyama, *2d (0,2) Quiver Gauge Theories and D-Branes*, *JHEP* **09** (2015) 072, [arXiv:1506.0381]. 2

[278] F. Benini and N. Bobev, *Two-dimensional SCFTs from wrapped branes and c-extremization*, *JHEP* **1306** (2013) 005, [arXiv:1302.4451]. 2

[279] C. Closset, S. Cremonesi, and D. S. Park, *The equivariant A-twist and gauged linear sigma models on the two-sphere*, *JHEP* **06** (2015) 076, [arXiv:1504.0630]. 2

[280] F. Benini and A. Zaffaroni, *A topologically twisted index for three-dimensional supersymmetric theories*, *JHEP* **07** (2015) 127, [arXiv:1504.0369]. 2

[281] K. A. Intriligator and N. Seiberg, *Mirror symmetry in three-dimensional gauge theories*, *Phys.Lett.* **B387** (1996) 513–519, [hep-th/9607207]. 5

[282] S. Lee and M. Yamazaki, *3d Chern-Simons Theory from M5-branes*, *JHEP* **12** (2013) 035, [arXiv:1305.2429]. 12

[283] J. Yagi, *3d TQFT from 6d SCFT*, *JHEP* **08** (2013) 017, [arXiv:1305.0291]. 12

[284] T. Dimofte, D. Gaiotto, and S. Gukov, *3-Manifolds and 3d Indices*, *Adv.Theor.Math.Phys.* **17** (2013) 975–1076, [arXiv:1112.5179]. 12

[285] N. J. Hitchin, *The Selfduality equations on a Riemann surface*, *Proc. Lond. Math. Soc.* **55** (1987) 59–131. 7

[286] H. K. Dreiner, C. Luhn, and M. Thormeier, *What is the discrete gauge symmetry of the MSSM?*, *Phys. Rev.* **D73** (2006) 075007, [hep-ph/0512163]. B.3